

SYNTHESIS AND REACTIVITY OF LOW- VALENT GROUP 13 COMPOUNDS

Dissertation

Zur Erlangung des Grades des Doktors der
Naturwissenschaften der Naturwissenschaftlich-Technischen
Fakultät der Universität des Saarlandes

von

M.Sc. Türkan Ilgin Demirer

Saarbrücken

2025

Tag des Kolloquiums: 25.04.2025

Dekan: Prof. Dr.-Ing. Dirk Bähre

Berichterstatter: Dr. Diego M. Andrada

Prof. Dr. David Scheschkewitz

Akad. Mitglied: Priv.-Doz. Dr. André Schäfer

Vorsitz: Prof. Dr. Aranzázu del Campo Bécares

This dissertation was done in the time between September 2019 and July 2023 at the Institute of General and Inorganic Chemistry of the Faculty of Natural Sciences and Engineering at the Saarland University in the group of Dr. Diego M. Andrada.

Die vorliegende Dissertation wurde in der Zeit zwischen September 2019 und Juli 2023 am Institut für Allgemeine und Anorganische Chemie der Naturwissenschaftlich-Technischen Fakultät an der Universität des Saarlandes in dem Arbeitskreis von Dr. Diego M. Andrada.

Abstract

Mixed species containing elements from both group 13 and 15 have been of interest for decades due to their potential application in the production of semiconducting materials. However, their synthesis remains challenging since they are highly reactive and tend to oligomerize. In this thesis, different approaches were followed for producing these highly reactive species. One of these approaches involves employing strong σ -donating Lewis bases, namely N-heterocyclic carbenes (NHCs). Novel phosphanyl-gallanes have been prepared from various phosphorous sources and studied for elimination reactions to afford group 13-15 multiple bonds. Additionally, their electronic properties were investigated both experimentally and by computational methods.

Another approach for stabilization of inherently instable and reactive species relies on employing sterically hindering ligand systems. Bis(silylamido)naphthalene and carbazole derivatives were used for the preparation of low-valent aluminum and gallium species. Further reactivity studies were conducted including Al(II) radical addition reaction to the benzene ring and oxidative cyclization of a gallylene with a π -component.

Finally, a low-valent mono-coordinated gallium (I) compound was synthesized, and its reactivity tested towards various substrates including transition metal complexes, Lewis bases, and unsaturated compounds. Moreover, its potential as a precursor to form Ga=N and Ga=P multiply bonded species was explored.

Zusammenfassung

Gemischte Verbindungen der Elemente der Gruppen 13 und 15 sind aufgrund ihres Potenzials in der Herstellung von Halbleitermaterialien von Interesse. Die Synthese dieser Verbindungen ist oft herausfordernd, da sie sehr reaktiv sind und zur Oligomerisierung neigen. Die vorliegende Dissertation konzentriert sich auf verschiedene Ansätze zur Herstellung dieser hochreaktiven Spezies. Im ersten Teil, N-heterozyklischer Carbene (NHC) wurden für die Synthese von neuartigen Phosphagallanen verwendet. Diese wurden auf Eliminierungsreaktionen untersucht, um Mehrfachbindungen zwischen Elementen der Gruppen 13 und 15 zu ermöglichen. Außerdem wurden ihre elektronischen Eigenschaften experimentell und mittels theoretischer Methoden untersucht.

Im zweiten Teil wurden sterische anspruchsvolle Ligandensysteme, z.B. Bis(silylamido)naphthalin- und Carbazol-Derivate, für die Herstellung von niedervalenten Aluminium- und Galliumspezies verwendet. Weitere Reaktivitätsstudien wurden durchgeführt, darunter die radikalische Al(II)-Additionsreaktion an Benzol und die oxidative Cyclisierung eines Gallylens mit einer π -Komponente.

Schließlich wurde eine niedrigvalente monokoordinierte Gallium(I)-Verbindung synthetisiert und ihre Reaktivität gegenüber verschiedenen Verbindungen, einschließlich ungesättigter Verbindungen, Lewis-Säuren und Basen, untersucht. Außerdem wurde ihr Potenzial als Vorläufer für die Bildung von Ga=N- und Ga=P-Mehrfachbindungen untersucht.

List of Publications

This thesis has been published in parts in:

- T. Ilgin Demirer, Dr. Bernd Morgenstern, Dr. Diego M. Andrada, Synthesis, Structure, and Bonding Analysis of Lewis Base and Lewis Acid/Base-Stabilized Phosphanylgallanes. *Eur. J. of Inorg. Chem.* **2022**.
<https://doi.org/10.1002/ejic.202200477>
- Depdeep Mandal, T. Ilgin Demirer, Tetiana Sergeieva, Bernd Morgenstern, Haakon T. A. Wiedemann, Christopher W. M. Kay, Diego M. Andrada, Evidence of Al(II) Radical Addition to Benzene, *Angew. Chem. Int. Ed.* **2023**.
<https://doi.org/10.1002/anie.202217184>

Other contributions:

A list of author's other contributions not included in this thesis:

- Tetiana Sergeieva, T. Ilgin Demirer, Axel Wuttke, Ricardo A. Mata, André Schäfer, Gerrit-Jan Linker, Diego M. Andra, Revisiting the Origin of the Bending in Group 2 Metallocenes Cp₂Ae (Ae= Be-Ba), *Phys. Chem. Chem. Phys.* **2023**.
<http://doi.org/10.1002/anie.202217184>
- Arne Merschel, Dennis Rottschäfer, Beate Neumann, Hans-Georg Stämmler, Maurice van Gastel, T. Ilgin Demirer, Diego M. Andrada, Rajendra Ghadwal, Crystalline Anions Based on Classical N-Heterocyclic Carbenes, *Angew. Chem. Int. Ed.* **2022**.
<https://doi.org/10.1002/anie.202215244>

Acknowledgements

Firstly, I would like to thank Dr. Diego M. Andrada for giving me the opportunity to be a part of his research group.

I would like to thank Prof. Dr. David Scheschkewitz to be my supervisor and taking his time to read and evaluate this work. I also would like to thank his entire group for their collaboration and a friendly environment.

I would like to thank Dr. André Schäfer for his constructive comments and support. His encouragement has been vital in guiding me through this journey.

I would especially like to thank Dr. Bernd Morgenstern for his help and guidance in X-ray crystallography. Additionally, I'd like to thank Dr. Michael Zimmer for the support in NMR spectroscopy and Susanne Harling for elemental analyses.

I would like to thank Dr. Carsten Präseing for useful suggestions and comments.

I would like to thank both Bianca Iannuzzi and Dominika Posse for their kind help throughout the years.

I would like to thank all the current and past group members, Dr. Anup Kumar Adhikari, Dr. Tetiena Sergeieva, Dr. Abhishek Koner, Dr. Debdeep Mandal, Sergi Danés, Enric Sabater, Dennis Wetterlich, Stavroula Pachoula, Pamela Hasanovic, and Dr. Marti Gimferrer for scientific discussions and friendly environment. Sergi Danés, Enric Sabater, Tetiena Sergeieva, and Dennis Wetterlich were not only colleagues but became dear friends to me and I always will cherish our time during our studies. Moreover, I would like to thank my friends Dr. Emiliano Martinez Vollbert and Anna-Lena Thömmes for their nice company. Lastly, I would like to thank Batuhan Koyuncu for his friendship and express my happiness that Saarbrücken reunited us.

I would like to thank my dear friends from Berlin, Dr. Alexandra Tsouka, Anna-Maria Tsirigoni, Antreas Vorcas, Mariafrancesca La Greca and Eleftheria Poulou for their support and friendship throughout the years.

I would like to express my heartfelt gratitude to my friends Daghan Berker, Doguscan Biyikli, Cem Ergören, and Yalin Yüksel for their many years of friendship, constant support, and unwavering presence in my life.

Additionally, I would like to thank one of my best friends Gökce Özkan for being there for me through both good and bad times.

Finally, I would like to thank my family (my mother, father, grandmother, and uncle) for their support and guidance throughout all my studies and encourage me for the best.

Content

LIST OF ABBREVIATIONS	XIX
LIST OF FIGURES	XXI
LIST OF SCHEMES	XXV
LIST OF TABLES	XXVIII
1. INTRODUCTION	1
1.1. N-Heterocyclic Carbenes (NHCs) and Cyclic (alkyl)(amino)carbenes (cAACs)	1
1.2. Synthesis and Properties of Phosphanlygallanes and Aminogallanes	7
1.3. Group 13 Metallylenes	10
1.3.1. Al(I) Compounds	10
1.3.2. Ga(I) Compounds	12
1.4. Carbazole-Stabilized Main Group Compounds	15
1.5. Group 13/15 Multiple Bonding Systems	22
2. OBJECTIVES	31
3. RESULTS AND DISCUSSION	33
3.1. Synthesis of Novel Phosphanlygallanes	33
3.1.1. Synthesis and Characterization of NHC-GaH ₂ (PCO) (NHC= IDip, IMes)	33
3.1.2. Synthesis and Characterization of IDip-GaCl ₂ P(TMS) ₂ 122 and CAAC-GaCl ₂ P(TMS) ₂ 123	35
3.1.3. Synthesis, Structure, and Bonding Analysis of Lewis Acid/Base-Stabilized Phosphanlygallanes	39
3.2. Synthesis of Group 13 Complexes and their Reactions	51
3.2.1. Synthesis of Gallium (I) Compound and its Reactions	51
3.2.2. Evidence of Al ^{II} Radical Addition to Benzene	63
4. CONCLUSION AND OUTLOOK	72

5. EXPERIMENTAL SECTION	75
5.1. General	75
5.1.1. Experimental Conditions	75
5.1.2. Solvent Purification	75
5.1.3. Analytical Methods	75
5.2. Starting Materials	75
5.2.1. Synthesis of IDip-GaH ₂ (PCO)	119
5.2.2. Synthesis of IMes-GaH ₂ (PCO)	120
5.2.3. Synthesis of IDip-GaCl ₂ (OTf)	121
5.2.4. Synthesis of IDip-GaCl ₂ P(TMS) ₂	122
5.2.5. Synthesis of ^{Me} 2CAAC.GaCl ₂ P(TMS) ₂	123
5.2.6. Synthesis of L-GaI ₂	124
5.2.7. Synthesis of L-Ga	125
5.2.8. Synthesis of L-GaCr(CO) ₅	126
5.2.9. Synthesis of L-GaMo(CO) ₅	127
5.2.10. Synthesis of L-GaW(CO) ₅	128
5.2.11. Synthesis of L-Ga(ⁱ Pr ₂ Me ₂)	129
5.2.12. Synthesis of L-Ga(C ₁₄ H ₈ O)	130
5.2.13. Synthesis of (L-GaN ₄ Ad ₂)	131
6. REFERENCES	84
7. APPENDIX	92
7.1. NMR Spectra	92
7.2. IR Spectra	107
7.3. Crystal Data and Structure Refinement	112
7.3.1. IDip-GaH ₂ (PCO)	119
7.3.2. IMes-GaH ₂ (PCO)	120
7.3.3. (ⁱ Pr ₂ Me ₂ -H)(PCO)	116
7.3.4. IDip-GaCl ₂ (OTf)	121
7.3.5. IDip-GaCl ₂ P(TMS) ₂	122
7.3.6. CAAC-GaCl ₂ P(TMS) ₂	123
7.3.7. L-GaI ₂	124
7.3.8. L-Ga	125

7.3.9. L-GaCr(CO) ₅ 126	127
7.3.10. L-GaMo(CO) ₅ 127	129
7.3.11. L-GaW(CO) ₅ 128	131
7.3.12. L-Ga(ⁱ Pr ₂ Me ₂) 129	133
7.3.13. L-Ga(C ₁₄ H ₈ O ₂) 130	135
7.3.14. L-GaN ₄ Ad ₂ 131	137
7.4. COMPUTATIONAL DETAILS	138
7.4.1. Optimized Structures, Cartesian xyz coordinates and Energies in Hartrees	139
7.4.2. Frontier Molecular Orbitals	185
7.4.4. NBO Results	192
7.4.5. EDA-NOCV	193
7.4.6. AIM Analysis	195
8. SYNTHESIS, STRUCTURE, AND BONDING ANALYSIS OF LEWIS BASE AND LEWIS ACID/BASE-STABILIZED PHOSPHANYLGALLANES	196
9. EVIDENCE OF AL^{II} ADDITION TO BENZENE	244

List of Abbreviations

Å	Angstrom
Ar	Aryl
BenzK	Benzyl Potassium
^t Bu	<i>tert</i> -butyl
^s Bu	<i>sec</i> -butyl
C°	Celcius
18-C-6	18-crown-6
CAAC	Cyclic (alkyl)(amino)carbene
Cp	Cyclopentadienyl
Cp*	1,2,3,4,5-pentamethylcyclopentadiene
⁵ Cp	pentaisopropylcyclopentadienyl
Cy	Cyclohexyl
CEt ₂	1,4-diethylcyclohexane
DFT	Density Functional Theory
DMAP	4-Dimethylamidopyridine
DMSO	Dimethylsulfoxide
Dip	2,6-diisopropylphenyl
Et ₂ O	Diethyl Ether
Et	Ethyl
Eq.	Equivalentents
h	hour
HOMO	Highest Occupied Molecular Orbital
HSAB	Hard and Soft Acids and Bases
Hz	Hertz
ⁱ Pr-bimy	1,3-diisopropylbenzimidazole
IR	Infrared
KC ₈	Potassium graphite
LA	Lewis acid
LB	Lewis base
LED	Light Emitting Diode
LUMO	Lowest Unoccupied Molecular Orbital
Me	Methyl
Mes	1,3,5-trimethylbenzene
Mes*	1,3,5-(<i>tri-tert</i> -butyl)benzene
Mes'	3,5-dimethylcumene
MO	Molecular Orbital
NacNac	[HC(CMe ₂ N(2,6- ⁱ Pr ₂ C ₆ H ₃) ₂)]
NBar ^F ₄	Sodium tetrakis[3,5-bis(trifluoromethyl)phenyl]borate
NHC	N-heterocyclic carbene
NMR	Nuclear Magnetic Resonance
NON	4,5-bis(2,6-diisopropylanilido)-2,7-di- <i>tert</i> -butyl-9,9-dimethylxanthene
OTf	trifluoromethanesulfonate
Ph	Phenyl
ppm	Parts per million

RT	Room temperature
Salen(^t Bu)	<i>N,N'</i> -ethylenebis(3,5-di- <i>tert</i> -butylsalicylideneimine)
^{Mes} Ter	1,3-dimesitylbenzene
TMS	Trimethylsilyl
TMP	2,2,6,6-Tetramethylpiperidine
THF	Tetrahydrofuran
Tip	C ₆ H ₂ -2,4,6- ⁱ Pr ₃
Tol.	Toluene
UV	Ultraviolet
VIS	visible
XRD	X-ray diffraction

List of Figures

- FIGURE 1.** THERMAL ELLIPSOID PLOTS (50%) OF **119**. HYDROGEN ATOMS EXCEPT FOR H_X AND H_Y ARE OMITTED FOR THE CLARITY. SELECTED BOND LENGTHS (Å) AND ANGLES (°): **119**: GA1-C1: 2.046(3), GA1-P1: 2.410(1), O1-C28: 1.172(5), O1-C28-P1: 177.4(5)°, C28-P1-GA1: 89.4(2)°. **120**: GA1A-C1: 2.027(3), GA1A-P1A: 2.393(2), C22A-O1A: 1.193(5), O1A-C22A-P1A: 173.4(5)°, GA1A-P1A-C22A: 89.1(2)°. _____ 34
- FIGURE 2.** THERMAL ELLIPSOID PLOTS (50%) OF **121**. HYDROGEN ATOMS ARE OMITTED FOR THE CLARITY. SELECTED BOND LENGTHS (Å) AND ANGLES (°): **121**: GA1-C1: 1.990(1), GA1-O1:1.908(1), GA1-CL1: 2.1468(4), GA1-CL2: 2.1480(4), C1-GA1-O1: 104.17(5). _____ 36
- FIGURE 3.** ¹H NMR SPECTRA OF IDIP-GACL₂P(TMS)₂ **122** IN C₆D₆. _____ 37
- FIGURE 4.** THERMAL ELLIPSOID PLOTS (50%) OF **122** AND **123**. HYDROGEN ATOMS ARE OMITTED FOR THE CLARITY. SELECTED BOND LENGTHS (Å) AND ANGLES (°): **122**: GA1-C1: 2.0537(9), GA1-P1:2.3082(3), GA1-CL1: 2.2082(3), GA1-CL2: 2.2230(3), C1-GA1-P1: 118.22(3); **123**: GA1-C1: 2.067(1), GA1-P1:2.3187(3), GA1-CL1: 2.2179(3), GA1-CL2: 2.2336(3), C1-GA1-P1: 115.05(3). ____ 38
- FIGURE 5.** SOLID STATE STRUCTURES OF COMPOUND **124** (LEFT) AND **125** (RIGHT). THERMAL ELLIPSOIDS SET TO 50% PROBABILITY. SELECTED EXPERIMENTAL AND THEORETICAL [B3LYP-D3(BJ)/DEF2-TZVP] BOND LENGTHS [Å] AND ANGLES [DEG]: **124**: N1-GA1: 1.875(3) [1.90], GA1-I1: 2.4540(6) [2.492], GA1-I2: 2.4936(9) [2.535], N1-GA1-I2: 110.5(1) [113.1], I1-GA1-I2: 122.38(2) [116.8], N1-GA1-I1: 124.5(1) [130]. **125**: N1-GA1: 2.010(2) [2.06]. HYDROGEN ATOMS ARE OMITTED FOR CLARITY. _____ 52
- FIGURE 6.** KS-MOLECULAR ORBITALS (ISOCONTOUR VALUE = 0.05 A.U.) OF COMPOUND **125** AT THE B3LYP-D3(BJ)/DEF2-SVP LEVEL OF THEORY. HYDROGEN ATOMS ARE OMITTED FOR CLARITY. ____ 54
- FIGURE 7.** MOLECULAR STRUCTURES OF **128** AND **129**. ELLIPSOIDS SET AT 50% PROBABILITY LEVEL. HYDROGEN ATOMS ARE OMITTED FOR CLARITY. _____ 56
- FIGURE 8.** 2D LAPLACIAN DISTRIBUTION ∇²P IN THE N-GA-M AND N-GA-C_{CAR} PLANE. DASHED RED LINES INDICATE AREAS OF CHARGE CONCENTRATION (∇²P<0) WHILE SOLID BLUE LINES SHOW AREAS OF CHARGE DEPLETION (∇²P>0), BOND PATHS (BLACK LINES), AND BCPS (BLACK DOTS). 58
- FIGURE 9.** ¹H NMR SPECTRA OF **131** IN C₆D₆. _____ 61
- FIGURE 10.** THERMAL ELLIPSOID PLOTS (50%) OF (L-GAN₄AD₂) **131**. HYDROGEN ATOMS ARE OMITTED FOR THE CLARITY. SELECTED BOND LENGTHS (Å) AND ANGLES (°): GA-N1: 1.852(1), GA1-N2:1.835(1), GA-N3: 1.816 (1), N2-N5: 1.375 (2), N3-N4: 1.377(2), N4-N5: 1.274(2). _____ 62
- FIGURE 11.** ¹H NMR (400 MHZ, C₆D₆, 300K) SPECTRUM OF IDIP-GAH₂(PCO) **119**. _____ 92
- FIGURE 12.** ³¹P NMR (400 MHZ, C₆D₆, 300K) SPECTRUM OF IDIP-GAH₂(PCO) **119**. _____ 92
- FIGURE 13.** ¹³C NMR (400 MHZ, C₆D₆, 300K) SPECTRUM OF IDIP-GAH₂(PCO) **119**. _____ 93
- FIGURE 14.** ¹H NMR (400 MHZ, C₆D₆, 300K) SPECTRUM OF IMES-GAH₂(PCO) **120**. _____ 93
- FIGURE 15.** ³¹P NMR (400 MHZ, C₆D₆, 300K) SPECTRUM OF IMES-GAH₂(PCO) **120**. _____ 94
- FIGURE 16.** ¹³C NMR (400 MHZ, C₆D₆, 300K) SPECTRUM OF IMES-GAH₂(PCO) **120**. _____ 94
- FIGURE 17.** ¹H NMR (400 MHZ, CDCL₃, 300K) SPECTRUM OF IDIP-GACL₂(OTF) **121**. _____ 95

FIGURE 18. ^1H NMR (400 MHz, C_6D_6 , 300K) SPECTRUM OF IDIP-GACL ₂ P(TMS) ₂ 122 .	95
FIGURE 19. ^{31}P NMR (400 MHz, C_6D_6 , 300K) SPECTRUM OF IDIP-GACL ₂ P(TMS) ₂ 122 .	96
FIGURE 20. ^{13}C NMR (400 MHz, C_6D_6 , 300K) SPECTRUM OF IDIP-GACL ₂ P(TMS) ₂ 122 .	96
FIGURE 21. ^{29}Si NMR (400 MHz, C_6D_6 , 300K) SPECTRUM OF IDIP-GACL ₂ P(TMS) ₂ 122 .	97
FIGURE 22. ^1H NMR (400 MHz, C_6D_6 , 300K) SPECTRUM OF $^{\text{ME}_2}\text{CAAC-GACL}_2\text{P(TMS)}_2$ 123 .	97
FIGURE 23. ^{31}P NMR (400 MHz, C_6D_6 , 300K) SPECTRUM OF $^{\text{ME}_2}\text{CAAC-GACL}_2\text{P(TMS)}_2$ 123 .	98
FIGURE 24. ^{13}C NMR (400 MHz, C_6D_6 , 300K) SPECTRUM OF $^{\text{ME}_2}\text{CAAC-GACL}_2\text{P(TMS)}_2$ 123 .	98
FIGURE 26. ^{13}C NMR (400 MHz, C_6D_6 , 300K) SPECTRUM OF L-GAl ₂ 124 .	99
FIGURE 27. ^1H NMR (400 MHz, C_6D_6 , 300K) SPECTRUM OF L-GA 125 . (• L-GAl ₂)	100
FIGURE 28. ^{13}C NMR (400 MHz, C_6D_6 , 300K) SPECTRUM OF L-GA 125 . (• L-GAl ₂ , * L-H)	100
FIGURE 30. ^{13}C NMR (400 MHz, C_6D_6 , 300K) SPECTRUM OF L-GACR(CO) ₅ 126 . (* L-H)	101
FIGURE 31. ^1H NMR (400 MHz, C_6D_6 , 300K) SPECTRUM OF L-GAMO(CO) ₅ 127 . (• L-GAl ₂ , * L-H, ○ L-GA)	102
FIGURE 33. ^1H NMR (400 MHz, C_6D_6 , 300K) SPECTRUM OF L-GAW(CO) ₅ 128 . (• L-GAl ₂ , * L-H, ○ L-GA)	103
FIGURE 34. ^{13}C NMR (400 MHz, C_6D_6 , 300K) SPECTRUM OF L-GAW(CO) ₅ 128 . (* L-H)	103
FIGURE 35. ^1H NMR (400 MHz, C_6D_6 , 300K) SPECTRUM OF L-GA(I'PR ₂ ME ₂) 129 .	104
FIGURE 36. ^{13}C NMR (400 MHz, C_6D_6 , 300K) SPECTRUM OF L-GA(I'PR ₂ ME ₂) 129 .	104
FIGURE 37. ^1H NMR (400 MHz, C_6D_6 , 300K) SPECTRUM OF L-GA(C ₁₄ H ₈ O) 130 . (• L-GAl ₂ , * L-H•)	105
FIGURE 38. ^{13}C NMR (400 MHz, C_6D_6 , 300K) SPECTRUM L-GA(C ₁₄ H ₈ O) 130 .	106
FIGURE 39. ^1H (400 MHz, C_6D_6 , 300K) NMR SPECTRA OF L-GAN ₄ AD ₂ 131 .	106
FIGURE 40. ^{13}C (400 MHz, C_6D_6 , 300K) NMR SPECTRA OF L-GAN ₄ AD ₂ 131 .	107
FIGURE 41. IR SPECTRUM OF IDIP-GAH ₂ (PCO) 119 .	107
FIGURE 42. IR SPECTRUM OF IMES-GAH ₂ (PCO) 120 .	108
FIGURE 43. IR SPECTRUM OF L-GAl ₂ 124 .	108
FIGURE 44. IR SPECTRUM OF L-GA 125 .	109
FIGURE 45. IR SPECTRUM OF L-GACR(CO) ₅ 126 .	109
FIGURE 46. IR SPECTRUM OF L-GAMO(CO) ₅ 127 .	110
FIGURE 47. IR SPECTRUM OF LGAW(CO) ₅ 128 .	110
FIGURE 48. IR SPECTRUM OF L-GA(NHC) 129 .	111
FIGURE 49. IR SPECTRUM OF L-GA(C ₁₄ H ₈ O ₂) 130 .	111
FIGURE 50. OPTIMIZED STRUCTURE AT THE B3LYP-D3(BJ)/DEF2SVP LEVEL OF THEORY FOR 124 . HYDROGEN ATOMS ARE OMITTED FOR CLARITY.	139
FIGURE 51. OPTIMIZED STRUCTURE AT THE B3LYP-D3(BJ)/DEF2SVP LEVEL OF THEORY FOR 125 . HYDROGEN ATOMS ARE OMITTED FOR CLARITY.	144
FIGURE 52. OPTIMIZED STRUCTURE AT THE B3LYP-D3(BJ)/DEF2SVP LEVEL OF THEORY FOR 126 . HYDROGEN ATOMS ARE OMITTED FOR CLARITY.	149
FIGURE 53. OPTIMIZED STRUCTURE AT THE B3LYP-D3(BJ)/DEF2SVP LEVEL OF THEORY FOR 127 . HYDROGEN ATOMS ARE OMITTED FOR CLARITY.	154

FIGURE 54. OPTIMIZED STRUCTURE AT THE B3LYP-D3(BJ)/DEF2SVP LEVEL OF THEORY FOR 128 . HYDROGEN ATOMS ARE OMITTED FOR CLARITY. _____	160
FIGURE 55. OPTIMIZED STRUCTURE AT THE B3LYP-D3(BJ)/DEF2SVP LEVEL OF THEORY FOR 129 . HYDROGEN ATOMS ARE OMITTED FOR CLARITY. _____	166
FIGURE 56. OPTIMIZED STRUCTURE AT THE B3LYP-D3(BJ)/DEF2SVP LEVEL OF THEORY FOR 130 . HYDROGEN ATOMS ARE OMITTED FOR CLARITY. _____	172
FIGURE 57. OPTIMIZED STRUCTURE AT THE B3LYP-D3(BJ)/DEF2SVP LEVEL OF THEORY FOR 131 . HYDROGEN ATOMS ARE OMITTED FOR CLARITY. _____	178
FIGURE 58. FRONTIER KS MOLECULAR ORBITALS (ISOVALUE 0.05 A.U.) OF COMPOUND 124 AT THE B3LYP-D3(BJ)/DEF2-SVP LEVEL OF THEORY. _____	185
FIGURE 59. FRONTIER KS MOLECULAR ORBITALS (ISOVALUE 0.05 A.U.) OF COMPOUND 125 AT THE B3LYP-D3(BJ)/DEF2-SVP LEVEL OF THEORY. _____	186
FIGURE 60. FRONTIER KS MOLECULAR ORBITALS (ISOVALUE 0.05 A.U.) OF COMPOUND 126 AT THE B3LYP-D3(BJ)/DEF2-SVP LEVEL OF THEORY. _____	187
FIGURE 61. FRONTIER KS MOLECULAR ORBITALS (ISOVALUE 0.05 A.U.) OF COMPOUND 127 AT THE B3LYP-D3(BJ)/DEF2-SVP LEVEL OF THEORY. _____	188
FIGURE 62. FRONTIER KS MOLECULAR ORBITALS (ISOVALUE 0.05 A.U.) OF COMPOUND 128 AT THE B3LYP-D3(BJ)/DEF2-SVP LEVEL OF THEORY. _____	189
FIGURE 63. FRONTIER KS MOLECULAR ORBITALS (ISOVALUE 0.05 A.U.) OF COMPOUND 129 AT THE B3LYP-D3(BJ)/DEF2-SVP LEVEL OF THEORY. _____	190
FIGURE 65. FRONTIER KS MOLECULAR ORBITALS (ISOVALUE 0.05 A.U.) OF COMPOUND 131 AT THE B3LYP-D3(BJ)/DEF2-SVP LEVEL OF THEORY. _____	192
FIGURE 66. PLOT OF DEFORMATION DENSITIES $\Delta\rho$ OF THE PAIRWISE ORBITAL INTERACTIONS BETWEEN L-GA AND CR(CO) ₅ FRAGMENT, ASSOCIATED ENERGIES ΔE (IN KCAL/MOL) AND EIGENVALUES N (IN A.U.). THE RED COLOR SHOWS THE CHARGE OUTFLOW, WHEREAS BLUE SHOWS CHARGE DENSITY ACCUMULATION. SHAPE OF THE MOST IMPORTANT INTERACTING OCCUPIED AND VACANT ORBITALS OF THE FRAGMENTS. CALCULATIONS ARE DONE AT BP86- D3(BJ)/TZ2P LEVEL OF THEORY. _____	193
FIGURE 67. PLOT OF DEFORMATION DENSITIES $\Delta\rho$ OF THE PAIRWISE ORBITAL INTERACTIONS BETWEEN L-GA AND MO(CO) ₅ FRAGMENT, ASSOCIATED ENERGIES ΔE (IN KCAL/MOL) AND EIGENVALUES N (IN A.U.). THE RED COLOR SHOWS THE CHARGE OUTFLOW, WHEREAS BLUE SHOWS CHARGE DENSITY ACCUMULATION. SHAPE OF THE MOST IMPORTANT INTERACTING OCCUPIED AND VACANT ORBITALS OF THE FRAGMENTS. CALCULATIONS ARE DONE AT BP86- D3(BJ)/TZ2P LEVEL OF THEORY. _____	193
FIGURE 68. PLOT OF DEFORMATION DENSITIES $\Delta\rho$ OF THE PAIRWISE ORBITAL INTERACTIONS BETWEEN L-GA AND W(CO) ₅ FRAGMENT, ASSOCIATED ENERGIES ΔE (IN KCAL · MOL ⁻¹) AND EIGENVALUES N (IN A.U.). THE RED COLOR SHOWS THE CHARGE OUTFLOW, WHEREAS BLUE SHOWS CHARGE DENSITY ACCUMULATION. SHAPE OF THE MOST IMPORTANT INTERACTING	

OCCUPIED AND VACANT ORBITALS OF THE FRAGMENTS. CALCULATIONS ARE DONE AT BP86-D3(BJ)/TZ2P LEVEL OF THEORY. _____ 194

FIGURE 69. LAPLACIAN DISTRIBUTION OF THE ELECTRON DENSITY OF **126-129**. CONTOUR LINE DIAGRAMS OF THE LAPLACIAN DISTRIBUTION $\nabla^2 P(R)$. DASHED RED LINES INDICATE AREAS OF CHARGE CONCENTRATION ($\nabla^2 P(R) < 0$) WHILE SOLID BLUE LINES SHOW AREAS OF CHARGE DEPLETION ($\nabla^2 P(R) > 0$) (B3LYP-D3(BJ)/DE2-TZVPP//B3LYP-D3(BJ)/DEF2-SVP). _____ 195

List of Schemes

SCHEME 1. SYNTHETIC ROUTE FOR THE NHC (2). _____	1
SCHEME 2. EXAMPLES OF NHCS AND CAACS AND THEIR ACRONYMS. _____	1
SCHEME 3. SYNTHESIS OF CARBENES. 3: R=ME; 4: R=ET; 5: R=PR; 6: R= ^t BU; 7: R=ME; 8: R=ET; 9: R=PR. _____	2
SCHEME 4. SOME EXAMPLES OF NHCS AND THEIR ACRONYMS. _____	2
SCHEME 5. USE OF NHCS IN STABILIZATION OF HIGHLY REACTIVE SPECIES. 10A: NHC= IDIP; 10B: NHC= IMES; 11A: R= ME; 11B: R=PR. _____	3
SCHEME 6. TWO ALTERNATIVE ROUTES FOR THE SYNTHESIS OF NHC GALLIUM HYDRIDES. 13: R=ME, R'=PR; 14: R= H, R'=DIP; 16: R=H, R'=MES. _____	4
SCHEME 7. SYNTHETIC ROUTE FOR THE NHC MONO- AND DICHLOROGALLANES. 17: R=DIP, R'=H; 18: R=DIP, R'= H ₂ ; 19: R= PR, R'= ME; 20: R=DIP, R'=H; 21: R=DIP, R'=H ₂ ; 22: R=PR, R'=ME; 23: R=DIP, R'=H; 24: R=DIP, R'=H ₂ ; 25: R=PR, R'=ME. _____	5
SCHEME 8. REACTIVITY OF CARBENE STABILIZED GALLANES TOWARDS CAAC. 25: X=H; 28: X=CL; 29: X=H; 30: X=CL. _____	6
SCHEME 9. REPRESENTATION OF MOST COMMON STRUCTURAL MOTIFS OF GROUP 13-15 ELEMENTS. _____	7
SCHEME 10. STERIC EFFECTS ON THE STABILIZATION OF MONOMERIC PHOSPHANYLGALLANES. 36: LB=PY; 37: LB=DMAP. _____	8
SCHEME 11. EXAMPLES OF LA/LB AND LB-STABILIZED PHOSPHANYLALANES AND -GALLANES. 33: M=AL; 34: M=GA. _____	9
SCHEME 12. EXAMPLES OF AL(I) COMPOUNDS. 36: R=H, ^t BU. _____	11
SCHEME 13. SYNTHESIS OF GACP 40 AND GACP* 41 . _____	12
SCHEME 14. EXAMPLES OF GALLYLENES REPORTED IN THE LITERATURE. 44: R=ME, ^t BU. _____	13
SCHEME 15. SYNTHESIS OF TERPHENYL-STABILIZED ORGANOGALLIUM (I) COMPOUNDS 47-49 . _____	14
SCHEME 16. SYNTHESIS OF COMPOUNDS 50-51 . 50: R= ME; 51: ET; 52: R=ME, 53: R=ET. _____	15
SCHEME 17. SYNTHESIS OF AMIDO(DICHLORO)GALLANES 54 AND 55 . 54: R=PH; 55: MES. _____	15
SCHEME 18. SYNTHESIS OF CARBOZYL-STABILIZED GROUP 14 SALTS. 59: E=GE; 60: E=SN; 61: E=PB. _____	16
SCHEME 19. FORMATION OF 63 FROM L-ALi ₂ 62 . R=3,5-DI-TERT-BUTYLPHENYL. _____	17
SCHEME 20. SYNTHESIS AND REACTIVITY STUDIES OF FREE ALUMINYLENE. R=3,5-DI-TERT-BUTYLPHENYL. _____	18
SCHEME 21. INTER- AND INTRAMOLECULAR ADDITION OF NHC-COORDINATED ALUMYLENE 68 . R=3,5-DI-TERT-BUTYLPHENYL, NHC= PR ₂ -BIMY. _____	19
SCHEME 22. REACTIVITY OF ALUMINYLENE 64 TOWARDS UNSATURATED SUBSTRATES. R=3,5-DI-TERT-BUTYLPHENYL. 73: R'= PH; 74: R'=ET. _____	20
SCHEME 23. SYNTHESIS OF CARBAZOL-STABILIZED GA(I) COMPOUND 75 . R=9-PHENYL-10-ANTHRACENE. _____	20

SCHEME 25. ISOLATION OF FIRST MONOMERIC ALUMINUM 78 AND GALLIUM IMIDES 79 . 78: M=AL; 79: M=GA. _____	22
SCHEME 26. ISOLATION OF MONOMERIC GALLIUM IMIDES 82 AND 83 . _____	23
SCHEME 27. EXAMPLES OF COMPOUNDS CONTAINING GA=P IN THE LITERATURE. 86A: R=H; 86B: R='PR. _____	23
SCHEME 28. EXAMPLES OF GA=AS IN THE LITERATURE. X = CL, BR. _____	24
SCHEME 29. EXAMPLES OF GA=SB IN THE LITERATURE. _____	24
SCHEME 30. REARRANGEMENT OF THE PHOSPHAKETENE 84A . _____	25
SCHEME 31. REACTIVITY OF THE PHOSPHANYLGALLENE 84B TOWARDS H ₂ AND CO ₂ . _____	25
SCHEME 32. REACTIVITY STUDIES OF 84B . R=NH'PR, NHPH, OH, CCPH, PHPH. _____	26
SCHEME 33. REACTIVITY STUDIES OF 85 . R= ME, PH; R'='PR, CY; 96: R"='PR; 97: R"=CY; 98: R"=ET; 99: R"='PR; 100: R"=CY; 101: R"=ET. _____	27
SCHEME 34. REACTIVITY OF ^{DIP} TERPGACP* 86A TOWARDS H ₂ O AND CO ₂ . _____	28
SCHEME 35. PREPARATION OF HETEROLEPTIC GA-P-C ALLYL CATION AND SYNTHESIS OF COMPOUNDS 105-106 . X=CL, BR; 102: AN= B{C ₆ H(CF ₃) ₂ } ₄ ; 103: AN= B(C ₆ F ₅) ₄ ; 104: AN= AL{OC(CF ₃) ₃ } ₄ . _____	29
SCHEME 36. SYNTHESIS OF COMPOUNDS 107-118 . _____	30
SCHEME 37. PLANNED ROUTE FOR THE SYNTHESIS OF NHC-STABILIZED GA-P MULTIPLE BONDS. _____	31
SCHEME 38. SYNTHESIS OF 119 AND 120 . 119: R=DIP; 120: R=MES. _____	33
SCHEME 39. ATTEMPTED SYNTHESIS OF NHC-GAH ₂ (PCO). (R= 'PR, ME). _____	35
SCHEME 40. SYNTHESIS OF IDIP-GACL ₂ P(TMS) ₂ 122 AND ^{ME2} CAAC-GACL ₂ P(TMS) ₂ 123 . _____	35
SCHEME 41. ATTEMPTED TMSCL ELIMINATION FROM 122 AND 123 . 122: L= IDIP; 123: L= ^{ME2} CAAC. _____	38
SCHEME 42. SYNTHESIS OF GALLYLENE 125 . R=2,6- <i>DI-TERT</i> -BUTYLPHENYL. _____	52
SCHEME 43. SYNTHESIS OF THE COMPOUNDS 126-128 IN C ₆ H ₆ . R= 2,6- <i>DI-TERT</i> -BUTYLPHENYL; 126: M=CR; 127: M=MO; 128: M=W. _____	55
SCHEME 44. SYNTHESIS OF 129 IN C ₆ H ₆ . R=2,6- <i>DI-TERT</i> -BUTYLPHENYL. _____	55
SCHEME 45. REACTION OF GALLYLENE 130 WITH PHENANTHRENE-9,10-DIONE (ABOVE) AND THE MOLECULAR STRUCTURE OF 130 (BELOW). ELLIPSOIDS SET AT 50% PROBABILITY LEVEL. HYDROGEN ATOMS ARE OMITTED FOR CLARITY. R= 2,6- <i>DI-TERT</i> -BUTYLPHENYL. _____	60
SCHEME 46. SYNTHESIS OF 131 . R= 2,6- <i>DI-TERT</i> -BUTYLPHENYL. _____	61
SCHEME 47. ATTEMPTS TO SYNTHESIZE GA=P. R= 2,6- <i>DI-TERT</i> -BUTYLPHENYL, R'= MES*, ^{DIP} TER, ^{ME} STER. _____	62
SCHEME 48. SYNTHESIZED AND STRUCTURALLY CHARACTERIZED NHC-STABILIZED PHOSPHANYLGALLANES. L= IDIP, IMES, ^{ME2} CAAC; X=CL, H, OTF; R=NCY ₂ , N'PR ₂ , TIP, MES; R"=PH,H. _____	72
SCHEME 49. ATTEMPTED SYNTHESIS OF PHOSPHANYLGALLENES VIA A) TMSCL ELIMINATION B) HCL ELIMINATION. X=CL, H; R=NCY ₂ , TIP. _____	73

SCHEME 50. ATTEMPTED SYNTHESIS OF GA=P AND GA=N DOUBLE BONDS FROM GALLYLENE **125**.

R=2,6-*DI-TERT*-BUTYLPHENYL; AR=DIP, TIP. _____ 73

SCHEME 51. FORMATION OF BIRCH-TYPE REDUCTION PRODUCT OF BENZENE. _____ 74

List of Tables

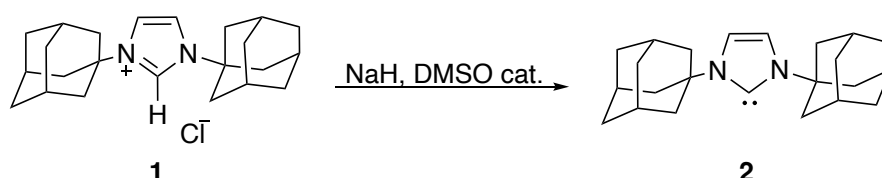
TABLE 1. GA-C _{CAR} BOND LENGTH OF NHC GALLIUM HYDRIDES, HALIDES, AND HYDROCHLORIDES IN Å.	5
TABLE 2. SELECTED EXPERIMENTAL BOND LENGTHS (Å) AND ANGLES (°) OF GALLYLENE-M(CO) ₅ COMPLEXES 126-128 AND GALLYLENE-NHC COMPLEX 129 (CALCULATED VALUES IN PARENTHESIS, B3LYP-D3(BJ)/DEF2-SVP).	57
TABLE 3. CALCULATED NBO CHARGE DISTRIBUTION AT B3LYP-D3(BJ)/DEF2-TZVPP.	57
TABLE 4. EDA-NOCV RESULTS OF THE M-GA AND GA-C _{CAR} BONDS IN COMPOUNDS 126-129 AT B3LYP-D3(BJ)/TZ2P. ALL VALUES ARE IN KCAL MOL ⁻¹ . THE VALUE IN PARENTHESES GIVES THE PERCENTAGE CONTRIBUTION TO THE TOTAL ATTRACTIVE INTERACTIONS $\Delta E_{\text{ELST}} + \Delta E_{\text{ORB}} + \Delta E_{\text{DISP}}$.	59

1. Introduction

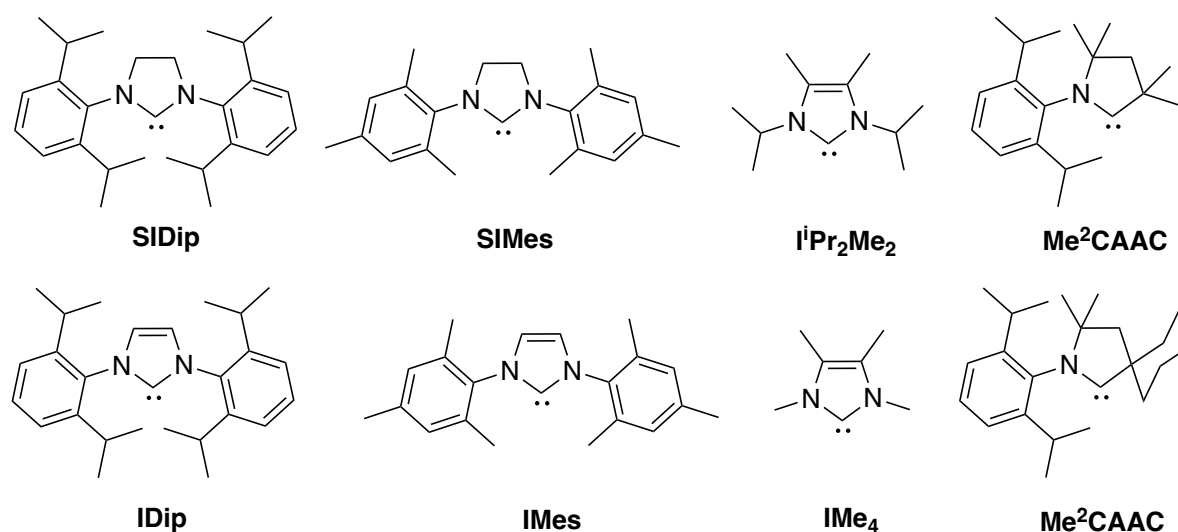
1.1. N-Heterocyclic Carbenes (NHCs) and Cyclic (alkyl)(amino)carbenes (CAACs)

Carbenes are neutral compounds containing a divalent carbon with six electrons in its valence shell.^[1] N-heterocyclic carbenes (NHCs) and cyclic (alkyl)(amino)carbenes (CAACs) are important classes of stable carbenes, known for their stability and extensive utilization in organometallic chemistry and catalysis. The significant difference in their electronic properties leads to a wide range of applications.

The first free and stable N-heterocyclic carbene was isolated by Arduengo et al. in 1991. The synthesis of imidazol-2-ylides was achieved by deprotonation of imidazolium chloride **1** with NaH in THF to produce the stable carbene **2** (Scheme 1).^[2]



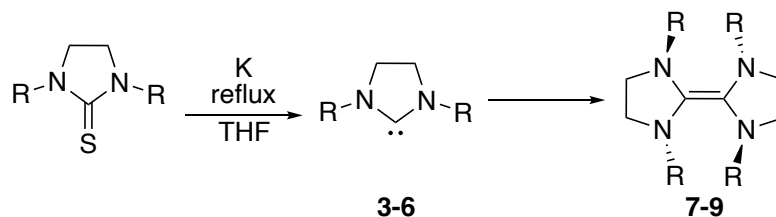
Scheme 1. Synthetic route for the NHC (**2**).



Scheme 2. Examples of NHCs and CAACs and their acronyms.

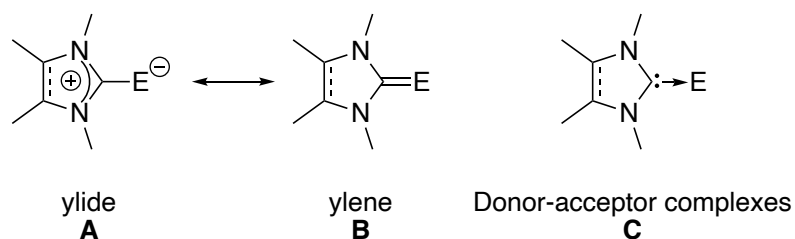
After the isolation of the first bottleable imidazoline-2-ylidene, many NHCs with different heteroatoms and sizes were reported, some examples of which are given in Scheme 2.^[3–6] Both electronic and steric factors play an important role in the stability of NHCs. Heinemann and Thiel applied theoretical methods and showed the importance of the singlet-triplet gap in carbenes for stabilization. This gap was influenced by the factors such as the geometry or the substituents used on the NHCs (Scheme 3).^[7] The effects of sterics was also discussed by Denk and his coworkers. They reported the synthesis of carbenes, the stability of which is dependent on the bulkiness of the substituents. For instance, in the case of R= Me, Et, ⁱPr,

carbenes **3-5** were obtained; however, they underwent dimerization in solution, yielding **7-9** within minutes. Carbene **6**, on the other hand, was stable indefinitely at room temperature.^[8]



Scheme 3. Synthesis of carbenes. **3:** R=Me; **4:** R=Et; **5:** R=ⁱPr; **6:** R=^tBu; **7:** R=Me; **8:** R=Et; **9:** R=ⁱPr.

It is crucial to understand how NHCs bind to metal centers. The nature of the E-C_{car} bonds can be either a dative (donor acceptor) or a double bond. They can be represented by ylide or ylone resonance structures (Scheme 4). In ylide resonance structure **A**, E possesses a formal negative charge, and positive charge delocalizes over the heterocycle. In ylone structure **B**, the C_{car}-E bond is a double bond.^[9,10]



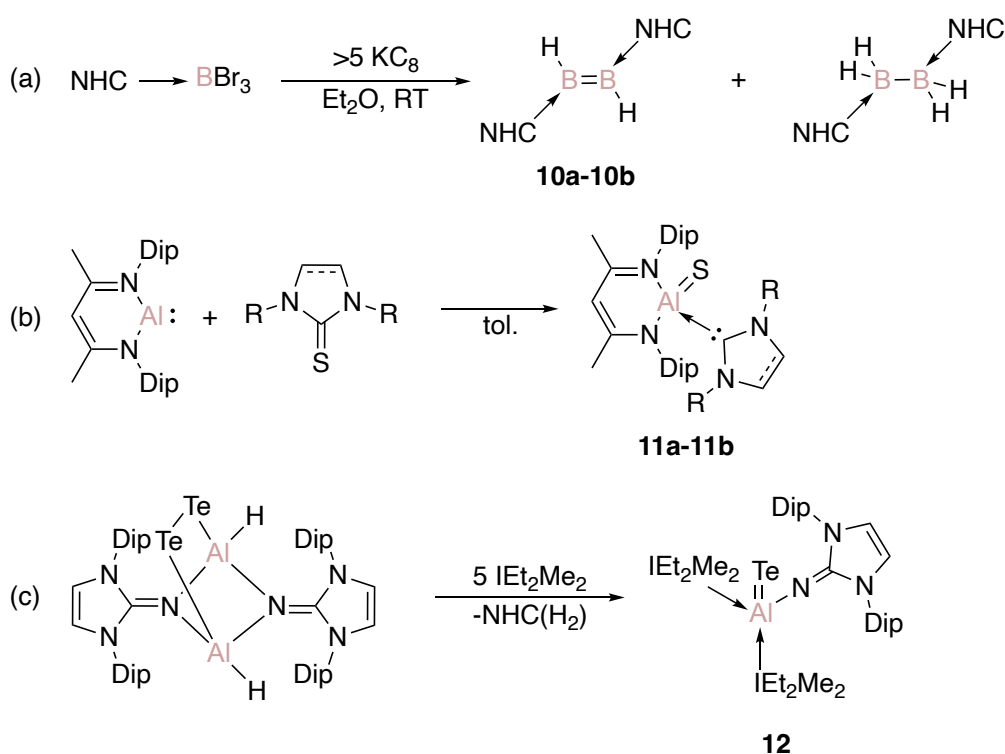
Scheme 4. Some examples of NHCs and their acronyms.

NHCs are commonly used in main group chemistry due to their strong σ -donator and weak π -acceptor properties, allowing them to form strong bonds without compromising the formal oxidation state. In Scheme 4, two different representations of a dative C_{car}-E are given (**A** and **C**). In this thesis, single C_{car}-Ga bonds are represented as in Scheme 4C, irrespective of the bond strength but keeping in mind the literature discourse on the appropriateness of donor-acceptor bonding graphical representations.^[11,12]

In contrast to NHCs, cyclic alkyl amino carbenes (CAACs) are somewhat stronger σ -donors and much stronger π -acceptors than NHCs. The replacement of nitrogen by a quaternary carbon led to both decreases in HOMO-LUMO and the singlet-triplet gap in comparison to classical NHCs (45 vs. 68 kcal/mol).^[13,14] While NHCs are widely used to stabilize low-coordinate elements in different oxidation states, there are several examples of CAACs leading to paramagnetic species.^[15]

NHCs as ligands play an important role in stabilization of group 13 elements in their different oxidation states. There are many examples where the preparation of stable adduct furnishes exotic compounds with the central elements in a low oxidation state. Robinson and coworkers,

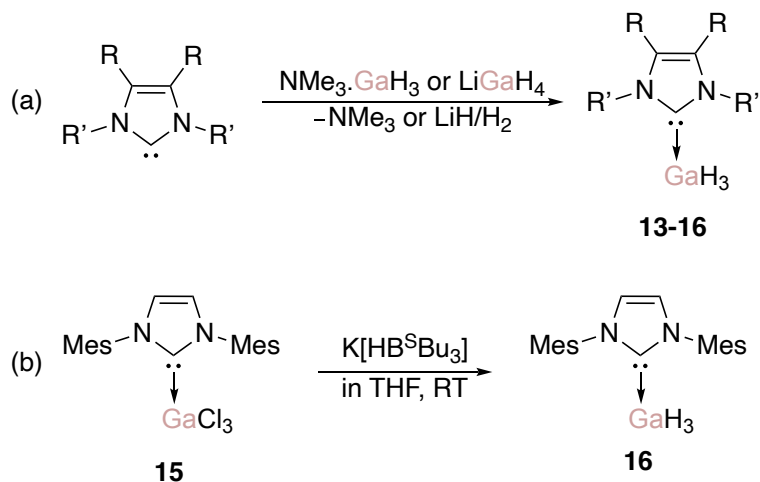
for instance, reported the first examples of stable species with B=B double bond **8a,b** by stabilizing it with IDip and IMes carbene species (Scheme 5a). These compounds were synthesized by reducing (NHC)-BBr₃ **7a,b** with KC₈ in diethyl ether.^[16] As another landmark example, the otherwise inevitable oligomerization of compounds such as aluminum sulfides **10a,b**^[17] and telluride **12**^[18] can be prevented by the coordination of NHCs, thus allowing for the isolation of the monomeric species (Scheme 5b,c). In this thesis, NHCs and Me₂CAAC are employed to stabilize monomeric phosphanyl-gallanes and demonstrate the electrophilic nature of the novel Ga(I) compound. For the synthesis of phosphanyl-gallanes, NHC gallium halides and hydrohalides were used as starting materials.



Scheme 5. Use of NHCs in stabilization of highly reactive species. **10a**: NHC= IDip; **10b**: NHC= IMes; **11a**: R= Me; **11b**: R=Pr.

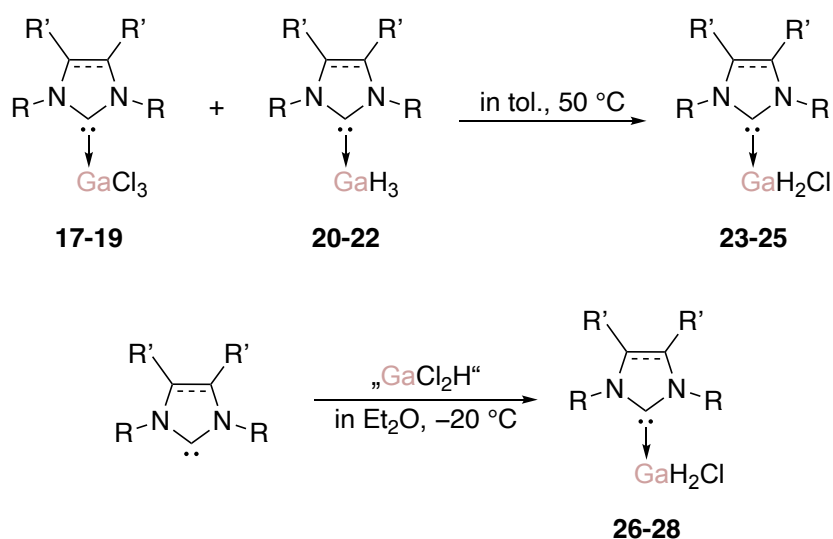
In 1998, Jones and coworkers reported two alternative routes for the synthesis of NHC gallium hydrides.^[19] They can be produced by either ligand exchange (amine/NHC) or in the presence of LiGaH₄ (Scheme 6a). Isolated NHC complexes **13-14**, **16** showed very good thermal stability in comparison to their other Lewis base analogs such as NMe₃-GaH₃.^[20-22] In addition, in 2017, Rivard and coworkers reported a novel route to access IMes-GaH₃ **16** since the previous procedure involved thermally unstable LiGaH₄ (Scheme 6b). Reacting IMes-GaCl₃ **15** with 3 equivalents of K[HB^sBu₃] in THF at room temperature resulted in the Cl/H exchange.^[23] Although there are no reports of the molecular structure of IMes-GaH₃ **16**, many other NHC gallium chlorides, hydrides, and hydrochlorides were characterized by XRD analysis (Table 1). In all structures, the gallium center adopts an approximate tetrahedral

geometry with a Ga-C_{car} bond length between 2.065-2.076 Å which is longer than a typical C-Ga single bond ($\sum_{cov} = 1.99$ Å).



Scheme 6. Two alternative routes for the synthesis of NHC gallium hydrides. **13**: R=Me, R'=iPr; **14**: R=H, R'=Dip; **16**: R=H, R'=Mes.

The group of Cole reported the synthesis of mono- and dichloro halides **23-28** and showed that the replacement of hydrogen atoms by halides increased stability with respect to dehydrogenation.^[24,25] Radius and coworkers then reported carbene-stabilized gallanes and chlorogallanes and further discussed the influence of halide substitution on the reactivity and overall stability of these compounds (Scheme 7). For the synthesis of monochlorogallanes **23-25**, NHC gallium chlorides **17-19** were reacted with 2 equivalents of the corresponding NHC gallium hydrides **20-22**. The desired products **23-25** were produced in good yields where NHC= IDip, SIDip, and (iPrMe)NHC. For the synthesis of NHC dichlorogallanes **26-28**, however, an alternative method was reported. *In situ* generated “GaCl₂H” was treated with the NHC to yield the desired NHC dichlorogallanes **26-28**.^[26] The products were collected in good yields, although in case of of SIDip-GaCl₂H **27**, dismutation of 2 equivalents of IDip-GaCl₃ **18** with IDip-GaH₃ **20** was shown to be more efficient.

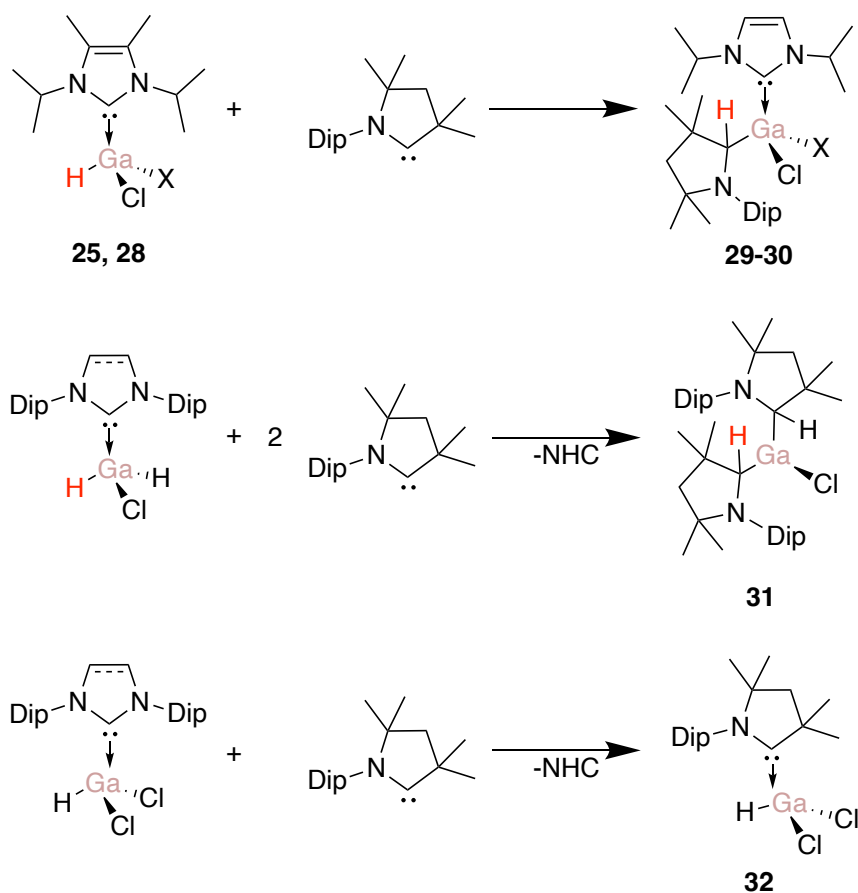


Scheme 7. Synthetic route for the NHC mono- and dichlorogallanes. **17**: R=Dip, R'=H; **18**: R=Dip, R'=H₂; R=*i*Pr, R'=Me; **20**: R=Dip, R'=H; **21**: R=Dip, R'=H₂; **22**: R=*i*Pr, R'=Me; **23**: R=Dip, R'=H; **24**: R=Dip, R'=H₂; **25**: R=*i*Pr, R'=Me.

Table 1. Ga-C_{car} bond length of NHC gallium hydrides, halides, and hydrochlorides in Å.

	(NHC)GaCl ₃	(NHC)GaCl ₂ H	(NHC)GaH ₂ Cl	(NHC)GaH ₃
IMes	1.954(4) ^[27]	2.005(6) ^[24]	2.030(3) ^[24]	-
SIMes	2.025(2) ^[28]	-	-	-
IDip	2.016(2) ^[27]	2.034(2) ^[26]	-	2.055(1) ^[24]
<i>i</i>PrMe	2.011(4) ^[27]	2.019(4) ^[26]	-	2.071(5) ^[19]
IMe₄	-	-	-	2.0537(2) ^[26]
SIDip	2.023(3) ^[28]	-	-	2.076(2) ^[26]

In the same report, the group of Radius described their attempt to prepare CAAC gallium hydrides (Scheme 8). The reaction of ^{Me₂}CAAC with *in situ* generated LiGaH₄, however, led to ^{Me₂}CAACH₂ instead. The alternative ligand exchange of the NHC in (NHC)-GaH₃ (NHC = *i*Pr₂Me, IMe₄, IDip) adducts and ^{Me₂}CAAC was explored without success as the reactions resulted in the insertion of ^{Me₂}CAAC into Ga-H bond. A similar approach was taken for the synthesis of (^{Me₂}CAAC)-GaH₂Cl. CAAC was reacted with (*i*Pr₂Me)-GaH₂Cl **25** and (*i*Pr₂Me)-GaCl₂H **28**, affording compounds **29** and **30**. Additionally, ligand exchange was attempted with (IDip)-GaH₂Cl, forming the chloro analogue of (^{Me₂}CAAC₂GaH). However, (IDip)-GaCl₂H led to a selective substitution of IDip, yielding (^{Me₂}CAAC)-GaCl₂H **32**.^[26]



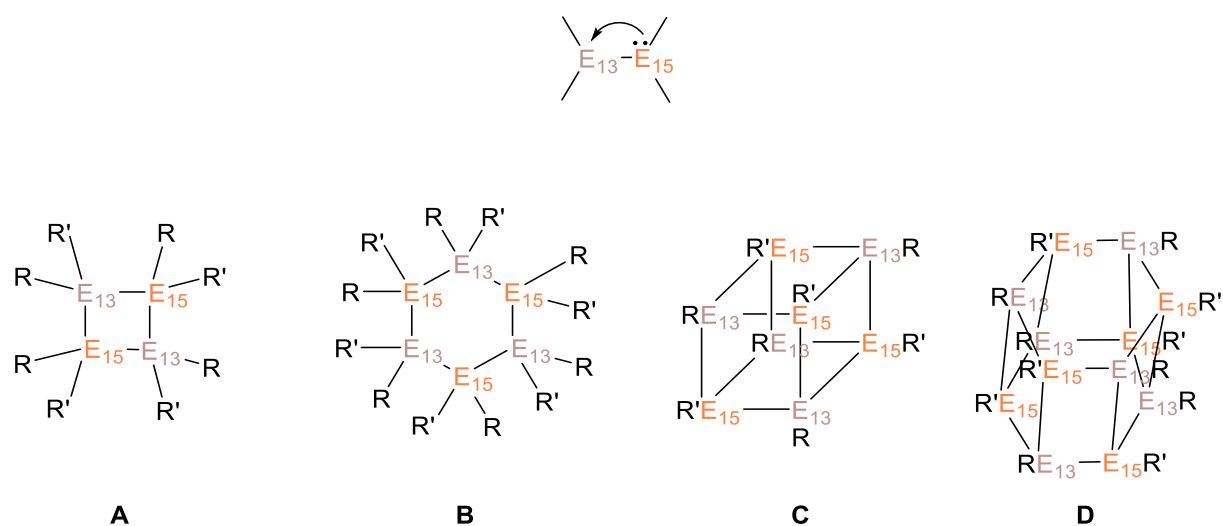
Scheme 8. Reactivity of carbene stabilized gallanes towards CAAC. **25:** X=H; **28:** X=Cl; **29:** X=H; **30:** X=Cl.

Gallanes stabilized by NHC or CAAC can be used as precursors for the synthesis of monomeric phosphanylgallanes and aminogallanes. In the next chapter, these examples are discussed in detail.

1.2. Synthesis and Properties of Phosphanylgallanes and Aminogallanes

Synthesis of compounds containing units with group 13 and 15 elements has attracted great attention due to their applications in material science. For instance, they can be used as precursors for semiconducting materials. Gallium nitrides (GaN) and Gallium phosphides (GaP) are used as emitting layer of LEDs^[29] whereas gallium arsenides (GaAs) are applied in lasers and semiconductors.^[30] The preparation of such materials by molecular beam epitaxy, however, is technically demanding, costly, and requires toxic and pyrophoric gases as precursors (e.g. GaMe₃, AsH₃, or PH₃). A different strategy has been suggested and explored to some extent taking advantage of the precise stoichiometry of the pre-established motifs of single source precursors, thus avoiding the use of hazardous gases.^[31]

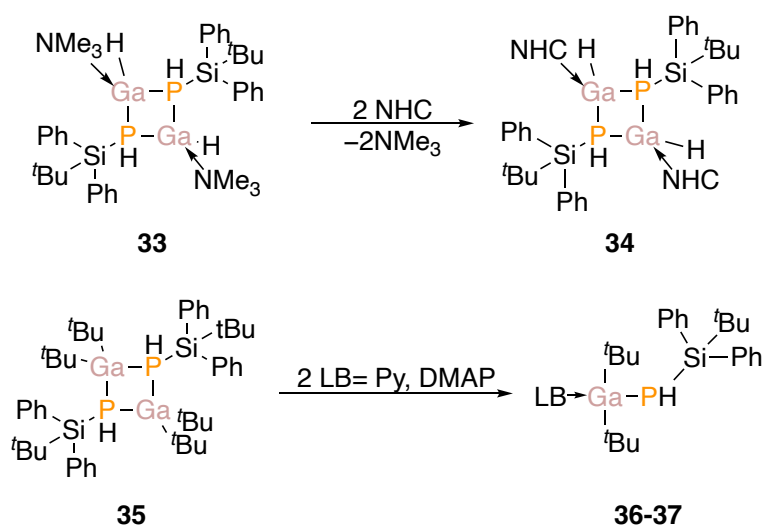
The synthesis of monomeric precursors featuring a multiple bond between 13-15 elements is desirable given the lower carbon content, but at the same time becomes more challenging due to their higher tendency to produce oligomers. This is a consequence of the weak π -bonding, which can be explained by the electropositive character and large size of the group 13 metal. The chemical bond has an increased ionic character and reduced orbital overlap, leaving a reactive functionality prone for self-aggregation.^[32] In Scheme 9, the most common structural motifs of the heavier group 13-15 compounds are given: four- (A) and six-membered (B) heterocycles, cubic (C) and hexagonal forms (D). The electron deficiency at the group 13 element is compensated with intramolecular Lewis/acid pair interaction.



Scheme 9. Representation of most common structural motifs of group 13-15 elements.

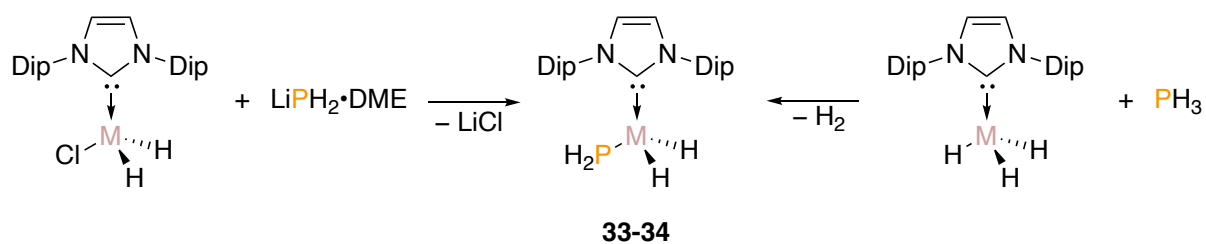
One of the most common methods to prevent oligomerization is the use of bulky substituents at the main group elements. The group of Schulz prepared DMAP-coordinated monomeric group 13/15 compounds [(DMAP)Me₂M-Pn(TMS)₂] (M=Ga, Al and Pn= P, As) by cleaving the four-membered ring with DMAP.^[33] Many years later, von Hänisch and coworkers attempted

a similar approach for the preparation of monomeric phosphanylgallanes. A four-membered cycle **33** was prepared by the reaction of $\text{NMe}_3\text{-MH}_3$ ($\text{M} = \text{Al}, \text{Ga}$) with $\text{H}_2\text{PSi}^t\text{BuPh}_2$. Methane elimination results in NMe_3 stabilized cyclic compounds, which were subsequently treated with NHC as an external Lewis base. Instead of the isolation of monomeric structure, however, NMe_3 was replaced by NHC, affording **34** (Scheme 10).^[34] Hydrogen atoms and NMe_3 groups on gallium atoms were replaced by bulkier *tert*-butyl groups to study the importance of sterics in the stabilization of the monomeric structures. **35** was treated with pyridine and DMAP, which resulted in the formation of **36** and **37**. It was indeed observed that increasing the steric demand at the group 13 metal center led to the successful isolation of the monomeric structure after introducing the external Lewis base.^[35]



Scheme 10. Steric effects on the stabilization of monomeric phosphanylgallanes. **36**: $\text{LB} = \text{Py}$; **37**: $\text{LB} = \text{DMAP}$.

In 2020, Scheer and coworkers accomplished the preparation of the first monomeric, exclusively Lewis base-stabilized phosphanylalanes **33** and -gallanes **34**. Initially, they studied the thermodynamic stability of the target molecules computationally with different Lewis bases such as DMAP, pyridine, and NHC. Both experimentally and computationally, they showed that NHC was able to stabilize the monomeric structures. These results indicate that stabilization can be achieved by using only a Lewis base, which is sterically bulky and strongly σ -donating such as IDip.^[36] Additionally, two routes for the preparation of unsubstituted phosphanylalanes and -gallanes were employed, H_2 and salt elimination the latter of which gave better yields (23% vs. 67%) (Scheme 11).



Scheme 11. Examples of LA/LB and LB-stabilized phosphanylalanes and -gallanes. **33:** M=Al; **34:** M=Ga.

The aforementioned studies suggested the use of NHC gallium chlorides and hydrochlorides as suitable precursors to prepare phosphanylgallanes. NHCs were used to provide enough stabilization to isolate monomeric structures for further application as starting materials in the planned synthesis of so far unknown stable compounds with Ga=P multiple bonds.

1.3. Group 13 Metallylenes

With the discovery that NHCs can stabilize otherwise elusive low-valent species, the synthesis of group 13 metallylenes has gained considerable attention due to their isolobal relationship to carbenes. The most common oxidation state for group 13 elements, except for thallium, is +3, which makes the synthesis of metallylenes challenging. For the stabilization of the +1 oxidation state, many efforts to find an appropriate ligand design have been made. In this thesis, the importance of the ligand design on the isolation of aluminum and gallium (I) complexes and their reactivity will be discussed.

1.3.1. Al(I) Compounds

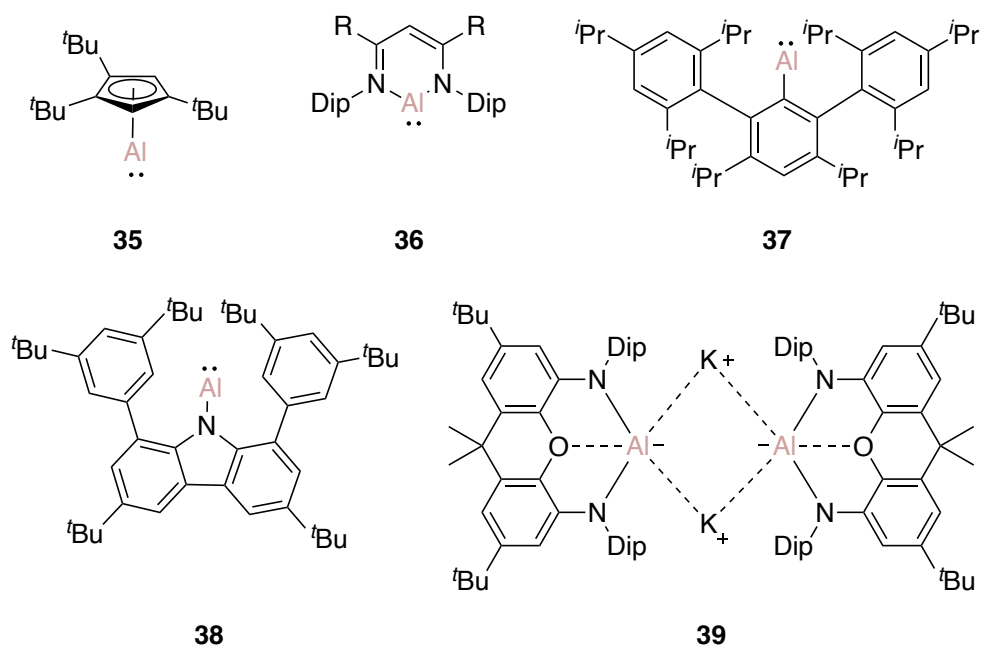
The first example of an Al(I) species was reported by Schnöckel group in 1991. The tetrameric, η^5 -coordinated aluminum (I) compound was prepared by reaction between AlCl and $[\text{Mg}(\text{Cp}^*)_2]$. The formation of the tetrameric compound was confirmed with XRD analysis. They further demonstrated the formation of monomeric units at elevated temperatures by using ^{27}Al -NMR spectroscopy. It was suggested that the formation of monomeric units depends on the temperature and the nature of Cp^{R} stabilizing ligand.^[37,38] This was much later proved by isolation of pure monomeric form **35** by increasing the steric demand ($\text{Cp}^{\text{R}} = \text{C}_5\text{H}_2^t\text{Bu}_3$), despite con X-ray structure were obtained.^[39] Most recently, Schäfer and his coworkers demonstrated the synthesis and isolation of monomeric cyclopentadienylalumylene by employing a very sterically demanding group, ^5Cp , where all substituents are *iso*-propyl groups.^[40]

Nevertheless, the preparation of alumylenes remains challenging, resulting in limited examples due to their high reactivity and tendency to disproportionate into Al^0 and Al^{3+} .^[41] In Scheme 12, some examples of reported alumylenes **35-39** are given. One notable breakthrough involves the stabilization of a monomeric Al(I) compound **36** by β -diketiminato ligand, as reported by Cui and Roesky.^[42] Additionally, Braunschweig group successfully synthesized an alumylene stabilized by two CAACs,^[43] while the Cowley group demonstrated the synthesis of transient aminophosphine-supported alumylene.^[44] Employing bulky ligands was proven to be an effective strategy for the synthesis of mono-coordinated alumylenes. Power utilized bulky terphenyl substituents **37**^[45] whereas Liu and Hinz groups independently reported on the carbazolyl-stabilized base-free alumylenes **38**.^[46,47] Synthesis of carbazolyl-based alumylenes will be further explored in the chapter 2.2. (Scheme 12).

In addition to the neutral alumylenes, there are examples of cationic^[48-50] and anionic alumylenes.^[51] Power group reported first “dialuminyne” species $\text{Na}_2(\text{AlAr}^{\text{iPr}_4})_2$ ($\text{Ar}^{\text{iPr}_4} = \text{C}_6\text{H}_3\text{-2,6-(C}_6\text{H}_3\text{-2,6-}^i\text{Pr}_2)_2$) and “cyclotrialuminene” $\text{Na}_2(\text{AlAr}^{\text{Me}_6})_3$ ($\text{Ar}^{\text{iPr}_4} = \text{C}_6\text{H}_3\text{-2,6-(C}_6\text{H}_3\text{-2,6-}^i\text{Pr}_2)_2$) by following a similar route for the preparation of their gallium counterparts.^[52-54] The dialuminyne $\text{Na}_2(\text{AlAr}^{\text{iPr}_4})_2$ was previously obtained as a transient dialuminene compound,

which activated toluene and benzene.^[55] It could not, however, be isolated due to its highly reactive nature. The molecular structure of $\text{Na}_2(\text{AlAr}^{\text{iPr}_4})_2$ shows an Al-Al bond (2.428(1) Å) with a multiple character. $\text{Tip}_2\text{AlAlTip}_2$ and R_2AlAIR_2 ($\text{R} = \text{CH}(\text{SiMe}_3)_2$), were treated with alkali metals to afford their radical anion complexes.^[56–58] Al(I) complexes, $[\text{KAl}(\text{NON}^{\text{Dip}})]_2$ **39** and $\text{K}[\text{Al}(\text{O}(\text{SiMe}_2\text{NDip})_2)]$ were stabilized by chelating ligand systems (Scheme 12).^[59,60] Coles, Hill, McMullin and coworkers reported the synthesis of $[\text{Al}\{\text{SiN}^{\text{Dip}}\}\text{K}]_2$.^[61]

Examples of cationic alumylenes are rarer compared to its anionic counterparts. The group of Crossing demonstrated the synthesis of $[\text{Al}(\text{AlCp}^*)_3]^+[\text{Al}(\text{OR}^{\text{F}})_4]^-$ ($\text{R}^{\text{F}} = \text{C}(\text{CF}_3)_3$) via salt metathesis between $[\text{AlCp}^*_4]$ and $\text{Li}[\text{Al}(\text{OR}^{\text{F}})_4]$.^[48] Surprisingly, $[\text{Al}(\text{AlCp}^*)_3]^+$ cation dimerizes in solid state as well as in concentrated solutions, but the addition of Lewis bases resulted in isolation of monomeric compounds.



Scheme 12. Examples of Al(I) compounds. **36:** $\text{R} = \text{H}$, tBu .

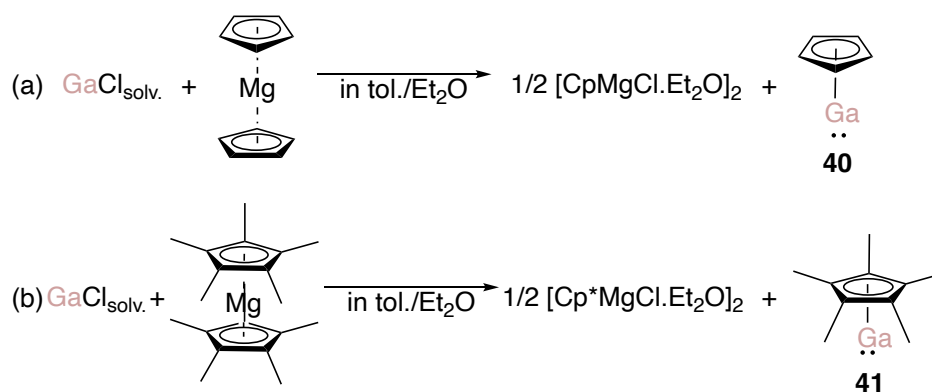
The Wiberg group accomplished the synthesis of the dialane R_2AlAIR_2 ($\text{R} = \text{Si}^{\text{tBu}}_3$) which dissociated into monoalanyl radicals R_2Al^* at 50 °C. Simultaneous cleavage of supersilyl group leads to $[\text{R}_2\text{Al-AIR}]^*$, formation of which was confirmed by EPR spectroscopy. By thermolysis of the dialane at 100 °C, $[\text{R}_4\text{Al}_3]^*$ and tetrahedral tetraalane R_4Al_4 were formed via radicals $[\text{R}_2\text{Al-AIR}]^*$.^[62,63]

Al(I) compounds exhibit intriguing reactivity profiles^[64,65] which involve oxidative addition,^[66] olefin coordination,^[67] C-C bond coupling^[68,69] as well as C-H and C-F bond activation.^[67,70] The synthesis of these compounds poses a significant challenge due to their inherent instability. In this thesis, this challenge is addressed by employing bulky silyl groups to stabilize

Al(II) radical species, examples of which are limited. In this context, the formation of Birch-type reduction product cyclohexa-1,3(or 4)-dienes will be investigated and discussed.

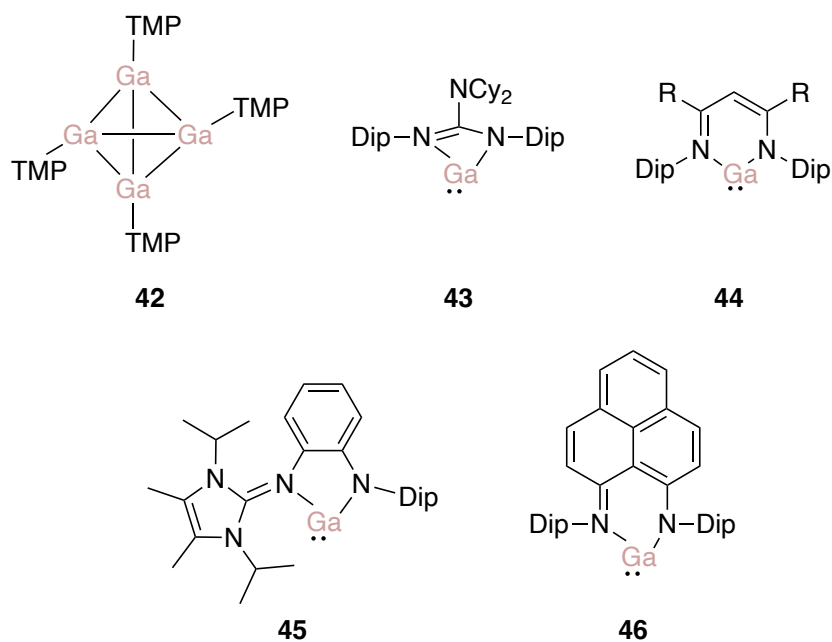
1.3.2. Ga(I) Compounds

The first report of a monovalent gallium (I) compound came from Schnöckel and coworkers in 1992. They treated a solution of GaCl with $[\text{MgCp}_2]$ to afford the desired monovalent gallium (I) compound, GaCp **40** (Scheme 13). The product was characterized by mass spectrometry as well as ^1H , ^{13}C , and ^{71}Ga NMR spectroscopy, but single crystals for x-ray diffraction could not be obtained.^[71] This was then followed by the synthesis of GaCp* **41** by the same group and the structure was successfully analyzed by XRD analysis showing that the metal atom is η^5 -bonded to the ring.^[72]



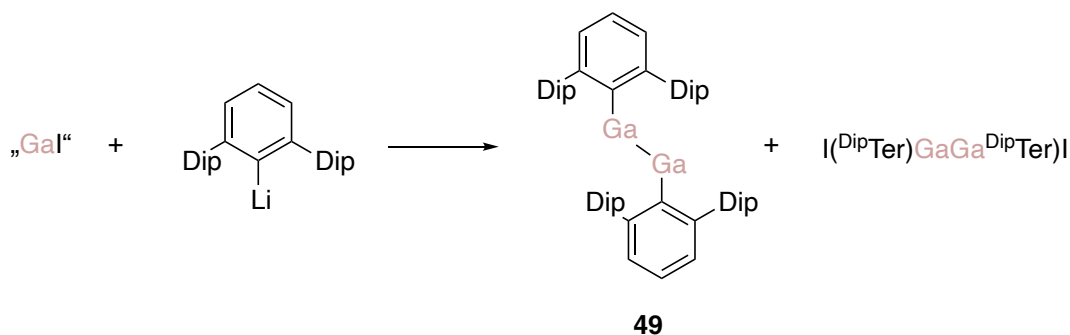
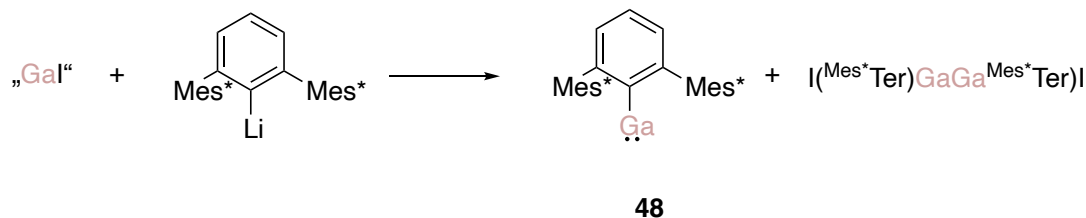
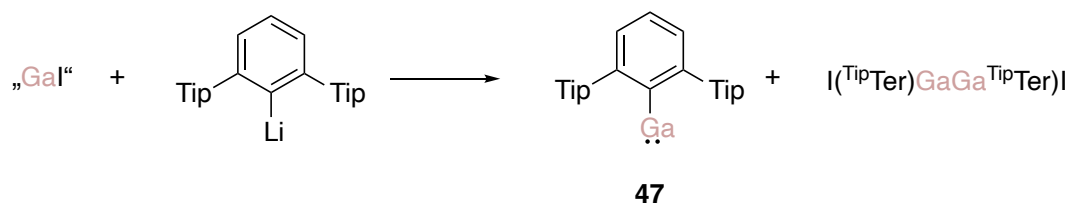
Scheme 13. Synthesis of GaCp **40** and GaCp* **41**.

Many examples of gallium (I) compounds have been reported since then and some of their structures **42-46** are shown in Scheme 14.^[73-81] Anionic *N,N'*-style bi- or tridentate ligands have been widely used for their synthesis due to their structural modularity and steric protection. In particular, β -ketiminate-type ligands (NacNac) have been extensively used for the preparation of group 13 metallylenes.^{[65,74,82][83-85]} In addition, they were further employed for the synthesis of group 13 – group 15 multiple bonds, which will be discussed in detail in the next chapter.



Scheme 14. Examples of gallylenes reported in the literature. **44:** R=Me, ^tBu.

Power and his coworkers showed the importance of steric protection for the stabilization of the mononuclear gallium (I) compounds and other low-valent species. Several gallium aryls were synthesized and characterized. “GaI”^[86] was reacted with (Et₂O)Li^{TiP}Ter,^[87] (Et₂O)Li^{Mes*}Ter and (Li^{Dip}Ter)₂^[88] to afford organogallium(I) compounds Ga^{TiP}Ter **47**, Ga^{Mes*}Ter **48**, and ^{Dip}TerGaGa^{Dip}Ter **49**,^[74] respectively (Scheme 15). Aryliodogallane derivatives were formed as by-products during the reactions; however, the products can be purified by recrystallization. Although Ga^{TiP}Ter **47** and Ga^{Mes*}Ter **48** were collected as green crystals, XRD analysis could not be done due to the low quality. Nonetheless, the reactivity studies suggested that Ga^{TiP}Ter **47** and Ga^{Mes*}Ter **48** are present in the solution as monomers rather than dimers. A dynamic equilibrium was suggested as a plausible explanation since the Ga-Ga bond is weak, given the large energy difference between the lone pair and the vacant p-orbital of the monomers.^[74]

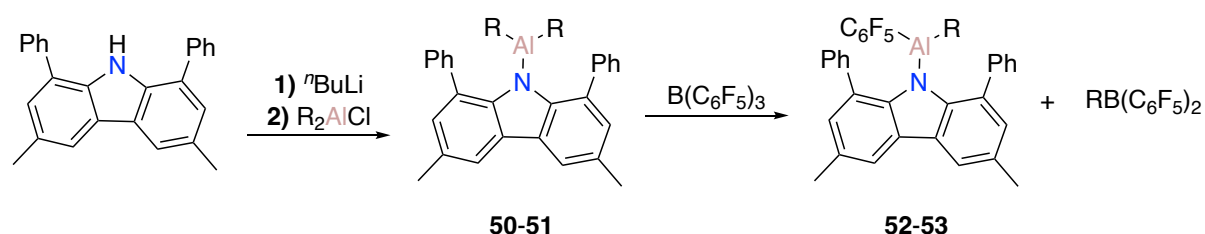


Scheme 15. Synthesis of terphenyl-stabilized organogallium (I) compounds **47-49**.

In this thesis, the synthesis of a monomeric gallylene is reported, as well as the reactivity towards different substrates including metal carbonyls. Furthermore, its application to generate novel gallium imides was investigated. To provide stability for this highly reactive, mono-coordinated Ga(I) compound, a carbazole-based ligand system was employed.

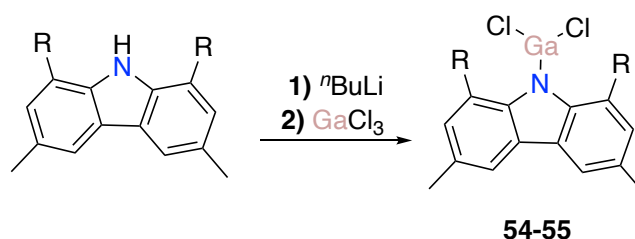
1.4. Carbazole-Stabilized Main Group Compounds

Carbazoles (L) have gained attention as ligand systems in main-group chemistry due to their bulky nature and the electronic donation by the nitrogen center.^[89] Although carbazoles are widely used in optoelectronics, examples of their use as ligands with main group elements are limited, especially with group 13. L-AlR₂ (R=Me (**50**), Et (**51**)) were prepared by the *N*-lithiation of the carbazole ligand and consecutive treatment with aluminum methyl chloride (Scheme 16). Further treatment of the alkyl aluminum compounds with Lewis and Brønsted acids, B(C₆F₅)₃ and [H(OEt₂)₂][B{3,5-(CF₃)₂C₆H₃]₄], led to alkyl/Ar^F exchange, forming cationic species, [LAIR]⁺, which then abstracts Ar^F from the counter-anion forming **52** and **53**. Additionally, solutions of cationic species, [LAIR]⁺ were reacted with 1 bar of ethylene. ¹H NMR spectrum of the reactions showed the formation of higher olefins.^[90]



Scheme 16. Synthesis of compounds **50-51**. **50**: R= Me; **51**: Et; **52**: R=Me, **53**: R=Et.

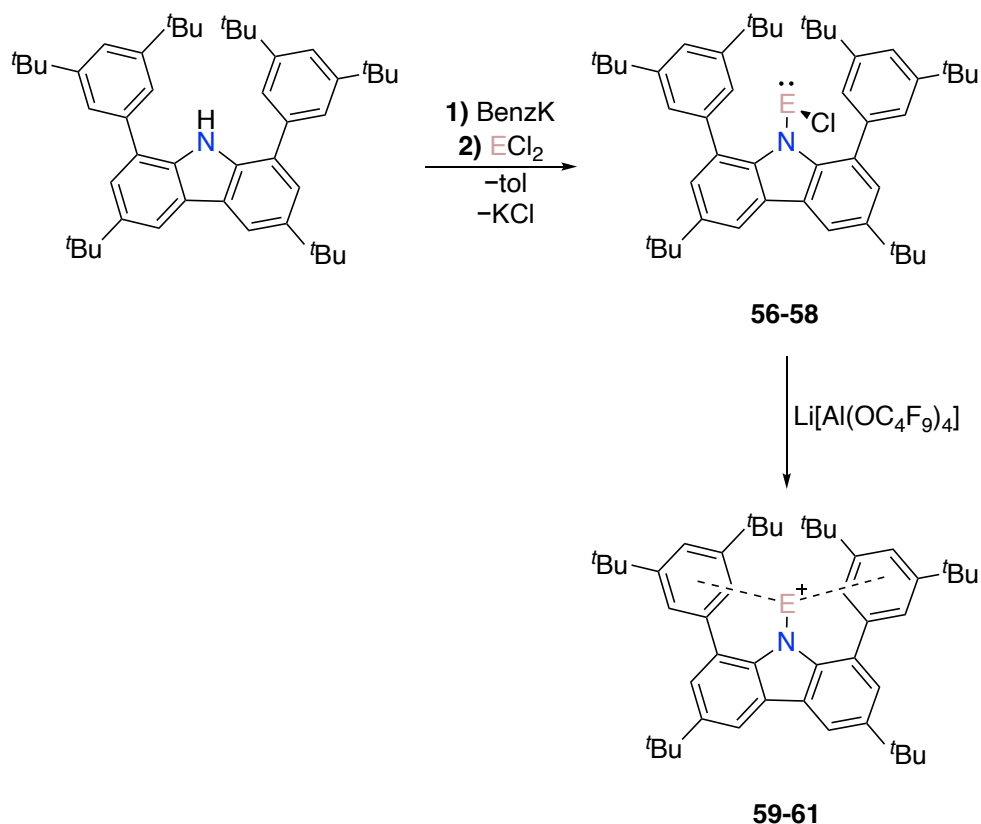
Aldridge and coworkers reported the synthesis of amido ligands containing 1,8-diarylcarbazol-9-yl backbone and their dichlorogallane complexes **54-55** (Scheme 17). This was the first example of monomeric three-coordinate amido(dihalo)gallanes reported in the literature. The synthesized compounds were characterized by multinuclear NMR spectroscopy and XRD analysis. It was shown that these ligand systems can be an alternative to sterically encumbered terphenyl ligands.^[91]



Scheme 17. Synthesis of amido(dichloro)gallanes **54** and **55**. **54**: R=Ph; **55**: Mes.

In 2019, Hinz reported the synthesis of 1,8-bis(3,5-*di-tert*-butylphenyl)-3,6-*di-tert*-butylcarbazole.^[92] He showed that such ligand systems can be used to stabilize mono-coordinated group 14 cations **59-61** (Scheme 18). The ligand was deprotonated with benzyl potassium followed by addition of group 14 chlorides ECl₂ (Sn, Pb, Ge) to the solution containing the potassium salt of the ligand. **56-58** were then reacted with Li[Al(OC₄F₉)₄] to

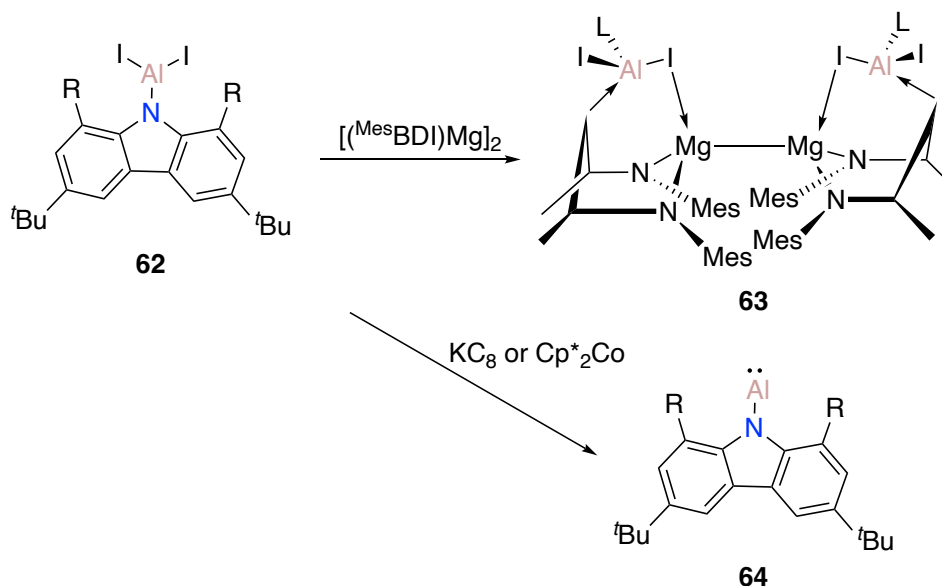
produce the desired salts, [(RE)(Al(OC₄F₉)₄)] **59-61**. A year later, he reported the synthesis of mono-substituted silicon (II) cation by implementing the same ligand system.^[93] These findings showed the ability of the carbazole ligand in the stabilization of highly reactive species.^[92]



Scheme 18. Synthesis of carbozyl-stabilized group 14 salts. **59**: E=Ge; **60**: E=Sn; **61**: E=Pb.

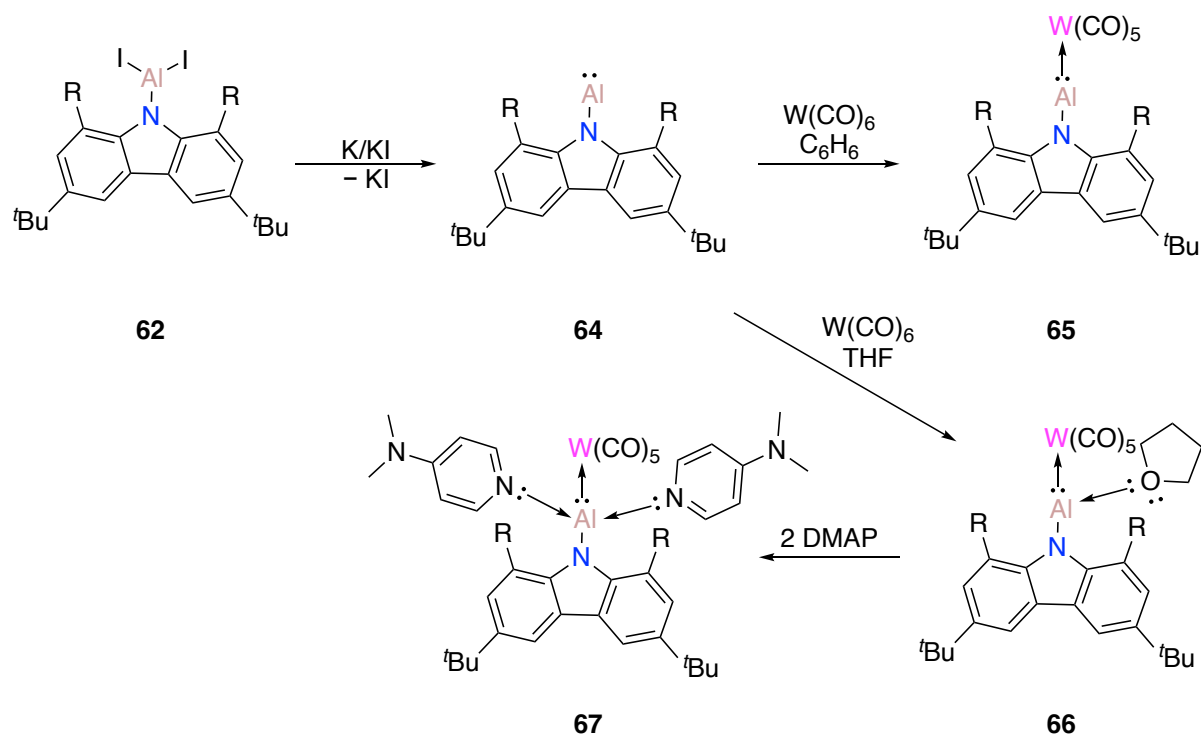
After establishing the synthesis of carbazole ligand and isolating its group 14 salts, Hinz et al. aimed to use this ligand system to synthesize the corresponding aluminum diiodides. L-AlI₂ (L= 1,8-bis(3,5-*di-tert*-butylphenyl)-3,6-*di-tert*-butylcarbazole) **62** was prepared from the potassium salt of the ligand and AlI₃ in toluene. It was obtained as a white crystalline solid which has poor solubility in solvents such as *n*-hexane and toluene. XRD analysis shows that there is a N-Al bond length of 1.830(3) Å and the aluminum atom has a short contact with one of the *o*-C atoms of the pending aryl groups. However, ¹H NMR spectra of the compound show that aryl-*t*Bu groups are equivalent to each other, confirming that this contact is weak and hence fluxional. L-AlI₂ **62** was further reduced to target the free alumylene with two different reducing agents, namely KC₈ and Cp₂Co. The reaction with KC₈ indeed afforded L-Al (**64**, Scheme 19, but the competitive elimination of the potassium salt of the ligand reduces the reaction yields significantly. The reduction with Cp₂Co led to better results allowing the isolation of the product. Additionally, the reduction of L-AlI₂ was attempted with Jones' compound [(^{Mes}BDI)Mg]₂ since it has been proven to be effective in reducing alanates and carbene-alane adducts.^{[94-96][97]} However, instead of reduction, addition of diiodoalane across

$[(^{\text{Mes}}\text{BDI})\text{Mg}]$ moieties had taken place, forming $[(\text{LAlI}_2)_2\{(^{\text{Mes}}\text{BDI})\text{Mg}\}_2]$ **63** as a product (Scheme 19).^[47]



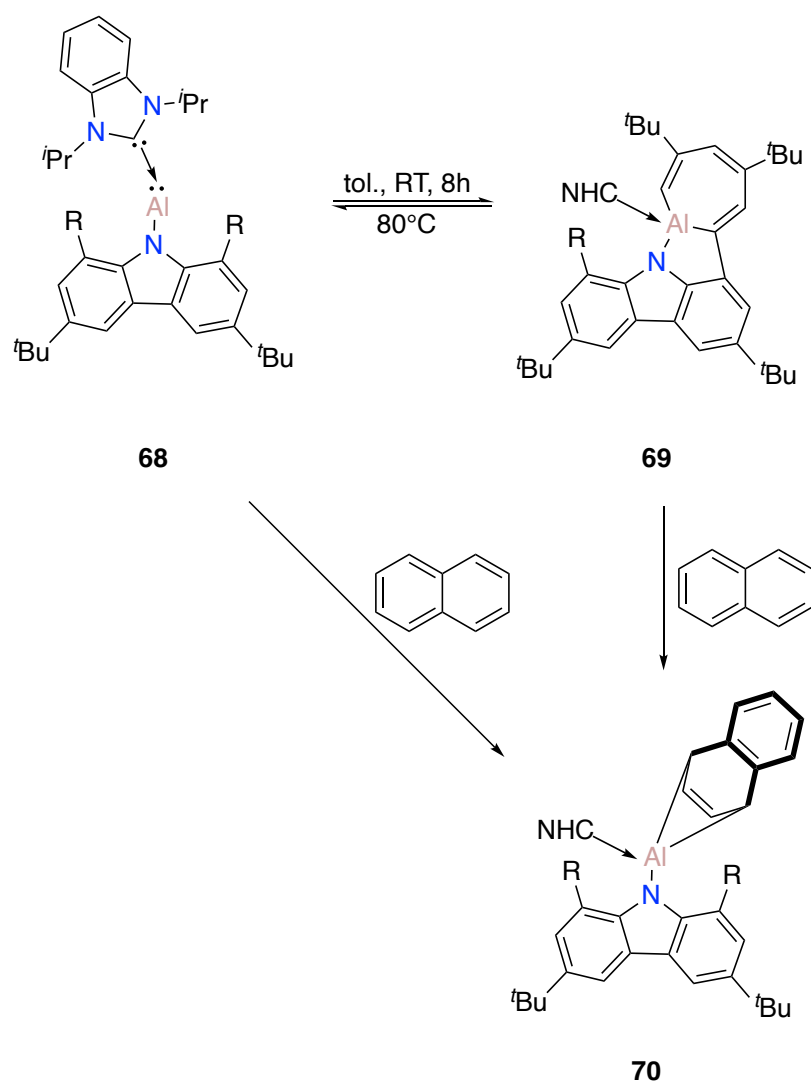
Scheme 19. Formation of **63** from L-AlI_2 **62**. $\text{R} = 3,5\text{-di-tert-butylphenyl}$.

The group of Liu independently showed that the alumylene derivatives can be prepared in acceptable yields from the reduction of carbonyl-substituted aluminum diiodides **62** with KI/K (Scheme 20).^[46] As expected, the reactivity of alumylene **64** is amphiphilic as it reacts with Lewis acids like metal carbonyls as well as Lewis bases such as DMAP. Coordination of tungsten pentacarbonyl to the aluminum center was possible in both benzene and THF upon photolysis. However, in the presence of THF, THF was also coordinated to the aluminum center. These results demonstrated that the aluminum center acts as a σ -donor as well as a π -acceptor. Additionally, $\text{L-Ga}(\text{THF})\text{W}(\text{CO})_5$ **66** was reacted with DMAP, which resulted in ligand exchange of THF. IR spectra showed that the coordination of THF and DMAP affects the electronic properties of the coordinated transition metals. With an increased number of ligands in **66** and **67** ($\text{L-Al}(\text{L}^2)_n\text{W}(\text{CO})_5$ where $\text{L}^2 = \text{THF}$ or DMAP and $n = 0-2$), Al-to-W σ -donation increases whereas CO stretching frequencies decrease. The IR bands of **65** (ν_{CO} 2046, 1958, and 1897 cm^{-1}) are shifted to higher energies compared to those in **66** and **67** due to the reduced electron-donating ability of the Al ligand in the absence of additional donors at the aluminum center.^[46]



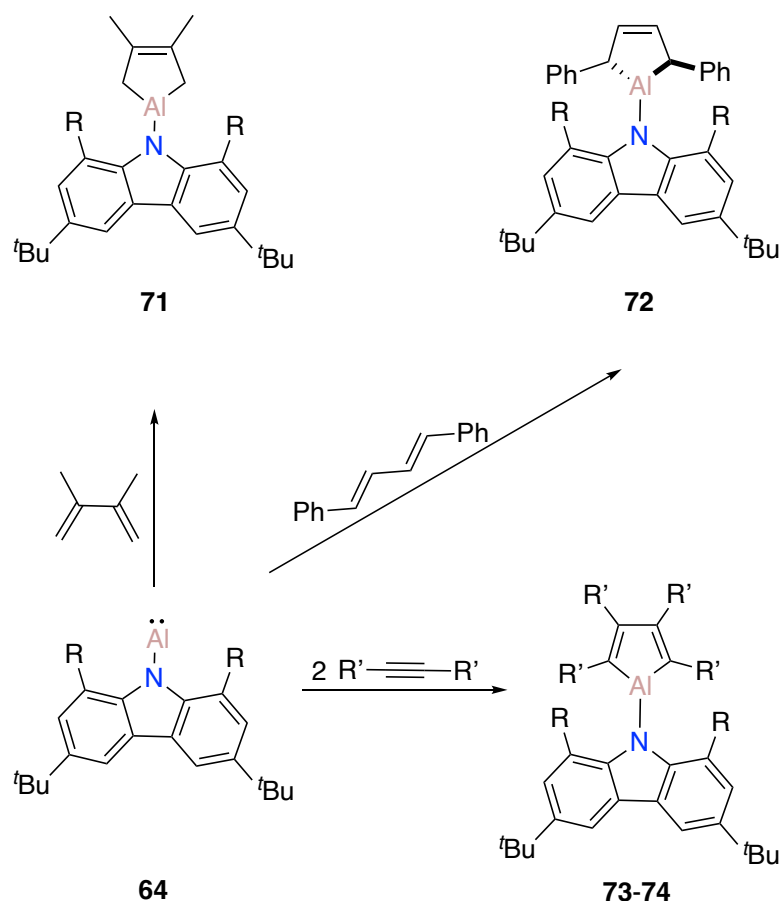
Scheme 20. Synthesis and reactivity studies of free alumylene. R=3,5-*di-tert*-butylphenyl.

Additionally, Liu's group boosted the redox activity of the alumylene by coordination of NHC ($i\text{Pr}_2\text{-bimy}$) to the aluminum center, which decreases the HOMO-LUMO gap. NHC-coordinated alumylene **68** is isoelectronic to singlet carbenes. It was reacted with biphenylene and naphthalene, which results in [1+4] cycloaddition reactions at room temperature (Scheme 21). It is important to note that free alumylene is inert towards both biphenylene and naphthalene. Moreover, a reversible intramolecular addition of the aluminum center to the flanking aromatic ring is observed in solution at high temperatures.^[98]



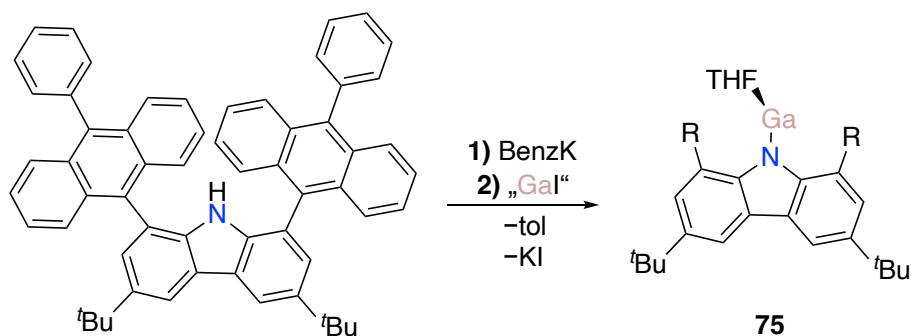
Scheme 21. Inter- and intramolecular addition of NHC-coordinated alumylene **68**. R=3,5-*di-tert*-butylphenyl, NHC= *i*Pr₂-bimy.

Free alumylene, L-Al **64** was also proven to be effective in transferring the Al-atom for the synthesis of a variety of aluminum heterocycles (Scheme 22).^[99] The alumylene **64** does not react with stable aromatic compounds but conjugated systems such as 2,3-dimethyl-1,3-butadiene and *E,E*-1,4-diphenyl-1,3-butadiene furnish [1,4]-addition products, **71** and **72**. The reaction of L-Al **64** and 3-hexyne (EtCCEt) in a 1:1 molar ratio yields two products, i.e. L-Al(CEt)₂ and L-Al(CEt)₄.^[51,100,101] The addition of one extra 3-hexyne equivalent led exclusively to a five-membered ring **74**. This evidence led to the plausible suggestion that the L-Al(CEt)₂ forms initially followed by a ring expansion upon the addition of a second equivalent of 3-hexyne. A similar observation was made for the reaction with diphenylethene, affording **73**.



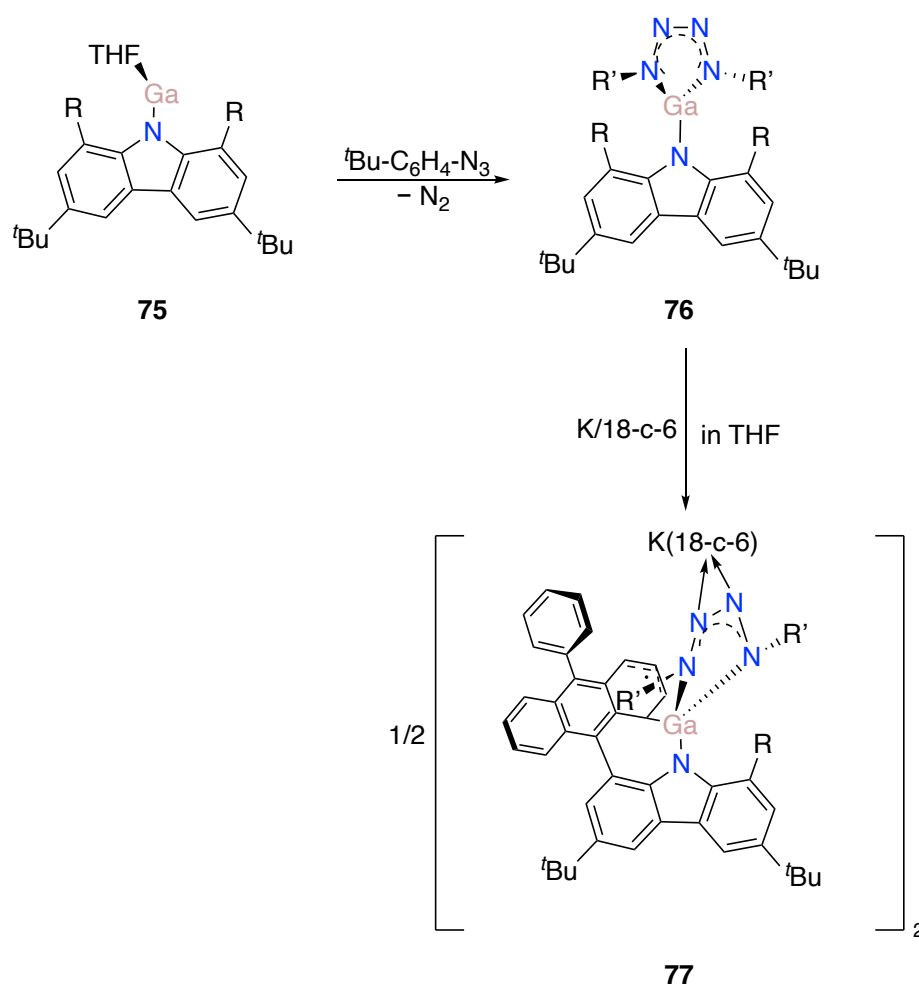
Scheme 22. Reactivity of aluminylene **64** towards unsaturated substrates. R=3,5-*di-tert*-butylphenyl. **73**: R'= Ph; **74**: R'=Et.

Recently, the mono-coordinated Ga(I) carbazole ligand compound has been reported by the group of Tan and its reactivity has been explored (Scheme 23).^[102] The carbazole was deprotonated with benzyl potassium and reacted with “Gal”, which was prepared *in situ*. The compound **75** was characterized by NMR spectroscopy and XRD analysis. While ¹H NMR spectra did not show any solvent molecule coordinated to the gallium center, the crystal characterization led to one THF molecule with a coordinative interaction. Further attempts to grow crystals in the absence of THF were unsuccessful.



Scheme 23. Synthesis of carbazol-stabilized Ga(I) compound **75**. R=9-phenyl-10-anthracene.

The reactivity of **75** towards organic azides has been explored with $t\text{Bu-C}_6\text{H}_4\text{-N}_3$ (Scheme 24). The reaction of the gallylene with two equivalents of azide afforded the first stable tetrazagallole LGaN_4Ar_2 **76**. It was suggested that $[\text{LGa}=\text{NR}']$ might form first during the reaction course, which further reacts with one more equivalent of the azide to yield the tetrazagallole **76**. It was noted that with one equivalent of azide, tetrazagallole **76** along with unreacted gallylene **75** was obtained suggesting the first addition to be rate-determining. The crystal structure shows a planar five-membered ring configuration with an N-N bond length between a single and a double bond. This molecule exhibits redox properties with the ability to incorporate an additional electron yielding a radical species, $\{[\text{K}(18\text{-C-6})]^+[\text{LGaN}_4\text{Ar}]^-\}_2$ **77**.

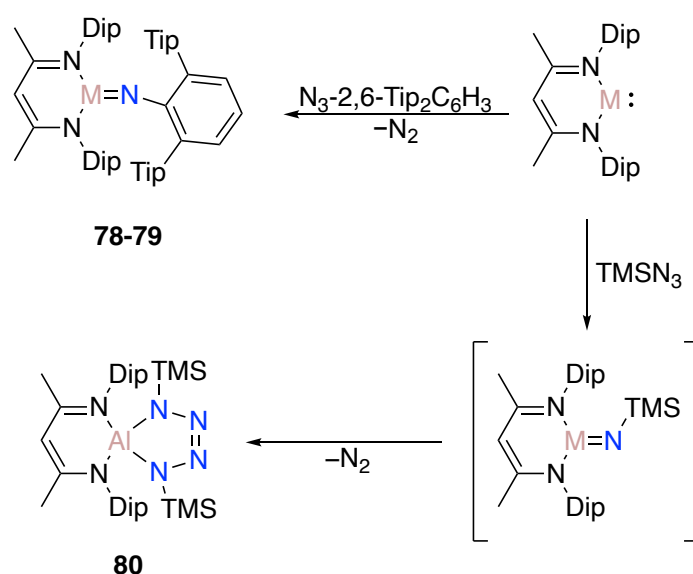


Scheme 24. Formation of tetrazagallole **76** and its radical dimer **77**. R=9-phenyl-10-anthracene, R'= $t\text{Bu-C}_6\text{H}_4$.

1.5. Group 13/15 Multiple Bonding Systems

The synthesis of compounds containing double bonds between group 13 and 15 elements was once thought inaccessible. This was explained with the “double bond rule” which suggests that elements with a principal quantum number three or higher are unable to form stable multiple bonds.^[103,104] A multiple bonding (double and triple bonds) by an overlap of the group 15 element lone pair with the formally empty p orbital of the group 13 element would be possible although much weaker than in the case of B-N interactions. The use of a bulky group has made the isolation of some examples possible, hindering the inherent reactivity of the bonding motif. As discussed in the previous section, this leads to head-to-tail oligomerization.

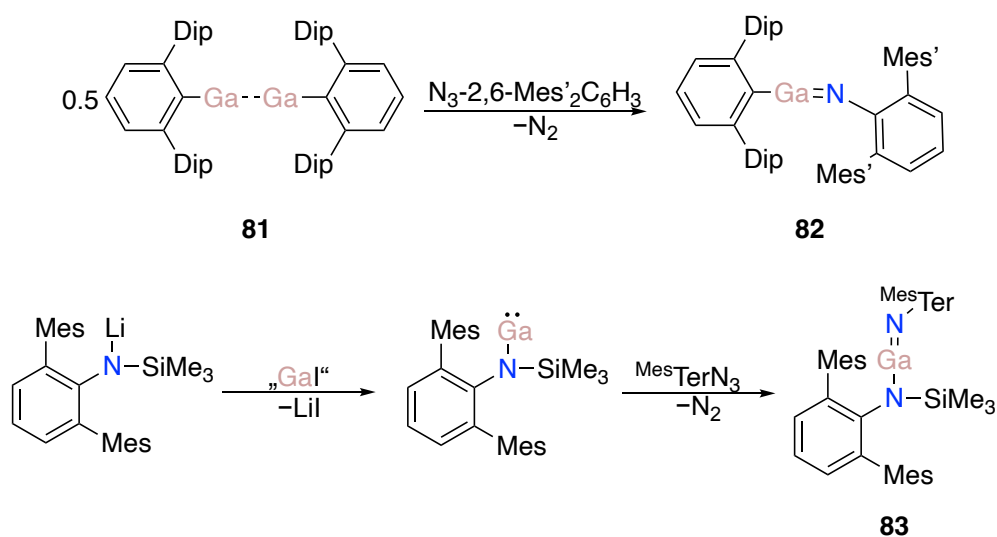
The reaction of $(^{\text{Dip}}\text{NacNac})\text{Al}$ with 2 equivalents of TMSN_3 led to the isolation of cyclic motif product **80** (Scheme 25).^[105] It was suggested that the imide $[\text{Al}=\text{N}]$ forms during the reaction; however, it further reacts with another equivalent of TMSN_3 to afford **80**. This hypothesis was later supported with the isolation of aluminum and gallium imides by using a bulkier azide. The reaction of monomeric $(^{\text{Dip}}\text{NacNac})\text{M}$ ($\text{M}=\text{Al}, \text{Ga}$) with $^{\text{Tip}}\text{TerN}_3$ led to the formation of **78** and **79**.^[106] Only gallium imide **79** was characterized by XRD analysis. The molecular structure bears a three-coordinate gallium center with a central Ga-N bond length of 1.742(3) Å.



Scheme 25. Isolation of first monomeric aluminum **78** and gallium imides **79**. **78**: M=Al; **79**: M=Ga.

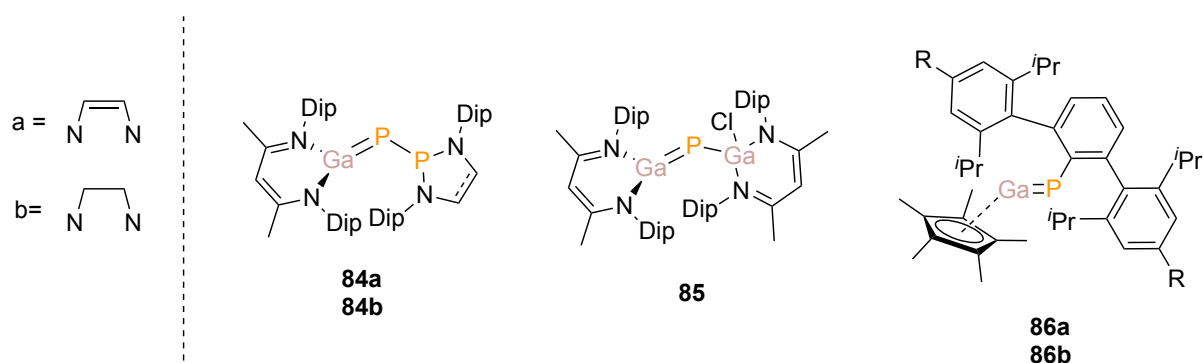
The group of Power followed this study and prepared group 13 imides, $[(^{\text{Dip}}\text{Ter})\text{M}=\text{N}^{\text{Mes}}\text{Ter}]$ **82** where $\text{M}=\text{Ga}$, as well as the monomeric amido-imide compound, $[(^{\text{Mes}}\text{Ter})\text{N}(\text{TMS})\text{-Ga}=\text{N}^{\text{Mes}}\text{Ter}]$ **83** (Scheme 26).^[107,108] Target imide **82** as well as its indium analogue were isolated from reactions of dimeric group 13 compounds, $(^{\text{Dip}}\text{TerM})_2$ ($\text{M}=\text{Ga}, \text{In}$) with $^{\text{Mes}}\text{TerN}_3$. Ga-N bond lengths in **82** and **83** (1.701(3) Å) are shorter compared to that in $(^{\text{Dip}}\text{NacNac})\text{GaN}^{\text{Tip}}\text{Ter}$ **79** (1.742(3) Å). Computational calculations on the model compounds

RGaNR (R= H, Ph) showed a double bond character where the HOMO is the Ga-N π -bond many localized at the N, while the LUMO consists of π^* -orbital with strong contribution of the 4p from the gallium atom.



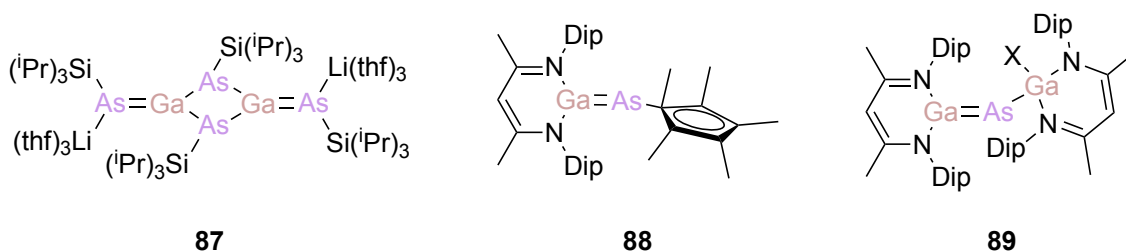
Scheme 26. Isolation of monomeric gallium imides **82** and **83**.

In 2020, Goicoechea and coworkers reported the first examples of phosphanylgallenes (**84a** and **84b**, Scheme 27). (^{Dip}NacNac)Ga was reacted with phosphanylphosphaketene to afford the target compounds upon CO release. The obtained compound features Ga-P bond lengths of 2.165(1) (**84a**) and 2.177(3) Å (**84b**).^[109] Schulz and coworkers directly demonstrated the synthesis of **85** by the reaction of gallium phosphaketene with (^{Dip}NacNac)Ga. The Ga-P bond length was reported to be 2.1613(6) Å, which is comparable to **84a/b**.^[110] Most recently, the use of Phospha-Wittig reagents was proven to be an effective route to form Ga=P containing compounds. Cp*Ga was reacted with ^{Dip}TerP(PMe)₃ and upon irradiation, PMe₃ was released to form the target phosphanylgallenes **86a** and **86b**. Ga-P bonds in the isolated phosphanylgallenes are relatively longer (2.2104(5)-2.2176(5) Å) than in **84a**, **84b** and **85**.^[111]



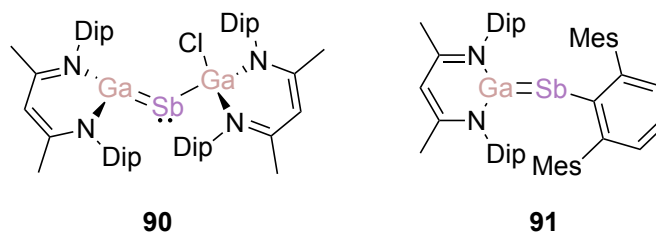
Scheme 27. Examples of compounds containing Ga=P in the literature. **86a**: R=H; **86b**: R=*i*Pr.

Beyond phosphanylgallenes and gallium imides, multiple bonds of gallium with heavier pnictogens have also been reported. Von Hänisch and Hampe reported the preparation of the first example of a Ga-As double bond via the reaction of GaCl₃ with Li₂As(SiⁱPr₃). A dimeric structure with a planar Ga₂As₂ ring **87** was isolated (Scheme 28).^[112] Schulz and coworkers reported the first monomeric compound which contains a Ga=As bond. Compound **88** was isolated upon the reaction of two equivalents of (^{Dip}NacNac)Ga with Cp*AsCl₂.^[113] Additionally, the same group showed the synthesis of another example of monomeric gallaarsenes **89** by the reaction of three equivalents of (^{Dip}NacNac)Ga with AsX₃.^[114]



Scheme 28. Examples of Ga=As in the literature. X = Cl, Br.

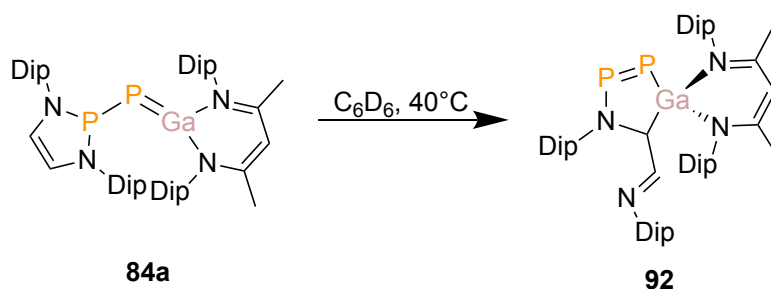
The authors reported the synthesis of **90**, which is the first compound containing Ga=Sb bond (Scheme 29). The synthesis was based on the reaction of (^{Dip}NacNac)Ga with half an equivalent of [Cp*₂SbCl₂], which affords [NacNac(Cl)Ga]₂Sb• radical. Reduction of [NacNac(Cl)Ga]₂Sb• radical with KC₈ afforded **90**.^[115] A year later, it was demonstrated that two equivalents of (^{Dip}NacNac)Ga with ^{Mes}TerSbCl₂ afforded Ga=Sb containing compound **91**. These results showed the importance of carbon-pnictogen bond strength and steric protection for efficient stabilization.^[116]



Scheme 29. Examples of Ga=Sb in the literature.

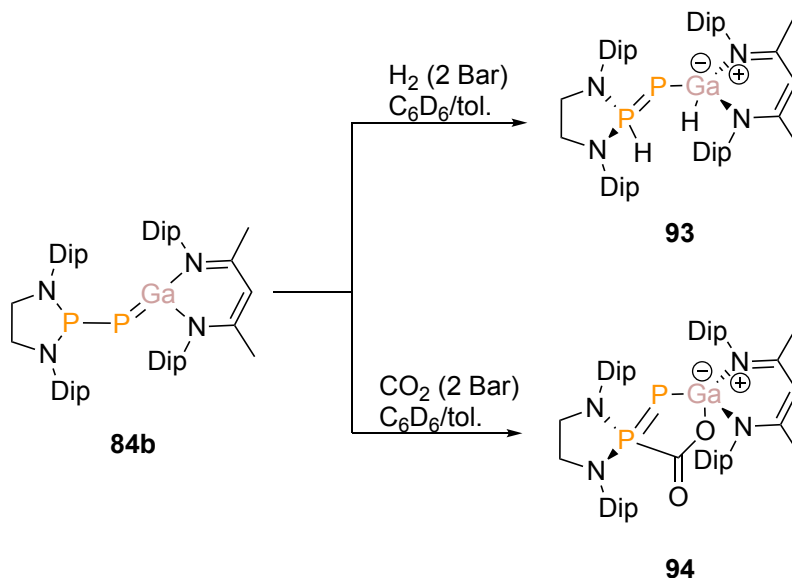
Upon isolation of compounds containing Ga-Pn (Pn= N-Sb) double bonds, reactivity studies were performed. There are a few reports on the reactivity of gallium imides. However, given the need for extremely bulky azides for the kinetic stability of a GaN unsaturated unit, the inherent reactivity is precluded. For examples, Power and coworkers tested the reactivity of gallium imide, ^{Dip}TerGaN^{Mes}Ter, towards Me₃SiCCMe₃Si, HCCPh, and PhN=NPh. Remarkably, even under reflux conditions, no reactions were observed.^[108]

The first report for the reactivity of multiple bonds of Ga-Pn was for a phosphanylgallene (Scheme 30). ^1H and ^{31}P NMR spectra of a solution containing **84a** showed the presence of two products. The conversion can be completed by heating the previously synthesized phosphanylgallene for 5 days at 40 °C. The product was characterized to be the rearrangement product **92** of the phosphanylgallene **84a**, where the Ga(I) center inserts into the unsaturated backbone of the phosphanyl group. Furthermore, using the phosphanyl moiety with a saturated backbone increases the stability, and such rearrangement was not observed for phosphanylgallene **84b**.^[109]



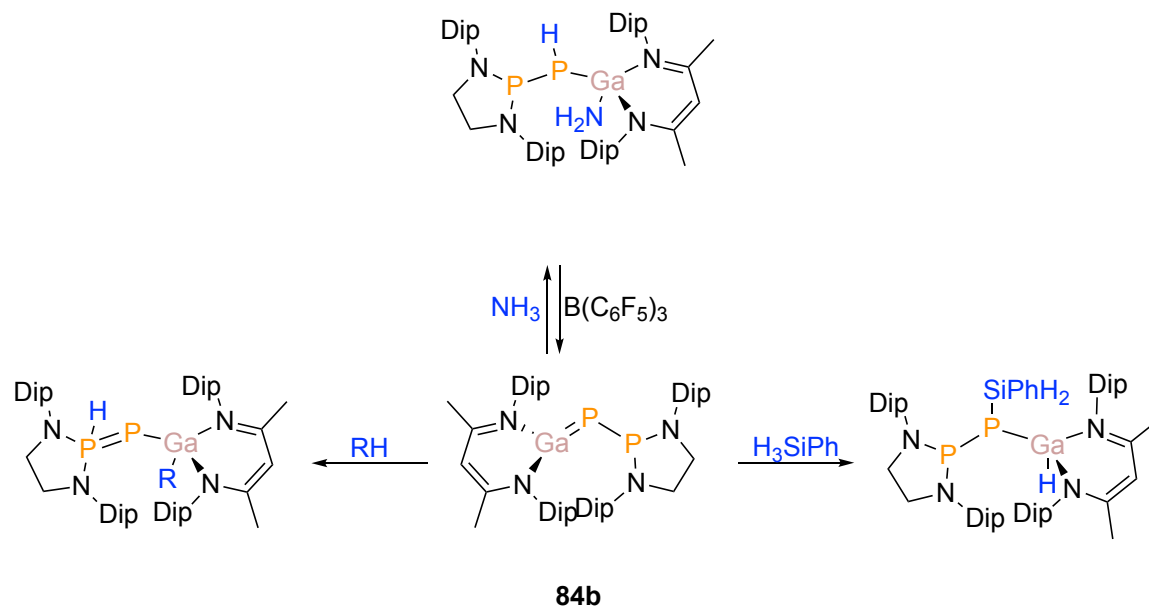
Scheme 30. Rearrangement of the phosphaketene **84a**.

In the same study, the reactivity of **84b** towards H_2 and CO_2 was demonstrated (Scheme 31). Exposing to H_2 resulted in the 1,3-hydrogenation product **93**, whereas with CO_2 , a five-membered ring **94** was isolated (Scheme 31). These results show that the phosphanyl phosphanylgallene acts as a Frustrated Lewis Pair towards both substrates. This type of reactivity can be observed where the lone pair of the phosphorus atom acts as the Lewis base and the formally empty p-orbital of the gallium acts as the Lewis acid.^[109]



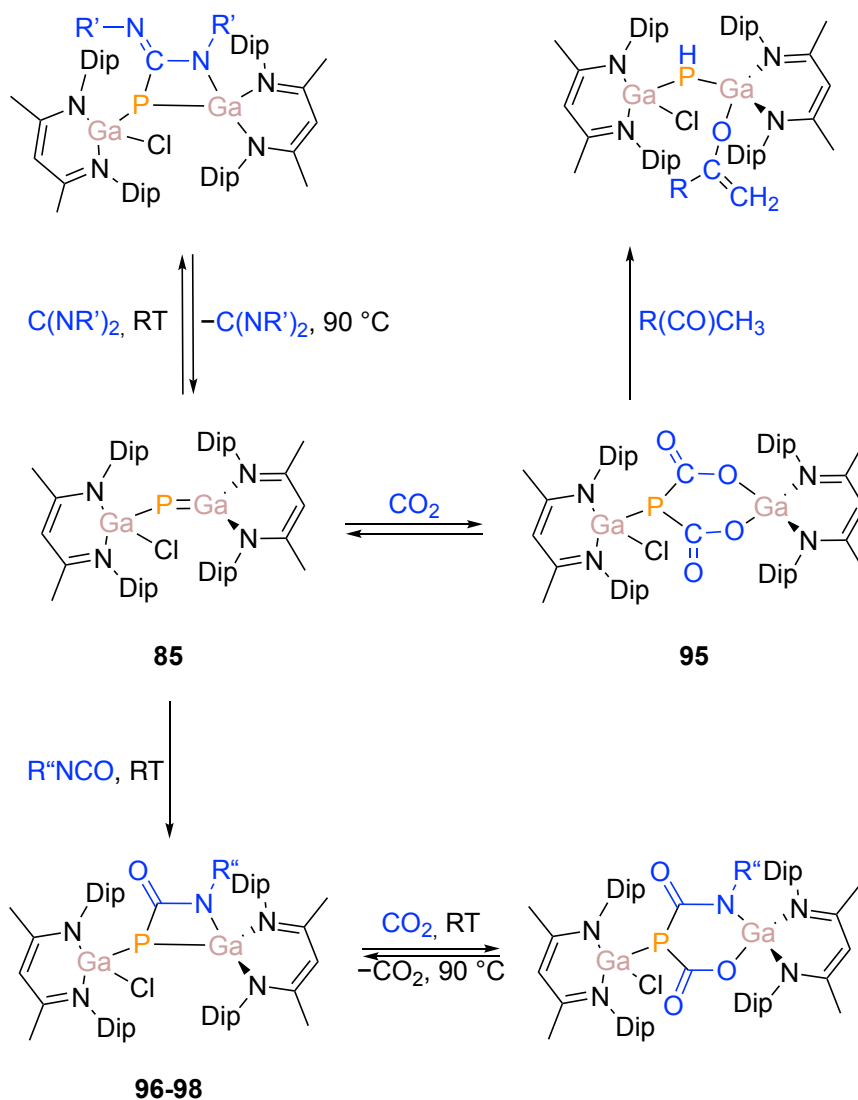
Scheme 31. Reactivity of the phosphanylgallene **84b** towards H_2 and CO_2 .

Goicoechea and coworkers further investigated the reactivity of Ga=P towards many substrates including ammonia, water, a series of primary amines, phenylacetylene, and phenylphosphine (Scheme 32). All reactions led to X-H activating (X= N, O, C, P) by [1,3]-addition to the P-P=Ga moiety. Moreover, the activation of the ammonia can be reversed by addition of B(C₆F₅)₃ as a strong Lewis acid. For phenylsilane, the 1,2-addition product was formed via a σ -bond metathesis unlike in the previous cases.^[117]



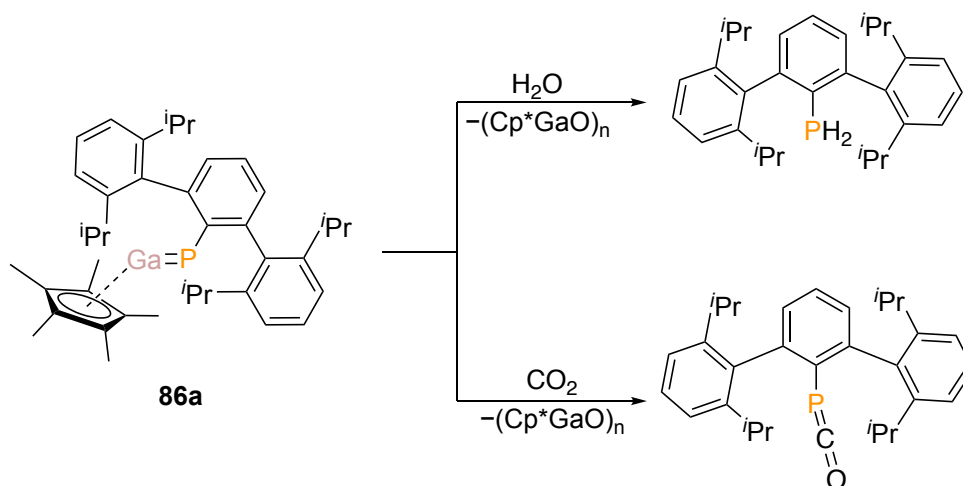
Scheme 32. Reactivity studies of **84b**. R=NHⁱPr, NPh, OH, CPh, PPh.

Reversible activation of CO₂ was reported by the group of Schulz for compounds containing Ga=P bonds (Scheme 33). Phosphanylgallene **85** was reacted with CO₂ to yield **95** containing a PC₂O₂Ga six-membered cycle. DFT calculations showed that addition of CO₂ is thermodynamically favored. Interestingly, the phosphanylgallene **85** can be regenerated by heating the product. Furthermore, they studied the reactivity of **85** towards acetophenone and acetone. Both reactions resulted in the C(sp³)-H activation.^[110] Activation of carbodiimide and isocyanite yielded [2+2] cycloaddition products, four-membered metallaheterocycles. **96-98** can further reversibly react with CO₂ via [2+2] cycloaddition at elevated temperatures, affording six-membered metallaheterocycles **99-101**. Similar to CO₂ reactions, carbodiimide activation is reversible and the phosphanylgallene can be retrieved quantitatively upon heating.^[118]



Scheme 33. Reactivity studies of **85**. R= Me, Ph; R'= *i*Pr, Cy; **96**: R''=*i*Pr; **97**: R''=Cy; **98**: R''=Et; **99**: R''=*i*Pr; **100**: R''=Cy; **101**: R''=Et.

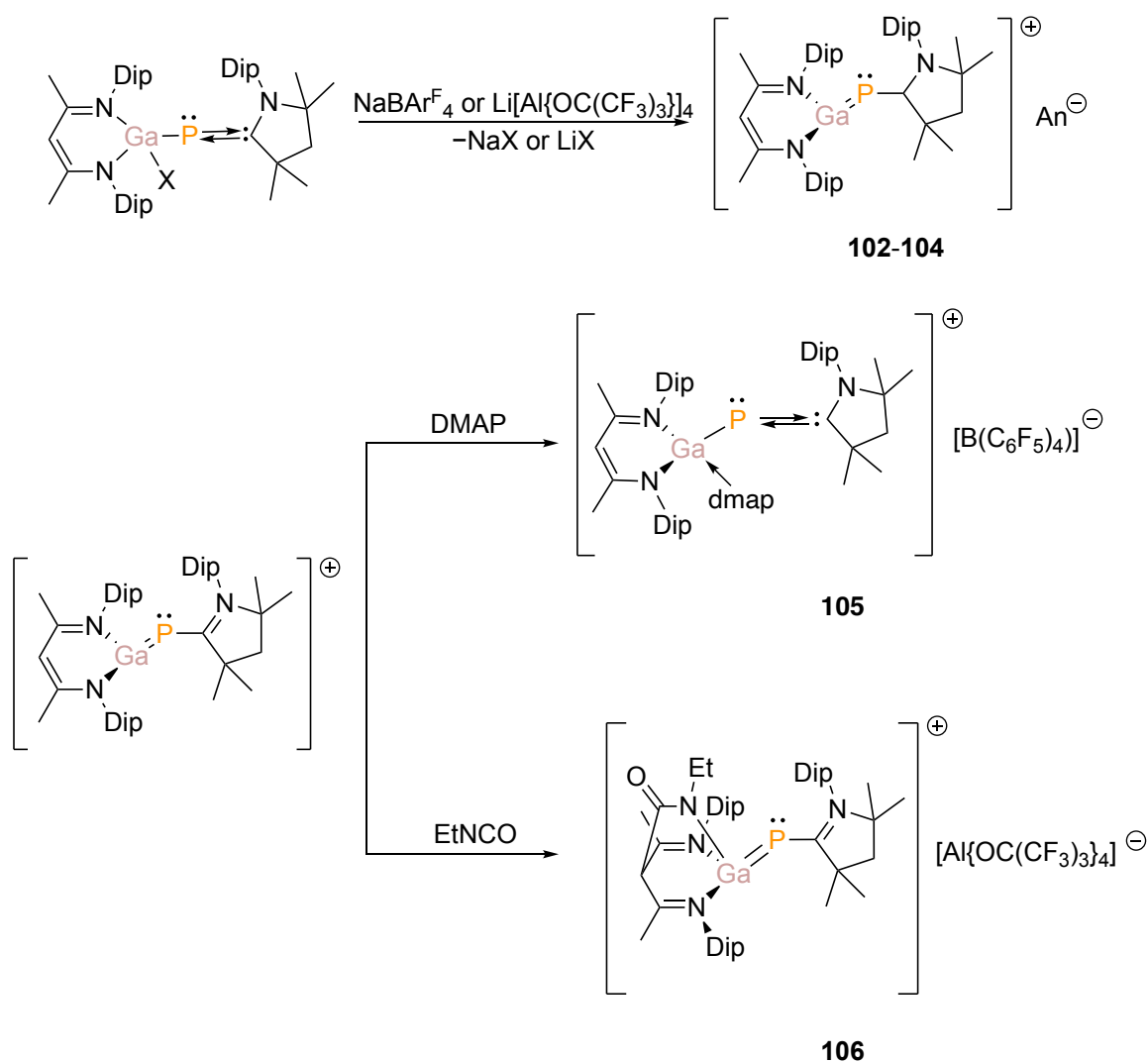
The group of Hering-Junghans explored the reactivity of $\text{Dip}^{\text{Ter}}\text{PGaCp}^*$ **86a** towards CO_2 and H_2O (Scheme 34). Upon exposure to CO_2 , the reaction mixture showed an immediate color change and ^{31}P and ^1H NMR confirmed the formation of $\text{Dip}^{\text{Ter}}\text{PCO}$ and various Cp^* containing species. A similar observation was made during the reaction of H_2O , which resulted in the formation of $\text{Dip}^{\text{Ter}}\text{PH}_2$.^[111]



Scheme 34. Reactivity of ^{Dip}TerPGaCp* **86a** towards H₂O and CO₂.

Schulz and coworkers reported the synthesis of cationic heteroallylic species containing Ga=P double bond. The preparation consists of a chlorine abstraction from previously synthesized phosphanylgallene, (^{Dip}NacNac)(Cl)GaPGa(^{Dip}NacNac). The almost equidistant Ga-P bond lengths (2.2026(4) Å and 2.1860(4) Å) indicate a delocalized π -system. The Lewis acidity properties of the heteroallylic cation were demonstrated by the addition of Lewis bases, DMAP and THF.^[110]

The same group showed that the reaction of (^{Dip}NacNac)Ga with ^{Dip}CAACPCl followed by chlorine abstraction yields the heteroleptic Ga-P-C allyl cation **102-104** with substantial Ga-P double bond character (Scheme 35). The Ga-P bond is 2.2396(6) Å, which is in between the lengths of Ga-P single and a double bond. To confirm the electrophilic character of the gallium, **103** was reacted with DMAP, which resulted in the formation of Lewis acid-base adduct **105**. Furthermore, its reaction with ethyl isocyanate led to unexpected formation of an adduct **106** containing a bicyclo[2.2.2]octane-like C₄N₃Ga heterocycle. This was formed by the reaction of **104** with ethyl isocyanate yielded an addition product by electrophilic attack of the isocyanate at the γ -carbon of the ^{Dip}NacNac ligand backbone.^[119]



Scheme 35. Preparation of heteroleptic Ga-P-C allyl cation and synthesis of compounds **105-106**. X=Cl, Br; **102**: An= $\text{B}\{\text{C}_6\text{H}(\text{CF}_3)_2\}_4$; **103**: An= $\text{B}(\text{C}_6\text{F}_5)_4$; **104**: An= $\text{Al}\{\text{OC}(\text{CF}_3)_3\}_4$.

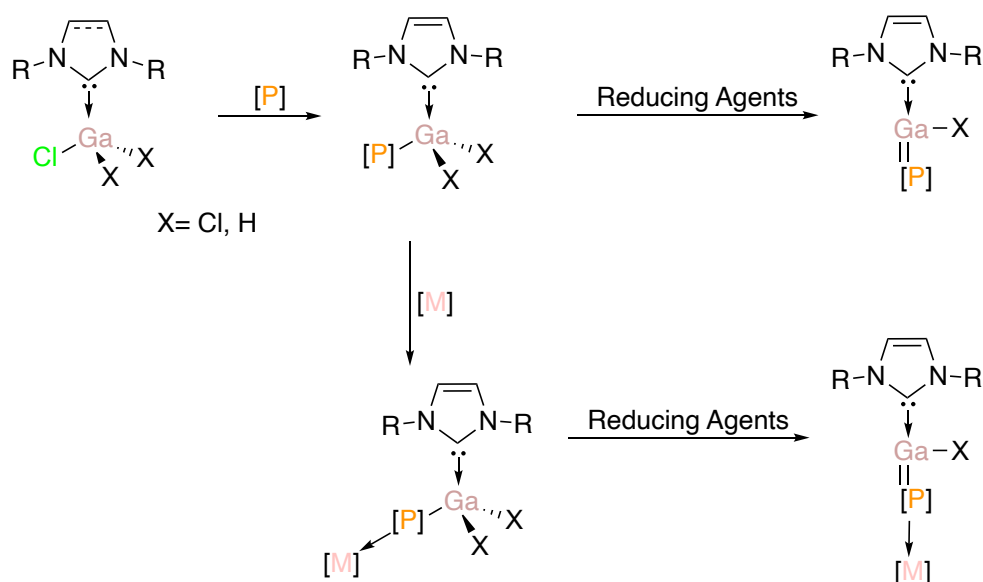
The ambiphilic nature of double bonds bearing heavier group 15 elements Ga-Pn (Pn=As, Sb) is manifest in their reactions with Lewis acids and bases (Scheme 36). Reactions of $(\text{DipNacNac})\text{GaEGa}(\text{Cl})(\text{DipNacNac})$ (E= As (**89**), Sb (**90**)) with strong acids (e.g. HCl in Et_2O , $[\text{H}(\text{OEt}_2)_2][\text{BAR}_4^{\text{F}}]$) led to protonation at the pnictogen atoms, forming species **107-110**. Their reactions with imidazolium salt led to the formation of pnictanides anions, **111** and **112**, which then react as nucleophiles. Treatment of **111** and **112** with MeI afforded the formation of methyl-substituted pnictanes **113-116**, which can also be access through treatment of **89** and **90** with MeI. Additionally, **111** and **112** are one-electron oxidizers. Their reaction with $[\text{FeCp}_2][\text{BAR}_4^{\text{F}}]$ results in the formation of corresponding radicals, **117** and **118**.^[120]

2. Objectives

Low-valent, low-coordinate, and unsaturated main group compounds have gained attention due to their ability to mimic the chemistry of transition metals, such as the activation of small molecules, while being environmentally friendly and consists of abundant elements..^[121–125] Although many examples of them have been reported until now, synthesis of these compounds remains challenging due to their highly reactive nature and tendency to oligomerize. There are different approaches used for the stabilization of such compounds. One of the most used strategies consists of Lewis base and/or-acid coordination to block the empty p-orbital on the group 13 element and/or the lone pair of the group 15 element, respectively. Another well-known strategy is the use of sterically demanding groups to provide kinetic stability. Finding the balance between stability and reactivity is a key ingredient to use low-valent and low-coordinate main group compounds as precursors to form unsaturated units.

Therefore, the following objectives arise:

- 1) Preparation of LA/LB and only LB-stabilized phosphanyl-gallanes to study the effects in stabilization of the monomeric compounds and understand the differences in the reaction behavior. Furthermore, their potential for the preparation of Ga-P multiple bonds is investigated. Ga-N bonds were not in the scope of this chapter since there were already attempts to isolate Ga-N multiple bonds with a similar ligand system in the literature. (Chapter 3.1.)^[23]



Scheme 37. Planned route for the synthesis of NHC-stabilized Ga-P multiple bonds.

- 2) Chapter 3.2. presents an alternative method for exploring the chemistry of low-valent aluminum and gallium. This thesis employs bulky ligands to isolate these inherently unstable and reactive compounds. Furthermore, the chapter focuses on synthesizing a novel

monomeric carbazole-based gallium(I) compound, along with studying its reactivity towards various substrates including Lewis bases and transition metal complexes. Computational methods are also employed to gain insights into the bonding and reactivity mechanisms involved. Additionally, in Chapter 3.2., the use of bulky silyl groups is employed to stabilize an aluminum (II) radical, followed by the demonstration of its addition reaction to benzene.

3. Results and Discussion

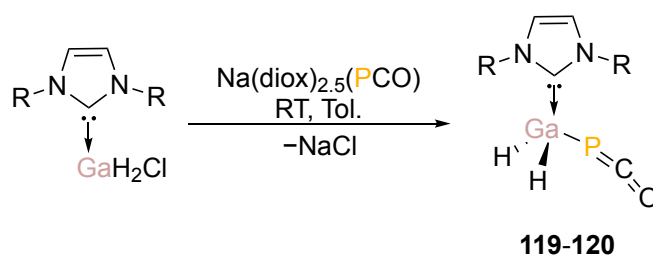
3.1. Synthesis of Novel Phosphanylgallanes

In this chapter, the synthesis of phosphanylgallanes stabilized by coordination of either both Lewis acids and bases or of just a Lewis base is described. NHC gallium chlorides and hydrochlorides were reacted with various phosphorous sources including 2-phosphaethynolate anion, PCO^- and phosphine boranes to isolate novel phosphanylgallanes. The obtained products were then characterized spectroscopically and the factors which influence their overall stability were discussed by theoretical methods. Additionally, their use as precursors for the preparation of Ga-P multiple bonds via different approaches such as salt elimination and decarbonylative photolysis.

3.1.1. Synthesis and Characterization of NHC-GaH₂(PCO) (NHC= IDip, IMes)

The phosphanylgallanes, specifically phosphaketenes, would be ideal candidates for the preparation of Ga-P multiple bonds since they possess a weak P-CO interaction. Upon photolytic decarbonylation, thermolysis or reactions with Lewis bases, Ga-P multiple bonds can be formed.^[126] This sparked an interest in synthesizing novel gallium phosphaketenes, in order to investigate their potential as precursors for preparation of phosphanylgallanes.

This type of compounds should be accessible through salt metathesis reactions between NHC stabilized gallium chlorides and $\text{Na}(\text{diox})_{2.5}(\text{PCO})$. Indeed, the equimolar reactions of NHC-GaH₂Cl (NHC = IDip, IMes) with $\text{Na}(\text{diox})_{2.5}(\text{PCO})$ afforded NHC-GaH₂(PCO) (NHC = IDip (**119**), IMes (**120**)) as yellow solids in 37% and 47% yield, respectively (Scheme 38).*



Scheme 38. Synthesis of **119** and **120**. **119**: R=Dip; **120**: R=Mes.

C_6D_6 solution of **119** shows a triplet at $\delta = -393$ ppm ($^2J(^{31}\text{P}-^1\text{H}) = 18.3$ Hz) in ^{31}P NMR, which is comparable to the free $[\text{PCO}]^-$ ion in water ($\delta = -396.4$ ppm).^[127] The triplet splitting is a strong indication for the coordination of the PCO^- moiety via the phosphorus terminus, which is in fact expected according to the HSAB principle. On the other hand, the ^{31}P NMR signal of **120**, appears as singlet at -393 ppm. Additionally, the ^{13}C NMR resonance of the PCO^- -moiety of **119** ($\delta = 174.98$ ppm) and **120** ($\delta = 181.3$ ppm) as well as the related $^1J(^{31}\text{P}-^{13}\text{C})$ of **119** (92.4

* The preparation of **120** has been conducted in cooperation with Dr. Anup Adhikari.

Hz) and **120** (92.2 Hz) coupling constants are consistent with the previously reported gallium phosphaketenes (180.76-186.50 ppm).^[110,128–130]

Crystal of **119** (Figure 1) and **120** suitable for XRD analysis were grown from saturated toluene solutions. The molecular structures of **119** and **120** prove the coordination via phosphorous. The Ga1-P1-C1 bond angles are close to 90° (**119**: 89.4(2)°; **120**: 89.1(2)°) and P1-C22-O1 bonds angles are nearly linear (**119**: 177.4(5)°, **120**: 173.4(5)°). The C=O bond lengths in the PCO unit are slightly shorter than a typical C=O bond, which can be explained with the electronic donating properties of IDip and IMes. PCO stretching vibrations in the IR spectra at 1898 cm⁻¹ (for both, **119** and **120**) are in accordance with the previously reported gallium phosphaketenes ((^{Mes}Ter)₂GaPCO):^[130] $\nu = 1898 \text{ cm}^{-1}$; Salen(^tBu)Ga(PCO):^[128] $\nu = 1910 \text{ cm}^{-1}$. The Ga-P bond lengths of **119** (2.410(1) Å) and **120** (2.393(2) Å) are consistent with the sum of the covalent radii (2.35 Å).

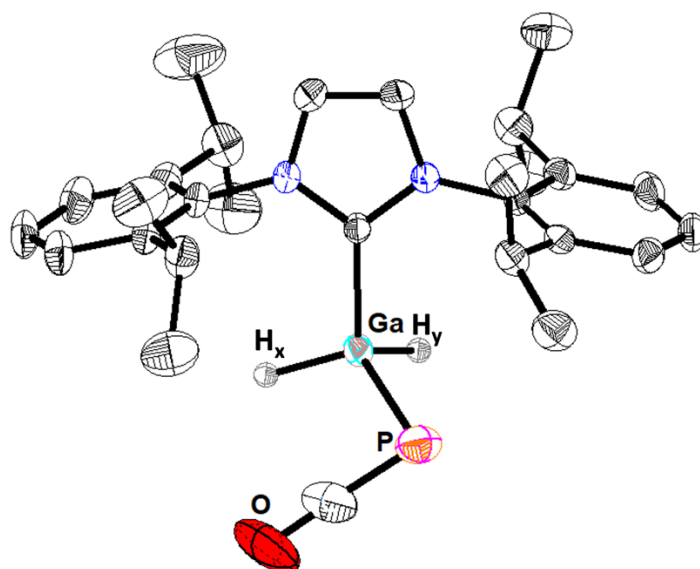
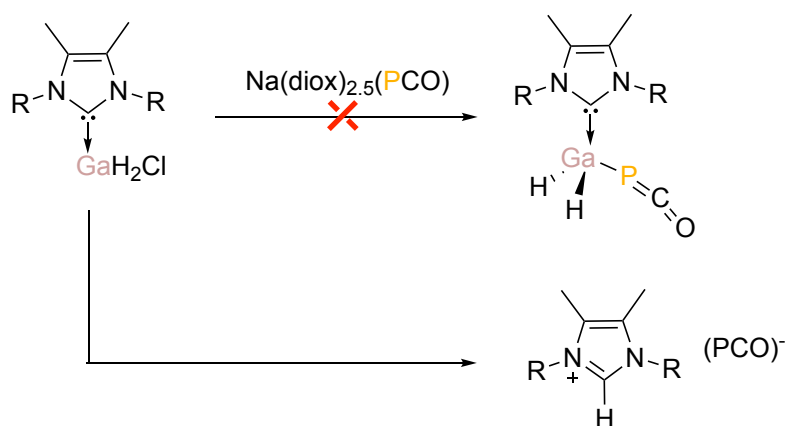


Figure 1. Thermal ellipsoid plots (50%) of **119**. Hydrogen atoms except for H_x and H_y are omitted for the clarity. Selected bond lengths (Å) and angles (°): **119**: Ga1-C1: 2.046(3), Ga1-P1: 2.410(1), O1-C28: 1.172(5), O1-C28-P1: 177.4(5)°, C28-P1-Ga1: 89.4(2)°. **120**: Ga1A-C1: 2.027(3), Ga1A-P1A: 2.393(2), C22A-O1A: 1.193(5), O1A-C22A-P1A: 173.4(5)°, Ga1A-P1A-C22A: 89.1(2)°.

The reaction of Na(diox)_{2.5}(PCO) with smaller Lewis based stabilized gallanes NHC-GaH₂Cl (NHC = 1,2,3,4-tetramethylimidazolin-2-ylidene^[131] and 1,3-bis(isopropyl)-4,5(dimethyl)imidazole-2-ylidene^[5]) did not afford the desired phosphaketenes (Scheme 39). ³¹P NMR spectra showed the presence of broad signals at -393 ppm, which is comparable to the chemical shift of the free phosphaketene anion;^[127] however, XRD analysis revealed the formation of [NHC-H⁺][PCO⁻] (NHC= ⁱPr₂Me₂, IMe₄), instead.

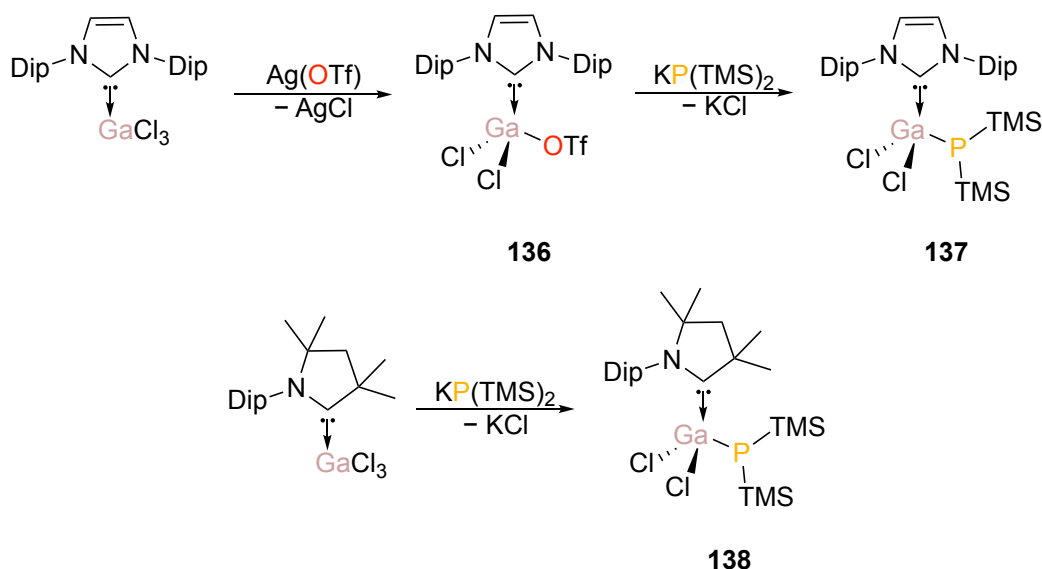


Scheme 39. Attempted synthesis of NHC-GaH₂(PCO). (R= *i*Pr, Me).

Heating or irradiation with UV/vis light resulted in the cleavage of CO for some of the main group phosphaketenes.^[129,132–138] However, upon irradiation of **119**, no reaction was observed whereas heating benzene solution of **119** to 50 °C resulted in decomposition to IDip=PH.^[139]

3.1.2. Synthesis and Characterization of IDip-GaCl₂P(TMS)₂ **122** and CAAC-GaCl₂P(TMS)₂ **123**

Another route which might lead to the desired Ga=P bond was trimethyl halide elimination from a suitable precursor. Therefore, IDip-GaCl₂P(TMS)₂ **122** and Me²CAAC-GaCl₂P(TMS)₂ (**122**) were prepared. For the synthesis of compound **122**, IDip-GaCl₂(OTf) **121** was prepared first and then reacted with KP(TMS)₂(thf)₂^[140] to avoid multiple substitution.



Scheme 40. Synthesis of IDip-GaCl₂P(TMS)₂ **122** and Me²CAAC-GaCl₂P(TMS)₂ **123**.

For the preparation of compound **121**, a THF solution of IDip-GaCl₃ was treated with a THF solution of Ag(OTf) at -70 °C. After stirring the reaction at room temperature overnight, the product was isolated. Compound **121** was collected as a white solid in 88% yield. The ¹H NMR shows characteristic signals of IDip, slightly downfield shifted in comparison to IDip-GaCl₃.

This can be explained with the replacement of a chlorine atom with a more electron withdrawing group such as triflate.

Slow diffusion of *n*-hexane into a THF solution of **121** afforded single crystals suitable for XRD analysis (Figure 2). **121** crystallizes in monoclinic space group $P2_1/n$ as colorless crystals. **121** has a wider $C_{\text{car}}\text{-Ga-O}$ angle and shorter Ga1-O1 bond than in IDip-GaH₂(OTf) (99.27(9)°), which is an indicative of stronger Ga-OTf interaction.^[141] Moreover, The Ga1-O1 bond (1.908(1) Å) is comparable to the sum of covalent radii of Ga-O single bond (1.87 Å),^[142] Ga1-C1 is slightly shorter than in IDip-GaCl₃, which can be explained by the replacement of chlorine with more electron-withdrawing triflate group.

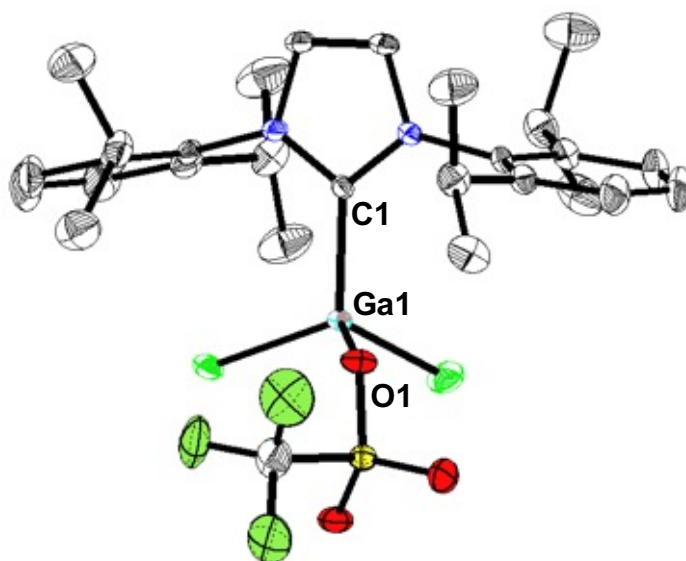


Figure 2. Thermal ellipsoid plots (50%) of **121**. Hydrogen atoms are omitted for the clarity. Selected bond lengths (Å) and angles (°): 1: Ga1-C1: 1.990(1), Ga1-O1:1.908(1), Ga1-Cl1: 2.1468(4), Ga1-Cl2: 2.1480(4), C1-Ga1-O1: 104.17(5).

IDip-GaCl₂(OTf) and ^{Me}2CAAC-GaCl₃ were reacted with KP(TMS)₂(thf)₂ in a 1:1 ratio to afford **122** and **123** in 68% yield and 57% yield, respectively. They are stable both in solid state and in solution for at least a month if moisture and air are excluded. The compounds were characterized by ¹H, ³¹P NMR and XRD analysis.

The ¹H NMR spectra of **122** and **123** show the expected resonances due to the organic ligands. ¹H NMR signals for the methyl groups of IDip appear as doublets at 0.96 and 1.54 ppm for **122** (Figure 3), while methyl groups of TMS groups appear as doublets at 0.45 ppm. Additionally, a septet signal can be seen at 2.88 ppm, which is characteristic for IDip. In **122** and **123**, ¹H chemical shifts of both IDip and ^{Me}2CAAC appear downfield compared to their chloride counterparts. ³¹P NMR shows the presence of broad signals at -253 ppm (**122**) and -242 ppm (**123**). The slightly downfield ³¹P NMR resonance of **123** can be explained by the more σ -donating nature of ^{Me}2CAAC in comparison to IDip.

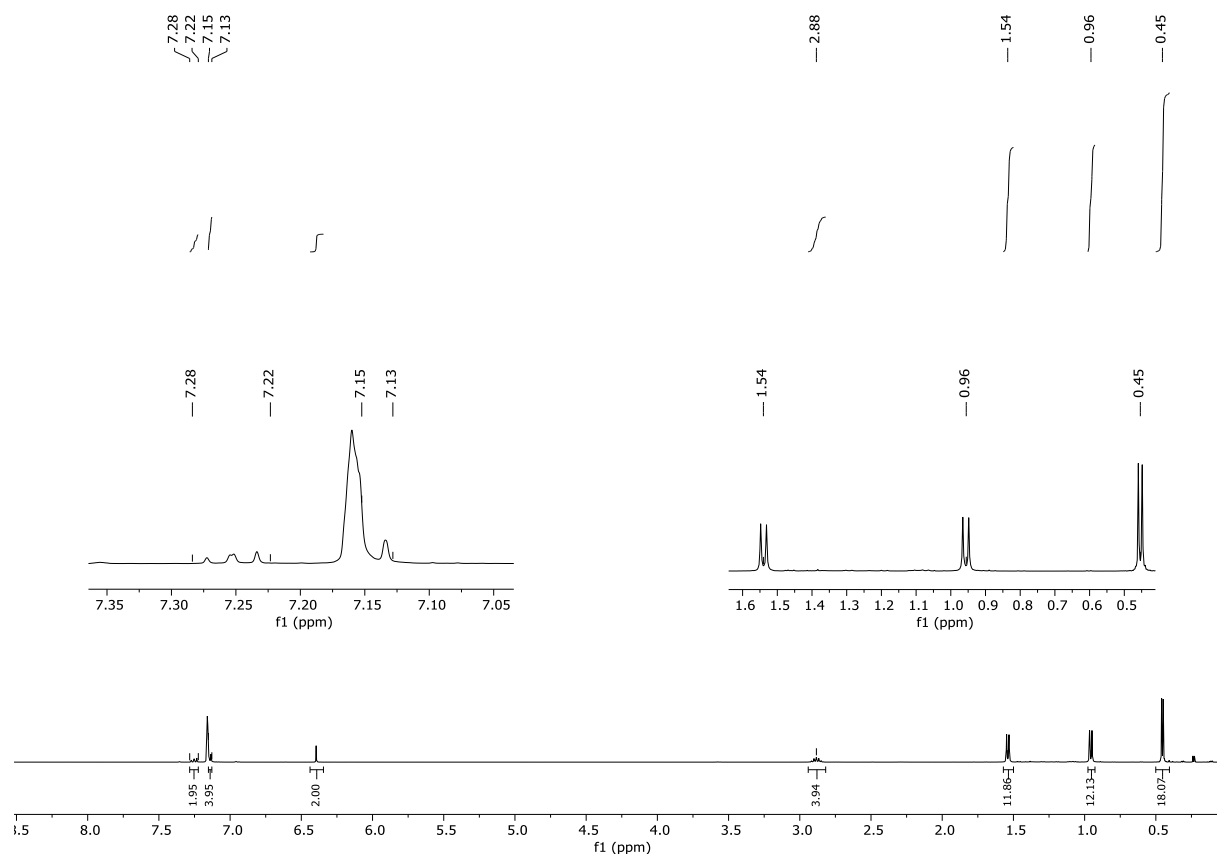


Figure 3. ^1H NMR spectra of IDip-GaCl₂P(TMS)₂ **122** in C₆D₆.

The molecular structures of **122** and **123** were determined by XRD (Figure 4). Single crystals of the compounds were grown from slow diffusion of *n*-hexane into their saturated THF solutions. **123** crystallizes in monoclinic space group P2₁/n, whereas **122** crystallizes in triclinic space group P-1. In both structures, gallium adapts distorted tetrahedral geometry. C1-Ga1 bond lengths 2.0537(9) (**122**) and 2.067(1) (**123**) are comparable to each other, slightly longer in **123**. Ga1-P1 bond length is slightly shorter in **122** (**122**: 2.3082(3), **123**: 2.3187(3)) but in both cases, they are in the expected Ga-P single bond range and shorter than in previously reported phosphanyl gallane, DMAP-Ga(^tBu)₂(TMS)₂ (2.372 Å) and DMAP-GaMe₂P(TMS)₂ (2.372 Å).^[33,143]

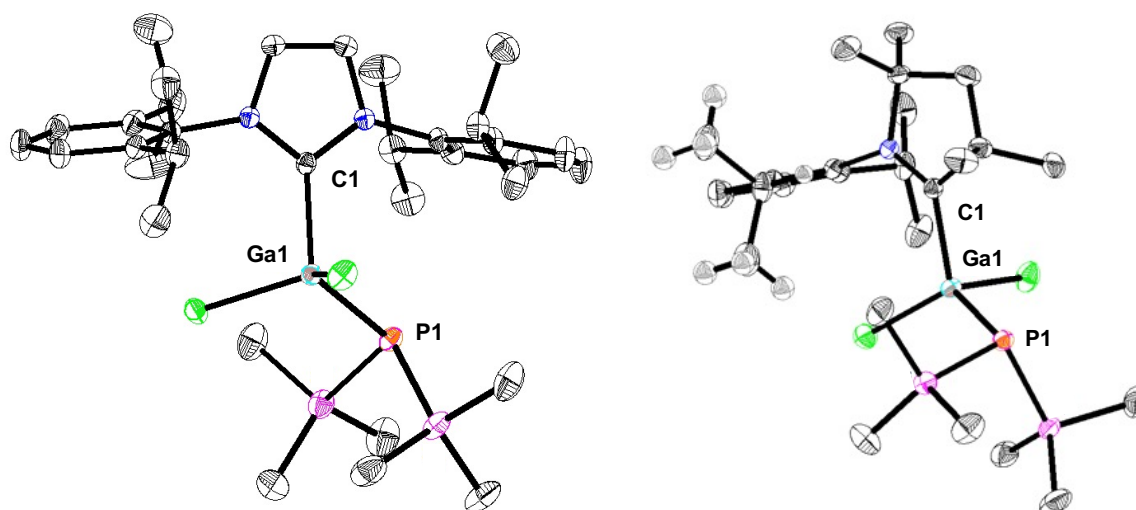
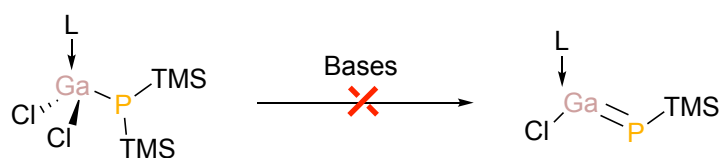


Figure 4. Thermal ellipsoid plots (50%) of **122** and **123**. Hydrogen atoms are omitted for the clarity. Selected bond lengths (Å) and angles (°): **122**: Ga1-C1: 2.0537(9), Ga1-P1:2.3082(3), Ga1-Cl1: 2.2082(3), Ga1-Cl2: 2.2230(3), C1-Ga1-P1: 118.22(3); **123**: Ga1-C1: 2.067(1), Ga1-P1:2.3187(3), Ga1-Cl1: 2.2179(3), Ga1-Cl2: 2.2336(3), C1-Ga1-P1: 115.05(3).

After the isolation of **122** and **123**, base-induced trimethylsilyl chloride elimination was explored. Both compounds were reacted with different bases including MeLi, ⁿBuLi, TBAF, DMAP and KO^tBu; however, these attempts were not successful. With MeLi, ⁿBuLi and TBAF, no reaction was observed, even when they were heated at 80 °C. The reactions with DMAP and ⁱPr₂Me₂ resulted in a ligand exchange. After the addition of the bases at room temperature, ¹H NMR spectra of the reaction solution showed the presence of free IDip.



Scheme 41. Attempted TMSCl elimination from **122** and **123**. **122**: L= IDip; **123**: L=^{Me}₂CAAC.

3.1.3. Synthesis, Structure, and Bonding Analysis of Lewis Acid/Base-Stabilized Phosphanylgallanes

- T. Ilgin Demirer, Dr. Bernd Morgenstern, Dr. Diego M. Andrada, Synthesis, Structure, and Bonding Analysis of Lewis Base and Lewis Acid/Base-Stabilized Phosphanylgallanes. *Eur. J. of Inorg. Chem.* **2022**.
<https://doi.org/10.1002/ejic.202200477>

The above cited article was published by Wiley-VCH GmbH as an „Open Access“ article and is licensed under a “Creative Commons Attribution 4.0 International” License. (<https://creativecommons.org/licenses/by/4.0/>)

The results described within this article are additionally concluded and put into context in the next chapter (7).

Contributions of the Authors:

T. Ilgin Demirer: Lead: Synthesis and characterization of all compounds, investigation, visualization, theoretical studies, writing.

Bernd Morgenstern: Lead: X-ray analysis.

Diego M. Andrada: Lead: Project administration, supervision, acquisition of funding and resources; Supporting: Writing – Review and Editing.

Synthesis, Structure, and Bonding Analysis of Lewis Base and Lewis Acid/Base-Stabilized Phosphyngallanes

T. Ilgin Demirel,^[a] Bernd Morgenstern,^[a] and Diego M. Andrada*^[a]

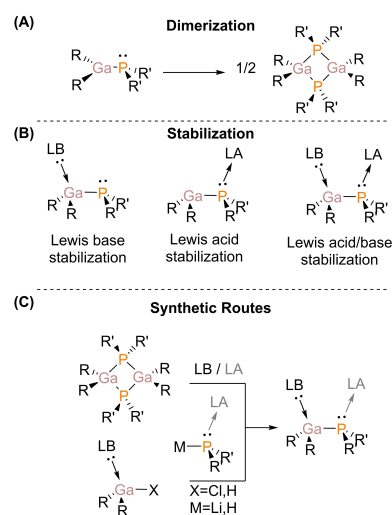
Phosphyngallane with hydrogen and halogen substituents (RXGa–PHR, R = organic substituent, X = halogen/hydrogen) are regarded as putative suitable precursors for accessing Ga=P doubly bonded species. Herein, we report on the synthesis, structure, and bonding analysis of a series of Lewis base- and Lewis acid/base-stabilized phosphyngallane bearing P–H and Ga–Cl/H substitution. To avoid oligomerization, the treatment of IDip.GaCl₃ and (IDip)GaH₂Cl (IDip = 1,3-bis(2,6-diisopropylphenyl)imidazole-2-ylidene) with LiPHR or LiPHR(BH₃) (R = Ph, Tip, Mes, NiPr₂, NCy₂) affords the corresponding Lewis base and

Lewis acid/base coordinated *H*,*Cl*-functionalized monomeric phosphyngallane, respectively. The structure of these derivatives were determined by spectroscopic and X-ray crystallographic analyses. The observed Ga–P bond lengths are comparable to those previously reported phosphyngallane analogues. The nature of the C^{Dip}-Ga coordination bond was assessed with Energy Decomposition Analysis, suggesting a relatively stable adduct. Reactions of the phosphyngallane with Brønsted bases were investigated.

Introduction

Unsaturated main group compounds containing a combination of heavier group 13 (E¹³) and group 15 (E¹⁵) elements are interesting precursors for preparing binary materials with applications in opto- and microelectronic devices.^[1] The pre-established 1:1 relationship between these elements has driven captivating investigations to prove their value as single source precursors using metal-organic chemical vapour deposition (MOCVD) or molecular beam epitaxy (MBE) methods.^[2] The intended E¹³=E¹⁵ functional groups are isoelectronic to C=C in alkenes, but their electronegative difference provides a marked tendency to form dimers, trimers, or tetramers (Scheme 1A). Nonetheless, particular interest has been placed on synthesizing monomeric [R₂E¹³=E¹⁵R₂] species, over the oligomers, because of their increased volatility and potentially simple deposition process.^[3]

In contrast to the lightest E¹³=E¹⁵ combination (B=N), their heavier congeners like Al=P or Ga=P have a significantly weak π-bond, making the monomeric forms synthetically challenging.^[4] A common stabilization strategy involves the use of sterically demanding organic substituents around the double bond, which provides kinetic and thermodynamic stability, but inevitably decreasing volatility.^[5] Another strategy is based on the stabilization provided through a Lewis base and/or acid



Scheme 1. Phosphyngallanes as example of group 13/15 multiple bonded compounds: (A) dimerization process, (B) different types of stabilization, (C) synthetic routes followed for the synthesis of monomeric species. LA = Lewis acid, LB = Lewis base, R = organic substituent.

[a] T. I. Demirel, Dr. B. Morgenstern, Dr. D. M. Andrada
Faculty of Natural Sciences and Technology, Department of Chemistry
Universität des Saarlandes
Campus C4.1, 66123 Saarbrücken, Germany
E-mail: diego.andrada@uni-saarland.de
http://inorg-comp-chem.com/

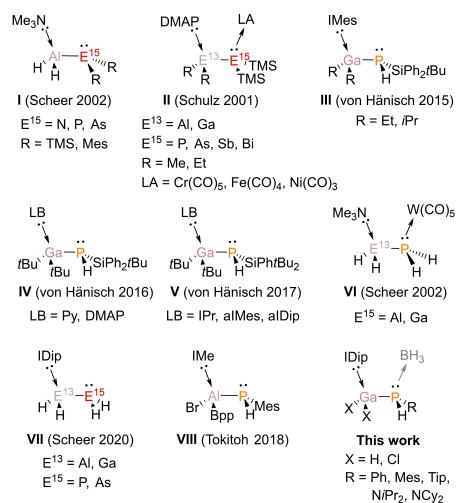
Supporting information for this article is available on the WWW under
https://doi.org/10.1002/ejic.202200477

Part of the "EurJIC Talents" Special Collection.

© 2022 The Authors. European Journal of Inorganic Chemistry published by
Wiley-VCH GmbH. This is an open access article under the terms of the
Creative Commons Attribution License, which permits use, distribution and
reproduction in any medium, provided the original work is properly cited.

coordination, which essentially blocks the empty p-orbital on E¹³ or the lone pair at E¹⁵ elements (Scheme 1B).^[6]

The oligomeric heterocycles have served as starting compounds for the generation of their monomeric forms (Scheme 1C).^[3,7] Despite some Lewis base stabilized adducts have been reported in the past (Scheme 2, I), Schulz and co-workers have introduced a general straightforward synthetic route towards the monomeric species via E¹³-E¹⁵ bond cleavage of the heterocycle with DMAP (4-dimethylamino-pyridine) as a



Scheme 2. Previously reported examples of Lewis stabilized group 13/15 species. Py = pyridine, DMAP = 4-dimethylamino-pyridine, IMe = 1,3,4,5-tetra methyl imidazole-2-ylidene, IPr = 1,3-diisopropyl-4,5-dimethylimidazole-2-ylidene, IMes = 1,3-bis-(2,4,6-trimethylphenyl) imidazole-2-ylidene, IDip = 1,3-bis(2,6-diisopropylphenyl) imidazole-2-ylidene, aIMes = abnormal IMes, alDiP = abnormal IDip, Mes = 2,4,6-Me₃C₆H₃, Tip = 2,4,6-*i*-Pr₃C₆H₃, Bbp = 2,6-[CH(SiMe₃)₂]₂C₆H₃.

Lewis base (Scheme 1C first reaction).^[8] With many examples, monomeric species (II) containing Al–P and Ga–P units have been isolated and characterized with this strategy, even involving a coordination transition metal on E¹³.^[9] However, not all the Lewis bases are able to cleave the heterocycles by coordinating the E¹³. The group of von Hänisch has addressed a thorough study to determine the limitations of the Lewis base stabilization for Ga–P-containing molecules.^[10] They have prepared monomeric species of galliumsilylphosphanide derivatives for relatively small substitutions on the Ga atom using the strong Lewis base IMes (1,3-bis-(2,4,6-trimethylphenyl)imidazole-2-ylidene, III).^[10e] Their attempts to create a doubly bonding Ga=P by thermal-induced elimination reactions resulted in the formation of heterocubane structure, pointing



Diego M. Andrada studied chemistry at the National University of Córdoba, Argentina, where he obtained his PhD degree under the supervision of Prof. Alejandro M. Granados. In 2012, he joined the group of Prof. Ricardo A. Mata at the Georg-August University of Göttingen, Germany. After a second postdoctoral stay at Philipps-University of Marburg with Prof. Gernot Frenking, he initiated his independent research career in 2018 at Saarland University. His research group focuses on the chemistry main group unsaturated compounds and the chemical bonding concepts.

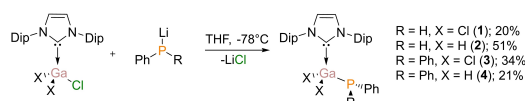
out the need for more demanding steric protection. However, when the substituents on Ga are bulkier, they observed that using a strong σ -donor Lewis base is not enough to cleave the oligomeric heterocycle when the steric demand is high. Thus, pyridine, DMAP and IPr (1,3-diisopropyl-4,5-dimethylimidazole-2-ylidene) can coordinate (IV).^[10c] Only IMes and IDip can provide such stabilization after a rearrangement if the group at the phosphorous terminal is large (V).^[10a]

A different approach has been employed by the group of Scheer, which essentially bypasses the generation of the heterocycle by directly reacting the corresponding adduct by salt, dihydrogen, and alkane elimination reactions, furnishing the Lewis base or Lewis acid/base pair compounds directly.^[11] In this manner, Scheer and co-workers synthesized several unsubstituted group 13/15 compounds, for instance (VI).^[11–12] Notably, this strategy allows the use of bulky NHC-stabilized gallium chlorides, hydrochlorides, and hydrides,^[13] giving access to the smallest stabilized phosphanylalanes and phosphanylgallanes (VII).^[12e]

The NHC as Lewis bases are very interesting not only for the stabilization provided on the group 13 element but also to enforce multiple chemical bonds in some cases.^[14] The group of Rivard has provided a detailed description of the synthesis of amido- and azide-functionalized gallium hydrides as potential precursors for Ga=N compounds.^[15] Recently, Tokitoh and co-workers have explored HBr elimination from Lewis base stabilized sterically hindered phosphanylalumane adduct (VIII).^[16] Herein, we report the synthesis of Lewis base and Lewis acid/base stabilized *H,H*- and *H,Cl*-functionalized phosphanylgallane. Furthermore, we assess their reactivity toward bases and the effect of the substituents at gallium and phosphorous sites on the overall stability of the monomeric compounds. These adducts have been fully characterized, and their electronic structures have been described by theoretical calculations.

Results and Discussion

We have selected the strong σ -donor Lewis base 1,3-bis(2,6-diisopropylphenyl) imidazole-2-ylidene (IDip) since it has been demonstrated its value to provide thermodynamic and kinetic stability to phosphagallanes.^[12e] Thus, we started our investigation by reacting LiPPh₂ with the Lewis base-stabilized trichloro-(IDip.GaCl₃) and mono-chlorogallane adducts (IDip.GaH₂Cl) in THF at –78 °C. These reactions afforded the mono substituted compounds **3** and **4**. The crystals can be isolated as a white solid stable at room temperatures in an inert atmosphere with yields of 34% (**3**) and 21% (**4**). The low yields are a consequence of the IDip elimination, similarly to the observations reported elsewhere.^[12e] ¹H NMR spectrum of compound **4** shows a doublet at 4.2 ppm (²J_{P,H} = 13.3 Hz) for the GaH₂-unit, while the ³¹P NMR spectrum gives a broad singlet at –59.1 ppm. This value is slightly upfield shifted compared to the dicyclohexylphosphane analogue reported by the group of Scheer (–56.1 ppm).^[12e] The chlorinated congener compound **3** shows a downfield shifted phosphorus chemical shift (–51.7 ppm), compared to hydride phosphagallane **4** (Scheme 3).



Scheme 3. Synthesis of compounds 1–4.

Likewise, with the aim to prepare the precursors for generating monomeric Lewis base stabilized phosphagallene compounds bearing Ga–P, we followed with the synthesis of 1,2 *H,H/H,Cl*-functionalized phosphanyl gallane **1** and **2** analogues. The reactions have been carried out in a similar fashion as with compounds **3** and **4**. Treatment of LiHPPH with IDip gallium hydrochlorides and chlorides adduct afforded products **1** and **2** in poor to moderate yields. The compounds were immediately isolated since longer reaction times led to an increasing amount of free IDip in the mixture together with unidentified side products. The ¹H NMR spectrum of **1** and **2** shows a doublet at 2.66 ppm (¹J_{P,H} = 196.6 Hz) and a doublet of triplets at 2.8 (²J_{H,P} = 188.7 Hz, ³J_{H,H} = 4.5 Hz) for the PH moiety, respectively. In the case of compound **2**, the signal corresponding to the GaH₂ moiety cannot be observed. The ³¹P NMR spectrum reveals a doublet at –130.3 ppm (¹J_{P,H} = 197.0 Hz) and a doublet of triplets at –142.9 ppm (¹J_{P,H} = 189.6 Hz, ²J_{P,H} = 16.4 Hz) for compound **1** and **2**, respectively. Additionally, the ¹³C{¹H} NMR spectra of all compounds **1–4** exhibit a doublet at 168.1 (**1**), 179.2 (**2**), 168.3 (**3**), and 178.8 (**4**) ppm assigned to the carbene carbon coordinated to the Ga center, which is high-field shifted compared to free IDip (220.6 ppm)^[17] and in good agreement with previously reported (IDip.GaH₃ 205.9 ppm, IDip.GaH₂Cl 181.6 ppm and IDip.GaHCl₂ 167.9 ppm).^[13c]

The IR spectra of compounds **2** and **4** display a strong, broad absorbance at 1825 and 1809 cm^{–1} (Figures S30 and S32 in the ESI), respectively, which are ascribed to the Ga–H stretching vibrational mode. These values are in good agreement with previously reported gallane adducts NMe₃.GaH₃ (1853 cm^{–1}),^[18] IPr.GaH₃ (1775 cm^{–1}, IPr),^[19] IDip.GaH₃ (1790 cm^{–1}),^[18] and IDip.GaH₂Cl (1877 cm^{–1}).^[13c] Notably, it has been suggested elsewhere that lower wavenumbers reflect a stronger donation from the Lewis base.^[19]

The solid-state structures of **1–4** were determined by single-crystal X-ray diffraction. Figure 1 shows the molecular structure, and the most important structural features are summarized in Table 1. The obtained Ga–P bond lengths are close to the sum of covalent radii (2.35 Å)^[20] and in accordance with the other representative adducts, i.e. IDip.GaH₂PCy₂ (2.3724(6) Å), IDip.GaH₂PH₂ (2.3373(6) Å),^[12e] and IMes.GaEt₂P(H)Si*t*BuPh₂ (2.4051(2) Å).^[10e] The Ga–C bond lengths are noticeably longer than the expected values for a single bond (Ga–C 1.99 Å).^[20] Moreover, these bond lengths are within the range of previously reported gallium complexes IDip.GaH₃ (2.076(2) Å), IDip.GaHCl₂ (2.034(2) Å),^[13c] IDip.GaH₂PCy₂ (2.090(2) Å), and IDip.GaH₂PH₂ (2.0507(2) Å),^[12e] but slightly shorter than the IMes.GaEt₂P(H)Si*t*BuPh₂ (2.1254(7) Å).^[10e]

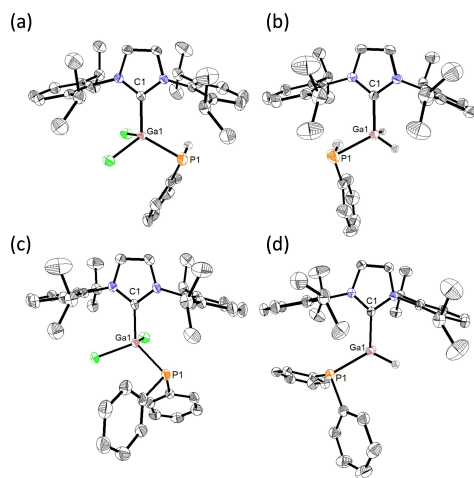


Figure 1. Molecular structures of Lewis base-stabilized phosphanyl gallane compounds **1** (a), **2** (b), **3** (c), and **4** (d). Ellipsoids set at 50% probability level. Hydrogen atoms, with the exception of those attached to gallium and phosphorous atoms, are omitted for clarity.

Table 1. Selected experimental and theoretical bond lengths (Å) and angles (°) for compounds **1–8**.^[a]

	Ga–C _{carb}	Ga–P	P–B	Σ/Ga ^[b]	Σ/P ^[b]
1	2.032(2) (2.082)	2.3258(6) (2.352)	—	325.2 (331.1)	281.2 (286.3)
2	2.057(2) (2.100)	2.334(1) (2.395)	—	330.9 (343.0)	245.4 (292.7)
3	2.047(2) (2.129)	2.3438(7) (2.388)	—	328.0 (328.6)	304.3 (310.2)
4	2.069(1) (2.139)	2.3738(4) (2.407)	—	338.5 (340.7)	307.0 (309.1)
5	2.042(2) (2.072)	2.3547(6) (2.369)	1.933(2) (1.944)	326.8 (324.7)	322.6 (312.8)
6	2.042(3) (2.116(6))	2.353(1) (2.29(1))	1.935(6) (1.91(2))	328.3 (323.9)	322.6 (319.2)
7	2.060(1) (2.076)	2.3694(3) (2.392)	1.959(2) (1.988)	336.5 (335.8)	318.6 (303.8)
8	2.052(2) (2.089)	2.3739(5) (2.405)	1.954(2) (1.974)	337.6 (338.6)	314.8 (311.3)

[a] All calculations were performed at the B3LYP-D3(BJ)/def2-SVP level of theory. [b] Sum of angles around Ga/P atom, disregarding the Lewis Acid or Base molecule.

The coordination of the Lewis base results in a different degree of pyramidalization of the gallium atom depending on the substituents, being the chlorinated adducts those with the lower sum of bond angles: 325.2 (**1**), 330.9 (**2**), 328.0 (**3**), and 336.5 (**4**). In the same vein, the phosphorus atoms are also pyramidal 281.2 (**1**), 245.4 (**2**), 304.3 (**3**), and 307.0 (**4**), which suggest that the coordination with the Lewis base precludes optimal π-conjugation.

To gain deeper insight into the electronic structure of compounds **1–4**, we carried out DFT calculations at the B3LYP-

D3(BJ)/def2-SVP level of theory (see Computational Details). The optimized geometries are in good agreement with the experimentally determined structures, as summarized in the Table 1. As a general observation, the computed bond lengths are slightly longer than the experimental ones.^[21] Inspection of the frontier Kohn-Sham molecular orbitals (KS-MO) identifies the HOMO as the lone pair located at the phosphorus atom, while LUMO is located at the π -system of the IDip ligand (Figures S38–S41 in the ESI).

We analyzed the electronic structures of 1–4 by Natural Bond Orbitals (NBO) analysis.^[22] Table 2 gathers the calculated natural atomic partial charges (Q) and Wiberg bond orders (P) of the Ga–C_{carb} and Ga–P bonds calculated at the B3LYP-D3(BJ)/def2-TZVPP level of theory on the previous optimized geometries. The localization of the orbitals shows the presence of a polarized Ga–P σ -bonds (Figures S46–S49). The contribution of phosphorous is between 66.07% and 70.41%, which is expected from Pauli electronegativities. (Ga: 1.41, P: 2.19).^[23] As a comparison, the aluminium analogues bear slightly more polarized bond i.e. 74 to 77% contribution of the phosphorus atom.^[7] Additionally, there is a lone pair (LP) on the phosphorus atom with p-character of around 50%, which is in agreement with the pyramidalization observed in the crystal structures. Natural population analyses (NPA) indicate a positive charge of ca. +0.60e on the Ga atom for the hydride derivatives, while chlorinated compounds bear a positive charge of about +1.10e (Table 2). The charge on the full carbene moiety (Q(IDip)) reveals no significant differences on electron density donated, i.e. about +0.30 e. Notably, the WBI between the gallium and the carbene carbon is slightly higher for 2 (0.54 au) and 4 (0.54 au) than for 1 (0.48 au) and 3 (0.49 au), in contrast to the expected from the comparison in of experimental bond lengths (Table 1).

We also analyzed the electron density distribution with atoms in molecules (QTAIM) using the B3LYP-D3(BJ)/def2-TZVPP electron density.^[24] The Laplacian distribution $\nabla^2\rho(r)$ in the C_{carb}–Ga–P plane is depicted in Figure 2b for compounds 3 and 4. The Laplacian plot shows an electron accumulation on the phosphorus atom localized on the σ -system and the electron density of the Ga–P bond critical point ($\rho^{\text{BCP}}=0.54/0.51\text{ e}/\text{\AA}^3$), which is shifted towards the P. In the case of the IDip-Ga the Laplacian distribution suggest a rather ionic bond with the electron density of the bond critical point ($\rho^{\text{BCP}}=0.55/0.52\text{ e}/\text{\AA}^3$). A similar picture is observed for the remaining series of compounds (Figure S54).

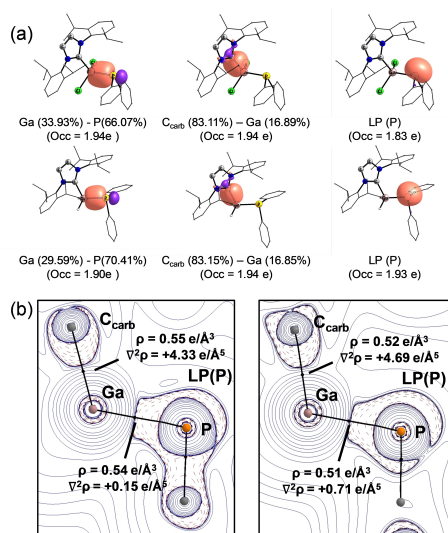


Figure 2. Bonding analysis of 3 and 4 (B3LYP-D3(BJ)/def2-TZVPP//B3LYP-D3(BJ)/def2-SVP). (a) NBOs. (b) 2D Laplacian distribution $\nabla^2\rho(r)$ in the P–Ga–C_{carb} plane. Dashed red lines indicate areas of charge concentration ($\nabla^2\rho(r) < 0$) while solid blue lines show areas of charge depletion ($\nabla^2\rho(r) > 0$), bond paths (black lines), and bcps (black dots).

To examine the strength of the IDip-Ga bonds in series of compounds 1–4, we have computed and compared the dissociation energies (D_0). Table 3 gives the bond energies at the BP86-D3(BJ)/TZ2P//B3LYP-D3(BJ)/def2-SVP level of theory. These computed bond dissociation energies suggest a relatively strong coordination of the Lewis base ligands to the phosphanyl-gallane moiety, which is comparable to those values computed for the carbene-alane compounds.^[7,12e,25] The values range from 45.5 kcal/mol (4) to 57.8 kcal/mol (1), being the chlorinated complexes those with larger dissociation energy values. More detailed information about the nature of the chemical bond is provided by the results of the Energy Decomposition Analysis (EDA) method.^[21] EDA has proven to be a useful tool to assess the nature of the chemical bond in main group compounds and transition metal compounds.^[26] None-

	Q(P)	Q(Ga)	Q(IDip)	P (Ga–P)	$\sigma(\text{Ga–P})$ contribution	P (C _{carb} –Ga)	$\sigma(\text{C}_{\text{carb}}\text{–Ga})$ contribution
1	–0.03	1.13	0.29	0.79	Ga (33.93%)–P(66.07%)	0.48	C _{carb} (83.11%)–Ga (16.89%)
2	–0.02	0.62	0.29	0.78	Ga (29.59%)–P(70.41%)	0.54	C _{carb} (83.15%)–Ga (16.85%)
3	0.25	1.12	0.30	0.78	Ga (33.23%)–P(66.77%)	0.49	C _{carb} (82.51%)–Ga (17.49%)
4	0.26	0.60	0.31	0.78	Ga (30.50%)–P(69.50%)	0.54	C _{carb} (82.79%)–Ga (17.21%)
5	0.73	1.13	0.30	0.71	Ga (30.59%)–P(69.41%)	0.49	C _{carb} (82.44%)–Ga (17.56%)
6	0.73	1.11	0.33	0.71	Ga (31.00%)–P(69.00%)	0.50	C _{carb} (81.86%)–Ga (18.14%)
7	0.45	0.64	0.33	0.72	Ga (26.18%)–P(73.82%)	0.56	C _{carb} (82.14%)–Ga (17.86%)
8	0.47	0.63	0.33	0.73	Ga (26.67%)–P(73.33%)	0.56	C _{carb} (82.06%)–Ga (17.94%)

Table 3. EDA-NOCV results of the C_{carb}-Ga bond in Lewis Base and Lewis Acid/Base-stabilized phosphanyl gallanes 1–8 at BP86-D3(BJ)/TZ2P.^[a] All values are in kcal/mol.

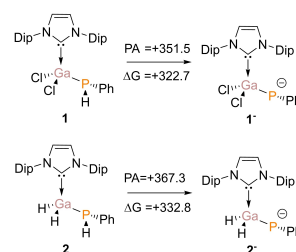
	1	2	3	4	5	6	7	8
ΔE_{int}	-72.8	-62.3	-75.8	-60.7	-78.3	-77.2	-77.2	-73.7
ΔE_{Pauli}	157.2	126.0	136.9	116.3	173.9	168.5	140.2	131.0
$\Delta E_{\text{elst}}^{\text{[b]}}$	-125.8 (55%)	-107.0 (57%)	-111.2 (52%)	-93.2 (53%)	-133.9 (53%)	-128.9 (52%)	-117.6 (54%)	-112.7 (55%)
$\Delta E_{\text{orb}}^{\text{[b]}}$	-77.0 (33%)	-60.0 (32%)	-72.9 (34%)	-59.4 (34%)	-85.1 (34%)	-85.9 (35%)	-69.1 (32%)	-65.8 (32%)
$\Delta E_{\text{disp}}^{\text{[b]}}$	-27.3 (12%)	-21.3 (11%)	-28.5 (12%)	-24.5 (13%)	-33.2 (13%)	-30.9 (13%)	-30.7 (14%)	-26.2 (13%)
$\Delta E_{\text{prep}}^{\text{GaP}}$	11.6	10.2	14.3	7.1	11.1	13.9	11.4	19.2
$\Delta E_{\text{prep}}^{\text{IDip}}$	3.4	1.8	6.3	3.5	3.6	3.9	2.4	2.2
$\Delta E_{\text{prep}}^{\text{tot}}$	15.0	12.0	20.6	10.6	14.7	17.8	13.8	21.4
$-\Delta E_{\text{e}}$	-57.8	-50.3	-55.1	-45.5	-63.6	-59.5	-63.4	-52.3

[a] All calculations were performed on the B3LYP-D3(BJ)/def2-SVP optimized structures. [b] The percentage values in the parentheses give the contribution to the total attractive interactions $\Delta E_{\text{elst}} + \Delta E_{\text{orb}} + \Delta E_{\text{disp}}$.

theless, a recent discussion has been placed about the path function nature of the energy components.^[26c,27] Within the EDA scheme, the interaction energy (ΔE_{int}) between two (or more) structurally and electronically unrelaxed fragments of a molecule is divided into four physical meaningful terms, namely, Pauli repulsion (ΔE_{Pauli}), electrostatic interaction (ΔE_{elst}), orbital interaction (ΔE_{orb}), and dispersion interaction (ΔE_{disp}). The dissociation energy is related to the interaction energy by the preparation energy (ΔE_{prep}), which is the energy needed to promote the fragments from their equilibrium geometry to the geometry and electronic state in the compounds.

Table 3 summarizes the numerical results of the EDA calculations performed for the heterolytic fragmentation resulting in IDip and the monomeric phosphagallane. The interaction energies ΔE_{int} follows the same trend as the dissociation energy, leading to stronger interaction for compounds 1 and 3 than for compounds 2 and 4. The preparation (ΔE_{prep}) of IDip does not carry particular energy penalties as the geometry is rather rigid, giving similar results along the series. The phosphagallanes moieties instead request more energy as a consequence of the pyramidalization of the gallium atom upon coordination. The dissection of the ΔE_{int} reveals that the bonding interactions are on average >50% ionic with an important contribution of the dispersion interaction >10%. Noteworthy, the orbital interaction values are higher for 1 and 3 than 2 and 4 by about 10 kcal/mol, given the higher effective acidity,^[28] which is partially compensated by the stronger Pauli repulsion.

We attempted to promote the formation of the Lewis base coordinated phosphagallane compounds bearing a Ga=P double, by reacting Brønsted bases with 1 and 2. However, all attempted reactions to induce elimination of HCl or H₂ by the addition of bases such as NEt₃, morpholine, K[N(SiMe₃)₂], and DBU (1,8-diazabicyclo[5.4.0]undeca-7-ene) were unsuccessful in the regard that no abstraction reaction was observed. Instead, either no reaction (NEt₃) or decomposition with the formation of phosphalkene (IDipPH), as observed by Blum et al.^[29] In order to further corroborate the inertness towards deprotonation, we have computed the proton affinity of compound 1–2. Previous studies have shown that the proton affinities (PA) are sensitive probe for the presence of chemically available or accessible lone pairs of a molecule.^[30] Scheme 4 gathers the calculated PAs of 1–2 at the B3LYP-D3(BJ)/def2-SVP level of

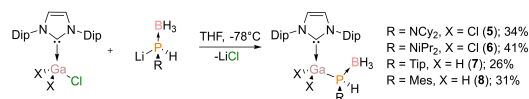


Scheme 4. Calculated Proton Affinities (in kcal/mol) and Gibbs energy (in THF) of compounds 1–2. DFT calculations were performed at the B3LYP-D3(BJ)/def2-SVP level of theory.

theory. The PA of all compounds are higher than 350 kcal/mol which suggest a highly basic nature of the elusive anion. Note that the calculated PA values follow the trend of the gallium Lewis acidity. The highest PA is for 2 (367.3 kcal/mol), while for 1 the PA is still high but there is a notable reduction of about 15 kcal/mol leading to 351.5 kcal/mol. In terms of Gibbs energy considering the solvent polarity (THF), the deprotonation is endergonic by 322.7 (1) and 332.8 (2) kcal/mol, which is comparable to the values computed by Agou and coworkers for the Lewis base stabilized phosphanylalumane congeners (VIII),^[16a] i.e. 323.3 kcal/mol.

Since the phosphorus atom of compound 1–4 bears a lone pair, we became interested to elucidate whether the HCl or H₂ elimination of phosphagallane compounds can be accessed by coordinated with a Lewis acid. Thus, we conducted the reaction of IDip.GaH₂Cl and IDip.GaCl₃ with the mono-lithiated phosphineboranes (RPHLi.BH₃)^[31] in THF at -78 °C afforded the compounds 5–8 (Scheme 5). The compounds were isolated immediately upon the addition of RPHLi.BH₃, since longer reaction times leads to an increasing amount of free phosphine H₂PR.

Compounds 5–8 were obtained as colourless crystalline solids, which are stable for weeks under inert gas atmosphere at ambient temperature, but they decompose rapidly when exposed to air. Indeed, the formation of side products are observed at short reaction scales for the compound 8. All compounds were fully characterized by multinuclear NMR, elemental analysis, and IR spectroscopy. The ¹H NMR spectra



Scheme 5. Synthesis of compounds 5–8.

exhibit two sets of resonances for the Dip groups for all compounds. Additionally, the PH moiety in 5 and 6 can be detected as doublet of quadruplets at 5.32 ($^1J_{\text{H,P}} = 339.8$ Hz, $^3J_{\text{H,H}} = 7.3$ Hz) and 5.3 ($^1J_{\text{H,P}} = 337.0$ Hz, $^3J_{\text{H,H}} = 7.3$ Hz), respectively. The same functionality appears as a doublet of multiplet for 7 at 5.4 ($^1J_{\text{H,P}} = 310.2$ Hz, $^3J_{\text{H,H}} = 7.0$ Hz), while 8 undergoes decomposition during NMR measurements. The phosphorous chemical shift is in general low-field shifted in comparison to compounds 1–4. The ^{31}P NMR spectra display broad doublets at -2.9 ($^1J_{\text{P,H}} = 342.4$ Hz), -6.71 ($^1J_{\text{P,H}} = 339.1$ Hz), -110.7 ($^1J_{\text{P,H}} = 309.4$ Hz), and -103.5 ($^1J_{\text{P,H}} = 316.8$ Hz) for compound 5, 6, 7, and 8, respectively. For all compounds, boron atoms appear in the ^{11}B NMR spectra as broad singlets in the range of -34.1 and -35.1 ppm.

In the IR spectra, both P–H and Ga–H stretching bands can be detected as in the case of compounds 1–4. The Ga–H stretching vibrations of 7 and 8 are observed at higher wavenumbers than compound 2 and 4, i.e. 1869 and 1871 cm^{-1} . According to the discussion elsewhere this can be associated to a weaker coordination of IDip.^[19]

The molecular structures of the compounds 5–8 were confirmed by single crystal X-ray diffraction. Figure 3 displays

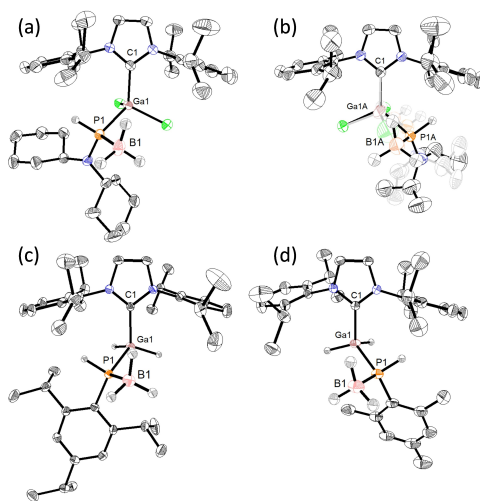


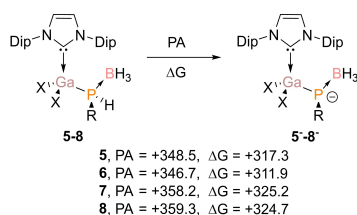
Figure 3. Molecular structures of Lewis acid/base-stabilized phosphanyl-gallane compounds 5 (a), 6 (b), 7 (c), and 8 (d). Ellipsoids set at 50% probability level. Hydrogen atoms, with the exception of those attached to gallium and phosphorous atoms, are omitted for clarity.

the molecular structure and Table 1 collects the most important structural parameters. The Lewis acid/base coordinated phosphagallane adducts possess a comparable degree of gallium atom pyramidalization with values of 326.6° (5) to 337.5° (8), while the phosphorus atom shows less pyramidalization leading to wider sum of angles, i.e. 314.6° (8) to 322.6° (6). The Ga–P bond lengths are in general longer for 5–8 than 1–4, indicating the absence of π -conjugation. At the same time, the C_{carb} –Ga bond length is slightly shorter when the Lewis acid is incorporated, suggesting a stronger coordination as a consequence of the push-pull effect of the Lewis pair.^[32]

It is interesting to remark the importance of the substituent on the phosphorus terminal. We attempted to prepare less sterically protected Lewis acid/base phosphagallane compounds such as $R = \text{Ph}$ or $t\text{Bu}$. However, the desired products could not be isolated. Upon addition of the RPHLi.BH_3 , mixture of compounds including $\text{IDip.GaX}_2\text{PHR.BH}_3$, $\text{IDip.GaX}_2\text{PHR}$ and H_2PR were detected in the reaction mixture. Longer reaction times indeed does not lead to full conversion, instead decomposition product into free phosphine is observed. This indicates that the stability of the adducts are highly influenced by the Lewis acidity of the phosphorus, which is enhanced by the presence of the nitrogen of NCy_2 and NiPr_2 functional groups in compound 5 and 6.^[33] Alternatively, Mes and Tip groups provides enough kinetic stability for isolation, however, decomposition is observed in solution.

Next, we have carried out DFT calculations to examine the electronic structure effects produced by the Lewis acid incorporation. The results are summarized in Table 2 and Table 3. The atomic partial charges show no significant effect on the gallium atom with a value of about $+1.10$ and $+0.60$ e for the chlorinated and hydride derivatives, respectively. As expected, the coordination to BH_3 results in a phosphorus atom bearing more positive charge. The Wiberg bond indices indicate a small reduction of the Ga–P bond order together with an increase in the polarization. Additionally, the coordination of IDip to the gallium atom is not significantly affected in polarization of bond order terms. We have applied EDA to gain insight into the coordination strength origins. The bond dissociation energy is in average 5 kcal/mol stronger for the Lewis acid/base pair adducts than for the Lewis base ones. This is reflected in the interaction energy (ΔE_{int}) rather than in the preparation energy (ΔE_{prep}). The Lewis acid incorporation increases mainly the electrostatic and orbital interaction, which is also partially compensated the higher Pauli repulsion.

The calculation of the proton affinity and Gibbs free energy of compound 5–8 are in agreement with the increase of the PH acidity. The Lewis acid coordination represent a lowering of



Scheme 6. Calculated Proton Affinities (in kcal/mol) and Gibbs energy (in THF) of compounds 5–8. DFT calculations were performed at the B3LYP-D3(BJ)/def2-SVP level of theory.

about 10 kcal/mol (Scheme 6). However, our attempts to induce H₂ or HCl elimination by reaction with different Brønsted bases were once more unsuccessful furnishing decomposition instead the intended phosphagallane adducts.

Conclusions

In this contribution, we have presented eight derivatives of monomeric phophanylgallanes stabilized by a strong σ -donor, and sterically demanding Lewis base, namely 1,3-bis(2,6-diisopropylphenyl) imidazole-2-ylidene. In addition to the species, which are only organosubstituted on the P atom, the parent compounds bearing H,H or H,Cl-functionalization were isolated coordinating to a Lewis base or a Lewis base/acid pair. The products were characterized by means of spectroscopy, single crystal X-ray diffraction and DFT methods. These compounds exhibit Ga–P bond lengths typical for a single bond and a slightly longer C_{carb}–Ga bond length than a single bond. The bonding analysis suggests a fairly stable interaction between the Lewis base and the phosphagallane, which is mainly dominated by the electrostatic interaction (>50%). Notably, the introduction of a Lewis acid at the phosphorus lone pair enhances the bond energy by 10 kcal/mol which is mainly due to a stronger orbital interaction. The Lewis base and Lewis acid/base-stabilized species do not show reactivity towards Brønsted bases due to their high proton affinity.

Experimental Section

General considerations. All syntheses and manipulations were carried out under argon atmosphere (Ar), using either Schlenk line techniques or a glovebox (MBraun Unilab Plus). The glassware was pre-dried in oven at 125 °C and heated *in vacuo* prior to use. Organic solvents THF, benzene and *n*-pentane were taken directly from solvent purification system (Innovative Technology PureSolv MD5). Deuterated benzene was dried over appropriate drying agents, distilled and, stored inside a glovebox. NMR-spectra were recorded at 300 K on a Bruker Avance III 300 and a Bruker Avance IV HD 400 spectrometer. (¹H: 400.13 MHz, ¹³C: 100.61 MHz, ¹¹B: 128.38 MHz, ³¹P: 121.5 MHz). Chemical shifts (in δ , ppm) are referenced to the residual solvent signal(s): C₆D₆ (¹H, 7.16; ¹³C, 128.06).^[34] Fourier-transform IR spectra were acquired on a Bruker Vertex 70 spectrometer in attenuated total reflectance (ATR) mode.

Elemental analyses were performed on an elemental analyzer Leco CHN-900 and/or an elemental 161vario Micro Cube. Single crystal X-ray diffraction analysis were carried out at low temperatures on Bruker AXS D8 Venture diffractometer operating with a microfocus sealed tube and a Photon II detector. Monochromated MoK α radiation (λ = 0.71073 Å) was used. Structure solution and refinement were performed using SHELX.^[35] These data can be obtained free of charge from The Cambridge Crystallographic Data Centre via <http://www.ccdc.cam.ac.uk>. ⁹BuLi (1.6 M in hexane, Alfa-Aesar), GaCl₃ (Sigma Aldrich), and PhPH₂ (10% wt. in hexane) (ABCR GmbH) were commercially available and used without further purification. Phosphine-boranes RPH₂BH₃,^[31] LiPPh₂,^[36] IDip.GaCl₃^[37] and IDip.GaH₂Cl^[38] were prepared according to the literature procedures.

Compound 1 (IDipGaCl₂PHPh): 10% weight in hexane solution of PhPH₂ (0.5 mL, 0.49 mmol) was added in 2 mL of THF and 1.6 M of ⁹BuLi (0.3 mL, 0.49 mmol) was added dropwise to the solution at –78 °C. After stirring at –78 °C for 30 minutes, it was added dropwise to the THF solution of IDip.GaCl₃ (250 mg, 0.44 mmol) at –78 °C. Upon addition, volatiles were evaporated under vacuum. The product was then extracted with 8 mL of benzene. Benzene was then removed under reduced pressure and the residue was washed with *n*-pentane (2 × 5 mL), leading to mg (128 mg, 20%) of a white solid. Colourless crystals were grown by slow evaporation of saturated toluene solution at room temperature. ¹H NMR (400 MHz, C₆D₆) δ ppm: 7.59–7.54 (m, 1H, Ar), 7.32–7.18 (m, 6H, Ar), 7.14–7.07 (m, 4H, Ar), 6.44 (s, 2H, NCH), 2.76 (sep, 3H, CH(CH₃)₂), 2.71 (sep, 4H, CH(CH₃)₂), 2.66 (d, ¹J_{H,P} = 196.6 Hz PPh) 1.51–1.41 (m, 12H, CH(CH₃)₂), 1–02–0.94 (m, 12H, CH(CH₃)₂) ppm. ¹³C{¹H} NMR (100.6 MHz, C₆D₆, 298 K): 168.1 (d, ²J_{C,P} = 14.9 Hz, NCN), 146.2 (Ar), 146.0 (Ar), 145.8 (Ar), 135.0 (d, 15.03 Hz), 131.7 (Ar), 126.4 (Ar), 125.7 (Ar), 125.3 (Ar), 124.9 (Ar), 124.6 (d, 5.43 Hz), 29.2 (CH(CH₃)₂), 25.9 (CH(CH₃)₂), 23.1 (CH(CH₃)₂) ppm. ³¹P NMR (161.9 MHz, C₆D₆, 298 K): –130.2 (d, ¹J_{P,H} = 197.0 Hz) ppm. EA (%): calcd. C: 62.10 H: 6.63 N: 4.39; found: C: 62.57, H: 6.30, N: 4.00; MP: 187 °C(decomp.). APPI-MS (*m/z*): 601.20 [M–Cl⁺ + H]⁺.

Compound 2 (IDipGaH₂PHPh). 10% weight in hexane solution of PhPH₂ (0.2 mL, 0.22 mmol) was added in 2 mL of THF and 1.6 M of ⁹BuLi (0.1 mL, 0.22 mmol) was added dropwise to the solution at –78 °C. After stirring at –78 °C for 30 minutes, it was added dropwise to the THF solution of IDip.GaH₂Cl (100 mg, 0.20 mmol) at –78 °C. Upon addition, volatiles were evaporated under vacuum. The product was then extracted with 8 mL of benzene. Benzene was then removed under reduced pressure and the residue was washed with *n*-pentane (2 × 5 mL) to afford the product as white solid (59 mg, 51%). Colourless crystals were grown by slow evaporation of saturated benzene solution at room temperature. ¹H NMR (400 MHz, C₆D₆) δ ppm: 7.44–7.39 (m, 2H, Ar), 7.29–7.24 (m, 3H, Ar), 7.14–7.11 (m, 6H, Ar), 6.45 (s, 2H, NCH), 2.77 (dt, ¹J_{H,P} = 188.7 Hz, ²J_{H,H} = 4.5 Hz 1H, PPh), 2.69 (sep, 4H, CH(CH₃)₂), 1.44 (d, 12H, CH(CH₃)₂), 1.04 (d, 12H, CH(CH₃)₂) ppm. ¹³C{¹H} NMR (100.6 MHz, C₆D₆, 298 K): 179.2 (d, ²J_{C,P} = 19.9 Hz, NCN), 145.7 (Ar), 142.5 (d, 20.9 Hz, Ar), 134.76 (Ar), 133.6 (d, 13.0 Hz, NCHCN), 130.9 (Ar), 124.7 (d, 7.8 Hz, Ar), 124.4 (Ar), 124.1 (d, 6.22 Hz, Ar), 123.7 (d, 5.1 Hz, Ar), 29.1 (CH(CH₃)₂), 25.4 (CH(CH₃)₂), 23.2 (d, 3.3 Hz, CH(CH₃)₂) ppm. ³¹P NMR (161.9 MHz, C₆D₆, 298 K): –142.7 (d, ¹J_{P,H} = 189.6 Hz, ²J_{P,H} = 16.4 Hz) ppm. EA (%): calcd. C: 69.61 H: 7.79 N: 4.92; found: C: 67.50, H: 7.22, N: 4.78; MP: 74 °C(decomp.). APPI-MS (*m/z*): 567.24 [M]⁺. Compound 2 consistently analyzed low for carbon over repeated analyses.

Compound 3 (IDipGaCl₂PPh₃). 5 mL THF solution of LiPPh₃ (70 mg, 0.36 mmol) was added dropwise to the solution of 5 mL THF solution of IDip.GaCl₃ (250 mg, 0.44 mmol) at –78 °C. Upon addition, volatiles were evaporated under vacuum. The product was then extracted with 8 mL of benzene. Benzene was then removed under reduced pressure and the remaining white solid is

washed with *n*-pentane (2×5 mL) to afford the product as white solid (97 mg, 34%). Colourless crystals were grown by slow evaporation of saturated benzene solution at room temperature. ¹H NMR (400 MHz, C₆D₆, 298 K): 7.65–7.59 (m, 4H, Ar), 7.24–7.19 (m, 2H, Ar), 7.11–7.06 (m, 4H, Ar), 7.05–6.99 (m, 4H, Ar), 6.98–6.92 (m, 2H, Ar), 6.43 (s, 2H, NCHCHN), 2.85 (sep, 4H, CH(CH₃)₂), 1.40 (d, 12H, CH(CH₃)₂), 0.96 (d, 12H, CH(CH₃)₂) ppm. ¹³C{¹H} NMR (100.6 MHz, C₆D₆, 298 K): 168.3 (d, ²J_{CP}=27.3 Hz, NCN), 145.9 (Ar), 138.0 (d, 21.0 Hz, Ar), 135.9 (d, 19.4 Hz, Ar), 134.3 (Ar), 134.0 (Ar), 131.5 (Ar), 127.1 (Ar), 125.6 (Ar), 124.7 (Ar), 29.2 (CH(CH₃)₂), 26.2 (CH(CH₃)₂), 22.9 (CH(CH₃)₂) ppm. ³¹P NMR (161.9 MHz, C₆D₆, 298 K): –51.7 ppm. EA (%): calcd. C: 65.57 H: 6.49 N: 3.92; found: C: 64.33, H: 6.10, N: 3.69; MP: 248 °C(decomp.). APPI-MS (*m/z*): 713.21 [M]⁺. Compound 3 consistently analyzed low for carbon over repeated analyses.

Compound 4 (IDipGaH₂PPh₂). 5 mL THF solution of LiPPh₂ (97 mg, 0.50 mmol) was added dropwise to the solution of 5 mL THF solution of IDip.GaH₂Cl (250 mg, 0.50 mmol) at –78 °C. Upon addition, volatiles were evaporated under vacuum. The product was then extracted with 8 mL of benzene. Benzene was then removed under reduced pressure and the remaining white solid is washed with *n*-pentane (2×5 mL) to afford the product as white solid (67 mg, 21%). Colourless crystals were grown by slow evaporation of saturated benzene solution at room temperature. ¹H NMR (400 MHz, C₆D₆, 298 K): 7.45–7.40 (m, 4H, Ar), 7.24–7.19 (m, 2H, Ar), 7.10–7.06 (m, 4H, Ar), 7.03–6.98 (m, 4H, Ar), 6.95–6.88 (m, 2H, Ar), 6.48 (s, 2H, NCHCHN), 4.23 (d, ²J_{PH}=13.3 Hz, GaH₂), 2.75 (sep, 4H, CH(CH₃)₂), 1.38 (d, 12H, CH(CH₃)₂), 1.01 (d, 12H, CH(CH₃)₂) ppm. ¹³C{¹H} NMR (100.6 MHz, C₆D₆, 298 K): 178.8 (d, ²J_{CP}=28.1 Hz, NCN), 145.6 (Ar), 144.4 (Ar), 144.2 (Ar), 134.9 (d, 16.5 Hz, Ar), 130.9, 127.7 (d, 5.8 Hz, Ar), 125.2 (Ar), 128.8 (d, 6.0 Hz, Ar), 124.4 Hz (Ar), 29.1 (CH(CH₃)₂), 25.5 (CH(CH₃)₂), 23.0 (CH(CH₃)₂) ppm. ³¹P NMR (161.9 MHz, C₆D₆, 298 K): –59.1 ppm. EA (%): calcd. C: 72.57 H: 7.50 N: 4.34; found: C: 69.98, H: 6.58, N: 3.71; MP: 196 °C(decomp.). APPI-MS (*m/z*): 643.27 [M]⁺. Compound 4 consistently analyzed low for carbon over repeated analyses.

Compound 5 (IDipGaCl₂PHNCy₂BH₃). (NCy₂)PH₂BH₃ (111 mg, 0.49 mmol) was dissolved in 3 mL of dry THF and cooled down to –78 °C. To this solution, 1.6 M of ⁹BuLi (0.3 mL, 0.49 mmol) solution in hexane was added dropwise. After stirring at –78 °C for 30 minutes, it was added dropwise to the THF solution of IDip.GaCl₃ (278 mg, 0.44 mmol) at –78 °C. After the addition is complete, volatiles were under vacuum. The products were then extracted with 10 mL of benzene and washed with *n*-pentane (2×10 mL) to yield the product as white powder (128 mg, 34%). Single crystals were grown by slow evaporation of saturated benzene solution at room temperature. ¹H NMR (400 MHz, C₆D₆, 298 K): 7.28–7.24 (m, 3H, Ar), 7.14–7.11 (m, 3H, Ar), 6.51 (s, 2H, NCH), 5.32 (dq, ¹J_{HP}=339.8 Hz, ³J_{HH}=7.3 Hz 1H, –PH), 3.00–2.90 (m, 2H, CyH), 2.82 (sep, 4H, CH(CH₃)₂), 1.97–1.79 (m, 6H, CyH), 1.60–1.51 (m, 17H, CH(CH₃)₂, CyH), 1.44–1.40 (m, 4H, CyH), 0.99–0.92 (m, 17H, CH(CH₃)₂, CyH) δ ppm. ¹³C{¹H} NMR (100.6 MHz, C₆D₆, 298 K): 165.8 (d, ²J_{CP}=32.0, NCN), 146.4 (d, 48.6 Hz, Ar), 133.8 (Ar), 131.8 (Ar), 126.0 (Ar), 124.6 (d, 26.7 Hz, Ar), 57.1 (d, 3.5 Hz, NCHCHN), 33.9 (NCHCH₂CH₂CH₃), 33.1 (NCHCH₂CH₂CH₃), 29.3 (d, 19.9 Hz, NCHCH₂CH₂CH₃), 26.6 (d, 4.2 Hz, NCHCH₂CH₂CH₃), 26.3 (d, 19.6 Hz, CH(CH₃)₂), 26.0 (CH(CH₃)₂), 23.0 (d, 22.1 Hz, CH(CH₃)₂) δ ppm. ³¹P NMR (161.9 MHz, C₆D₆, 298 K): –2.9 ppm (bd, ¹J_{PH}=342.4 Hz), ¹¹B{¹H} NMR (128.4 MHz, C₆D₆, 298 K) δ: –34.1 ppm. EA (%): calcd. C:62.01 H:8.27 N:5.56; found: C:62.05, H:7.77, N:5.13. MP: 108 °C(decomp.).

Compound 6 (IDipGaCl₂PHNiPr₂BH₃). (NiPr₂)PH₂BH₃ (65 mg, 0.43 mmol) was dissolved in 3 mL of dry THF and cooled down to –78 °C. To this solution, 1.6 M of ⁹BuLi (0.3 mL, 0.48 mmol) solution in hexane was added dropwise. After stirring at –78 °C for 30 minutes, it was added dropwise to the THF solution of IDip.GaCl₃ (250 mg, 0.44 mmol) at –78 °C. After the addition is complete, volatiles were

under vacuum. The products were then extracted with 10 mL of benzene and washed with *n*-pentane (2×10 mL) to yield the product as white powder (124 mg, 41%). Single crystals were grown by slow evaporation of saturated benzene solution at room temperature. ¹H NMR (400 MHz, C₆D₆, 298 K) δ ppm: 7.27–7.23 (m, 2H, Ar), 7.15–1.11 (m, 4H, Ar), 5.28 (dq, ¹J_{HP}=337.0 Hz, ³J_{HH}=7.3 Hz 1H, –PH), 3.33 (sep, 2H, CH(CH₃)₂), 2.95–2.73 (m, 4H, CH(CH₃)₂), 1.57 (t, 12H, CH(CH₃)₂), 1.03 (d, 6H, CH(CH₃)₂), 0.96 (t, 18H, CH(CH₃)₂) ppm. ¹³C{¹H} NMR (100.6 MHz, C₆D₆, 298 K): 146.4 (d, ²J_{CP}=38.7 Hz, NCN), 133.8 (Ar), 131.7 (Ar), 126.0 (Ar), 124.6 (d, 24.7 Hz, Ar), 48.2 (d, 3.96 Hz, NCHCH₂), 29.3 (d, 16.8 Hz, CH(CH₃)₂), 26.3 (d, 13.5 Hz, CH(CH₃)₂), 23.1 (d, 10.3 Hz, CH(CH₃)₂), 22.8 (d, 2.4 Hz, NCH(CH₃)₂), 22.5 (d, 2.7 Hz, NCH(CH₃)₂) δ ppm. ³¹P NMR (161.9 MHz, C₆D₆, 298 K): –6.7 (bd, ¹J_{PH}=339.1 Hz) ppm. ¹¹B{¹H} NMR (128.4 MHz, C₆D₆, 298 K) δ: –34.2 ppm. EA (%): calcd. C:58.70 H:8.06 N: 6.22; found: C:57.27, H:7.77, N:5.86; MP: 132 °C(decomp.). Compound 6 consistently analyzed low for carbon over repeated analyses.

Compound 7 (IDipGaH₂PHTip.BH₃). TipPH₂BH₃ (41 mg, 0.16 mmol) was dissolved in 3 mL of dry THF and cooled down to –78 °C. To this solution, 1.6 M of ⁹BuLi (0.1 mL, 0.16 mmol) solution in hexane was added dropwise. After stirring at –78 °C for 30 minutes, it was added dropwise to the THF solution of IDip.GaH₂Cl (100 mg, 0.20 mmol) at –78 °C. After the addition is complete, volatiles were under vacuum. The products were then extracted with 10 mL of benzene and washed with *n*-pentane (2×10 mL) to yield the product as white powder (30 mg, 26%). Single crystals were grown by vapour diffusion into a saturated toluene solution at room temperature. ¹H NMR (400 MHz, C₆D₆, 298 K) δ ppm: 7.29–7.21 (m, 2H, Ar), 7.15–7.09 (m, 4H, Ar), 7.02 (s, 2H, NCH), 4.28 (dt, ¹J_{HP}=310.2 Hz, ³J_{HH}=7.0 Hz 1H, –PH), 3.31 (sept, 2H, CH(CH₃)₂), 2.93 (sept, 2H, CH(CH₃)₂), 2.77–2.51 (m, 3H, CH(CH₃)₂), 1.45 (d, 12H, CH(CH₃)₂), 1.31 (d, 6H, CH(CH₃)₂), 1.24 (d, 6H, CH(CH₃)₂), 1.12 (d, 6H, CH(CH₃)₂), 1.04–0.93 (m, 12H, CH(CH₃)₂) ppm. ¹³C{¹H} NMR (100.6 MHz, C₆D₆, 298 K): 174.8 (d, ²J_{CP}=13.1 Hz, NCN), 152.1 (d, 8.4 Hz, Ar), 148.4 (d, 2.4 Hz, Ar), 145.9 (d, 17.5 Hz, Ar), 134.7 (Ar), 131.1 (Ar), 125.0 (Ar), 124.6 (Ar), 124.4 (Ar), 121.7 (d, 7.0 Hz, Ar), 34.5 (CH(CH₃)₂), 32.7 (d, 8.2 Hz, CH(CH₃)₂), 29.0 (d, 22.1 Hz, CH(CH₃)₂), 25.9 (CH(CH₃)₂), 25.7 (d, 15.0 Hz, CH(CH₃)₂), 24.7 (CH(CH₃)₂), 24.1 (d, 3.6 Hz, CH(CH₃)₂), 23.5 (CH(CH₃)₂), 23.0 (CH(CH₃)₂) ppm. ³¹P NMR (161.9 MHz, C₆D₆, 298 K): –110.7 (bd, ¹J_{PH}=309.4 Hz) ppm. ¹¹B{¹H} NMR (128.4 MHz, C₆D₆, 298 K): –33.10 δ ppm. EA (%): calcd. C:71.10 H:9.23 N:3.95; found: C:67.17, H:7.96, N:3.55; MP: 180 °C(decomp.). APPI-MS (*m/z*): 693.38 [M-BH₃]⁺. Compound 7 consistently analyzed low for carbon over repeated analyses.

Compound 8 (IDipGaH₂PHMes.BH₃). MesPH₂BH₃ (83.7 mg, 0.50 mmol) was dissolved in 3 mL of dry THF and cooled down to –78 °C. To this solution, 1.6 M of ⁹BuLi (0.4 mL, 0.64 mmol) solution in hexane was added dropwise. After stirring at –78 °C for 30 minutes, it was added dropwise to the THF solution of IDip.GaH₂Cl (250 mg, 0.50 mmol) at –78 °C. After the addition is complete, volatiles were under vacuum. The products were then extracted with 10 mL of benzene and washed with *n*-pentane (2×10 mL) to yield the product as white powder (97 mg, 31%). Single crystals were grown by slow evaporation of saturated benzene solution at room temperature. ¹H NMR (400 MHz, C₆D₆, 298 K) δ ppm: 7.26–7.21 (m, 3H), 7.13–7.09 (m, 5H), 6.48 (s, 2H), 2.88 (sept, 2H), 2.68 (sept, 2H), 2.34 (s, 6H), 1.96 (s, 3H), 1.48–1.44 (m, 12H), 1.01–0.95 (m, 12H) ppm. ¹³C{¹H} NMR (100.6 MHz, C₆D₆, 298 K): 174.4 (d, ²J_{CP}=10.2 Hz, NCN), 145.9 (Ar, d, 18.0 Hz), 141.1.1 (Ar, d, 7.2 Hz), 136.9 (Ar), 134.6 (Ar), 131.2 (Ar), 129.2 (Ar, d, 7.1 Hz), 125.1 (Ar), 124.7 (Ar), 124.4 (Ar), 34.4 (NCHCHN), 29.2 (CH(CH₃)₂, d, 15.0), 25.7 (o-PhCH₃, d, 23.5 Hz), 23.6 (p-PhCH₃, d, 6.0 Hz), 23.4 (CH(CH₃)₂), 23.1 ppm (CH(CH₃)₂). ³¹P NMR (161.9 MHz, C₆D₆, 298 K): –103.5 ppm (d, ¹J_{PH}=316.8 Hz) ppm. ¹¹B{¹H} NMR (128.4 MHz, C₆D₆, 298 K): –35.1 δ ppm. EA (%): calcd. C:69.15 H:8.54 N:4.48; found: C:67.01, H:7.31, N:3.83; MP:

98 °C(decomp.). APPI-MS (*m/z*): 609.29 [M-BH₃]⁺. Compound **8** consistently analyzed low for carbon over repeated analyses.

Computational Details. All geometry optimizations were performed using the Gaussian 16.C01 software.^[39] All geometry optimizations were computed using the functional B3LYP^[40] functional with Grimme dispersion corrections D3^[41] and the Becke-Jonson damping function^[42] in combination with the def2-SVP basis set.^[43] The stationary points were located with the Bery algorithm^[44] using redundant internal coordinates. Analytical Hessians were computed to determine the nature of stationary points (one and zero imaginary frequencies for transition states and minima, respectively)^[45] and to calculate unscaled zero-point energies (ZPEs) as well as thermal corrections and entropy effects using the standard statistical-mechanics relationships for an ideal gas.

The atomic partial charges were estimated with the natural bond orbital (NBO)^[22] method using NBO 7.0.^[46] The topological quantum theory of atoms in molecules (QTAIM),^[24] and Laplacian of the electron density analyses were carried out with AIMAll.^[47] The calculations were performed at the B3LYP-D3(BJ)/def2-TZVP level of theory.

The nature of the chemical bonds were investigated by means of the Energy Decomposition Analysis (EDA) method, which was developed by Morokuma^[48] and by Ziegler and Rauk.^[49] The bonding analysis focuses on the instantaneous interaction energy ΔE_{int} of a bond A–B between two fragments A and B in the particular electronic reference state and in the frozen geometry AB. This energy is divided into four main components (Eq 1).

$$\Delta E_{\text{int}} = \Delta E_{\text{elst}} + \Delta E_{\text{Pauli}} + \Delta E_{\text{orb}} + \Delta E_{\text{disp}} \quad (1)$$

The term ΔE_{elst} corresponds to the classical electrostatic interaction between the unperturbed charge distributions of the prepared atoms (or fragments) and it is usually attractive. The Pauli repulsion ΔE_{Pauli} is the energy change associated with the transformation from the superposition of the unperturbed wave functions (Slater determinant of the Kohn-Sham orbitals) of the isolated fragments to the wave function $\Psi^0 = N\hat{A}[\Psi_A\Psi_B]$, which properly obeys the Pauli principle through explicit antisymmetrization (\hat{A} operator) and renormalization ($N = \text{constant}$) of the product wave function. It comprises the destabilizing interactions between electrons of the same spin on either fragment. The orbital interaction ΔE_{orb} accounts for charge transfer and polarization effects.^[50] In the case that the Grimme dispersion corrections^[41–42] are computed the term ΔE_{disp} is added to equation 1. Further details on the EDA method can be found in the literature.^[51] In the case of the dimers, relaxation of the fragments to their equilibrium geometries at the electronic ground state is termed ΔE_{prep} because it may be considered as preparation energy for chemical bonding. The addition of ΔE_{prep} to the intrinsic interaction energy ΔE_{int} gives the total energy ΔE , which is, by definition, the opposite sign of the bond dissociation energy D_e :

$$\Delta E(-D_e) = \Delta E_{\text{int}} + \Delta E_{\text{prep}} \quad (2)$$

The EDA–NOCV method combines the EDA with the natural orbitals for chemical valence (NOCV) to decompose the orbital interaction term ΔE_{orb} into pairwise contributions. The NOCVs Ψ_i are defined as the eigenvector of the valence operator, \hat{V} , given by Equation (3).

$$\hat{V}\Psi_i = \nu_i\Psi_i \quad (3)$$

In the EDA–NOCV scheme the orbital interaction term, ΔE_{orb} , is given by Equation (4),

$$\Delta E_{\text{orb}} = \sum_k \Delta E_k = \sum_{k=1}^{N/2} \nu_k [-F_{-k,k}^{\text{TS}} + -F_{k,k}^{\text{TS}}] \quad (4)$$

in which $F_{-k,-k}^{\text{TS}}$ and $F_{k,k}^{\text{TS}}$ are diagonal transition state Kohn–Sham matrix elements corresponding to NOCVs with the eigenvalues $-\nu_k$ and ν_k , respectively. The ΔE_k^{orb} term for a particular type of bond is assigned by visual inspection of the shape of the deformation density $\Delta\rho_k$. The latter term is a measure of the size of the charge deformation and it provides a visual notion of the charge flow that is associated with the pairwise orbital interaction. The EDA–NOCV scheme thus provides both qualitative and quantitative information about the strength of orbital interactions in chemical bonds. The EDA–NOCV calculations were carried out with ADF2019. The basis sets for all elements have triple- ζ quality augmented by two sets of polarizations functions and one set of diffuse function. Core electrons were treated by the frozen-core approximation. This level of theory is denoted BP86-D3(BJ)/TZ2P.^[52] Scalar relativistic effects have been incorporated by applying the zeroth-order regular approximation (ZORA).^[53]

Deposition Numbers 2182156 (for **1**), 2182157 (for **2**), 2182158 (for **3**), 2182159 (for **4**), 2182160 (for **5**), 2182162 (for **6**), 2182163 (for **7**), 2182165 (for **8**) contain the supplementary crystallographic data for this paper. These data are provided free of charge by the joint Cambridge Crystallographic Data Centre and Fachinformationszentrum Karlsruhe Access Structures service www.ccdc.cam.ac.uk/structures.

Acknowledgements

We thank ERC StG (EU805113) and University of Saarland for financial support. DMA thanks Prof. Dr. Scheschkewitz for his kind support. Instrumentation and technical assistance for this work were provided by the Service Center X-ray Diffraction, with financial support from Saarland University and German Science Foundation (project number INST 256/506-1). Open Access funding enabled and organized by Projekt DEAL.

Conflict of Interest

The authors declare no conflict of interest.

Data Availability Statement

The data that support the findings of this study are available in the supplementary material of this article.

Keywords: Carbene · Chemical bonding · Donor-Acceptor · Lewis base · Theoretical calculations

- [1] a) F. Dimroth, *Phys. Status Solidi C* **2006**, *3*, 373–379; b) A. M. Glass, *Science* **1987**, *235*, 1003–1009.
[2] a) A. H. Cowley, R. A. Jones, *Angew. Chem. Int. Ed. Engl.* **1989**, *28*, 1208–1215; b) D. A. Neumayer, A. H. Cowley, A. Decken, R. A. Jones, V. Lakhotia, J. G. Ekerdt, *J. Am. Chem. Soc.* **1995**, *117*, 5893–5894; c) F. Maury, *Adv. Mater.* **1991**, *3*, 542–548; d) R. L. Wells, W. L. Gladfelter, *J. Cluster Sci.* **1997**, *8*, 217–238.

- [3] S. Schulz, in *Advances in Organometallic Chemistry, Vol 49, Vol. 49* (Eds.: R. West, A. F. Hill), **2003**, pp. 225–317.
- [4] a) R. T. Paine, H. Noth, *Chem. Rev.* **1995**, *95*, 343–379; b) F. A. Cotton, A. H. Cowley, X. J. Feng, *J. Am. Chem. Soc.* **1998**, *120*, 1795–1799; c) R. J. Wright, A. D. Phillips, T. L. Allen, W. H. Fink, P. P. Power, *J. Am. Chem. Soc.* **2003**, *125*, 1694–1695; d) G. He, O. Shynkaruk, M. W. Lui, E. Rivard, *Chem. Rev.* **2014**, *114*, 7815–7880; e) F. Dankert, C. Hering-Junghans, *Chem. Commun.* **2022**, *58*, 1242–1262; f) M. Fischer, S. Nees, T. Kupfer, J. T. Goettel, H. Braunschweig, C. Hering-Junghans, *J. Am. Chem. Soc.* **2021**, *143*, 4106–4111; g) S. Nees, F. Fantuzzi, T. Wellnitz, M. Fischer, J. E. Siewert, J. T. Goettel, A. Hofmann, M. Harterich, H. Braunschweig, C. Hering-Junghans, *Angew. Chem. Int. Ed.* **2021**, *60*, 24318–24325.
- [5] a) P. P. Power, *Chem. Rev.* **1999**, *99*, 3463–3504; b) R. C. Fischer, P. P. Power, *Chem. Rev.* **2010**, *110*, 3877–3923; c) P. P. Power, *Acc. Chem. Res.* **2011**, *44*, 627–637.
- [6] E. Rivard, *Dalton Trans.* **2014**, *43*, 8577–8586.
- [7] W. Haider, M. D. Calvin-Brown, I.-A. Bischoff, V. Huch, B. Morgenstern, C. Müller, T. Sergeieva, D. M. Andrada, A. Schäfer, *Inorg. Chem.* **2022**, *61*, 1672–1684.
- [8] a) F. Thomas, S. Schulz, M. Nieger, *Eur. J. Inorg. Chem.* **2001**, 161–166; b) A. Kuczowski, F. Thomas, S. Schulz, M. Nieger, *Organometallics* **2000**, *19*, 5758–5762; c) S. Schulz, M. Nieger, *Organometallics* **2000**, *19*, 2640–2642.
- [9] F. Thomas, S. Schulz, M. Nieger, K. Nättinen, *Chem. Eur. J.* **2002**, *8*, 1915–1924.
- [10] a) M. Balmer, M. Kapitein, C. von Hänisch, *Dalton Trans.* **2017**, *46*, 7074–7081; b) M. Kapitein, M. Balmer, L. Niemeier, C. von Hänisch, *Dalton Trans.* **2016**, *45*, 6275–6281; c) M. Kapitein, M. Balmer, C. von Hänisch, *Z. Anorg. Allg. Chem.* **2016**, *642*, 1275–1281; d) M. Kapitein, M. Balmer, C. von Hänisch, *Phosphorus Sulfur Silicon Relat. Elem.* **2016**, *191*, 641–644; e) M. Kapitein, C. von Hänisch, *Eur. J. Inorg. Chem.* **2015**, 837–844.
- [11] U. Vogel, A. Y. Timoshkin, M. Scheer, *Angew. Chem. Int. Ed.* **2001**, *40*, 4409–4412; *Angew. Chem.* **2001**, *113*, 4541–4544.
- [12] a) M. Bodensteiner, A. Y. Timoshkin, E. V. Peresypkina, U. Vogel, M. Scheer, *Chem. Eur. J.* **2013**, *19*, 957–963; b) M. Bodensteiner, U. Vogel, A. Y. Timoshkin, M. Scheer, *Angew. Chem. Int. Ed.* **2009**, *48*, 4629–4633; *Angew. Chem.* **2009**, *121*, 4700–4704; c) U. Vogel, P. Hoemensch, K. C. Schwan, A. Y. Timoshkin, M. Scheer, *Chem. Eur. J.* **2003**, *9*, 515–519; d) U. Vogel, A. Y. Timoshkin, K. C. Schwan, M. Bodensteiner, M. Scheer, *J. Organomet. Chem.* **2006**, *691*, 4556–4564; e) M. A. K. Weinhart, A. S. Lisovenko, A. Y. Timoshkin, M. Scheer, *Angew. Chem. Int. Ed.* **2020**, *59*, 5541–5545; *Angew. Chem.* **2020**, *132*, 5586–5590; f) M. A. K. Weinhart, M. Seidl, A. Y. Timoshkin, M. Scheer, *Angew. Chem. Int. Ed.* **2021**, *60*, 3806–3811; *Angew. Chem.* **2021**, *133*, 3850–3855; g) E. Leiner, M. Scheer, *Organometallics* **2002**, *21*, 4448–4453; h) U. Vogel, K. C. Schwan, M. Scheer, *Eur. J. Inorg. Chem.* **2004**, 2062–2065.
- [13] a) M. L. Cole, S. K. Furfari, M. Kloth, *J. Organomet. Chem.* **2009**, *694*, 2934–2940; b) S. G. Alexander, M. L. Cole, S. K. Furfari, M. Kloth, *Dalton Trans.* **2009**, 2909–2911; c) A. Hock, L. Werner, C. Luz, U. Radius, *Dalton Trans.* **2020**, *49*, 11108–11119.
- [14] a) V. Nesterov, D. Reiter, P. Bag, P. Frisch, R. Holzner, A. Porzelt, S. Inoue, *Chem. Rev.* **2018**, *118*, 9678–9842; b) M. M. D. Roy, A. A. Omaña, A. S. S. Wilson, M. S. Hill, S. Aldridge, E. Rivard, *Chem. Rev.* **2021**, *121*, 12784–12965.
- [15] A. K. Swarnakar, M. J. Ferguson, R. McDonald, E. Rivard, *Dalton Trans.* **2017**, *46*, 1406–1412.
- [16] a) T. Agou, S. Ikeda, T. Sasamori, N. Tokitoh, *Eur. J. Inorg. Chem.* **2018**, *2018*, 1984–1987; b) T. Agou, S. Ikeda, T. Sasamori, N. Tokitoh, *Eur. J. Inorg. Chem.* **2016**, 623–627.
- [17] X. Bantreil, S. P. Nolan, *Nat. Protoc.* **2011**, *6*, 69–77.
- [18] P. L. Baxter, A. J. Downs, D. W. H. Rankin, *J. Chem. Soc. Dalton Trans.* **1984**, 1755–1758.
- [19] M. D. Francis, D. E. Hibbs, M. B. Hursthouse, C. Jones, N. A. Smithies, *J. Chem. Soc. Dalton Trans.* **1998**, 3249–3254.
- [20] P. Pyykko, *J. Chem. Phys. A* **2015**, *119*, 2326–2337.
- [21] L. L. Zhao, M. von Hopfgarten, D. M. Andrada, G. Frenking, *WIREs Comput. Mol. Sci.* **2018**, *8*, e13450.
- [22] a) A. E. Reed, R. B. Weinstock, F. Weinhold, *J. Chem. Phys.* **1985**, *83*, 735–746; b) A. E. Reed, L. A. Curtiss, F. Weinhold, *Chem. Rev.* **1988**, *88*, 899–926.
- [23] J. Emsley, *The elements*, Clarendon Press; Oxford University Press, Oxford; New York, **1998**.
- [24] R. F. W. Bader, *Atoms in Molecules: A Quantum Theory*, Clarendon, Oxford, **1990**.
- [25] S. Dutta, S. M. De, S. Bose, E. Mahal, D. Koley, *Eur. J. Inorg. Chem.* **2020**, 638–655.
- [26] a) W. Haider, D. M. Andrada, I.-A. Bischoff, V. Huch, A. Schäfer, *Dalton Trans.* **2019**, *48*, 14953–14957; b) T. Yang, D. M. Andrada, G. Frenking, *Mol. Phys.* **2019**, *117*, 1306–1314; c) D. M. Andrada, C. Foroutan-Nejad, *Phys. Chem. Chem. Phys.* **2020**, *22*, 22459–22464.
- [27] J. Poater, D. M. Andrada, M. Solà, C. Foroutan-Nejad, *Phys. Chem. Chem. Phys.* **2022**, *24*, 2344–2348.
- [28] P. Erdmann, L. Greb, *Angew. Chem. Int. Ed.* **2022**, *61*, e202114550.
- [29] M. Blum, J. Kappler, S. H. Schlindwein, M. Nieger, D. Gudat, *Dalton Trans.* **2018**, *47*, 112–119.
- [30] a) N. Takagi, G. Frenking, *Theor. Chem. Acc.* **2011**, *129*, 615–623; b) N. Takagi, T. Shimizu, G. Frenking, *Chem. Eur. J.* **2009**, *15*, 8593–8604; c) N. Takagi, T. Shimizu, G. Frenking, *Chem. Eur. J.* **2009**, *15*, 3448–3456; d) N. Takagi, R. Tonner, G. Frenking, *Chem. Eur. J.* **2012**, *18*, 1772–1780; e) S. Klein, R. Tonner, G. Frenking, *Chem. Eur. J.* **2010**, *16*, 10160–10170.
- [31] G. B. de Jong, N. Ortega, M. Lutz, K. Lammertsma, J. C. Slootweg, *Chem. Eur. J.* **2020**, *26*, 15944–15952.
- [32] M. M. D. Roy, E. Rivard, *Acc. Chem. Res.* **2017**, *50*, 2017–2025.
- [33] E. Buncel, I. H. Um, *Tetrahedron* **2004**, *60*, 7801–7825.
- [34] G. R. Fulmer, A. J. M. Miller, N. H. Sherden, H. E. Gottlieb, A. Nudelman, B. M. Stoltz, J. E. Bercaw, K. I. Goldberg, *Organometallics* **2010**, *29*, 2176–2179.
- [35] a) G. M. Sheldrick, *Acta Crystallogr. Sect. A* **2008**, *64*, 112–122; b) G. M. Sheldrick, *Acta Crystallogr. Sect. C* **2015**, *71*, 3–8.
- [36] P. W. Clark, *Org. Prep. Proced. Int.* **1979**, *11*, 103–106.
- [37] N. Marion, E. C. Escudero-Adán, J. Benet-Buchholz, E. D. Stevens, L. Fensterbank, M. Malacria, S. P. Nolan, *Organometallics* **2007**, *26*, 3256–3259.
- [38] A. Hock, L. Werner, C. Luz, U. Radius, *Dalton Trans.* **2020**, *49*, 11108–11119.
- [39] M. J. Frisch, G. W. Trucks, H. B. Schlegel, G. E. Scuseria, M. A. Robb, J. R. Cheeseman, G. Scalmani, V. Barone, G. A. Petersson, H. Nakatsuji, X. Li, M. Caricato, A. V. Marenich, J. Bloino, B. G. Janesko, R. Gomperts, B. Mennucci, H. P. Hratchian, J. V. Ortiz, A. F. Izmaylov, J. L. Sonnenberg, D. Williams-Young, F. Ding, F. Lipparini, F. Egidi, J. Goings, B. Peng, A. Petrone, T. Henderson, D. Ranasinghe, V. G. Zakrzewski, J. Gao, N. Rega, G. Zheng, W. Liang, M. Hada, M. Ehara, K. Toyota, R. Fukuda, J. Hasegawa, M. Ishida, T. Nakajima, Y. Honda, O. Kitao, H. Nakai, T. Vreven, K. Throssell, J. J. A. Montgomery, J. E. Peralta, F. Ogliaro, M. J. Bearpark, J. J. Heyd, E. N. Brothers, K. N. Kudin, V. N. Staroverov, T. A. Keith, R. Kobayashi, J. Normand, K. Raghavachari, A. P. Rendell, J. C. Burant, S. S. Iyengar, J. Tomasi, M. Cossi, J. M. Millam, M. Klene, C. Adamo, R. Cammi, J. W. Ochterski, R. L. Martin, K. Morokuma, O. Farkas, J. B. Foresman, D. J. Fox, Gaussian 16, Revision C.01. Gaussian, Inc., Wallingford CT, **2019**.
- [40] a) A. D. Becke, *J. Chem. Phys.* **1993**, *98*, 5648–5652; b) C. Lee, W. Yang, R. G. Parr, *Phys. Rev. B* **1988**, *37*, 785–789.
- [41] S. Grimme, J. Antony, S. Ehrlich, H. Krieg, *J. Chem. Phys.* **2010**, 132.
- [42] S. Grimme, S. Ehrlich, L. Goerigk, *J. Comb. Chem.* **2011**, *32*, 1456–1465.
- [43] F. Weigend, R. Ahlrichs, *Phys. Chem. Chem. Phys.* **2005**, *7*, 3297–3305.
- [44] C. Y. Peng, P. Y. Ayala, H. B. Schlegel, M. J. Frisch, *J. Comb. Chem.* **1996**, *17*, 49–56.
- [45] J. W. McIver, A. Komornic, *J. Am. Chem. Soc.* **1972**, *94*, 2625–2633.
- [46] E. D. Glendening, C. R. Landis, F. Weinhold, *J. Comb. Chem.* **2019**, *40*, 2234–2241.
- [47] T. A. Keith, T. K. Gristmill, 19.02.13 ed., Overland Park KS, USA (aim.tkgristmill.com), **2019**.
- [48] K. Morokuma, *J. Chem. Phys.* **1971**, *55*, 1236–1244.
- [49] a) T. Ziegler, A. Rauk, *Inorg. Chem.* **1979**, *18*, 1558–1565; b) T. Ziegler, A. Rauk, *Inorg. Chem.* **1979**, *18*, 1755–1759.
- [50] F. M. Bickelhaupt, N. M. M. Nibbering, E. M. Van Wezenbeek, E. J. Baerends, *J. Phys. Chem.* **1992**, *96*, 4864–4873.
- [51] a) F. M. Bickelhaupt, E. J. Baerends, in *Reviews in Computational Chemistry, Vol. 15* (Eds.: K. B. Lipkowitz, D. B. Boyd), **2000**, pp. 1–86; b) G. te Velde, F. M. Bickelhaupt, E. J. Baerends, C. Fonseca Guerra, S. J. A. van Gisbergen, J. G. Snijders, T. Ziegler, *J. Comb. Chem.* **2001**, *22*, 931–967.
- [52] J. Krijn, E. J. Baerends, *Fit Functions in the HFS-Method* **1984**.
- [53] E. Van Lenthe, E. J. Baerends, J. G. Snijders, *J. Chem. Phys.* **1993**, *99*, 4597–4610.

Manuscript received: July 26, 2022
Revised manuscript received: August 29, 2022
Accepted manuscript online: August 30, 2022

- [18] S. Brand, H. Elsen, J. Langer, W. A. Donaubauer, F. Hampel, S. Harder, *Angew. Chem. Int. Ed.* **2018**, *57*, 14169–14173; *Angew. Chem.* **2018**, *130*, 14365–14369.
- [19] T. X. Gentner, B. Rösch, G. Ballmann, J. Langer, H. Elsen, S. Harder, *Angew. Chem. Int. Ed.* **2019**, *58*, 607–611; *Angew. Chem.* **2019**, *131*, 617–621.
- [20] D. Dhara, F. Fantuzzi, M. Härterich, R. D. Dewhurst, I. Kruppenacher, M. Arrowsmith, C. Prancevicius, H. Braunschweig, *Chem. Sci.* **2022**, *13*, 9693–9700.
- [21] N. J. Roberts, E. R. Johnson, S. S. Chitnis, *Organometallics* **2022**, *41*, 2180–2187.
- [22] a) K. M. Marcenko, J. A. Zurakowski, K. L. Bamford, J. W. M. MacMillan, S. S. Chitnis, *Angew. Chem. Int. Ed.* **2019**, *58*, 18096–18101; *Angew. Chem.* **2019**, *131*, 18264–18269; b) K. M. Marcenko, S. S. Chitnis, *Chem. Commun.* **2020**, *56*, 8015–8018; c) A. Koner, T. Sergeieva, B. Morgenstern, D. M. Andrada, *Inorg. Chem.* **2021**, *60*, 14202–14211.
- [23] Deposition numbers 2193647 (for 2), 2193648 (for 3), 2193649 (for 4), and 2193650 (for 5) contain the supplementary crystallographic data for this paper. These data are provided free of charge by the joint Cambridge Crystallographic Data Centre and Fachinformationszentrum Karlsruhe Access Structures service.
- [24] P. Pyykko, *J. Chem. Phys. A* **2015**, *119*, 2326–2337.
- [25] P. Federmann, T. Bosse, S. Wolff, B. Cula, C. Herwig, C. Limberg, *Chem. Commun.* **2022**, *58*, 13451–13454.
- [26] a) P. P. Power, *Chem. Rev.* **2003**, *103*, 789–810; b) J. Moilanen, P. P. Power, H. M. Tuononen, *Inorg. Chem.* **2010**, *49*, 10992–11000.
- [27] W. Uhl, A. Vester, W. Kaim, J. Poppe, *J. Organomet. Chem.* **1993**, *454*, 9–13.
- [28] W. Kaim, *J. Am. Chem. Soc.* **1984**, *106*, 1712–1716.
- [29] J. R. M. Giles, B. P. Roberts, *J. Chem. Soc. Chem. Commun.* **1981**, 1167–1168.
- [30] M. Nakamoto, T. Yamasaki, A. Sekiguchi, *J. Am. Chem. Soc.* **2005**, *127*, 6954–6955.
- [31] N. Wiberg, T. Blank, W. Kaim, B. Schwederski, G. Linti, *Eur. J. Inorg. Chem.* **2000**, 1475–1481.

Manuscript received: November 22, 2022

Accepted manuscript online: January 3, 2023

Version of record online: February 17, 2023

3.2. Synthesis of Group 13 Complexes and their Reactions

In chapter 3.1., synthesis of NHC- and CAAC-stabilized phosphanylgallanes were described and their potential as precursors to form compounds with multiple bonds between group 13 and 15 elements was discussed. It was observed that weak C_{car}-Ga bonds in these phosphanylgallanes made the isolation of Ga=P challenging. Therefore, possible alternative routes were to be explored to achieve the desired multiple bonds.

In this section, the synthesis of low-valent gallium and aluminum (I) compounds, which were proven to be excellent starting materials for the isolation of E¹³-E¹⁵ multiple bonds, are described.^[122] A carbazole-based ligand system and a bis(silylamido)naphthalene derivative were used for the preparation of low-valent gallium and aluminum species, respectively. Additionally, their reactivity profile such as small molecular activation and coordination to transition metals is discussed.

3.2.1. Synthesis of Gallium (I) Compound and its Reactions

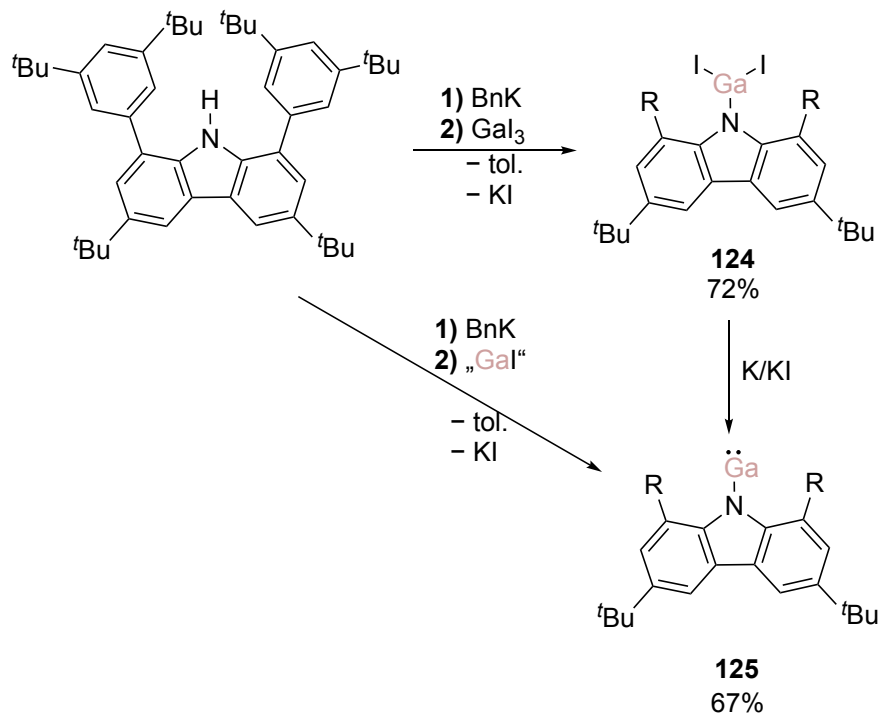
The 1,8-bis(3,5-*di-tert*-butylphenyl)-3,6-*di-tert*-butylcarbazole (L) was prepared as a supporting ligand and its deprotonation with benzyl potassium afforded the potassium salt of the ligand.^[92] L-K was subsequently reacted with GaI₃ to afford **124** as a yellow solid in 72% yield (Scheme 42) and its molecular structure was unambiguously characterized by single-crystal XRD analysis (Figure 5).

The molecular structure of **124** exhibits a tricoordinate Ga1 atom which is slightly pyramidalized ($\Sigma < = 357.3^\circ$) and a short contact to one of the *ortho*-carbons of the flanking substituent (2.856(5) Å) to passivate the Lewis acidity, similarly to the situation of the aluminum analogue.^[46] Consequently, the coordination of Ga1 atom to the anchoring N1 atom is not directly in the plane of the carbazole moiety but slightly shifted with the dihedral angle of 34° between the two planes. Additionally, the Ga1-N1 bond length is 1.874(3) Å, which is shorter than typical Ga-N single bond lengths (1.95 Å).^[7]

In order to prepare the corresponding gallylene species **125**, several reduction conditions including KC₈, K/KI and {(Dip)NacNac}Mg₂^[97] were performed. Among these conditions, the reduction with K/KI in benzene led to full conversion. However, the ¹H NMR spectrum reveals free gallylene **125** together with the free potassium carbazolide ligand in the mixture. The spectroscopically obtained yield was lower (51%) than the route described above.

An alternative route was followed to isolate the mono-coordinated gallylene by using “Gal” as gallium source.^[86] Gallium metal was sonicated with I₂ in toluene to prepare “Gal” *in-situ*, which was then treated with potassium carbazolide ligand, L-K to afford **125** in 67% yield. Compound **125** is soluble in solvents such as toluene and benzene; but in THF, slow decomposition into

free ligand was observed over time. The formation of a uniform product was confirmed by ^1H NMR spectroscopy. The ^1H NMR resonances of the *tert*-butyl groups were found at 1.52 for the carbazole moiety and at 1.20 ppm for the ones on phenyl groups in the spectrum obtained in C_6D_6 .



Scheme 42. Synthesis of gallylene **125**. R=2,6-*di-tert*-butylphenyl.

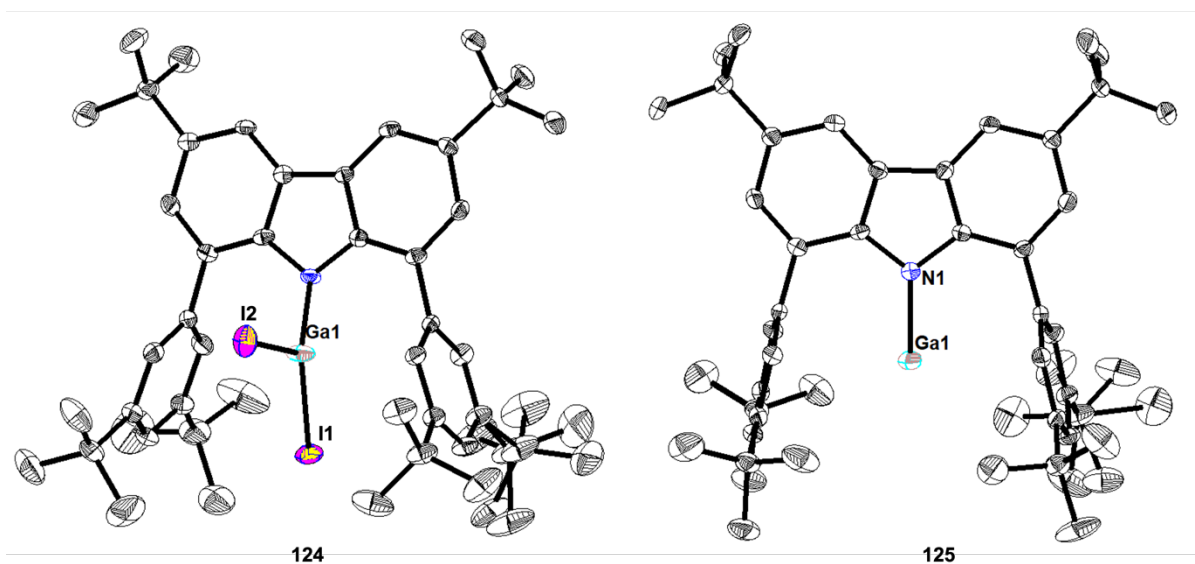


Figure 5. Solid state structures of compound **124** (left) and **125** (right). Thermal ellipsoids set to 50% probability. Selected experimental and theoretical [B3LYP-D3(BJ)/def2-TZVP] bond lengths [Å] and angles [deg]: **124**: N1-Ga1: 1.875(3) [1.90], Ga1-I1: 2.4540(6) [2.492], Ga1-I2: 2.4936(9) [2.535], N1-

Ga1-I2: 110.5(1) [113.1], I1-Ga1-I2: 122.38(2) [116.8], N1-Ga1-I1: 124.5(1) [130]. **125**: N1-Ga1: 2.010(2) [2.06]. Hydrogen atoms are omitted for clarity.

Single crystals of **125** suitable for XRD were obtained from its concentrated diethyl ether solution at room temperature overnight (Figure 5). The molecule shows a mono-coordinated gallium atom. The molecule has a C_{2v} symmetry with the gallium atom placed between the two flanking 3,5-*di-tert*-butylphenyl rings and within the plane of the carbazolyl moiety. The bond length for N-Ga bond is 2.010(2) Å, which is elongated compared to the expected Ga-N single bond (1.95 Å). This is shorter than carbazole ligand supported gallylene **75** reported by Tan (2.091(8) Å)^[102] and (Nacnac)Ga **44** (R=Me) reported by Power (2.053(1) and 2.056(1) Å).^[82]

We analyzed the electronic structure of **125** within the DFT framework at the B3LYP-D3(BJ)/def2-SVP level of theory. The equilibrium geometry is in very good agreement with the structure determined by SC-XRD, although the Ga-N distance is slightly longer than the one observed experimentally. The KS-frontier molecular orbitals of **125** (Figure 6) consist of HOMO-2 which involves the non-bonding lone pair whereas HOMO is distributed on the π -system of the ligand. LUMO and LUMO+6 consist of vacant in-plane and out-of-plane p-orbitals of the gallium atom. In addition, NBO analysis show that gallium carries a positive charge (+0.60 a.u.) whereas the nitrogen atom of the ligand is negatively charged (-0.74 a.u.). Wiberg bond index (WBI) of the Ga-N bond is 0.27 which is comparable with the Jones' four-membered gallylene, whereas significantly lower than the carbazol-supported Ga(I) compounds reported by Tan group.^[102]

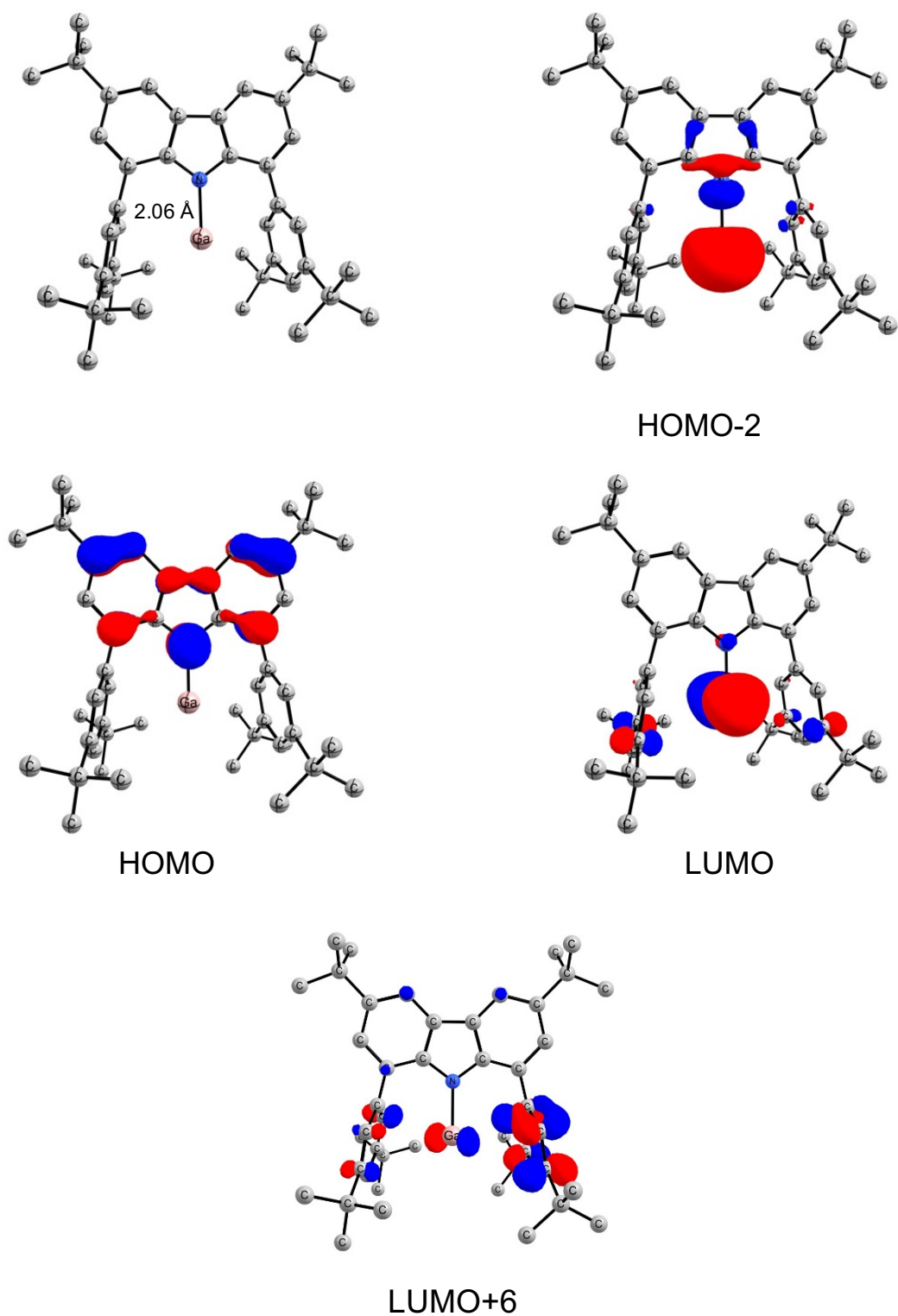
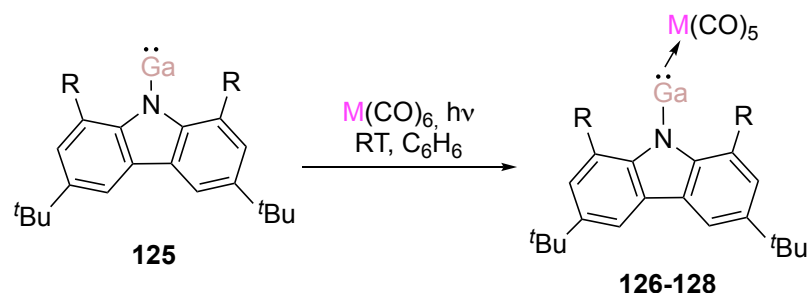


Figure 6. KS-Molecular orbitals (isocontour value = 0.05 a.u.) of compound **125** at the B3LYP-D3(BJ)/def2-SVP level of theory. Hydrogen atoms are omitted for clarity.

Coordination properties of **125** with a series of transition metal complexes of group 6 was explored (Scheme 43). The metal complexes were added to a benzene solution of **125**. Upon irradiation, CO was released, and the reaction mixtures turned to an intense yellow color.

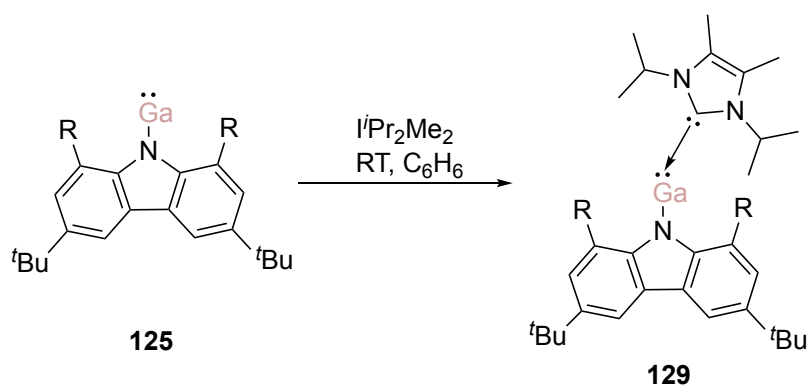
Corresponding metal carbonyl complexes **126**, **127** and **128** were isolated as yellow solids in moderate yields (34-74%).



Scheme 43. Synthesis of the compounds **126-128** in C₆H₆. R= 2,6-*di-tert*-butylphenyl; **126**: M=Cr; **127**: M=Mo; **128**: M=W.

The crystals were grown from saturated benzene solutions at room temperature. The molecular structure of **128** is shown in Figure 7 and important bond lengths and angles are given in Table 2. Ga-M (M= W, Mo) bond lengths are comparable for the complexes **127** and **128** (**127**: 2.5243(2) Å, **128**: 2.5165(3) Å), whereas the Ga-Cr (2.3744(4) Å) bond is significantly shorter than the former two. The N1-Ga1-M1 bond angles (W: 161.22(7)°, Cr: 154.17(5)°, Mo: 152.72(3)°) deviate more from linearity in the order of W, Cr and Mo. Furthermore, N1-Ga bond lengths are similar in all compounds and in accordance with the Ga-N single bonds. In addition, IR spectra of the metal complexes show strong absorption for CO stretching frequencies at 1923 (M=Cr), 1930 (M=W), and 1937 (M=Mo) cm⁻¹, and are comparable with previously reported transition-metal complexes Cp*GaCr(CO)₅ (1918 cm⁻¹), Cp*GaFe(CO)₅ (1966 cm⁻¹), and (tmp)GaCr(CO)₅ (1924 cm⁻¹).^[144,145]

The combination of **125** with ⁱPr^{Me}NHC in benzene at room temperature resulted in the formation of compound **129** (Scheme 44). The product was collected as a yellow solid in 70% yield. In the ¹H NMR spectrum of **129**, the signals for the methyl groups of ⁱPr^{Me}NHC appear at 1.40 and 1.29 ppm whereas an ⁱPr-CH septet signal was observed at 3.89 ppm. These chemical shifts are slightly shifted downfield compared to free ⁱPr^{Me}NHC.^[5]



Scheme 44. Synthesis of **129** in C₆H₆. R=2,6-*di-tert*-butylphenyl.

Crystals suitable for XRD analysis were grown from a saturated benzene solution. The molecular structure of **129** is given in Figure 7. The bond lengths of N1-Ga1 and Ga1-C25 are 2.066(2) and 2.270(3), respectively. N1-Ga1 is elongated in comparison to **125** (Ga1-N1: 2.010(2) Å).^[98] Additionally, the HOMO-LUMO gap (**125**: 3.84 eV, **129**: 3.69 eV) slightly decreases, which can be explained with the changes in electronic structure upon coordination of NHC to the gallium center. HOMO of **129** consists of σ -lone pair of gallium whereas LUMO has contributions from both π and π^* orbitals over gallium and $i\text{Pr}^{\text{Me}}\text{NHC}$. Additionally, through NBO analysis, natural charges of the gallium and the nitrogen atom of the ligand were found. Gallium carries more positive charge in **125** (**129**: Ga1: 0.17, N1: -0.21; **125**: Ga: 0.28, N1: -0.21). NBO analysis of **129** provide Wiberg bond indices (WBIs) of Ga1-N1 (**129**: 0.28, **125**: 0.30).

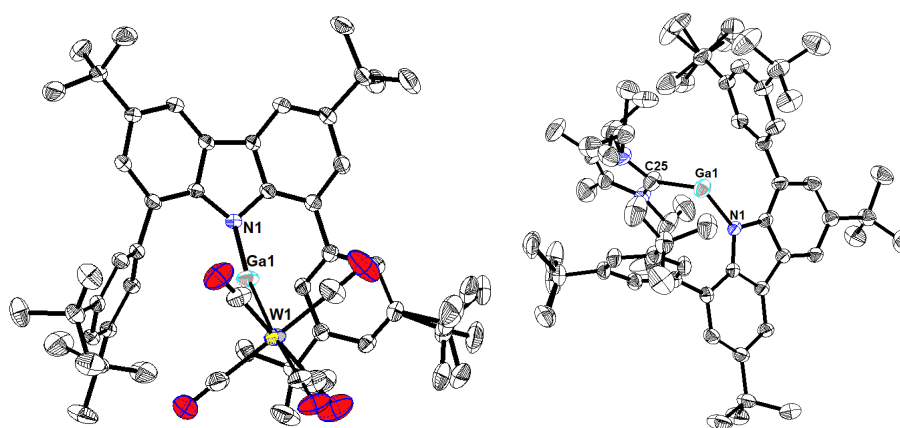


Figure 7. Molecular structures of **128** and **129**. Ellipsoids set at 50% probability level. Hydrogen atoms are omitted for clarity.

Table 2. Selected experimental bond lengths (Å) and angles (°) of gallylene-M(CO)₅ complexes **126-128** and gallylene-NHC complex **129** (calculated values in parenthesis, B3LYP-D3(BJ)/def2-SVP).

	N1-Ga1	Ga1-M/Ga-C _{car}	N1-Ga1-M1
126 (M = Cr)	1.895(2) (1.93)	2.3744(4) (2.42)	154.17(5) (153.3)
127 (M= Mo)	1.894(1) (1.93)	2.5243(3) (2.57)	152.72(3) (153.2)
128 (M=W)	1.880(2) (1.93)	2.5165(3) (2.59)	161.22(7) (153.4)
129 (M-C_{car})	2.066(2) (2.12)	2.270(3) (2.36)	95.05(9) (94.0)

In Table 2, experimentally determined and calculated bond lengths and angles are given. As frequently observed for DFT functionals, the computed bond lengths are slightly longer than the experimental ones. On the other hand, M-Ga bond lengths are much shorter than expected for a single bond based on the covalent radii (W-Ga: 2.65 Å; Cr-Ga: 2.70 Å; Mo-Ga: 2.75 Å).

We analyzed the electronic structures of **126-129** by Natural Bonding Orbital (NBO) analysis. Table 3 shows the calculated natural atomic partial charges (Q) and Wiberg bond orders of the Ga-M (M= W, Cr, Mo) and Ga-N bonds calculated at the B3LYP-D3(BJ)/def2-TZVPP level of theory on the optimized geometries. The lone pair (LP) at gallium has an s-character of larger than 95% (W: 95.34%; Cr: 97.11%; Mo: 96.12%). Natural population analyses NPA indicate that the positive charge at the Ga atom increases in the order of W, Mo and Cr (Table 2). The charge at the metal carbonyl moiety (M(CO)₅) shows no significant differences on electron density donated, i.e. about -0.50 e. Notably, the WBI between the gallium and the metal atom is slightly higher for **128** (0.50 au) than for **126** and **127** (0.48 au), which was not expected from the comparison of experimental bond lengths (Table 2) and is yet another manifestation of the widely recognized fact that bond lengths are an unreliable indicator for bond strength.^[146] The WBI values of the M-CO bonds indicate that CO ligand in *trans*-position to the LGa moiety is bonded more weakly than the CO ligands in the *cis*-position.

Table 3. Calculated NBO charge distribution at B3LYP-D3(BJ)/def2-TZVPP.

M	WBI (M-Ga)	WBI (Ga-N1)	Q(M(CO) ₅)	Q(Ga)	Q(M)
126 (M=Cr)	0.48	0.30	-0.58	1.21	-1.74
127 (M=Mo)	0.48	0.30	-0.50	1.17	-1.27
128 (M=W)	0.50	0.32	-0.51	1.13	-1.02

We also analyzed the electron density distribution in **126-129** with Bader's quantum theory on atoms in molecules (QTAIM) at the B3LYP-D3(BJ)/def2-TZVPP level of theory. The Laplacian distribution $\nabla^2\rho(r)$ in the N1-Ga1-M1 plane is shown in Figure 8 for compounds **128** and **129**. The Laplacian plot shows an electron accumulation at the nitrogen atom. A similar observation was made for the remaining series of the compounds. The Laplacian distribution of Ga-M suggest a covalent character with the electron density of the bond critical point ($\rho^{\text{BCP}}=0.36-0.53 \text{ e}/\text{\AA}^3$), whereas $\text{C}_{\text{car}}\text{-Ga}$ shows rather ionic contributions. Similar observation was made for Ga-N bonds in **126-129**, where the Ga-N bond in **129** exhibits a more ionic character.

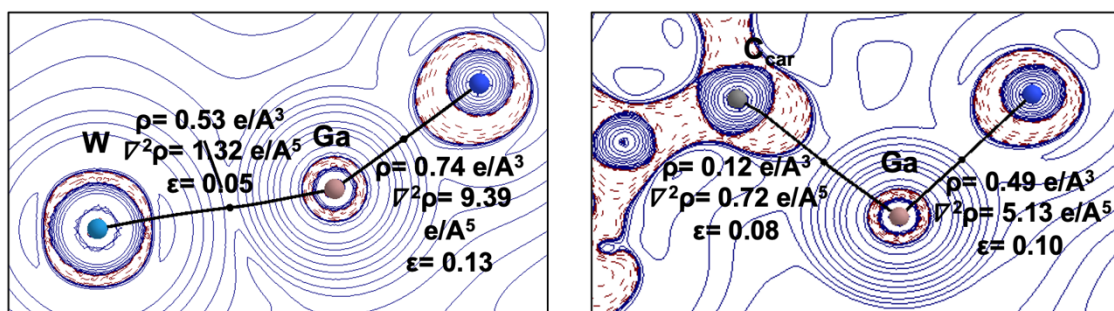


Figure 8. 2D Laplacian distribution $\nabla^2\rho$ in the N-Ga-M and N-Ga-C_{car} plane. Dashed red lines indicate areas of charge concentration ($\nabla^2\rho < 0$) while solid blue lines show areas of charge depletion ($\nabla^2\rho > 0$), bond paths (black lines), and bcps (black dots).

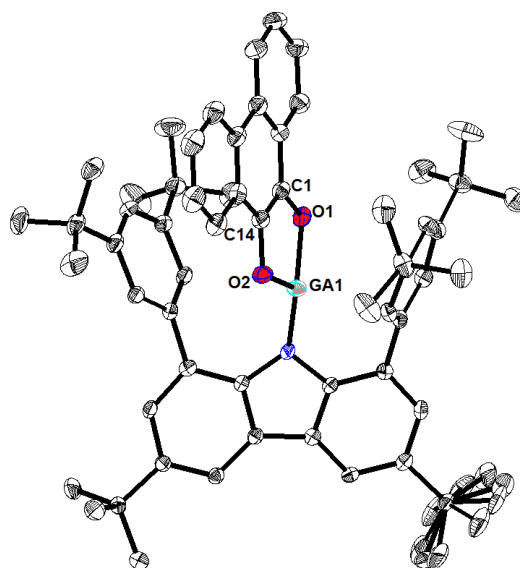
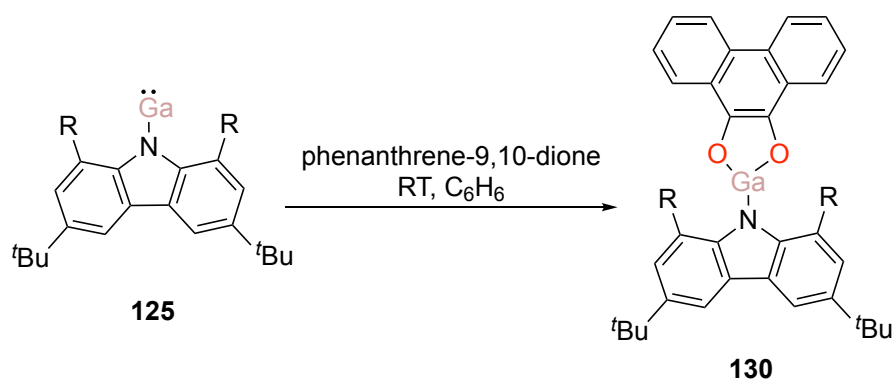
To examine the strength of the Ga-M bonds in series of compounds **141-144**, we performed an Energy Decomposition Analysis (EDA).^[147,148] EDA has proven to be a useful tool to assess the nature of the chemical bond in main group compounds and transition metal compounds. Within the EDA scheme, the interaction energy (ΔE_{int}) between two (or more) structurally and electronically unrelaxed fragments of a molecule is divided into four physical meaningful terms, namely, Pauli repulsion (ΔE_{Pauli}), electrostatic interaction (ΔE_{elst}), orbital interaction (ΔE_{orb}), and dispersion interaction (ΔE_{disp}). The dissociation energy (D_e) is related to the interaction energy by the preparation energy (ΔE_{prep}), which is the energy needed to promote the fragments from their equilibrium geometry to the geometry and electronic state in the compounds. The addition of ΔE_{prep} to the interaction energy (ΔE_{int}) gives the total energy ($-D_e$), which is the opposite sign of the dissociation energy.^[149]

Table 4. EDA-NOCV results of the M-Ga and Ga-C_{car} bonds in compounds **126-129** at B3LYP-D3(BJ)/TZ2P. All values are in kcal·mol⁻¹. The value in parentheses gives the percentage contribution to the total attractive interactions $\Delta E_{\text{elst}} + \Delta E_{\text{orb}} + \Delta E_{\text{disp}}$.

	126 (M = Cr)	127 (M = Mo)	128 (M = W)	129 (NHC)
ΔE_{int}	-55.0	-54.3	-60.6	-42.0
ΔE_{Pauli}	95.6	90.1	97.8	127.1
ΔE_{elst}	-67.2 (45%)	-66.5 (46%)	-75.1 (47%)	-79.7 (47%)
ΔE_{orb}	-56.7 (38%)	-49.6 (34%)	-54.0 (34%)	-52.2 (31%)
ΔE_{disp}	-26.6 (18%)	-28.3 (20%)	-29.2 (19%)	-37.1 (22%)
ΔE_{prep}	6.5	6.3	7.1	5.7
$-D_e$	-48.5	-48.1	-53.5	-36.3

Table 4 summarizes the numerical results of EDA calculations performed for fragmentation of Ga-M. The dissociation energy is higher for the Ga-M bond in **128** than **126** and **127**. The interaction energy, ΔE_{int} follow the trend as $W > Cr > Mo$, which indicates stronger interaction in the order of W, Cr and Mo. The distribution of the ΔE_{int} shows that the electrostatic interaction terms, ΔE_{elst} , are larger than orbital interactions, ΔE_{orb} , which indicates that the interaction is governed by electrostatic interactions. It is important to note that ΔE_{Pauli} is the largest for the tungsten complex **128**.

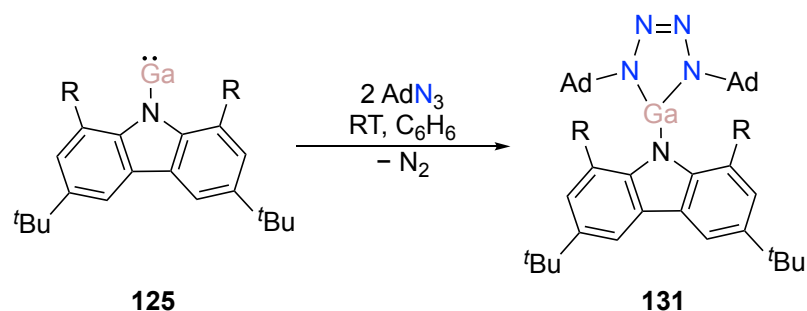
It is well-established that metallocenes are highly reactive towards unsaturated substrates.^[98,102,150,151] Compound **130** was reacted with α - β unsaturated phenanthrene-9,10-dione in toluene at room temperature (Scheme 45). The reaction indeed led to formation of gallacycle **130**. Suitable crystals for XRD analysis were grown from a saturated toluene solution. Ga1-N3 (1.839(2) Å) shortened significantly in comparison to **125** while O1-Ga1 (1.8491(19) Å) and O2-Ga2 (1.830(2) Å) bond lengths elongated upon coordination to the gallium. Ga-O bonds lengths are in between typical single and double Ga-O bonds. These bond lengths are quite comparable with the ones in [ONO]Al(*o*-O₂C₆Cl₄)(py) (Al-O: 1.900(1)-1.922(2) Å, Al-N: 2.038(2) Å) and [ONO]Al(*o*-O₂C₁₆H₈)(py) (Al-O: 1.866(2)-1.864(2) Å, Al-N: 1.966(2) Å). C1-C14 (1.360(4) Å) bond length shortens as expected upon formation of **130**.^[152] The heterocycle is sandwiched between the aryl groups of the carbazole ligand.



Scheme 45. Reaction of gallylene **130** with phenanthrene-9,10-dione (above) and the molecular structure of **130** (below). Ellipsoids set at 50% probability level. Hydrogen atoms are omitted for clarity. R= 2,6-*di-tert*-butylphenyl.

In summary, a Ga (I) monocoordinate compound was synthesized via two routes. Its reactivity towards metal carbonyls and the Lewis base, ⁱPrMeNHC, demonstrated its ambiphilic nature. Additionally, it underwent cycloaddition reaction with phenanthrene-9,10-dione.

L-Ga **125** was reacted with azides to investigate whether carbazole-based ligand system provide enough stability to isolate [Ga=N] bonds. **125** was initially reacted with commercially available AdN₃ in a 1:1 molar ratio in benzene at room temperature. Upon the addition of the azide, gas evolution was observed suggesting the elimination of molecular dinitrogen. ¹H NMR showed about 50% unreacted gallylene in the reaction mixture. Upon addition of one more equivalent of AdN₃, complete conversion to [L-Ga(N₄Ad₂)] **131** was confirmed by ¹H NMR spectroscopy (Scheme 46).



Scheme 46. Synthesis of **131**. R= 2,6-di-*tert*-butylphenyl.

^1H NMR spectra of compound **131** obtained in C_6D_6 show that the *tert*-butyl groups of the carbazole ligand appear as sharp singlets at 1.33 and 1.29 ppm while the adamantyl groups appear as broad signals, probably due to hindered rotation (Figure 9).

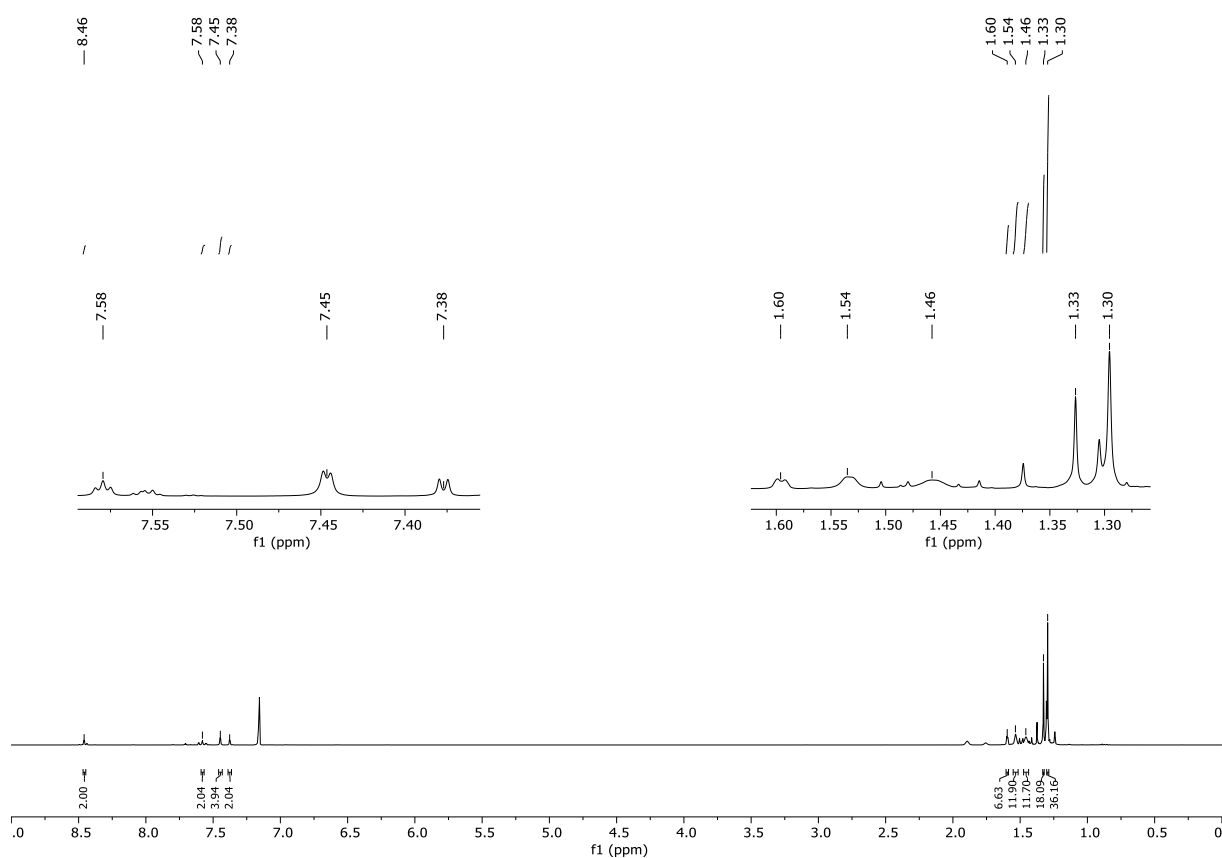


Figure 9. ^1H NMR spectra of **131** in C_6D_6 .

Crystals suitable for XRD analysis were grown from a saturated benzene solution of **131** at room temperature (Figure 10). Ga1-N1 bond length was determined to 1.852(1), which is much shorter than in L-Ga. N2-N5 (1.375(2) $^\circ$) and N3-N4 (1.377(2) $^\circ$) bond lengths are comparable to each other and longer than the N4-N5 bond length (1.274(2) $^\circ$). All N-N bond distances in the ring are in between Ga-N single and double bonds which suggests electron delocalization across the four nitrogen atoms. Additionally, the structural parameters are comparable with the previously reported tetrazagallole; however, Ga-N bond lengths are

shorter in **131** (1.826(1), 1.835(1), 1.852(1) Å) than in tetrazagallole **76** (1.845(2), 1.836(2), 1.832(2) Å).^[102]

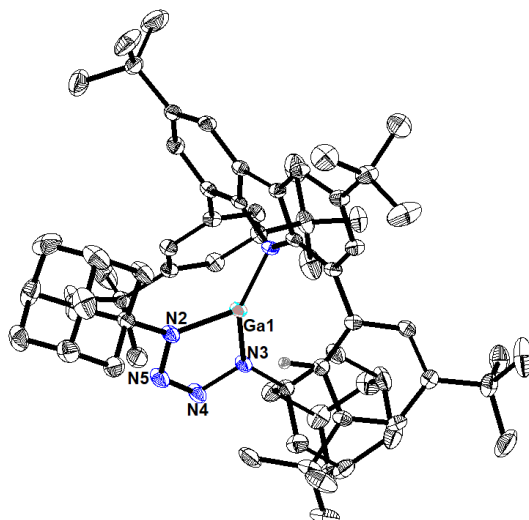
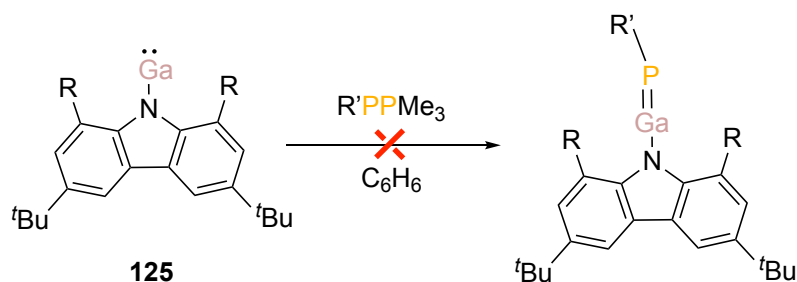


Figure 10. Thermal ellipsoid plots (50%) of (L-GaN₄Ad₂) **131**. Hydrogen atoms are omitted for the clarity. Selected bond lengths (Å) and angles (°): Ga-N1: 1.852(1), Ga1-N2:1.835(1), Ga-N3: 1.816 (1), N2-N5: 1.375 (2), N3-N4: 1.377(2), N4-N5: 1.274(2).

The synthesis of Ga=P containing compounds was attempted by the following similar route.[†] Previously, the Hering-Junghans group successfully isolated a stable compound with Ga=P bond by reacting Cp*Ga with phosphanylenephosphoranes, ^{Ar}TerP(PMe₃) (Ar= Dip, Tip). Upon irradiation, PMe₃ was released and formation of phosphanylgallenes ^{Ar}TerP=GaCp* (Ter= Dip, Ter) observed.^[111] Phosphanylenephosphoranes RPPMe₃ (R= ^{Mes}Ter, ^{Dip}Ter, Mes*)^[153] were reacted with L-Ga **125** in benzene and the solutions were irradiated at 435 nm. No reaction was observed for ^{Mes}TerPPMe₃ and ^{Mes}*PPMe₃ while decomposition to free ligand L-H was observed from the reaction with ^{Dip}TerPPMe₃. In addition, the solutions were heated at 80 °C, however, only unreacted starting materials were found in ¹H NMR.



Scheme 47. Attempts to synthesize Ga=P. R= 2,6-*di-tert*-butylphenyl, R'= Mes*, ^{Dip}Ter, ^{Mes}Ter.

[†] In cooperation with the group of PD. Dr. Hering-Junghans

3.2.2. Evidence of Al^{II} Radical Addition to Benzene

- Dr. Debdeep Mandal, T. Ilgin Demirer, Dr. Tetiana Sergeieva, Dr. Bernd Morgenstern, Haakon T. A. Wiedemann, Prof. Dr. Christopher W. M. Kay, Dr. Diego M. Andrada, Evidence of Al^{II} Radical Addition to Benzene. *Angew. Chem. Int. Ed.* **2023**.
<https://doi.org/10.1002/anie.202217184>

The above cited article was published by Wiley-VCH GmbH as an „Open Access“ article and is licensed under a “Creative Commons Attribution 4.0 International” License. (<https://creativecommons.org/licenses/by/4.0/>)

The results described within this article are additionally concluded and put into context in the next chapter (7).

Contributions of the Authors:

Dr. Debdeep Mandal: Lead: Conceptualization, Visualization, Writing – Review and Editing, Investigation, Methodology, Data Curation, Synthesis.

T. Ilgin Demirer: Lead: Characterization of the aluminum species, Investigation, Formal Analysis.

Dr. Tetiana Sergeieva: Lead: Theoretical Studies.

Dr. Bernd Morgenstern: Lead: X-ray analysis.

Haakon T. A. Wiedemann: Lead: EPR studies.

Prof. Dr. Christopher W. M. Kay: Lead: Project administration, supervision, acquisition of funding and resources; Supporting: Writing – Review and Editing.

Diego M. Andrada: Lead: Project administration, supervision, acquisition of funding and resources; Supporting: Writing – Review and Editing.

Evidence of Al^{II} Radical Addition to Benzene

Debdeep Mandal, T. Ilgin Demirer, Tetiana Sergeieva, Bernd Morgenstern, Haakon T. A. Wiedemann, Christopher W. M. Kay,* and Diego M. Andrada*

Abstract: Electrophilic Al^{III} species have long dominated the aluminum reactivity towards arenes. Recently, nucleophilic low-valent Al^I aluminyl anions have showcased oxidative additions towards arenes C–C and/or C–H bonds. Herein, we communicate compelling evidence of an Al^{II} radical addition reaction to the benzene ring. The electron reduction of a ligand stabilized precursor with KC₈ in benzene furnishes a double addition to the benzene ring instead of a C–H bond activation, producing the corresponding cyclohexa-1,3(ori,4)-dienes as Birch-type reduction product. X-ray crystallographic analysis, EPR spectroscopy, and DFT results suggest this reactivity proceeds through a stable Al^{II} radical intermediate, whose stability is a consequence of a rigid scaffold in combination with strong steric protection.

various catalytic cycles involving bond activation processes.^[3]

The first Al^I species was reported more than thirty years ago by Schnöckel in the form of a tetrameric species (**I**), which upon thermal conditions, dissociates into its monomeric units.^[4] The isolation of the pure monomeric form has been accomplished by increasing the steric demand AlCp^R (Cp^R = C₅H₂/Bu₃).^[5] Ten years later, the first monomeric neutral Al^I compound (**II**) was isolated and characterized by Roesky.^[6] The bulky β-diketiminato (NacNac) supporting ligand was the key to providing enough electronic and steric protection to the aluminum center. Over the years, this compound has evolved from a lab curiosity into a valuable reagent, given its ability to participate in various bond activations via oxidative addition.^[7] In 2018, the groups of Aldridge and Goicoechea expanded the scope by synthesizing the anionic Al^I nucleophilic species, aluminyl anions (**III**), which demonstrate unprecedented reactivity in the oxidative addition on non-polarized C–H and C–C bonds of aromatic hydrocarbons (Scheme 1). Since then, several amido- and alkyl-substituted aluminyl compounds have been prepared and their reactivity has been explored.^[8] Recently, examples of neutral mono-coordinated aluminyls Al^I compounds **IV–V** have been reported by Liu, Hinz, and Power taking advantage of sterically demanding carbazolyl and terphenyl ligands respectively.^[9]

The exotic reactivity of aluminyl anions is currently in the spotlight for the activation of small molecules. Notably, the reaction outcome sharply depends on the nature of the counter cation and its coordination nature with the anionic moiety.^[10] The extent of the interaction between the cation and the flanking aryl substituents plays a crucial role in the formation of aluminyl species.^[8c,f,11] In this vein, we envisage that bulky silyl groups, instead of aromatic groups, may provide sufficient kinetic stability to isolate Al^{II} radical species, preventing ionic interactions in favor of aluminyl anions. Compared to Al^I, dicoordinated Al^{II} radicals are even rarer. This is partially due to the inherent instability of mononuclear neutral Al^{II}/Al^I radical species, which prefers to dimerize forming Al–Al single bonded compounds, **VI–IX**.^[8h,k,12] Thus, a suitable ligand that not only stabilizes the elusive Al^{II} radical but also destabilize dimer form is indispensable for the successful isolation of aluminum radical species. To date, only a few examples **X–XI**^[13] are known for neutral monomeric aluminum radicals, using cyclic(alkyl)(amino)carbene (CAAC) as stabilization units of the radical centers.

Herein, we report on the unusual *trans* 1,4-addition of two aluminum(II) species to a benzene furnishing a 1,4-

Introduction

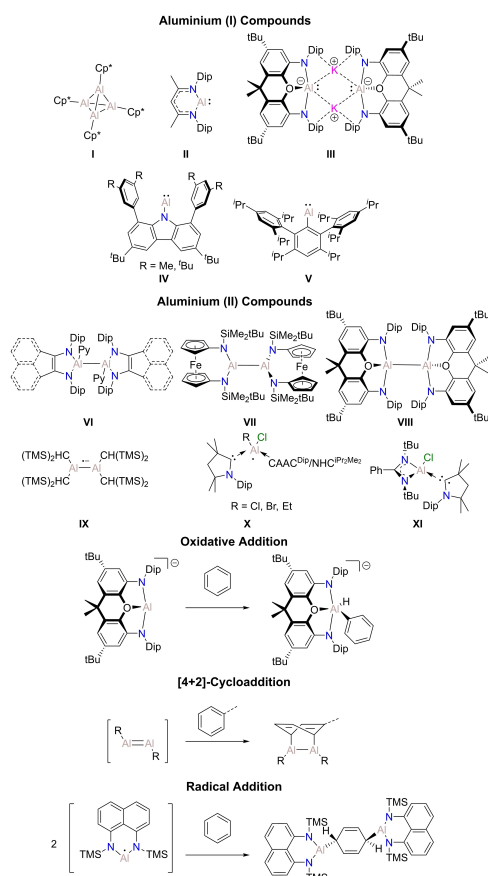
The preference of aluminum to adopt its oxidation state Al^{III} has been extensively exploited in the design of trivalent species as Lewis acid catalysts in various organic transformations.^[1] In contrast, and despite significant progress in the field, low oxidation states such as Al^{II} and Al^I are still considered exotic, and their applications are considerably less numerous.^[2] Efforts in this area have been driven by their proven potential to replace transition metals in

[*] Dr. D. Mandal, T. I. Demirer, Dr. T. Sergeieva, Dr. B. Morgenstern, Dr. D. M. Andrada
 General and Inorganic Chemistry Department, University of Saarland
 Campus C4.1, 66123 Saarbrücken (Germany)
 E-mail: diego.andrada@uni-saarland.de

H. T. A. Wiedemann, Prof. Dr. C. W. M. Kay
 Physical Chemistry Department, University of Saarland
 Campus B2.2, 66123 Saarbrücken (Germany)
 E-mail: christopher.kay@uni-saarland.de

Prof. Dr. C. W. M. Kay
 London Centre for Nanotechnology, University College London
 17-19 Gordon Street, London WC1H 0AH (UK)

© 2023 The Authors. Angewandte Chemie International Edition published by Wiley-VCH GmbH. This is an open access article under the terms of the Creative Commons Attribution License, which permits use, distribution and reproduction in any medium, provided the original work is properly cited.



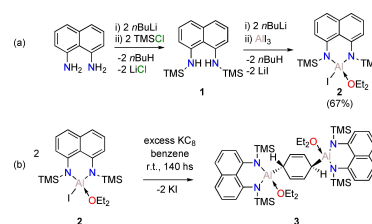
Scheme 1. Selected structures of Al^{I} and Al^{II} compounds. Oxidative addition, [4+2]-cycloaddition, and radical addition. R: $\text{Ar}^{\text{R}} = 2,6\text{-Dip}_2\text{C}_6\text{H}_3$, $\text{Ar}^{\text{R}^*} = 2,6\text{-Dip}_2\text{-}4\text{-TMS-C}_6\text{H}_2$, $\text{Bbp} = 2,6\text{-[CH-(TMS)}_2\text{]}_2\text{C}_6\text{H}_3$, $\text{Tbp} = 2,6\text{-[CH-(TMS)}_2\text{]}_2\text{-}4\text{-tBu-C}_6\text{H}_2$, $\text{Dip} = 2,6\text{-[iPr]}_2\text{C}_6\text{H}_3$, $\text{TMS} = \text{Trimethylsilyl}$.

cyclohexadiene system as a Birch-type reduction reaction product (Scheme 1). The Birch reduction of aromatic compounds is well-established in organic chemistry to produce *cis* and/or *trans* 1,4-disubstituted-cyclohexadienes as hydro, alkyl or silyl derivatives.^[14] The groups of Power and Tokitoh have described a *cis* 1,4-addition to toluene and benzene via [4+2]-cycloaddition of a transient dialuminene compound,^[15] which has been later stabilized as a dianion^[16] or by coordination to Lewis bases.^[17] The group of Harder has shown that the combination of the nucleophilic Al^{I} compound (II) with the highly Lewis acidic $(\text{NacNac})\text{Ca}^+$ analogue reduces benzene.^[18] Notably, the isolobal Mg compound can also undergo a Birch-type benzene reduction, when the dimerization of the intermediate Mg^{I} radical is

prevented by a super bulky spectator ligand ($(\text{HC}[\text{C}(\text{Me})\text{N}-[2,6\text{-}(3\text{-pentyl})\text{-phenyl}]]_2)_2$) and a coordinating species, TME-DA (N,N,N',N' -tetramethylethylenediamine).^[19] In the course of the development of this work, the group of Braunschweig reported a similar outcome, in which the aluminum center is coordinated to an *N*-heterocyclic carbene (NHC) and stabilized by a redox-active ferrocenyl substituent.^[20] Although it was not possible to isolate or characterize a radical addition to arenes, the authors proposed a plausible radical-based mechanism. We now provide compelling evidence of an in situ generated diamino-substituted Al^{I} radical as a key reactive species for such Birch-type reduction of aromatic molecule.

Results and Discussion

Bis(silylamido)naphthalene derivatives have been recently established as attractive ligands given their unexpectedly high degree of thermodynamic and kinetic stability.^[21] This framework provides a characteristic interplay between steric repulsion and dispersive attraction, allowing the isolation of exotic chemical bonds.^[22] Thus, the *N*-trimethylsilyl substituted diamino naphthyl amine has been chosen as the supporting ligand for synthesizing the aluminum precursor. Compound **2** was prepared in 67% yield from a salt metathesis reaction of the respective dithiated ligand with AlI_3 (Scheme 2a). The molecular structure of compound **2** exhibits a tetra-coordinated aluminum atom located out of the naphthalene plane (Figure 1).^[23] The diethylether molecule coordinates to the acidic aluminum center with a bond length of 1.884(4) Å, which is in the range of an $\text{Al}-\text{O}$ single bond (1.89 Å).^[24] This structure is reminiscent to the aluminum iodide stabilized by xanthene ligand (precursor of compound **III**), but the rigid structure carries a longer $\text{Al}-\text{O}$ bond length (1.967(2) Å).^[8a] The $\text{Al}-\text{N}$ bond lengths are 1.797(5) and 1.803(5) Å, fall in between the typical $\text{Al}-\text{N}$ single and double bonds (1.97 and 1.73 Å, respectively),^[24] indicative of a weak $\text{N} \pi$ -donation. The nitrogen atoms are planar ($\Sigma_4 = 359.5^\circ$), underlining that the location of the aluminum is a consequence of the relatively small bonding pocket of the ligand, i.e. 2.06 Å compared to the xanthene scaffold 4.55 Å in **III**.^[25] Note that precursor **III** analogue has longer $\text{Al}-\text{N}$ bond lengths (1.847(2) Å).^[8a]



Scheme 2. (a) Synthesis of **1** and **2**. (b) Reduction of **2** with excess of K_8 .

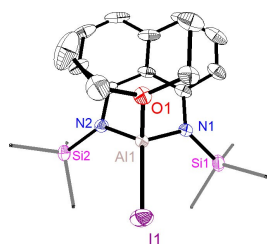


Figure 1. Molecular structure of **2** in the solid state as determined by X-ray crystallography. Thermal ellipsoids set at 50% probability. Hydrogen atoms were omitted for clarity. Selected experimental bond lengths (Å) and bond angles (°): Al1–N1 1.797(5), Al1–N2 1.803(5), Al1–O1 1.884(4), Al1–I1 2.520(2), N1–Si1 1.739(5), N2–Si2 1.742(5), N2–Al1–N1 103.7(2), N1–Al1–I1 118.2(2), N2–Al1–I1 124.0(2).

In order to prepare the corresponding reduced species (Al^{II} radical or aluminyl Al^I anion), we attempted various reducing conditions. The reduction of **2** with conventional reducing agents like metallic Mg, K(mirror), or KC₈ in ethereal solvents (THF, diethyl ether) afforded either an unidentified mixture or decomposition products. Also, reduction of compound **2** with equimolar Jones Mg^I reagent or cobaltocene (Co(Cp)₂) led to no reaction in benzene solution. While reducing **2** with one equivalent of KC₈ led to incomplete reduction even after several days, stirring a reaction mixture containing compound **2** with an excess of KC₈ (2 equivalents) at room temperature in benzene for 140 hs gave rise to complete conversion (Scheme 2a). The initially expected formation of an aluminyl anion or dialumane species could rapidly be ruled out based on the NMR spectra indicating the occurrence of six new protons symmetrically distributed. In ¹H NMR, alongside the expected trimethylsilyl groups (δ (H)=0.44 ppm (s)) and the coordinated diethyl ether (δ (H)=3.79 (sept) and 0.40 ppm(t)), two distinctive singlets at 5.89 (4H) and 2.37 (2H) ppm were observed. In confirmation of the ¹H NMR data, the ¹³C NMR spectrum shows two new signals at chemical shifts of 124.6 and 29.9 ppm. These NMR spectroscopic data compare favorably with the reported quinoid type benzene moiety suggesting a Birch-type reduction product of benzene.^[14a,19,20]

After the filtration of the insoluble precipitate from the reaction mixture, an orange solution was obtained. Pale yellow crystals of **3** were grown from concentrated solution after 1 week at 4 °C and the structure was confirmed by X-ray diffraction (Figure 2). As predicted from the ¹H NMR chemical shifts, a benzene molecule reacts with two molecules of reduced intermediate of compound **2**, and the resulting molecule **3** exhibits a C₂ symmetry. While the tetra-coordinated environment around aluminum center from compound **2** is preserved, the bond lengths with the surrounding atoms become longer in **3**, probably because of the steric repulsion with the new C₆H₆ moiety. In this sense, the Al–N bonds to the supporting ligands in **3** (1.8293(8) Å) are longer than in **2**. Also, the coordinating ether molecule

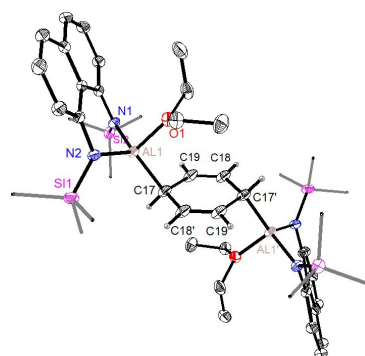


Figure 2. Molecular structure of **3** in the solid state as determined by X-ray crystallography. Thermal ellipsoids set at 50% probability. Nonessential hydrogen atoms were omitted for clarity. Selected experimental and theoretical [TPSSh/def2-SVP] bond lengths (Å) and bond angles (°): Al1–N1 1.8293(8) [1.848], Al1–N2 1.8319(8) [1.850], Al1–O1 1.9151(7) [1.971], Al1–C17 1.9925(9) [2.016], C17–C19 1.503(1) [1.506], C18–C19 1.333(2) [1.349], N1–Al1–N2 101.56(2) [101.7], N1–Al1–C17 121.19(8) [124.4], N1–Al1–C17 124.49(2) [123.0].

has a 1.9151(7) Å bond length, while the distortion degree ($\Sigma_a=347^\circ$) supports a weak interaction ($D_c=29.1$ and 25.6 kcal mol⁻¹ for **2** and **3**, respectively). The bond lengths between the aluminum atom and the carbon atom of the benzene (1.9925(9) Å) in **3** are slightly shorter than the expected Al–C single bond (2.01 Å)^[24] and also than those reported for the Birch reduction by Brand et al. 2.060(3)/2.073(3) Å,^[18] by Dhara et al. 2.064(3)/2.059(3) Å,^[20] and also from the products resulting from the [4+2]-cycloaddition, i.e. 2.000(2)/2.003(2) Å,^[15a] and 2.028(5)/2.020(5) Å.^[15b] As in the case of compound **2**, the Al atom in **3** remains out of the plane of the ligand. Notably, the C18–C19 bond length of 1.333(2) Å is comparable to the double bond (1.34 Å), while the C17–C19 bond length of 1.503(1) indicates a C–C single bond (1.50 Å).

The new adduct **3** is indefinitely stable at ambient temperature in the solid state under argon atmosphere. Notably, the addition of the aluminum units to the benzene ring in the 1,4 fashion leading to the quinoid type of structure through de-aromatization benzene can only be explained by the presence of an *in situ* generated Al^{II} radical species.^[14b] We explored the reaction paths using density functional theory (DFT) at the PCM(benzene)-TPSSh/def2-TZVPP/TPSSh/def2-SVP level of theory (see Supporting Information for further details). Figure 3 shows the computed reaction profiles along with some key optimized structures. The reaction starts with one electron reduction of compound **2**, with the elimination of iodine in the form of KI to generate a new radical species **INT1**, where the ether molecule is coordinated. The corresponding radical anion of **2** is computed as an unstable species which is prone to the elimination of iodine ($\Delta G=-11.4$ kcal mol⁻¹). The strength of the bond between Al and O in **INT1** is significantly reduced, and its release is endergonic by 2.6 kcal mol⁻¹,

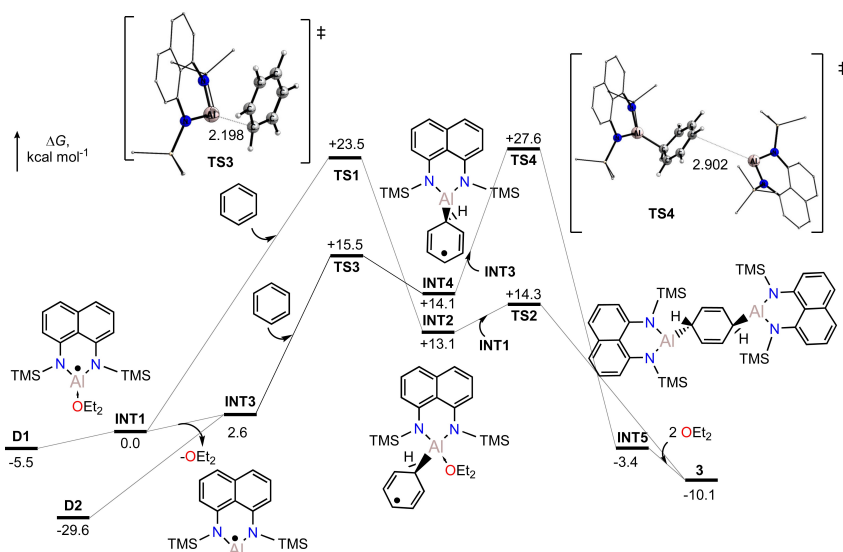


Figure 3. Gibbs free energy (ΔG in kcal mol^{-1}) profile at the PCM(benzene)-TPSSH/def2-TZVPP//TPSSH/def2-SVP level of theory for the reduction of **2** in benzene solvent. Transition state structures are shown, where nonessential hydrogens were omitted for clarity.

forming the radical species **INT3**. Despite not being experimentally isolated, both **INT1** and **INT3** can dimerize to form their respective dialumane **D1** and **D2** since the process is exergonic by 5.5 and 29.6 kcal mol^{-1} , respectively. The monomer and dimer species can exist in equilibrium.^[26] Nonetheless, the probability of meeting a benzene solvent molecule is higher than meeting another **INT1** or **INT3** to dimerize, similar to the situation of a heterobimetallic Ca/Al Birch-reduction.^[18] Thus, the radical addition to a molecule of benzene is the first step of the reaction. While the most stable radical species **INT1** requires 23.5 kcal mol^{-1} , the corresponding addition from **INT3** has lower energy barrier 15.5 kcal mol^{-1} . The energy needed to form the intermediate **INT2** and **INT4** is 13.1 and 14.1 kcal mol^{-1} , respectively. The formed intermediates are thermodynamically unfavored, and they can easily collapse back to **INT1** or **INT3**, as the difference in energy to **TS3** is very small. However, in a high-pressure regime where molecular collisions are efficient enough to cool the otherwise rovibrationally hot intermediates, causing it to be in thermal equilibrium with the environment. To produce the observed product **3**, a second **INT1** or **INT3** must meet **INT2** or **INT4**. The second step of the reaction course is computed to be fast when the ether molecule is coordinated **TS3**, while the **INT4** and **INT3** react via **TS4** with a Gibbs energy of 27.6 kcal mol^{-1} relative to the reactants. The overall thermodynamics of the reaction is favorable by 10.1 kcal mol^{-1} . Potentially, different isomers are possible according to the position and geometry of the second radical addition. Our calculations suggest the

observed *trans*- structure in **3** as the most stable isomer (see Figure S32).

The optimized structure for **3** is in good agreement with the crystal structure (Figure 2). The calculated NPA charge of +2.14 (Al) is in line with previously assigned Al^{III} .^[18] The total charge on the $\text{C}_6\text{H}_6^{2-}$ fragment ($-1.37 e$) is in agreement with its strongly reduced nature. While the C atoms directly attached to the Al atoms bear a ($\text{C17} = -0.89 e$), the vinylic C atoms has only ($\text{C18/C19} = -0.22 e$). The chemical bond Al–C is rather ionic (Figure S33 and Table S5) with a Wiberg bond order of 0.41 au.

It is noteworthy that the experimental conditions and the computational calculations agree on a rather slow reduction process under the given conditions. The rate-determining step is computed as the first step consisting of the radical addition of aluminum species to the benzene molecule with an energy of 15.5 kcal mol^{-1} , and a second step with 13.5 kcal mol^{-1} . Therefore, this result predicts the presence of relatively stable radical species **INT1–4** in solution. In order to prove the radical addition reaction, we recorded the time dependence of the reduction of **2** with continuous wave (cw) EPR spectroscopy at X-band frequencies. For that, dry C_6H_6 was added to the solid mixture of compound **2** and KC_8 (1:2.2 ratio) at room temperature under inert conditions. An aliquot of reaction mixture (supernatant solution) was transferred into a quartz EPR tube at various time intervals. The aliquot was then diluted with dry C_6H_6 , and the EPR spectra were measured. This procedure was repeated over several days. Figure 4a shows

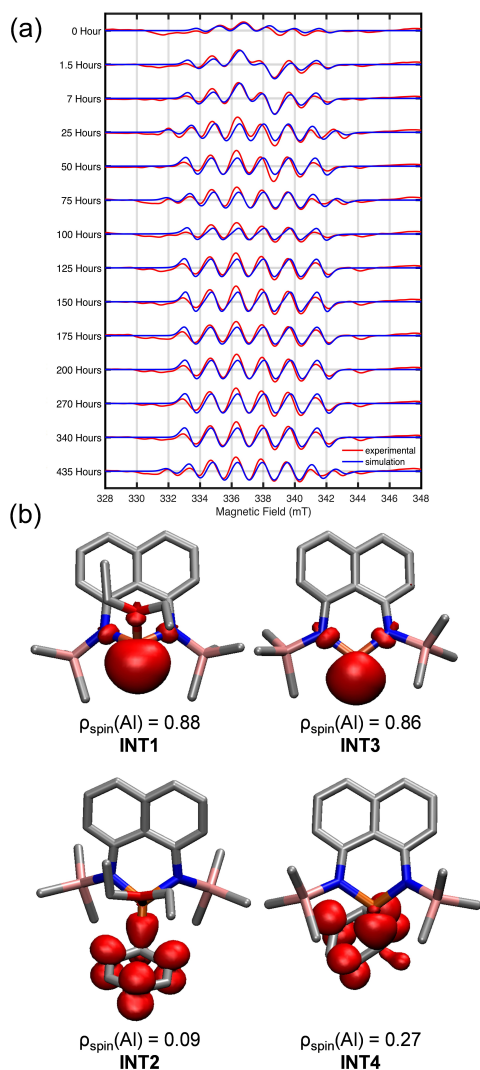


Figure 4. (a) EPR spectra of (1:2) reduction reaction between compound **2** and KC_8 at various time intervals. Simulation parameters: $g_{iso} = 2.0057$, $A_{iso}(^{27}Al) = 1.63$ mT. (b) Spin density (isovalue 0.004 a.u.) and Mulliken spin-density plots of **INT1–4**. H atoms have been omitted for clarity.

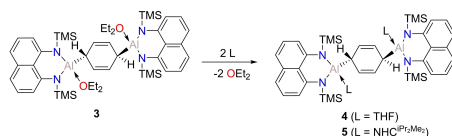
the experimentally obtained EPR spectra together with their simulations.

All EPR spectra are dominated by the sextet that results from the coupling of the unpaired electron with the aluminum center (^{27}Al , 100% natural abundance, $I = 5/2$). At early times, our simulations suggest the presence of two

species with g_{iso} of 2.0057 and 2.0051 and isotropic hyperfine couplings (hfc), $A_{iso}(^{27}Al)$ of 1.63 mT and 1.54 mT, respectively. However, on a longer times scale, the EPR radical formation corresponds mainly to one species (g_{iso} of 2.0057 and $A_{iso}(^{27}Al)$ of 1.63 mT). Note that after 50 hours of reaction a third 11 lines species is detected with g_{iso} of 2.00638 and $A_{iso}(^{27}Al)$ of 1.30/1.26 mT. The magnitude of the hfc in this species is larger than those reported for metal-base spin aluminum radicals such as $[R_2AlAIR_2]^+$ (1.11 mT),^[27] and carbene-stabilized aluminum radicals (0.93–1.25 mT).^[13a,c] In contrast, aluminum radical complexes with ligand-based spin have smaller $A(^{27}Al)$ values (0.13–0.46 mT).^[28] The hfc s of Al centered radicals strongly depend on the s -orbital character via pyramidalization.^[29] For instance, the radical anion $[AlH_3]^+$ displays an isotropic hfc of 15.4 mT with a deviation from planarity of $\Sigma_\alpha = 331.8^\circ$, while the $[Al(SiMetBu_2)_3]^+$ which is more planar $\Sigma_\alpha = 358.4^\circ$ exhibits a hfc of 6.2 mT.^[30] Furthermore, the resulting cyclohexadienyl radical adduct from the $[AlH_3]^+$ addition to benzene affords an $A_{iso}(^{27}Al)$ of 5.4 mT.^[29] The stronger participation of the s -orbital character has also been suggested as responsible for the higher hfc s of $[R_2AlAIR]^+$ ($A_{iso}(^{27}Al)$ of 2.18 and 1.89 mT), compared to the aforementioned $[R_2AlAIR_2]^+$.^[31] Figure 4b shows the calculated spin density of the main radical species **INT1–4**. In general, the calculations indicate the presence of an unpaired electron mainly located at the aluminum atom, with a small contribution of the nitrogen atoms of the supporting ligand (Table S7). EPR calculations provided an estimated hfc of 36.6 mT and 41.8 mT for **INT1** and **INT3**, respectively, in line with the strong s -orbital character of the unpaired electron. On the other hand, the **INT2** and **INT4** display a smaller hfc , namely 7.7 mT and 8.8 mT, respectively. Note, that the predicted hfc s depend on a rather flat potential energy surface. We have also considered the dialanes **D1⁻** and **D2⁻** radical anion species (Table S7). The calculations suggest g_{iso} of 2.00212 and $A_{iso}(^{27}Al)$ of -0.10 mT for **D1⁻** and g_{iso} of 2.00174 and $A_{iso}(^{27}Al)$ of 10.1/9.8 mT **D2⁻**. The EPR signal consisting of 11 lines is probably due to **D2⁻**, which under the reaction conditions dissociates ($\Delta G = -28.0$ kcal mol⁻¹) to give **INT3**. However, given the mismatch between the experimental and theoretical hfc values, the EPR cannot be unambiguously assigned.

The manipulation of adduct **3** in different solvents indicated that the ether molecule can be easily exchanged. Therefore, we envisioned the use of stronger σ -donors such NHC or CAAC for stabilizing the radical species and re-aromatizing the benzene molecule. However, the reaction process led only to a ligand exchange with 1,3-disopropyl-4,5-dimethylimidazol-2-ylidene (NHC^{IPr2Me2}), while CAAC^{DIP} shows no reaction (Scheme 3).

Furthermore, all our attempts to isolate the radical species or activate different aromatic compounds such as toluene, xylene and biphenyl with the in situ generated Al^{II} radical were unsuccessful. In contrast to former benzene reductions,^[15b,18] leaving a C_6D_6 solution of compounds **3**, **4**, or **5** at room temperature does not lead to any detectable decrease of the NMR signals corresponding to the C_6H_6 moiety. This observation holds even after heating for 24 hrs



Scheme 3. Ligand exchange reaction of **3**.

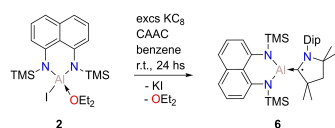
at 60 °C, thus indicating the intermolecular exchange of the C₆H₆ molecule is not possible.

The low reactivity of the intermediates is advantageous for the EPR detection, but the lifetime measurements by other spectroscopic methods like UV/Vis are precluded by the absorption of **2**. Additionally, due to the reaction setup, TEMPO cannot be used as radical scavenger. Instead, to trap or examine the transient radical, we conducted the reduction of **2** with KC₈ in the presence of 1 equiv of CAAC^{Dip} in benzene at room temperature, which afforded a deep yellow solution (Scheme 4). The related product is NMR silent, and unfortunately, despite numerous crystallization attempts no crystals could be obtained. Nonetheless, the formation of **6** was confirmed by Fourier-transform ion cyclotron resonance-mass spectrometry showing a peak at *m/z* 613.38 [Al(cAAC)]⁺ (Figure S25). Although the ether molecule could bind to the Al center, our calculations suggest a very weak coordination energy ($D_e = 11.6 \text{ kcal mol}^{-1}$).

We were also able to monitor the progress of this reaction via EPR spectroscopy. In this case, the EPR spectra show a broad four-line asymmetric signal shape (Figure 5a). The simulations suggest the occurrence of two species. At short reaction time (1.5 hrs), a radical with $g = 2.0033(2)$ and $A(^{14}\text{N}) = 0.48 \text{ mT}$ is the major radical species, probably the CAAC^{Dip} radical anion. A minor component increases with time, with $g = 2.0026(3)$ and $A_{\text{iso}}(^{27}\text{Al}) = 0.47 \text{ mT}$. Our theoretical calculations suggest a *hfc* of **6** of $A_{\text{iso}}(^{27}\text{Al}) = 0.34 \text{ mT}$ (Figure 5b). This result is in good agreement with previous ligand-base radical of aluminum **XI** with a experimental $A_{\text{iso}}(^{27}\text{Al}) = 0.93 \text{ mT}$.^[13c]

Conclusion

In conclusion, we have described a new reaction mode of aluminum(II) species. In great contrast to the well-known Al^{III} and Al^I reactions towards arenes, the designed aluminum complex produces a stable radical intermediate upon



Scheme 4. Reduction of **2** with excess of KC₈ in the presence of CAAC^{Dip}.

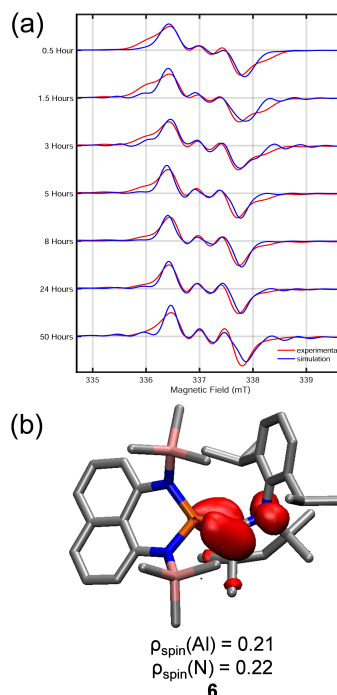


Figure 5. (a) EPR spectra of (1:2) reduction reaction of compound **2** with KC₈ in the presence of CAAC^{Dip} at various time intervals. Simulation parameters, **6**: $g_{\text{iso}} = 2.0026(3)$ (2.00261), $A_{\text{iso}}(^{27}\text{Al}) = 0.47 \text{ mT}$ (0.34 mT), $A_{\text{iso}}(^{14}\text{N}) = 0.48 \text{ mT}$ (0.62 mT); [CAAC^{Dip}]^{•-}: $g_{\text{iso}} = 2.0033(2)$, $A_{\text{iso}}(^{14}\text{N}) = 0.48 \text{ mT}$, $A_{\text{iso}}(^1\text{H}) = 0.21 \text{ mT}$. (b) Spin density (isovalue 0.003 a.u.) and Mulliken spin-density plots of **6**. H atoms have been omitted for clarity.

reduction, leading to a Birch reduction type reaction. This result is a consequence of the rigid scaffold of the supporting ligand in combination with silyl protecting groups. Thus, the absence of protecting aromatic substituent on the neighboring nitrogen atoms probably prevents the formation of an ionic pair between a putative aluminyli anion and counter cations, leaving room for an aluminum radical. Current efforts are directed at the isolation and further spectroscopic characterization of the aluminum radical.

Acknowledgements

The work at University of Saarland has been supported by the ERC StG (EU805113). DM thanks the Alexander von Humboldt Foundation for the postdoctoral fellowship. DMA thanks Prof. Dr. Scheschkewitz for his kind support. All authors gratefully acknowledge the suggestions from M.Sc. S. Danés, M.Sc. E. Sabater, Dr. H.-G. Korth, and Prof. Dr. Simon Aldridge. Instrumentation and technical

assistance for this work were provided by the Service Center Mass Spectrometry and the Service Center X-ray Diffraction, with financial support from Saarland University and the German Science Foundation (project number INST 256/506-1). EPR spectroscopy was performed on spectrometers purchased with support of the State of Saarland and the German Science Foundation (project number INST 256/535-1) Open Access funding enabled and organized by Projekt DEAL.

The authors declare no conflict of interest. Data Availability Statement

The data that support the findings of this study are available in the supplementary material of this article.

Conflict of Interest

The authors declare no conflict of interest.

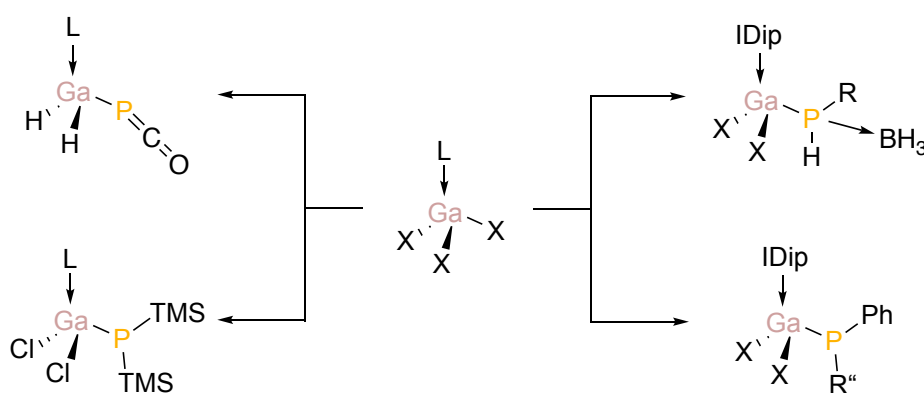
Keywords: Aluminum · EPR Spectroscopy · Low-Valent Compounds · Radicals · Structure Elucidation

- [1] a) T. Krahl, E. Kemnitz, *Catal. Sci. Technol.* **2017**, *7*, 773–796; b) T. Krahl, E. Kemnitz, *J. Fluorine Chem.* **2006**, *127*, 663–678; c) S. Saito, in *Main Group Metals in Organic Synthesis*, Wiley-VCH, Weinheim, **2004**, pp. 189–306; d) G. A. Olah, V. P. Reddy, G. K. S. Prakash, in *Kirk-Othmer Encyclopedia of Chemical Technology*, Wiley, Hoboken, **2000**; e) V. P. Reddy, G. K. S. Prakash, in *Kirk-Othmer Encyclopedia of Chemical Technology*, Wiley, Hoboken, **2000**, pp. 1–49.
- [2] a) P. P. Power, *Nature* **2010**, *463*, 171–177; b) M. Melaimi, R. Jazzar, M. Soleilhavoup, G. Bertrand, *Angew. Chem. Int. Ed.* **2017**, *56*, 10046–10068; *Angew. Chem.* **2017**, *129*, 10180–10203; c) R. L. Melen, *Science* **2019**, *363*, 479–484; d) Y. Su, R. Kinjo, *Chem. Soc. Rev.* **2019**, *48*, 3613–3659; e) C. Weetman, S. Inoue, *ChemCatChem* **2018**, *10*, 4213–4228; f) P. Bellotti, M. Koy, M. N. Hopkinson, F. Glorius, *Nat. Chem. Rev.* **2021**, *5*, 711–725.
- [3] a) C. Weetman, H. Xu, S. Inoue, in *Encyclopedia of Inorganic and Bioinorganic Chemistry*, Wiley, Hoboken, **2011**, pp. 1–20; b) K. Hobson, C. J. Carmalt, C. Bakewell, *Chem. Sci.* **2020**, *11*, 6942–6956.
- [4] a) C. Dohmeier, C. Robl, M. Tacke, H. Schnöckel, *Angew. Chem. Int. Ed. Engl.* **1991**, *30*, 564–565; *Angew. Chem.* **1991**, *103*, 594–595; b) H. Sitzmann, M. F. Lappert, C. Dohmeier, C. Üffing, H. Schnöckel, *J. Organomet. Chem.* **1998**, *561*, 203–208.
- [5] A. Hofmann, T. Tröster, T. Kupfer, H. Braunschweig, *Chem. Sci.* **2019**, *10*, 3421–3428.
- [6] C. Cui, H. W. Roesky, H.-G. Schmidt, M. Noltemeyer, H. Hao, F. Cimpoesu, *Angew. Chem. Int. Ed.* **2000**, *39*, 4274–4276; *Angew. Chem.* **2000**, *112*, 4444–4446.
- [7] Y. Liu, J. Li, X. Ma, Z. Yang, H. W. Roesky, *Coord. Chem. Rev.* **2018**, *374*, 387–415.
- [8] a) J. Hicks, P. Vasko, J. M. Goicoechea, S. Aldridge, *Nature* **2018**, *557*, 92–95; b) M. M. D. Roy, J. Hicks, P. Vasko, A. Heilmann, A.-M. Baston, J. M. Goicoechea, S. Aldridge, *Angew. Chem. Int. Ed.* **2021**, *60*, 22301–22306; *Angew. Chem.* **2021**, *133*, 22475–22480; c) R. J. Schwamm, M. D. Anker, M. P. Coles, *Angew. Chem. Int. Ed.* **2019**, *58*, 1489–1493; *Angew. Chem.* **2019**, *131*, 1503–1507; d) R. J. Schwamm, M. P. Coles, M. S. Hill, M. F. Mahon, C. L. McMullin, N. A. Rajabi, A. S. S. Wilson, *Angew. Chem. Int. Ed.* **2020**, *59*, 3928–3932; *Angew. Chem.* **2020**, *132*, 3956–3960; e) M. J. Evans, M. D. Anker, M. G. Gardiner, C. L. McMullin, M. P. Coles, *Inorg. Chem.* **2021**, *60*, 18423–18431; f) T. X. Gentner, M. J. Evans, A. R. Kennedy, S. E. Neale, C. L. McMullin, M. P. Coles, R. E. Mulvey, *Chem. Commun.* **2022**, *58*, 1390–1393; g) S. Kurumada, S. Takamori, M. Yamashita, *Nat. Chem.* **2020**, *12*, 36–39; h) K. Koshino, R. Kinjo, *J. Am. Chem. Soc.* **2020**, *142*, 9057–9062; i) S. Grams, J. Eysel, J. Langer, C. Färber, S. Harder, *Angew. Chem. Int. Ed.* **2020**, *59*, 15982–15986; *Angew. Chem.* **2020**, *132*, 16116–16120; j) S. Kurumada, K. Sugita, R. Nakano, M. Yamashita, *Angew. Chem. Int. Ed.* **2020**, *59*, 20381–20384; *Angew. Chem.* **2020**, *132*, 20561–20564; k) I. L. Fedushkin, M. V. Moskalev, A. N. Lukoyanov, A. N. Tishkina, E. V. Baranov, G. A. Abakumov, *Chem. Eur. J.* **2012**, *18*, 11264–11276.
- [9] a) J. D. Queen, A. Lehmann, J. C. Fetting, H. M. Tuononen, P. P. Power, *J. Am. Chem. Soc.* **2020**, *142*, 20554–20559; b) X. Zhang, L. L. Liu, *Angew. Chem. Int. Ed.* **2021**, *60*, 27062–27069; *Angew. Chem.* **2021**, *133*, 27268–27275; c) A. Hinz, M. P. Müller, *Chem. Commun.* **2021**, *57*, 12532–12535.
- [10] a) J. Hicks, P. Vasko, J. M. Goicoechea, S. Aldridge, *J. Am. Chem. Soc.* **2019**, *141*, 11000–11003; b) J. Hicks, P. Vasko, J. M. Goicoechea, S. Aldridge, *Angew. Chem. Int. Ed.* **2021**, *60*, 1702–1713; *Angew. Chem.* **2021**, *133*, 1726–1737; c) J. Hicks, P. Vasko, A. Heilmann, J. M. Goicoechea, S. Aldridge, *Angew. Chem. Int. Ed.* **2020**, *59*, 20376–20380; *Angew. Chem.* **2020**, *132*, 20556–20560.
- [11] S. Grams, J. Mai, J. Langer, S. Harder, *Dalton Trans.* **2022**, *51*, 12476–12483.
- [12] a) P. Henke, T. Pankewitz, W. Klopper, F. Breher, H. Schnöckel, *Angew. Chem. Int. Ed.* **2009**, *48*, 8141–8145; *Angew. Chem.* **2009**, *121*, 8285–8290; b) V. A. Dodonov, W. Chen, L. Liu, V. G. Sokolov, E. V. Baranov, A. A. Skatova, Y. Zhao, B. Wu, X.-J. Yang, I. L. Fedushkin, *Inorg. Chem.* **2021**, *60*, 14602–14612; c) Y. Zhao, Y. Liu, L. Yang, J.-G. Yu, S. Li, B. Wu, X.-J. Yang, *Chem. Eur. J.* **2012**, *18*, 6022–6030; d) W. Uhl, *Z. Naturforsch. B* **1988**, *43*, 1113–1118.
- [13] a) B. Li, S. Kundu, A. C. Stückl, H. Zhu, H. Keil, R. Herbst-Irmer, D. Stalke, B. Schwederski, W. Kaim, D. M. Andraga, G. Frenking, H. W. Roesky, *Angew. Chem. Int. Ed.* **2017**, *56*, 397–400; *Angew. Chem.* **2017**, *129*, 407–411; b) S. Kundu, S. Sinhababu, S. Dutta, T. Mondal, D. Koley, B. Ditttrich, B. Schwederski, W. Kaim, A. C. Stückl, H. W. Roesky, *Chem. Commun.* **2017**, *53*, 10516–10519; c) M. M. Siddiqui, S. Banerjee, S. Bose, S. K. Sarkar, S. K. Gupta, J. Kretsch, N. Graw, R. Herbst-Irmer, D. Stalke, S. Dutta, D. Koley, H. W. Roesky, *Inorg. Chem.* **2020**, *59*, 11253–11258; d) B. Li, B. L. Geoghegan, H. M. Weinert, C. Wolper, G. E. Cutsail, S. Schulz, *Chem. Commun.* **2022**, *58*, 4372–4375.
- [14] a) P. W. Rabideau, Z. Marciniow, The Birch Reduction of Aromatic Compounds. In *Organic Reactions*, **2004**, pp. 1–334, <https://doi.org/10.1002/0471264180.or042.01>; b) H. E. Zimmerman, *Acc. Chem. Res.* **2012**, *45*, 164–170.
- [15] a) R. J. Wright, A. D. Phillips, P. P. Power, *J. Am. Chem. Soc.* **2003**, *125*, 10784–10785; b) T. Agou, K. Nagata, N. Tokitoh, *Angew. Chem. Int. Ed.* **2013**, *52*, 10818–10821; *Angew. Chem.* **2013**, *125*, 11018–11021.
- [16] R. J. Wright, M. Brynda, P. P. Power, *Angew. Chem. Int. Ed.* **2006**, *45*, 5953–5956; *Angew. Chem.* **2006**, *118*, 6099–6102.
- [17] a) P. Bag, A. Porzelt, P. J. Altmann, S. Inoue, *J. Am. Chem. Soc.* **2017**, *139*, 14384–14387; b) C. Weetman, A. Porzelt, P. Bag, F. Hanusch, S. Inoue, *Chem. Sci.* **2020**, *11*, 4817–4827.

4. Conclusion and Outlook

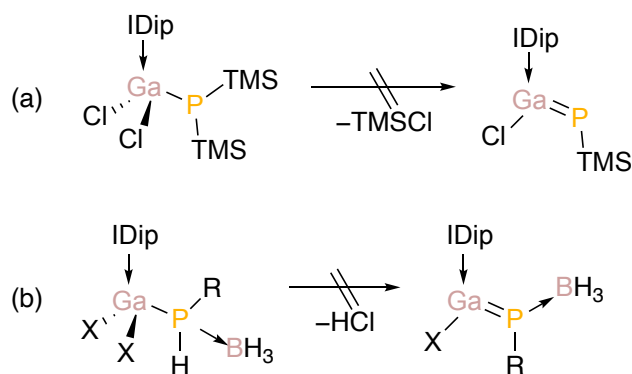
The growing interest in the preparation of compounds featuring group 13-15 multiple bonds is driven by their applications, especially in novel phosphanylgallenes and gallium imides. So far, there are limited examples in the literature due to significant synthetic challenges.

In the first chapter of this thesis, several NHC-stabilized phosphanylgallanes were prepared via salt metathesis of NHC gallium chlorides and hydrochlorides with various phosphorous salts ($\text{Na}(\text{diox})_{2.5}(\text{PCO})$, $\text{KP}(\text{TMS})_2$, $\text{LiPHR}\cdot\text{BH}_3$ ($\text{R} = \text{NCy}_2$, N^iPr_2 , Mes, Tip) (Scheme 48), LiPPh , LiPPH_2). They were characterized by x-ray crystallography, NMR and IR spectroscopy. Additionally, their bonding was studied using theoretical calculations and their reactivity in reduction reactions and towards bases was explored.



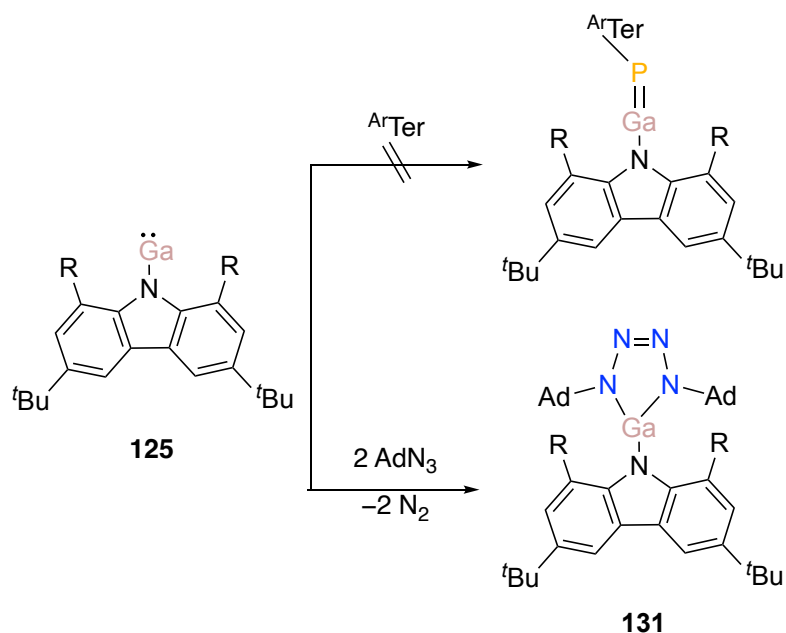
Scheme 48. Synthesized and structurally characterized NHC-stabilized phosphanylgallanes. L= IDip, IMes, Me_2CAAC ; X=Cl, H, OTf; R= NCy_2 , N^iPr_2 , Tip, Mes; R''=Ph,H.

These substances feature distinct Ga-P single bonds, along with slightly elongated $\text{C}_{\text{car}}\text{-Ga}$ bonds. DFT studies indicate a relatively stable interaction between the Lewis base and the phosphanylgallane, primarily driven by electrostatic attraction (>50%). Importantly, incorporating a Lewis acid and utilizing the phosphorus lone pair boosts the bond energy by 10 kcal/mol, largely attributable to a more robust orbital interaction. Furthermore, several approaches including HCl or TMSCl elimination did not afford NHC-stabilized phosphanylgallenes (Scheme 49). Treatment with different bases or reducing agents resulted in the breakage of either Ga-P or $\text{C}_{\text{car}}\text{-Ga}$ bonds.



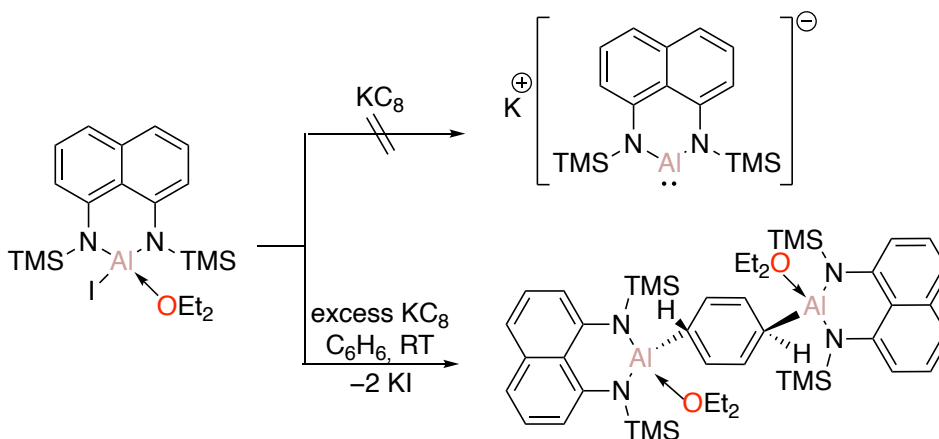
Scheme 49. Attempted synthesis of phosphanylgallenes via a) TMSCl elimination b) HCl elimination. X=Cl, H; R=NCy₂, Tip.

Since NHCs were not able to provide enough stability for Ga=P double bonds, the focus shifted to employing sterically hindering carbazole ligand systems. In the second part of this thesis, a monocoordinate gallium (I) compound was prepared by 1,8-bis(3,5-*di-tert*-butylphenyl)-3,6-*di-tert*butylcarbazole. The reactivity of the resulting gallylene towards metal carbonyl complexes, Lewis bases along with unsaturated substrates was then systematically investigated. Moreover, the potential of the gallylene **125** to access compounds with Ga=N and Ga=P multiple bonds was evaluated. Gallylene **125** was thus reacted with phospho-Wittig reagents (phosphanyliedenephosporanes, ^{Ar}TerP(PMe₃); Ar= Dip, Tip), but no reaction was observed neither upon photolysis nor at elevated temperatures (Scheme 50). For isolating gallium imides, **125** was reacted with AdN₃, which then formed tetrazagallole **141**.



Scheme 50. Attempted synthesis of Ga=P and Ga=N double bonds from gallylene **125**. R=2,6-*di-tert*-butylphenyl; Ar=Dip, Tip.

Bis(silylamido)naphthalene derivatives were used to prepare low-valent aluminum species (Al(II) radical or alumanyl Al(I) anion). The precursor with the tetra-coordinated aluminum atom was attempted to be reduced with various reducing agents such as KC_8 or magnesium (Scheme 51), yet only unidentified mixtures or decomposition products were obtained. In contrast, treatment with excess KC_8 produced a Al(II) radical intermediate, which then affords a Birch-type reduction product of benzene.



Scheme 51. Formation of Birch-type reduction product of benzene.

5. Experimental Section

5.1. General

5.1.1. Experimental Conditions

All manipulations, if not indicated otherwise were carried out under an argon atmosphere using standard Schlenk techniques or a glovebox. The protection gas was Argon 5.0 supplied by Air Liquide and was used without further purification.

All glassware was cleaned in a KOH/*n*-propanol bath, neutralized, and kept in a drying oven at 120°C overnight prior to use. All setups were evacuated and purged with argon three times. The high vacuum was generated with a slide vane rotary vacuum pump RZ 6 from Vacuubrand.

5.1.2. Solvent Purification

n-hexane, tetrahydrofuran (thf), benzene, and toluene were taken directly from a solvent purification system (Innovative Technology PureSolv MD7). C₆D₆ was refluxed over potassium and distilled prior to use. CDCl₃ was refluxed over calcium hydride and distilled prior to use.

5.1.3. Analytical Methods

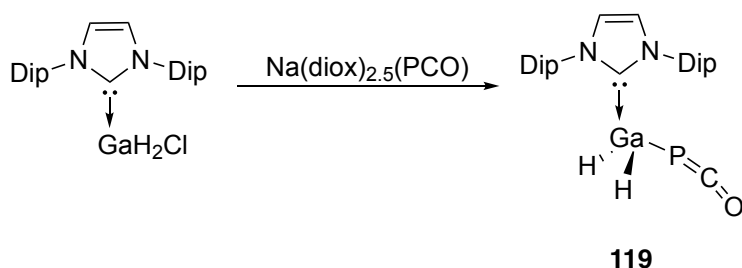
NMR spectra were recorded at 300 K on a Bruker Avance III 300 (¹H: 300.13 MHz, ¹³C: 75.47 MHz, ³¹P: 121.5 MHz, ²⁹Si: 59.6 MHz) and a Bruker Avance III HD 400 (¹H: 400.13 MHz, ¹³C: 100.61 MHz, ³¹P: 121.5 MHz, ²⁹Si: 79.5 MHz). ¹H and ¹³C NMR spectra were referenced to the peaks of the residual protons of deuterated solvents or the deuterated solvent itself (CDCl₃: δH: 7.26 ppm, δC: 77.16 ppm; C₆D₆: δH: 7.16 ppm, δC: 128.06 ppm). All chemical shifts are reported in parts per million (ppm). Coupling constants are reported in Hertz (Hz). The multiplicity and shape of the observed signals are given as s = singlet, d = doublet, t = triplet, sept = septet, m = multiplet or convoluted signals, br = broad signal. UV/Vis spectra were measured using a Shimadzu UV-2600 spectrometer in quartz cells with a path length of 1 mm. The corresponding UV/Vis spectra were measured with a Jasco V-650 spectrometer. Quantum yields were measured using Hamamatsu QuantaurusQY C11347-11. Fourier-Transform IR spectra were acquired on a Bruker Vertex 70 spectrometer in attenuated total reflectance (ATR) mode. Melting points were determined under argon in closed NMR tubes and are uncorrected. NMR spectra were run directly afterwards on a solution of the cooled down melt. Elemental analysis was carried out on an elemental vario Micro Cube.

5.2. Starting Materials

The following compounds are either purchased from commercial sources or prepared according to the literature procedures. Na(diox)_{2.5}(PCO),^[154] KP(thf)₂(TMS)₂,^[140] Me₂CAAC-

GaCl₃,^[155] IDip-GaCl₃,^[27] and IMes-GaCl₃,^[27] IDip-GaH₂Cl,^[26] GaCl₃ (Sigma Aldrich), GaI₃ (Sigma Aldrich), BenzK,^[156] 1,8-bis(3,5-*di-tert*-butylphenyl)-3,6-*di-tert*butylcarbazole,^[46,92] Gal,^[157] AdN₃ (Sigma Aldrich), CS₂ (Sigma Aldrich), Ag(OTf) (Sigma Aldrich), CO₂, and C₂H₄.

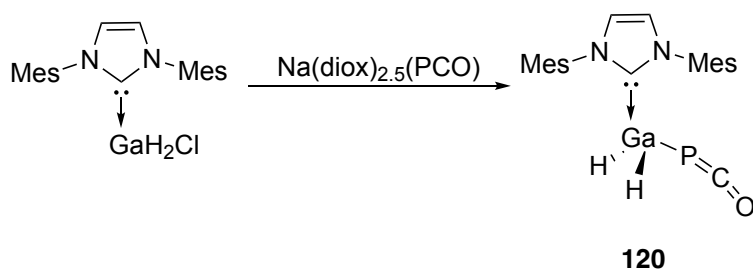
5.2.1. Synthesis of IDip-GaH₂(PCO) 119



IDip-GaH₂Cl (500 mg, 1.01 mmol, 1 eq.) and Na(diox)_{2.5}(PCO) (228.5 mg, 1.01 mmol, 1 eq.) are mixed in 35 mL of dry toluene and stirred at room temperature for 2 hours. The solution is filtered off and the volatiles are dried under vacuum. The remaining solid is then washed with dry hexane (2 x 10 mL) and dried under vacuum.

¹H NMR (400 MHz, C₆D₆) δ ppm: 7.25-7.21 (m, 2H, Ar), 7.10-7.07 (m, 4H, Ar), 6.42 (s, 2H, NCH), 2.63 (sep, 4H, CH(CH₃)₂), 1.40 (d, 12H, CH(CH₃)₂), 0.98 (d, 12H, CH(CH₃)₂) ppm. **¹³C{¹H} NMR (100.6 MHz, C₆D₆, 298K):** 174.98 (d, ²J_{C,P} = 10.6 Hz, NCN), 145.51 (Ar), 134.13 (Ar), 131.20 (Ar), 124.49 (Ar), 29.15 (CH(CH₃)₂), 25.45 (CH(CH₃)₂), 23.05 (CH(CH₃)₂) ppm. **³¹P NMR (161.9 MHz, C₆D₆, 298K):** -393.4 (t, ¹J_{P,H} = 18.3 Hz) ppm. **EA (%):** calcd. C: 64.76 H: 7.38 N: 5.39; found: C: 65.33, H: 7.49, N: 5.19. **MP:** decomp.; Yield: 37%.

5.2.2. Synthesis of IMes-GaH₂(PCO) 120

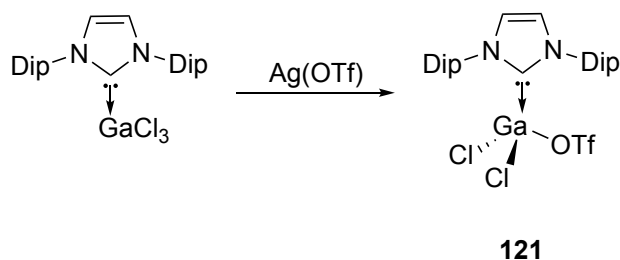


IMes-GaH₂Cl (500 mg, 1.21 mmol, 1 eq.) and Na(diox)_{2.5}(PCO) (274 mg, 1.21 mmol, 1 eq.) are mixed in 35 mL of dry toluene and stirred at room temperature for 2 hours. The solution is filtered off and the volatiles are dried under vacuum. The remaining solid is then washed with dry hexane (2 x 10 mL) and dried under vacuum.

¹H NMR (400 MHz, C₆D₆) δ ppm: 6.72 (s, 4H, Ar), 5.95 (s, 2H, NCH), 2.06 (s, 6H, *o*-CH₃), 2.01 (s, 12H, *o*-CH₃) ppm. **¹³C{¹H} NMR (100.6 MHz, C₆D₆, 298K):** 181.3 (d, ²J_{C,P} = 91.4 Hz, -PCO), 140.1, (NCN), 137.5 (Ar), 134.9 (Ar), 129.7 (Ar), 122.9 (Ar), 21.1 (CH(CH₃)₂), 19.1 (*o*-

$\text{CH}_3)_2$, 17.8 (*p*- CH_3) ppm. ^{31}P NMR (161.9 MHz, C_6D_6 , 298K): -393.3 ppm. EA (%): calcd. C: 60.70 H: 6.02 N: 6.44; found: C: 60.34, H: 5.87, N: 6.64. MP: decomp. Yield: 47%.

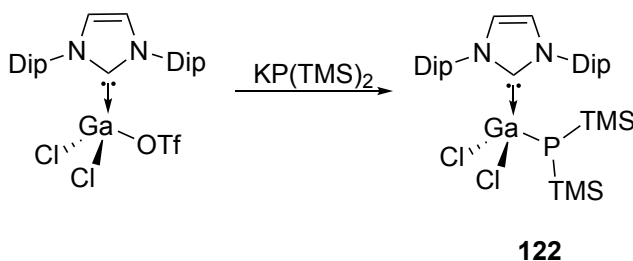
5.2.3. Synthesis of IDip-GaCl₂(OTf) 121



IDip.GaCl₃ (1 g, 1.8 mmol, 1 eq.) was dissolved in 40 mL of dry dichloromethane and was slowly added to a Schlenk flask containing Ag(OTf) (455 mg, 1.8 mmol, 1 eq.) in 30 mL of dry dichloromethane at -70 °C. The reaction mixture was warmed to room temperature and stirred overnight. The solvent was then removed under vacuum and the remaining white solid was washed with *n*-hexane (2 x 30 mL). The product was further dried under vacuum and collected as white solid (1 g) in 88% yield.

^1H NMR (400 MHz, C_6D_6) δ ppm: 7.25-7.21 (m, 2H, Ar), 7.10-7.07 (m, 4H, Ar), 6.42 (s, 2H, NCH), 2.63 (sep, 4H, $\text{CH}(\text{CH}_3)_2$), 1.40 (d, 12H, $\text{CH}(\text{CH}_3)_2$), 0.98 (d, 12H, $\text{CH}(\text{CH}_3)_2$) ppm. MP: decomp. Yield: 88%.

5.2.4. Synthesis of IDip-GaCl₂P(TMS)₂ 122

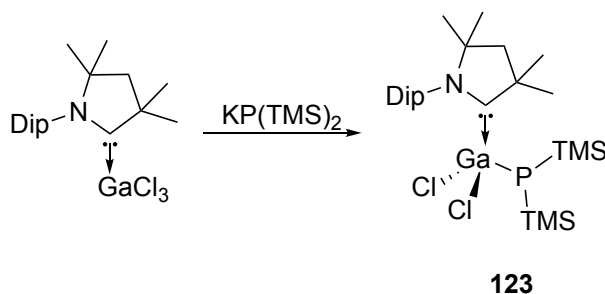


IDip-GaCl₂(OTf) (1 g, 1.5 mmol, 1 eq.) was dissolved in 40 mL of THF and 10 mL of THF solution of K(thf)₂P(TMS)₂ (541 mg, 1.5 mmol, 1 eq.) was slowly added to it at -70 °C. The reaction mixture was warmed to room temperature and stirred overnight. The solvent was then removed under vacuum and the remaining solid was washed with *n*-hexane (2 x 30 mL). The product was further dried under vacuum and collected as white solid (1.02 g) in 68% yield.

^1H NMR (400 MHz, C_6D_6) δ ppm: 7.28-7.22 (m, 2H, Ar), 7.15-7.13 (m, 4H, Ar), 6.40 (s, 2H, NCH), 2.88 (sep, 4H, $\text{CH}(\text{CH}_3)_2$), 1.54 (d, 12H, $\text{CH}(\text{CH}_3)_2$), 0.96 (d, 12H, $\text{CH}(\text{CH}_3)_2$), 0.45 (d, 18H, -Si(CH_3)₂) ppm. $^{13}\text{C}\{^1\text{H}\}$ NMR (100.6 MHz, C_6D_6 , 298K): 167.63 (d, $^2J_{\text{C,P}} = 32.1$ Hz, NCN), 145.81 (Ar), 131.22 (Ar), 125.48 (Ar), 124.47 (Ar), 29.22 ($\text{CH}(\text{CH}_3)_2$), 26.25 ($\text{CH}(\text{CH}_3)_2$), 23.06

(CH(CH₃)₂), 4.90 (d, 11.54 Hz, -Si(CH₃)₂ ppm. ³¹P NMR (161.9 MHz, C₆D₆, 298K): -252.0 ppm. ²⁹Si NMR (59.6 MHz, C₆D₆, 298K): 4.52 (d, J_{Si-P} = 33.37 Hz). MP: 250 < °C. Yield: 68%.

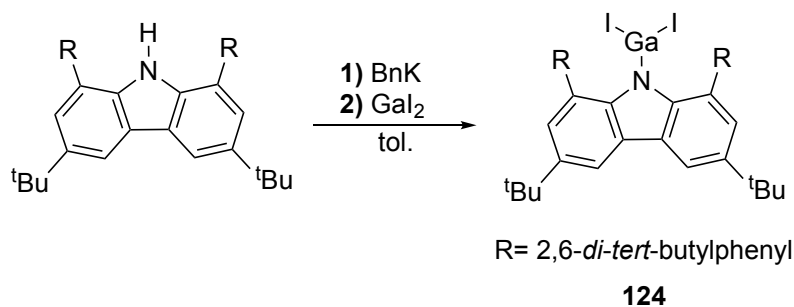
5.2.5. Synthesis of Me₂CAAC.GaCl₂P(TMS)₂ 123



Me₂CAAC.GaCl₃ (1 g, 2.2 mmol, 1 eq.) was dissolved in 40 mL of THF and 10 mL of THF solution of K(thf)₂P(TMS)₂ (781 mg, 2.2 mmol, 1 eq.) was slowly added to it at -70 °C. The reaction mixture was warmed to room temperature and stirred overnight. The solvent was then removed under vacuum and the remaining solid was washed with *n*-hexane (2 x 30 mL). The product was further dried under vacuum and collected as white solid (668 mg) in 57% yield.

¹H NMR (400 MHz, C₆D₆) δ ppm: 7.15-7.10 (m, 1H, Ar), 7.05-7.02 (m, 2H, Ar), 2.74 (sep, 2H, CH(CH₃)₂), 1.75 (s, 6H, -CH₃), 1.54 (d, 6H, -CH₃), 1.31 (s, 2H, -NCCCH₂), 1.07 (d, 6H, -CH₃), 0.82 (s, 6H, -CH₃), 0.62 (d, 18H, -Si(CH₃)₂) ppm. ¹³C{¹H} NMR (100.6 MHz, C₆D₆, 298K): 145.27 (Ar), 145.81 (Ar), 130.38 (Ar), 125.71 (Ar), 82.57, 29.85 (d, 9.70 Hz), 29.34, 28.57, 27.91, 24.88, 5.43 (d, 10.96 Hz, -Si(CH₃)₂) ppm. ³¹P NMR (161.9 MHz, C₆D₆, 298K): -241.6 ppm. MP: 250 < °C.

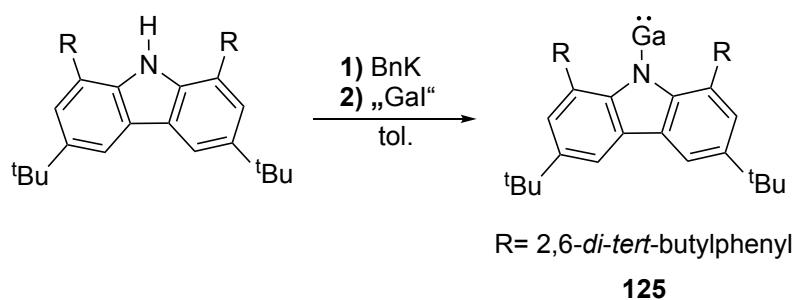
5.2.6. Synthesis of L-Gal₂ 124



The potassium carbazolidine ligand derivative, L-K (1 eq., 1.6 g, 2.3 mmol), was dissolved in dry toluene and toluene solution of Gal₃ (1 eq., 1.0 g, 2.3 mmol) was added slowly at -30 °C. The reaction mixture was warmed to room temperature and stirred overnight. The solution was filtered off and toluene was evaporated under vacuum. The remaining solid was washed with *n*-hexane and dried under vacuum to yield 1.60 g of L-Gal₂ **124** as light-yellow powder. L-Gal₂ is stored at -30 °C and with exclusion of moisture and oxygen to avoid decomposition. ¹H NMR (400 MHz, C₆D₆) δ ppm: 8.43 (d, J_{HH} = 1.91 Hz, 2H, C^{2,7}H), 7.70 (t,

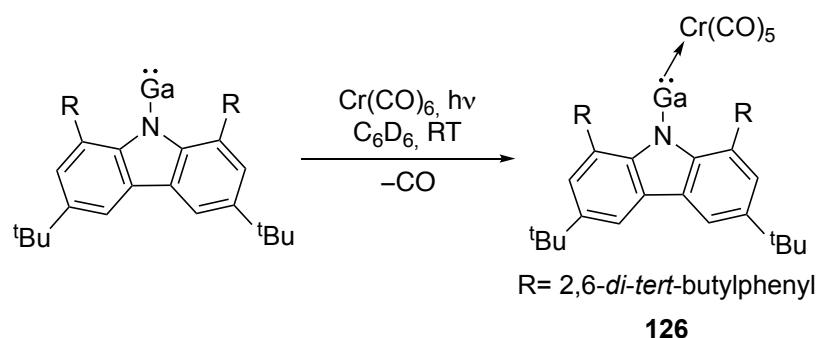
J_{HH} = 2.05 Hz, 2H, Ar *p*-CH), 7.60 (d, J_{HH} = 1.81 Hz, 4H, *o*-CH), 7.55 (d, J_{HH} = 2.03 Hz, 2H, C^{4,5}H), 1.37 (s, 18H, Carb(CH₃)₃), 1.30 (s, 36H, Ar(CH₃)₃). **¹³C{¹H} NMR (100.6 MHz, C₆D₆, 298K)**: 153.5 (s, Ar), 144.8 (s, Ar), 143.7 (s, Ar), 137.2 (s, Ar), 127.6 (s, Ar), 127.2 (s, Ar), 126.3 (s, Ar), 124.9 (s, Ar), 116.0 (s, Ar), 35.3 (s, C(CH₃)₃), 35.0 (s, C(CH₃)₃), 32.2 (s, C(CH₃)₃). **IR (cm⁻¹)**: 2951 (s), 2900 (w), 2861 (w), 1590 (m), 1360 (m), 1286 (s), 1241 (s). **HRMS (m/z)**: [M]⁺ calcd. For C₄₈H₆₄GaNi₂, 724.43673; found 724.45356. **MP**: > 300 °C (decomp.) **Yield**: 72%. **EA (%)**: calcd. C: 58.91 H: 6.59 N: 1.43; found: C: 59.87 H: 6.00, N: 1.21.

5.2.7. Synthesis of L-Ga 125



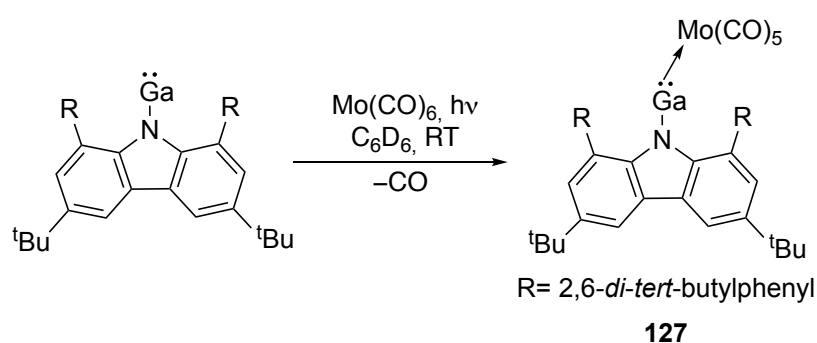
“Gal” was prepared according to the literature procedure.^[86] (1.05 eq., 1.26 g, 6.4 mmol) Toluene solution of the potassium salt of the ligand (1 eq., 4.2 g, 6.1 mmol) was added dropwise to the suspension of “Gal” in toluene at -30 °C. The reaction mixture was slowly warmed to room temperature and stirred overnight at room temperature. The solution was then filtered off and toluene was evaporated under vacuum. The remaining solid was washed with *n*-hexane to afford 2.96 g of L-Ga **125** as pale-yellow powder. Crystals suitable for XRD analysis were grown from saturated diethyl ether solution of **125** at room temperature by slow evaporation. L-Ga is stored at -30 °C and with exclusion of moisture and oxygen to avoid decomposition. **¹H NMR (400 MHz, C₆D₆) δ ppm**: 8.54 (d, J_{HH} = 1.57 Hz, 2H, Ar), 7.61 (d, J_{HH} = 2.10 Hz, 2H, Ar), 7.49 (d, J_{HH} = 1.65 Hz, 4H, Ar), 7.45 (t, J_{HH} = 1.82 Hz, 4H, Ar), 1.52 (s, 18H, C(CH₃)₃), 1.20 (s, 36H, C(CH₃)₃). **¹³C{¹H} NMR (100.6 MHz, C₆D₆, 298K)**: 154.8 (s, Ar-C^tBu), 148.4 (s), 144.1 (s), 141.3 (s), 125.1 (s), 124.2 (s, -CH), 122.8 (s, -CH), 122.2 (s, -CH), 115.9 (s, -CH), 35.3 (s, C(CH₃)₃), 35.0 (s, C(CH₃)₃), 32.2 (s, C(CH₃)₃). **IR (cm⁻¹)**: 2959 (s), 2902 (w), 2864 (w), 1586 (m), 1478 (m), 1224 (m). **HRMS (m/z)**: [M]⁺ calcd. For C₄₈H₆₄GaN, 978.24567; found 978.26515. **MP**: 300 °C < (decomp.) **Yield**: 67%. **EA (%)**: Compound **125** consistently analyzed low for carbon over repeated analyses. C: 79.55 H: 8.90 N: 1.93; found: C: 73.24 H: 7.33, N: 1.48.

5.2.8. Synthesis of L-GaCr(CO)₅ **126**



Compound **126** (1 eq., 30 mg, 0.04 mmol) and Cr(CO)₆ (1 eq., 9.11 mg, 0.04 mmol) were placed in a quartz NMR tube and 0.7 mL of C₆D₆ was added via syringe. The reaction mixture was irradiated at 345 nm for 28 hours at room temperature. The reaction progress was monitored by ¹H NMR. After the completion of the reaction, the solution was transferred to a glass vial. Slow evaporation of the benzene solution afforded yellow crystals, which was then characterized as **126**. The crystals were collected, washed with *n*-hexane and dried under vacuum. 27.1 mg of product was collected. ¹H NMR (400 MHz, C₆D₆) δ ppm: 8.31 (d, *J*_{HH}=2.01 Hz, 2H, Ar), 8.06 (d, *J*_{HH}=81.3 Hz, 4H, Ar), 7.64 (t, *J*_{HH}=1.67 Hz, 2H, Ar), 7.58 (d, *J*_{HH}=1.95 Hz, 2H, Ar), 1.40 (s, 54H, C(CH₃)₃). ¹³C{¹H} NMR (100.6 MHz, C₆D₆, 298K): 216.1 (s), 144.4 (s, Ar), 142.9 (s, Ar), 142.5 (s, Ar), 142.0 (s, Ar), 130.6 (s, Ar), 128.6 (s, Ar), 126.9 (s, Ar), 126.4 (s, Ar), 116.2 (s, Ar), 35.5 (s, C(CH₃)₃), 34.8 (s, C(CH₃)₃), 32.1 (s, C(CH₃)₃). IR (cm⁻¹): 2959 (s), 2867 (w), 1923 (s), 1246 (m), 1223 (m), 1204 (w). MP: >300 °C (decomp.) Yield: 72%. EA (%): calcd. C: 69.43 H: 7.04 N: 1.53; found: C: 68.75 H: 6.49, N: 1.26.

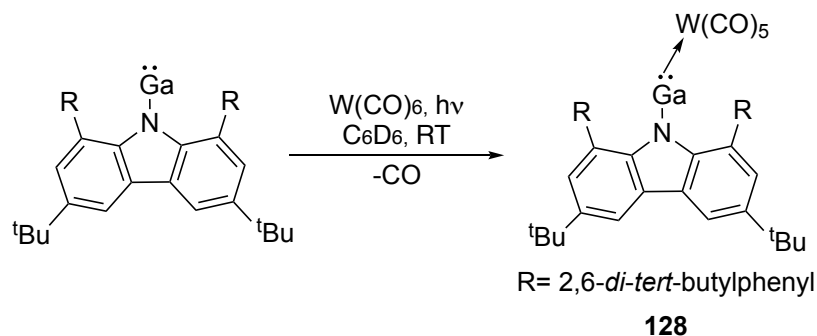
5.2.9. Synthesis of L-GaMo(CO)₅ **127**



A similar procedure as in the synthesis of **126** was followed. From compound **125** (1 eq., 30 mg, 0.04 mmol) and Mo(CO)₆ (1 eq., 10.8 mg, 0.04 mmol), 18.8 mg of **127** was isolated. ¹H NMR (400 MHz, C₆D₆) δ ppm: 8.31 (d, 2H, *J*_{HH}=2.16 Hz, Ar), 8.04 (d, *J*_{HH}=87.7 Hz, 4H, Ar), 7.64 (t, *J*_{HH}=1.73 Hz, 2H, Ar), 7.58 (d, *J*_{HH}=1.94 Hz, 2H, Ar), 1.40 (s, 54H, C(CH₃)₃). ¹³C{¹H} NMR (100.6 MHz, C₆D₆, 298K): 210.0 (s, -CO), 205.4 (s, Ar), 144.3 (s, Ar), 143.2 (s, Ar), 142.8 (s, Ar), 142.3 (s, Ar), 130.6 (s, Ar), 127.0 (s, Ar), 126.3 (s, Ar), 126.0 (s, Ar), 123.3 (s, Ar),

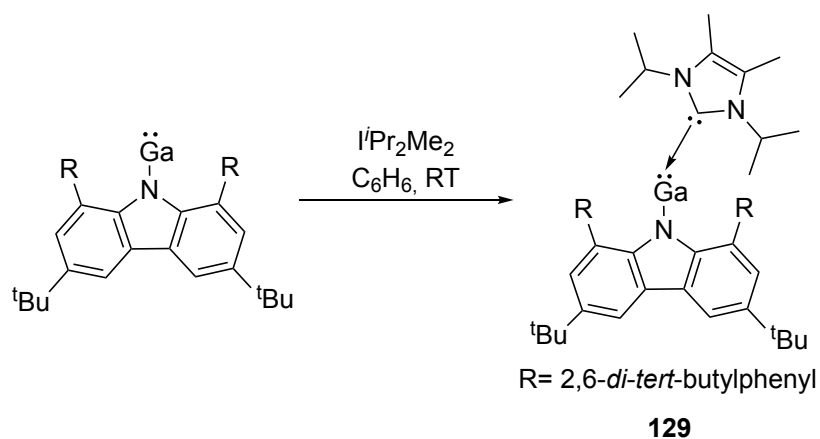
121.4 (s, Ar), 116.2 (s, Ar), 35.5 (s, C(CH₃)₃), 34.8 (s, C(CH₃)₃), 32.1 (s, C(CH₃)₃). **IR (cm⁻¹):** 2955 (s), 2865 (w), 1937 (s), 1247 (m), 1220 (m). **EA (%):** calcd. C: 66.26 H: 6.71 N: 1.46; found: C: 65.43 H: 6.47, N: 1.42. **MP:** >300 °C (decomp.). **Yield:** 48% (isolated).

5.2.10. Synthesis of L-GaW(CO)₅ **128**



The same procedure as above was followed. From **125** (1 eq., 500 mg, 0.69 mmol) and W(CO)₆ (1 eq., 243 mg, 0.69 mmol), 180 mg of **128** was isolated. (Irradiation was done with 254 nm of LED.) **¹H NMR (400 MHz, C₆D₆) δ ppm:** 8.30 (d, 2H, *J*_{HH}=1.93 Hz, Ar), 8.02 (d, 4H, *J*_{HH}=80.1 Hz, Ar), 7.65 (t, *J*_{HH}=1.87 Hz, 2H, Ar), 7.57 (d, *J*_{HH}=2.09 Hz, 2H, Ar), 1.40 (s, 54H, C(CH₃)₃). **¹³C{¹H} NMR (100.6 MHz, C₆D₆, 298K):** 197.7 (s, -CO), 195.6 (s, Ar), 144.5 (s, Ar), 142.9 (s, Ar), 142.6 (s, Ar), 142.1 (s, Ar), 130.6 (s, Ar), 127.1 (s, Ar), 126.6 (s, Ar), 126.0 (s, Ar), 116.2 (s), 35.5 (s, C(CH₃)₃), 32.0 (s, C(CH₃)₃), 31.6 (s, C(CH₃)₃). **IR (cm⁻¹):** 2955 (w), 1929 (s), 1247 (w), 1220 (w). **EA (%):** calcd. C: 60.7 H: 6.17 N: 1.34; found: C: 60.71 H: 5.71, N: 1.06. **MP:** 264 °C (decomp.). **Yield:** 34%.

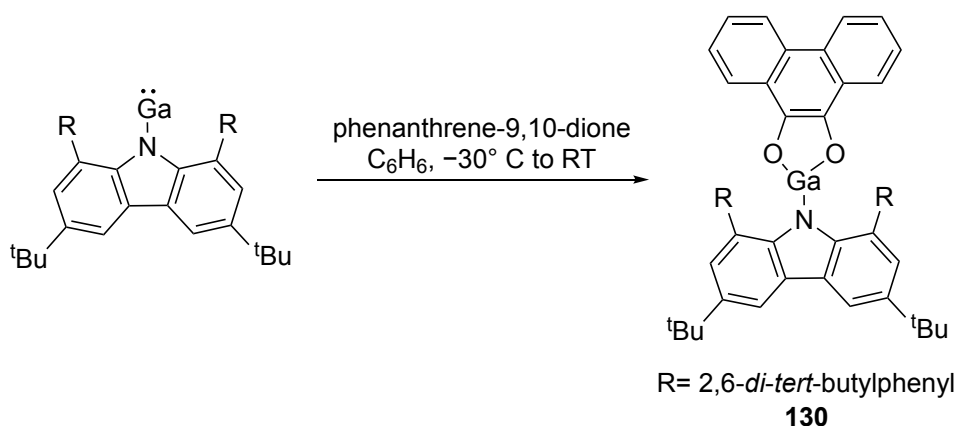
5.2.11. Synthesis of L-Ga(ⁱPr₂Me₂) **129**



To a benzene solution of L-Ga (1 eq., 500 mg, 0.69 mmol), benzene solution of ⁱPrMe₂NHC (1.05 eq., 131 mg, 0.72 mmol) was added. The reaction mixture was stirred for 1 hour at room temperature. Benzene was then evaporated under vacuum and the remaining solid was washed with *n*-hexane. 438 mg of **129** was collected as orange powder. **¹H NMR (400 MHz, C₆D₆) δ ppm:** 8.55 (d, 2H, *J*_{HH}=1.86 Hz, Ar), 7.61 (d, *J*_{HH}=1.86 Hz, 2H, Ar), 7.55 (m, *J*_{HH}=1.72

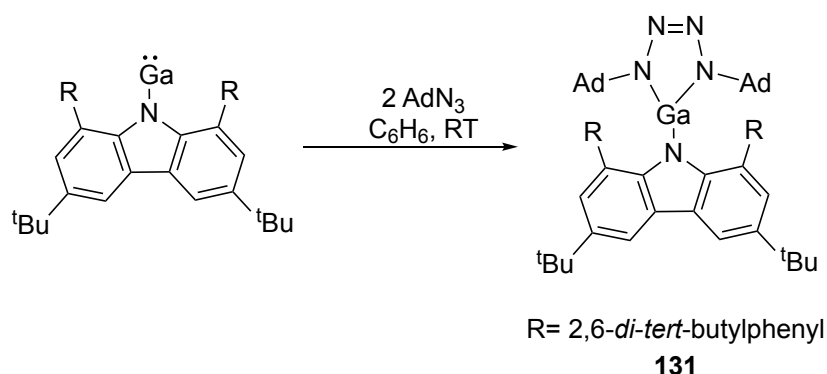
Hz, 4H, Ar), 7.46 (t, $J_{HH}=1.86$ Hz, 2H, Ar), 3.89 (sept, $J_{HH}=6.82$ Hz, 2H, $-CH(CH_3)_2$), 1.53 (s, 18H, $C(CH_3)_3$), 1.40 (s, 6H, $-CH_3$), 1.29 (s, 12H, $CH(CH_3)_2$), 1.22 (s, 36H, $C(CH_3)_3$). $^{13}C\{^1H\}$ NMR (100.6 MHz, C_6D_6 , 298K): 154.4 (s, NCN), 151.4 (s, Ar), 150.0 (s, Ar), 147.1 (s, Ar), 132.5 (s, Ar), 129.7 (s, Ar), 129.5 (s, Ar), 125.3 (s, Ar), 123.5 (s, Ar), 122.4 (s, Ar), 121.7 (s, Ar), 114.8 (s, Ar), 48.7 (s, $C(CH_3)_2$), 35.2 (s, $C(CH_3)_3$), 32.5 (s, $C(CH_3)_3$), 31.7 (s, $C(CH_3)_3$), 24.4 (s, $CH(CH_3)_2$), 8.86 (s, $CH(CH_3)_2$). IR (cm^{-1}): 2952 (m), 2865 (w), 1465 (m), 1201 (m), 865 (m). HRMS (m/z): $[M]^+$ calcd. For $C_{59}H_{84}GaN_3$, 903.59; found 902.58216. MP: 197 °C (decomp.). Yield: 70%.

5.2.12. Synthesis of L-Ga($C_{14}H_8O$) **130**



Toluene solution of phenanthrene-9,10-dione was added slowly to toluene solution of L-Ga (1 eq., 100 mg, 0.14 mmol) at -30 °C. Upon addition of phenanthrene-9,10-dione (1 eq., 28.7 mg, 0.14 mmol), the color of reaction mixture turns from yellow to dark brown. After warming the reaction mixture slowly to room temperature, the solution was stirred for 30 minutes at room temperature. The solution was then filtered off and toluene solution was placed at -30 °C. The product **130** (63.5 mg) precipitates as beige/brown solid. 1H NMR (400 MHz, C_6D_6) δ ppm: 8.53-8.49 (m, 4H, Ar), 8.28 (d, $J_{HH}=8.07$ Hz, 2H, Ar), 7.61-7.53 (m, 12H, Ar), 1.43 (s, 18H, $C(CH_3)_3$), 0.95 (s, 36H, $C(CH_3)_3$). $^{13}C\{^1H\}$ NMR (100.6 MHz, C_6D_6 , 298K): 156.5 (s, Ar), 142.9 (s, Ar), 140.9 (s, Ar), 139.9 (s, Ar), 129.3 (s, Ar), 127.1 (s, Ar), 126.9 (s, Ar), 125.9 (s, Ar), 125.7 (s, Ar), 124.8 (s), 124.7 (s, Ar), 123.3 (s, Ar), 123.0 (s, Ar), 122.3 (s, Ar), 35.3 (s, $C(CH_3)_3$), 32.2 (s, $C(CH_3)_3$), 31.0 (s, $C(CH_3)_3$). IR (cm^{-1}): 2954 (s), 2868 (w), 1586 (m), 1477 (w), 1461 (w), 1239 (s), 1026 (m). EA (%): calcd. C: 79.82 H: 7.78 N: 1.50; found: C: 74.23 H: 6.12 N: 1.33. MP: 300 °C < (decomp.). Yield: 20%.

5.2.13. Synthesis of (L-GaN₄Ad₂) **131**



L-Ga (1 eq., 94 mg, 0.130 mmol), was dissolved in dry benzene, and benzene solution of AdN₃ (2 eq., 46 mg, 0.260 mmol) was added to it slowly at room temperature. Upon the addition of the azide, evolution of N₂ was observed. The reaction solution was stirred for 1 hour and benzene was then evaporated under vacuum. The remaining solid was washed with *n*-hexane and dried under vacuum to yield **131** (69 mg) as yellow powder.

¹H NMR (400 MHz, C₆D₆) δ ppm: 8.46 (d, ¹J_{H-H} = 2.02 Hz, 2H, Ar), 7.58 (t, ¹J_{H-H} = 1.78 Hz, 2H, Ar), 7.45 (d, ¹J_{H-H} = 1.95 Hz, 4H, Ar), 7.38 (d, ¹J_{H-H} = 2.12 Hz, 2H, Ar), 1.60 (br, 6H, Ad), 1.54 (br, 12H, Ad), 1.46 (br, 12H, Ad), 1.33 (s, 18H, C(CH₃)₃), 1.30 (s, 36H, C(CH₃)₃). **¹³C NMR (100.6 MHz, C₆D₆, 298K):** 153.5 (s, Ar), 152.0 (s, Ar), 144.5 (s, Ar), 144.2 (s, Ar), 140.2 (s, Ar), 130.3 (s, Ar), 129.3 (s, Ar), 126.0 (s, Ar), 122.6 (s, Ar), 115.8 (s, Ar), 55.1 (s, C_{Ad}), 44.2 (s, C_{Ad}), 41.6 (s, CH_{Ad}), 36.6 (s, CH_{Ad}), 35.9 (s, CH_{Ad}), 35.2 (s, CH_{Ad}), 34.8 (s, CH_{2Ad}), 32.0 (s, CH_{2Ad}), 31.7 (s, C(CH₃)₃), 31.6 (s, C(CH₃)₃), 30.1 (s, C(CH₃)₃), 30.0 (s, C(CH₃)₃). **MP:** decomp. **Yield:** 29%.

6. References

- [1] D. Bourissou, O. Guerret, F. P. Gabbaï, G. Bertrand, *Chem. Rev.* **2000**, *100*, 39–91.
- [2] A. J. Arduengo III, R. L. Harlow, M. Kline, *J. Am. Chem. Soc.* **1991**, *113*, 361–363.
- [3] A. J. Arduengo III, H. V. R. Dias, R. L. Harlow, M. Kline, *J. Am. Chem. Soc.* **1992**, *114*, 5530–5534.
- [4] V. Lavallo, Y. Canac, C. Präsang, B. Donnadiou, G. Bertrand, *Angew. Chemie Int. Ed.* **2005**, *44*, 5705–5709.
- [5] T. Kuhn, N. Kratz, *Synthesis (Stuttg.)* **1993**, *1993*, 561–562.
- [6] A. J. Arduengo III, R. Krafczyk, R. Schmutzler, H. A. Craig, J. R. Goerlich, W. J. Marshall, M. Unverzagt, *ChemInform* **2000**, *31*.
- [7] C. Heinemann, W. Thiel, *Chem. Phys. Lett.* **1994**, *217*, 11–16.
- [8] M. K. Denk, A. Thadani, K. Hatano, A. J. Lough, *Angew. Chemie Int. Ed. English* **1997**, *36*, 2607–2609.
- [9] A. Haaland, *Angew. Chemie Int. Ed. English* **1989**, *28*, 992–1007.
- [10] V. Nesterov, D. Reiter, P. Bag, P. Frisch, R. Holzner, A. Porzelt, S. Inoue, *Chem. Rev.* **2018**, *118*, 9678–9842.
- [11] D. Himmel, I. Krossing, A. Schnepf, *Angew. Chemie Int. Ed.* **2014**, *53*, 370–374.
- [12] G. Frenking, *Angew. Chemie Int. Ed.* **2014**, *53*, 6040–6046.
- [13] N. Holzmann, D. M. Andrada, G. Frenking, *J. Organomet. Chem.* **2015**, *792*, 139–148.
- [14] D. Munz, *Organometallics* **2018**, *37*, 275–289.
- [15] M. Melaimi, R. Jazzar, M. Soleilhavoup, G. Bertrand, *Angew. Chemie* **2017**, *129*, 10180–10203.
- [16] Y. Wang, B. Quillian, P. Wei, C. S. Wannere, Y. Xie, R. B. King, H. F. Schaefer, P. v. R. Schleyer, G. H. Robinson, *J. Am. Chem. Soc.* **2007**, *129*, 12412–12413.
- [17] T. Chu, S. F. Vyboishchikov, B. Gabidullin, G. I. Nikonov, *Angew. Chemie Int. Ed.* **2016**, *55*, 13306–13311.
- [18] D. Franz, T. Szilvási, E. Irran, S. Inoue, *Nat. Commun.* **2015**, *6*, 10037.
- [19] M. D. Francis, D. E. Hibbs, M. B. Hursthouse, C. Jones, N. A. Smithies, *J. Chem. Soc. Dalt. Trans.* **1998**, 3249–3254.
- [20] M. G. Gardiner, C. L. Raston, *Coord. Chem. Rev.* **1997**, *166*, 1–34.

- [21] C. L. Raston, *J. Organomet. Chem.* **1994**, 475, 15–24.
- [22] A.J. Downs, *Chemistry of Aluminium, Gallium, Indium and Thallium*, Blackie Academic & Professional, 97, **1993**.
- [23] A. K. Swarnakar, M. J. Ferguson, R. McDonald, E. Rivard, *Dalt. Trans.* **2017**, 46, 1406–1412.
- [24] M. L. Cole, S. K. Furfari, M. Kloth, *J. Organomet. Chem.* **2009**, 694, 2934–2940.
- [25] S. G. Alexander, M. L. Cole, S. K. Furfari, M. Kloth, *Dalt. Trans.* **2009**, 2909–2911.
- [26] A. Hock, L. Werner, C. Luz, U. Radius, *Dalt. Trans.* **2020**, 49, 11108–11119.
- [27] N. Marion, E. C. Escudero-Adán, J. Benet-Buchholz, E. D. Stevens, L. Fensterbank, M. Malacria, S. P. Nolan, *Organometallics* **2007**, 26, 3256–3259.
- [28] S. Tang, J. Monot, A. El-Hellani, B. Michelet, R. Guillot, C. Bour, V. Gandon, *Chemistry* **2012**, 18, 10239–10243.
- [29] S. P. Denbaars, *Proc. IEEE* **1997**, 85, 1740–1749.
- [30] A. M. Glass, *Optical Materials*, American Association For The Advancement Of Science, **1987**.
- [31] A. H. Cowley, R. A. Jones, *Angew. Chemie Int. Ed. English* **1989**, 28, 1208–1215.
- [32] P. P. Power, *Chem. Rev.* **1999**, 99, 3463–3503.
- [33] F. Thomas, S. Schulz, M. Nieger, K. Nättinen, *Chem. - A Eur. J.* **2002**, 8, 1915–1924.
- [34] M. Kapitein, M. Balmer, L. Niemeier, C. von Hänisch, *Dalt. Trans.* **2016**, 45, 6275–6281.
- [35] M. Kapitein, M. Balmer, C. von Hänisch, **2016**, 642, 1275–1281.
- [36] M. A. K. Weinhart, A. S. Lisovenko, A. Y. Timoshkin, M. Scheer, *Angew. Chemie Int. Ed.* **2020**, 59, 5541–5545.
- [37] C. Dohmeier, C. Robl, M. Tacke, H. Schnöckel, *Angew. Chemie* **1991**, 103, 594–595.
- [38] H. Sitzmann, M. F. Lappert, C. Dohmeier, C. Üffing, H. Schnöckel, *J. Organomet. Chem.* **1998**, 561, 203–208.
- [39] A. Hofmann, T. Tröster, T. Kupfer, H. Braunschweig, *Chem. Sci.* **2019**, 10, 3421–3428.
- [40] I.-A. Bischoff, S. Danés, P. Thoni, B. Morgenstern, D. M. Andrada, C. Müller, J. Lambert, E. C. J. Gießelmann, M. Zimmer, A. Schäfer, *Nat. Chem.* **2024**, 1093–1110.
- [41] S. Aldridge, A. J. Downs, *The Group 13 Metals Aluminium, Gallium, Indium and Thallium: Chemical Patterns and Peculiarities*, Wiley, Chichester, UK, **2011**.

- [42] C. Cui, H. W. Roesky, H.-G. Schmidt, M. Noltemeyer, H. Hao, F. Cimpoesu, *Angew. Chemie Int. Ed.* **2000**, *39*, 4274–4276.
- [43] S. K. Mellerup, Y. Cui, F. Fantuzzi, P. Schmid, J. T. Goettel, G. Bélanger-Chabot, M. Arrowsmith, I. Krummenacher, Q. Ye, V. Engel, B. Engels, H. Braunschweig, *J. Am. Chem. Soc.* **2019**, *141*, 16954–16960.
- [44] R. L. Falconer, K. M. Byrne, G. S. Nichol, T. Krämer, M. J. Cowley, *Angew. Chemie Int. Ed.* **2021**, *60*, 24702–24708.
- [45] J. D. Queen, A. Lehmann, J. C. Fettingner, H. M. Tuononen, P. P. Power, *J. Am. Chem. Soc.* **2020**, *142*, 20554–20559.
- [46] X. Zhang, L. L. Liu, *Angew. Chemie Int. Ed.* **2021**, *60*, 27062–27069.
- [47] A. Hinz, M. P. Müller, *Chem. Commun.* **2021**, *57*, 12532–12535.
- [48] P. Dabringhaus, J. Willrett, I. Krossing, *Nat. Chem.* **2022**, *14*, 1151–1157.
- [49] C. Klemp, G. Stößer, I. Krossing, H. Schnöckel, *Angew. Chemie Int. Ed.* **2000**, *39*, 3691–3694.
- [50] D. Franz, S. Inoue, *Chem. – A Eur. J.* **2019**, *25*, 2898–2926.
- [51] J. Hicks, P. Vasko, J. M. Goicoechea, S. Aldridge, *Angew. Chemie Int. Ed.* **2021**, *60*, 1702–1713.
- [52] X.-W. Li, W. T. Pennington, G. H. Robinson, *J. Am. Chem. Soc.* **1995**, *117*, 7578–7579.
- [53] J. Su, X.-W. Li, R. C. Crittendon, G. H. Robinson, *J. Am. Chem. Soc.* **1997**, *119*, 5471–5472.
- [54] R. J. Wright, M. Brynda, P. P. Power, *Angew. Chemie Int. Ed.* **2006**, *45*, 5953–5956.
- [55] R. J. Wright, A. D. Phillips, P. P. Power, *J. Am. Chem. Soc.* **2003**, *125*, 10784–10785.
- [56] R. J. Wehmschulte, K. Ruhlandt-Senge, M. M. Olmstead, H. Hope, B. E. Sturgeon, P. P. Power, *Inorg. Chem.* **1993**, *32*, 2983–2984.
- [57] C. Pluta, K. R. Pörschke, C. Krüger, K. Hildenbrand, *Angew. Chemie Int. Ed.* **1993**, *32*, 388–390.
- [58] W. Uhl, *Angew. Chemie Int. Ed.* **1993**, *32*, 1386–1397.
- [59] J. Hicks, P. Vasko, J. M. Goicoechea, S. Aldridge, *Nature* **2018**, *557*, 92–95.
- [60] R. J. Schwamm, M. D. Anker, M. Lein, M. P. Coles, *Angew. Chemie Int. Ed.* **2019**, *58*, 1489–1493.
- [61] R. J. Schwamm, M. P. Coles, M. S. Hill, M. F. Mahon, C. L. McMullin, N. A. Rajabi, A.

- S. S. Wilson, *Angew. Chemie Int. Ed.* **2020**, *59*, 3928–3932.
- [62] N. Wiberg, T. Blank, W. Kaim, B. Schwederski, G. Linti, *Eur. J. Inorg. Chem.* **2000**, 1475–1481.
- [63] N. Wiberg, K. Amelunxen, T. Blank, H. Nöth, J. Knizek, *Organometallics* **1998**, *17*, 5431–5433.
- [64] H. W. Roesky, S. S. Kumar, *Chem. Commun.* **2005**, 4027–4038.
- [65] M. Zhong, S. Sinhababu, H. W. Roesky, *Dalt. Trans.* **2020**, *49*, 1351–1364.
- [66] T. Chu, I. Korobkov, G. I. Nikonov, *J. Am. Chem. Soc.* **2014**, *136*, 9195–9202.
- [67] C. Bakewell, A. J. P. White, M. R. Crimmin, *Chem. Sci.* **2019**, *10*, 2452–2458.
- [68] S. J. Urwin, G. S. Nichol, M. J. Cowley, *Chem. Commun.* **2018**, *54*, 378–380.
- [69] R. Y. Kong, M. R. Crimmin, *Chem. Commun.* **2019**, *55*, 6181–6184.
- [70] C. Bakewell, A. J. P. White, M. R. Crimmin, *Angew. Chemie Int. Ed.* **2018**, *57*, 6638–6642.
- [71] D. Loos, H. Schnöckel, J. Gauss, U. Schneider, *Angew. Chemie Int. Ed.* **1992**, *31*, 1362–1364.
- [72] D. Loos, E. Baum, A. Ecker, H. Schnöckel, A. J. Downs, *Angew. Chemie Int. Ed. English* **1997**, *36*, 860–862.
- [73] M. C. Kuchta, J. B. Bonanno, G. Parkin, *J. Am. Chem. Soc.* **1996**, *118*, 10914–10915.
- [74] N. J. Hardman, R. J. Wright, A. D. Phillips, P. P. Power, *J. Am. Chem. Soc.* **2003**, *125*, 2667–2679.
- [75] Z. Zhu, R. C. Fischer, B. D. Ellis, E. Rivard, W. A. Merrill, M. M. Olmstead, P. P. Power, J. D. Guo, S. Nagase, L. Pu, *Chem. – A Eur. J.* **2009**, *15*, 5263–5272.
- [76] A. Seifert, G. Linti, *Eur. J. Inorg. Chem.* **2007**, *2007*, 5080–5086.
- [77] R. J. Wright, M. Brynda, J. C. Fettinger, A. R. Betzer, P. P. Power, *J. Am. Chem. Soc.* **2006**, *128*, 12498–12509.
- [78] L. Denker, B. Trzaskowski, R. Frank, *Chem. Commun.* **2021**, *57*, 2816–2819.
- [79] N. J. Hardman, A. D. Phillips, P. P. Power, *ACS Symp. Ser.* **2002**, *822*, 2.
- [80] J. Kretsch, A. Kreyenschmidt, T. Schillmöller, C. Sindlinger, R. Herbst-Irmer, D. Stalke, *Inorg. Chem.* **2021**, *60*, 7389–7398.
- [81] H. Li, Y. He, C. Liu, G. Tan, *Dalt. Trans.* **2021**, *50*, 12674–12680.

- [82] N. J. Hardman, B. E. Eichler, P. P. Power, *Chem. Commun.* **2000**, 1991–1992.
- [83] Y.-C. Tsai, *Coord. Chem. Rev.* **2012**, 256, 722–758.
- [84] L. Bourget-Merle, M. F. Lappert, J. R. Severn, *Chem. Rev.* **2002**, 102, 3031–3066.
- [85] D. Dange, S. L. Choong, C. Schenk, A. Stasch, C. Jones, *Dalt. Trans.* **2012**, 41, 9304–9315.
- [86] M. L. H. Green, P. Mountford, G. J. Smout, S. R. Speel, *Polyhedron* **1990**, 9, 2763–2765.
- [87] B. Schiemenz, P. P. Power, *Organometallics* **1996**, 15, 958–964.
- [88] B. Schiemenz, P. P. Power, *Angew. Chemie Int. Ed. English* **1996**, 35, 2150–2152.
- [89] D. L. Kays, *Chem. Soc. Rev.* **2016**, 45, 1004–1018.
- [90] S. K. Spitzmesser, V. C. Gibson, *J. Organomet. Chem.* **2003**, 673, 95–101.
- [91] N. D. Coombs, A. Stasch, A. Cowley, A. L. Thompson, S. Aldridge, *Dalt. Trans.* **2008**, 332–337.
- [92] A. Hinz, *Chem. – A Eur. J.* **2019**, 25, 3267–3271.
- [93] A. Hinz, *Angew. Chemie Int. Ed.* **2020**, 59, 19065–19069.
- [94] S. P. Green, C. Jones, A. Stasch, *Science (80-.)*. **2007**, 318, 1754–1757.
- [95] S. J. Bonyhady, D. Collis, G. Frenking, N. Holzmann, C. Jones, A. Stasch, *Nat. Chem.* **2010**, 2, 865–869.
- [96] C. Jones, *Nat. Rev. Chem.* **2017**, 1, 59.
- [97] J. Hicks, M. Juckel, A. Paparo, D. Dange, C. Jones, *Organometallics* **2018**, 37, 4810–4813.
- [98] X. Zhang, L. L. Liu, *Angew. Chemie Int. Ed.* **2022**, 61, e202116658.
- [99] X. Zhang, H. Wang, X. Lan, Y. Mei, D. Ruiz, *CCS Chem.* **2022**, 5, 1–20.
- [100] H. Zhu, J. Chai, H. Fan, H. W. Roesky, C. He, V. Jancik, H.-G. Schmidt, M. Noltemeyer, W. A. Merrill, P. P. Power, *Angew. Chemie Int. Ed.* **2005**, 44, 5090–5093.
- [101] C. Cui, S. Köpke, R. Herbst-Irmer, H. W. Roesky, M. Noltemeyer, H.-G. Schmidt, B. Wrackmeyer, *J. Am. Chem. Soc.* **2001**, 123, 9091–9098.
- [102] Q. Yu, L. Zhang, Y. He, J. Pan, H. Li, G. Bian, X. Chen, G. Tan, *Chem. Commun.* **2021**, 57, 9268–9271.
- [103] R. S. Mulliken, *J. Am. Chem. Soc.* **1950**, 72, 4493–4503.

- [104] K. S. Pitzer, *J. Am. Chem. Soc.* **1948**, *70*, 2140–2145.
- [105] C. Cui, H. W. Roesky, H.-G. Schmidt, M. Noltemeyer, *Angew. Chemie Int. Ed.* **2000**, *39*, 4531–4533.
- [106] N. J. Hardman, C. Cui, H. W. Roesky, W. H. Fink, P. P. Power, *Angew. Chemie Int. Ed.* **2001**, *40*, 2172–2174.
- [107] R. J. Wright, A. D. Phillips, T. L. Allen, W. H. Fink, P. P. Power, *J. Am. Chem. Soc.* **2003**, *125*, 1694–1695.
- [108] R. J. Wright, M. Brynda, J. C. Fettinger, A. R. Betzer, P. P. Power, *J. Am. Chem. Soc.* **2006**, *128*, 12498–12509.
- [109] D. W. N. N. Wilson, J. Feld, J. M. Goicoechea, *Angew. Chemie Int. Ed.* **2020**, *59*, 20914–20918.
- [110] M. K. Sharma, C. Wölper, G. Haberhauer, S. Schulz, *Angew. Chemie Int. Ed.* **2021**, *60*, 6784–6790.
- [111] T. Taeufer, F. Dankert, D. Michalik, J. Pospesch, J. Bresien, C. Hering-Junghans, *Chem. Sci.* **2023**, *14*, 3018–3023.
- [112] C. von Hänisch, O. Hampe, *Angew. Chemie Int. Ed.* **2002**, *41*, 2095–2097.
- [113] C. Helling, C. Wölper, S. Schulz, *J. Am. Chem. Soc.* **2018**, *140*, 5053–5056.
- [114] J. Schoening, L. John, C. Wölper, S. Schulz, *Dalt. Trans.* **2019**, *48*, 17729–17734.
- [115] C. Ganesamoorthy, C. Helling, C. Wölper, W. Frank, E. Bill, G. E. Cutsail, S. Schulz, *Nat. Commun.* **2018**, *9*, 87.
- [116] C. Helling, C. Wölper, Y. Schulte, G. E. I. I. I. Cutsail, S. Schulz, *Inorg. Chem.* **2019**, *58*, 10323–10332.
- [117] J. Feld, D. W. N. Wilson, J. M. Goicoechea, *Angew. Chemie Int. Ed.* **2021**, *60*, 22057–22061.
- [118] M. K. Sharma, C. Wölper, G. Haberhauer, S. Schulz, *Angew. Chemie Int. Ed.* **2021**, *60*, 21784–21788.
- [119] B. Li, C. Wölper, G. Haberhauer, S. Schulz, *Angew. Chemie Int. Ed.* **2021**, *60*, 1986–1991.
- [120] J. Krüger, C. Wölper, S. Schulz, *Angew. Chemie Int. Ed.* **2021**, *60*, 3572–3575.
- [121] P. P. Power, *Nature* **2010**, *463*, 171–177.
- [122] F. Dankert, C. Hering-Junghans, *Chem. Commun.* **2022**, *58*, 1242–1262.

- [123] C. Weetman, *Chem. – A Eur. J.* **2021**, *27*, 1941–1954.
- [124] P. P. Power, *Chem. Rec.* **2012**, *12*, 238–255.
- [125] T. Chu, G. I. Nikonov, *Chem. Rev.* **2018**, *118*, 3608–3680.
- [126] J. M. Goicoechea, H. Grützmacher, *Angew. Chemie Int. Ed.* **2018**, *57*, 16968–16994.
- [127] F. F. Puschmann, D. Stein, D. Heift, C. Hendriksen, Z. A. Gal, H.-F. Grützmacher, H. Grützmacher, *Angew. Chemie Int. Ed.* **2011**, *50*, 8420–8423.
- [128] Y. Mei, J. E. Borger, D.-J. Wu, H. Grützmacher, *Dalt. Trans.* **2019**, *48*, 4370–4374.
- [129] D. W. N. Wilson, W. K. Myers, J. M. Goicoechea, *Dalt. Trans.* **2020**, *49*, 15249–15255.
- [130] D. Duvinage, M. Janssen, E. Lork, H. Grützmacher, S. Mebs, J. Beckmann, *Dalt. Trans.* **2022**, *51*, 7622–7629.
- [131] C. Barnett, M. L. Cole, J. B. Harper, *Eur. J. Inorg. Chem.* **2021**, *2021*, 4954–4958.
- [132] N. Del Rio, A. Baceiredo, N. Saffon-Merceron, D. Hashizume, D. Lutters, T. Müller, T. Kato, *Angew. Chemie Int. Ed.* **2016**, *55*, 4753–4758.
- [133] Y. Wu, L. L. Liu, J. Su, J. Zhu, Z. Ji, Y. Zhao, *Organometallics* **2016**, *35*, 1593–1596.
- [134] S. Yao, Y. Xiong, T. Szilvási, H. Grützmacher, M. Driess, *Angew. Chemie Int. Ed.* **2016**, *55*, 4781–4785.
- [135] A. Hinz, J. M. Goicoechea, *Chem. – A Eur. J.* **2018**, *24*, 7358–7363.
- [136] C. Li, A. Hinz, *Chem. – An Asian J.* **2023**, *18*, e202300698.
- [137] Y. Xiong, S. Yao, T. Szilvási, E. Ballester, H. Grützmacher, M. Driess, *Angew. Chemie Int. Ed.* **2017**, *56*, 4333–4336.
- [138] D. C. H. Do, A. V. Protchenko, P. Vasko, J. Campos, E. L. Kolychev, S. Aldridge, *Zeitschrift für Anorg. und Allg. Chemie* **2018**, *644*, 1238–1242.
- [139] A. Doddi, D. Bockfeld, T. Bannenberg, P. G. Jones, M. Tamm, *Angew. Chemie Int. Ed.* **2014**, *53*, 13568–13572.
- [140] F. Uhlig, R. Hummeltenberg, *J. Organomet. Chem.* **1993**, *452*, C9–C10.
- [141] R. Szlosek, M. Seidl, G. Balázs, M. Scheer, *Chem. – A Eur. J.* **2023**, *29*, e202301752.
- [142] P. Pyykkö, M. Atsumi, *Chemistry* **2009**, *15*, 12770–12779.
- [143] M. Matar, S. Schulz, U. Flörke, *Zeitschrift für Anorg. und Allg. Chemie* **2007**, *633*, 162–165.
- [144] A. Seifert, G. Linti, *Inorg. Chem.* **2008**, *47*, 11398–11404.

- [145] P. Jutzi, B. Neumann, G. Reumann, H.-G. Stammler, *Organometallics* **1998**, *17*, 1305–1314.
- [146] M. Kaupp, D. Danovich, S. Shaik, *Coord. Chem. Rev.* **2017**, *344*, 355–362.
- [147] K. Morokuma, *J. Chem. Phys.* **1971**, *55*, 1236–1244.
- [148] A. Michalak, M. Mitoraj, T. Ziegler, *J. Phys. Chem. A* **2008**, *112*, 1933–1939.
- [149] L. Zhao, M. von Hopffgarten, D. M. Andrada, G. Frenking, *WIREs Comput. Mol. Sci.* **2018**, *8*, e1345.
- [150] T. Kodama, N. Mukai, M. Tobisu, *Inorg. Chem.* **2023**, *62*, 6554–6559.
- [151] M. Asay, C. Jones, M. Driess, *Chem. Rev.* **2011**, *111*, 354–396.
- [152] G. Szigethy, A. F. Heyduk, *Dalt. Trans.* **2012**, *41*, 8144–8152.
- [153] F. Dankert, M. Fischer, C. Hering-Junghans, *Dalt. Trans.* **2022**, *51*, 11267–11276.
- [154] D. Heift, Z. Benkő, H. Grützmacher, *Dalt. Trans.* **2014**, *43*, 831–840.
- [155] A. El-Hellani, J. Monot, S. Tang, R. Guillot, C. Bour, V. Gandon, *Inorg. Chem.* **2013**, *52*, 11493–11502.
- [156] S. Kundu, S. Sinhababu, M. M. Siddiqui, A. V Luebben, B. Dittrich, T. Yang, G. Frenking, H. W. Roesky, *J. Am. Chem. Soc.* **2018**, *140*, 9409–9412.
- [157] R. J. Baker, H. Bettentrup, C. Jones, *Eur. J. Inorg. Chem.* **2003**, *2003*, 2446–2451.

7. Appendix

7.1. NMR Spectra

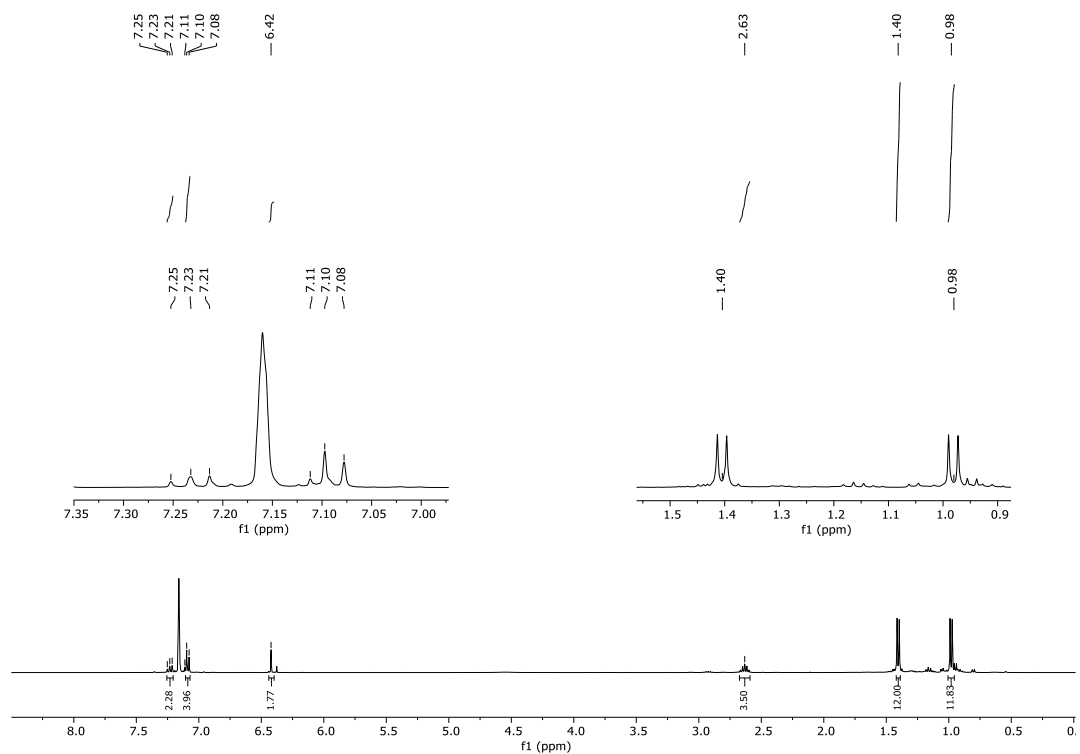


Figure 11. ^1H NMR (400 MHz, C_6D_6 , 300K) spectrum of IDip-GaH₂(PCO) **119**.

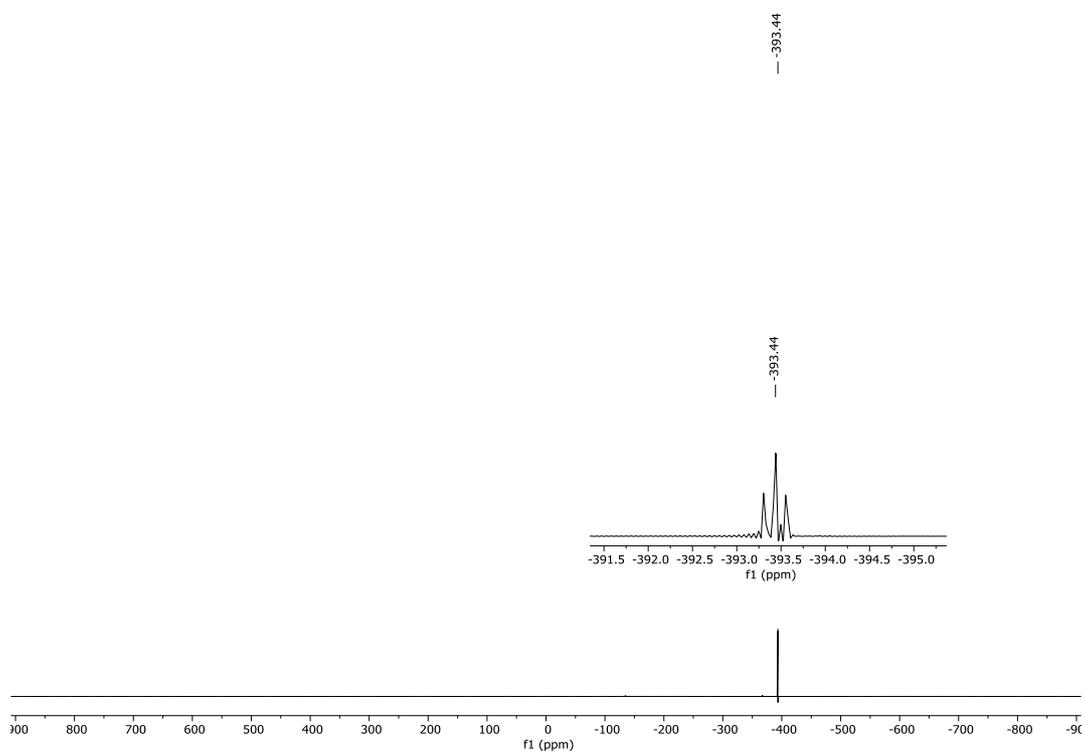


Figure 12. ^{31}P NMR (400 MHz, C_6D_6 , 300K) spectrum of IDip-GaH₂(PCO) **119**.

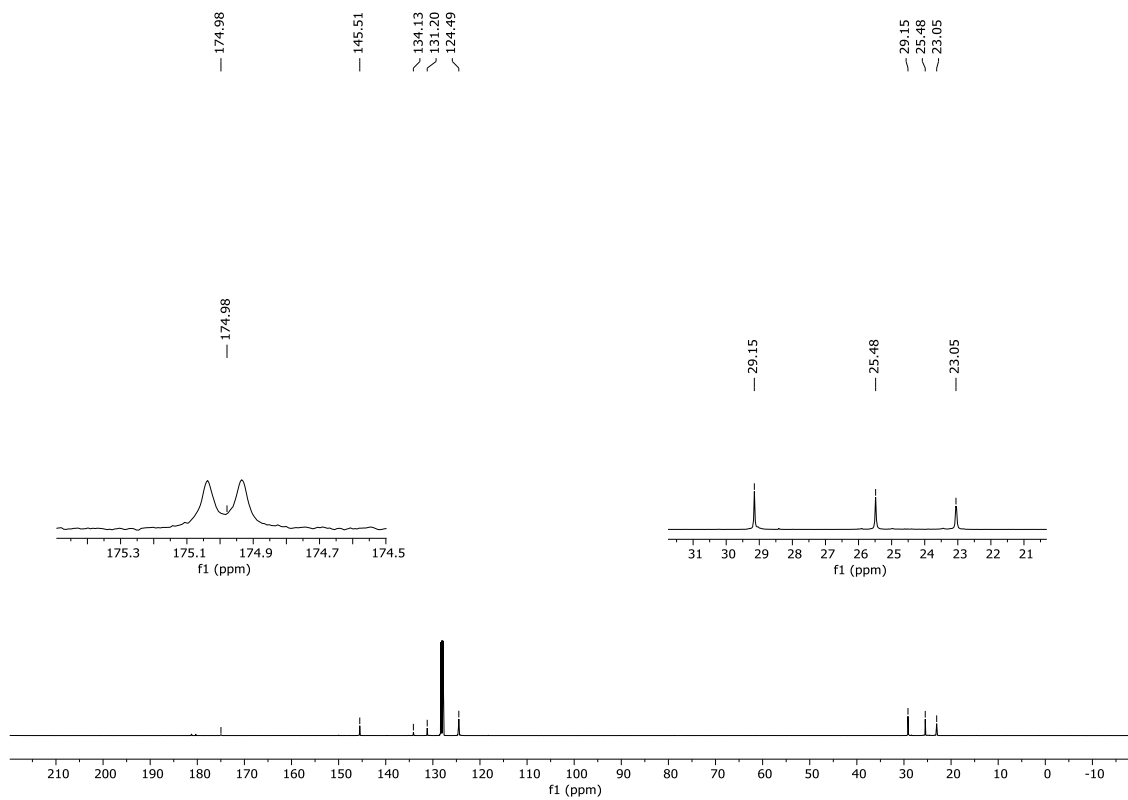


Figure 13. ^{13}C NMR (400 MHz, C_6D_6 , 300K) spectrum of IDip-GaH₂(PCO) **119**.

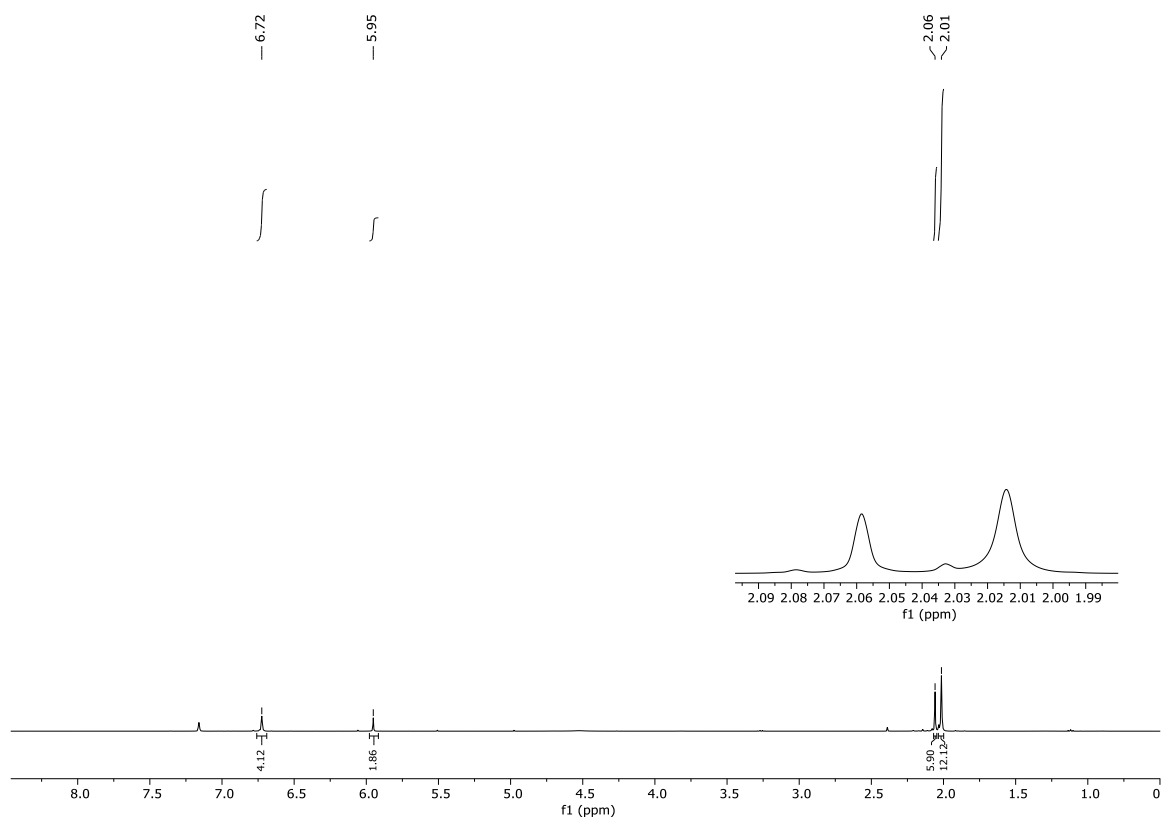


Figure 14. ^1H NMR (400 MHz, C_6D_6 , 300K) spectrum of IMes-GaH₂(PCO) **120**.

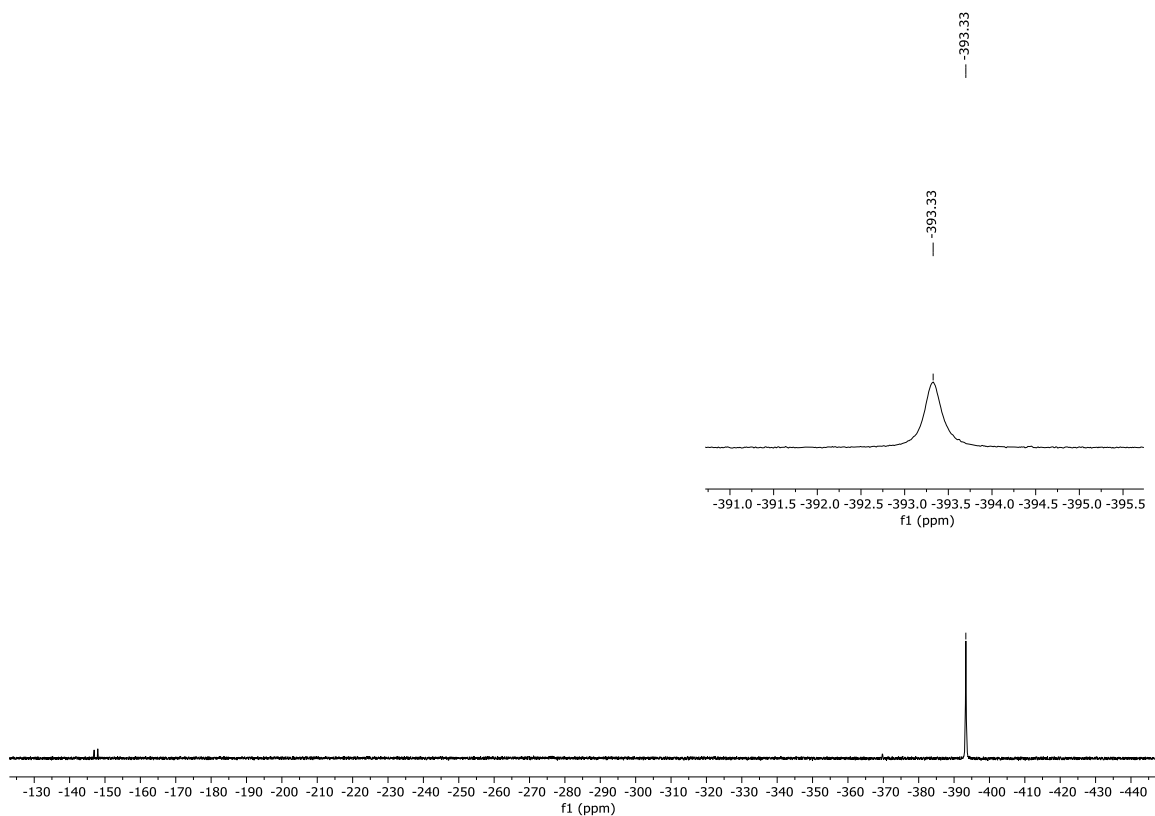


Figure 15. ^{31}P NMR (400 MHz, C_6D_6 , 300K) spectrum of IMes-GaH₂(PCO) **120**.

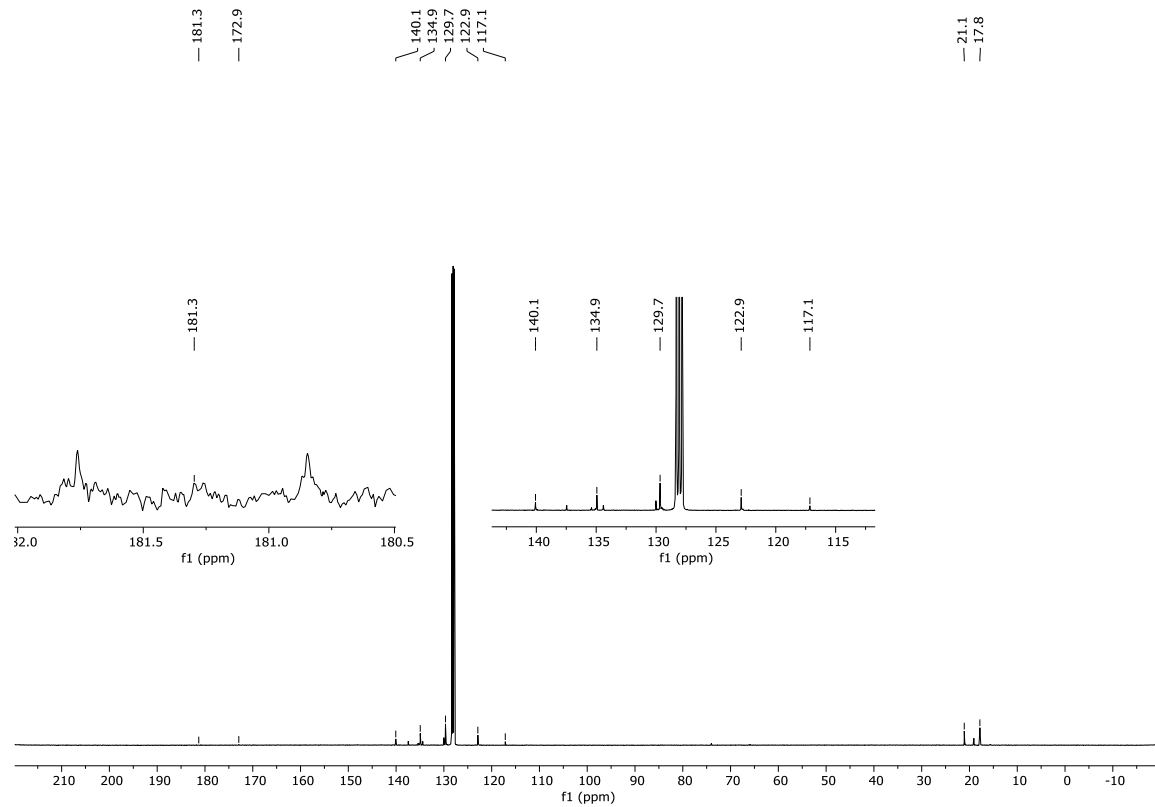


Figure 16. ^{13}C NMR (400 MHz, C_6D_6 , 300K) spectrum of IMes-GaH₂(PCO) **120**.

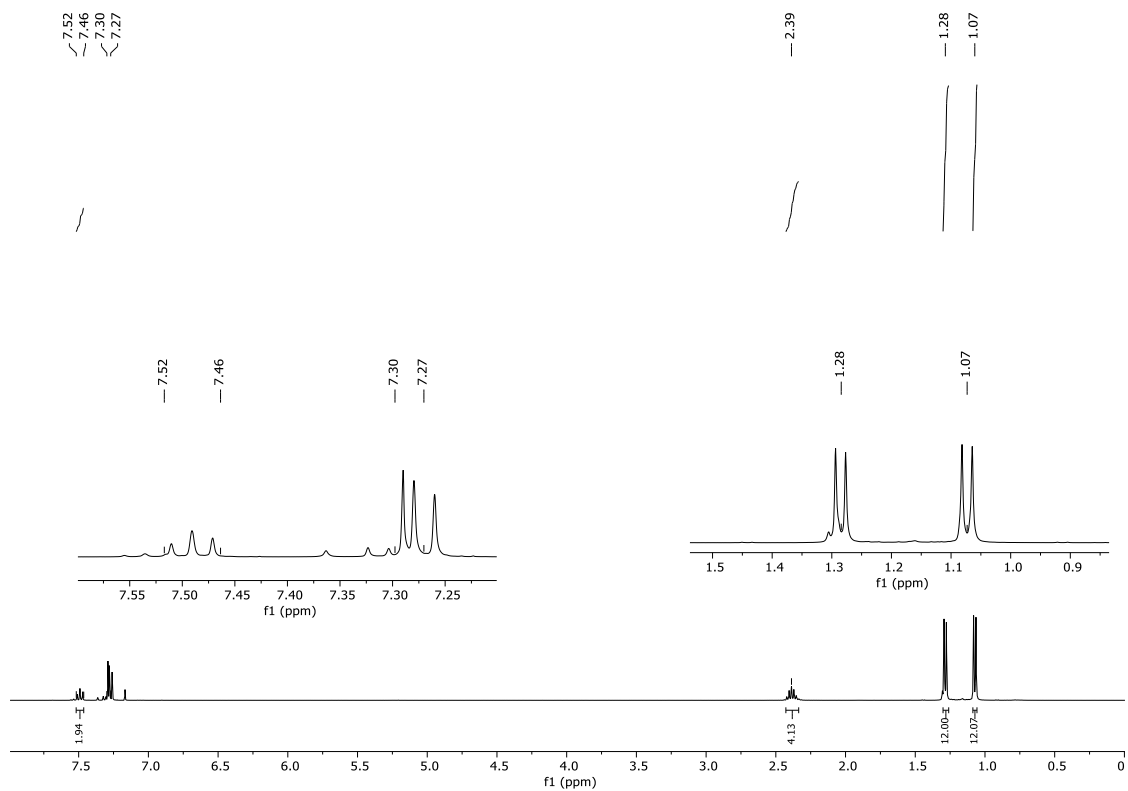


Figure 17. ^1H NMR (400 MHz, CDCl_3 , 300K) spectrum of IDip-GaCl₂(OTf) **121**.

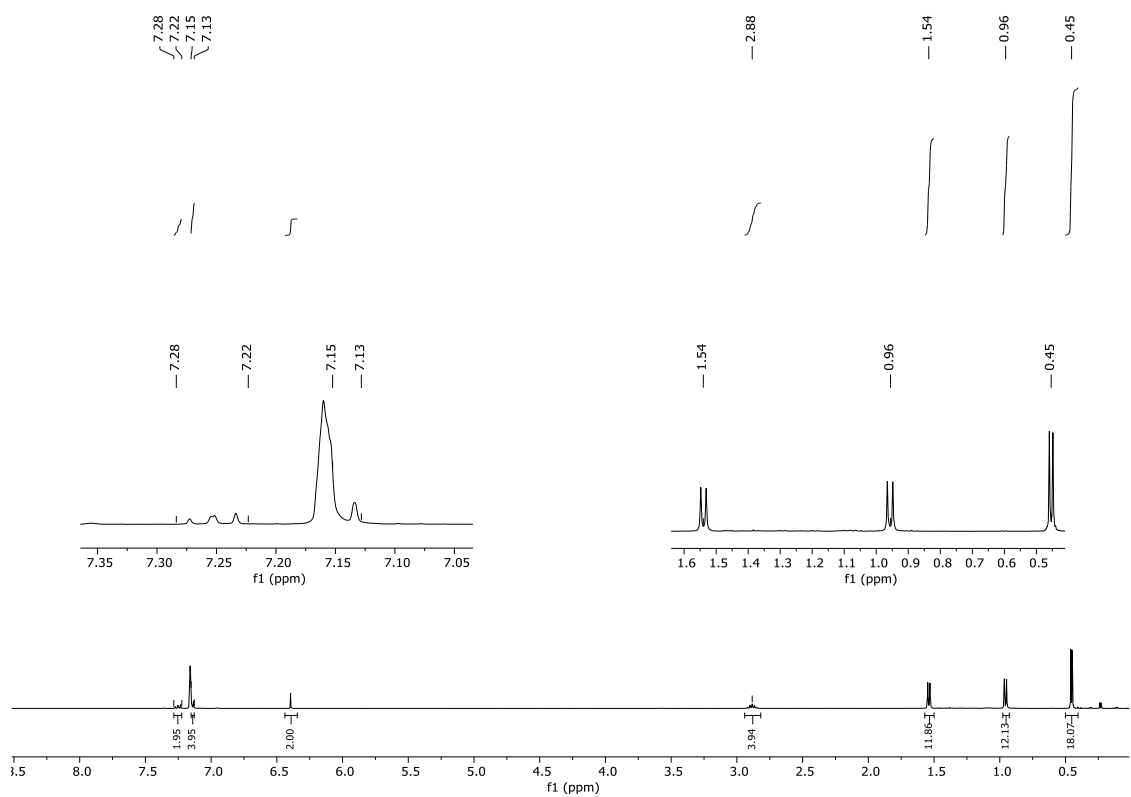


Figure 18. ^1H NMR (400 MHz, C_6D_6 , 300K) spectrum of IDip-GaCl₂P(TMS)₂ **122**.

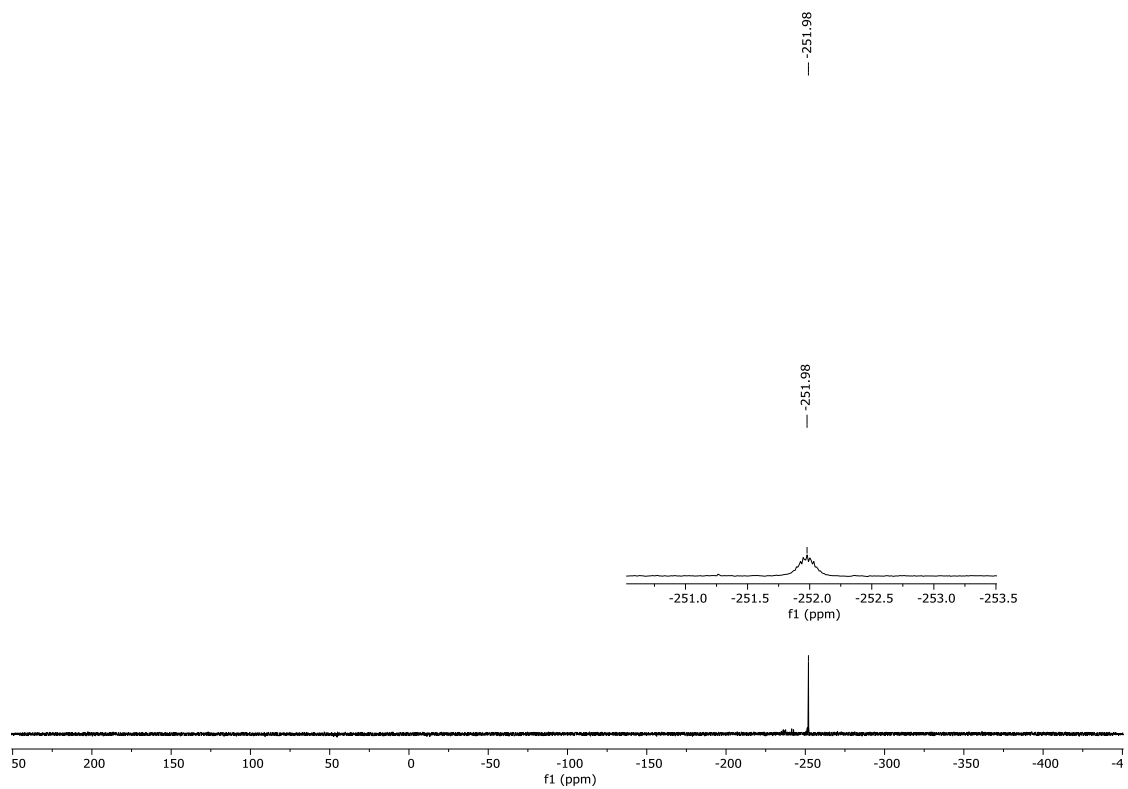


Figure 19. ^{31}P NMR (400 MHz, C_6D_6 , 300K) spectrum of IDip-GaCl₂P(TMS)₂ **122**.

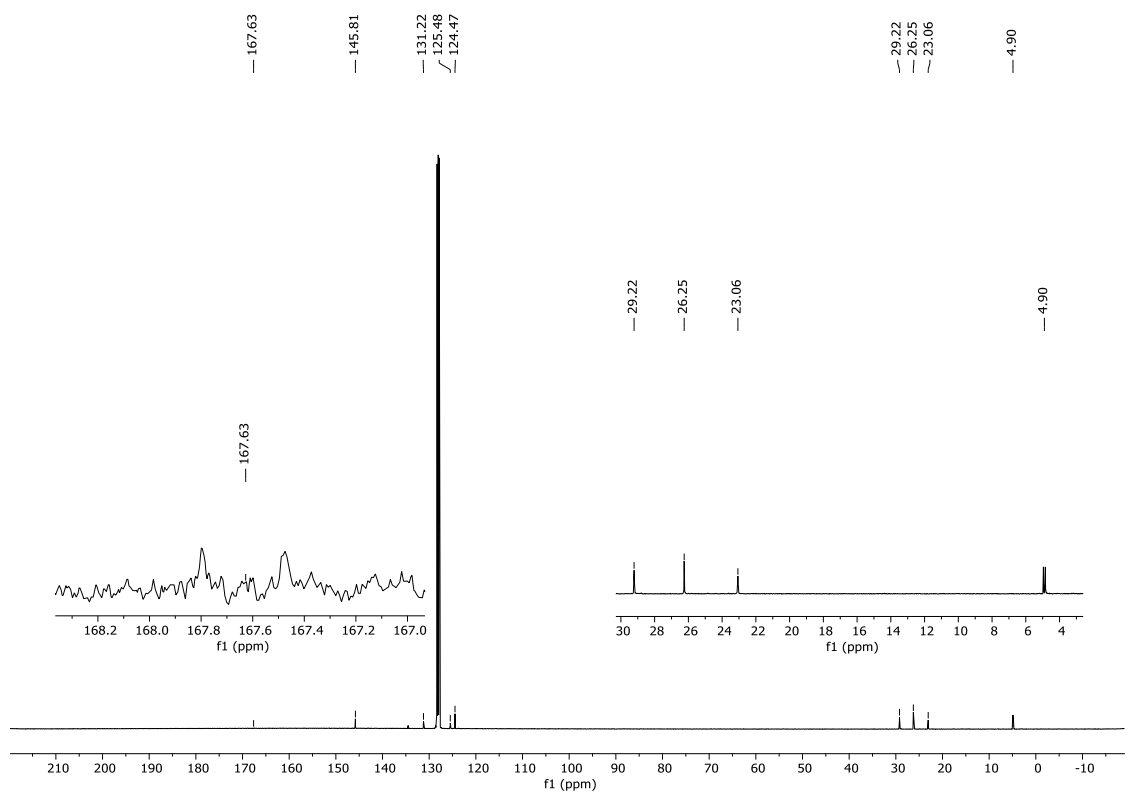


Figure 20. ^{13}C NMR (400 MHz, C_6D_6 , 300K) spectrum of IDip-GaCl₂P(TMS)₂ **122**.

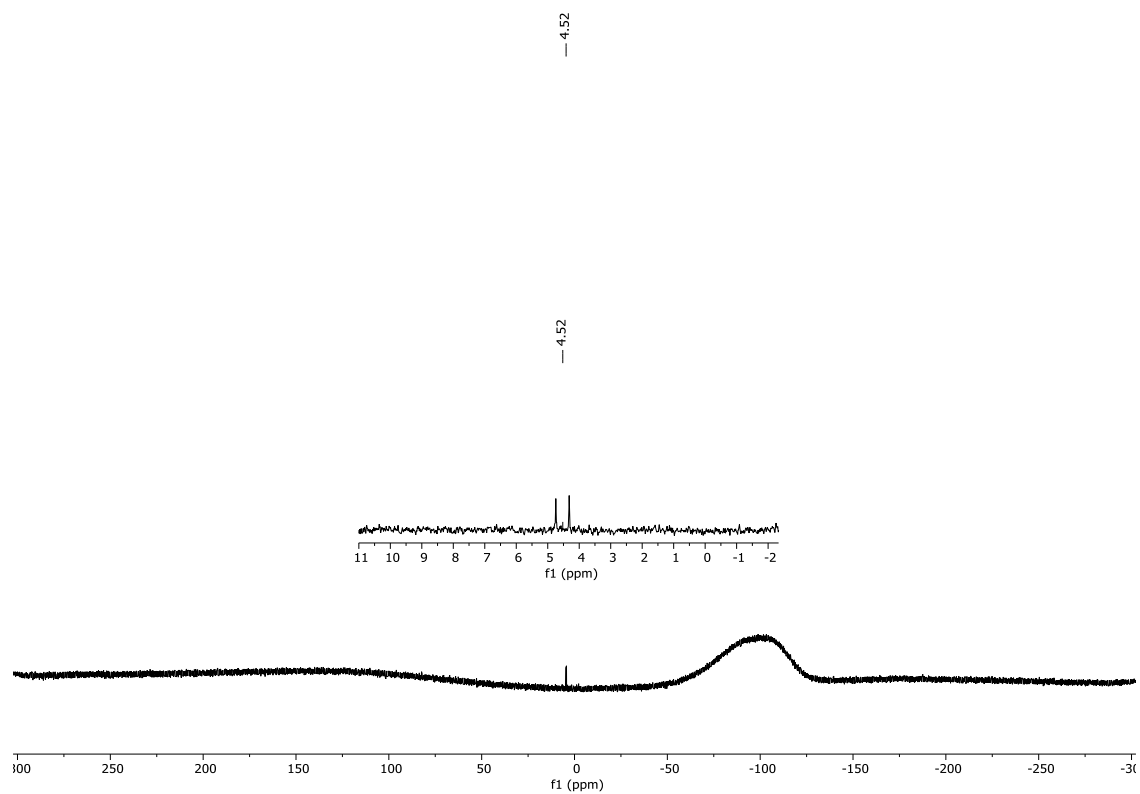


Figure 21. ^{29}Si NMR (400 MHz, C_6D_6 , 300K) spectrum of IDip-GaCl₂P(TMS)₂ **122**.

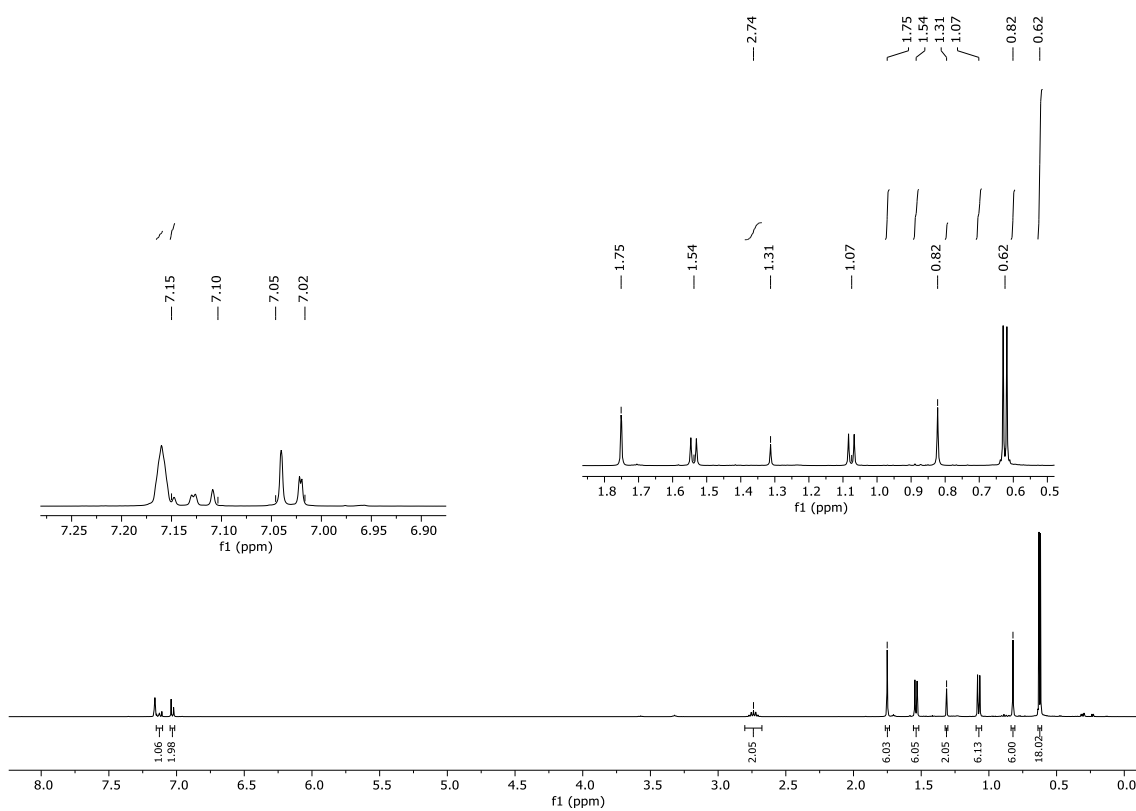


Figure 22. ^1H NMR (400 MHz, C_6D_6 , 300K) spectrum of $\text{Me}_2\text{CAAC-GaCl}_2\text{P(TMS)}_2$ **123**.

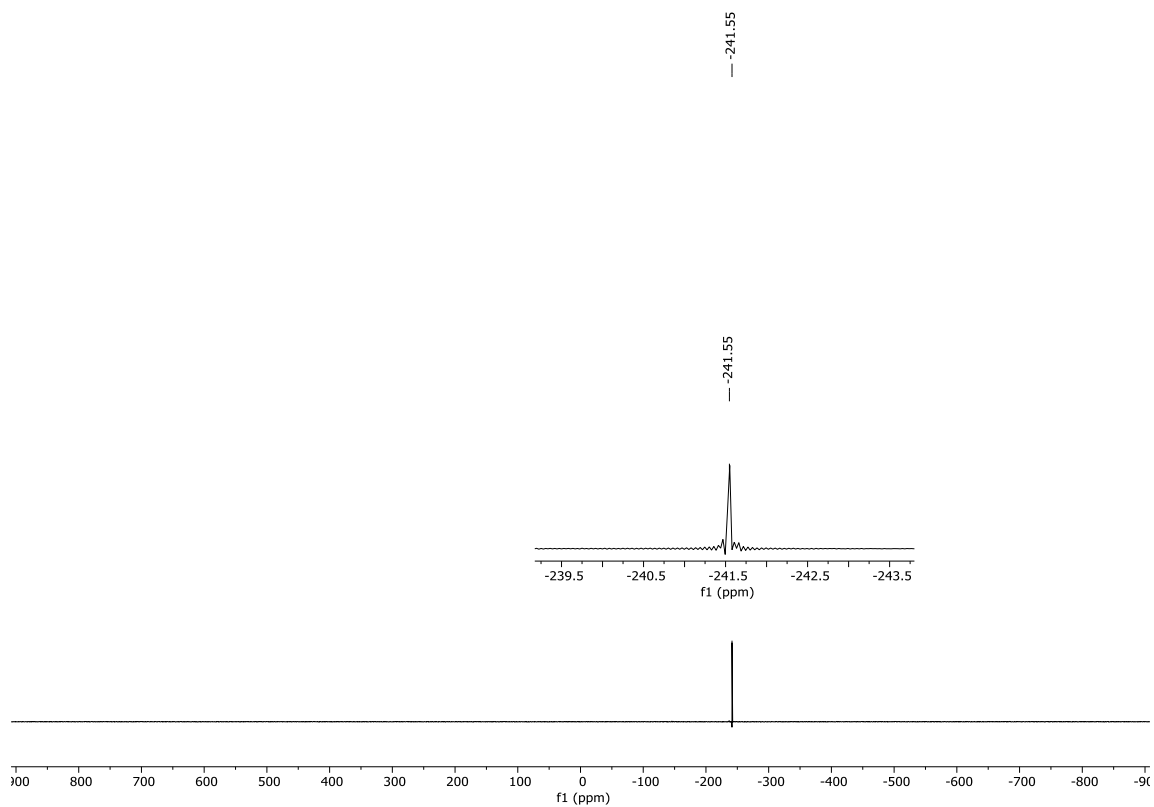


Figure 23. ^{31}P NMR (400 MHz, C_6D_6 , 300K) spectrum of $\text{Me}_2\text{CAAC-GaCl}_2\text{P(TMS)}_2$ **123**.

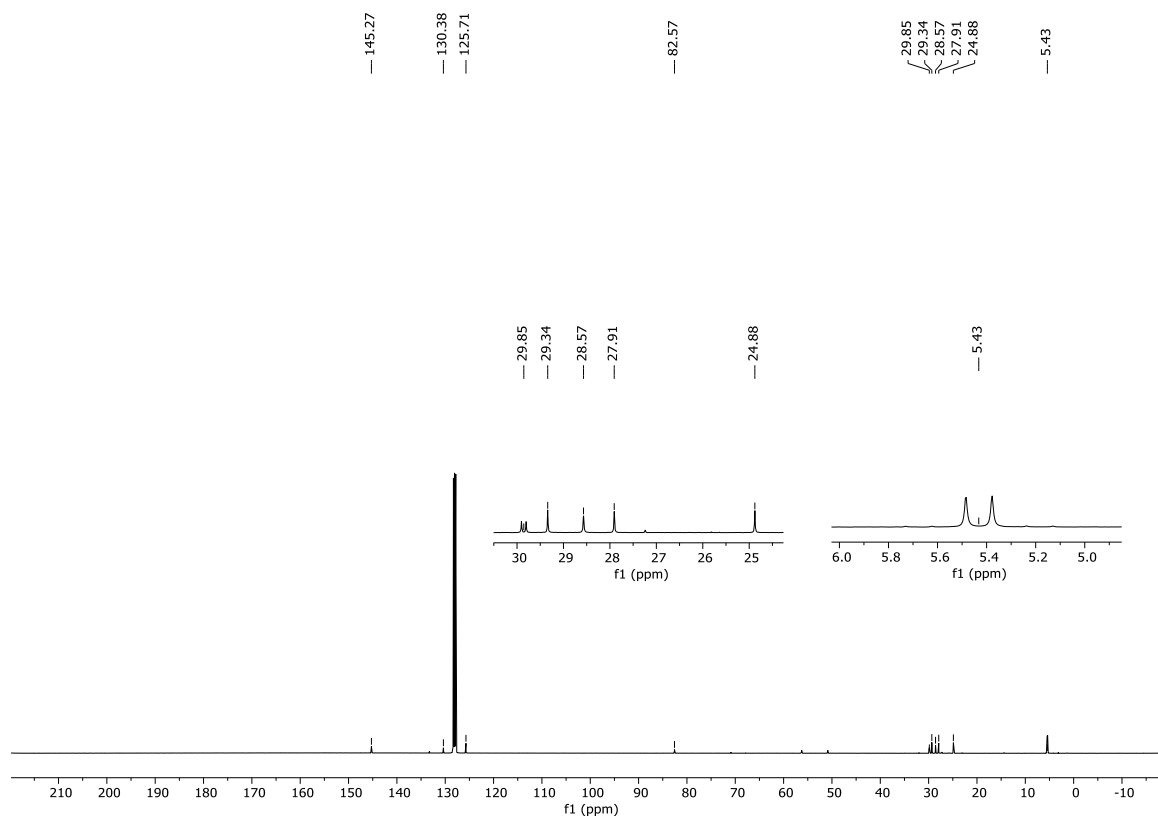


Figure 24. ^{13}C NMR (400 MHz, C_6D_6 , 300K) spectrum of $\text{Me}_2\text{CAAC-GaCl}_2\text{P(TMS)}_2$ **123**.

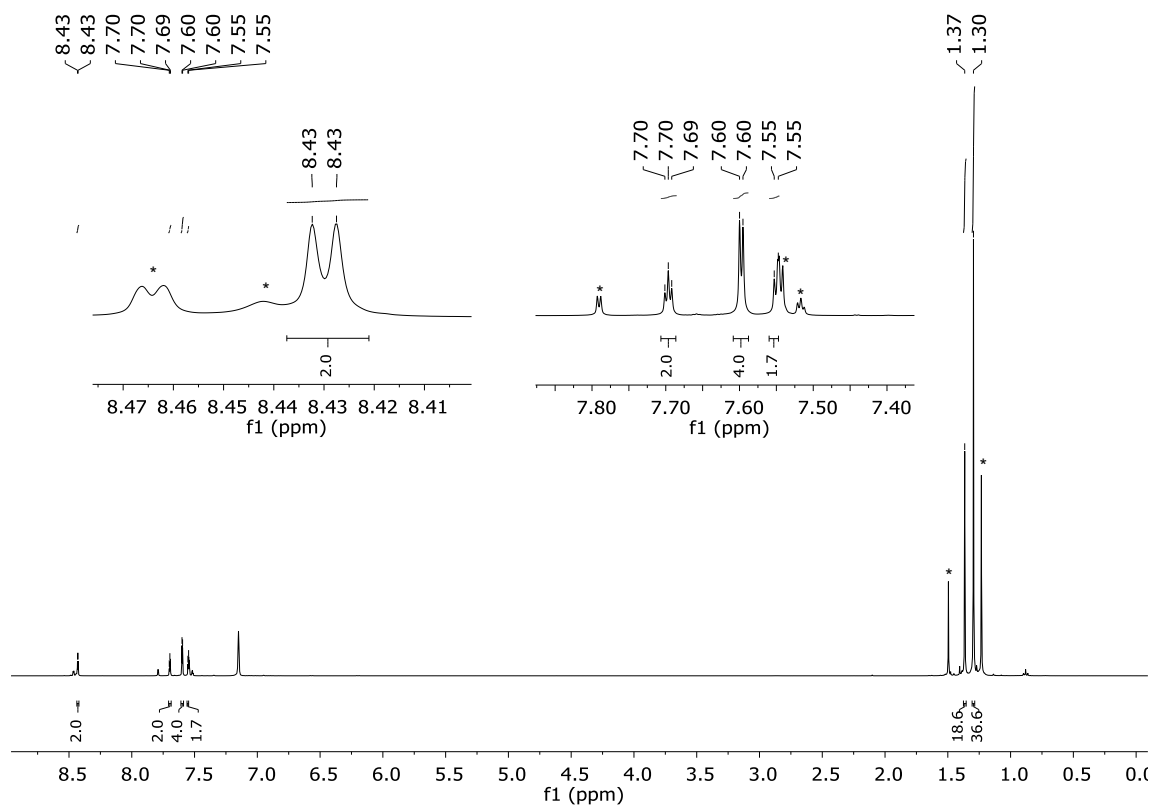


Figure 25. ^1H NMR (400 MHz, C_6D_6 , 300K) spectrum of L-Gal₂ **124**. (* Free ligand L-H)

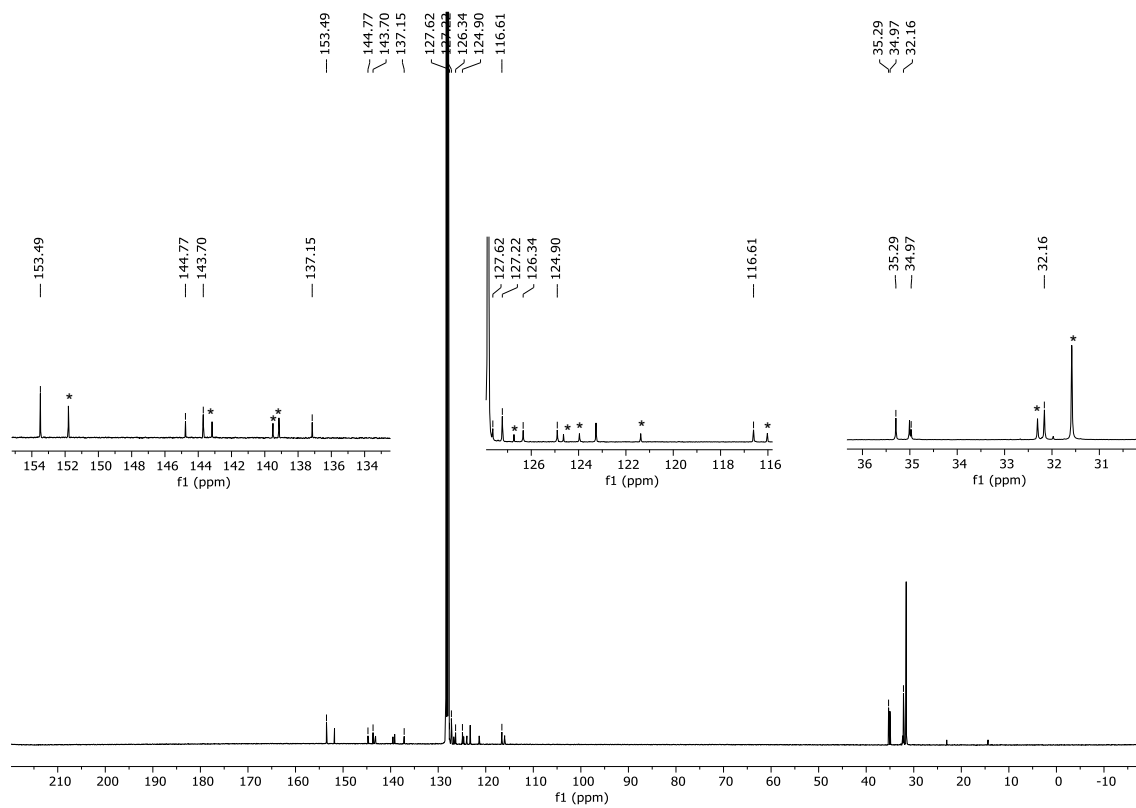


Figure 26. ^{13}C NMR (400 MHz, C_6D_6 , 300K) spectrum of L-Gal₂ **124**.

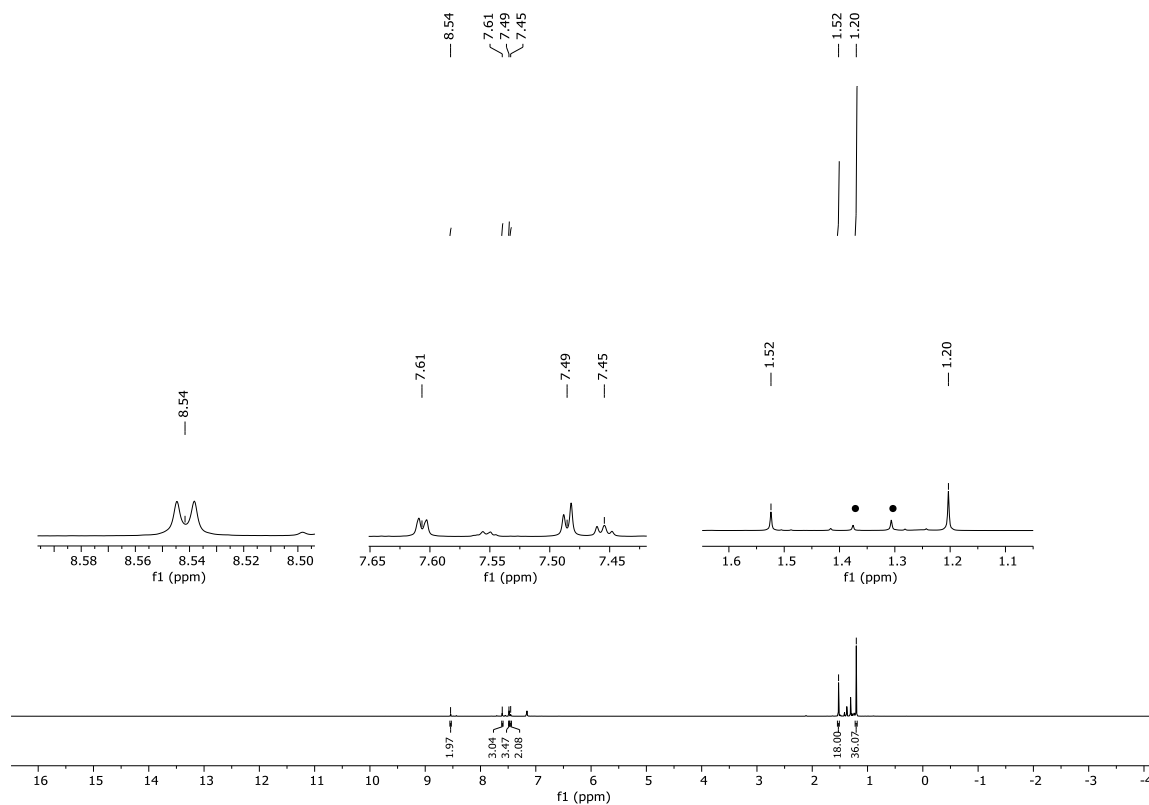


Figure 27. ^1H NMR (400 MHz, C_6D_6 , 300K) spectrum of L-Ga **125**. (• L-Gal₂)

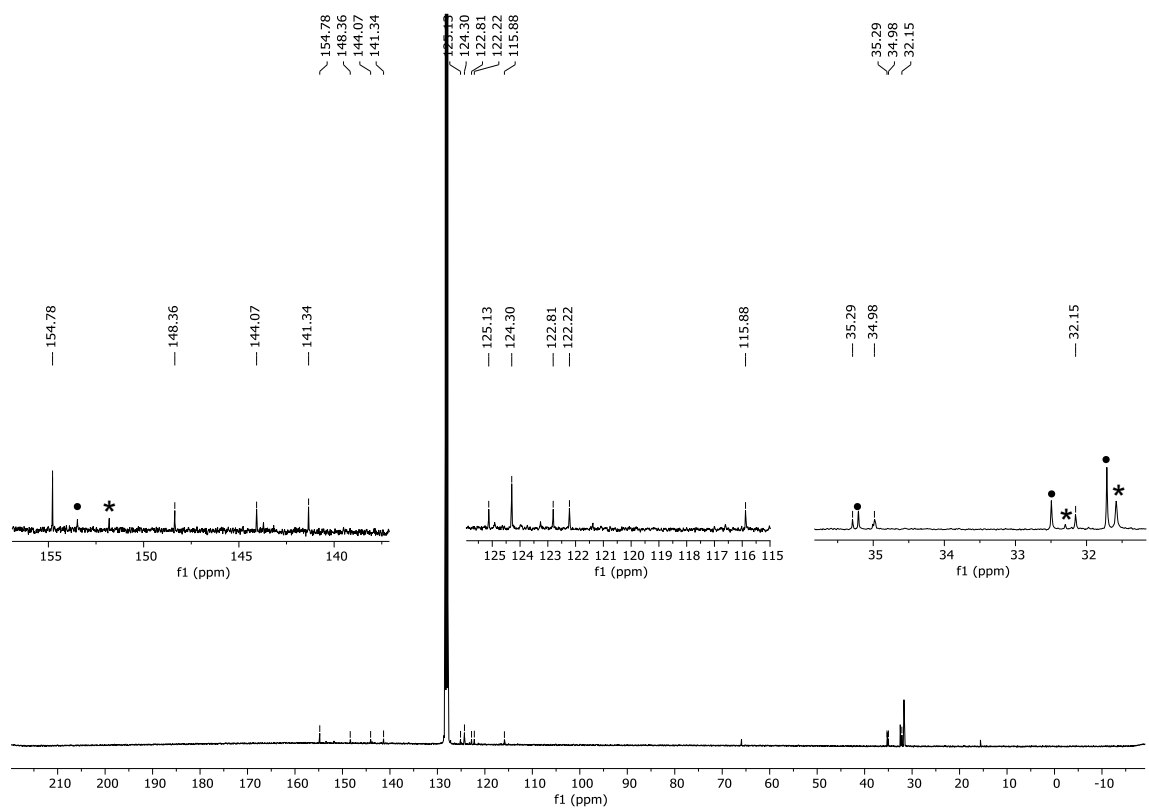


Figure 28. ^{13}C NMR (400 MHz, C_6D_6 , 300K) spectrum of L-Ga **125**. (• L-Gal₂, * L-H)

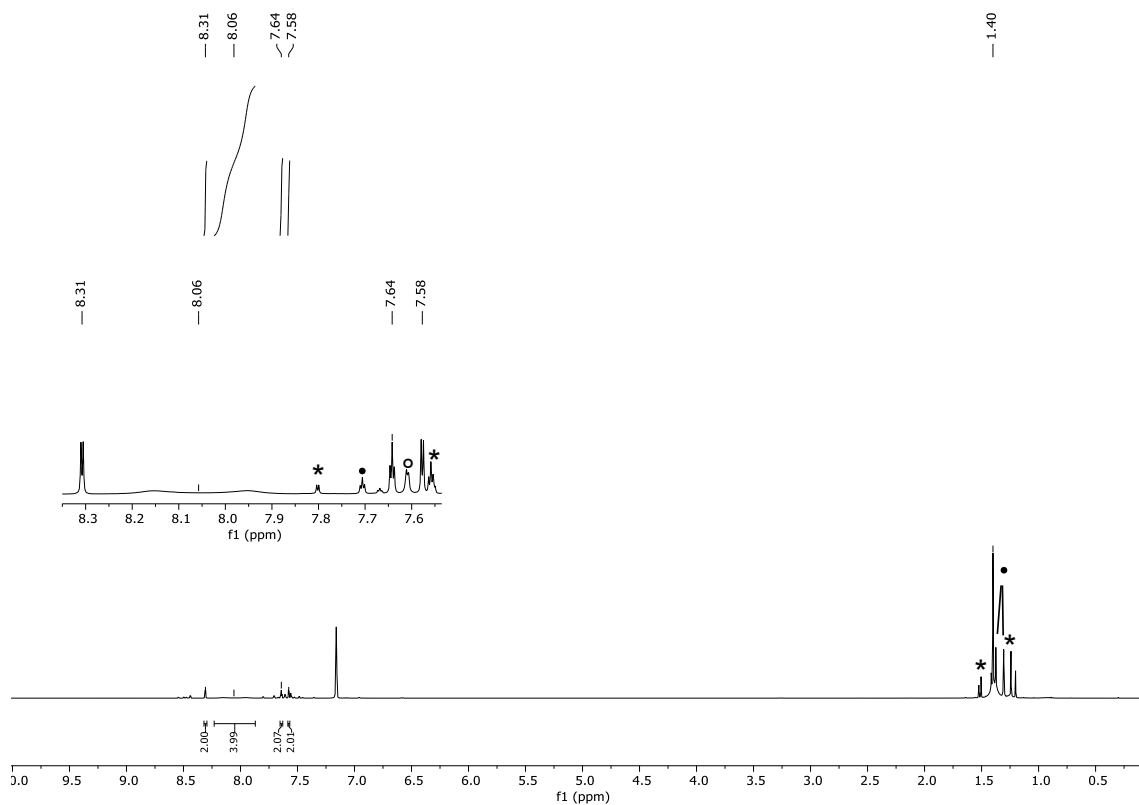


Figure 29. ^1H NMR (400 MHz, C_6D_6 , 300K) spectrum of L-GaCr(CO)₅ **126**. (• L-GaI2, * L-H, ○ L-Ga)

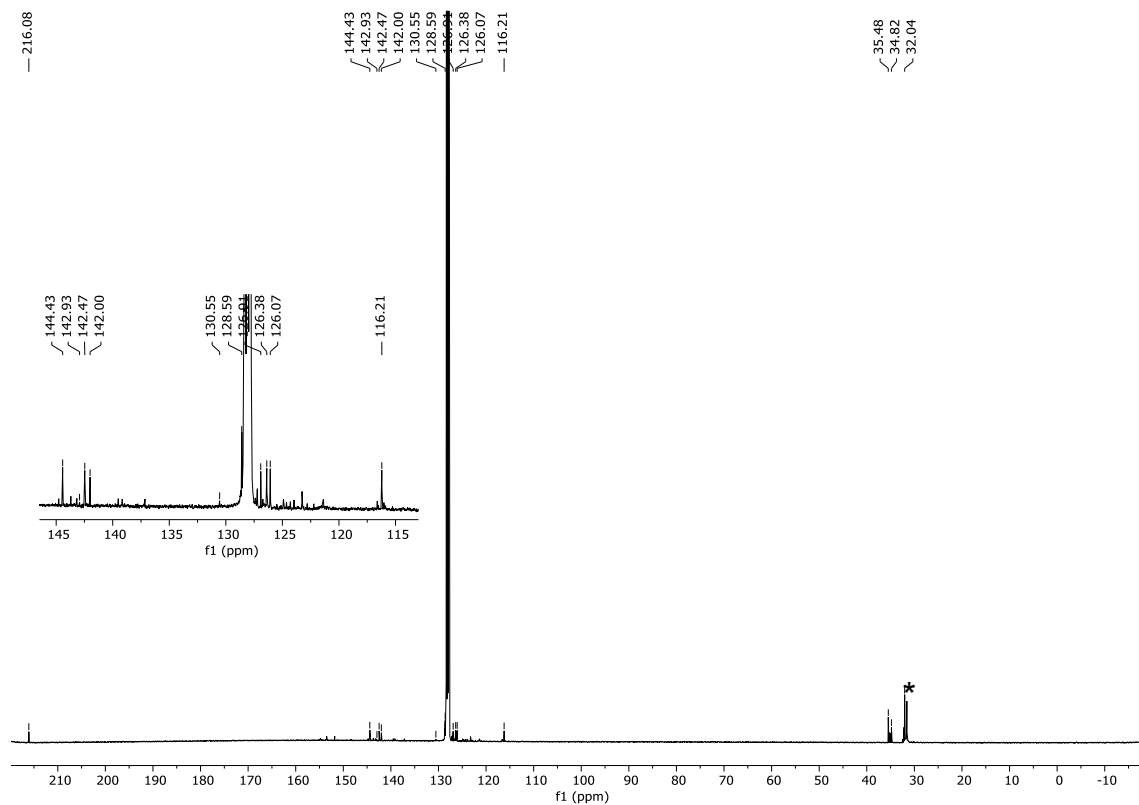


Figure 30. ^{13}C NMR (400 MHz, C_6D_6 , 300K) spectrum of L-GaCr(CO)₅ **126**. (* L-H)

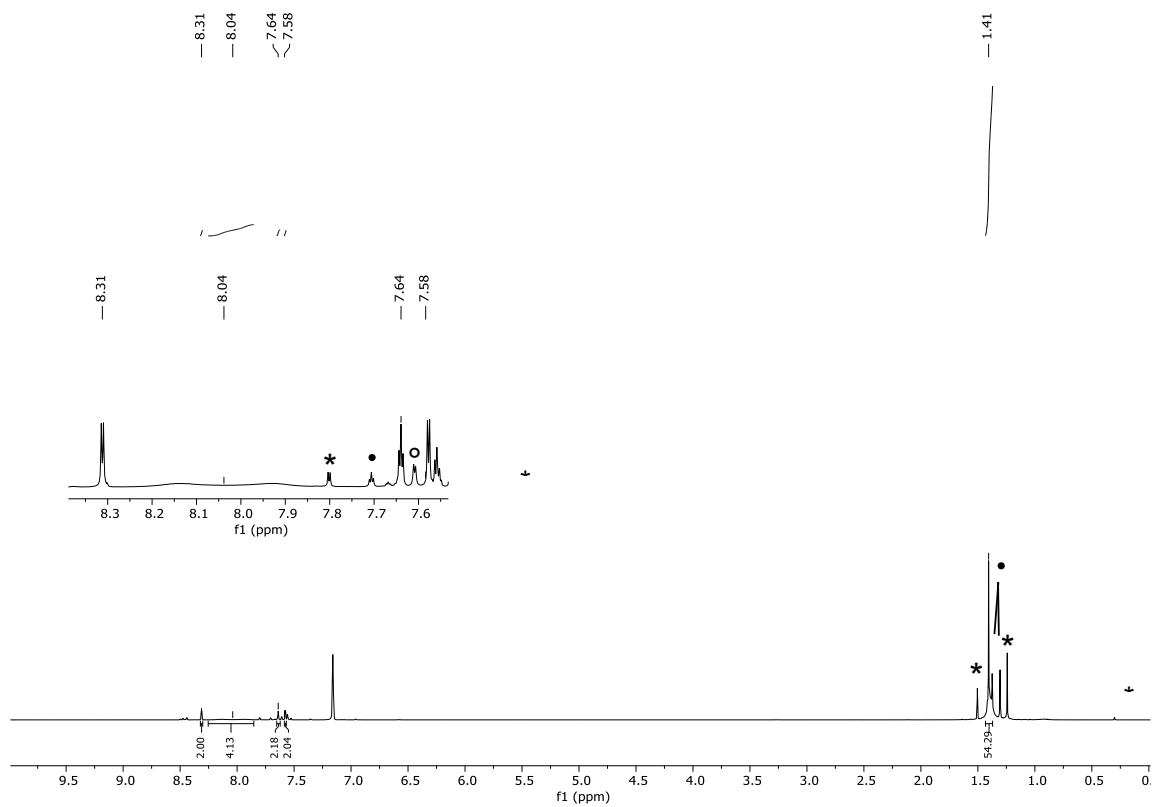


Figure 31. ^1H NMR (400 MHz, C_6D_6 , 300K) spectrum of L-GaMo(CO)₅ 127. (• L-Ga₂, * L-H, ○ L-Ga)

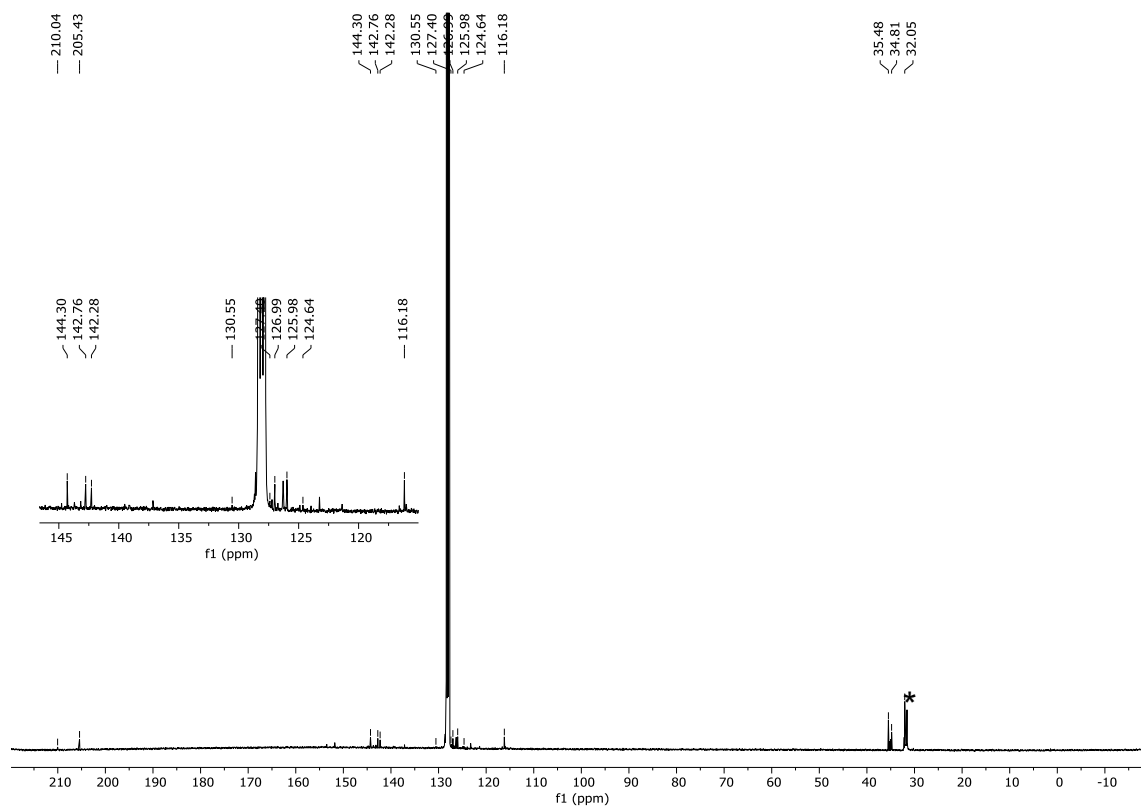


Figure 32. ^{13}C NMR (400 MHz, C_6D_6 , 300K) spectrum of L-GaMo(CO)₅ 127. (* L-H)

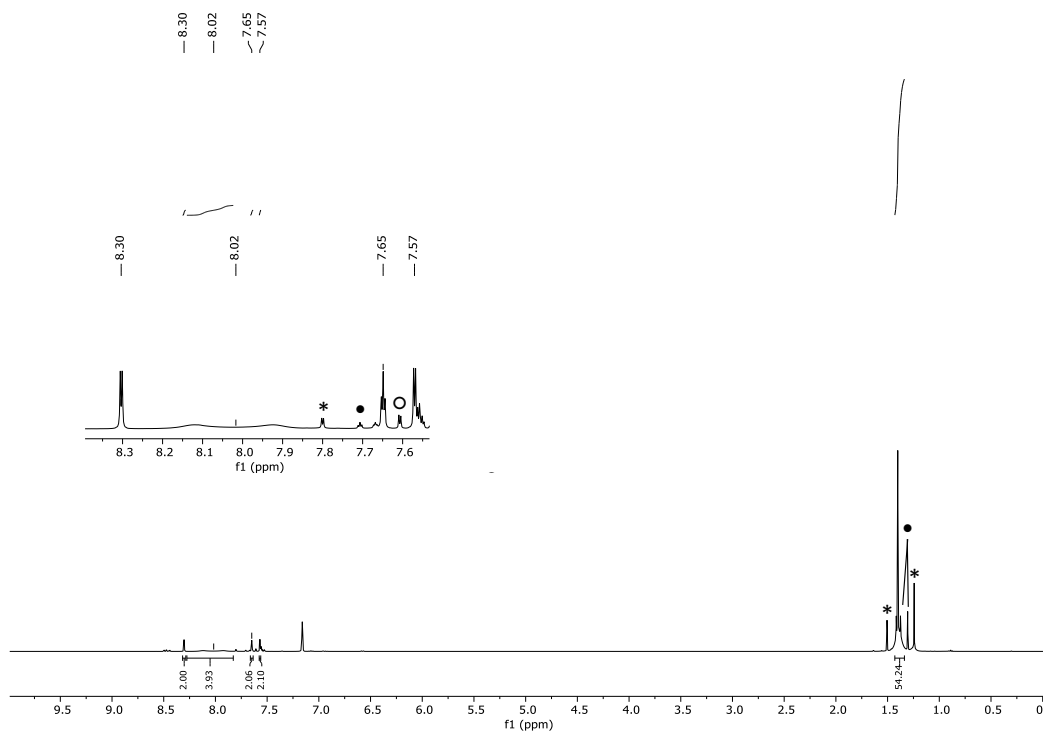


Figure 33. ^1H NMR (400 MHz, C_6D_6 , 300K) spectrum of L-GaW(CO)₅ **128**. (• L-Gal₂, * L-H, ○ L-Ga)

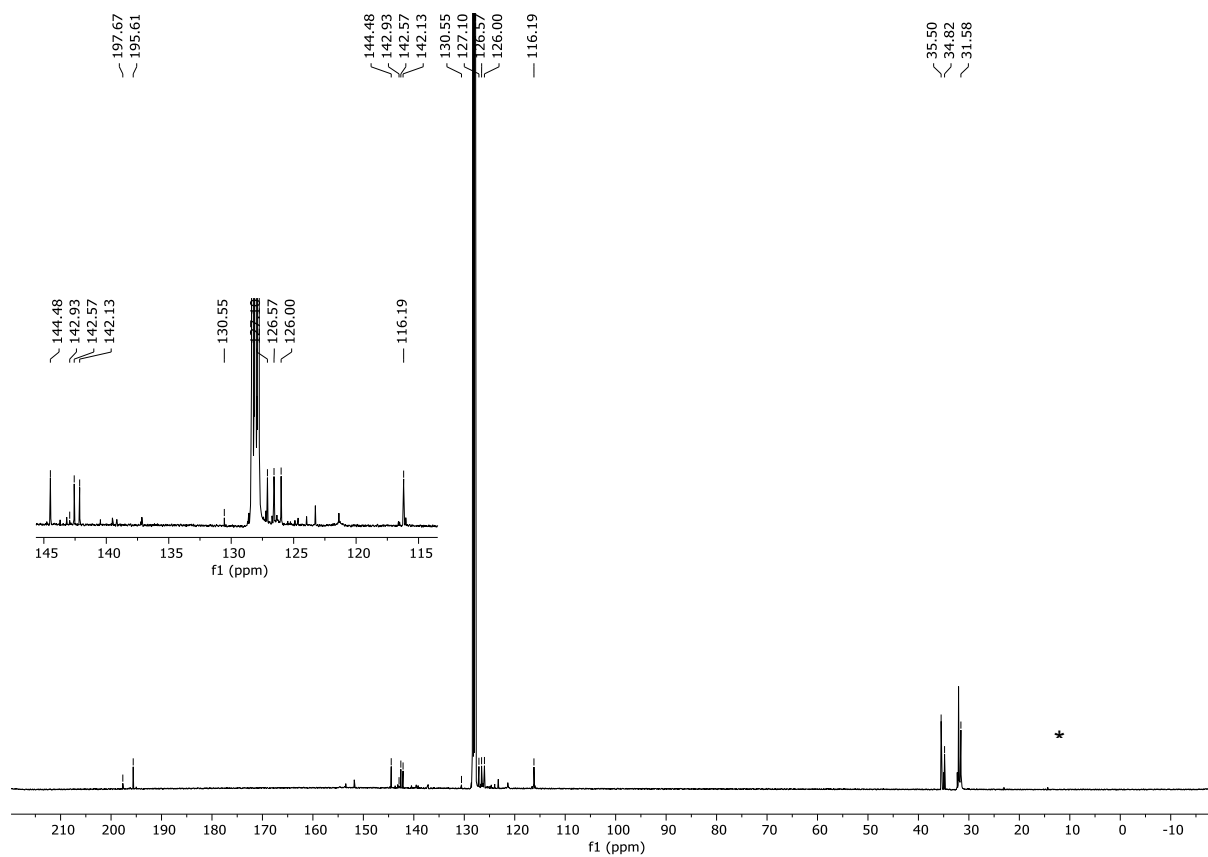


Figure 34. ^{13}C NMR (400 MHz, C_6D_6 , 300K) spectrum of L-GaW(CO)₅ **128**. (* L-H)

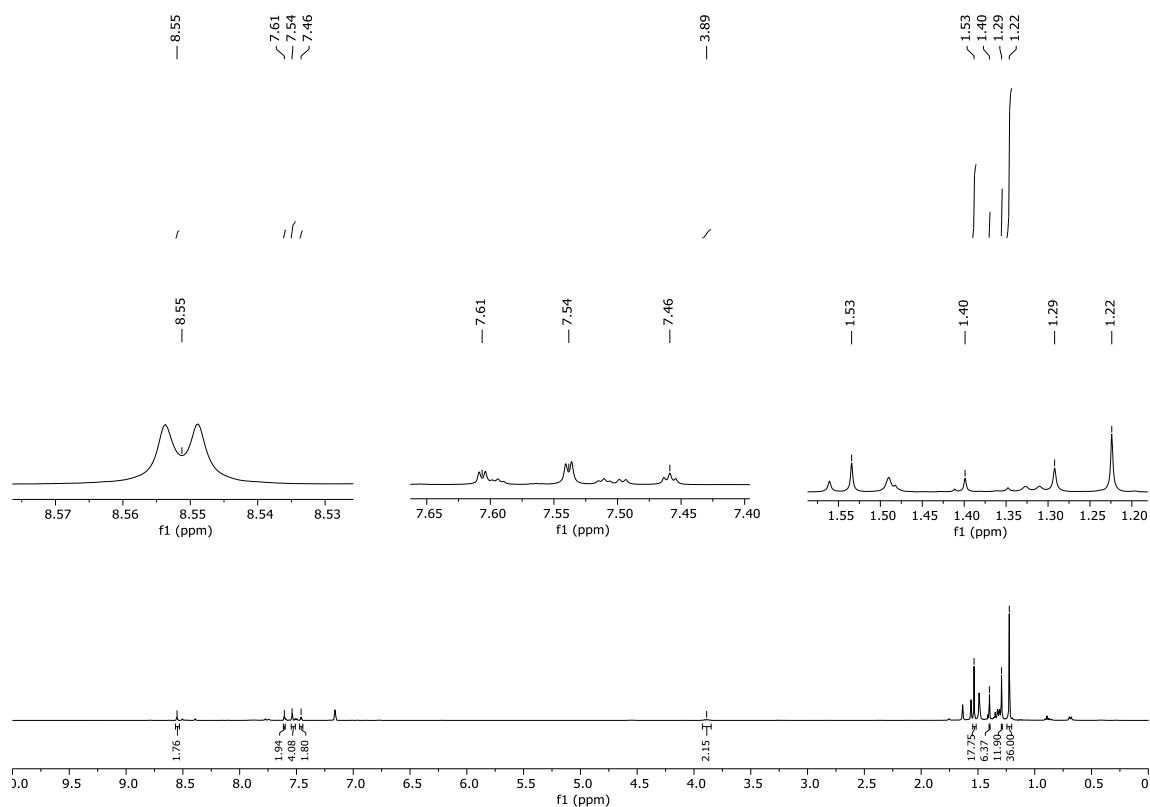


Figure 35. ^1H NMR (400 MHz, C_6D_6 , 300K) spectrum of L-Ga(I'Pr₂Me₂) **129**.

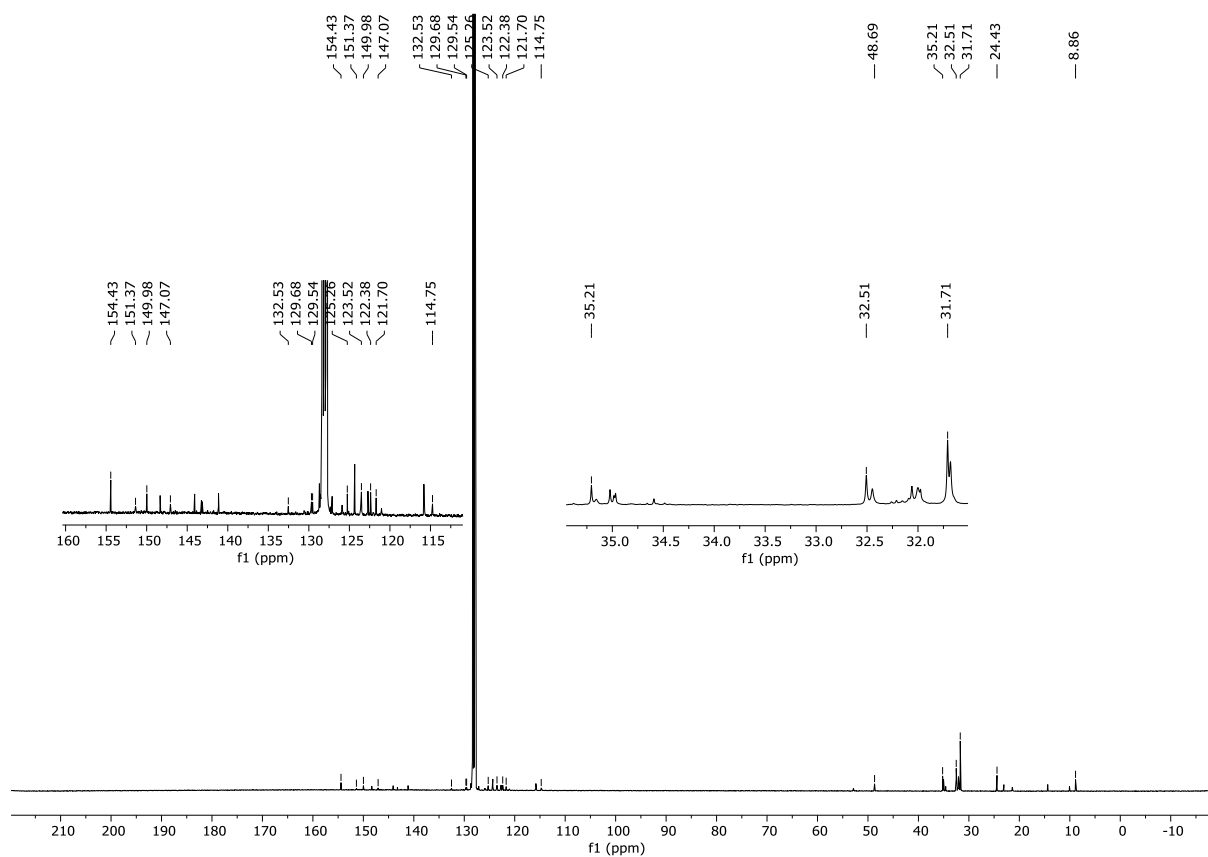


Figure 36. ^{13}C NMR (400 MHz, C_6D_6 , 300K) spectrum of L-Ga(I'Pr₂Me₂) **129**.

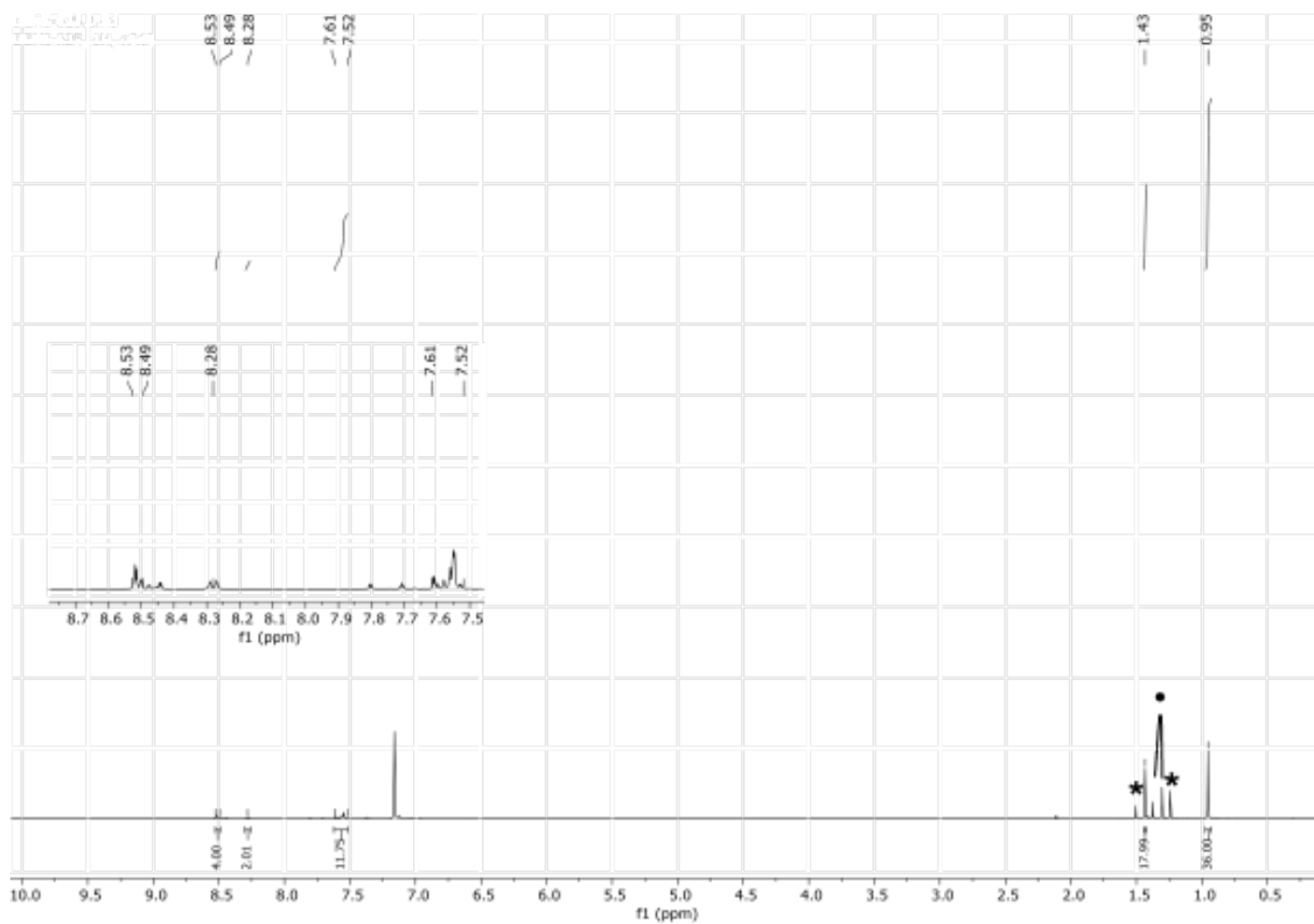


Figure 37. ¹H NMR (400 MHz, C₆D₆, 300K) spectrum of L-Ga(C₁₄H₈O) **130**. (• L-Gal₂, * L-H•)

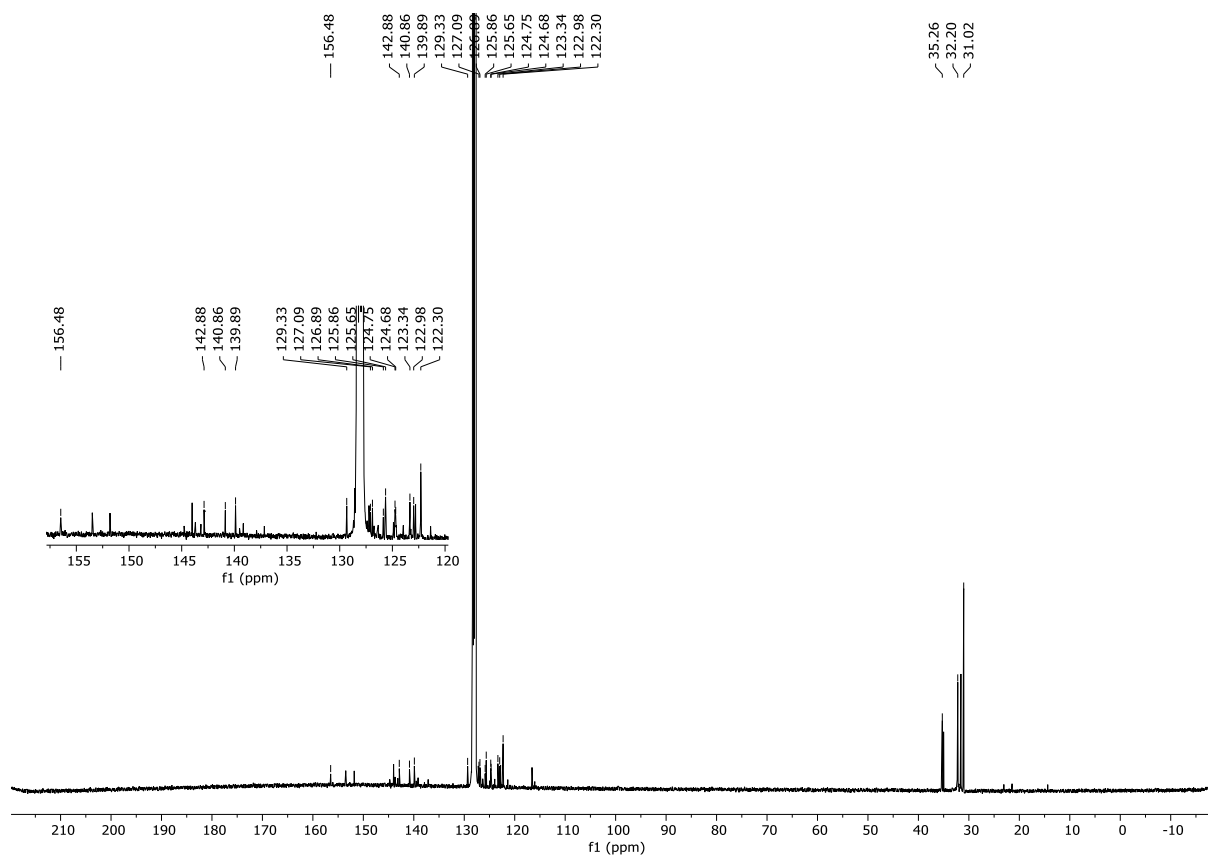


Figure 38. ^{13}C NMR (400 MHz, C_6D_6 , 300K) spectrum L-Ga($\text{C}_{14}\text{H}_8\text{O}$) **130**.

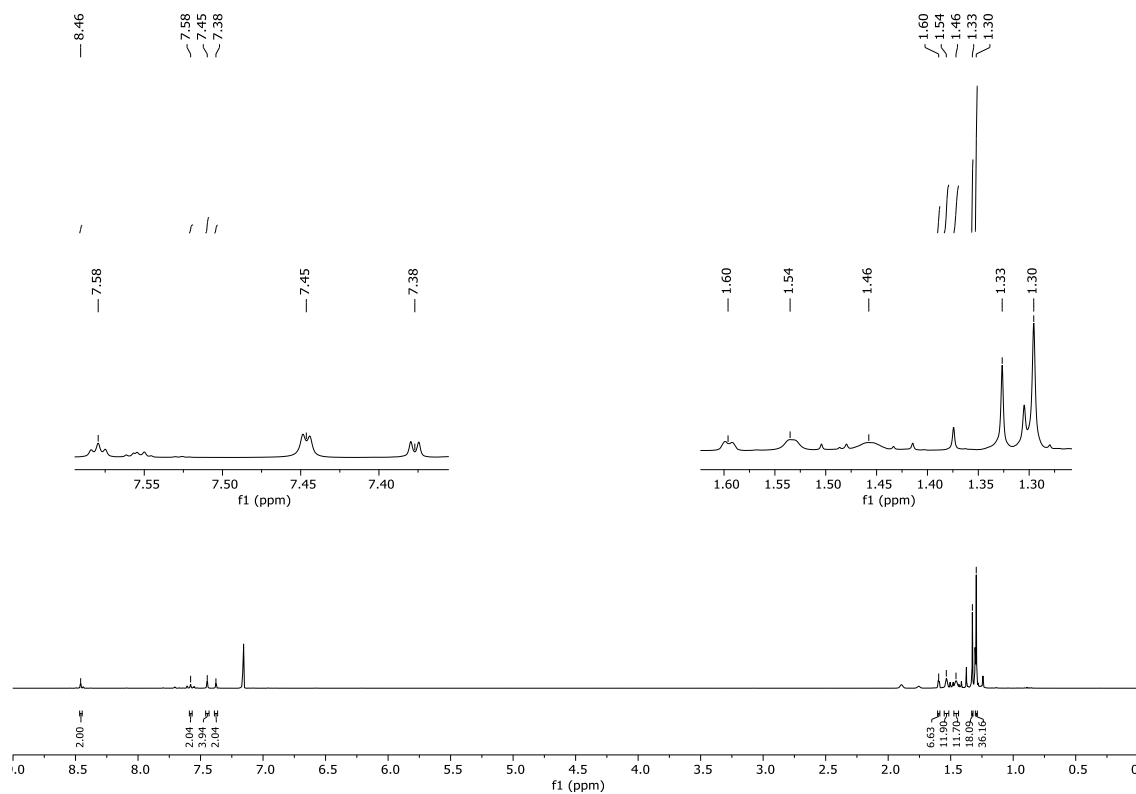


Figure 39. ^1H (400 MHz, C_6D_6 , 300K) NMR spectra of L-GaN₄Ad₂ **131**.

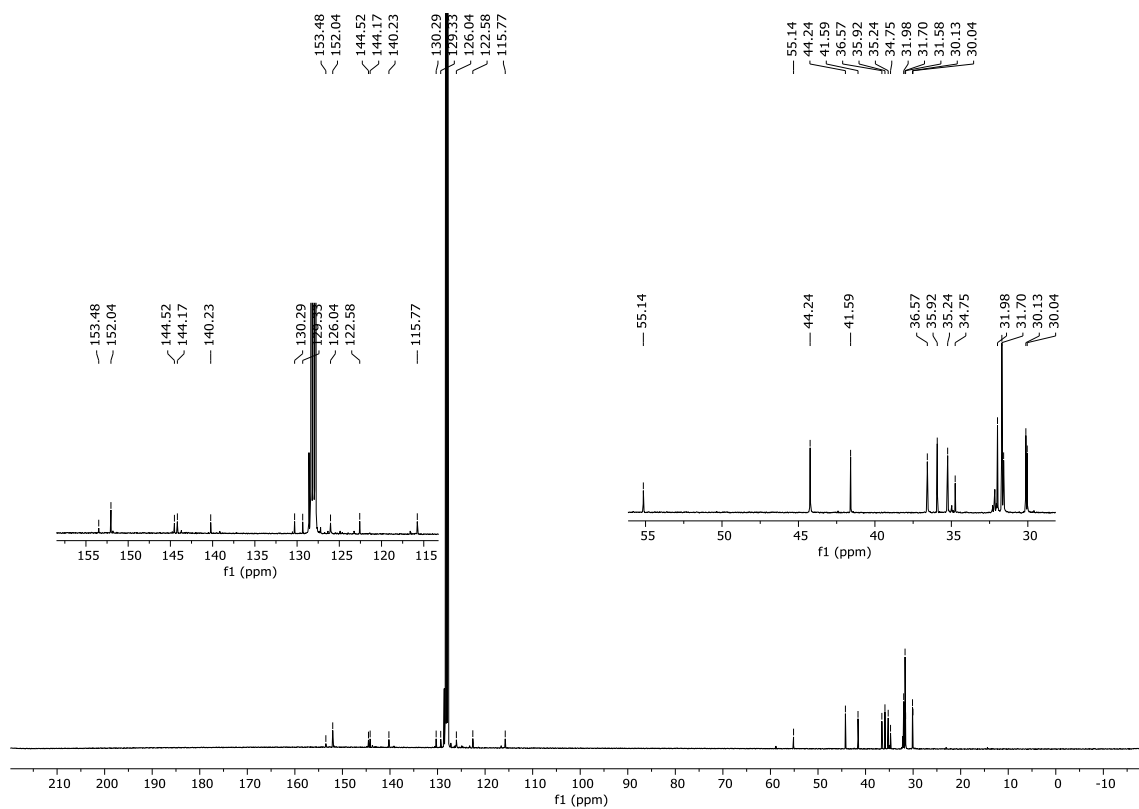


Figure 40. ^{13}C (400 MHz, C_6D_6 , 300K) NMR spectra of L-GaN₄Ad₂ **131**.

7.2. IR Spectra

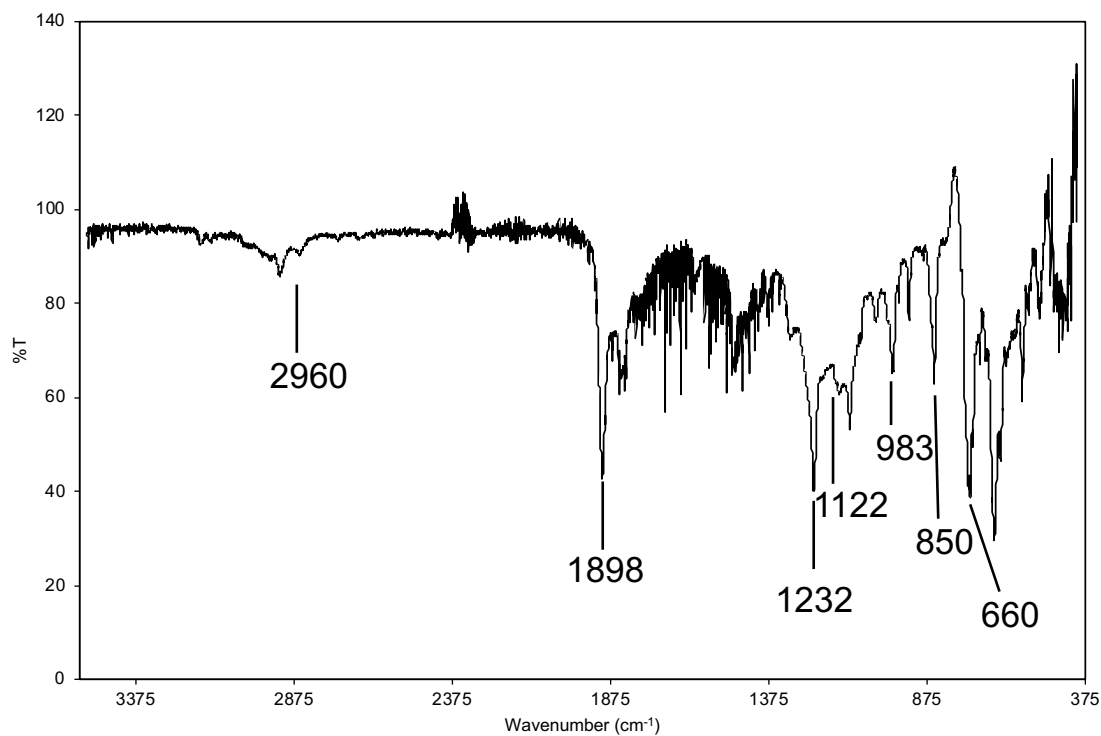


Figure 41. IR spectrum of IDip-GaH₂(PCO) **119**.

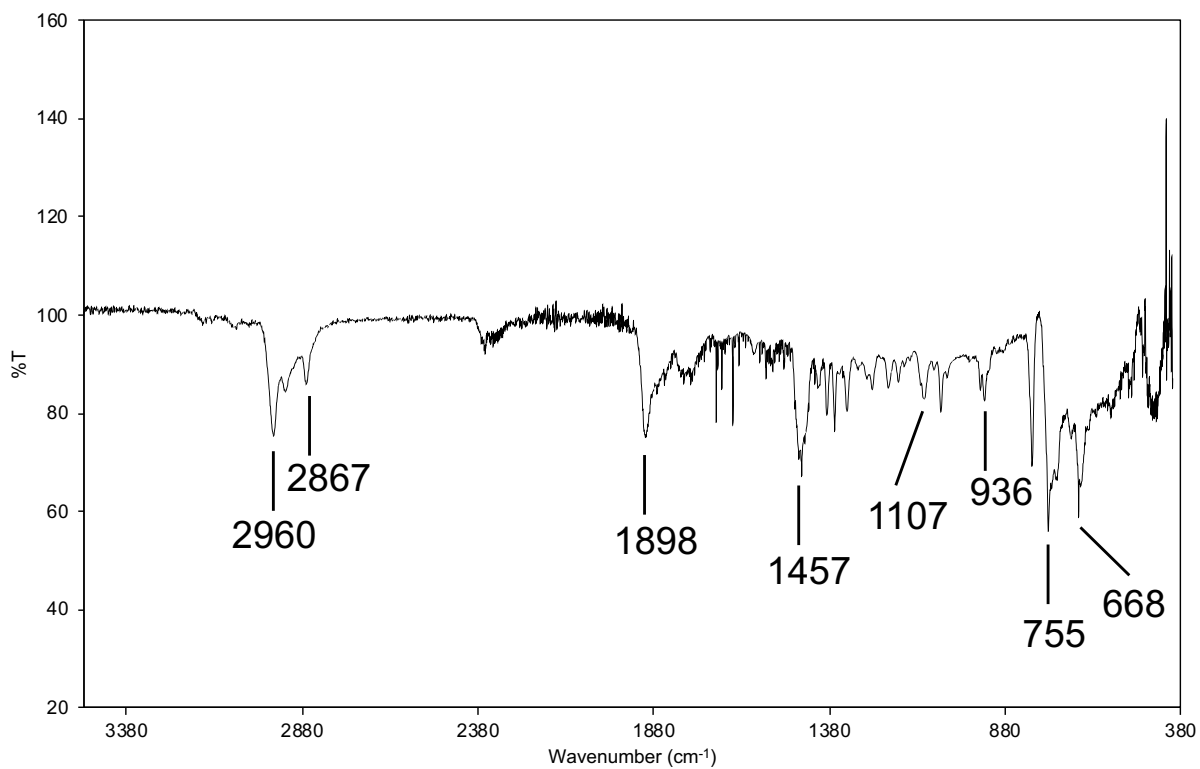


Figure 42. IR spectrum of IMes-GaH₂(PCO) 120.

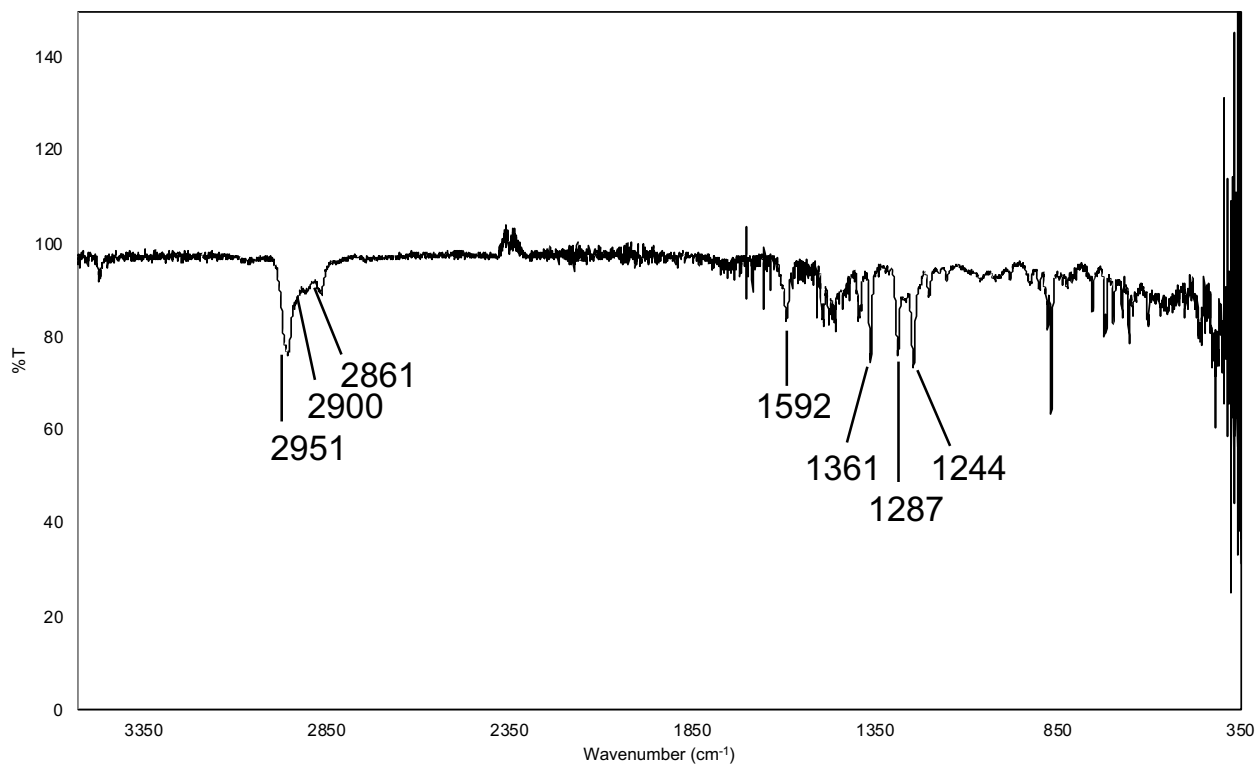


Figure 43. IR spectrum of L-Gal₂ 124.

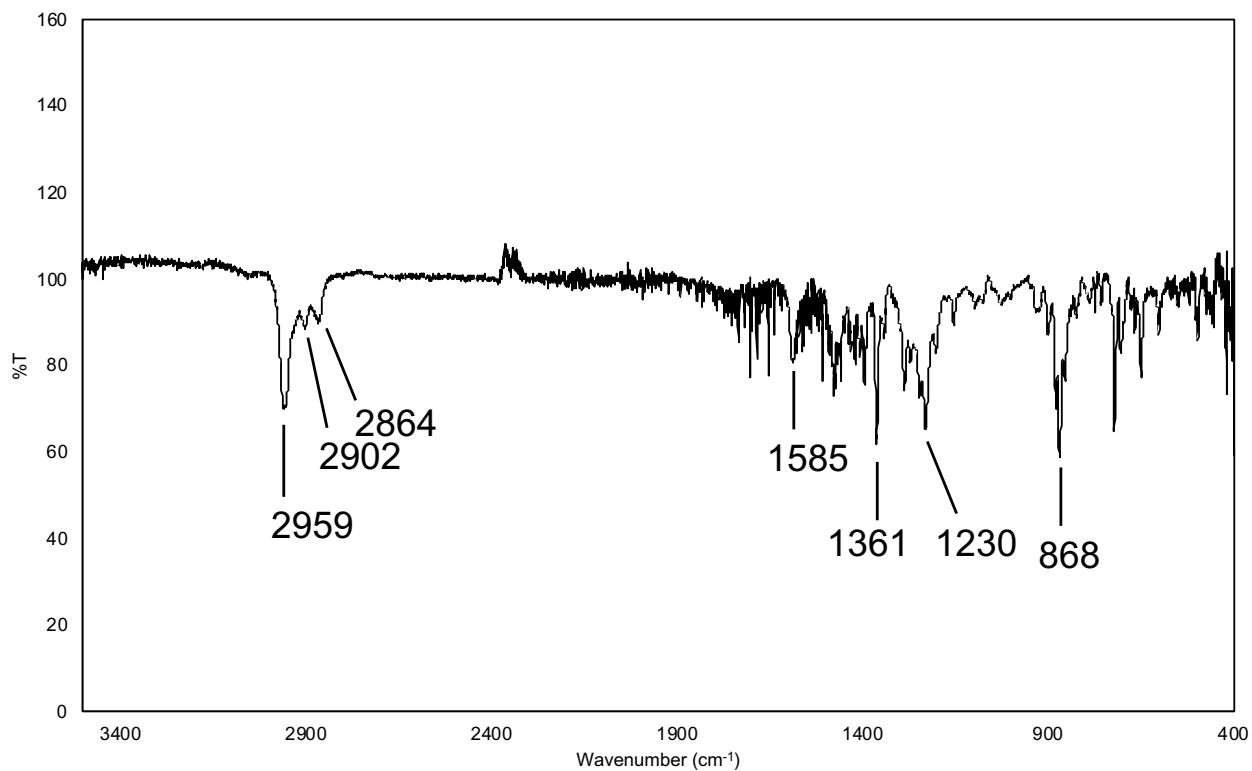


Figure 44. IR spectrum of L-Ga **125**.

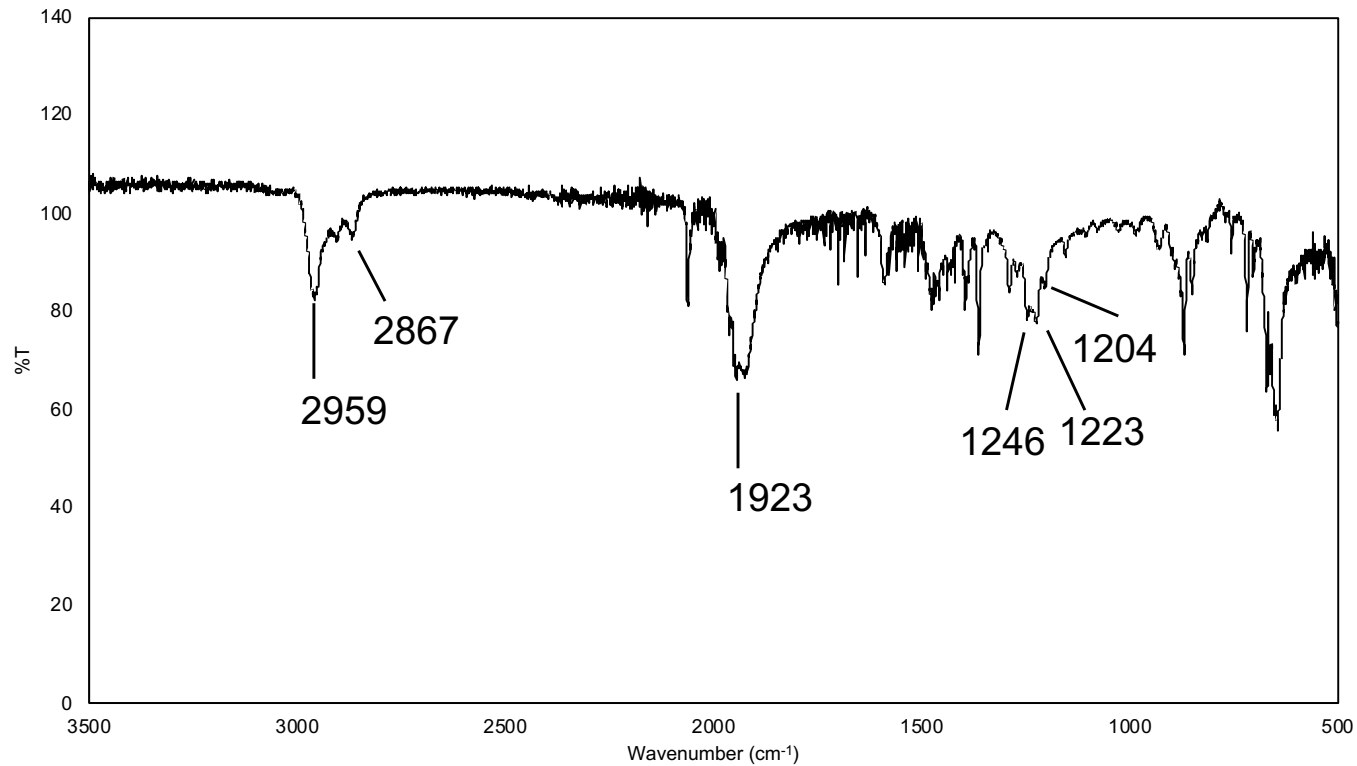


Figure 45. IR spectrum of L-GaCr(CO)₅ **126**.

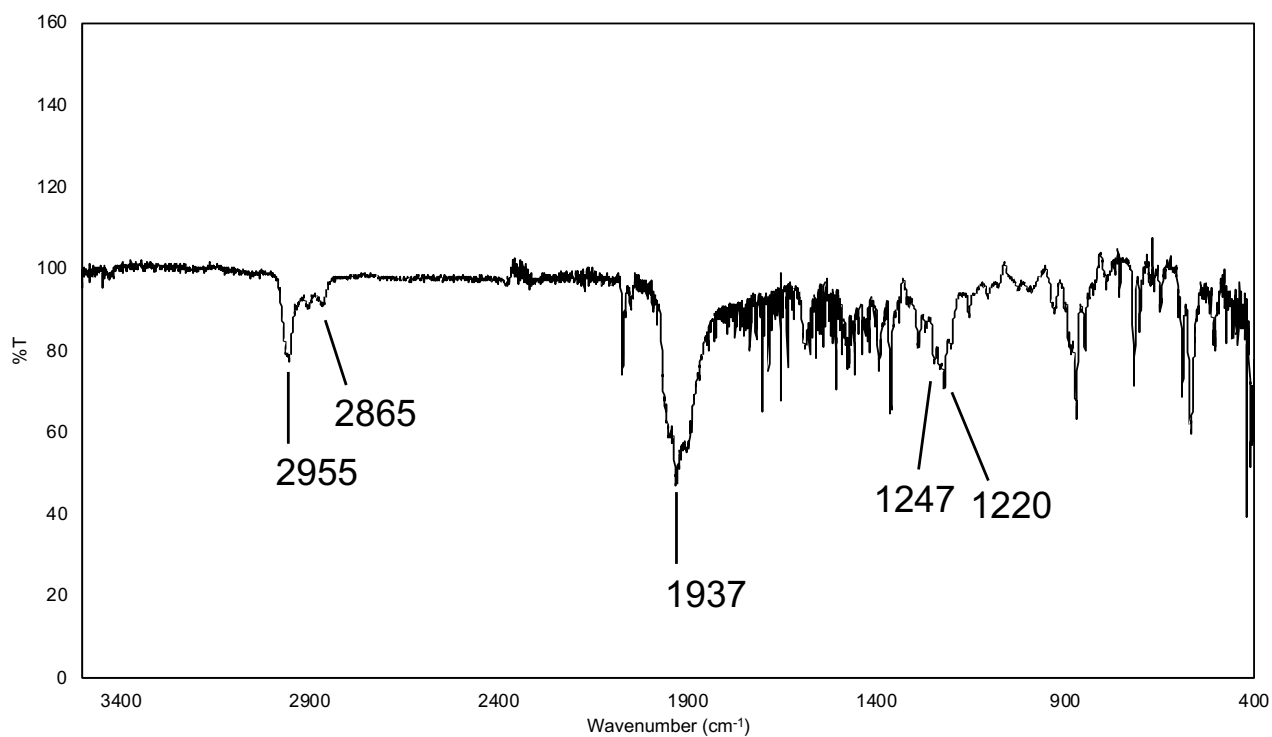


Figure 46. IR spectrum of L-GaMo(CO)₅ 127.

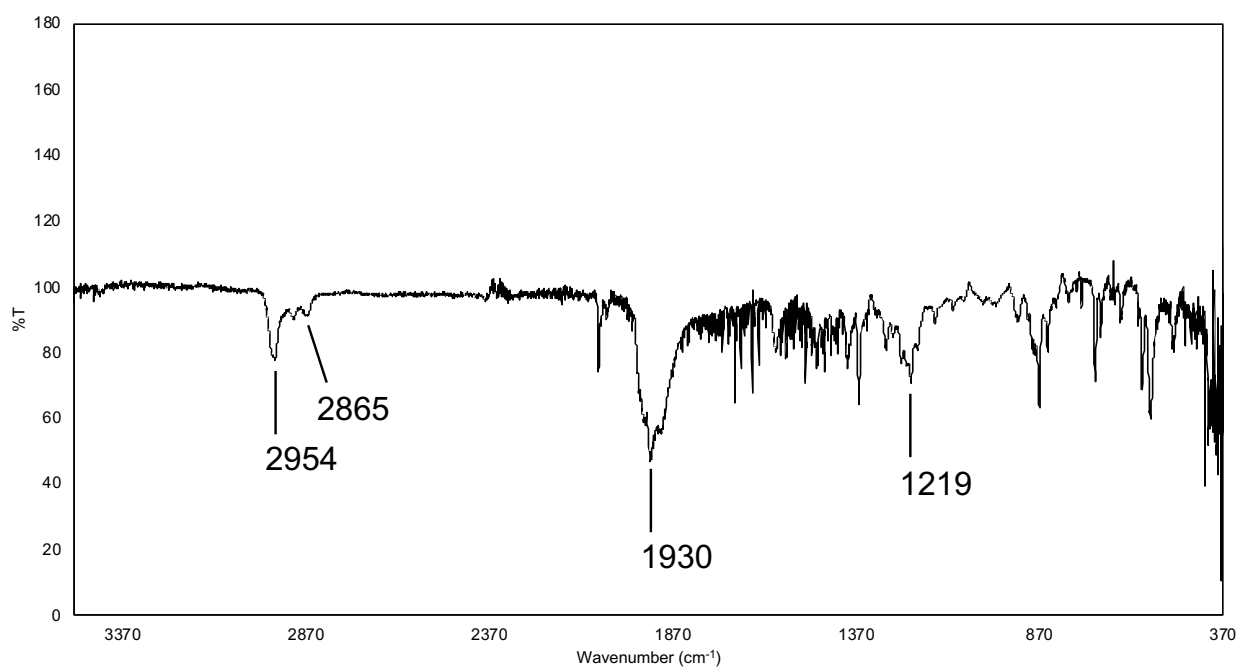


Figure 47. IR spectrum of LGaW(CO)₅ 128.

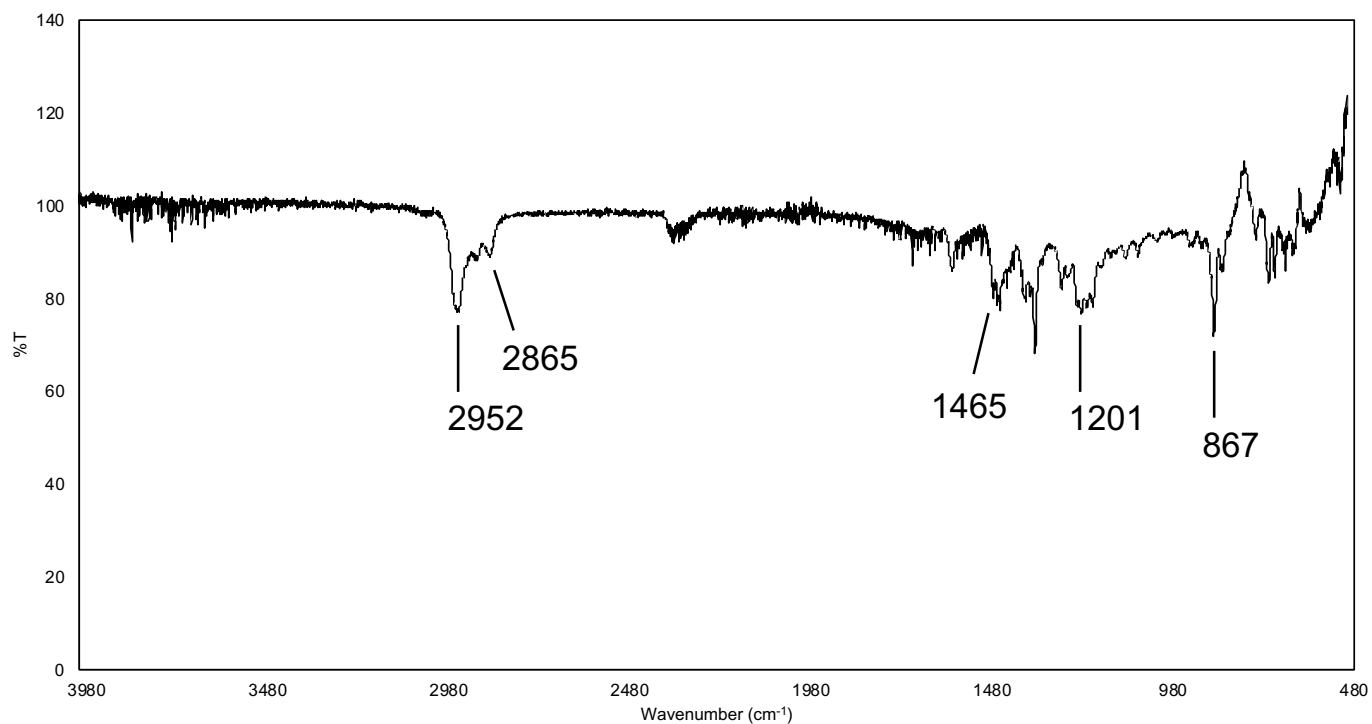


Figure 48. IR spectrum of L-Ga(NHC) **129**.

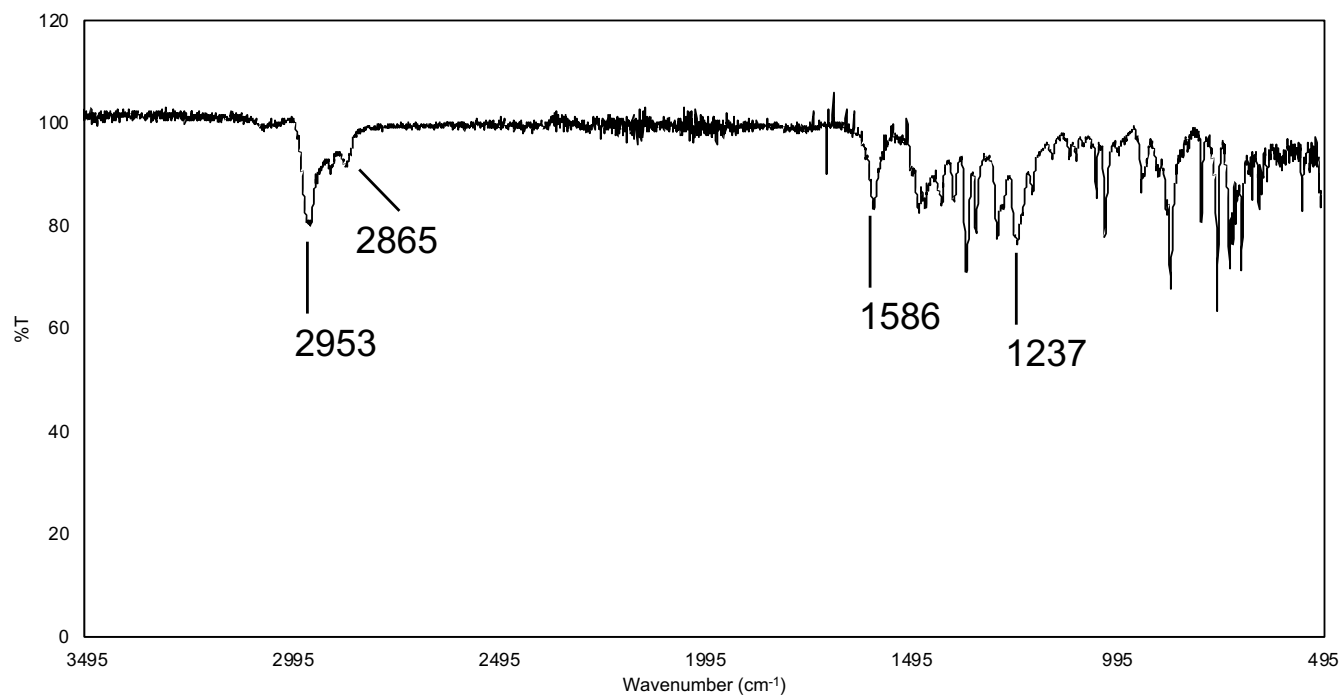


Figure 49. IR spectrum of L-Ga(C₁₄H₈O₂) **130**.

7.3. Crystal Data and Structure Refinement

7.3.1. IDip-GaH₂(PCO) 119

Identification code	sh4617_a	
Empirical formula	C ₂₈ H ₃₈ Ga N ₂ O P	
Formula weight	519.29	
Temperature	133(2) K	
Wavelength	0.71073 Å	
Crystal system	Triclinic	
Space group	P-1	
Unit cell dimensions	a = 10.3739(5) Å	a = 103.6900(10)°.
	b = 14.6502(6) Å	b = 102.9410(10)°.
	c = 20.5121(8) Å	g = 100.2890(10)°.
Volume	2862.3(2) Å ³	
Z	4	
Density (calculated)	1.205 Mg/m ³	
Absorption coefficient	1.038 mm ⁻¹	
F(000)	1096	
Crystal size	0.140 x 0.086 x 0.069 mm ³	
Theta range for data collection	2.053 to 27.907°.	
Index ranges	-13<=h<=13, -19<=k<=19, -27<=l<=26	
Reflections collected	111098	
Independent reflections	13682 [R(int) = 0.0849]	
Completeness to theta = 25.242°	100.0 %	
Absorption correction	Semi-empirical from equivalents	
Max. and min. transmission	0.7456 and 0.7068	
Refinement method	Full-matrix least-squares on F ²	
Data / restraints / parameters	13682 / 168 / 683	

Goodness-of-fit on F^2	1.034
Final R indices [$I > 2\sigma(I)$]	R1 = 0.0512, wR2 = 0.1169
R indices (all data)	R1 = 0.0795, wR2 = 0.1344
Extinction coefficient	n/a
Largest diff. peak and hole	1.356 and -1.548 e.Å ⁻³

7.3.2. IMes-GaH₂(PCO) 120

Identification code	sh4302	
Empirical formula	C ₂₂ H ₂₆ Ga N ₂ O P, 0.5(C ₇ H ₈)	
Formula weight	481.20	
Temperature	130(2) K	
Wavelength	0.71073 Å	
Crystal system	Monoclinic	
Space group	P2 ₁ /n	
Unit cell dimensions	a = 7.7838(5) Å	α = 90°.
	b = 17.9214(13) Å	β = 91.466(2)°.
	c = 18.1395(10) Å	γ = 90°.
Volume	2529.6(3) Å ³	
Z	4	
Density (calculated)	1.264 Mg/m ³	
Absorption coefficient	1.169 mm ⁻¹	
F(000)	1004	
Crystal size	0.330 x 0.165 x 0.050 mm ³	
Theta range for data collection	2.273 to 27.911°.	
Index ranges	-10 ≤ h ≤ 10, -23 ≤ k ≤ 23, -23 ≤ l ≤ 23	
Reflections collected	120966	
Independent reflections	6052 [R(int) = 0.0540]	
Completeness to theta = 25.242°	100.0 %	
Absorption correction	Semi-empirical from equivalents	
Max. and min. transmission	0.7456 and 0.6739	
Refinement method	Full-matrix least-squares on F ²	
Data / restraints / parameters	6052 / 143 / 323	
Goodness-of-fit on F ²	1.028	
Final R indices [I > 2σ(I)]	R1 = 0.0422, wR2 = 0.1079	
R indices (all data)	R1 = 0.0506, wR2 = 0.1139	

Extinction coefficient	n/a
Largest diff. peak and hole	0.680 and -0.558 e.Å ⁻³

7.3.3. (I¹Pr₂Me₂-H)(PCO)

Empirical formula	C ₁₂ H ₂₁ N ₂ O P	
Formula weight	240.28	
Temperature	132(2) K	
Wavelength	0.71073 Å	
Crystal system	Monoclinic	
Space group	P2 ₁ /n	
Unit cell dimensions	a = 8.21560(10) Å	a = 90°.
	b = 7.46930(10) Å	b = 92.9070(10)°.
	c = 22.3405(5) Å	g = 90°.
Volume	1369.16(4) Å ³	
Z	4	
Density (calculated)	1.166 Mg/m ³	
Absorption coefficient	0.185 mm ⁻¹	
F(000)	520	
Crystal size	0.371 x 0.265 x 0.196 mm ³	
Theta range for data collection	1.825 to 32.653°.	
Index ranges	-12<=h<=12, -11<=k<=11, -33<=l<=33	
Reflections collected	29264	
Independent reflections	5014 [R(int) = 0.0300]	
Completeness to theta = 25.242°	100.0 %	
Absorption correction	Semi-empirical from equivalents	
Max. and min. transmission	0.7464 and 0.7225	
Refinement method	Full-matrix least-squares on F ²	
Data / restraints / parameters	5014 / 0 / 151	
Goodness-of-fit on F ²	1.049	
Final R indices [I>2sigma(I)]	R1 = 0.0364, wR2 = 0.0966	
R indices (all data)	R1 = 0.0495, wR2 = 0.1044	
Extinction coefficient	n/a	
Largest diff. peak and hole	0.480 and -0.207 e.Å ⁻³	

7.3.4. IDip-GaCl₂(OTf) 121

Identification code	sh4398_a	
Empirical formula	C ₂₈ H ₃₆ Cl ₂ F ₃ Ga N ₂ O ₃ S	
Formula weight	678.27	
Temperature	132(2) K	
Wavelength	0.71073 Å	
Crystal system	Monoclinic	
Space group	P2 ₁ /n	
Unit cell dimensions	a = 12.1489(2) Å	a = 90°.
	b = 18.9530(4) Å	b = 97.1660(10)°.
	c = 14.1587(3) Å	g = 90°.
Volume	3234.69(11) Å ³	
Z	4	
Density (calculated)	1.393 Mg/m ³	
Absorption coefficient	1.128 mm ⁻¹	
F(000)	1400	
Crystal size	0.279 x 0.198 x 0.142 mm ³	
Theta range for data collection	2.002 to 31.497°.	
Index ranges	-17<=h<=17, -27<=k<=27, -20<=l<=20	
Reflections collected	57908	
Independent reflections	10757 [R(int) = 0.0551]	
Completeness to theta = 25.242°	100.0 %	
Absorption correction	Semi-empirical from equivalents	
Max. and min. transmission	0.7463 and 0.6996	
Refinement method	Full-matrix least-squares on F ²	
Data / restraints / parameters	10757 / 0 / 370	
Goodness-of-fit on F ²	1.008	
Final R indices [I>2sigma(I)]	R1 = 0.0342, wR2 = 0.0706	
R indices (all data)	R1 = 0.0557, wR2 = 0.0791	

Extinction coefficient	n/a
Largest diff. peak and hole	0.446 and -0.343 e.Å ⁻³

7.3.5. IDip-GaCl₂P(TMS)₂ 122

Empirical formula	C ₃₃ H ₅₄ Cl ₂ Ga N ₂ P Si ₂	
Formula weight	706.55	
Temperature	133(2) K	
Wavelength	0.71073 Å	
Crystal system	Monoclinic	
Space group	P2 ₁ /n	
Unit cell dimensions	a = 15.4395(5) Å	a = 90°.
	b = 15.2335(4) Å	b = 113.8060(10)°.
	c = 18.3285(6) Å	g = 90°.
Volume	3944.0(2) Å ³	
Z	4	
Density (calculated)	1.190 Mg/m ³	
Absorption coefficient	0.957 mm ⁻¹	
F(000)	1496	
Crystal size	0.343 x 0.265 x 0.184 mm ³	
Theta range for data collection	1.982 to 31.520°.	
Index ranges	-22 ≤ h ≤ 22, -21 ≤ k ≤ 22, -26 ≤ l ≤ 26	
Reflections collected	110586	
Independent reflections	13142 [R(int) = 0.0328]	
Completeness to theta = 25.242°	99.9 %	
Absorption correction	Semi-empirical from equivalents	
Max. and min. transmission	0.7462 and 0.6979	
Refinement method	Full-matrix least-squares on F ²	
Data / restraints / parameters	13142 / 0 / 384	
Goodness-of-fit on F ²	1.027	
Final R indices [I > 2σ(I)]	R1 = 0.0244, wR2 = 0.0588	
R indices (all data)	R1 = 0.0307, wR2 = 0.0620	

Extinction coefficient	n/a
Largest diff. peak and hole	0.561 and -0.331 e.Å ⁻³

7.3.6. CAAC-GaCl₂P(TMS)₂ 123

Empirical formula	C ₂₆ H ₄₉ Cl ₂ Ga N P Si ₂	
Formula weight	603.43	
Temperature	133(2) K	
Wavelength	0.71073 Å	
Crystal system	Triclinic	
Space group	P-1	
Unit cell dimensions	a = 9.2478(5) Å	a = 93.879(2)°.
	b = 9.5656(6) Å	b = 96.110(2)°.
	c = 20.3150(13) Å	g = 116.397(2)°.
Volume	1587.17(17) Å ³	
Z	2	
Density (calculated)	1.263 Mg/m ³	
Absorption coefficient	1.176 mm ⁻¹	
F(000)	640	
Crystal size	0.284 x 0.269 x 0.229 mm ³	
Theta range for data collection	2.033 to 31.532°.	
Index ranges	-12<=h<=13, -14<=k<=14, -29<=l<=29	
Reflections collected	74394	
Independent reflections	10591 [R(int) = 0.0593]	
Completeness to theta = 25.242°	99.9 %	
Absorption correction	Semi-empirical from equivalents	
Max. and min. transmission	0.7462 and 0.6919	
Refinement method	Full-matrix least-squares on F ²	
Data / restraints / parameters	10591 / 0 / 312	
Goodness-of-fit on F ²	1.051	
Final R indices [I>2sigma(I)]	R1 = 0.0258, wR2 = 0.0654	
R indices (all data)	R1 = 0.0288, wR2 = 0.0675	

Extinction coefficient	n/a
Largest diff. peak and hole	0.473 and -0.480 e.Å ⁻³

7.3.7. L-Gal₂ 124

Identification code	sh4927_a_tw	
Empirical formula	C ₅₄ H ₇₀ Ga I ₂ N	
Formula weight	1056.63	
Temperature	133(2) K	
Wavelength	0.71073 Å	
Crystal system	Triclinic	
Space group	P-1	
Unit cell dimensions	a = 13.5357(19) Å	a = 89.553(6)°.
	b = 14.116(2) Å	b = 87.438(5)°.
	c = 14.988(2) Å	g = 63.451(5)°.
Volume	2558.9(7) Å ³	
Z	2	
Density (calculated)	1.371 Mg/m ³	
Absorption coefficient	1.778 mm ⁻¹	
F(000)	1076	
Crystal size	0.200 x 0.070 x 0.020 mm ³	
Theta range for data collection	2.115 to 26.371°.	
Index ranges	-16<=h<=16, -17<=k<=17, 0<=l<=18	
Reflections collected	17269	
Independent reflections	17269 [R(int) = ?]	
Completeness to theta = 25.242°	99.8 %	
Absorption correction	Semi-empirical from equivalents	
Max. and min. transmission	0.1870 and 0.1493	
Refinement method	Full-matrix least-squares on F ²	
Data / restraints / parameters	17269 / 135 / 582	
Goodness-of-fit on F ²	1.143	

Final R indices [$I > 2\sigma(I)$]	R1 = 0.0446, wR2 = 0.0827
R indices (all data)	R1 = 0.0522, wR2 = 0.0852
Extinction coefficient	n/a
Largest diff. peak and hole	0.548 and -0.877 e.Å ⁻³

7.3.8. L-Ga 125

Identification code	sh5290_a	
Empirical formula	C ₅₂ H ₇₄ Ga N O	
Formula weight	798.84	
Temperature	152(2) K	
Wavelength	0.71073 Å	
Crystal system	Triclinic	
Space group	P-1	
Unit cell dimensions	a = 11.9872(7) Å	a = 112.793(2)°.
	b = 13.0309(8) Å	b = 94.866(2)°.
	c = 16.3985(10) Å	g = 95.167(2)°.
Volume	2331.8(2) Å ³	
Z	2	
Density (calculated)	1.138 Mg/m ³	
Absorption coefficient	0.626 mm ⁻¹	
F(000)	864	
Crystal size	0.200 x 0.200 x 0.040 mm ³	
Theta range for data collection	1.359 to 27.144°.	
Index ranges	-15<=h<=15, -16<=k<=16, -21<=l<=21	
Reflections collected	34893	
Independent reflections	10303 [R(int) = 0.0638]	
Completeness to theta = 25.242°	100.0 %	
Absorption correction	Semi-empirical from equivalents	
Max. and min. transmission	0.7467 and 0.3735	
Refinement method	Full-matrix least-squares on F ²	
Data / restraints / parameters	10303 / 48 / 547	

Goodness-of-fit on F^2	1.010
Final R indices [$I > 2\sigma(I)$]	R1 = 0.0496, wR2 = 0.1012
R indices (all data)	R1 = 0.0957, wR2 = 0.1180
Extinction coefficient	n/a
Largest diff. peak and hole	0.392 and -0.541 e.Å ⁻³

7.3.9. L-GaCr(CO)₅ 126

Identification code	sh5092_a	
Empirical formula	C ₅₉ H ₇₀ Cr Ga N O ₅	
Formula weight	994.88	
Temperature	143(2) K	
Wavelength	0.71073 Å	
Crystal system	Monoclinic	
Space group	C2/c	
Unit cell dimensions	a = 30.3997(7) Å	a = 90°.
	b = 12.3494(3) Å	b = 102.2580(10)°.
	c = 29.6518(7) Å	g = 90°.
Volume	10878.0(4) Å ³	
Z	8	
Density (calculated)	1.215 Mg/m ³	
Absorption coefficient	0.742 mm ⁻¹	
F(000)	4208	
Crystal size	0.340 x 0.080 x 0.060 mm ³	
Theta range for data collection	1.972 to 27.102°.	
Index ranges	-38<=h<=35, -15<=k<=15, -38<=l<=38	
Reflections collected	133619	
Independent reflections	11954 [R(int) = 0.0446]	
Completeness to theta = 25.242°	99.8 %	
Absorption correction	Semi-empirical from equivalents	
Max. and min. transmission	0.7457 and 0.6846	
Refinement method	Full-matrix least-squares on F ²	
Data / restraints / parameters	11954 / 181 / 740	
Goodness-of-fit on F ²	1.120	

Final R indices [$I > 2\sigma(I)$]	R1 = 0.0360, wR2 = 0.0891
R indices (all data)	R1 = 0.0422, wR2 = 0.0920
Extinction coefficient	n/a
Largest diff. peak and hole	0.384 and -0.432 e.Å ⁻³

7.3.10. L-GaMo(CO)₅ 127

Crystal data and structure refinement for sh5107_a.

Identification code	sh5107_a	
Empirical formula	C ₅₉ H ₇₀ Ga Mo N O ₅	
Formula weight	1038.82	
Temperature	144(2) K	
Wavelength	0.71073 Å	
Crystal system	Monoclinic	
Space group	C2/c	
Unit cell dimensions	a = 30.3480(9) Å	a = 90°.
	b = 12.3800(4) Å	b = 102.6840(10)°.
	c = 29.7888(7) Å	g = 90°.
Volume	10918.8(5) Å ³	
Z	8	
Density (calculated)	1.264 Mg/m ³	
Absorption coefficient	0.770 mm ⁻¹	
F(000)	4352	
Crystal size	0.200 x 0.140 x 0.100 mm ³	
Theta range for data collection	1.970 to 31.545°.	
Index ranges	-44 ≤ h ≤ 44, -18 ≤ k ≤ 18, -37 ≤ l ≤ 43	
Reflections collected	240511	
Independent reflections	18221 [R(int) = 0.0513]	
Completeness to theta = 25.242°	99.9 %	
Absorption correction	Semi-empirical from equivalents	
Max. and min. transmission	0.7462 and 0.7107	
Refinement method	Full-matrix least-squares on F ²	
Data / restraints / parameters	18221 / 222 / 709	

Goodness-of-fit on F^2	1.038
Final R indices [$I > 2\sigma(I)$]	R1 = 0.0320, wR2 = 0.0683
R indices (all data)	R1 = 0.0447, wR2 = 0.0750
Extinction coefficient	n/a
Largest diff. peak and hole	0.440 and -0.630 e.Å ⁻³

7.3.11. L-GaW(CO)₅ 128

Empirical formula	C53 H64 Ga N O5 W	
Formula weight	1048.62	
Temperature	143(2) K	
Wavelength	0.71073 Å	
Crystal system	Triclinic	
Space group	P-1	
Unit cell dimensions	a = 13.2686(4) Å	a = 63.1390(10)°.
	b = 14.4074(5) Å	b = 72.0600(10)°.
	c = 15.8636(6) Å	g = 71.8470(10)°.
Volume	2520.20(15) Å ³	
Z	2	
Density (calculated)	1.382 Mg/m ³	
Absorption coefficient	2.859 mm ⁻¹	
F(000)	1068	
Crystal size	0.160 x 0.080 x 0.060 mm ³	
Theta range for data collection	2.062 to 27.903°.	
Index ranges	-17<=h<=17, -18<=k<=18, -20<=l<=20	
Reflections collected	56912	
Independent reflections	12017 [R(int) = 0.0491]	
Completeness to theta = 25.242°	99.8 %	
Absorption correction	Semi-empirical from equivalents	
Max. and min. transmission	0.7456 and 0.6687	
Refinement method	Full-matrix least-squares on F ²	
Data / restraints / parameters	12017 / 147 / 602	
Goodness-of-fit on F ²	1.095	
Final R indices [I>2sigma(I)]	R1 = 0.0271, wR2 = 0.0629	

R indices (all data)	R1 = 0.0323, wR2 = 0.0653
Extinction coefficient	n/a
Largest diff. peak and hole	0.992 and -0.718 e.Å ⁻³

7.3.12. L-Ga(ⁱPr₂Me₂) 129

Empirical formula	C ₆₅ H ₉₀ Ga N ₃
Formula weight	983.11
Temperature	153(2) K
Wavelength	0.71073 Å
Crystal system	Orthorhombic
Space group	Ibam
Unit cell dimensions	a = 18.3759(11) Å a = 90°. b = 23.7864(16) Å b = 90°. c = 26.3408(18) Å g = 90°.
Volume	11513.5(13) Å ³
Z	8
Density (calculated)	1.134 Mg/m ³
Absorption coefficient	0.519 mm ⁻¹
F(000)	4256
Crystal size	0.260 x 0.200 x 0.180 mm ³
Theta range for data collection	2.086 to 27.908°.
Index ranges	-23 ≤ h ≤ 24, -31 ≤ k ≤ 31, -34 ≤ l ≤ 34
Reflections collected	223263
Independent reflections	7053 [R(int) = 0.0771]
Completeness to theta = 25.242°	99.9 %
Absorption correction	Semi-empirical from equivalents
Max. and min. transmission	0.7456 and 0.7018
Refinement method	Full-matrix least-squares on F ²
Data / restraints / parameters	7053 / 119 / 409
Goodness-of-fit on F ²	1.056
Final R indices [I > 2σ(I)]	R1 = 0.0467, wR2 = 0.1348

R indices (all data)	R1 = 0.0615, wR2 = 0.1499
Extinction coefficient	n/a
Largest diff. peak and hole	0.366 and -0.866 e.Å ⁻³

7.3.13. L-Ga(C₁₄H₈O₂) 130

Crystal data and structure refinement for sh5238_a.

Identification code	sh5238_a	
Empirical formula	C ₆₂ H ₇₂ Ga N O ₂	
Formula weight	932.93	
Temperature	143(2) K	
Wavelength	0.71073 Å	
Crystal system	Monoclinic	
Space group	P2 ₁ /n	
Unit cell dimensions	a = 15.6524(5) Å	a = 90°.
	b = 15.9288(5) Å	b = 100.5730(10)°.
	c = 20.9537(7) Å	g = 90°.
Volume	5135.6(3) Å ³	
Z	4	
Density (calculated)	1.207 Mg/m ³	
Absorption coefficient	0.580 mm ⁻¹	
F(000)	1992	
Crystal size	0.320 x 0.080 x 0.010 mm ³	
Theta range for data collection	1.971 to 25.027°.	
Index ranges	-18<=h<=18, -17<=k<=18, -24<=l<=24	
Reflections collected	106694	
Independent reflections	9065 [R(int) = 0.1066]	
Completeness to theta = 25.027°	100.0 %	
Absorption correction	Semi-empirical from equivalents	
Max. and min. transmission	0.7455 and 0.6626	
Refinement method	Full-matrix least-squares on F ²	
Data / restraints / parameters	9065 / 370 / 688	

Goodness-of-fit on F^2	1.028
Final R indices [$I > 2\sigma(I)$]	R1 = 0.0472, wR2 = 0.1078
R indices (all data)	R1 = 0.0691, wR2 = 0.1200
Extinction coefficient	n/a
Largest diff. peak and hole	1.884 and -0.539 e.Å ⁻³

7.3.14. L-GaN₄Ad₂ 131

Crystal data and structure refinement for sh4975_a.

Identification code	sh4975_a	
Empirical formula	C ₈₀ H ₁₀₆ Ga N ₅	
Formula weight	1207.41	
Temperature	152(2) K	
Wavelength	0.71073 Å	
Crystal system	Monoclinic	
Space group	P2 ₁ /c	
Unit cell dimensions	a = 13.7237(3) Å	a = 90°.
	b = 19.2690(3) Å	b = 101.6960(10)°.
	c = 26.3833(5) Å	g = 90°.
Volume	6832.0(2) Å ³	
Z	4	
Density (calculated)	1.174 Mg/m ³	
Absorption coefficient	0.450 mm ⁻¹	
F(000)	2608	
Crystal size	0.390 x 0.260 x 0.140 mm ³	
Theta range for data collection	1.318 to 27.102°.	
Index ranges	-17<=h<=17, -24<=k<=18, -33<=l<=33	
Reflections collected	75595	
Independent reflections	15068 [R(int) = 0.0419]	
Completeness to theta = 25.242°	100.0 %	
Absorption correction	Semi-empirical from equivalents	
Max. and min. transmission	0.7456 and 0.7074	
Refinement method	Full-matrix least-squares on F ²	
Data / restraints / parameters	15068 / 133 / 848	
Goodness-of-fit on F ²	1.018	
Final R indices [I>2sigma(I)]	R1 = 0.0384, wR2 = 0.0871	

R indices (all data)	R1 = 0.0574, wR2 = 0.0950
Extinction coefficient	n/a
Largest diff. peak and hole	0.453 and -0.425 e.Å ⁻³

7.4. Computational Details

Geometry optimizations were performed using the Gaussian 16 C0.1 software. All geometry optimizations were computed using the functional B3LYP functional with Grimme dispersion corrections D3 and the Becke-Jonson damping function in combination with the def2-TZVP basis set. The stationary points were located with the Berny algorithm¹⁵ using redundant internal coordinates. Analytical Hessians were computed to determine the nature of stationary points (one and zero imaginary frequencies for transition states and minima, respectively) and to calculate unscaled zero-point energies (ZPEs) as well as thermal corrections and entropy effects using the standard statistical-mechanics relationships for an ideal gas. For the calculation in benzene, the solvent was described by nonspecific solvent effects within the self-consistent reaction field (SCRF) approach in Tomasi's formalism.

TD-DFT calculations were performed using the ORCA 5.0.4 software. Single point PCM/TD-B3LYP/def2-TZVPP calculations were performed to estimate the change in the UV/Vis spectrum of **2** in the presence of benzene solvent.

The atomic partial charges were estimated with the natural bond orbital (NBO) method using NBO 7.0. The topological quantum theory of atoms in molecules (QTAIM), and Laplacian of the electron density analyses were carried out with AIMAll. All these analyses were performed at the B3LYP-D3(BJ)/def2-TZVPP level of theory.

The nature of the chemical bonds was investigated by means of the Energy Decomposition Analysis (EDA) method, which was described in detail in Chapter X.

The EDA-NOCV calculations were carried out with ADF2019.101. The basis sets for all elements have triple- ζ quality augmented by two sets of polarizations functions and one set of diffuse function. Core electrons were treated by the frozen-core approximation. This level of theory is denoted BP86-D3(BJ)/TZ2P. Scalar relativistic effects have been incorporated by applying the zeroth-order regular approximation (ZORA).

7.4.1. Optimized Structures, Cartesian xyz coordinates and Energies in Hartrees

L-Gal₂

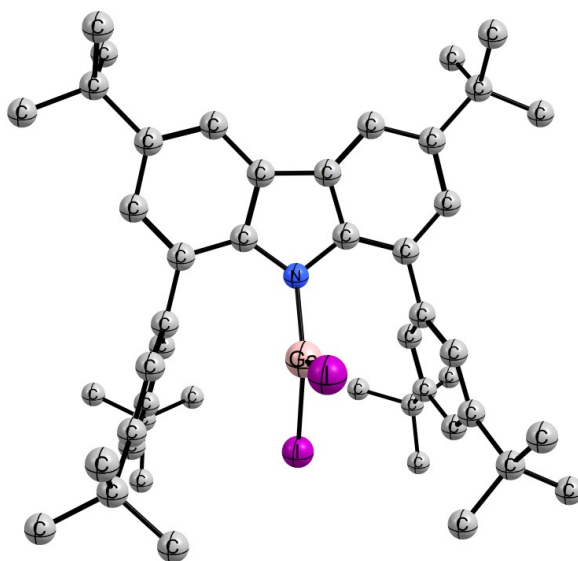


Figure 50. Optimized structure at the B3LYP-D3(BJ)/def2SVP level of theory for **124**. Hydrogen atoms are omitted for clarity.

Energy (B3LYP-D3(BJ)/def2SVP) = -4441.80 Hartree

I	-0.000897000000	0.300234000000	-3.020350000000
Ga	-0.000065000000	0.458293000000	-0.490441000000
C	2.470677000000	-1.715171000000	0.339955000000
C	0.727078000000	-3.441667000000	0.372589000000
I	-0.000316000000	2.747960000000	0.493513000000
N	0.000316000000	-1.236830000000	0.362658000000
C	1.121234000000	-2.077249000000	0.358212000000
C	-1.120340000000	-2.077623000000	0.358167000000
C	-0.725733000000	-3.441900000000	0.372523000000
C	-2.469915000000	-1.716007000000	0.339809000000
C	3.417735000000	-2.747113000000	0.326727000000
C	2.862096000000	-0.277993000000	0.368655000000

C	1.699550000000	-4.444752000000	0.371121000000
C	-1.697855000000	-4.445330000000	0.370784000000
C	-3.416612000000	-2.748269000000	0.326282000000
C	-2.861887000000	-0.278985000000	0.369043000000
C	3.062274000000	-4.112585000000	0.341837000000
C	3.179344000000	0.407528000000	-0.819427000000
C	2.946443000000	0.393098000000	1.594867000000
C	-3.060680000000	-4.113631000000	0.341271000000
C	-3.180321000000	0.406813000000	-0.818535000000
C	-2.945559000000	0.391667000000	1.595577000000
C	4.115270000000	-5.234323000000	0.330099000000
C	3.596740000000	1.745072000000	-0.789016000000
C	3.347096000000	1.733870000000	1.662834000000
C	-4.113277000000	-5.235726000000	0.329206000000
C	-3.598105000000	1.744228000000	-0.787332000000
C	-3.346737000000	1.732205000000	1.664339000000
C	5.550436000000	-4.686447000000	0.295543000000
C	3.907048000000	-6.117052000000	-0.918515000000
C	3.959371000000	-6.096169000000	1.600665000000
C	3.665953000000	2.379881000000	0.460579000000
C	3.943621000000	2.528588000000	-2.064686000000
C	3.462661000000	2.433222000000	3.026721000000
C	-3.904502000000	-6.118184000000	-0.919509000000
C	-3.957267000000	-6.097716000000	1.599661000000
C	-5.548655000000	-4.688396000000	0.294513000000
C	-3.666680000000	2.378554000000	0.462524000000
C	-3.945885000000	2.528106000000	-2.062519000000
C	-3.461668000000	2.431040000000	3.028550000000

C	5.317025000000	3.211575000000	-1.901776000000
C	4.006477000000	1.616859000000	-3.300242000000
C	2.857391000000	3.599871000000	-2.298434000000
C	4.724024000000	1.896286000000	3.737070000000
C	3.586078000000	3.958629000000	2.881683000000
C	2.223462000000	2.135240000000	3.895478000000
C	-2.859882000000	3.599567000000	-2.296560000000
C	-5.319279000000	3.210871000000	-1.898593000000
C	-4.009307000000	1.616757000000	-3.298306000000
C	-2.222070000000	2.132726000000	3.896574000000
C	-4.722731000000	1.893835000000	3.739267000000
C	-3.585152000000	3.956499000000	2.884137000000
H	4.467279000000	-2.456412000000	0.313294000000
H	1.386238000000	-5.490733000000	0.385779000000
H	-1.384169000000	-5.491206000000	0.385429000000
H	-4.466259000000	-2.457946000000	0.312782000000
H	3.118836000000	-0.139496000000	-1.758166000000
H	3.969006000000	3.424195000000	0.490109000000
H	2.696240000000	-0.160323000000	2.500349000000
H	6.105731000000	2.468285000000	-1.705584000000
H	5.324694000000	3.938270000000	-1.076111000000
H	5.580594000000	3.755993000000	-2.822509000000
H	4.286085000000	2.210484000000	-4.184214000000
H	3.035730000000	1.146793000000	-3.512458000000
H	4.757974000000	0.821065000000	-3.178872000000
H	2.784783000000	4.293532000000	-1.447236000000
H	1.870136000000	3.134301000000	-2.434394000000
H	3.088254000000	4.188817000000	-3.201026000000

H	5.627249000000	2.103552000000	3.142208000000
H	4.663030000000	0.807533000000	3.887255000000
H	4.844670000000	2.371307000000	4.724506000000
H	4.509166000000	4.252269000000	2.359688000000
H	3.612182000000	4.426089000000	3.877942000000
H	2.730463000000	4.380491000000	2.331784000000
H	2.117211000000	1.063176000000	4.114836000000
H	1.301501000000	2.469097000000	3.397347000000
H	2.305409000000	2.660463000000	4.860204000000
H	-3.120211000000	-0.139769000000	-1.757558000000
H	-3.970092000000	3.422744000000	0.492687000000
H	-2.694399000000	-0.161991000000	2.500647000000
H	-1.872648000000	3.134108000000	-2.433036000000
H	-2.786943000000	4.293081000000	-1.445276000000
H	-3.091215000000	4.188646000000	-3.198944000000
H	-5.326614000000	3.937171000000	-1.072576000000
H	-6.107802000000	2.467401000000	-1.702341000000
H	-5.583395000000	3.755696000000	-2.818932000000
H	-3.038612000000	1.146873000000	-3.511165000000
H	-4.289481000000	2.210617000000	-4.181939000000
H	-4.760632000000	0.820826000000	-3.176785000000
H	-1.300364000000	2.466965000000	3.398201000000
H	-2.115549000000	1.060552000000	4.115251000000
H	-2.303623000000	2.657345000000	4.861666000000
H	-4.842910000000	2.368468000000	4.726950000000
H	-4.661680000000	0.805020000000	3.888979000000
H	-5.626223000000	2.101381000000	3.144866000000
H	-2.729843000000	4.378522000000	2.333897000000

H	-3.610702000000	4.423585000000	3.880584000000
H	-4.508523000000	4.250366000000	2.362788000000
H	6.267447000000	-5.521984000000	0.285947000000
H	5.773204000000	-4.067382000000	1.178104000000
H	5.734593000000	-4.079775000000	-0.604328000000
H	4.012387000000	-5.522324000000	-1.839284000000
H	2.907736000000	-6.577154000000	-0.930253000000
H	4.651258000000	-6.929831000000	-0.946560000000
H	4.704413000000	-6.908597000000	1.611323000000
H	2.961562000000	-6.555744000000	1.661359000000
H	4.102808000000	-5.486362000000	2.506382000000
H	-2.904991000000	-6.577863000000	-0.931147000000
H	-4.009937000000	-5.523358000000	-1.840204000000
H	-4.648370000000	-6.931268000000	-0.947798000000
H	-2.959282000000	-6.556888000000	1.660490000000
H	-4.701970000000	-6.910460000000	1.610034000000
H	-4.101142000000	-5.488117000000	2.505449000000
H	-5.771862000000	-4.069702000000	1.177224000000
H	-6.265332000000	-5.524218000000	0.284508000000
H	-5.732885000000	-4.081516000000	-0.605203000000

L-Ga

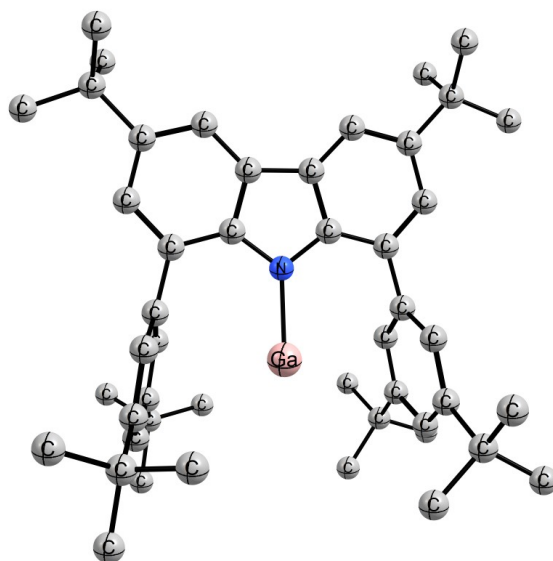


Figure 51. Optimized structure at the B3LYP-D3(BJ)/def2SVP level of theory for **125**. Hydrogen atoms are omitted for clarity.

Energy (B3LYP-D3(BJ)/def2SVP) = -3846.09 Hartree

C	-3.185834000000	-0.114659000000	-0.038089000000
C	-1.915930000000	-0.761250000000	-0.016053000000
N	-0.871895000000	0.162473000000	-0.028019000000
C	-1.479751000000	1.416477000000	-0.069356000000
C	-2.900898000000	1.307944000000	-0.074649000000
C	-3.692730000000	2.459338000000	-0.098610000000
C	-0.866926000000	2.679717000000	-0.086932000000
C	-3.100600000000	3.730801000000	-0.113269000000
C	-1.690526000000	3.810729000000	-0.104575000000
C	-4.359651000000	-0.872917000000	-0.014672000000
C	-1.836772000000	-2.162709000000	0.019242000000
C	-3.031567000000	-2.889976000000	0.046948000000
C	-4.302384000000	-2.273682000000	0.032027000000

Ga	1.140269000000	-0.233644000000	0.194477000000
C	0.619590000000	2.762006000000	-0.066467000000
C	1.355169000000	2.543573000000	-1.242903000000
C	1.300637000000	2.940910000000	1.146873000000
H	0.800929000000	2.386510000000	-2.167033000000
H	0.705301000000	3.081926000000	2.047623000000
C	2.758106000000	2.515107000000	-1.226676000000
C	2.702178000000	2.915503000000	1.202515000000
C	3.400558000000	2.713603000000	0.003831000000
H	4.489991000000	2.684290000000	0.034308000000
C	-0.493999000000	-2.805760000000	0.012489000000
C	0.201128000000	-2.958716000000	-1.196671000000
C	0.144499000000	-3.154162000000	1.210827000000
H	-0.305376000000	-2.666625000000	-2.118060000000
H	-0.401562000000	-3.008848000000	2.144494000000
C	1.512230000000	-3.456050000000	-1.228958000000
C	1.457654000000	-3.651629000000	1.220809000000
C	2.115843000000	-3.797794000000	-0.008887000000
H	3.135125000000	-4.171095000000	-0.015863000000
H	-5.324900000000	-0.361526000000	-0.030949000000
H	-2.952679000000	-3.976214000000	0.074642000000
H	-4.780506000000	2.358214000000	-0.102156000000
H	-1.199688000000	4.783292000000	-0.115642000000
C	-3.993967000000	4.983460000000	-0.138305000000
C	-5.609107000000	-3.085867000000	0.061198000000
C	2.135289000000	-3.967767000000	2.562684000000
C	3.593234000000	2.262640000000	-2.490937000000
C	2.236910000000	-3.583974000000	-2.577405000000

C	3.478690000000	3.043068000000	2.521628000000
C	-3.175781000000	6.284158000000	-0.148030000000
H	-2.542377000000	6.374905000000	0.747772000000
H	-2.526711000000	6.351863000000	-1.034565000000
H	-3.854347000000	7.151334000000	-0.165203000000
C	-4.874087000000	4.960446000000	-1.405779000000
H	-5.526194000000	5.848831000000	-1.442596000000
H	-4.250474000000	4.953496000000	-2.313455000000
H	-5.518598000000	4.069328000000	-1.436662000000
C	-4.897765000000	4.994635000000	1.112570000000
H	-5.543772000000	4.105124000000	1.155433000000
H	-4.291348000000	5.011917000000	2.031699000000
H	-5.549657000000	5.883922000000	1.113200000000
C	-5.354042000000	-4.600287000000	0.113393000000
H	-4.795008000000	-4.950940000000	-0.767710000000
H	-4.790005000000	-4.888513000000	1.013759000000
H	-6.313956000000	-5.139576000000	0.134866000000
C	-6.431629000000	-2.781089000000	-1.208526000000
H	-6.685031000000	-1.712993000000	-1.281973000000
H	-5.866798000000	-3.053674000000	-2.113784000000
H	-7.375355000000	-3.351332000000	-1.206595000000
C	-6.428903000000	-2.694101000000	1.308651000000
H	-5.862289000000	-2.903908000000	2.229394000000
H	-6.681953000000	-1.623408000000	1.309023000000
H	-7.372768000000	-3.262755000000	1.347914000000
C	2.549527000000	3.299580000000	3.717850000000
H	1.839532000000	2.472367000000	3.868966000000
H	3.146269000000	3.396343000000	4.637868000000

H	1.972260000000	4.228661000000	3.594322000000
C	4.242462000000	1.724705000000	2.773402000000
H	4.961622000000	1.511343000000	1.968538000000
H	4.801364000000	1.777755000000	3.721791000000
H	3.544504000000	0.874545000000	2.829773000000
C	4.479304000000	4.212900000000	2.424163000000
H	3.954333000000	5.162964000000	2.238642000000
H	5.045955000000	4.311760000000	3.363980000000
H	5.205537000000	4.065611000000	1.611108000000
C	4.361049000000	3.552764000000	-2.847081000000
H	3.663340000000	4.380408000000	-3.048733000000
H	5.024590000000	3.865258000000	-2.026387000000
H	4.980970000000	3.398547000000	-3.745305000000
C	2.716661000000	1.862498000000	-3.688070000000
H	2.013403000000	2.660922000000	-3.968280000000
H	3.352398000000	1.660006000000	-4.563631000000
H	2.135615000000	0.951478000000	-3.478024000000
C	4.597620000000	1.120598000000	-2.228581000000
H	5.164623000000	0.892394000000	-3.145110000000
H	5.324625000000	1.380164000000	-1.445480000000
H	4.075149000000	0.206410000000	-1.908683000000
C	1.299376000000	-5.015916000000	3.326001000000
H	1.221774000000	-5.950549000000	2.748750000000
H	1.768683000000	-5.249045000000	4.295369000000
H	0.278467000000	-4.658650000000	3.525802000000
C	3.557095000000	-4.520678000000	2.381797000000
H	4.216169000000	-3.797181000000	1.878102000000
H	3.997682000000	-4.740711000000	3.366312000000

H	3.561329000000	-5.454515000000	1.798789000000
C	2.222777000000	-2.669197000000	3.394245000000
H	2.712587000000	-2.864002000000	4.362056000000
H	2.805191000000	-1.902071000000	2.860007000000
H	1.226605000000	-2.249979000000	3.599839000000
C	2.288117000000	-2.198860000000	-3.256465000000
H	1.282256000000	-1.793904000000	-3.441328000000
H	2.829120000000	-1.477436000000	-2.626173000000
H	2.807298000000	-2.262459000000	-4.226265000000
C	3.677260000000	-4.093729000000	-2.418711000000
H	4.157438000000	-4.163978000000	-3.406798000000
H	4.284253000000	-3.414118000000	-1.800990000000
H	3.709502000000	-5.094875000000	-1.962327000000
C	1.463549000000	-4.572029000000	-3.475492000000
H	1.962054000000	-4.674607000000	-4.452975000000
H	1.414072000000	-5.568253000000	-3.008875000000
H	0.432376000000	-4.234653000000	-3.657137000000

L-GaCr(CO)₅

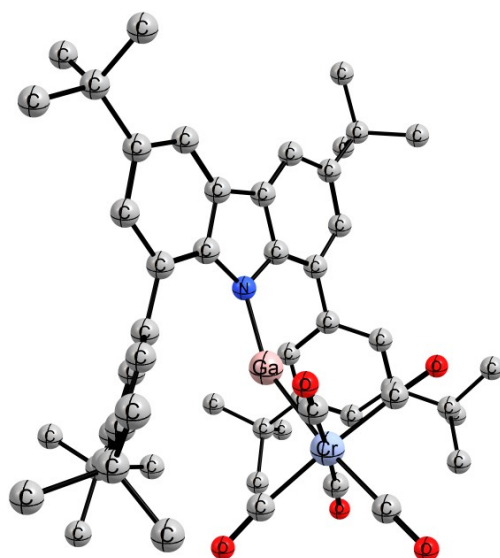


Figure 52. Optimized structure at the B3LYP-D3(BJ)/def2SVP level of theory for **126**. Hydrogen atoms are omitted for clarity.

Energy (B3LYP-D3(BJ)/def2SVP) = -5456.84 Hartree

Cr	-0.023702000000	-2.339911000000	-1.651766000000
Ga	0.036278000000	-0.505592000000	-0.076815000000
O	2.262606000000	-0.945244000000	-3.105103000000
O	1.851958000000	-4.233760000000	-0.190374000000
O	-0.111839000000	-4.326437000000	-3.914138000000
O	-2.125633000000	-3.974464000000	-0.180196000000
O	-2.077072000000	-0.725410000000	-3.220367000000
N	0.100157000000	1.368670000000	0.389159000000
C	1.261297000000	2.165193000000	0.362815000000
C	2.608145000000	1.772415000000	0.392657000000
C	3.579308000000	2.779128000000	0.278596000000
H	4.620477000000	2.461870000000	0.311000000000
C	3.267221000000	4.147318000000	0.153362000000

C	1.915161000000	4.513222000000	0.135569000000
H	1.624863000000	5.561052000000	0.034623000000
C	0.919317000000	3.537665000000	0.231579000000
C	-0.527333000000	3.595658000000	0.180972000000
C	-1.430381000000	4.654143000000	0.014189000000
H	-1.043030000000	5.669158000000	-0.068285000000
C	-2.801391000000	4.397457000000	-0.058319000000
C	-3.231219000000	3.056238000000	0.059989000000
H	-4.299133000000	2.832612000000	0.031661000000
C	-2.361773000000	1.975643000000	0.243890000000
C	-0.985625000000	2.258814000000	0.289024000000
C	4.352229000000	5.231416000000	0.039164000000
C	5.770819000000	4.641730000000	0.069299000000
H	6.512060000000	5.451006000000	-0.019382000000
H	5.940463000000	3.942781000000	-0.764118000000
H	5.972165000000	4.108382000000	1.010988000000
C	4.214441000000	6.218265000000	1.217396000000
H	4.335968000000	5.697144000000	2.179877000000
H	3.229504000000	6.708580000000	1.224297000000
H	4.981991000000	7.006918000000	1.153674000000
C	4.175034000000	5.991944000000	-1.291868000000
H	4.942339000000	6.776738000000	-1.394082000000
H	3.189505000000	6.476740000000	-1.356202000000
H	4.267734000000	5.306665000000	-2.148875000000
C	-3.849201000000	5.505156000000	-0.250640000000
C	-4.805955000000	5.522713000000	0.960162000000
H	-5.333376000000	4.564234000000	1.077193000000
H	-5.566408000000	6.311746000000	0.840632000000

H	-4.252595000000	5.717012000000	1.892233000000
C	-4.654191000000	5.230254000000	-1.538303000000
H	-3.991114000000	5.212145000000	-2.417301000000
H	-5.412258000000	6.014964000000	-1.695069000000
H	-5.177834000000	4.263637000000	-1.493677000000
C	-3.203095000000	6.893355000000	-0.374162000000
H	-2.635370000000	7.160909000000	0.530221000000
H	-3.983451000000	7.657183000000	-0.514957000000
H	-2.521712000000	6.950236000000	-1.236894000000
C	3.018806000000	0.354538000000	0.535803000000
C	3.924329000000	-0.211746000000	-0.377344000000
H	4.246911000000	0.397660000000	-1.218864000000
C	4.390656000000	-1.518386000000	-0.218625000000
C	3.931521000000	-2.253207000000	0.890077000000
H	4.293865000000	-3.269903000000	1.021057000000
C	3.020294000000	-1.735173000000	1.813048000000
C	2.558464000000	-0.420731000000	1.612286000000
H	1.892717000000	0.047393000000	2.340596000000
C	5.382264000000	-2.165807000000	-1.197577000000
C	4.741644000000	-3.423753000000	-1.821374000000
H	5.451598000000	-3.909025000000	-2.510028000000
H	3.840051000000	-3.161183000000	-2.393921000000
H	4.451976000000	-4.160752000000	-1.059136000000
C	6.658755000000	-2.566166000000	-0.428091000000
H	7.389333000000	-3.025258000000	-1.113326000000
H	6.445731000000	-3.293687000000	0.369325000000
H	7.129730000000	-1.685269000000	0.035606000000
C	5.777418000000	-1.211174000000	-2.334832000000

H	6.485539000000	-1.714654000000	-3.010782000000
H	6.270918000000	-0.303907000000	-1.953464000000
H	4.904123000000	-0.907513000000	-2.929855000000
C	2.536506000000	-2.529589000000	3.035213000000
C	3.146648000000	-3.938165000000	3.095315000000
H	4.243570000000	-3.902887000000	3.180124000000
H	2.885345000000	-4.530544000000	2.206925000000
H	2.762856000000	-4.469812000000	3.979582000000
C	2.929972000000	-1.769183000000	4.319348000000
H	4.021709000000	-1.638638000000	4.377354000000
H	2.602690000000	-2.328270000000	5.210656000000
H	2.469555000000	-0.770839000000	4.362366000000
C	1.003763000000	-2.669533000000	2.972807000000
H	0.696065000000	-3.246586000000	2.089696000000
H	0.509380000000	-1.688136000000	2.925552000000
H	0.621555000000	-3.186354000000	3.866715000000
C	-2.911077000000	0.605720000000	0.411722000000
C	-2.681908000000	-0.108685000000	1.603359000000
H	-2.056847000000	0.354204000000	2.366433000000
C	-3.331155000000	-1.327989000000	1.847797000000
C	-4.163364000000	-1.837487000000	0.840029000000
H	-4.660922000000	-2.792327000000	1.010451000000
C	-4.399979000000	-1.165109000000	-0.367729000000
C	-3.763858000000	0.067414000000	-0.561465000000
H	-3.922784000000	0.639772000000	-1.472857000000
C	-3.230585000000	-2.065200000000	3.193687000000
C	-2.358816000000	-1.304677000000	4.204539000000
H	-2.309614000000	-1.866557000000	5.149802000000

H	-2.770396000000	-0.308919000000	4.429125000000
H	-1.328452000000	-1.176015000000	3.845680000000
C	-2.636104000000	-3.471038000000	2.980079000000
H	-1.626890000000	-3.412293000000	2.550756000000
H	-3.248480000000	-4.073555000000	2.294921000000
H	-2.570765000000	-4.007617000000	3.940356000000
C	-4.646999000000	-2.196496000000	3.795092000000
H	-4.600039000000	-2.701337000000	4.773418000000
H	-5.314107000000	-2.784046000000	3.147539000000
H	-5.105022000000	-1.205832000000	3.941030000000
H	-4.615632000000	-3.821261000000	-1.119847000000
C	1.402058000000	-1.446590000000	-2.530071000000
C	1.187554000000	-3.461291000000	-0.722922000000
C	-0.076842000000	-3.570650000000	-3.047973000000
C	-1.371822000000	-3.300156000000	-0.724111000000
C	-1.307422000000	-1.306819000000	-2.594469000000
C	-5.360748000000	-1.767720000000	-1.406539000000
C	-5.578303000000	-0.829072000000	-2.604005000000
H	-6.281110000000	-1.292897000000	-3.313111000000
H	-6.008350000000	0.135435000000	-2.292439000000
H	-4.641106000000	-0.632484000000	-3.143344000000
C	-6.728658000000	-2.026673000000	-0.740324000000
H	-7.438400000000	-2.437999000000	-1.475816000000
H	-6.654461000000	-2.746517000000	0.088195000000
H	-7.152948000000	-1.092948000000	-0.339139000000
C	-4.785811000000	-3.099516000000	-1.931120000000
H	-5.481488000000	-3.555172000000	-2.653883000000
H	-3.825227000000	-2.937859000000	-2.442047000000

L-GaMo(CO)₅

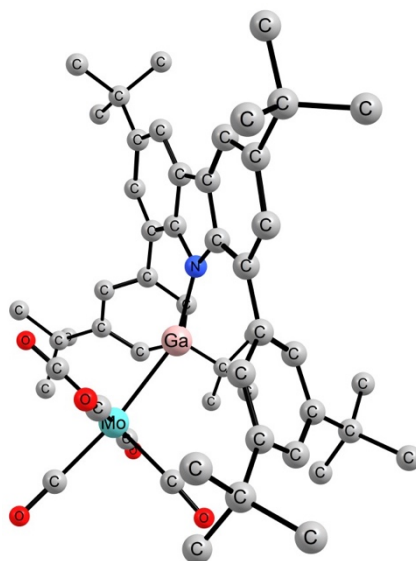


Figure 53. Optimized structure at the B3LYP-D3(BJ)/def2SVP level of theory for **127**. Hydrogen atoms are omitted for clarity.

Energy (B3LYP-D3(BJ)/def2SVP) = -4480.75 Hartree

Mo	-0.011659000000	-2.411264000000	-1.548053000000
Ga	0.017974000000	-0.390530000000	0.043354000000
O	2.342039000000	-0.906200000000	-3.114947000000
O	1.988362000000	-4.322487000000	0.059140000000
O	-0.033893000000	-4.543471000000	-3.879321000000
O	-2.215538000000	-4.153462000000	-0.011618000000
O	-2.168175000000	-0.756958000000	-3.243237000000
N	0.079015000000	1.503938000000	0.427307000000
C	1.234923000000	2.305704000000	0.366660000000
C	2.584994000000	1.922376000000	0.397858000000
C	3.548142000000	2.931394000000	0.242345000000
H	4.591678000000	2.622157000000	0.275957000000
C	3.226305000000	4.292738000000	0.074547000000

C	1.871846000000	4.649477000000	0.056242000000
H	1.573872000000	5.691477000000	-0.077531000000
C	0.883334000000	3.671377000000	0.192892000000
C	-0.564069000000	3.718817000000	0.149400000000
C	-1.475467000000	4.764790000000	-0.048524000000
H	-1.095856000000	5.779337000000	-0.165600000000
C	-2.844859000000	4.496159000000	-0.108573000000
C	-3.264904000000	3.156083000000	0.052013000000
H	-4.331202000000	2.923954000000	0.031548000000
C	-2.387033000000	2.088371000000	0.267382000000
C	-1.012575000000	2.383191000000	0.302806000000
C	4.303329000000	5.378966000000	-0.085964000000
C	5.725931000000	4.799496000000	-0.047744000000
H	6.461152000000	5.609929000000	-0.169765000000
H	5.893400000000	4.073967000000	-0.858584000000
H	5.938323000000	4.299381000000	0.909627000000
C	4.168931000000	6.404939000000	1.058725000000
H	4.301961000000	5.918048000000	2.037473000000
H	3.180861000000	6.888952000000	1.057226000000
H	4.930669000000	7.195804000000	0.961365000000
C	4.110136000000	6.092015000000	-1.440867000000
H	4.871515000000	6.877480000000	-1.576756000000
H	3.120986000000	6.568205000000	-1.513353000000
H	4.199993000000	5.378086000000	-2.274476000000
C	-3.901033000000	5.589815000000	-0.333042000000
C	-4.854637000000	5.639127000000	0.879377000000
H	-5.374641000000	4.681035000000	1.028484000000
H	-5.621194000000	6.418405000000	0.737006000000

H	-4.300163000000	5.867084000000	1.803124000000
C	-4.707576000000	5.268694000000	-1.609021000000
H	-4.046643000000	5.226777000000	-2.488823000000
H	-5.471137000000	6.043096000000	-1.788696000000
H	-5.224894000000	4.300691000000	-1.532135000000
C	-3.265225000000	6.977929000000	-0.502496000000
H	-2.696617000000	7.277915000000	0.391086000000
H	-4.051440000000	7.731418000000	-0.664777000000
H	-2.586934000000	7.012317000000	-1.368850000000
C	3.010137000000	0.513136000000	0.584180000000
C	3.913573000000	-0.074906000000	-0.317990000000
H	4.224342000000	0.509629000000	-1.181495000000
C	4.397656000000	-1.369430000000	-0.118025000000
C	3.953048000000	-2.072428000000	1.017269000000
H	4.329312000000	-3.079321000000	1.180870000000
C	3.048251000000	-1.530785000000	1.932912000000
C	2.571703000000	-0.228291000000	1.692641000000
H	1.909619000000	0.258254000000	2.412188000000
C	5.403426000000	-2.032954000000	-1.071818000000
C	4.792450000000	-3.327554000000	-1.648057000000
H	5.510077000000	-3.816890000000	-2.325687000000
H	3.878968000000	-3.110762000000	-2.220976000000
H	4.530373000000	-4.046153000000	-0.858763000000
C	6.686088000000	-2.377321000000	-0.285065000000
H	7.427566000000	-2.847190000000	-0.951022000000
H	6.485993000000	-3.077734000000	0.539455000000
H	7.137690000000	-1.469659000000	0.145023000000
C	5.784473000000	-1.113203000000	-2.242218000000

H	6.505498000000	-1.627252000000	-2.896212000000
H	6.258905000000	-0.183451000000	-1.892169000000
H	4.909289000000	-0.847667000000	-2.851989000000
C	2.586820000000	-2.287440000000	3.187363000000
C	3.236046000000	-3.674807000000	3.305820000000
H	4.332020000000	-3.605057000000	3.381562000000
H	2.987231000000	-4.314795000000	2.447552000000
H	2.871857000000	-4.176451000000	4.215533000000
C	2.957108000000	-1.466427000000	4.440569000000
H	4.044767000000	-1.303902000000	4.494433000000
H	2.643601000000	-1.999143000000	5.352693000000
H	2.469375000000	-0.480324000000	4.445074000000
C	1.058884000000	-2.470576000000	3.128176000000
H	0.767077000000	-3.079069000000	2.260851000000
H	0.540130000000	-1.503981000000	3.049403000000
H	0.688012000000	-2.969897000000	4.036761000000
C	-2.921656000000	0.717401000000	0.470668000000
C	-2.675422000000	0.032800000000	1.676227000000
H	-2.058450000000	0.524427000000	2.427815000000
C	-3.295639000000	-1.196057000000	1.946982000000
C	-4.121224000000	-1.743142000000	0.953536000000
H	-4.599967000000	-2.703422000000	1.146015000000
C	-4.385714000000	-1.094439000000	-0.261882000000
C	-3.771128000000	0.144133000000	-0.485732000000
H	-3.947837000000	0.695769000000	-1.406807000000
C	-3.172480000000	-1.903240000000	3.306944000000
C	-2.314866000000	-1.101867000000	4.298144000000
H	-2.247700000000	-1.643497000000	5.254024000000

H	-2.749688000000	-0.112181000000	4.504967000000
H	-1.289584000000	-0.955126000000	3.931891000000
C	-2.546089000000	-3.298412000000	3.116897000000
H	-1.544974000000	-3.224083000000	2.670983000000
H	-3.153835000000	-3.932019000000	2.456388000000
H	-2.452138000000	-3.810795000000	4.087897000000
C	-4.582503000000	-2.056229000000	3.918081000000
H	-4.518769000000	-2.540953000000	4.905570000000
H	-5.238621000000	-2.671773000000	3.285501000000
H	-5.063079000000	-1.074012000000	4.047627000000
H	-4.644437000000	-3.776711000000	-0.943123000000
C	1.504719000000	-1.431949000000	-2.529493000000
C	1.315026000000	-3.580853000000	-0.503778000000
C	-0.025351000000	-3.774512000000	-3.023381000000
C	-1.465381000000	-3.472459000000	-0.550950000000
C	-1.403944000000	-1.333928000000	-2.608272000000
C	-5.366159000000	-1.721309000000	-1.267858000000
C	-5.606527000000	-0.812612000000	-2.483890000000
H	-6.323333000000	-1.293614000000	-3.167028000000
H	-6.030874000000	0.159270000000	-2.188000000000
H	-4.680914000000	-0.629142000000	-3.046875000000
C	-6.721466000000	-1.955924000000	-0.566749000000
H	-7.447519000000	-2.384734000000	-1.275889000000
H	-6.632309000000	-2.652294000000	0.280152000000
H	-7.134033000000	-1.009541000000	-0.183457000000
C	-4.809933000000	-3.069772000000	-1.768107000000
H	-5.516073000000	-3.532704000000	-2.475795000000
H	-3.850799000000	-2.931593000000	-2.288476000000

L-GaW(CO)₅

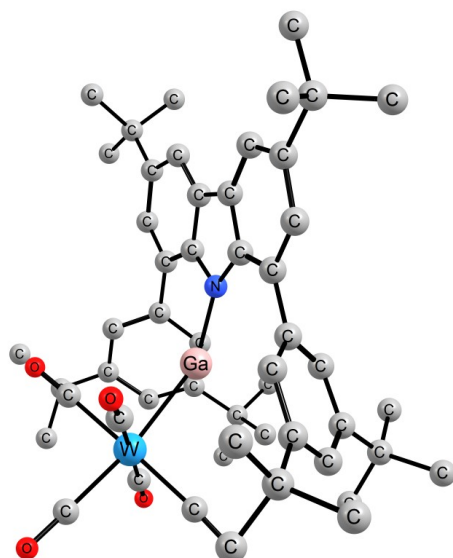


Figure 54. Optimized structure at the B3LYP-D3(BJ)/def2SVP level of theory for **128**. Hydrogen atoms are omitted for clarity.

Energy (B3LYP-D3(BJ)/def2SVP) = -4479.63 Hartree

W	-0.017784000000	-2.327846000000	-1.377883000000
Ga	0.019970000000	-0.229704000000	0.147357000000
O	2.361727000000	-0.870577000000	-2.984508000000
O	1.985457000000	-4.195142000000	0.308433000000
O	-0.050119000000	-4.542547000000	-3.652965000000
O	-2.242727000000	-3.997772000000	0.241534000000
O	-2.179469000000	-0.707221000000	-3.129682000000
N	0.088049000000	1.671621000000	0.463732000000
C	1.247562000000	2.465863000000	0.375994000000
C	2.595365000000	2.076941000000	0.420835000000
C	3.563419000000	3.075308000000	0.231378000000
H	4.605488000000	2.762553000000	0.275771000000
C	3.247753000000	4.431614000000	0.017142000000

C	1.894959000000	4.794058000000	-0.014154000000
H	1.602139000000	5.832298000000	-0.183599000000
C	0.901673000000	3.825944000000	0.155265000000
C	-0.545744000000	3.877868000000	0.109087000000
C	-1.453388000000	4.919626000000	-0.125080000000
H	-1.070298000000	5.928309000000	-0.276339000000
C	-2.823725000000	4.653765000000	-0.177089000000
C	-3.248954000000	3.321412000000	0.028352000000
H	-4.316043000000	3.092441000000	0.014502000000
C	-2.374921000000	2.258744000000	0.280715000000
C	-0.999933000000	2.550373000000	0.307631000000
C	4.329885000000	5.506824000000	-0.179236000000
C	5.749727000000	4.922175000000	-0.122189000000
H	6.488713000000	5.724649000000	-0.271040000000
H	5.913439000000	4.169517000000	-0.908703000000
H	5.960173000000	4.452950000000	0.851112000000
C	4.200481000000	6.570381000000	0.931222000000
H	4.331720000000	6.115263000000	1.925384000000
H	3.214554000000	7.058459000000	0.914050000000
H	4.965690000000	7.354230000000	0.807848000000
C	4.139715000000	6.175902000000	-1.556795000000
H	4.904966000000	6.952640000000	-1.718523000000
H	3.152980000000	6.654485000000	-1.644746000000
H	4.225725000000	5.434553000000	-2.366527000000
C	-3.875742000000	5.742991000000	-0.439322000000
C	-4.830546000000	5.836147000000	0.769592000000
H	-5.354468000000	4.885568000000	0.949795000000
H	-5.593884000000	6.613183000000	0.600348000000

H	-4.276303000000	6.092609000000	1.685975000000
C	-4.681904000000	5.382151000000	-1.704882000000
H	-4.020094000000	5.308589000000	-2.581940000000
H	-5.442520000000	6.152760000000	-1.911318000000
H	-5.202711000000	4.419057000000	-1.596378000000
C	-3.234903000000	7.122476000000	-0.654209000000
H	-2.666214000000	7.450125000000	0.229560000000
H	-4.018356000000	7.872806000000	-0.842375000000
H	-2.555643000000	7.125728000000	-1.520480000000
C	3.010926000000	0.672119000000	0.655175000000
C	3.912191000000	0.047550000000	-0.224198000000
H	4.229511000000	0.600220000000	-1.106106000000
C	4.386032000000	-1.243076000000	0.020658000000
C	3.933260000000	-1.904224000000	1.177679000000
H	4.301723000000	-2.907655000000	1.376201000000
C	3.030396000000	-1.325518000000	2.072177000000
C	2.564007000000	-0.028412000000	1.786811000000
H	1.904605000000	0.487276000000	2.488322000000
C	5.389526000000	-1.945653000000	-0.907169000000
C	4.769814000000	-3.253766000000	-1.442121000000
H	5.483876000000	-3.768874000000	-2.104206000000
H	3.857367000000	-3.049311000000	-2.021042000000
H	4.503494000000	-3.945342000000	-0.630486000000
C	6.666862000000	-2.273922000000	-0.105073000000
H	7.406357000000	-2.771838000000	-0.752579000000
H	6.458529000000	-2.944765000000	0.741686000000
H	7.124707000000	-1.356095000000	0.295878000000
C	5.781548000000	-1.067985000000	-2.105916000000

H	6.500927000000	-1.608826000000	-2.739794000000
H	6.261922000000	-0.130814000000	-1.784918000000
H	4.910414000000	-0.816445000000	-2.727123000000
C	2.558421000000	-2.037067000000	3.348823000000
C	3.209070000000	-3.417824000000	3.523756000000
H	4.304345000000	-3.342855000000	3.604699000000
H	2.967583000000	-4.089981000000	2.688390000000
H	2.838937000000	-3.885787000000	4.448881000000
C	2.913855000000	-1.171266000000	4.575802000000
H	4.000423000000	-1.003298000000	4.634768000000
H	2.592902000000	-1.672882000000	5.502813000000
H	2.422982000000	-0.187325000000	4.541631000000
C	1.031553000000	-2.225616000000	3.279984000000
H	0.750497000000	-2.866290000000	2.432692000000
H	0.512348000000	-1.263580000000	3.159020000000
H	0.651641000000	-2.691103000000	4.202629000000
C	-2.912389000000	0.896505000000	0.529912000000
C	-2.670754000000	0.254422000000	1.759725000000
H	-2.055364000000	0.771354000000	2.495542000000
C	-3.295625000000	-0.962115000000	2.072357000000
C	-4.119512000000	-1.542124000000	1.096375000000
H	-4.601766000000	-2.493347000000	1.321998000000
C	-4.378742000000	-0.936723000000	-0.142254000000
C	-3.760331000000	0.291637000000	-0.408130000000
H	-3.933088000000	0.810758000000	-1.348641000000
C	-3.182644000000	-1.618426000000	3.458449000000
C	-2.318314000000	-0.789429000000	4.420641000000
H	-2.257157000000	-1.296295000000	5.395788000000

H	-2.743927000000	0.211170000000	4.590834000000
H	-1.291450000000	-0.665788000000	4.050462000000
C	-2.573000000000	-3.027370000000	3.324204000000
H	-1.570763000000	-2.983554000000	2.876998000000
H	-3.187678000000	-3.679097000000	2.688297000000
H	-2.486563000000	-3.502150000000	4.314803000000
C	-4.596074000000	-1.731255000000	4.070788000000
H	-4.540777000000	-2.178718000000	5.076225000000
H	-5.257694000000	-2.362557000000	3.459809000000
H	-5.065229000000	-0.739200000000	4.161348000000
H	-4.639890000000	-3.640716000000	-0.734734000000
C	1.517528000000	-1.379957000000	-2.392499000000
C	1.312333000000	-3.476029000000	-0.285378000000
C	-0.037913000000	-3.748557000000	-2.818491000000
C	-1.486990000000	-3.349425000000	-0.331394000000
C	-1.415544000000	-1.271326000000	-2.481105000000
C	-5.357982000000	-1.596520000000	-1.128130000000
C	-5.597376000000	-0.728061000000	-2.373428000000
H	-6.314293000000	-1.230864000000	-3.040557000000
H	-6.021319000000	0.253202000000	-2.109549000000
H	-4.671585000000	-0.563770000000	-2.941772000000
C	-6.714179000000	-1.808642000000	-0.421627000000
H	-7.438789000000	-2.260960000000	-1.117496000000
H	-6.626274000000	-2.476828000000	0.447795000000
H	-7.127938000000	-0.850379000000	-0.070465000000
C	-4.800532000000	-2.960531000000	-1.582766000000
H	-5.503580000000	-3.445161000000	-2.278878000000
H	-3.838588000000	-2.839998000000	-2.102196000000

L-Ga(NHC)

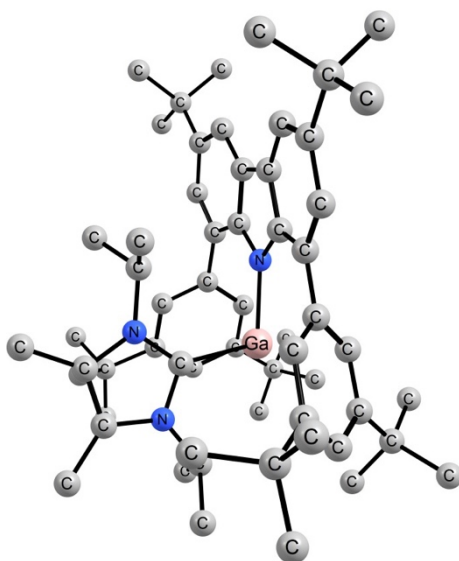


Figure 55. Optimized structure at the B3LYP-D3(BJ)/def2SVP level of theory for **129**. Hydrogen atoms are omitted for clarity.

Energy (B3LYP-D3(BJ)/def2SVP) = -4386.51 Hartree

C	-1.878470000000	2.958089000000	-0.611763000000
C	-1.853142000000	1.531026000000	-0.700431000000
N	-0.556966000000	1.062776000000	-0.876635000000
C	0.262706000000	2.182195000000	-0.893911000000
C	-0.501720000000	3.381664000000	-0.729444000000
C	0.121247000000	4.627317000000	-0.619760000000
C	1.672193000000	2.264448000000	-0.928427000000
C	1.518071000000	4.725758000000	-0.654865000000
C	2.256323000000	3.534627000000	-0.805354000000
C	-3.073361000000	3.644626000000	-0.378248000000
C	-3.050778000000	0.809829000000	-0.515476000000
C	-4.225688000000	1.533070000000	-0.276263000000
C	-4.273261000000	2.942686000000	-0.211005000000

Ga	0.000508000000	-0.979438000000	-0.888389000000
C	2.546521000000	1.070575000000	-1.021412000000
C	2.392769000000	0.124630000000	-2.053877000000
C	3.577905000000	0.888123000000	-0.093749000000
H	1.640095000000	0.317871000000	-2.815709000000
H	3.693240000000	1.630133000000	0.696766000000
C	3.244360000000	-0.985541000000	-2.156065000000
C	4.443275000000	-0.211289000000	-0.153813000000
C	4.248336000000	-1.141921000000	-1.184299000000
H	4.906276000000	-2.006782000000	-1.252158000000
C	-3.075429000000	-0.679615000000	-0.479847000000
C	-3.060278000000	-1.447508000000	-1.651769000000
C	-3.106171000000	-1.335585000000	0.758015000000
H	-3.031893000000	-0.924572000000	-2.608911000000
H	-3.131603000000	-0.722630000000	1.658868000000
C	-3.063590000000	-2.848731000000	-1.606033000000
C	-3.110307000000	-2.733071000000	0.849259000000
C	-3.082835000000	-3.466914000000	-0.346761000000
H	-3.078329000000	-4.551613000000	-0.295403000000
H	-3.056374000000	4.735387000000	-0.313833000000
H	-5.136006000000	0.952701000000	-0.129071000000
H	-0.494568000000	5.519836000000	-0.484737000000
H	3.344080000000	3.577226000000	-0.840861000000
C	2.191638000000	6.101334000000	-0.515702000000
C	-5.578808000000	3.712685000000	0.050963000000
C	-3.187290000000	-3.398883000000	2.233086000000
C	3.118455000000	-2.010586000000	-3.297203000000
C	-3.012358000000	-3.649506000000	-2.916955000000

C	5.564944000000	-0.330204000000	0.891113000000
C	0.806005000000	-0.945005000000	1.329223000000
N	0.542466000000	-0.198377000000	2.430411000000
N	1.373805000000	-2.085634000000	1.805921000000
C	1.454053000000	-2.065241000000	3.199749000000
C	0.934508000000	-0.857940000000	3.595000000000
C	1.986105000000	-3.168977000000	4.051985000000
H	3.079691000000	-3.272034000000	3.973557000000
H	1.746725000000	-2.972437000000	5.105359000000
H	1.540514000000	-4.140643000000	3.790645000000
C	0.759274000000	-0.327512000000	4.978912000000
H	-0.300086000000	-0.309940000000	5.280664000000
H	1.299188000000	-0.959658000000	5.696228000000
H	1.148838000000	0.695396000000	5.081568000000
C	1.741311000000	-3.190721000000	0.895185000000
H	1.785084000000	-2.704975000000	-0.087475000000
C	0.646307000000	-4.253323000000	0.836779000000
C	3.123940000000	-3.775972000000	1.164976000000
H	3.864739000000	-2.980388000000	1.307994000000
H	3.145456000000	-4.445301000000	2.035337000000
H	3.431765000000	-4.366527000000	0.289904000000
H	0.505152000000	-4.751579000000	1.808355000000
H	0.917422000000	-5.022896000000	0.097658000000
H	-0.307850000000	-3.805072000000	0.525424000000
C	-0.007523000000	1.169260000000	2.312506000000
H	-0.260028000000	1.232022000000	1.253275000000
C	1.051437000000	2.233152000000	2.596510000000
C	-1.299316000000	1.375345000000	3.100495000000

H	-1.994915000000	0.540739000000	2.936910000000
H	-1.133431000000	1.489241000000	4.181650000000
H	-1.790636000000	2.289163000000	2.734982000000
H	1.313765000000	2.296072000000	3.664448000000
H	0.673965000000	3.215469000000	2.276025000000
H	1.961462000000	2.027503000000	2.018637000000
C	3.724430000000	6.009574000000	-0.574301000000
H	4.127407000000	5.385509000000	0.238321000000
H	4.071615000000	5.590433000000	-1.531050000000
H	4.163032000000	7.014522000000	-0.471184000000
C	1.720764000000	7.023941000000	-1.659223000000
H	2.187114000000	8.019627000000	-1.574322000000
H	1.991522000000	6.599158000000	-2.638446000000
H	0.629267000000	7.161542000000	-1.645726000000
C	1.800478000000	6.725770000000	0.840560000000
H	0.711773000000	6.858843000000	0.927431000000
H	2.126481000000	6.082384000000	1.673231000000
H	2.271191000000	7.715165000000	0.965360000000
C	-6.786198000000	2.776366000000	0.214251000000
H	-6.956928000000	2.170266000000	-0.688576000000
H	-6.659301000000	2.091144000000	1.066508000000
H	-7.696611000000	3.368989000000	0.395810000000
C	-5.862299000000	4.660312000000	-1.133492000000
H	-5.047284000000	5.385440000000	-1.276636000000
H	-5.970790000000	4.091154000000	-2.069955000000
H	-6.792786000000	5.227735000000	-0.965013000000
C	-5.435461000000	4.540814000000	1.345427000000
H	-5.233019000000	3.884606000000	2.206687000000

H	-4.609710000000	5.264547000000	1.275121000000
H	-6.360172000000	5.104879000000	1.552434000000
C	4.947311000000	-0.374331000000	2.306063000000
H	4.257165000000	-1.223583000000	2.415896000000
H	5.736863000000	-0.469348000000	3.069165000000
H	4.374628000000	0.538102000000	2.526981000000
C	6.429670000000	-1.583346000000	0.685341000000
H	6.921518000000	-1.577995000000	-0.299208000000
H	7.219210000000	-1.621961000000	1.451679000000
H	5.844421000000	-2.510901000000	0.765829000000
C	6.485330000000	0.904679000000	0.779830000000
H	5.934959000000	1.839797000000	0.959454000000
H	7.300488000000	0.845670000000	1.519443000000
H	6.934760000000	0.967150000000	-0.223395000000
C	4.458283000000	-2.091599000000	-4.057805000000
H	4.732268000000	-1.108997000000	-4.472588000000
H	5.281278000000	-2.423039000000	-3.406959000000
H	4.381921000000	-2.807467000000	-4.892298000000
C	2.014168000000	-1.631201000000	-4.296588000000
H	2.213764000000	-0.660378000000	-4.775340000000
H	1.957391000000	-2.390408000000	-5.091992000000
H	1.029951000000	-1.583917000000	-3.807538000000
C	2.774050000000	-3.395949000000	-2.711052000000
H	2.714797000000	-4.147808000000	-3.514410000000
H	3.534665000000	-3.733610000000	-1.991370000000
H	1.798970000000	-3.364501000000	-2.201388000000
C	-4.561449000000	-3.075758000000	2.857907000000
H	-5.378032000000	-3.459615000000	2.226796000000

H	-4.651527000000	-3.535861000000	3.855806000000
H	-4.706311000000	-1.990724000000	2.969825000000
C	-3.036948000000	-4.926178000000	2.154469000000
H	-2.078526000000	-5.218756000000	1.700346000000
H	-3.074519000000	-5.356753000000	3.167195000000
H	-3.846903000000	-5.387863000000	1.569902000000
C	-2.071781000000	-2.848135000000	3.145368000000
H	-2.109666000000	-3.334161000000	4.133786000000
H	-1.079659000000	-3.027476000000	2.711804000000
H	-2.167458000000	-1.765284000000	3.305114000000
C	-1.720995000000	-3.290626000000	-3.682308000000
H	-1.675859000000	-2.219606000000	-3.927660000000
H	-0.829824000000	-3.521044000000	-3.079879000000
H	-1.665184000000	-3.857896000000	-4.625844000000
C	-3.018447000000	-5.166304000000	-2.672231000000
H	-2.985548000000	-5.698229000000	-3.635606000000
H	-2.143827000000	-5.487553000000	-2.085817000000
H	-3.926741000000	-5.492998000000	-2.142598000000
C	-4.240673000000	-3.292151000000	-3.779325000000
H	-4.220875000000	-3.852174000000	-4.728520000000
H	-5.175417000000	-3.540931000000	-3.252565000000
H	-4.268109000000	-2.219925000000	-4.023247000000

L-Ga(C₁₄H₈O₂)

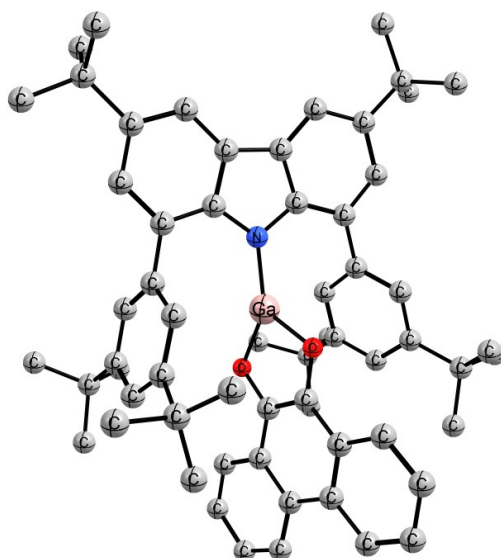


Figure 56. Optimized structure at the B3LYP-D3(BJ)/def2SVP level of theory for **130**. Hydrogen atoms are omitted for clarity.

Energy (B3LYP-D3(BJ)/def2SVP) = -4534.51 Hartree

Ga	0.101624000000	-0.097859000000	-0.009538000000
O	-1.363897000000	-0.752474000000	0.895279000000
C	-2.453126000000	-0.409244000000	0.155638000000
O	-0.962077000000	0.600644000000	-1.346243000000
N	1.946949000000	0.074176000000	0.115485000000
C	-2.241098000000	0.302019000000	-1.011787000000
C	2.653903000000	1.281636000000	0.154028000000
C	2.884726000000	-0.937358000000	-0.094748000000
C	-3.773459000000	-0.776043000000	0.567216000000
C	-3.330407000000	0.698444000000	-1.850072000000
C	2.146031000000	2.577831000000	0.329643000000
C	4.037742000000	1.046436000000	-0.035728000000
C	4.192207000000	-0.393460000000	-0.171663000000

C	2.647026000000	-2.306673000000	-0.222696000000
C	-3.983227000000	-1.531981000000	1.745259000000
C	-4.892381000000	-0.369016000000	-0.227220000000
C	-4.667689000000	0.388227000000	-1.451106000000
C	-3.091732000000	1.395021000000	-3.058918000000
C	3.060707000000	3.630656000000	0.253570000000
C	0.706272000000	2.778597000000	0.631930000000
C	4.927119000000	2.130189000000	-0.082942000000
C	5.279998000000	-1.254841000000	-0.346924000000
C	3.760713000000	-3.139116000000	-0.385371000000
C	1.244164000000	-2.804305000000	-0.212086000000
C	-5.258994000000	-1.883545000000	2.145057000000
C	-6.182442000000	-0.744217000000	0.217823000000
C	-5.718311000000	0.832173000000	-2.289215000000
C	-4.144544000000	1.804757000000	-3.855477000000
C	4.447905000000	3.437916000000	0.045827000000
C	-0.108883000000	3.593192000000	-0.164635000000
C	0.152215000000	2.137370000000	1.758454000000
C	5.080950000000	-2.640659000000	-0.445452000000
C	0.722511000000	-3.477430000000	0.895748000000
C	0.424095000000	-2.596705000000	-1.345033000000
C	-6.369134000000	-1.483986000000	1.374060000000
C	-5.469346000000	1.527331000000	-3.461527000000
C	5.368844000000	4.667839000000	-0.013152000000
C	-1.461839000000	3.781707000000	0.144780000000
C	-1.189648000000	2.342674000000	2.125680000000
C	6.296572000000	-3.566867000000	-0.627817000000
C	-0.594802000000	-3.961459000000	0.895499000000

C	-0.876795000000	-3.126528000000	-1.403091000000
C	6.835786000000	4.279934000000	-0.253260000000
C	4.918537000000	5.588889000000	-1.166728000000
C	5.285378000000	5.437239000000	1.322116000000
C	-1.973603000000	3.144602000000	1.287433000000
C	-2.352489000000	4.722890000000	-0.682089000000
C	-1.730578000000	1.827734000000	3.468997000000
C	7.033753000000	-3.193185000000	-1.931029000000
C	7.253247000000	-3.396597000000	0.571058000000
C	-1.363747000000	-3.781616000000	-0.261010000000
C	-1.129059000000	-4.682244000000	2.141865000000
C	-1.687103000000	-3.121241000000	-2.709350000000
C	-1.849365000000	4.848545000000	-2.130930000000
C	-2.307375000000	6.114742000000	-0.013036000000
C	-3.812149000000	4.229398000000	-0.720005000000
C	-3.255580000000	1.624728000000	3.427006000000
C	-1.071366000000	0.499429000000	3.885703000000
C	-1.398943000000	2.903334000000	4.529228000000
C	-0.291438000000	-5.956903000000	2.379787000000
C	-2.602458000000	-5.091309000000	1.991592000000
C	-0.997731000000	-3.747544000000	3.363362000000
C	-1.435596000000	-4.481831000000	-3.399938000000
C	-3.196299000000	-2.969998000000	-2.445372000000
C	-1.237901000000	-1.995304000000	-3.657278000000
H	-3.112070000000	-1.822074000000	2.328991000000
H	-5.405742000000	-2.468248000000	3.056371000000
H	-7.379549000000	-1.757636000000	1.686268000000
H	-7.057449000000	-0.450912000000	-0.362653000000

H	-6.752437000000	0.624896000000	-2.013105000000
H	-6.304720000000	1.856354000000	-4.083859000000
H	-3.951718000000	2.346350000000	-4.784560000000
H	-2.057129000000	1.599700000000	-3.335318000000
H	2.672700000000	4.641691000000	0.391120000000
H	5.988764000000	1.935223000000	-0.230144000000
H	6.287304000000	-0.837413000000	-0.404639000000
H	3.574537000000	-4.207869000000	-0.481649000000
H	6.964974000000	3.743049000000	-1.205573000000
H	7.227652000000	3.644354000000	0.555600000000
H	7.459126000000	5.186519000000	-0.294749000000
H	5.567015000000	6.478193000000	-1.226696000000
H	3.884113000000	5.938034000000	-1.030428000000
H	4.969781000000	5.060285000000	-2.131423000000
H	5.601867000000	4.798263000000	2.161303000000
H	4.261931000000	5.782471000000	1.531387000000
H	5.940019000000	6.323800000000	1.298843000000
H	7.910330000000	-3.844675000000	-2.080415000000
H	7.389136000000	-2.152084000000	-1.914111000000
H	8.133103000000	-4.051271000000	0.459926000000
H	7.615050000000	-2.361426000000	0.660204000000
H	6.369192000000	-3.306141000000	-2.801826000000
H	0.334906000000	4.062786000000	-1.041051000000
H	-3.018299000000	3.298614000000	1.543136000000
H	0.815406000000	1.558610000000	2.402727000000
H	-0.860763000000	5.327596000000	-2.188165000000
H	-2.545650000000	5.470903000000	-2.713832000000
H	-1.786700000000	3.863866000000	-2.614966000000

H	-1.278375000000	6.506095000000	0.015186000000
H	-2.678330000000	6.066987000000	1.022622000000
H	-2.933740000000	6.831134000000	-0.569580000000
H	-3.879687000000	3.203116000000	-1.104445000000
H	-4.406706000000	4.879613000000	-1.379950000000
H	-4.287139000000	4.257157000000	0.271475000000
H	-3.551900000000	0.951517000000	2.612078000000
H	-3.796698000000	2.574445000000	3.303237000000
H	-3.598072000000	1.180970000000	4.374360000000
H	-1.219715000000	-0.270914000000	3.117764000000
H	-1.513825000000	0.147537000000	4.830513000000
H	0.009237000000	0.610557000000	4.062257000000
H	-0.312166000000	3.064145000000	4.603894000000
H	-1.769808000000	2.592749000000	5.519797000000
H	-1.865872000000	3.867082000000	4.273099000000
H	1.366958000000	-3.617549000000	1.764695000000
H	-2.378391000000	-4.169275000000	-0.282304000000
H	0.863500000000	-2.110265000000	-2.216474000000
H	-0.364544000000	-4.625882000000	-3.611641000000
H	-1.985418000000	-4.533707000000	-4.353851000000
H	-1.770006000000	-5.316807000000	-2.764837000000
H	-3.738709000000	-2.938173000000	-3.402552000000
H	-3.416742000000	-2.045386000000	-1.900506000000
H	-3.606375000000	-3.811955000000	-1.869049000000
H	-0.213402000000	-2.153921000000	-4.026987000000
H	-1.276843000000	-1.013193000000	-3.168775000000
H	-1.897775000000	-1.966784000000	-4.537411000000
H	-0.366551000000	-6.640967000000	1.520026000000

H	-0.651158000000	-6.489771000000	3.274810000000
H	0.772886000000	-5.723516000000	2.532756000000
H	-2.744156000000	-5.806214000000	1.166592000000
H	-3.253465000000	-4.224377000000	1.809203000000
H	-2.946029000000	-5.582231000000	2.915135000000
H	0.051413000000	-3.491713000000	3.571904000000
H	-1.408693000000	-4.233389000000	4.262708000000
H	-1.539044000000	-2.805241000000	3.199187000000
C	5.894303000000	-5.047469000000	-0.712423000000
H	6.793497000000	-5.670480000000	-0.836950000000
H	5.380345000000	-5.384195000000	0.200984000000
H	5.233238000000	-5.243657000000	-1.570433000000
H	6.747987000000	-3.657133000000	1.514239000000

L-Ga(N₄Ad₂)

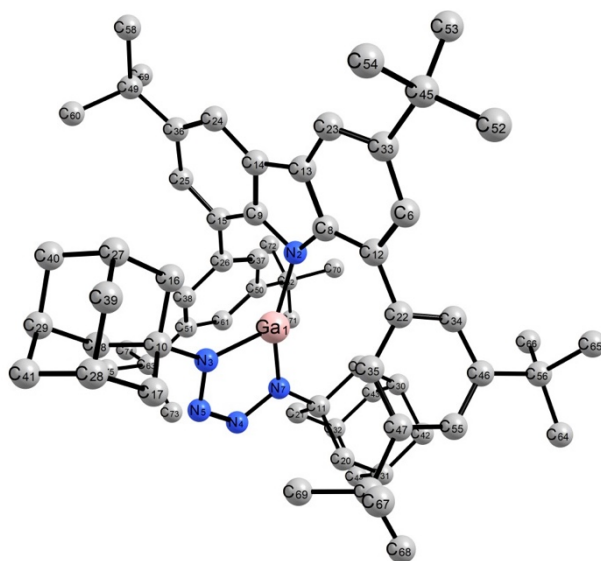


Figure 57. Optimized structure at the B3LYP-D3(BJ)/def2SVP level of theory for **131**. Hydrogen atoms are omitted for clarity.

Energy (B3LYP-D3(BJ)/def2SVP) = -4844.74 Hartree

Ga	0.113552000000	-0.188766000000	0.391530000000
N	-0.684091000000	0.693533000000	-1.060897000000
N	-0.679200000000	-0.421009000000	2.060723000000
N	1.069443000000	-1.799267000000	2.271286000000
N	0.030614000000	-1.304469000000	2.808627000000
C	0.093433000000	4.365455000000	-1.235554000000
N	1.367139000000	-1.393651000000	1.003865000000
C	-0.670967000000	2.092744000000	-1.211744000000
C	-1.980801000000	0.270106000000	-1.415872000000
C	-1.820119000000	0.208350000000	2.738316000000
C	2.650999000000	-1.864384000000	0.477283000000
C	0.356284000000	3.012809000000	-0.965022000000
C	-1.935421000000	2.547231000000	-1.680333000000

C	-2.785246000000	1.378521000000	-1.772367000000
C	-2.527960000000	-1.023149000000	-1.368267000000
C	-2.568487000000	1.091715000000	1.726947000000
C	-1.351658000000	1.095173000000	3.911180000000
C	-2.805160000000	-0.849765000000	3.277818000000
C	2.845483000000	-1.265186000000	-0.924164000000
C	3.813239000000	-1.403334000000	1.379757000000
C	2.690456000000	-3.400777000000	0.369631000000
C	1.695946000000	2.649897000000	-0.423467000000
C	-2.161952000000	3.902165000000	-1.929835000000
C	-4.152549000000	1.217673000000	-2.032793000000
C	-3.900872000000	-1.139889000000	-1.605327000000
C	-1.713630000000	-2.252120000000	-1.145474000000
C	-3.767930000000	1.783734000000	2.391974000000
C	-2.553764000000	1.773151000000	4.588675000000
C	-4.010168000000	-0.169988000000	3.947871000000
C	4.194453000000	-1.717818000000	-1.511310000000
C	5.159344000000	-1.863558000000	0.802768000000
C	4.037651000000	-3.861293000000	-0.213058000000
C	-1.142734000000	4.838546000000	-1.716541000000
C	2.818114000000	2.710870000000	-1.258918000000
C	1.873893000000	2.405975000000	0.947703000000
C	-4.738468000000	-0.045354000000	-1.922293000000
C	-0.923337000000	-2.733527000000	-2.196757000000
C	-1.832275000000	-3.006029000000	0.032779000000
C	-3.280535000000	2.656995000000	3.559892000000
C	-4.737572000000	0.712462000000	2.918812000000
C	-3.519373000000	0.699277000000	5.118004000000

C	5.334650000000	-1.245446000000	-0.593781000000
C	4.232993000000	-3.251099000000	-1.610311000000
C	5.180718000000	-3.397709000000	0.705640000000
C	-1.402801000000	6.328146000000	-1.995651000000
C	4.115039000000	2.569839000000	-0.749294000000
C	3.158659000000	2.259699000000	1.498641000000
H	0.999046000000	2.428813000000	1.600260000000
C	-6.242552000000	-0.287387000000	-2.120361000000
C	-0.291472000000	-3.982614000000	-2.115292000000
C	-1.184183000000	-4.238355000000	0.167672000000
C	-0.170261000000	7.198996000000	-1.706882000000
C	-1.785447000000	6.510255000000	-3.479378000000
C	-2.561108000000	6.818929000000	-1.101784000000
C	4.255982000000	2.334679000000	0.627646000000
C	5.320235000000	2.775284000000	-1.682789000000
C	3.337202000000	2.170761000000	3.024230000000
C	-6.992715000000	1.006403000000	-2.470900000000
C	-6.461238000000	-1.298917000000	-3.264727000000
C	-6.835759000000	-0.851680000000	-0.811536000000
C	-0.432386000000	-4.705275000000	-0.923468000000
C	0.422065000000	-4.574100000000	-3.341869000000
C	-1.298636000000	-5.102020000000	1.433978000000
C	6.660819000000	2.514482000000	-0.977912000000
C	5.308383000000	4.243001000000	-2.165662000000
C	5.217913000000	1.839857000000	-2.904569000000
C	3.001833000000	3.562227000000	3.608571000000
C	4.777552000000	1.809942000000	3.423214000000
C	2.387384000000	1.127784000000	3.639426000000

C	1.176884000000	-3.482853000000	-4.126113000000
C	1.417450000000	-5.680293000000	-2.948543000000
C	-0.657000000000	-5.189016000000	-4.261178000000
C	0.106383000000	-5.363042000000	2.014478000000
C	-1.970133000000	-6.441592000000	1.065660000000
C	-2.131189000000	-4.414799000000	2.525370000000
H	0.904466000000	5.066018000000	-1.042040000000
H	-2.922182000000	0.472571000000	0.891948000000
H	-1.883403000000	1.849474000000	1.310830000000
H	-0.786385000000	0.477957000000	4.625513000000
H	-0.662000000000	1.862114000000	3.522831000000
H	-2.279376000000	-1.502447000000	3.989094000000
H	-3.145050000000	-1.479680000000	2.441711000000
H	2.815289000000	-0.163907000000	-0.863450000000
H	2.014535000000	-1.587086000000	-1.574837000000
H	3.659738000000	-1.809078000000	2.390446000000
H	3.786884000000	-0.308503000000	1.448700000000
H	1.853834000000	-3.735348000000	-0.258987000000
H	2.538591000000	-3.830832000000	1.368898000000
H	-3.142949000000	4.219297000000	-2.289593000000
H	-4.748007000000	2.094014000000	-2.286584000000
H	-4.326114000000	-2.143812000000	-1.553968000000
H	-4.275269000000	2.409920000000	1.640095000000
H	-2.194848000000	2.395063000000	5.425739000000
H	-4.697642000000	-0.945598000000	4.324549000000
H	4.313581000000	-1.277799000000	-2.515154000000
H	5.973206000000	-1.519532000000	1.463394000000
H	4.041401000000	-4.962115000000	-0.285855000000

H	2.657743000000	2.920445000000	-2.317448000000
H	-0.863104000000	-2.137369000000	-3.107357000000
H	-2.445283000000	-2.608936000000	0.837157000000
H	-2.599940000000	3.441157000000	3.186376000000
H	-4.134949000000	3.169662000000	4.033460000000
H	-5.104561000000	0.094749000000	2.081607000000
H	-5.618327000000	1.190282000000	3.380567000000
H	-3.010235000000	0.070184000000	5.867364000000
H	-4.376403000000	1.176068000000	5.623379000000
H	6.309636000000	-1.530549000000	-1.024309000000
H	5.319880000000	-0.148863000000	-0.512499000000
H	5.197515000000	-3.575677000000	-2.036407000000
H	3.448300000000	-3.606826000000	-2.292907000000
H	5.063962000000	-3.840532000000	1.708931000000
H	6.151170000000	-3.741655000000	0.309015000000
H	0.689089000000	6.910517000000	-2.331489000000
H	0.136669000000	7.136280000000	-0.651640000000
H	-0.400597000000	8.253536000000	-1.924019000000
H	-1.979723000000	7.572345000000	-3.701441000000
H	-2.691213000000	5.942274000000	-3.739070000000
H	-0.973164000000	6.164429000000	-4.137653000000
H	-2.767453000000	7.885942000000	-1.286209000000
H	-2.311139000000	6.696299000000	-0.036297000000
H	-3.488988000000	6.259887000000	-1.294452000000
H	5.255236000000	2.234907000000	1.040620000000
H	-6.899903000000	1.759928000000	-1.673789000000
H	-8.064578000000	0.792451000000	-2.603068000000
H	-6.623507000000	1.450315000000	-3.408205000000

H	-6.042583000000	-0.916745000000	-4.208879000000
H	-7.537260000000	-1.484040000000	-3.415754000000
H	-5.982426000000	-2.266397000000	-3.052802000000
H	-6.363271000000	-1.804025000000	-0.528083000000
H	-7.917481000000	-1.032385000000	-0.922014000000
H	-6.688526000000	-0.144306000000	0.019837000000
H	0.052585000000	-5.675851000000	-0.835220000000
H	7.487587000000	2.659092000000	-1.690086000000
H	6.729649000000	1.486517000000	-0.592778000000
H	6.823832000000	3.207527000000	-0.138762000000
H	5.371582000000	4.935936000000	-1.312169000000
H	4.389364000000	4.478481000000	-2.722733000000
H	6.166322000000	4.435922000000	-2.830050000000
H	6.065956000000	2.011369000000	-3.586538000000
H	4.293118000000	2.009403000000	-3.475021000000
H	5.235842000000	0.784643000000	-2.598746000000
H	3.655719000000	4.338348000000	3.180755000000
H	3.135733000000	3.561398000000	4.702522000000
H	1.959536000000	3.844126000000	3.394859000000
H	5.499774000000	2.583680000000	3.121419000000
H	5.093264000000	0.851912000000	2.983239000000
H	4.841893000000	1.711653000000	4.517478000000
H	2.476780000000	1.139361000000	4.737010000000
H	2.609036000000	0.112019000000	3.293380000000
H	1.338709000000	1.330335000000	3.397317000000
H	1.884907000000	-2.941310000000	-3.482993000000
H	0.493168000000	-2.744072000000	-4.568013000000
H	1.744813000000	-3.935999000000	-4.953511000000

H	1.970566000000	-6.020126000000	-3.837523000000
H	0.908708000000	-6.559940000000	-2.527648000000
H	2.148976000000	-5.325956000000	-2.208176000000
H	-1.381790000000	-4.425996000000	-4.584136000000
H	-1.213478000000	-5.980747000000	-3.736051000000
H	-0.196195000000	-5.629201000000	-5.160990000000
H	0.766205000000	-5.861912000000	1.288879000000
H	0.032393000000	-6.012843000000	2.901457000000
H	0.577781000000	-4.416811000000	2.316714000000
H	-2.975392000000	-6.275129000000	0.647113000000
H	-2.071795000000	-7.077098000000	1.960254000000
H	-1.384636000000	-7.002513000000	0.321376000000
H	-1.668215000000	-3.469262000000	2.838326000000
H	-2.192048000000	-5.067760000000	3.409718000000
H	-3.161117000000	-4.210858000000	2.193594000000

7.4.2. Frontier Molecular Orbitals

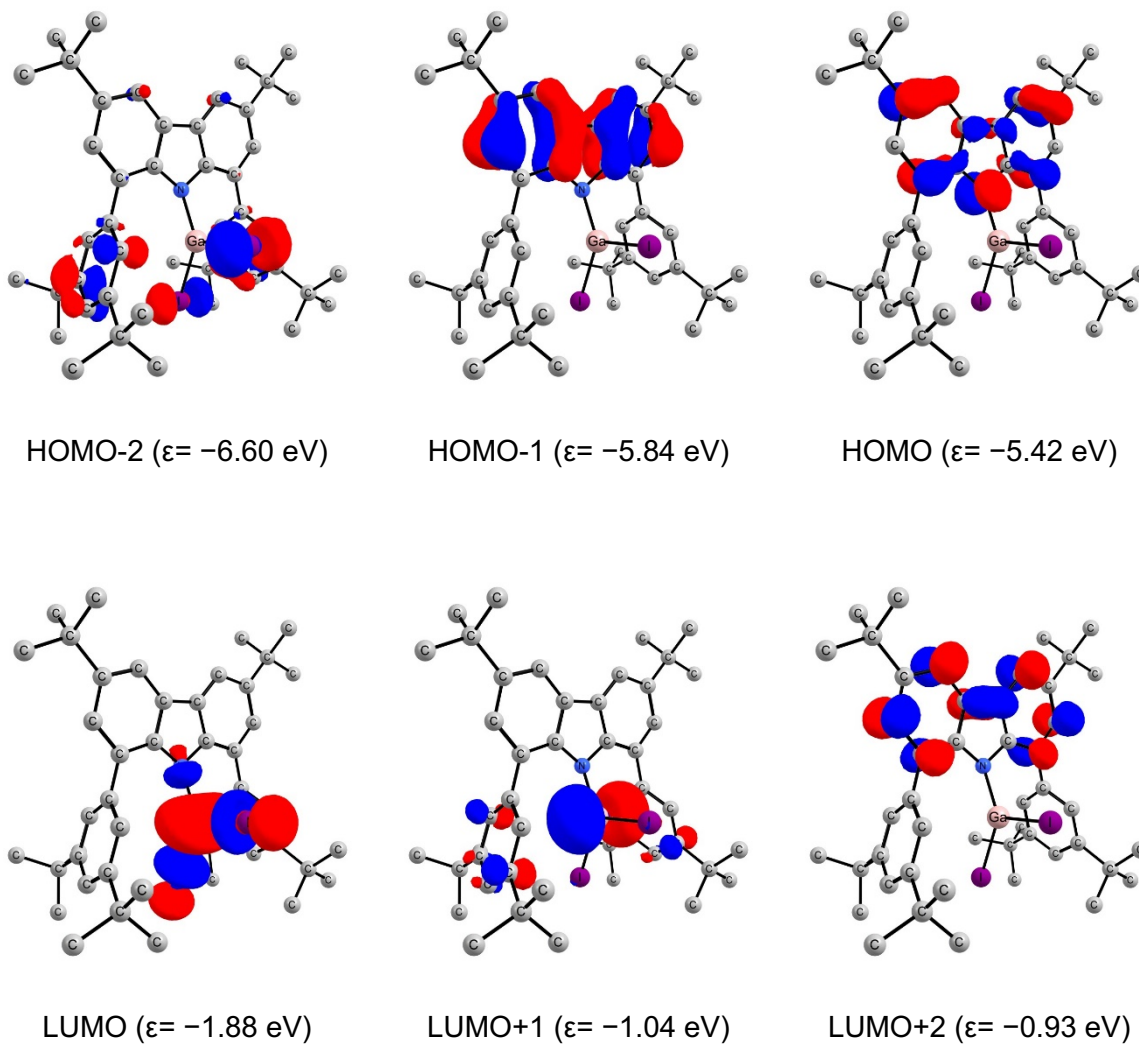


Figure 58. Frontier KS molecular orbitals (isovalue 0.05 a.u.) of compound **124** at the B3LYP-D3(BJ)/def2-SVP level of theory.

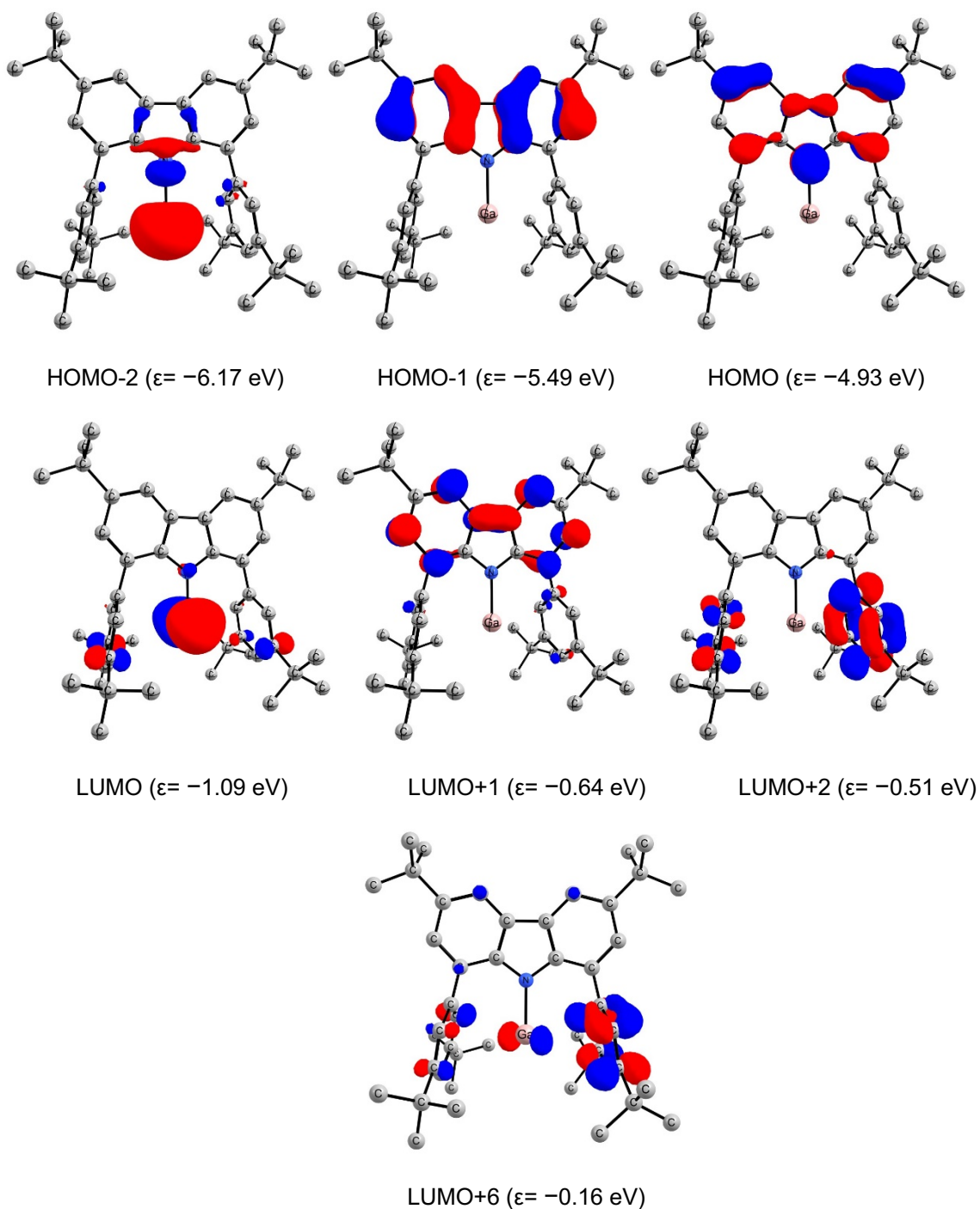


Figure 59. Frontier KS molecular orbitals (isovalue 0.05 a.u.) of compound **125** at the B3LYP-D3(BJ)/def2-SVP level of theory.

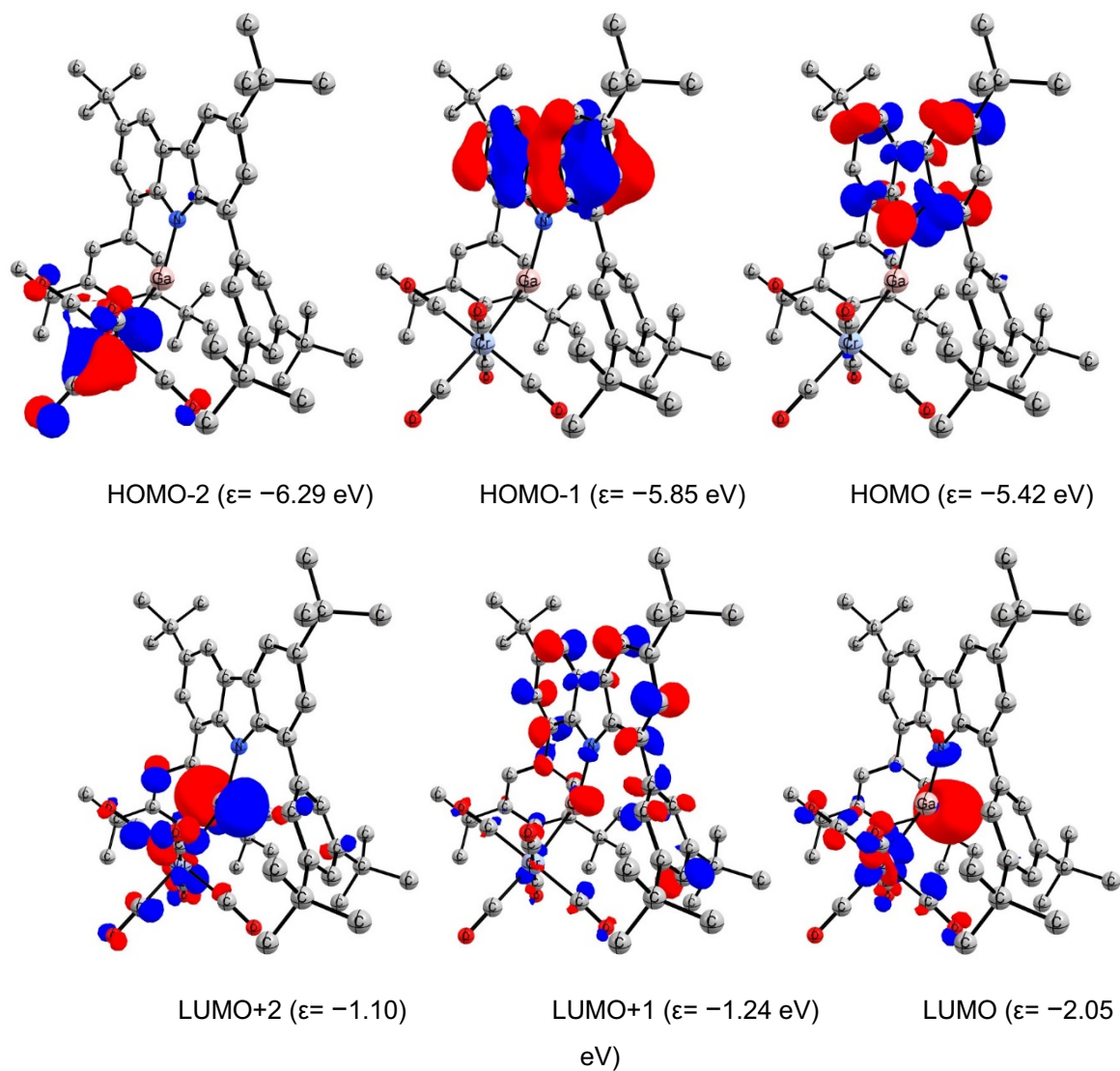


Figure 60. Frontier KS molecular orbitals (isovalue 0.05 a.u.) of compound **126** at the B3LYP-D3(BJ)/def2-SVP level of theory.

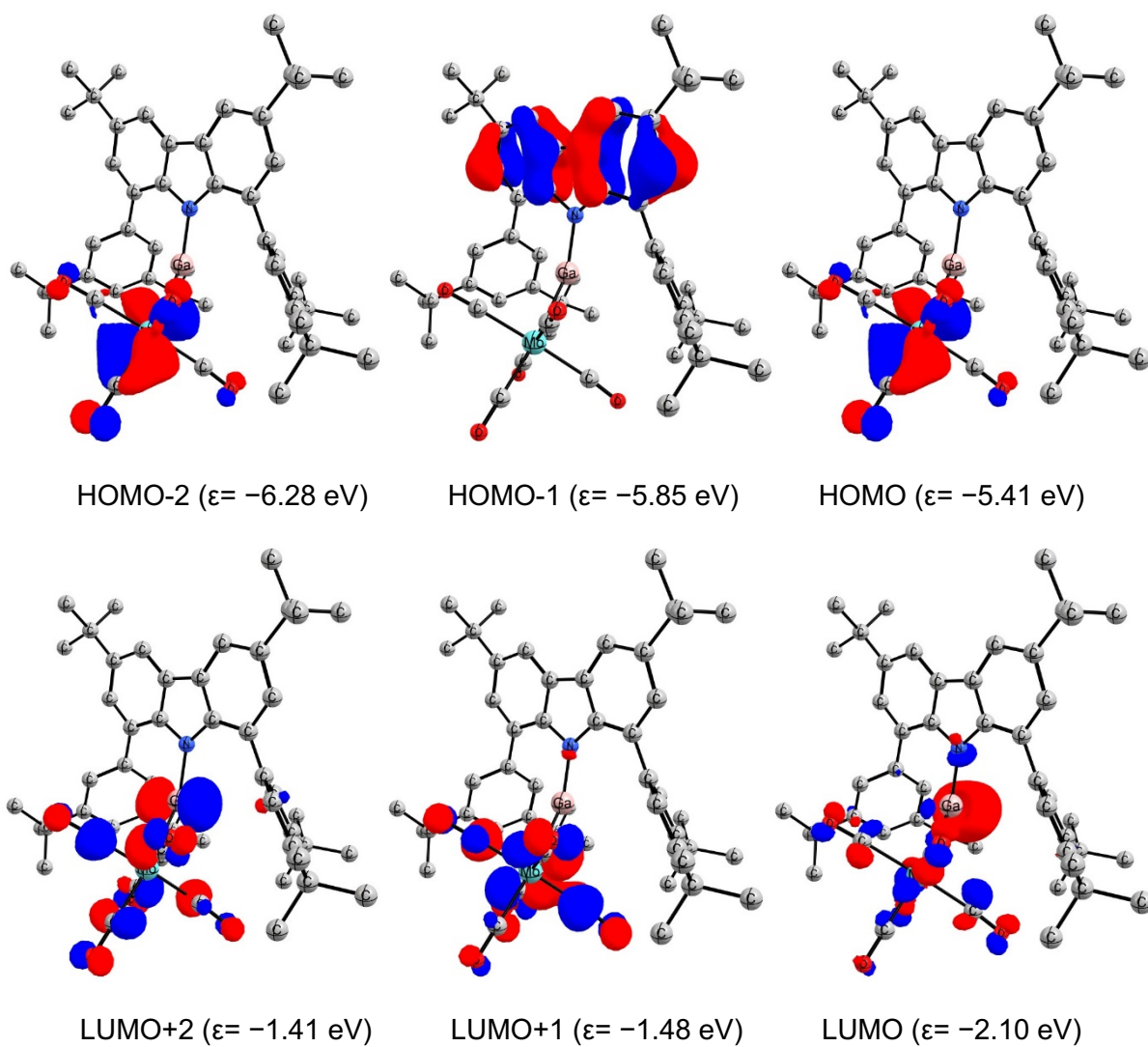


Figure 61. Frontier KS molecular orbitals (isovalue 0.05 a.u.) of compound **127** at the B3LYP-D3(BJ)/def2-SVP level of theory.

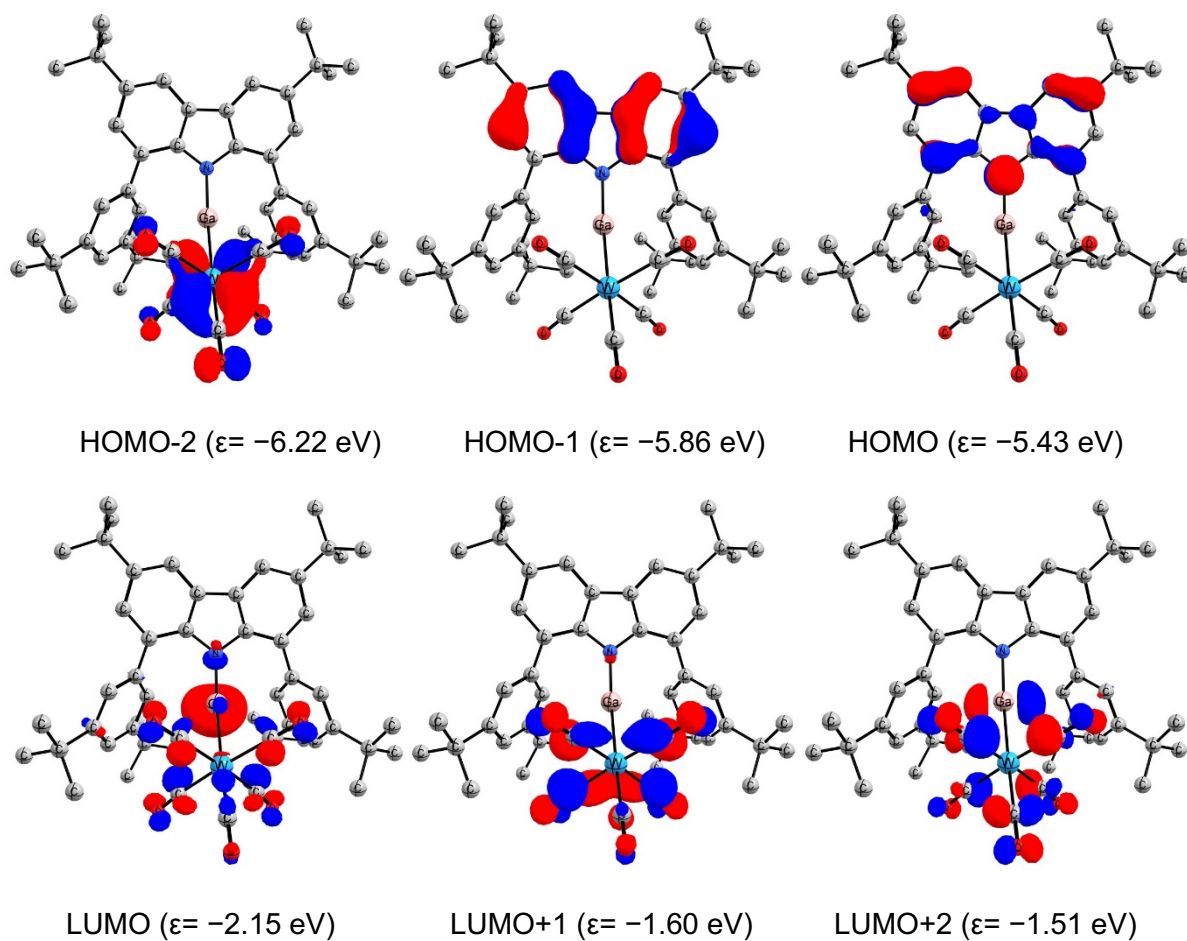


Figure 62. Frontier KS molecular orbitals (isovalue 0.05 a.u.) of compound **128** at the B3LYP-D3(BJ)/def2-SVP level of theory.

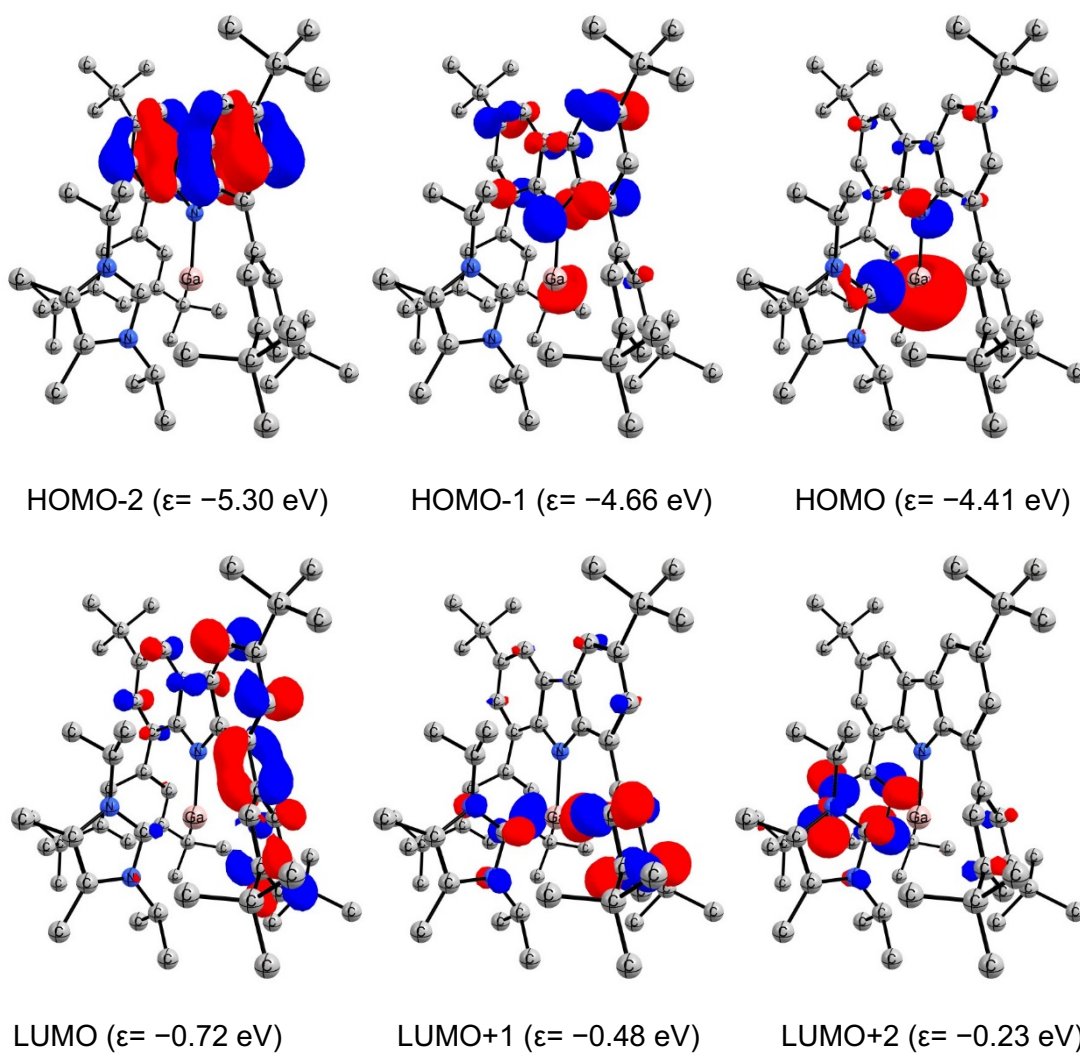


Figure 63. Frontier KS molecular orbitals (isovalue 0.05 a.u.) of compound **129** at the B3LYP-D3(BJ)/def2-SVP level of theory.

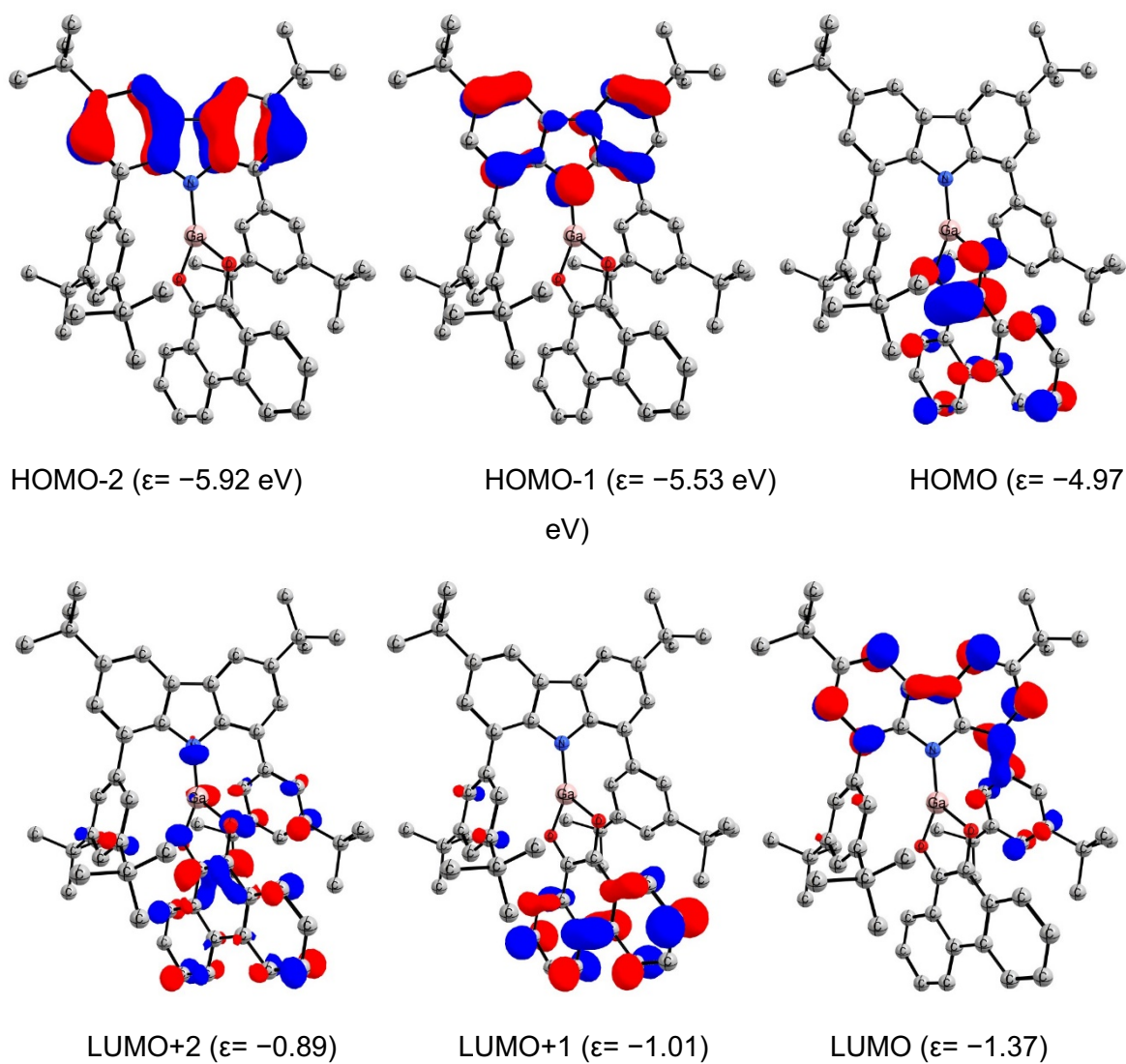


Figure 64. Frontier KS molecular orbitals (isovalue 0.05 a.u.) of compound **130** at the B3LYP-D3(BJ)/def2-SVP level of theory.

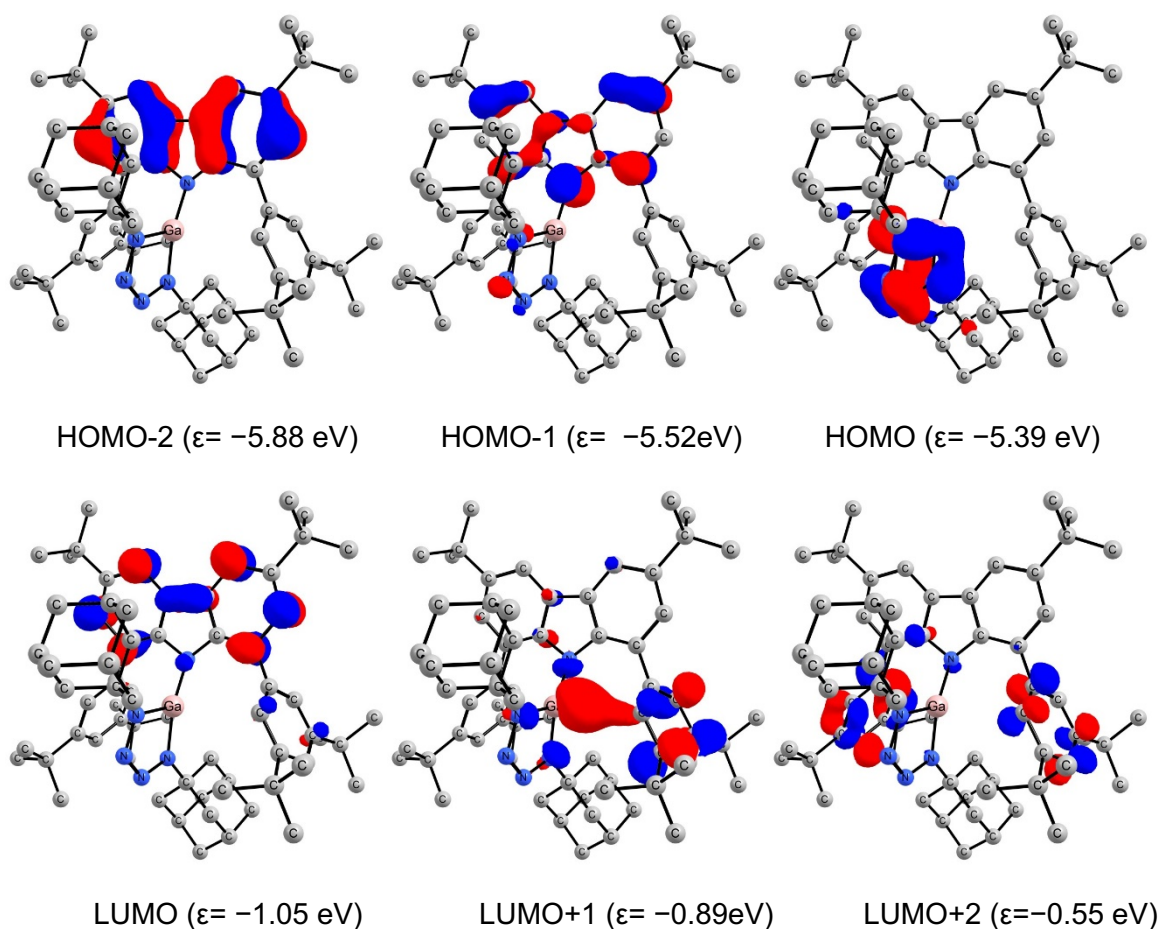


Figure 65. Frontier KS molecular orbitals (isovalue 0.05 a.u.) of compound **131** at the B3LYP-D3(BJ)/def2-SVP level of theory.

7.4.4. NBO Results

Table 5. Natural Partial Charges (q in a.u.) and Wiberg bond orders (P in a.u.) of compounds **126-127** at the B3LYP-D3(BJ)/def2-TZVPP//B3LYP-D3(BJ)/def2-SVP level of theory.

Property	126 (M=Cr)	127 (M=Mo)	128 (M= W)
$Q(M(CO)_5)$	0.40	-0.50	0.52
$Q(Ga)$	1.21	1.14	1.13
$P(Ga-M)$	0.48	0.48	0.50
$P(N-Ga)$	0.30	0.30	0.32

7.4.5. EDA-NOCV

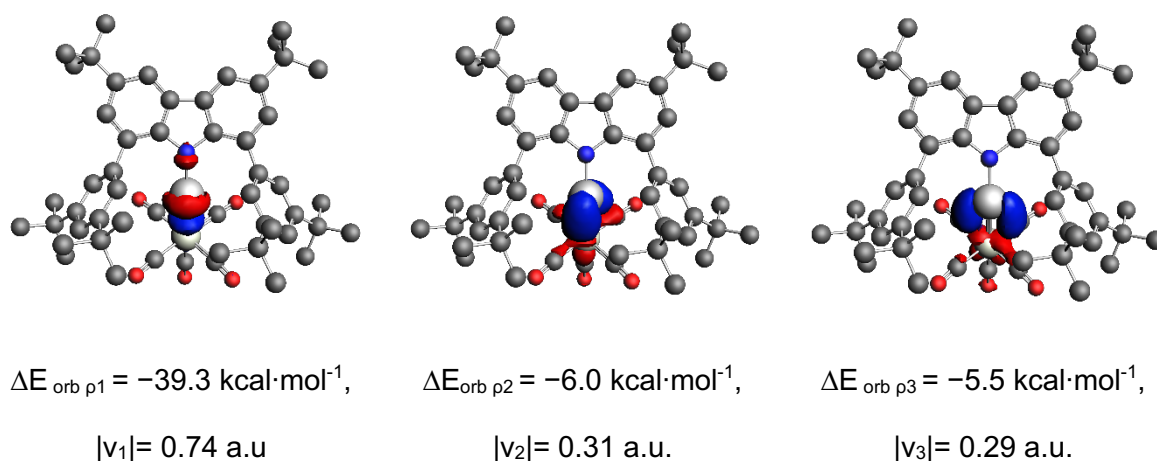


Figure 66. Plot of deformation densities $\Delta\rho$ of the pairwise orbital interactions between L-Ga and $\text{Cr}(\text{CO})_5$ fragment, associated energies ΔE (in kcal/mol) and eigenvalues v (in a.u.). The red color shows the charge outflow, whereas blue shows charge density accumulation. Shape of the most important interacting occupied and vacant orbitals of the fragments. Calculations are done at BP86-D3(BJ)/TZ2P level of theory.

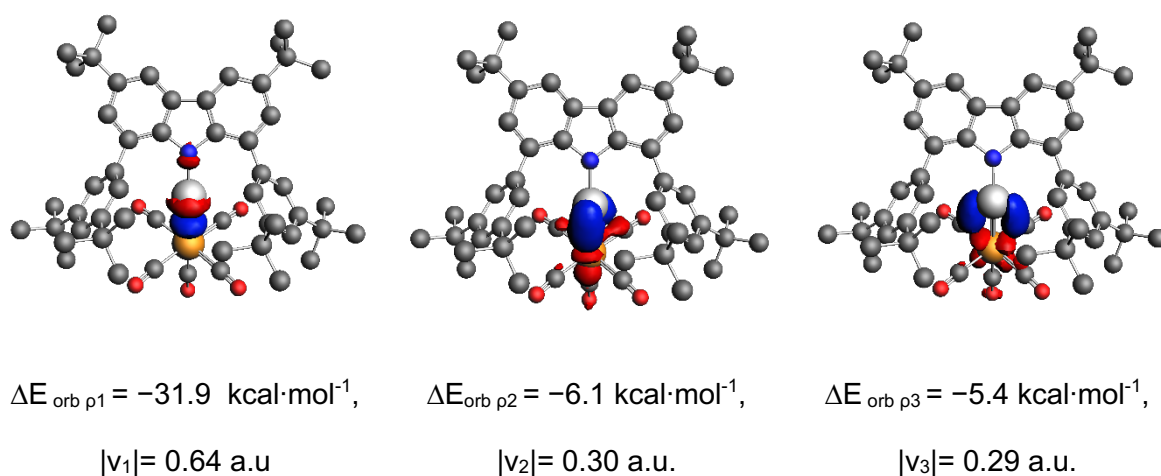


Figure 67. Plot of deformation densities $\Delta\rho$ of the pairwise orbital interactions between L-Ga and $\text{Mo}(\text{CO})_5$ fragment, associated energies ΔE (in kcal/mol) and eigenvalues v (in a.u.). The red color shows the charge outflow, whereas blue shows charge density accumulation. Shape of the most important interacting occupied and vacant orbitals of the fragments. Calculations are done at BP86-D3(BJ)/TZ2P level of theory.

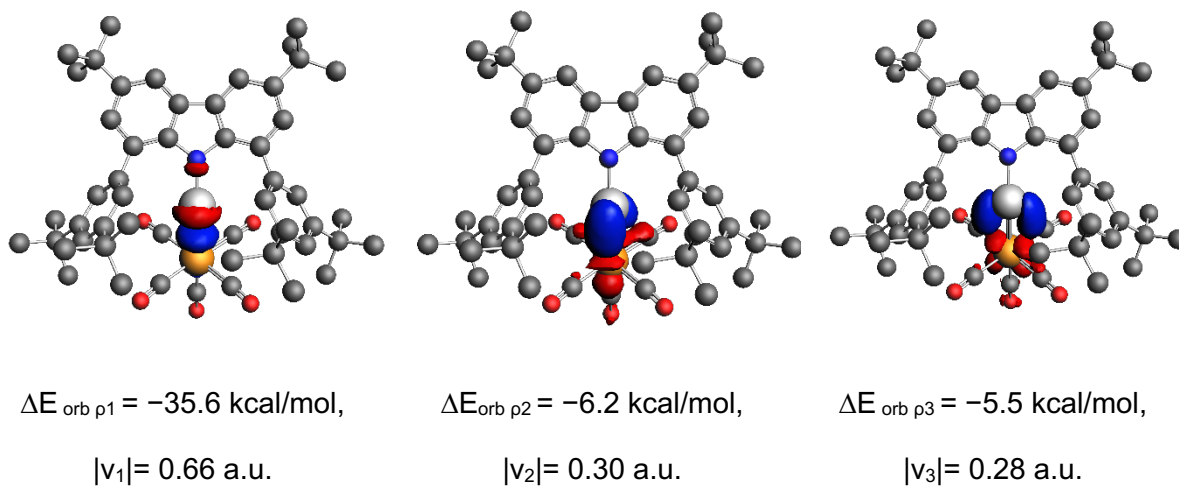


Figure 68. Plot of deformation densities $\Delta\rho$ of the pairwise orbital interactions between L-Ga and $\text{W}(\text{CO})_5$ fragment, associated energies ΔE (in $\text{kcal}\cdot\text{mol}^{-1}$) and eigenvalues v (in a.u.). The red color shows the charge outflow, whereas blue shows charge density accumulation. Shape of the most important interacting occupied and vacant orbitals of the fragments. Calculations are done at BP86-D3(BJ)/TZ2P level of theory.

7.4.6. AIM Analysis

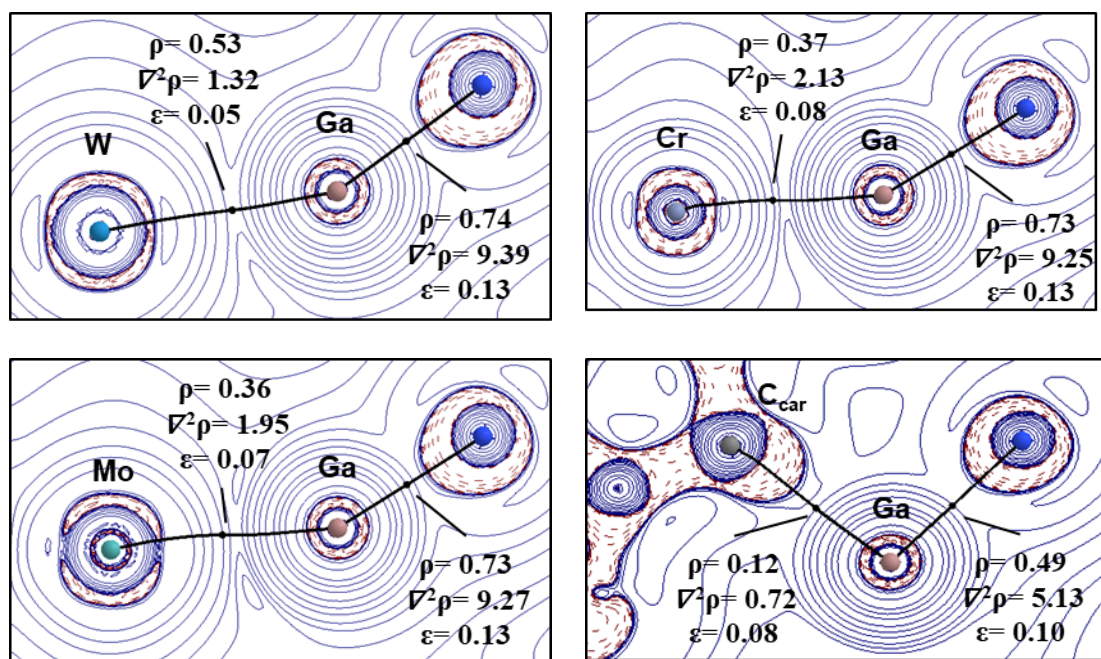


Figure 69. Laplacian distribution of the electron density of **126-129**. Contour line diagrams of the Laplacian distribution $\nabla^2\rho(r)$. Dashed red lines indicate areas of charge concentration ($\nabla^2\rho(r) < 0$) while solid blue lines show areas of charge depletion ($\nabla^2\rho(r) > 0$) (B3LYP-D3(BJ)/de2-TZVPP//B3LYP-D3(BJ)/def2-SVP).

8. Synthesis, Structure, and Bonding Analysis of Lewis Base and Lewis Acid/Base-Stabilized Phosphanylgallanes

European Journal of Inorganic Chemistry

Supporting Information

Synthesis, Structure, and Bonding Analysis of Lewis Base and Lewis Acid/Base-Stabilized Phosphanylgallanes

T. Ilgin Demirer, Bernd Morgenstern, and Diego M. Andrada*

Table of Contents

Experimental Procedures and NMR Spectra for Compounds 1-8.....	S2
IR Spectra.....	S27
Crystallographic Details.....	S31
Computational Details.....	S34

NMR Spectra for Compounds 1-8

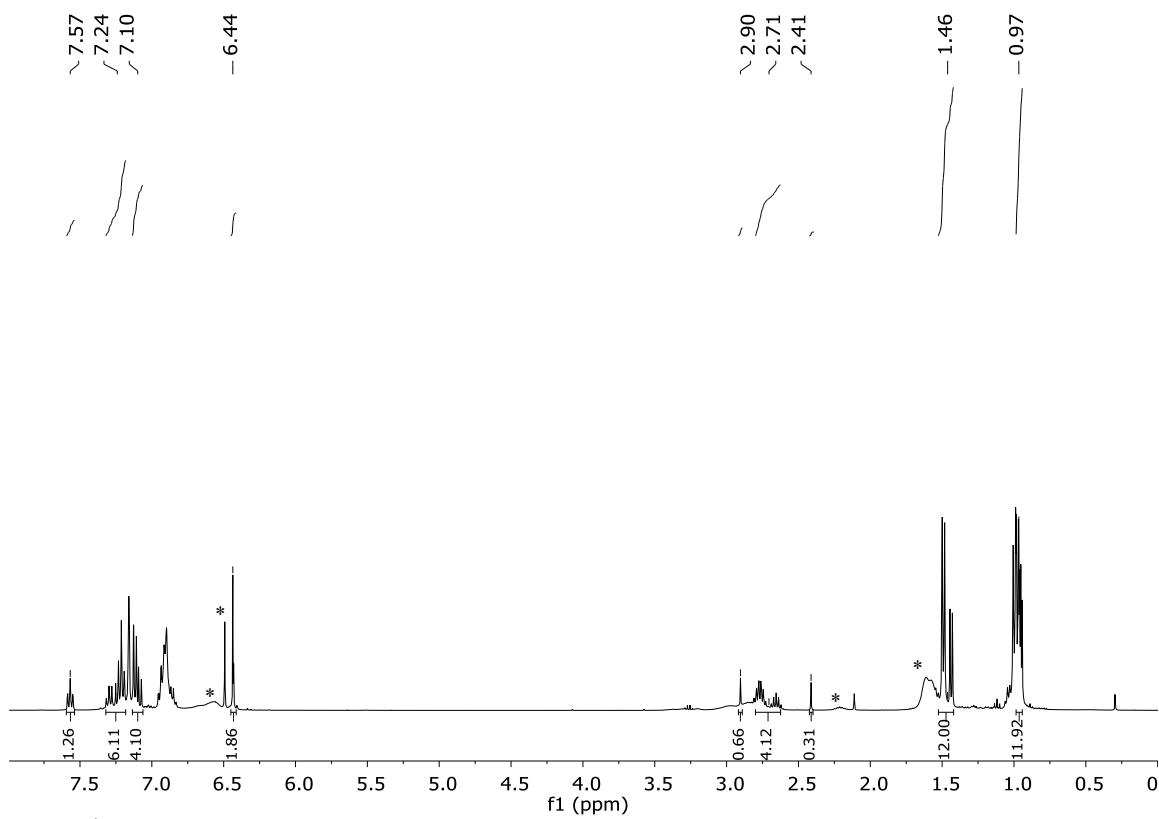


Figure S1. ^1H NMR (400.1 MHz, C_6D_6 , 300K) spectrum of 1. * = IDip. GaCl_3 + unidentified impurity.

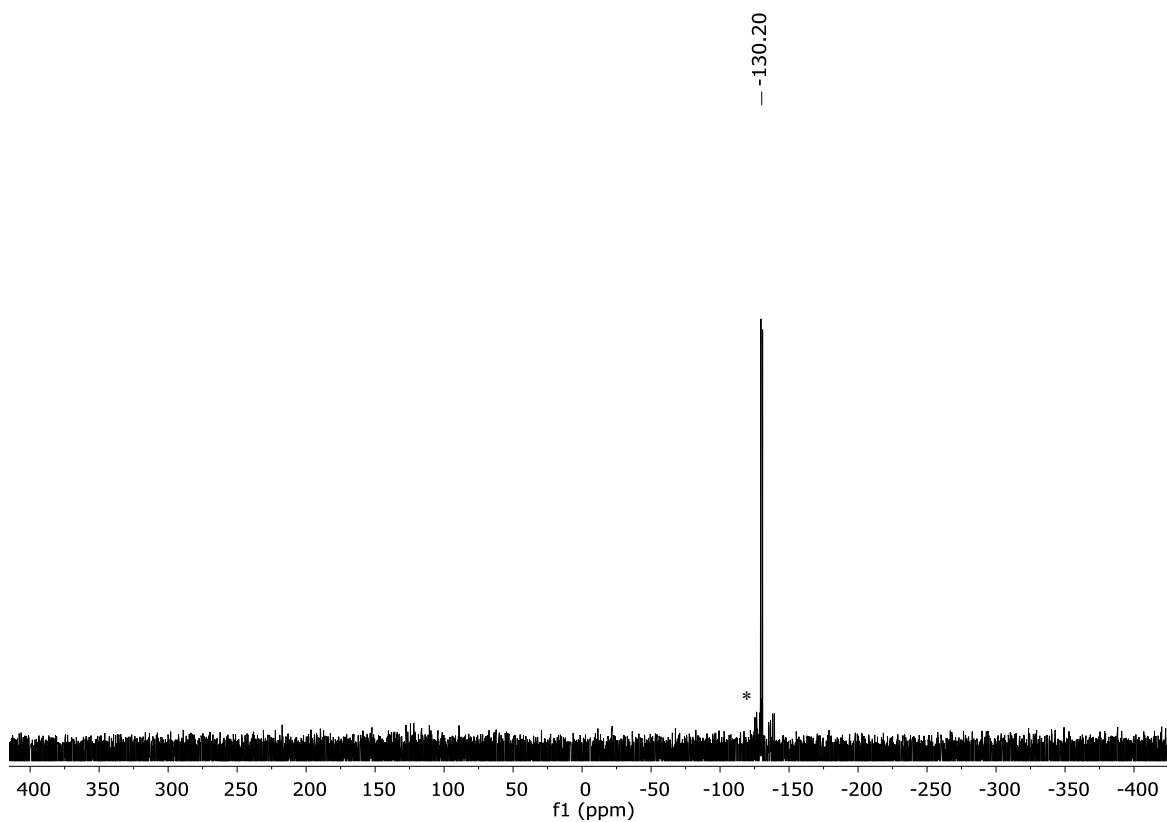


Figure S2. ^{31}P NMR (161.9 MHz, C_6D_6 , 300K) spectrum of **1**. * = PH_2Ph .

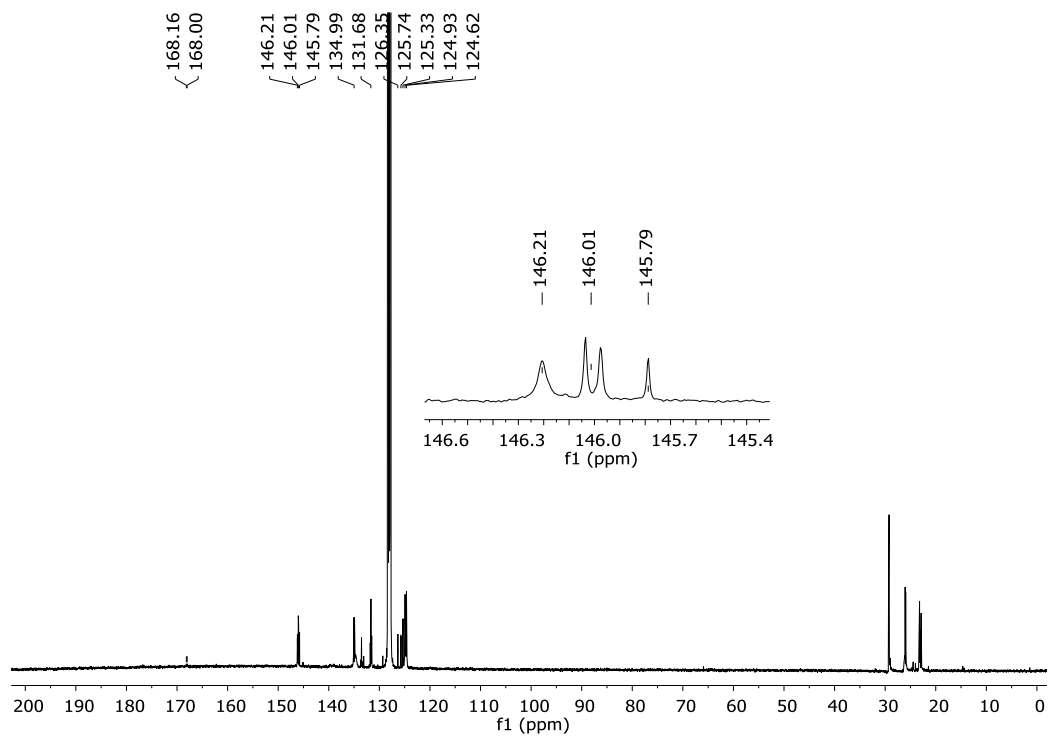


Figure S3. $^{13}\text{C}\{^1\text{H}\}$ NMR (100.6 MHz, C_6D_6 , 300K) spectrum of 1.

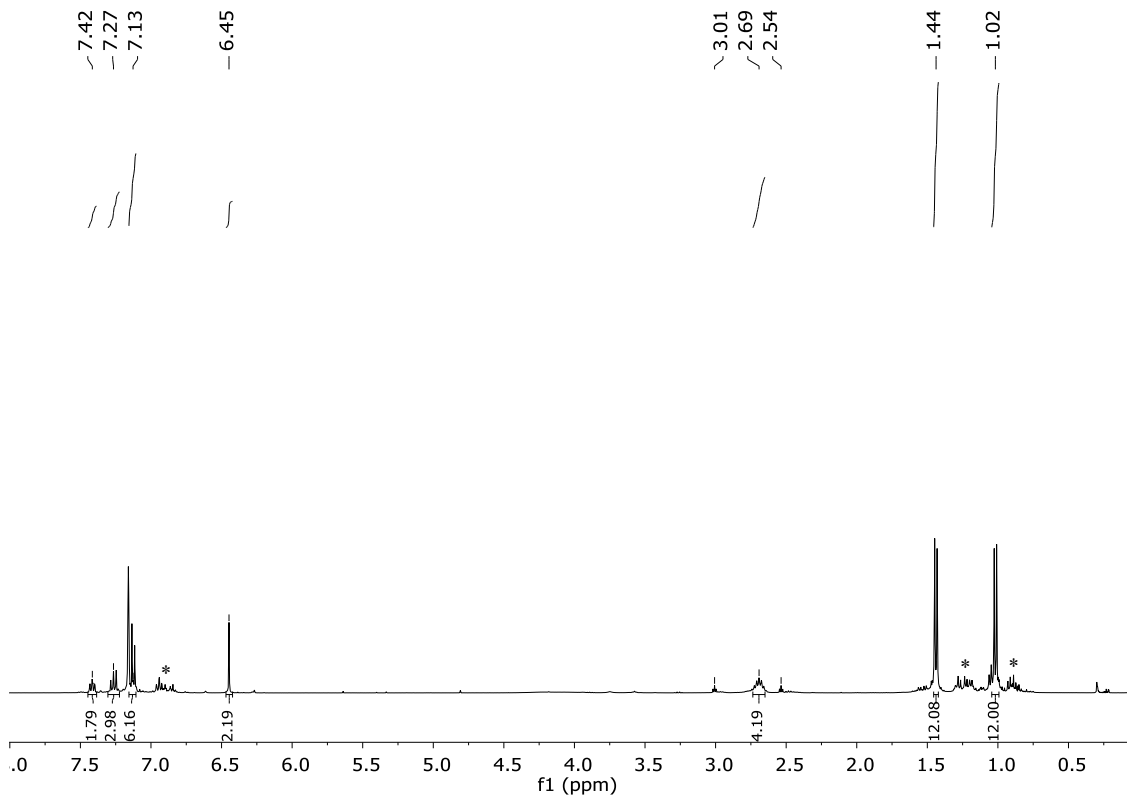


Figure S4. ^1H NMR (400.1 MHz, C_6D_6 , 300K) spectrum of 2. * = PH_2Ph + unidentified impurities.

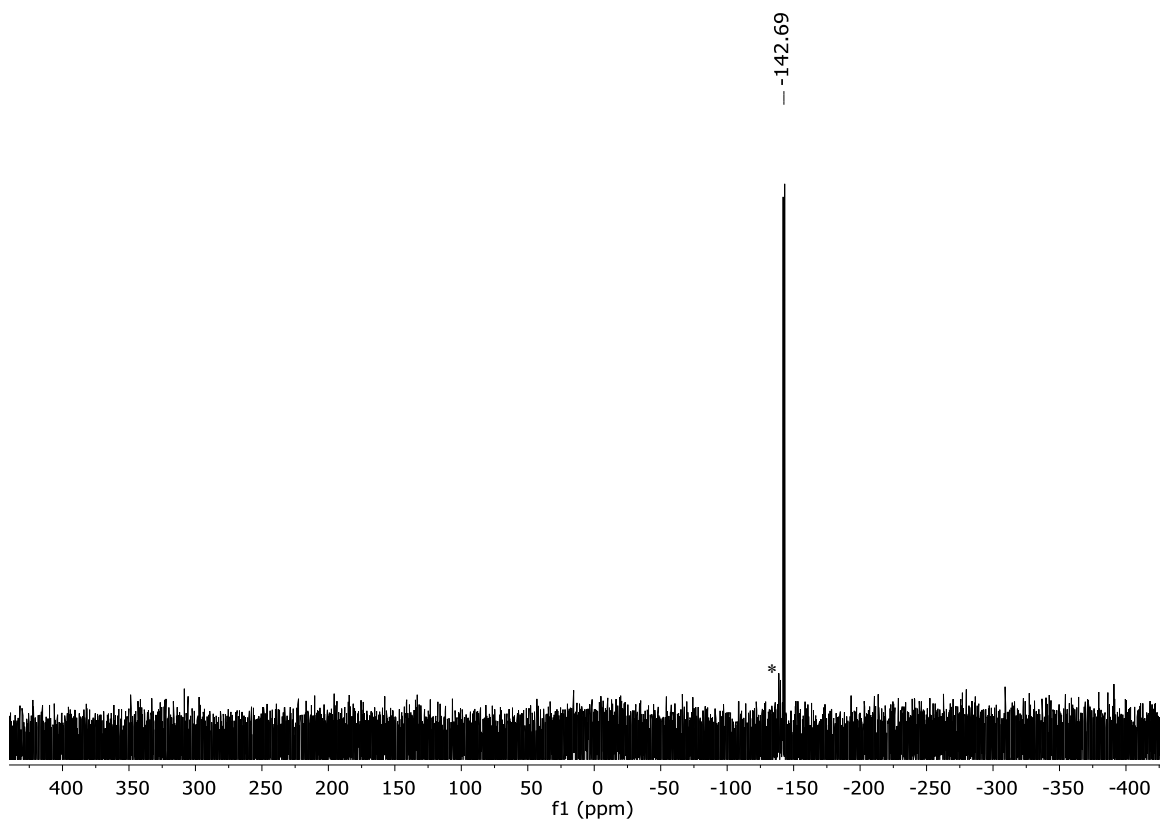


Figure S5. ^{31}P NMR (161.9 MHz, C_6D_6 , 300K) spectrum of 2. * = PH_2Ph .

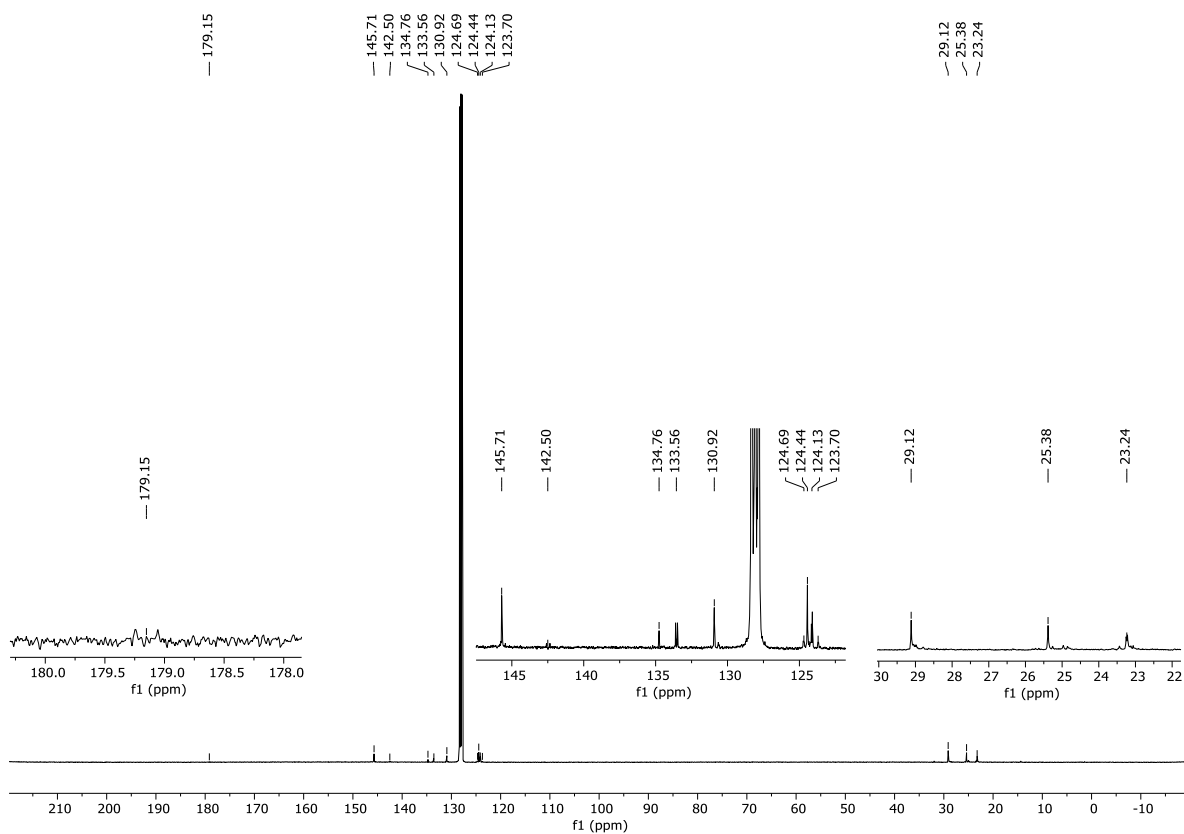


Figure S6. ^{13}C (^1H) NMR (100.6 MHz, C_6D_6 , 300K) spectrum of 2.

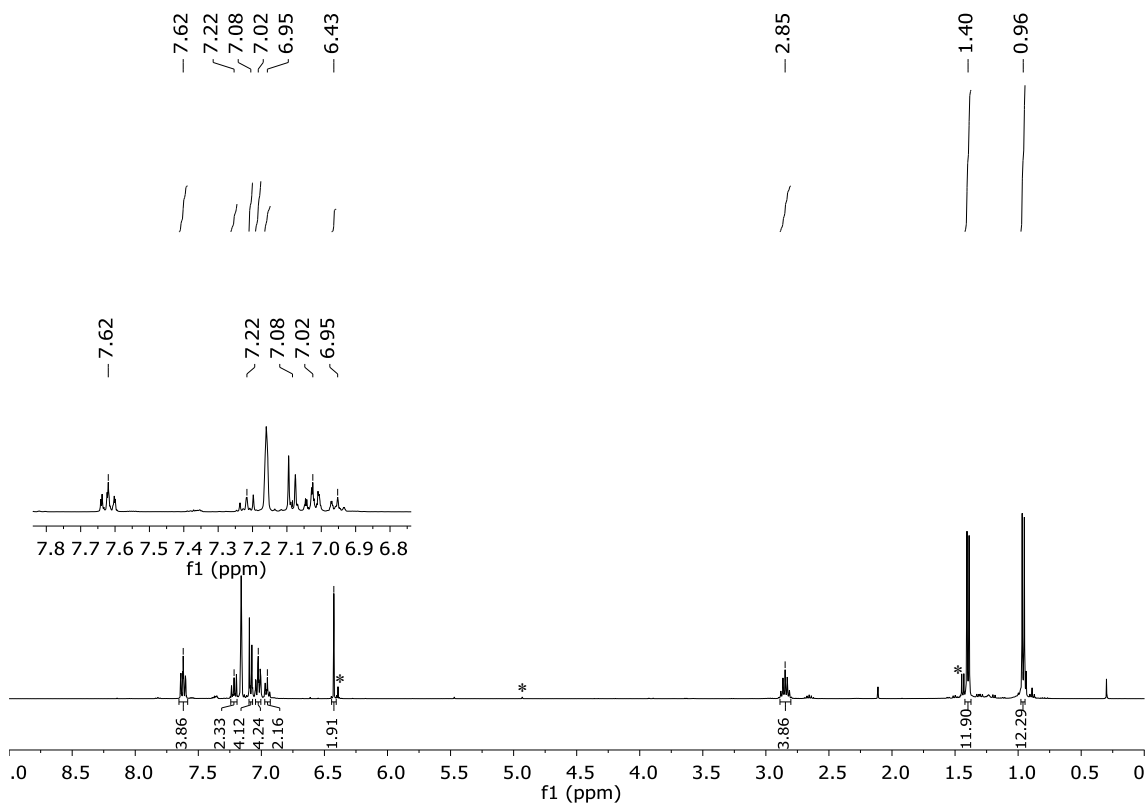


Figure S7. ^1H NMR (400.1 MHz, C_6D_6 , 300K) spectrum of **3**. * = PPh_2 + unidentified impurities.

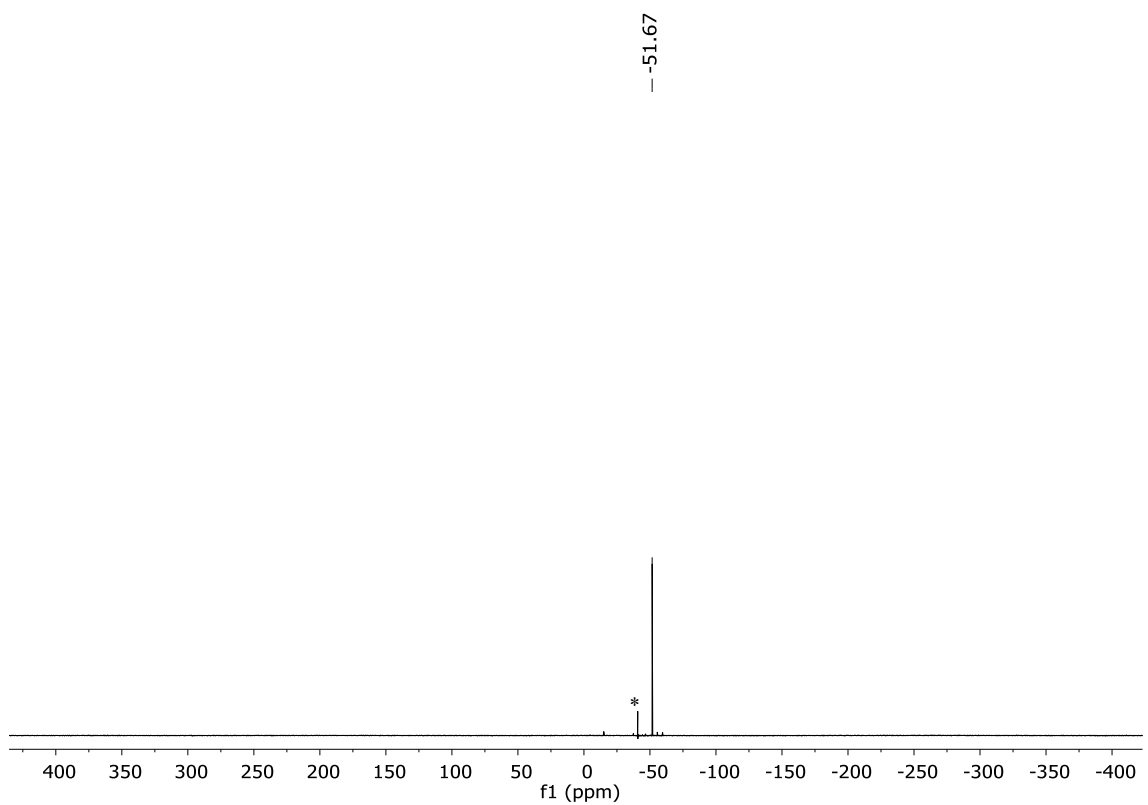


Figure S8. ^{31}P NMR (161.9 MHz, C_6D_6 , 300K) spectrum of **3**. * = PPh_2 .

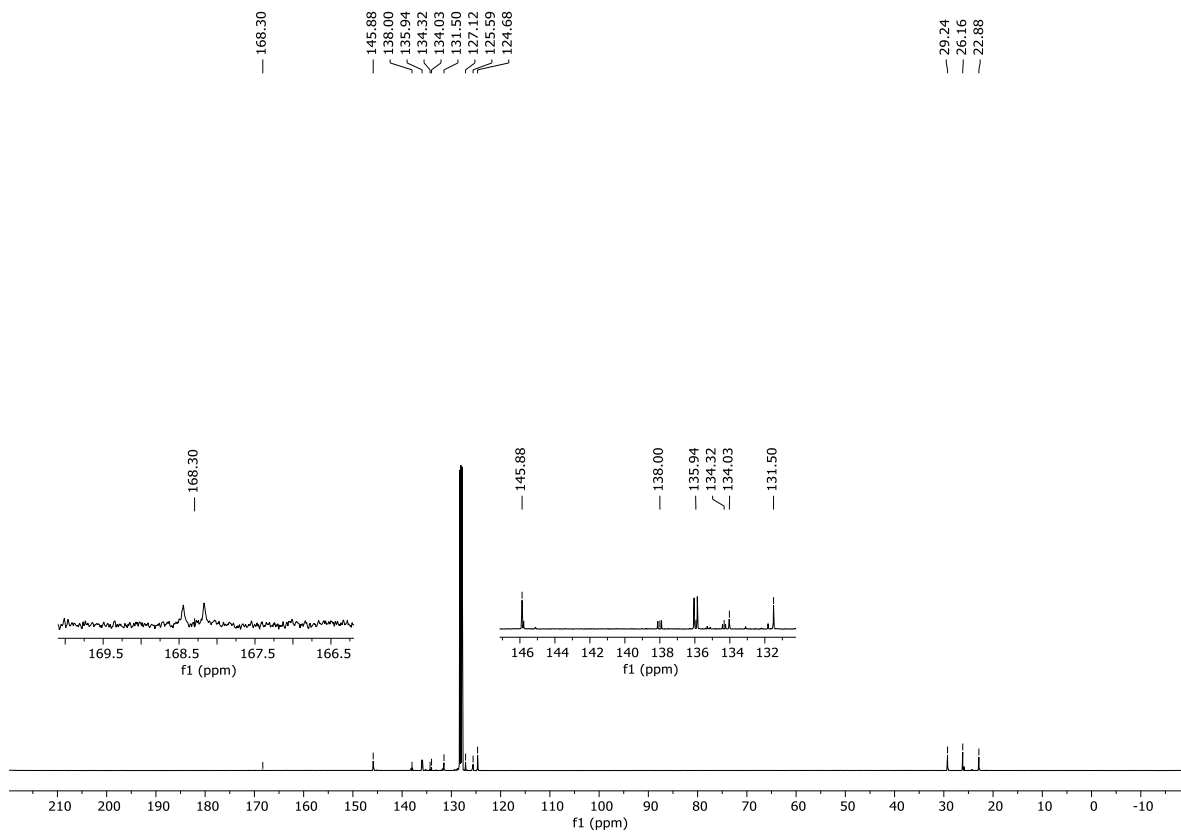


Figure S9. ^{13}C (^1H) NMR (100.6 MHz, C_6D_6 , 300K) spectrum of **3**.

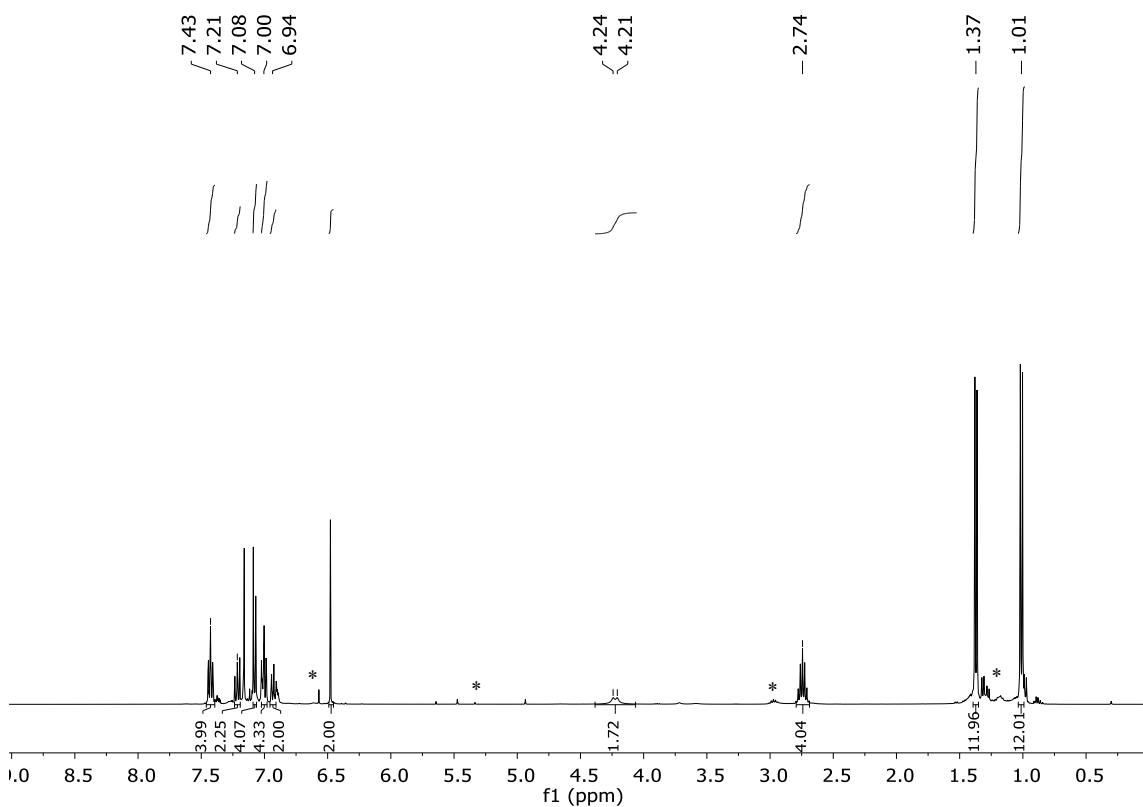


Figure S10. ^1H NMR (400.1 MHz, C_6D_6 , 300K) spectrum of **4**. * = PPh_2 + unidentified impurities.

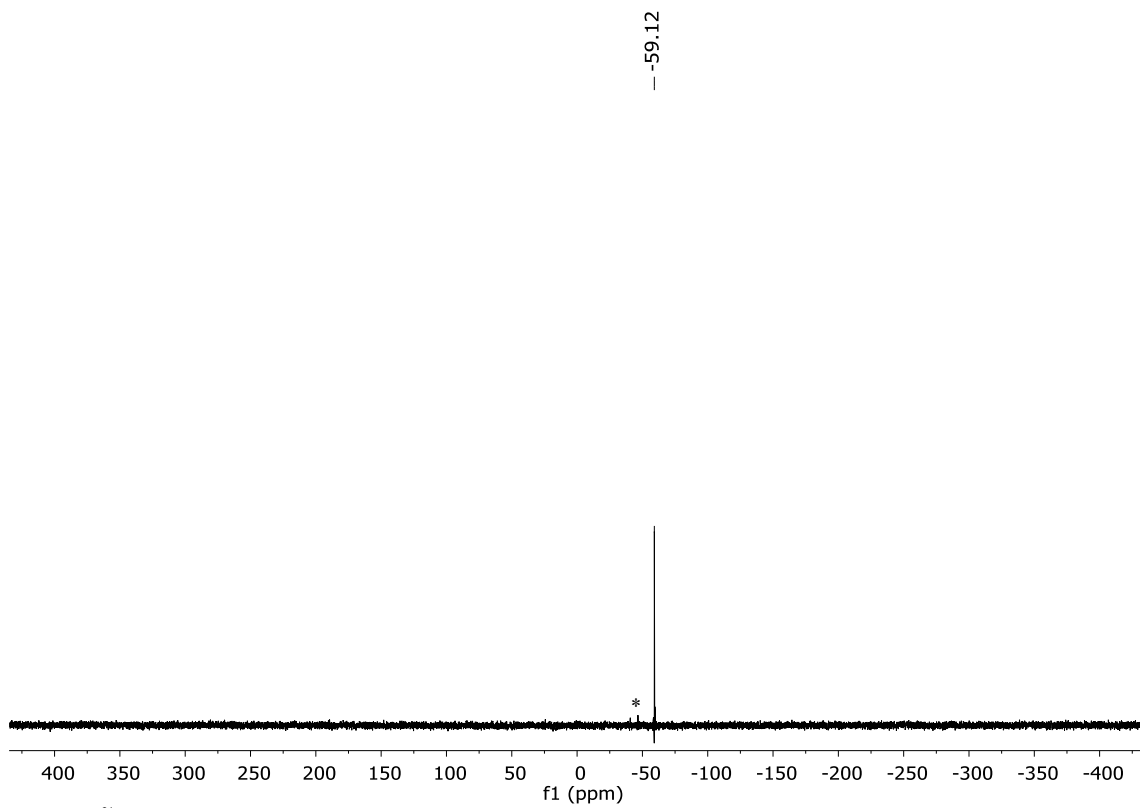


Figure S11. ³¹P NMR (161.9 MHz, C₆D₆, 300K) spectrum of **4**. * = PPh₂.

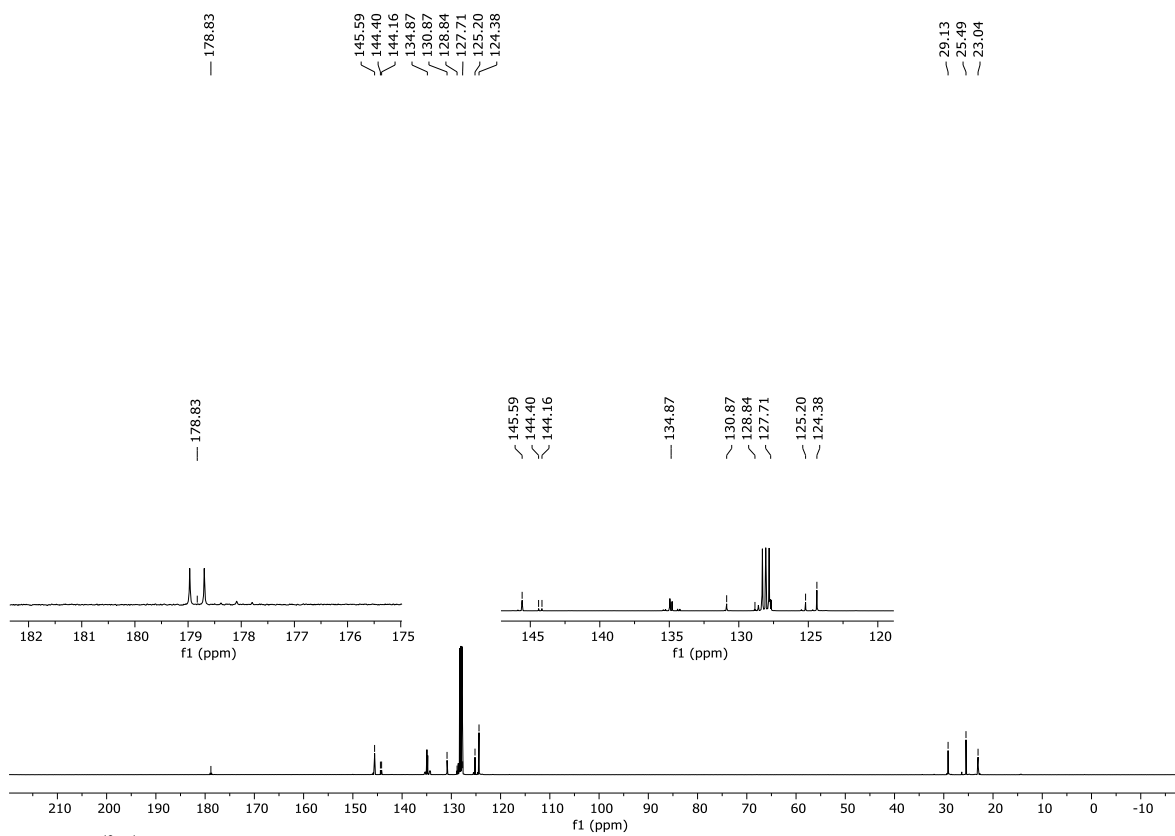


Figure S12. ¹³C{¹H} NMR (100.6 MHz, C₆D₆, 300K) spectrum of **4**.

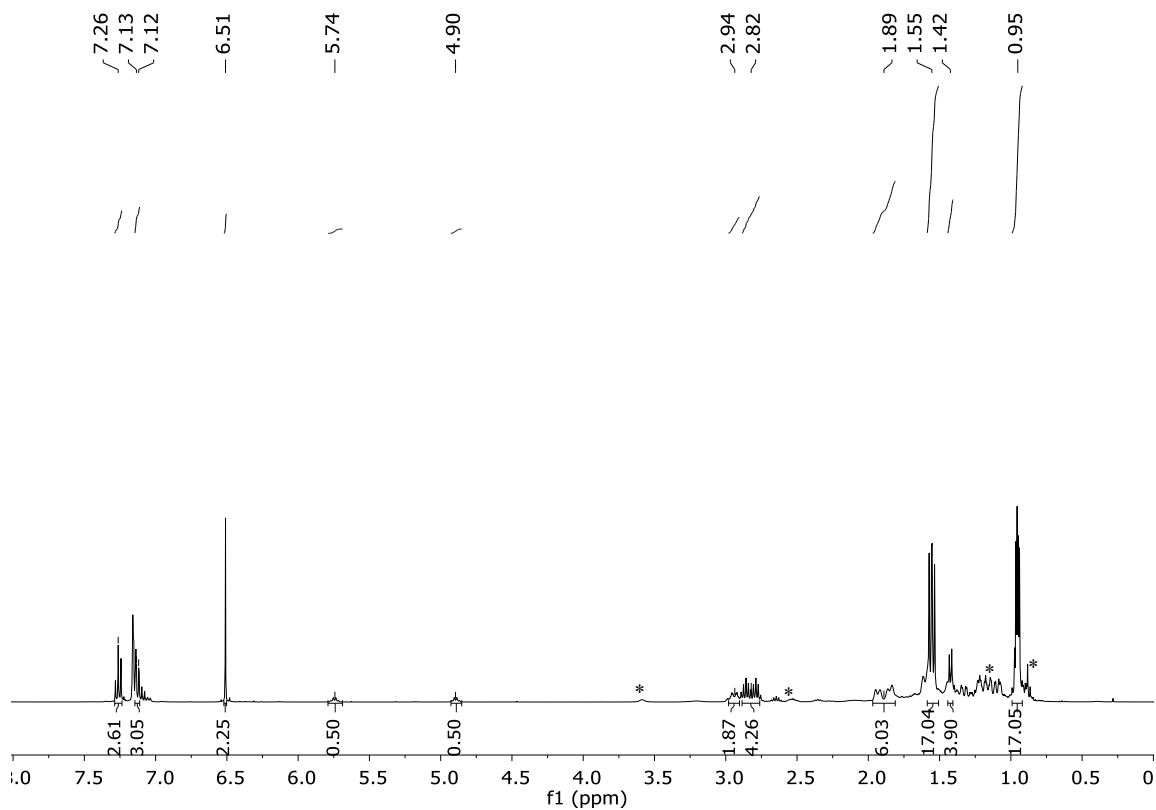


Figure S13. ^1H NMR (400.1 MHz, C_6D_6 , 300K) spectrum of **5**. * = $\text{PH}_2\text{NCy}_2\text{BH}_3$ + unidentified impurities.

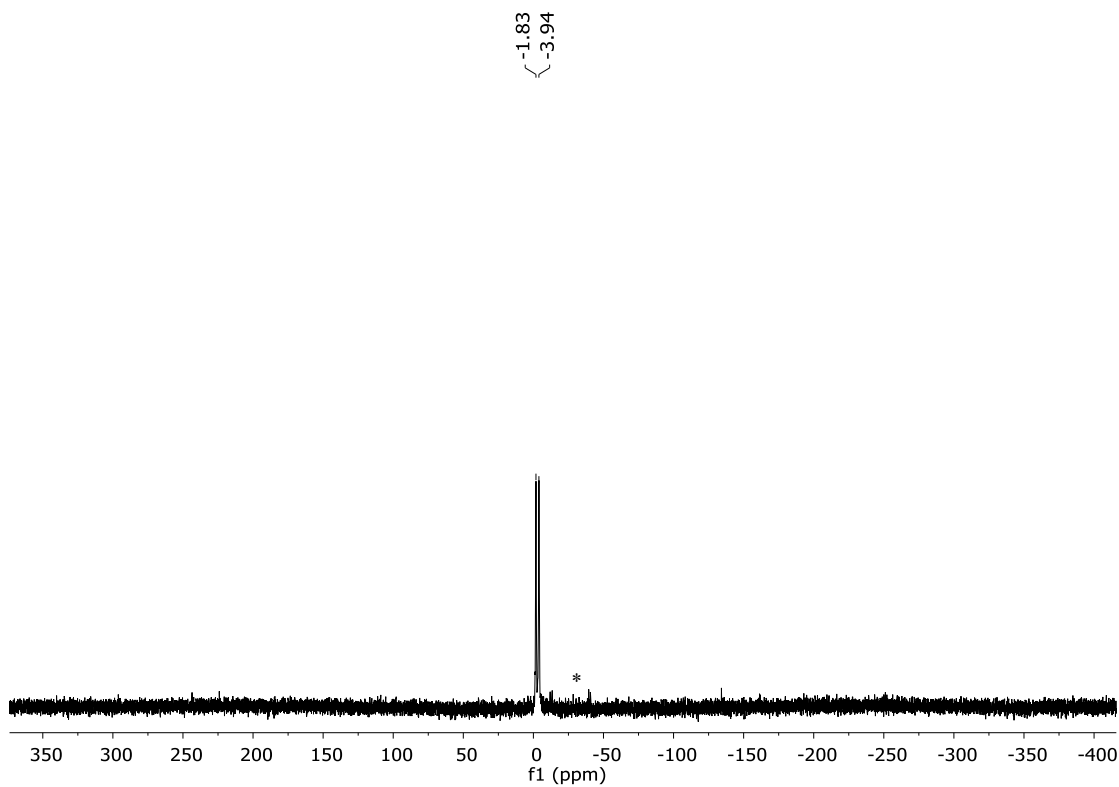


Figure S14. ^{31}P NMR (161.9 MHz, C_6D_6 , 300K) spectrum of **5**. * = $\text{PH}_2\text{NCy}_2\text{BH}_3$.

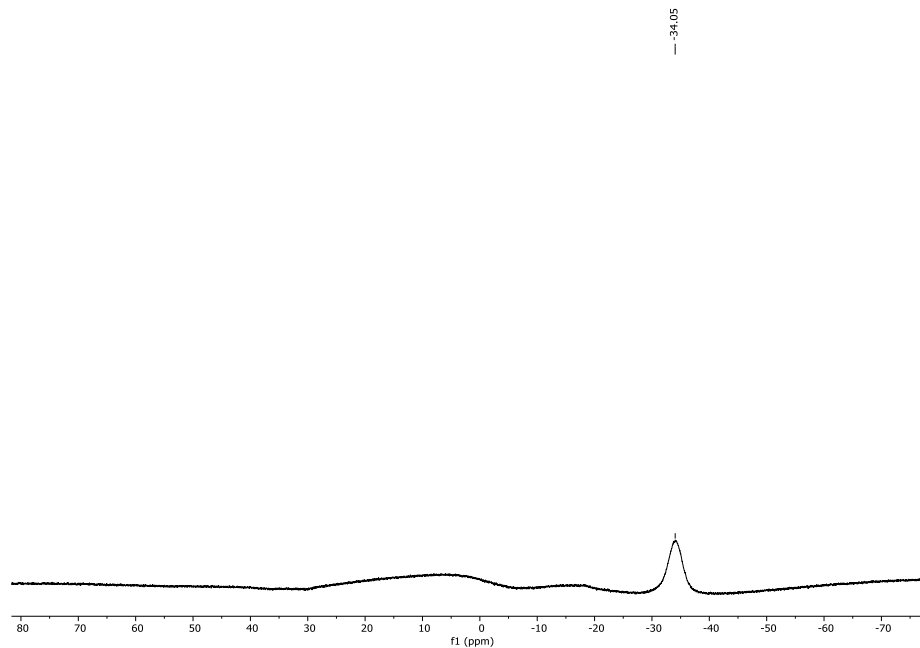


Figure S15. ^{11}B $\{^1\text{H}\}$ NMR (128.3 MHz, C_6D_6 , 300K) spectrum of **5**.

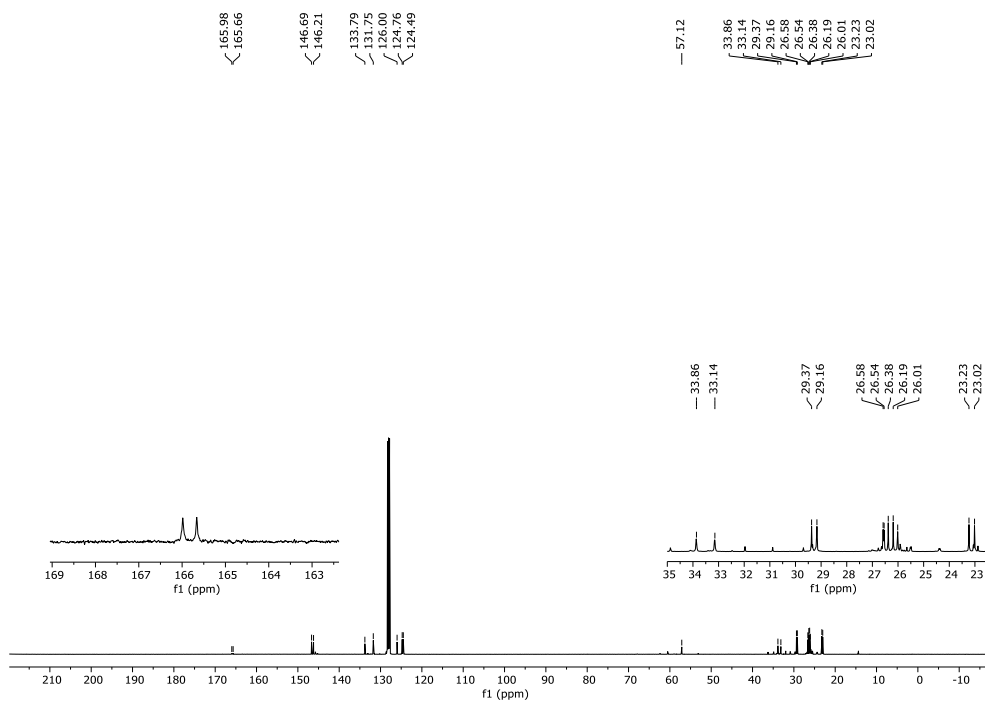


Figure S16. ^{13}C $\{^1\text{H}\}$ NMR spectrum (100.6 MHz, C_6D_6 , 300K) of **5**.

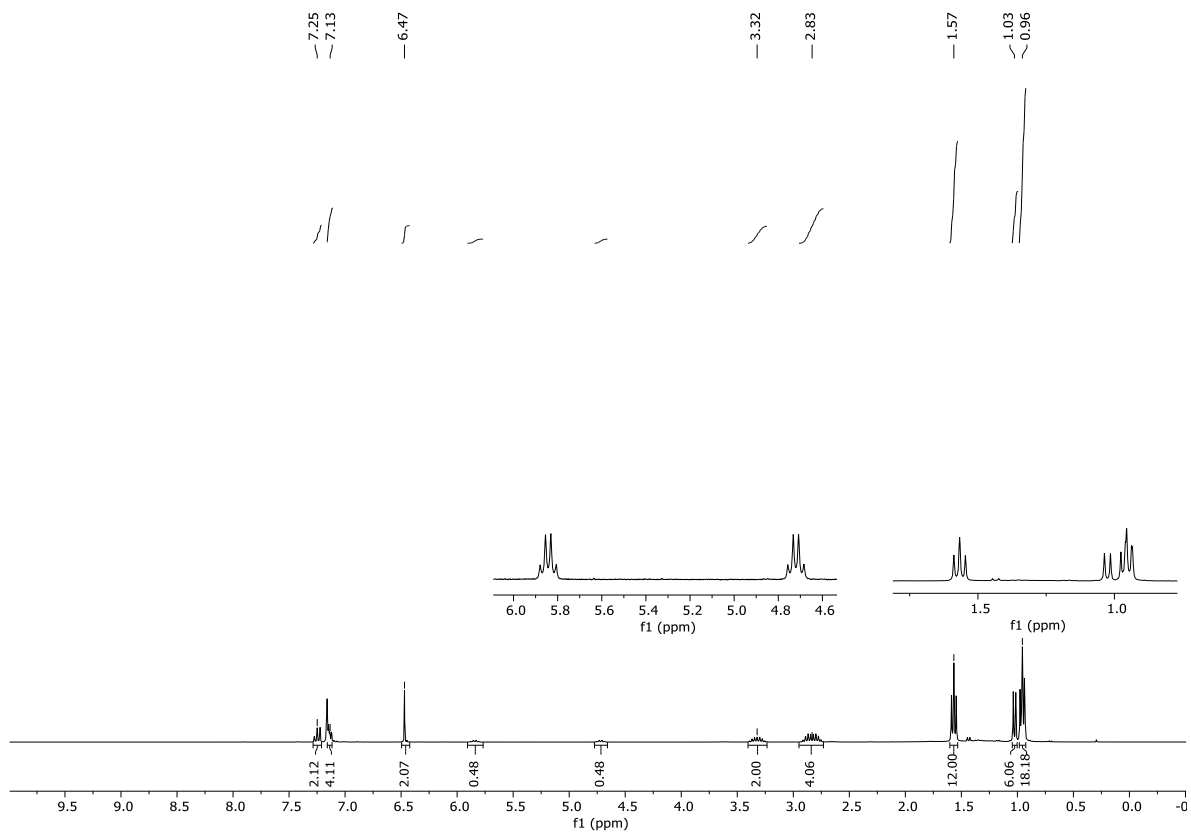


Figure S17. ^1H NMR (400.1 MHz, C_6D_6 , 300K) spectrum of **6**.

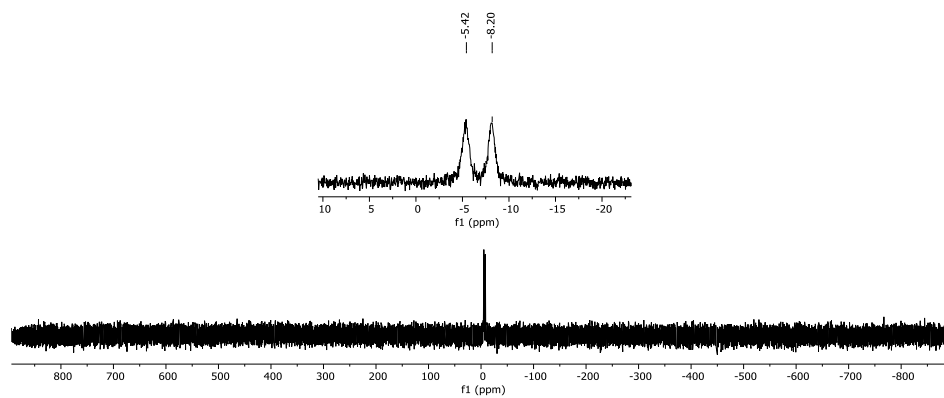


Figure S18. ^{31}P NMR (161.9 MHz, C_6D_6 , 300K) spectrum of **6**.

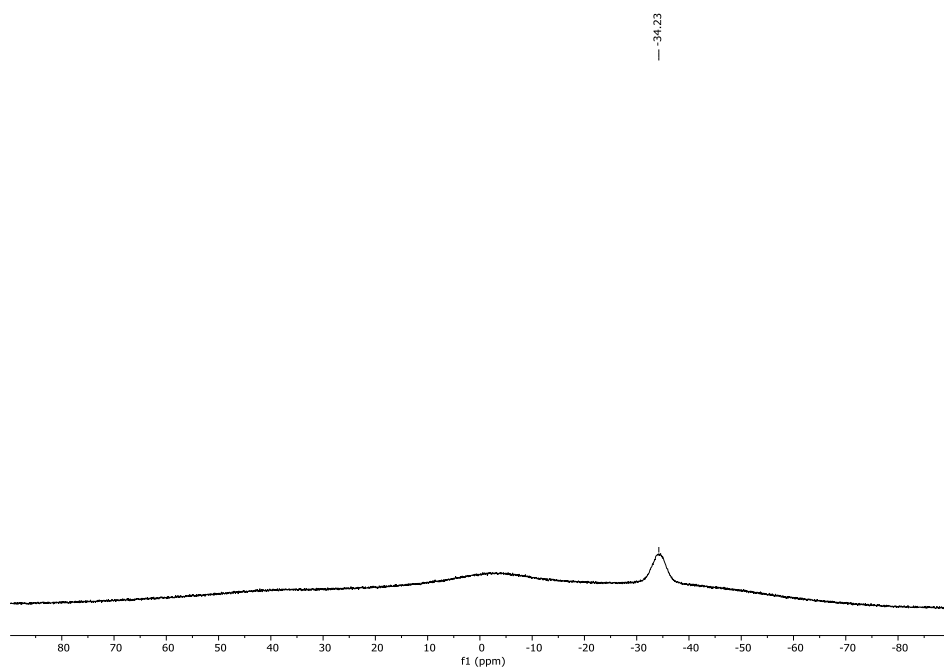


Figure S19. $^{11}\text{B}\{^1\text{H}\}$ NMR (128.3 MHz, C_6D_6 , 300K) spectrum of **6**.

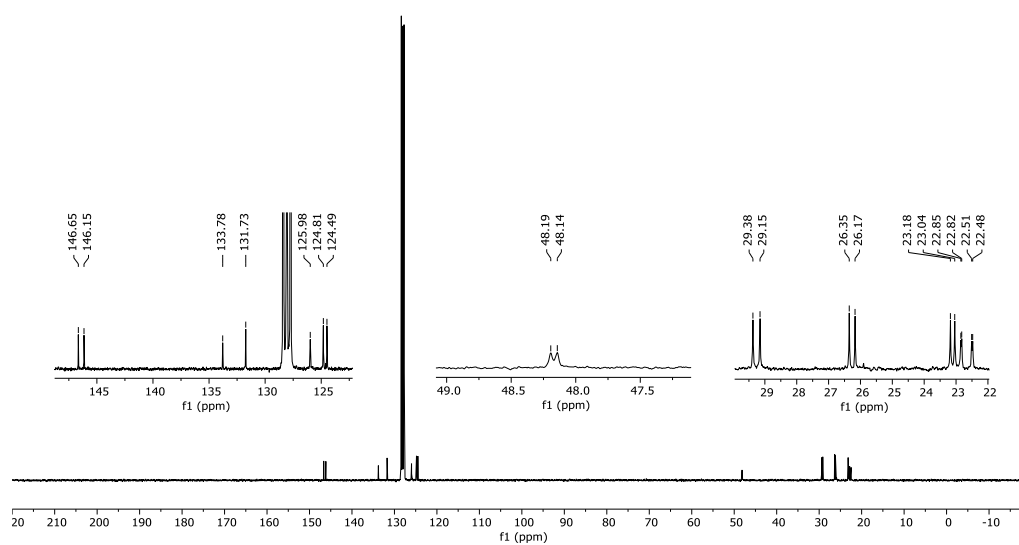


Figure S20. ^{13}C $\{^1\text{H}\}$ NMR (100.6 MHz, C_6D_6 , 300K) spectrum of 6.

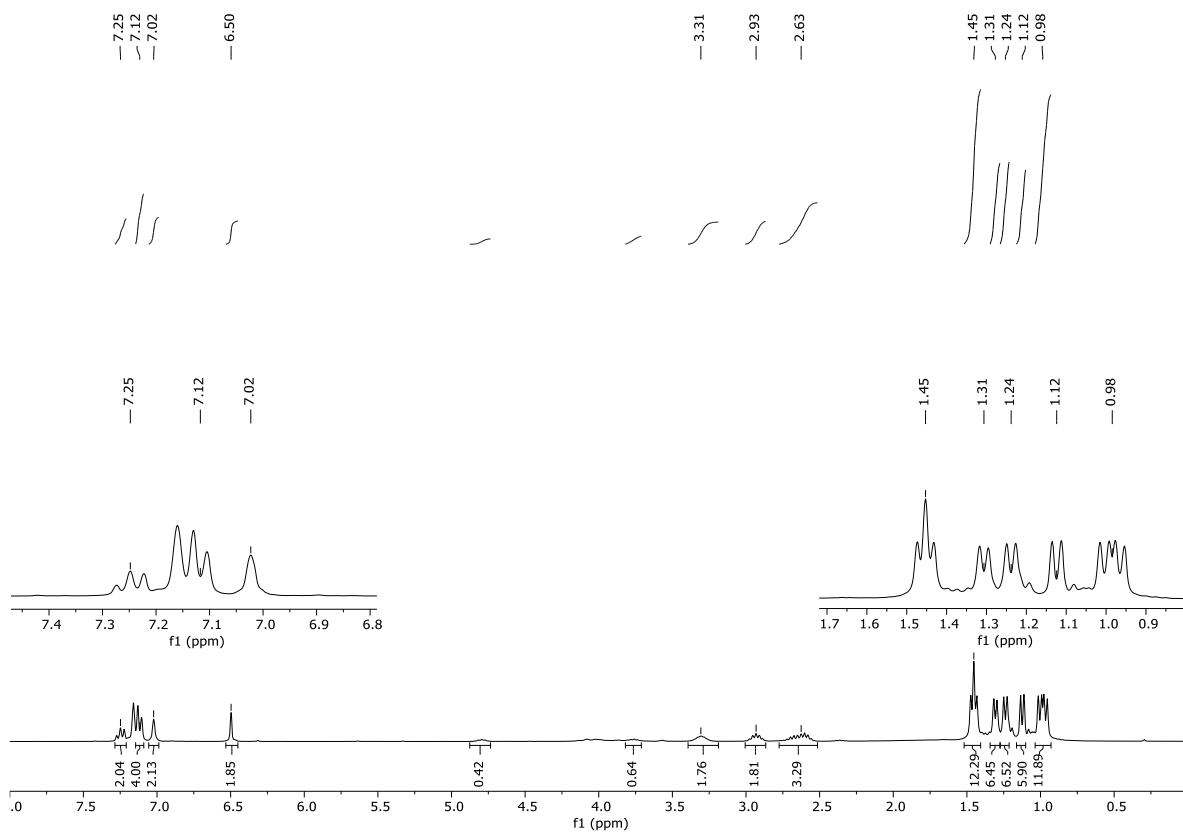


Figure S21. ^1H NMR (400.1 MHz, C_6D_6 , 300K) spectrum of 7.

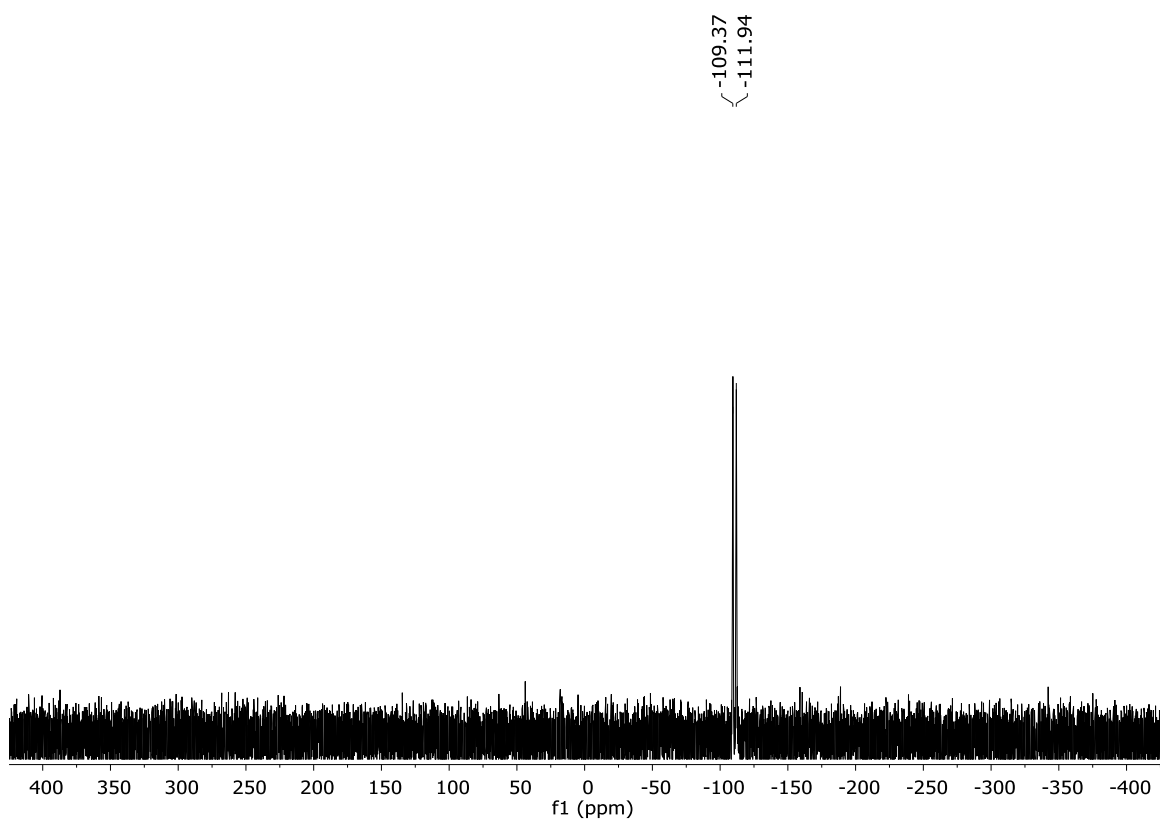


Figure S22. ^{31}P NMR (161.9 MHz, C_6D_6 , 300K) spectrum of 7.

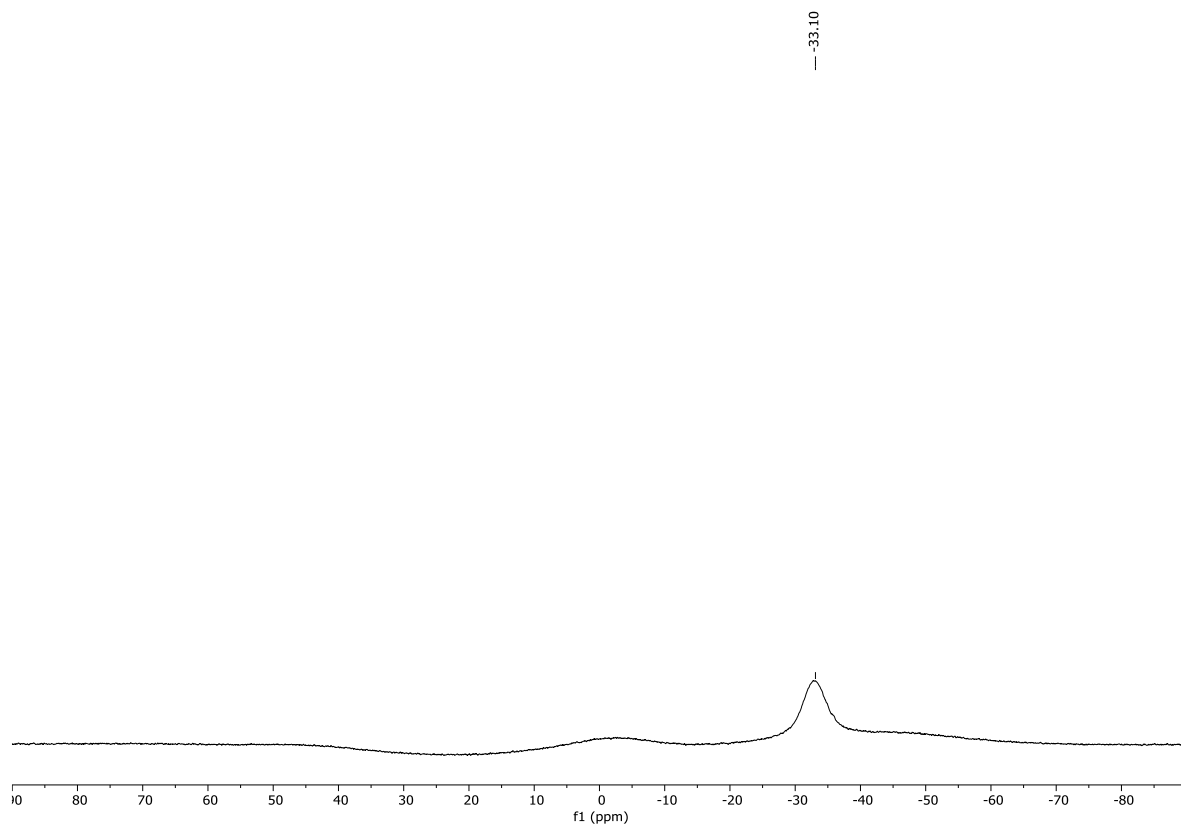


Figure S23. $^{11}\text{B}\{^1\text{H}\}$ NMR (128.3 MHz, C_6D_6 , 300K) of **7**.

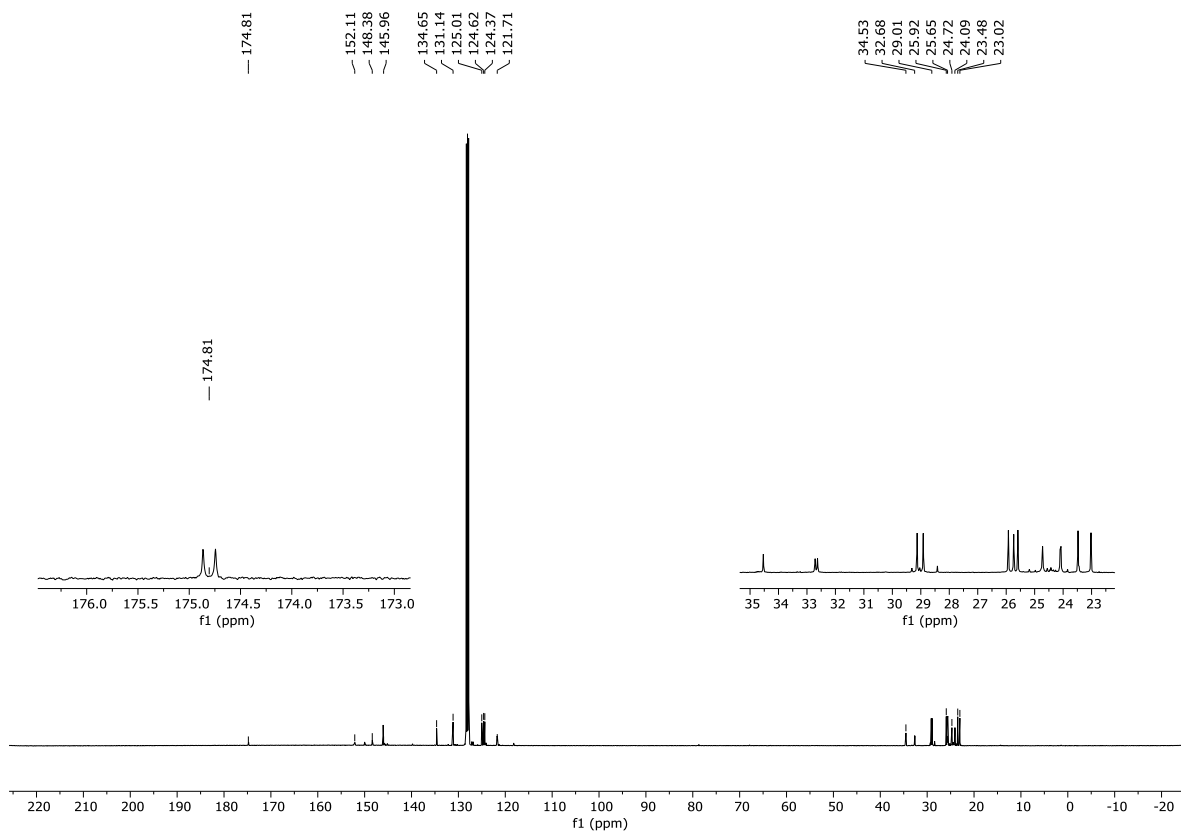


Figure S24. ^{13}C $\{^1\text{H}\}$ NMR spectrum (100.6 MHz, C_6D_6 , 300K) of **7**.

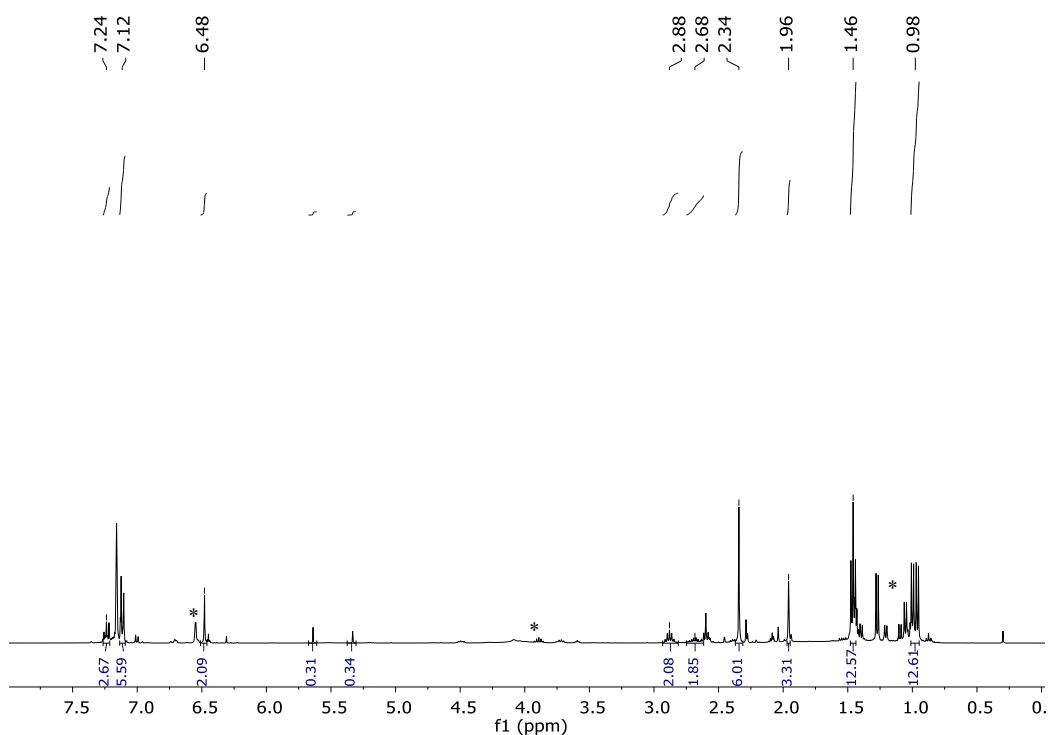


Figure S25. ^1H NMR (400.1 MHz, C_6D_6 , 300K) spectrum of **8**. * = PH_2Mes + $\text{PH}_2\text{MesBH}_3$ + unidentified impurities.

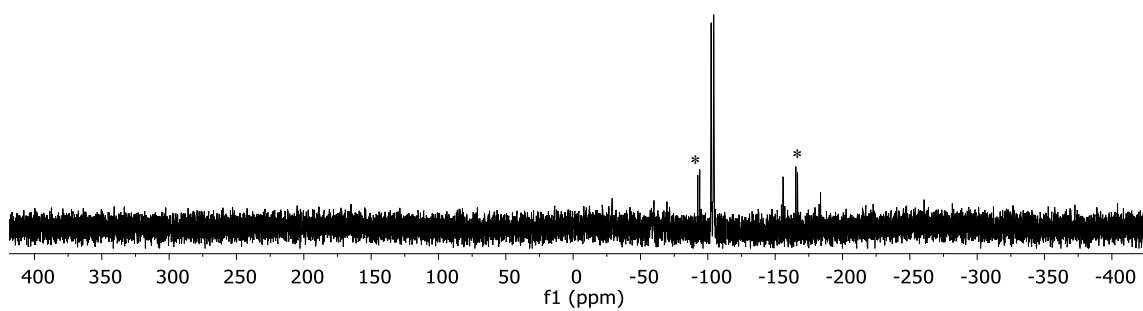


Figure S26. ^{31}P NMR spectrum (161.9 MHz, C_6D_6 , 300K) of **8**. * = PH_2Mes + $\text{PH}_2\text{MesBH}_3$ + unidentified impurities.

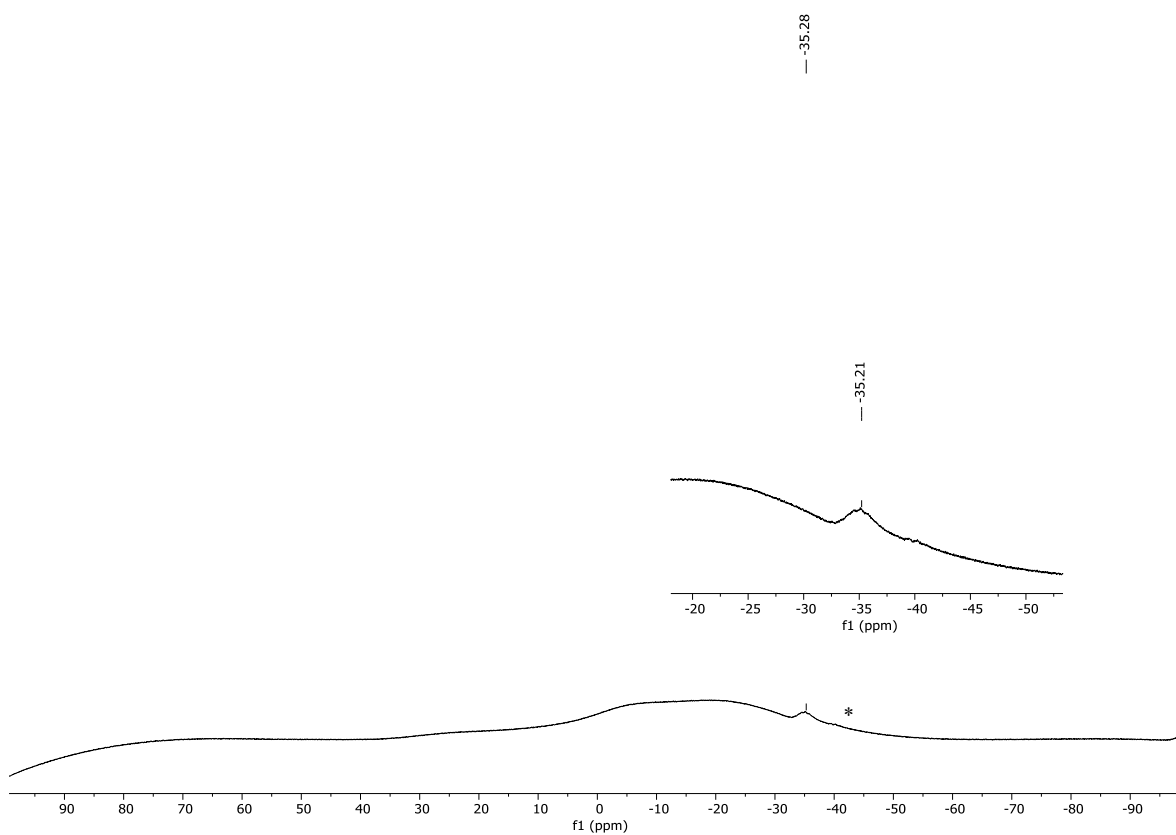


Figure S27. ^{11}B (^1H) NMR spectrum (128.3 MHz, C_6D_6 , 300K) of **8**. * = $\text{PH}_2\text{MesBH}_3$.

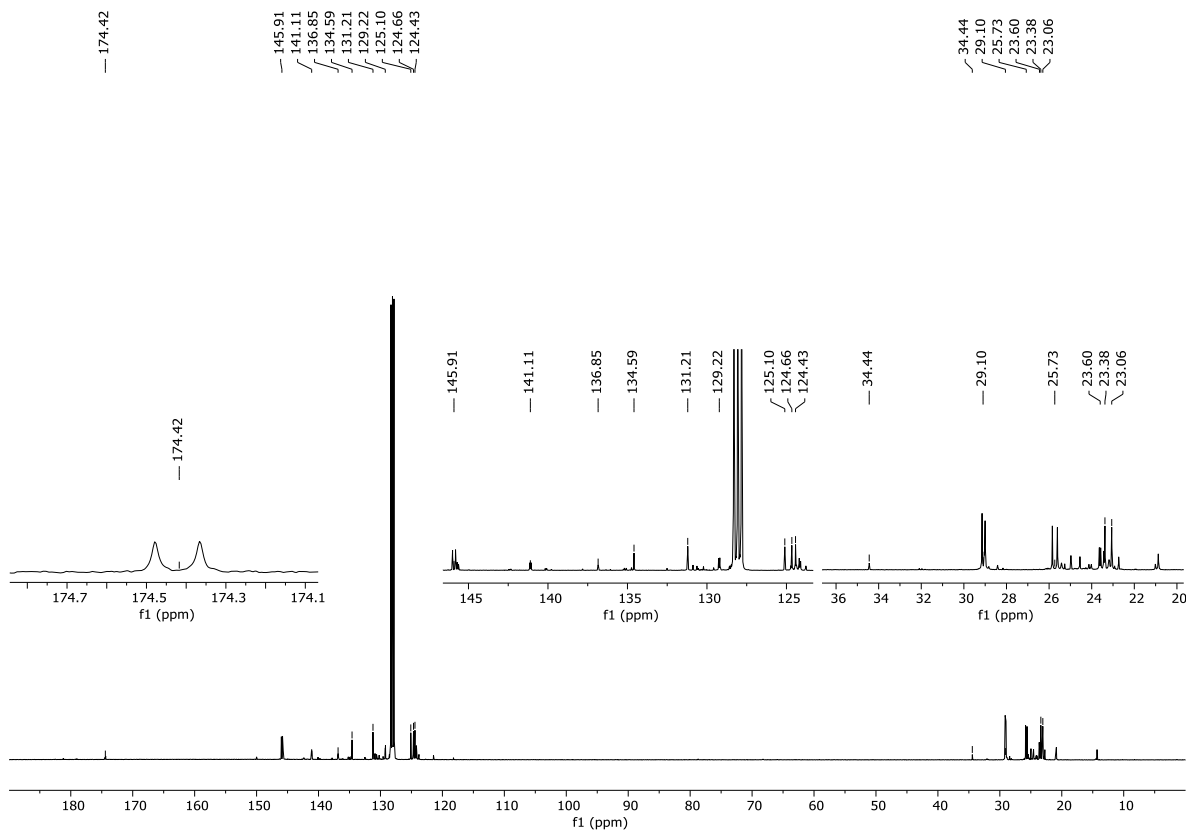


Figure S28. ^{13}C (^1H) NMR spectrum (100.6 MHz, C_6D_6 , 300K) of **8**.

IR Spectra

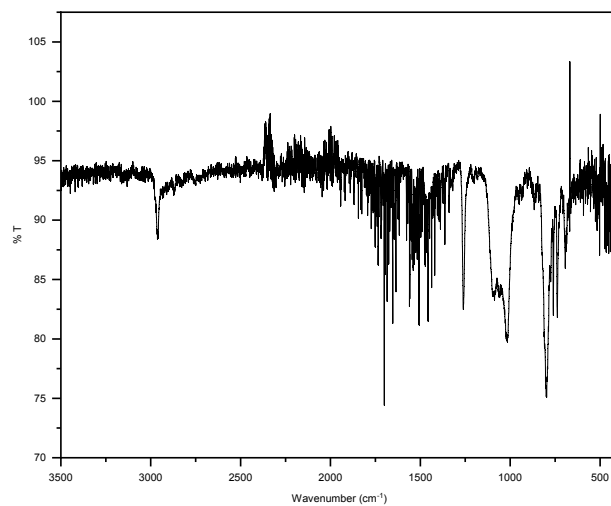


Figure S29. IR spectrum of 1.

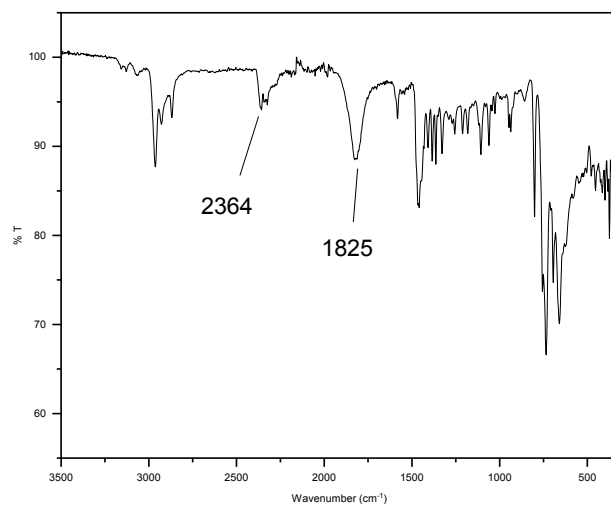


Figure S30. IR spectrum of 2.

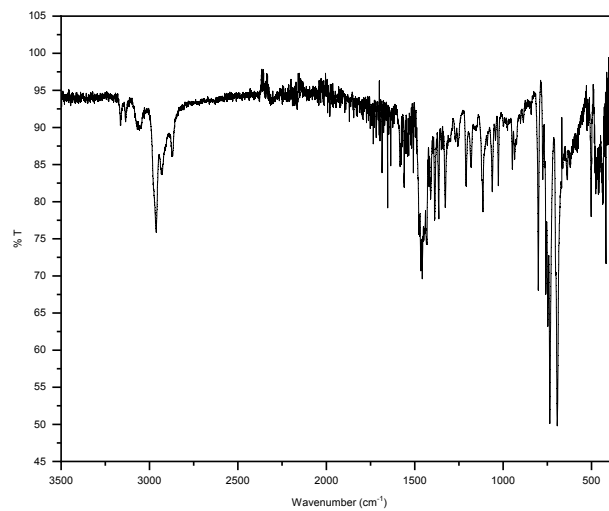


Figure S31. IR spectrum of 3.

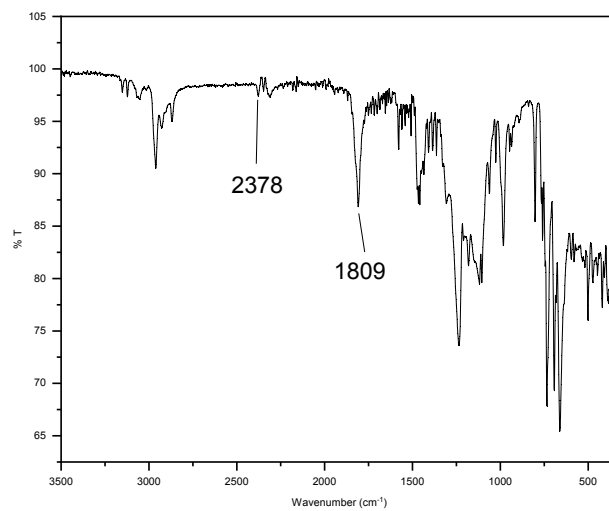


Figure S32. IR spectrum of 4.

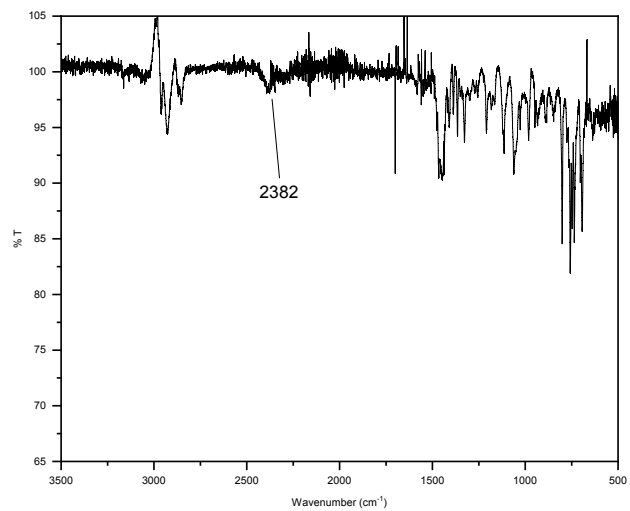


Figure S33. IR spectrum of 5.

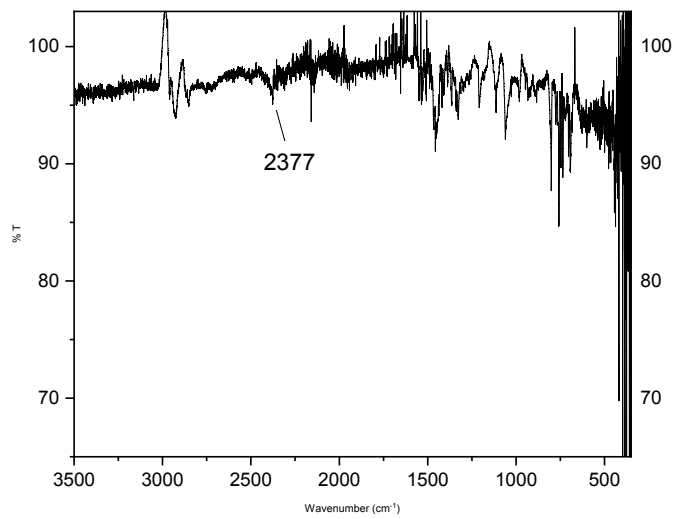


Figure S34. IR spectrum of 6.

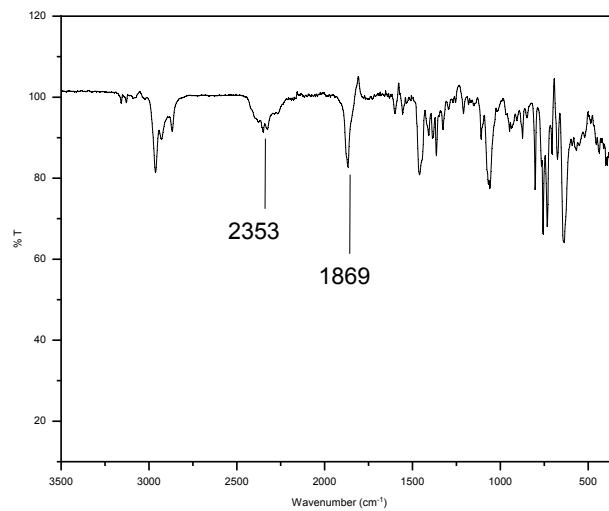


Figure S35. IR spectrum of 7.

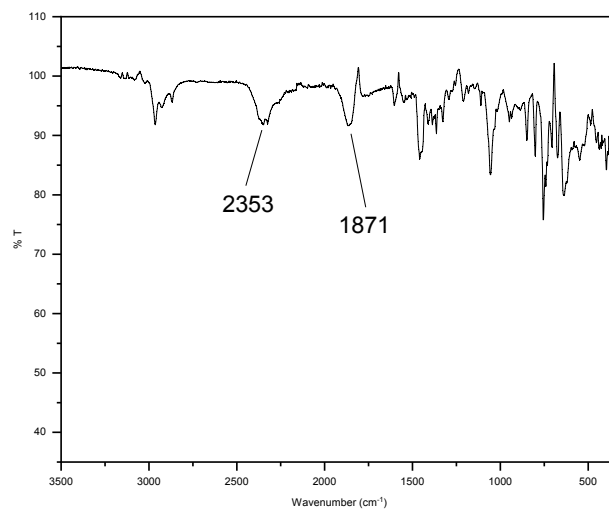
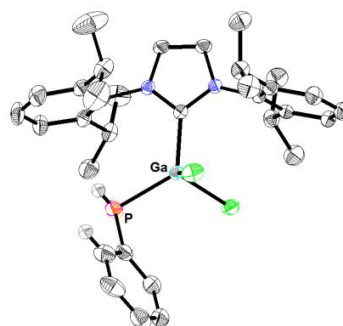


Figure S36. IR spectrum of 8.

Crystallographic Details

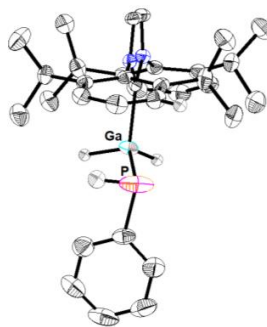
The boron, gallium and phosphorous bonded H atoms were located on the electron density maps and their positional parameters were refined using isotropic displacement parameters which were set at 1.2 times the Ueq value (P, Ga) or 1.5 times the Ueq value (B) of the corresponding parent atoms. Disorder: The GaCl2PHBH3N(CH(CH3)2) residue on C1 was split over two positions. The major component refined to 0.88.

Compound 1



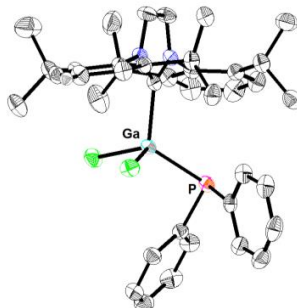
Sum Formula: $C_{33}H_{42}Cl_2GaN_2P$, mol. wt.: 638.27 g/mol, space group: $P 2_1 2_1 2_1$, $Z = 4$, $a = 13.6168(3) \text{ \AA}$, $b = 15.1257(5) \text{ \AA}$, $c = 16.4422(5) \text{ \AA}$, $\alpha = 90^\circ$, $\beta = 90^\circ$, $\gamma = 90^\circ$, $V = 3386.50(17) \text{ \AA}^3$, $d_c = 1.252 \text{ g cm}^{-3}$, $\mu = 1.041 \text{ mm}^{-1}$, $T = 133 \text{ K}$, transmission factors (min./max.) 0.715/0.746, $\theta_{max} = 27.886^\circ$, no. of unique data = 365, $R(\text{reflections}) = 0.0243(7679)$, $wR2(\text{reflections}) = 0.0608(8074)$, data completeness = 1.80/1.00, CCDC reference number: 2182156 (sh4775_a).

Compound 2



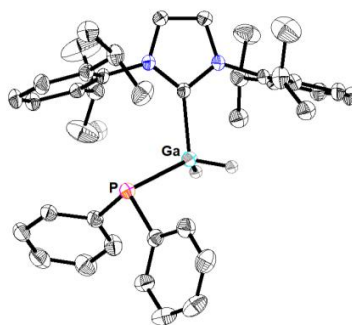
Sum Formula: $C_{33}H_{44}GaN_2P$, mol. wt.: 569.39 g/mol, space group: $P 4_1$, $Z = 4$, $a = 13.8123(4) \text{ \AA}$, $b = 13.8123(4) \text{ \AA}$, $c = 16.8084(8) \text{ \AA}$, $\alpha = 90^\circ$, $\beta = 90^\circ$, $\gamma = 90^\circ$, $V = 3206.7(2) \text{ \AA}^3$, $d_c = 1.179 \text{ g cm}^{-3}$, $\mu = 0.930 \text{ mm}^{-1}$, $T = 133 \text{ K}$, transmission factors (min./max.) 0.661/0.746, $\theta_{max} = 27.138^\circ$, no. of unique data = 352, $R(\text{reflections}) = 0.0276(6599)$, $wR2(\text{reflections}) = 0.0707(7017)$, data completeness = 1.91/0.99, CCDC reference number: 2182157 (sh4854_a).

Compound 3



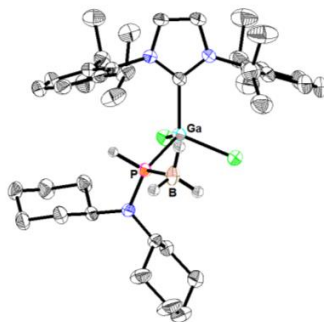
Sum Formula: $C_{81}H_{95}Cl_4Ga_2N_4P_2$, mol. wt.: 1467.78 g/mol, space group: $P-1$, $Z = 2$, $a = 10.4116(5) \text{ \AA}$, $b = 15.2713(7) \text{ \AA}$, $c = 24.5808(11) \text{ \AA}$, $\alpha = 92.200(2)^\circ$, $\beta = 101.262(2)^\circ$, $\gamma = 95.192(2)^\circ$, $V = 3811.0(3) \text{ \AA}^3$, $d_c = 1.279 \text{ g cm}^{-3}$, $\mu = 0.934 \text{ mm}^{-1}$, $T = 133 \text{ K}$, transmission factors (min./max.) 0.640/0.746, $\theta_{max} = 28.005^\circ$, no. of unique data = 882, $R(\text{reflections}) = 0.0402(14642)$, $wR2(\text{reflections}) = 0.1162(18191)$, data completeness = 0.987, CCDC reference number: 2182158 (sh4792_a).

Compound 4



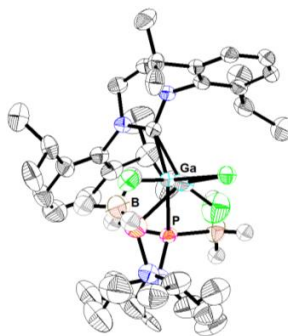
Sum Formula: $C_{39}H_{48}GaN_2P$, mol. wt.: 645.48 g/mol, space group: $P2_1/n$, $Z = 4$, $a = 10.6429(2) \text{ \AA}$, $b = 25.3550(4) \text{ \AA}$, $c = 13.7965(3) \text{ \AA}$, $\alpha = 90^\circ$, $\beta = 106.589(1)^\circ$, $\gamma = 90^\circ$, $V = 3568.04(12) \text{ \AA}^3$, $d_c = 1.202 \text{ g cm}^{-3}$, $\mu = 0.844 \text{ mm}^{-1}$, $T = 133 \text{ K}$, transmission factors (min./max.) 0.702/0.746, $\theta_{max} = 27.893^\circ$, no. of unique data = 402, $R(\text{reflections}) = 0.0322(7430)$, $wR2(\text{reflections}) = 0.0879(8476)$, data completeness = 0.997, CCDC reference number: 2182159 (sh4821_a).

Compound 5



Sum Formula: $C_{99}H_{148}B_2Cl_4Ga_2N_6P_2$, mol. wt.: 1787.03 g/mol, space group: $P-1$, $Z = 2$, $a = 16.0234(7) \text{ \AA}$, $b = 17.4571(8) \text{ \AA}$, $c = 18.5730(8) \text{ \AA}$, $\alpha = 87.470(2)^\circ$, $\beta = 88.808(2)^\circ$, $\gamma = 75.139(1)^\circ$, $V = 5016.4(4) \text{ \AA}^3$, $d_c = 1.183 \text{ g cm}^{-3}$, $\mu = 0.721 \text{ mm}^{-1}$, $T = 133 \text{ K}$, transmission factors (min./max.) 0.720/0.746, $\theta_{max} = 27.929^\circ$, no. of unique data = 1327, R (reflections) = 0.0392 (18190), $wR2$ (reflections) = 0.1014 (23974), data completeness = 0.998, CCDC reference number: 2182160 (sh4610_a).

Compound 6



Sum Formula: $C_{33}H_{54}BCl_2GaN_3P$, mol. wt.: 675.19 g/mol, space group: $P 2_1/n$, $Z = 4$, $a = 10.5075(4) \text{ \AA}$, $b = 17.2020(7) \text{ \AA}$, $c = 20.9277(7) \text{ \AA}$, $\alpha = 90.0^\circ$, $\beta = 103.778(1)^\circ$, $\gamma = 90^\circ$, $V = 9673.8(2) \text{ \AA}^3$, $d_c = 1.221 \text{ g cm}^{-3}$, $\mu = 0.963 \text{ mm}^{-1}$, $T = 133 \text{ K}$, transmission factors (min./max.) 0.680/0.746, $\theta_{max} = 26.372^\circ$, no. of unique data = 456, R (reflections) = 0.0519 (6004), $wR2$ (reflections) = 0.1444 (7503), data completeness = 0.999, CCDC reference number: 2182162 (sh4912_a).

Compound 7

Computational Details

Optimized Structures

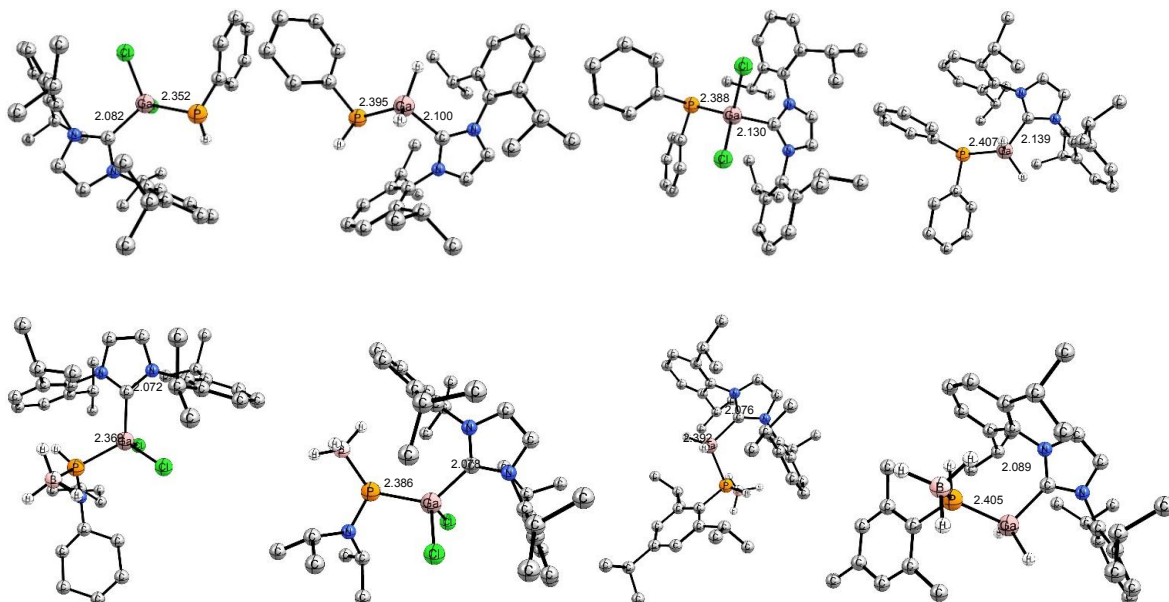
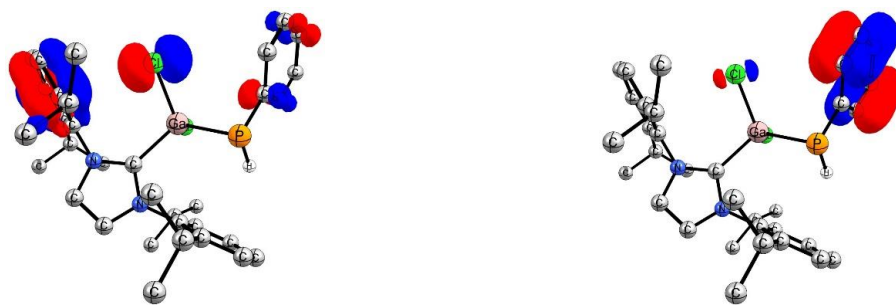


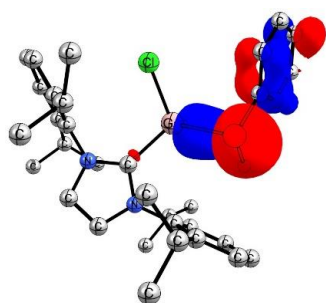
Figure S37. Optimized structures of **1-8** at the B3LYP-D3(BJ)/def2-SVP level of theory. The bond lengths are in Å. The hydrogen atoms except for the ones attached to phosphorous and gallium atoms are omitted for clarity.

Frontier Molecular Orbitals

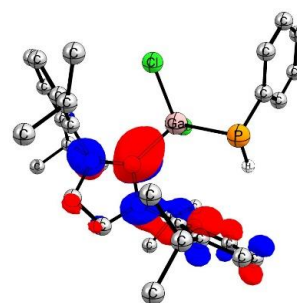


HOMO-2 ($\epsilon = -6.68$ eV)

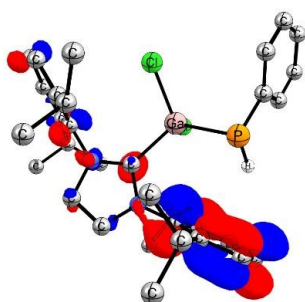
HOMO-1 ($\epsilon = -6.31$ eV)



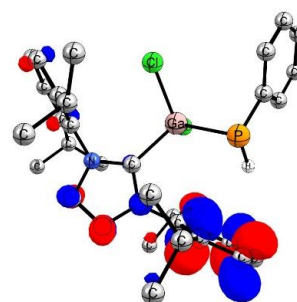
HOMO ($\epsilon = -5.35$ eV)



LUMO ($\epsilon = -1.14$ eV)

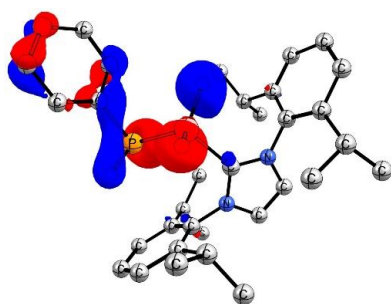


LUMO-1 ($\epsilon = -0.93$ eV)

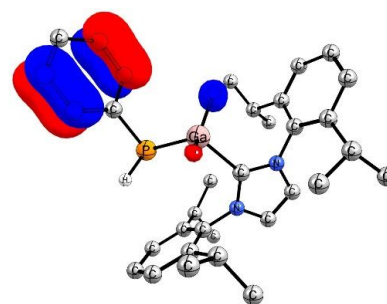


LUMO-2 ($\epsilon = -0.77$ eV)

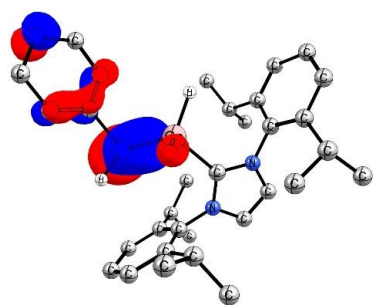
Figure S38. Frontier KS molecular orbitals (isovalue 0.05 a.u.) of compound **1** at the B3LYP-D3(BJ)/def2-TZVPP//B3LYP-D3(BJ)/def2-SVP level of theory.



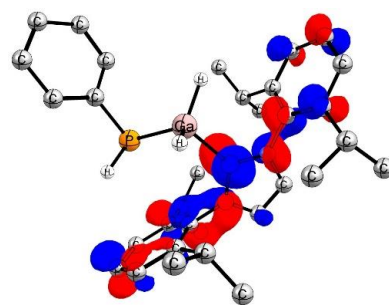
HOMO-2 ($\epsilon = -6.46$ eV)



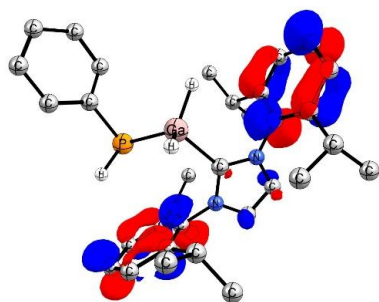
HOMO-1 ($\epsilon = -6.24$ eV)



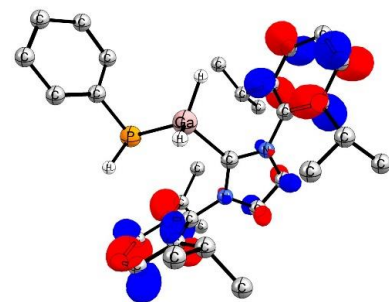
HOMO ($\epsilon = -4.77$ eV)



LUMO ($\epsilon = -0.85$ eV)

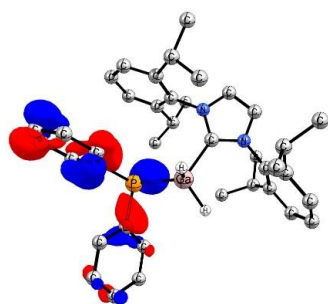


LUMO-1 ($\epsilon = -0.77$ eV)

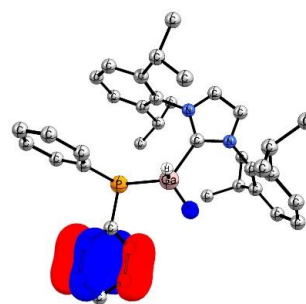


LUMO-2 ($\epsilon = -0.61$ eV)

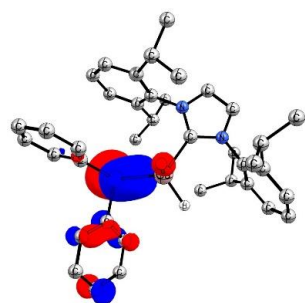
Figure S39. Frontier KS molecular orbitals (isovalue 0.05 a.u.) of compound **2** at the B3LYP-D3(BJ)/def2-TZVPP//B3LYP-D3(BJ)/def2-SVP level of theory.



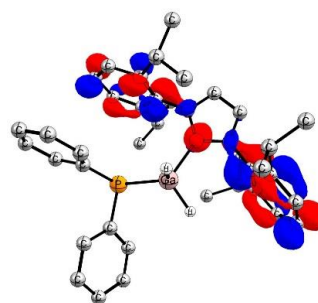
HOMO-2 ($\epsilon = -6.55$ eV)



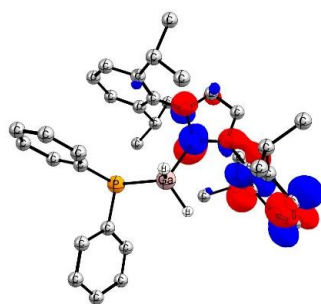
HOMO-1 ($\epsilon = -6.32$ eV)



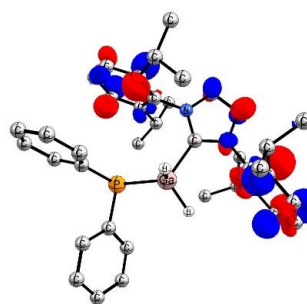
HOMO ($\epsilon = -5.15$ eV)



LUMO ($\epsilon = -1.16$ eV)

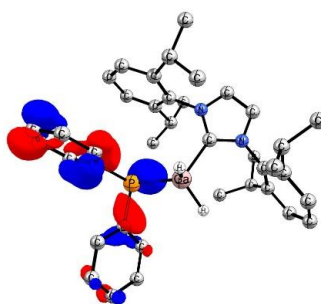


LUMO-1 ($\epsilon = -0.84$ eV)

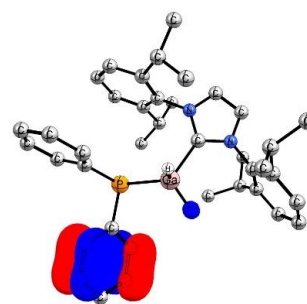


LUMO-2 ($\epsilon = -0.71$ eV)

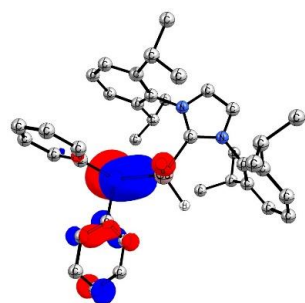
Figure S40. Frontier KS molecular orbitals (isovalue 0.05 a.u.) of compound **3** at the B3LYP-D3(BJ)/def2-TZVP//B3LYP-D3(BJ)/def2-SVP level of theory.



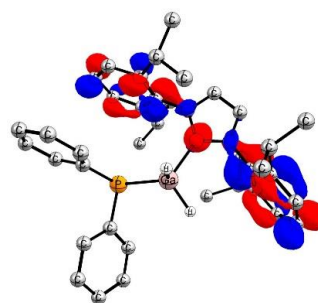
HOMO-2 ($\epsilon = -6.22$ eV)



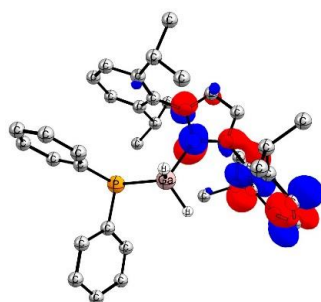
HOMO-1 ($\epsilon = -6.21$ eV)



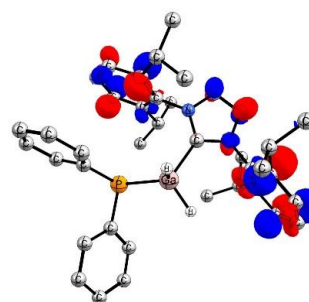
HOMO ($\epsilon = -4.64$ eV)



LUMO ($\epsilon = -0.80$ eV)

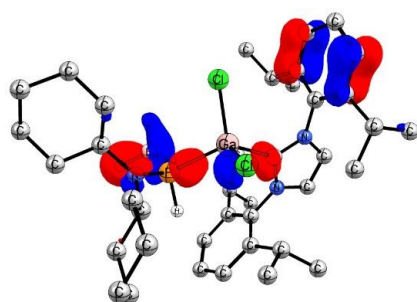


LUMO-1 ($\epsilon = -0.75$ eV)

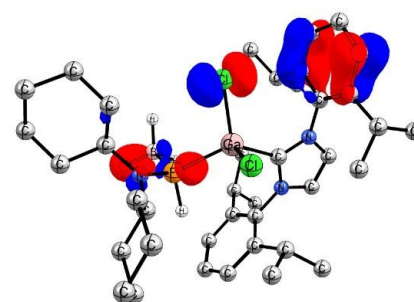


LUMO-2 ($\epsilon = -0.64$ eV)

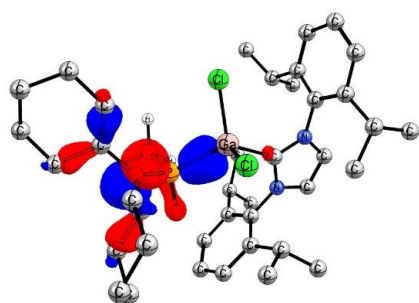
Figure S41. Frontier KS molecular orbitals (isovalue 0.05 a.u.) of compound **4** at the B3LYP-D3(BJ)/def2-TZVPP//B3LYP-D3(BJ)/def2-SVP level of theory.



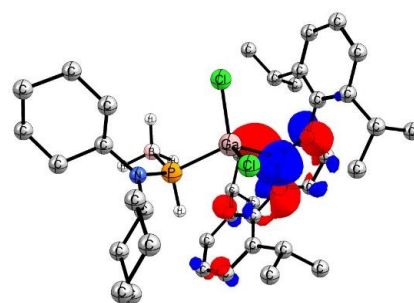
HOMO-2 ($\epsilon = -6.89$ eV)



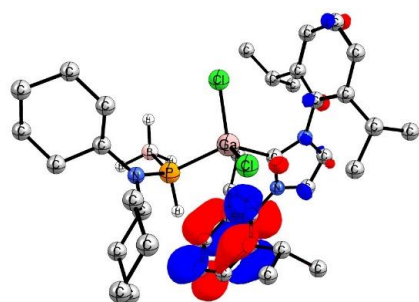
HOMO-1 ($\epsilon = -6.77$ eV)



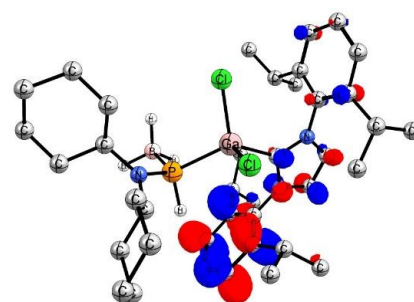
HOMO ($\epsilon = -5.23$ eV)



LUMO ($\epsilon = -1.37$ eV)

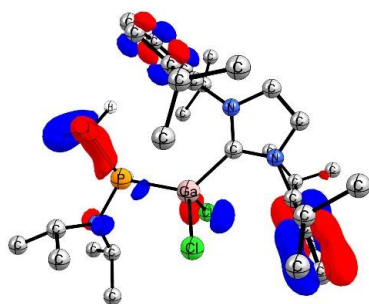


LUMO-1 ($\epsilon = -1.09$ eV)

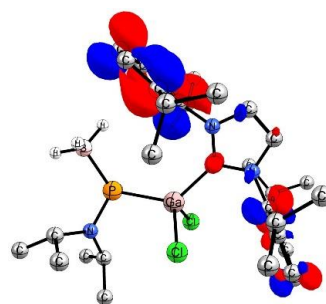


LUMO-2 ($\epsilon = -0.91$ eV)

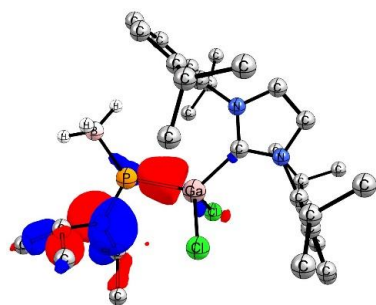
Figure S42. Frontier KS molecular orbitals (isovalue 0.05 a.u.) of compound **5** at the B3LYP-D3(BJ)/def2-TZVPP//B3LYP-D3(BJ)/def2-SVP level of theory.



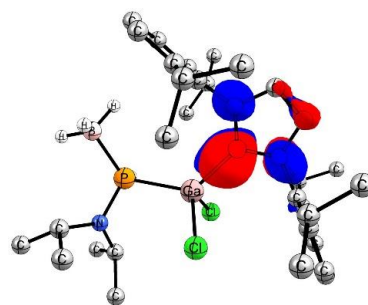
HOMO-2 ($\epsilon = -6.72$ eV)



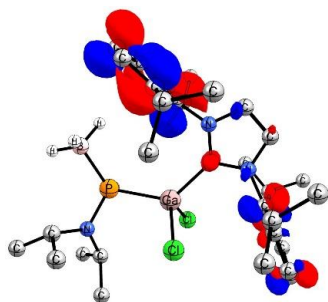
HOMO-1 ($\epsilon = -6.72$ eV)



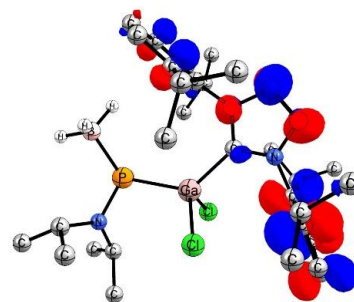
HOMO ($\epsilon = -5.38$ eV)



LUMO ($\epsilon = -1.28$ eV)

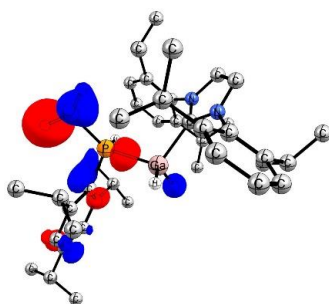


LUMO-1 ($\epsilon = -0.85$ eV)

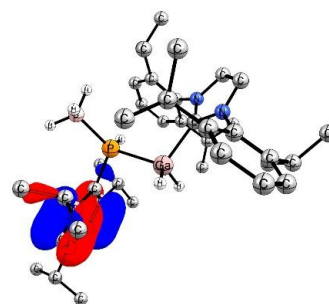


LUMO-2 ($\epsilon = -0.71$ eV)

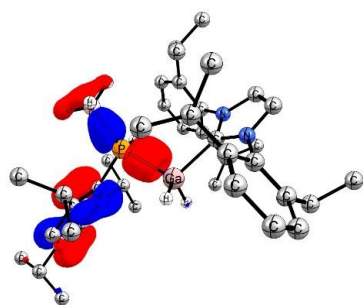
Figure S43. Frontier KS molecular orbitals (isovalue 0.05 a.u.) of compound **6** at the B3LYP-D3(BJ)/def2-TZVPP//B3LYP-D3(BJ)/def2-SVP level of theory.



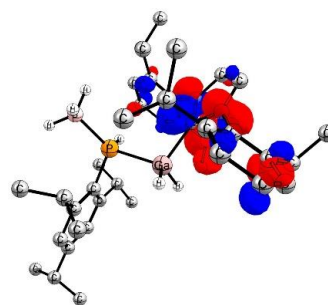
HOMO-2 ($\epsilon = -6.56$ eV)



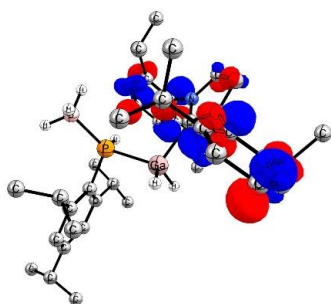
HOMO-1 ($\epsilon = -6.09$ eV)



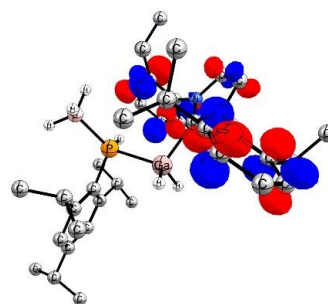
HOMO ($\epsilon = -5.64$ eV)



LUMO ($\epsilon = -1.06$ eV)

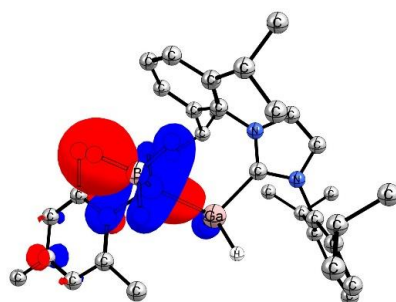


LUMO-1 ($\epsilon = -0.90$ eV)

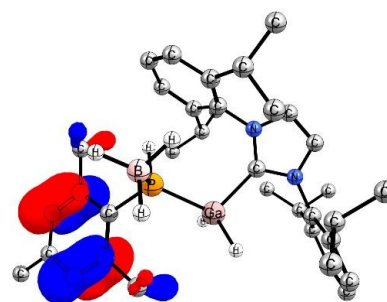


LUMO-2 ($\epsilon = -0.74$ eV)

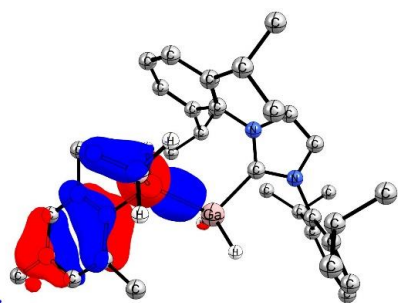
Figure S44. Frontier KS molecular orbitals (isovalue 0.05 a.u.) of compound 7 at the B3LYP-D3(BJ)/def2-TZVPP//B3LYP-D3(BJ)/def2-SVP level of theory.



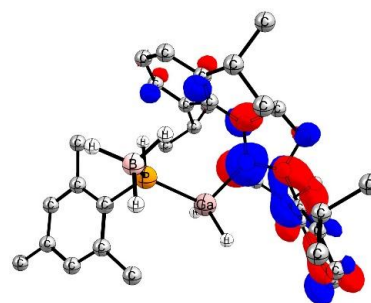
HOMO-2 ($\epsilon = -6.42$ eV)



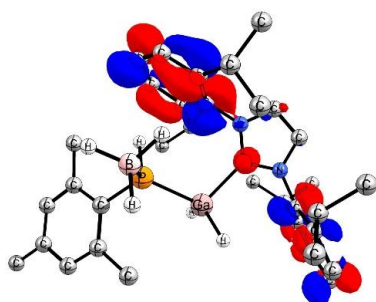
HOMO-1 ($\epsilon = -6.09$ eV)



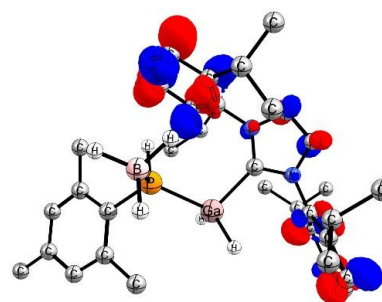
HOMO ($\epsilon = -5.62$ eV)



LUMO ($\epsilon = -1.01$ eV)



LUMO-1 ($\epsilon = -0.90$ eV)



LUMO-2 ($\epsilon = -0.77$ eV)

Figure S45. Frontier KS molecular orbitals (isovalue 0.05 a.u.) of compound **8** at the B3LYP-D3(BJ)/def2-TZVPP//B3LYP-D3(BJ)/def2-SVP level of theory.

NBO Results

Table S1. Natural Partial Charges (q in a.u.) and Wiberg bond orders (P in a.u.) of compound **1-8** at the B3LYP-D3(BJ)/def2-TZVPP//B3LYP-D3(BJ)/def2-SVP level of theory.

Property	1	2	3	4	5	6	7	8
Q(P)	-0.03	-0.02	0.25	0.26	0.73	0.73	0.45	0.47
Q(Ga)	1.13	0.62	1.12	0.60	1.13	1.11	0.64	0.63
Q(C _{car})	0.29	0.44	0.30	0.67	0.28	0.76	0.48	0.50
$P(\text{Ga-P})$	0.79	0.78	0.78	0.78	0.71	0.71	0.72	0.73
$P(\text{C}_{\text{car}}\text{-Ga})$	0.48	0.54	0.49	0.54	0.49	0.50	0.56	0.56

Orbital	Occ.	Contribution of the Atoms to the Orb.	Atomic Orbitals
---------	------	---------------------------------------	-----------------

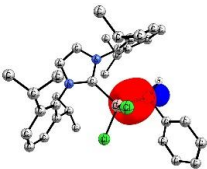
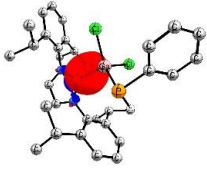
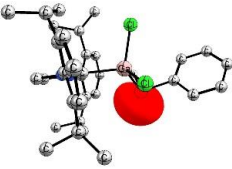
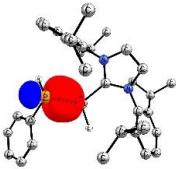
	1.94	Ga (33.93%) - P(66.07%)	Ga: s(65.79%), p(34.06%), d(0.12%) P: s(15.22%), p(84.04%), d(0.69%)
	1.94	C _{carb} (83.11%) - Ga (16.89%)	C: s(42.26%), p(57.70%), d(0.02%) Ga: s(33.53%), p(66.26%), d(0.20%)
	1.93	LP(P)	P: s(53.59%), p(46.33%), d(0.08%)

Figure S46. NBO results at the B3LYP-D3(BJ)/def2-TZVPP//B3LYP-D3(BJ)/def2-SVP level of theory of compound 1.

Orbital	Occ.	Contribution of the Atoms to the Orb.	Atomic Orbitals
	1.90	Ga (29.59%) - P(70.41%)	Ga: s(23.73%), p(76.08%), d(0.16%) P: s(16.15%), p(83.45%), d(0.39%)

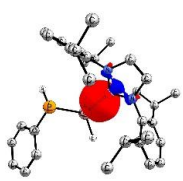
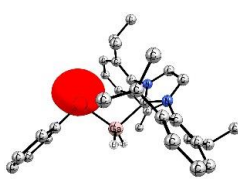
	1.94	C _{carb} (83.15%) – Ga (16.85%)	C: s(44.55%), p(55.43%), d(0.01%) Ga: s(14.09%), p(85.70%), d(0.20%)
	1.93	LP(P)	P: s(52.67%), p(47.28%), d(0.05%)

Figure S47. NBO results at the B3LYP-D3(BJ)/def2-TZVPP//B3LYP-D3(BJ)/def2-SVP level of theory of compound 2.

Orbital	Occ.	Contribution of the Atoms to the Orb.	Atomic Orbitals
---------	------	---------------------------------------	-----------------

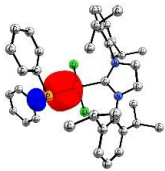
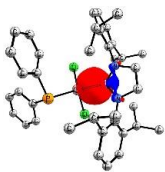
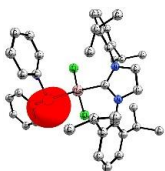
	1.90	Ga (33.23%) - P(66.77%)	Ga: s(50.93%), p(48.87%), d(0.16%) P: s(14.99%), p(84.37%), d(0.63%)
	1.94	C _{carb} (82.51%) - Ga (17.49%)	C: s(41.63%), p(58.34%), d(0.02%) Ga: s(33.80%), p(65.99%), d(0.20%)
	1.89	LP(P)	P: s(50.30%), p(49.65%), d(0.03%)

Figure S48. NBO results at the B3LYP-D3(BJ)/def2-TZVPP//B3LYP-D3(BJ)/def2-SVP level of theory of compound 3.

Orbital	Occ.	Contribution of the Atoms to the Orb.	Atomic Orbitals
---------	------	---------------------------------------	-----------------

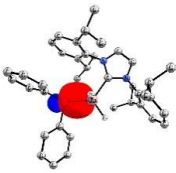
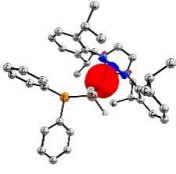
	1.90	Ga (30.50%) - P(69.50%)	Ga: s(25.28%), p(74.53%), d(0.16%) P: s(17.13%), p(82.49%), d(0.37%)
	1.94	C _{car} (82.79%) - Ga (17.21%)	C: s(43.97%), p(56.01%), d(0.01%) Ga: s(14.46%), p(85.34%), d(0.20%)
	1.89	LP(P)	P: s(49.08%), p(50.88%), d(0.04%)

Figure S49. NBO results at the B3LYP-D3(BJ)/def2-TZVPP//B3LYP-D3(BJ)/def2-SVP level of theory of compound 4.

Orbital	Occ.	Contribution of the Atoms to the Orb.	Atomic Orbitals
---------	------	---------------------------------------	-----------------

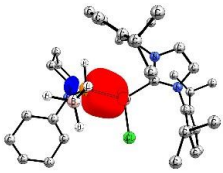
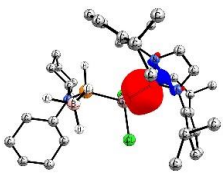
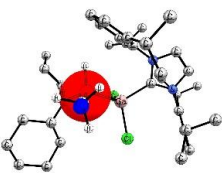
	1.94	Ga (30.59%) - P(69.41%)	Ga: s(46.44%), p(53.40%), d(0.15%) P: s(24.70%), p(74.48%), d(0.82%)
	1.94	C _{car} (82.44%) - Ga (17.56%)	C: s(82.44%), p(58.20%), d(0.02%) Ga: s(36.59%), p(63.22%), d(0.18%)
	1.97	P (61.45%) - B (38.55%)	P: s(36.02%), p(63.60%), d(0.35%) B: s(20.41%), p(79.41%), d(0.17%)

Figure S50. NBO results at the B3LYP-D3(BJ)/def2-TZVPP//B3LYP-D3(BJ)/def2-SVP level of theory of compound 5.

Orbital	Occ.	Contribution of the Atoms to the Orb.	Atomic Orbitals
---------	------	---------------------------------------	-----------------

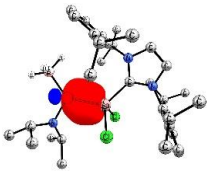
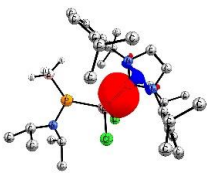
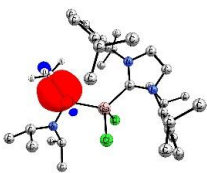
	1.94	Ga (31.00%) - P(69.00%)	Ga: s(47.06%), p(52.77%), d(0.16%) P: s(24.92%), p(74.30%), d(0.77%)
	1.94	C _{car} (81.86%) - Ga (18.14%)	C: s(41.36%), p(58.60%), d(0.02%) Ga: s(38.02%), p(61.80%), d(0.18%)
	1.97	P (61.47%) - B (38.53%)	P: s(37.20%), p(62.42%), d(0.35%) B: s(20.23%), p(79.58%), d(0.17%)

Figure S51. NBO results at the B3LYP-D3(BJ)/def2-TZVPP//B3LYP-D3(BJ)/def2-SVP level of theory of compound 6.

Orbital	Occ.	Contribution of the Atoms to the Orb.	Atomic Orbitals
---------	------	---------------------------------------	-----------------

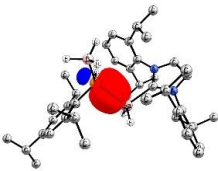
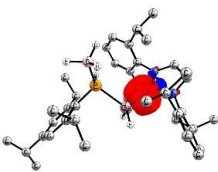
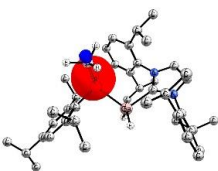
	1.93	Ga (26.18%) - P(73.82%)	Ga: s(20.74%), p(79.06%), d(0.17%) P: s(26.78%), p(72.90%), d(0.32%)
	1.94	C _{car} (82.14%) - Ga (17.86%)	C: s(44.09%), p(55.89%), d(0.01%) Ga: s(16.45%), p(83.38%), d(0.17%)
	1.97	P (63.53%) - B (36.47%)	P: s(34.89%), p(64.87%), d(0.23%) B: s(19.56%), p(80.26%), d(0.16%)

Figure S52. NBO results at the B3LYP-D3(BJ)/def2-TZVPP//B3LYP-D3(BJ)/def2-SVP level of theory of compound 7.

Orbital	Occ.	Contribution of the Atoms to the Orb.	Atomic Orbitals
---------	------	---------------------------------------	-----------------

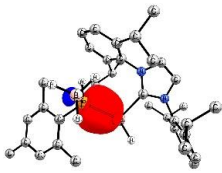
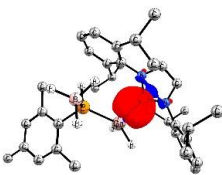
	1.94	Ga (26.67%) - P(73.33%)	Ga: s(21.90%), p(77.90%), d(0.17%) P: s(27.34%), p(72.31%), d(0.35%)
	1.94	C _{car} (82.06%) - Ga (17.94%)	C: s(44.06%), p(55.91%), d(0.01%) Ga: s(16.16%), p(83.66%), d(0.16%)
	1.97	P (62.97%) - B (37.03%)	P: s(33.79%), p(65.95%), d(0.25%) B: s(19.75%), p(80.06%), d(0.17%)

Figure S53. NBO results at the B3LYP-D3(BJ)/def2-TZVPP//B3LYP-D3(BJ)/def2-SVP level of theory of compound **8**.

AIM Analysis

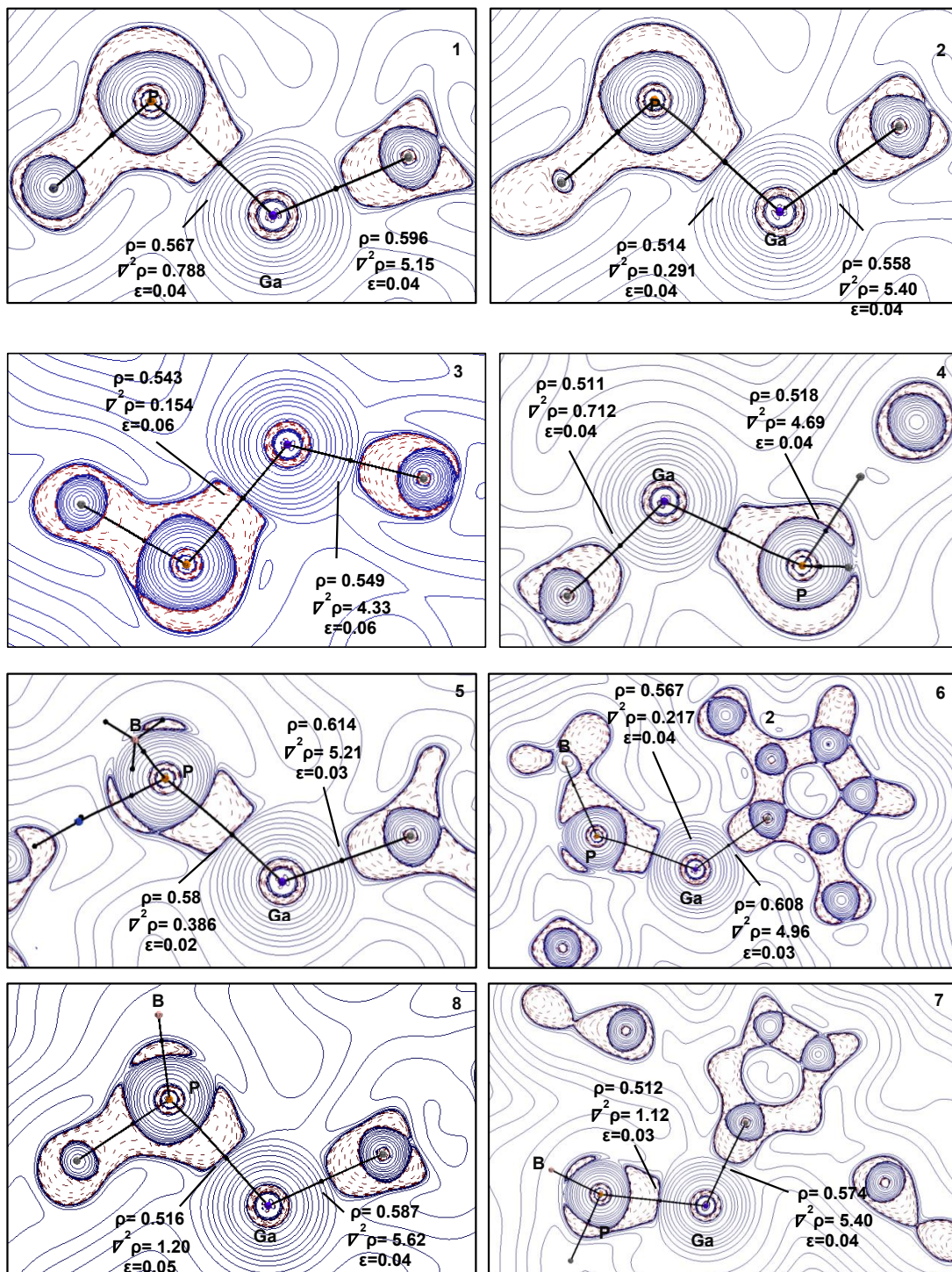


Figure S54. 2D Laplacian distribution ($\nabla^2\rho(r)>0$) on the C_{car} -Ga-P plane for compounds 1-8. Red areas are charge concentration ($\nabla^2\rho(r)<0$) and blue areas are charge depletion ($\nabla^2\rho(r)>0$), bond paths (black lines), and Bond Critical Points (black dots).

9. Evidence of Al^{II} Addition to Benzene



Supporting Information

Evidence of Al^{II} Radical Addition to Benzene

D. Mandal, T. I. Demirel, T. Sergeieva, B. Morgenstern, H. T. A. Wiedemann, C. W. M. Kay,
D. M. Andrada**

Supporting Information

for

Evidence of Al(II) Radical Addition to Benzene

Debdeep Mandal,^[a] T. Ilgin Demirer,^[a] Tetiana Sergeieva,^[a] Bernd Morgenstern,^[a] Haakon T. A. Wiedemann,^[b] Christopher W. M. Kay*,^[b] and Diego M. Andrada*,^[a]

^[a]*Inorganic and Computational Chemistry Group, Allgemeine und Anorganische Chemie, Universität des Saarlandes, Campus C4.1, D-66123 Saarbrücken, Germany*

^[b]*Physical and Educational Chemistry Group, Physikalische Chemie und Didaktik der Chemie, Universität des Saarlandes, Campus B2.2, D-66123 Saarbrücken, Germany*

*E-Mail: christopher.kay@uni-saarland.de; diego.andrada@uni-saarland.de;

<https://inorg-comp-chem.com/>

Tel: +49 681 302-71665

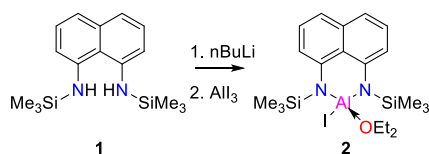
Table of Contents

Materials and Method	S2
Synthesis of 2.	S2
Synthesis of 3.	S3
Synthesis of 4.	S3
Synthesis of 5.	S4
<i>NMR Spectra</i>	S5
<i>UV-Visible Spectra</i>	S14
<i>IR Spectra</i>	S16
<i>XRD structure</i>	S18 S17
<i>Crystallographic Details</i>	S19 S18
<i>EPR Details</i>	S23 S22
<i>Computational Details</i>	S25 S23
<i>Cartesian xyz coordinates and Energies in Hartrees</i>	S30 S25
<i>References</i>	S88 S70

Materials and Method

All syntheses and manipulations were carried out under an inert gas atmosphere (Ar or N₂) using standard *Schlenk* techniques or a glove box (MBraun Unilab Plus). Organic solvents Benzene, and Mesitylene were dried over K/benzophenone, distilled and stored under an atmosphere of argon. *n*-hexane, Et₂O, THF and toluene were taken directly from a solvent purification system (Innovative Technology PureSolv MD7). Deuterated solvents were dried over appropriate drying agents, distilled, and stored inside a glove box. NMR spectra were recorded at 300 K on a Bruker Avance IV HD 400 (¹H: 400.13 MHz, ¹³C: 100.61 MHz, ²⁷Al: 104.26 MHz, ²⁹Si: 59.6 MHz) or on a BrukerNanoBay 300 MHz (¹H: 300.13 MHz, ¹³C: 75.468 MHz, ²⁷Al: 78.204 MHz, ²⁹Si: 59.627 MHz) NMR spectrometer. Chemical shifts (in δ , ppm) are referenced to the residual^[1] solvent signal(s): C₆D₆ (¹H, 7.16; ¹³C, 128.06), Fourier-transform IR spectra were acquired on a Bruker Vertex 70 spectrometer in attenuated total reflectance (ATR) mode. Elemental analyses were performed on an elemental analyzer Leco CHN-900 and/or an elemental vario Micro Cube. Single crystal X-ray diffraction analysis were carried out at low temperatures on Bruker AXS X8 Apex CCD and Bruker AXS D8 Venture diffractometers operating with graphite monochromated Mo K α radiation. Structure solution and refinement was performed using SHELX.^[2] These data can be obtained free of charge from The Cambridge Crystallographic Data Centre via <http://www.ccdc.cam.ac.uk>. UV/Vis spectra were measured using a Shimadzu UV-2600 spectrometer in quartz cells with a path length of 0.1 cm. 1,8-diamino naphthalene (Sigma Aldrich), TMSCl (Sigma Aldrich), *n*BuLi (1.6 M in *n*-hexane) (Alfa aesar), AlI₃ (abcr GmbH), Naphthalene (Alfa aesar), Durene (Alfa aesar), Biphenyl (Alfa aesar) were purchased from commercial sources and used without further purification. KC₈ were synthesized according to literature procedure.^[3] Ligand **1** was synthesized following the literature procedure.^[4]

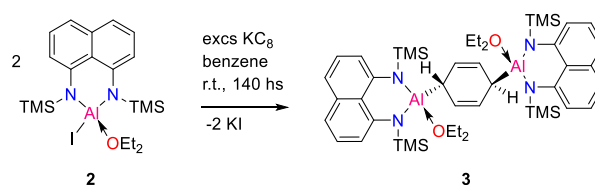
Synthesis of **2**.



In a 250 mL Schlenk flask, 4.93g (16.3 mmol) ligand **1** was dissolved in about 100 mL dry diethylether. The solution was cooled down to $-78\text{ }^{\circ}\text{C}$ and 20.5 mL 1.6 M *n*BuLi solution in *n*hexane (32.8 mmol) was added dropwise to it. The reaction mixture was slowly allowed to reach room temperature in 1h followed by stirred for 1h to get dark orange red color solution. In another 250 mL Schlenk flask, 6.64 g (16.3 mmol) of anhydrous AlI₃ was dissolved in about 70 mL dry diethylether. The solution was again cooled down to $-78\text{ }^{\circ}\text{C}$ and the diluted ligand **1** solution was added to it very slowly. During addition, the temperature was maintained at $-78\text{ }^{\circ}\text{C}$. The reaction mixture was slowly allowed to reach room temperature and then stirred overnight. After removing all the volatiles, the residue was extracted with 200 mL dry toluene. After evaporation of the filtrate, the residue was washed with 100 mL dry *n*-hexane to get compound **2** as gray color powder. Isolated yield = 5.76g (10.9 mmol, 66.86%). Crystals suitable for single crystal XRD measurement were obtained by keeping concentrated *n*hexane

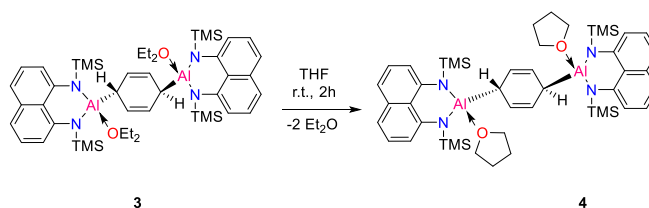
solution of **2** at 4 °C for overnight. ^1H NMR (C_6D_6 , 400 MHz), $\delta = 7.30\text{-}7.26$ (m, 2H, Ar-*H*), 7.17-7.11 (m, 2H, Ar-*H*), 6.87-6.83 (m, 2H, Ar-*H*), 3.39 (q, 4H, MeCH_2 , coordinated diethylether), 0.56 (s, 18H, $\text{Si}(\text{CH}_3)_3$), 0.35 (t, 6H, CH_3CH_2 , coordinated diethylether) ppm. $^{13}\text{C}\{^1\text{H}\}$ NMR (C_6D_6 , 100.61 MHz), $\delta = 150.23$ (2C, C_{10}H_8 , CN), 138.38 (2C, C_{10}H_8 , ArC), 125.76 (2C, C_{10}H_8 , ArCH), 120.73 (2C, C_{10}H_8 , ArCH), 119.32 (2C, C_{10}H_8 , ArCH), 67.0 (2C, CH_2 , coordinated diethylether), 12.19 (2C, CH_3 , coordinated diethylether), 4.08 (6C, $\text{Si}(\text{CH}_3)_3$) ppm. $^{29}\text{Si}\{^1\text{H}\}$ NMR (C_6D_6 , 79.5 MHz), $\delta = +1.78$ ppm. Elemental analysis (%), calcd for **2** (528.56): C: 45.45, H: 6.48, N: 5.30; found: C: 45.57, H: 6.50, N: 5.69. **MP**: 182 °C. UV/VIS (Benzene): λ_{max} (ϵ) = 357 nm (14606 L mol $^{-1}$ cm $^{-1}$).

Synthesis of 3.



About 20 mL dry benzene was added into the mixture of 2.11 g (4.0 mmol) of **2** and 1.14 g (8.43 mmol) KC_8 at 0 °C. After addition of benzene the cold bath was removed and the reaction mixture was stirred at room temperature. After 140hrs of stirring, complete consumption of starting material was observed. The reaction mixture was filtered through D4 frit and the resultant orange color filtrate was concentrated to about 2 mL. Pale yellow color crystal of compound **3** was isolated on keeping the concentrated solution at 4 °C for 1 week. Isolated yield = 0.310 g (0.351 mmol, 17% with respect to **2**). ^1H NMR (^1H , C_6D_6 , 400 MHz), $\delta = 7.33\text{-}7.28$ (m, 4H, Ar-*H*), 7.23-7.18 (m, 4H, Ar-*H*), 6.95-6.90 (t, 4H, Ar-*H*), 5.89 (s, 4H, $\text{CH}(\text{CH}=\text{CH})_2\text{CH}$), 3.80 (q, 8H, MeCH_2 , coordinated diethylether), 2.37 (s, 2H, $\text{CH}(\text{CH}=\text{CH})_2\text{CH}$), 0.44 (s, 36H, $\text{Si}(\text{CH}_3)_3$), 0.40 (t, 12H, CH_3CH_2 , coordinated diethylether) ppm. $^{13}\text{C}\{^1\text{H}\}$ NMR (C_6D_6 , 100.61 MHz), $\delta = 151.47$ (4C, C_{10}H_8 , CN), 138.56 (4C, C_{10}H_8 , ArC), 125.83 (4C, C_{10}H_8 , ArCH), 124.58 (4C, $\text{AlCH}(\text{CH}=\text{CH})_2\text{CHAl}$), 120.44 (4C, C_{10}H_8 , ArCH), 119.15 (4C, C_{10}H_8 , ArCH), 66.21 (4C, CH_2 , coordinated diethylether), 29.88 (2C, $\text{AlCH}(\text{CH}=\text{CH})_2\text{CHAl}$), 11.69 (4C, CH_3 , coordinated diethylether), 2.98 (12C, $\text{Si}(\text{CH}_3)_3$) ppm. $^{29}\text{Si}\{^1\text{H}\}$ NMR (C_6D_6 , 79.5 MHz), $\delta = -2.08$ ppm. Elemental analysis (%), calcd for **3** (881.43) : C: 62.68, H: 8.46, N: 6.36; found: C: 61.87, H: 7.80, N: 6.25. **MP**: 171 °C UV/VIS (Benzene): λ_{max} (ϵ) = 355 nm (28852 L mol $^{-1}$ cm $^{-1}$).

Synthesis of 4.



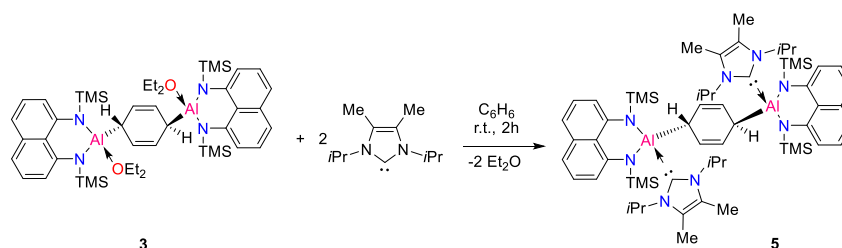
About 100 mg (0.11 mMol) of compound **3** was dissolved in about 10 mL dry THF. The solution was stirred for 2hrs. ^1H NMR of reaction mixture in C_6D_6 indicated complete replacement of the coordinated diethylether in **3**

with THF. All the volatiles were evaporated to get off white powder as product, **4**. Colorless crystals of compound **4** was isolated on keeping the concentrated THF solution at $-33\text{ }^{\circ}\text{C}$ for 2 days.

Yield = Quantitative.

^1H NMR (C_6D_6 , 300 MHz), $\delta = 7.36\text{--}7.17$ (m, 8H, Ar-H), 6.97-6.89 (m, 4H, Ar-H), 5.82 (s, 4H, $\text{CH}(\text{CH}=\text{CH})_2\text{CH}$), 3.86 (m, 8H, CH_2 , coordinated THF), 2.19 (s, 2H, $\text{CH}(\text{CH}=\text{CH})_2\text{CH}$), 0.73 (m, 8H, CH_2 , coordinated THF), 0.42 (s, 36H, $\text{Si}(\text{CH}_3)_3$), ppm. $^{13}\text{C}\{^1\text{H}\}$ NMR (C_6D_6 , 75.46 MHz), $\delta = 151.58$ (4C, C_{10}H_8 , CN), 138.58 (4C, C_{10}H_8 , ArC), 125.82 (4C, C_{10}H_8 , ArCH), 124.70 (4C, $\text{AlCH}(\text{CH}=\text{CH})_2\text{CHAl}$), 120.21 (4C, C_{10}H_8 , ArCH), 118.71 (4C, C_{10}H_8 , ArCH), 72.93 (4C, CH_2 , coordinated THF), 30.79 (2C, $\text{AlCH}(\text{CH}=\text{CH})_2\text{CHAl}$), 24.38 (4C, CH_2 , coordinated THF), 2.38 (12C, $\text{Si}(\text{CH}_3)_3$) ppm. $^{29}\text{Si}\{^1\text{H}\}$ NMR (C_6D_6 , 59.62 MHz), $\delta = -2.29$ ppm. Elemental analysis (%), calcd for **4** (877.40) : C: 62.97, H: 8.04, N: 6.39; found: C: 62.42, H: 7.51, N: 6.04. **MP**: $198\text{ }^{\circ}\text{C}$

Synthesis of **5**.



A solution of 0.0108 g (0.06 mMol) of $\text{NHC}^{\text{iPr}_2\text{Me}_2}$ in 0.5 mL dry C_6H_6 was added to the 0.026 g (0.03 mMol) of **3** in 0.5 mL C_6H_6 dropwise. The reaction mixture was stirred for 2 hrs. ^1H NMR of reaction mixture in C_6D_6 indicated complete replacement of the coordinated diethyl ether in **3** with $\text{NHC}^{\text{iPr}_2\text{Me}_2}$. All the volatiles were evaporated to get compound **5** pale yellow powder as desired product. Colorless crystals of compound **3** was isolated on keeping the concentrated THF solution at $-33\text{ }^{\circ}\text{C}$ for 2 days. yield = Quantitative.

^1H NMR (C_6D_6 , 300 MHz), $\delta = 7.25\text{--}7.10$ (m, 8H, Ar-H), 6.95-6.86 (m, 4H, Ar-H), 5.73 (s, 4H, $\text{CH}(\text{CH}=\text{CH})_2\text{CH}$), 5.66 (sept, 4H, $\text{CH}(\text{CH}_3)_2$), 2.08 (s, 2H, $\text{CH}(\text{CH}=\text{CH})_2\text{CH}$), 1.43 (s, 12H, CCH_3), 1.25 (d, 24H, $\text{CH}(\text{CH}_3)_2$), 0.43 (s, 36H, $\text{Si}(\text{CH}_3)_3$) ppm. $^{13}\text{C}\{^1\text{H}\}$ NMR (C_6D_6 , 75.46 MHz), $\delta = 152.50$ (4C, C_{10}H_8 , CN), 138.58 (4C, C_{10}H_8 , ArC), 126.27 (4C, CCH_3), 125.94 (4C, $\text{AlCH}(\text{CH}=\text{CH})_2\text{CHAl}$), 125.06 (4C, C_{10}H_8 , ArCH), 120.35 (4C, C_{10}H_8 , ArCH), 119.89 (4C, C_{10}H_8 , ArCH), 51.30 (4C, $\text{CH}(\text{CH}_3)_2$), 30.38 (2C, $\text{AlCH}(\text{CH}=\text{CH})_2\text{CHAl}$), 23.76 (8C, $\text{CH}(\text{CH}_3)_2$), 10.29 (4C, CCH_3), 3.66 (12C, $\text{Si}(\text{CH}_3)_3$) ppm. $^{29}\text{Si}\{^1\text{H}\}$ NMR (C_6D_6 , 59.62 MHz), $\delta = -2.91$ ppm. Elemental analysis (%), calcd for **5** qsdnm, : C: 65.89, H: 8.66, N: 10.24; found: C: 65.03, H: 8.18, N: 9.69. **MP**: above $200\text{ }^{\circ}\text{C}$

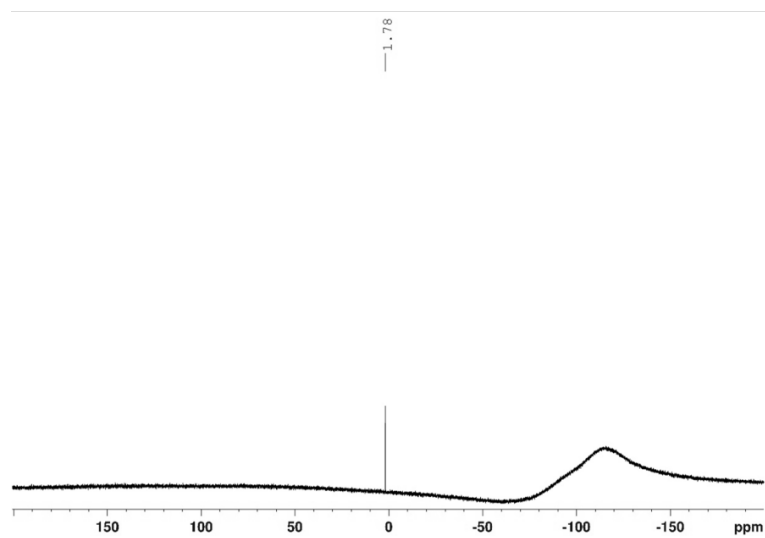


Figure S3. $^{29}\text{Si}\{^1\text{H}\}$ NMR (79.5 MHz, C_6D_6 , 300 K) spectrum of compound **2**.

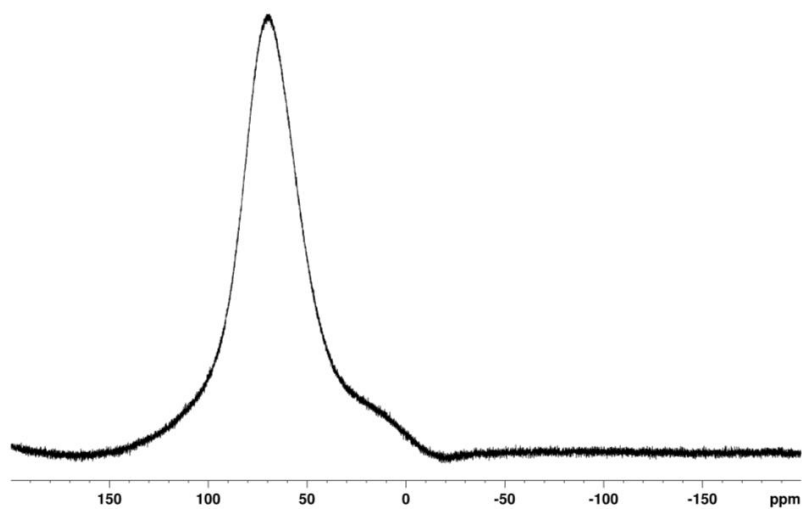


Figure S4. $^{27}\text{Al}\{^1\text{H}\}$ NMR (104.26 MHz, C_6D_6 , 300 K) spectrum of compound **2**.

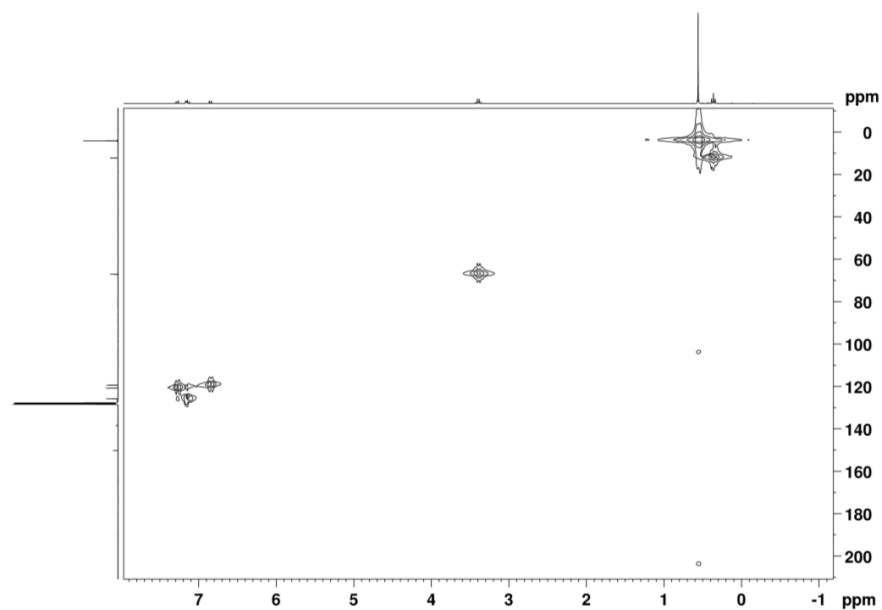


Figure S5. ^1H - ^{13}C HMQC NMR (C_6D_6 , 300 K) spectrum of compound 2.

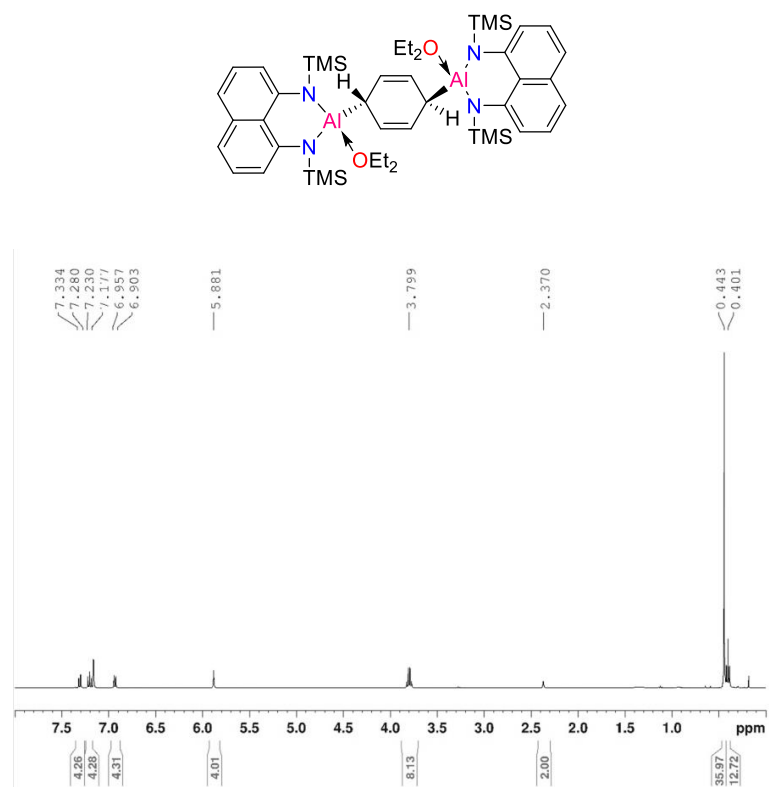


Figure S6. ^1H NMR (400.13 MHz, C_6D_6 , 300 K) spectrum of compound 3.

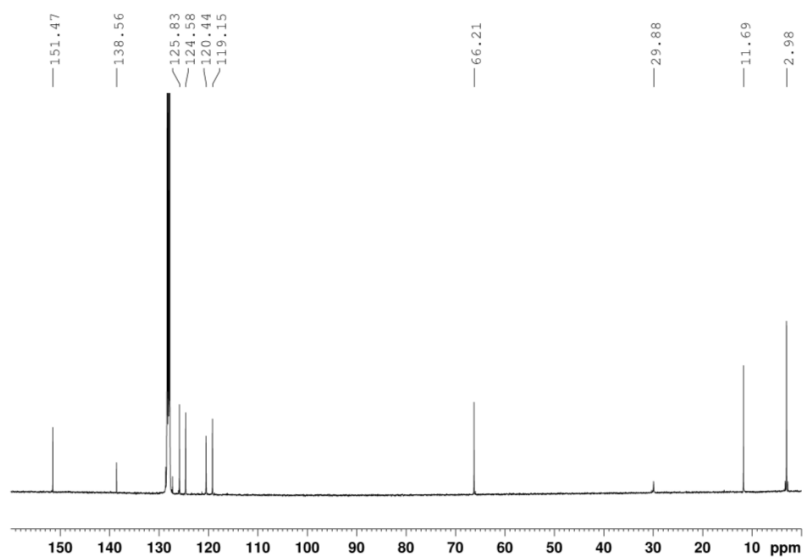


Figure S7. $^{13}\text{C}\{^1\text{H}\}$ NMR (100.61 MHz, C_6D_6 , 300 K) spectrum of compound **3**.

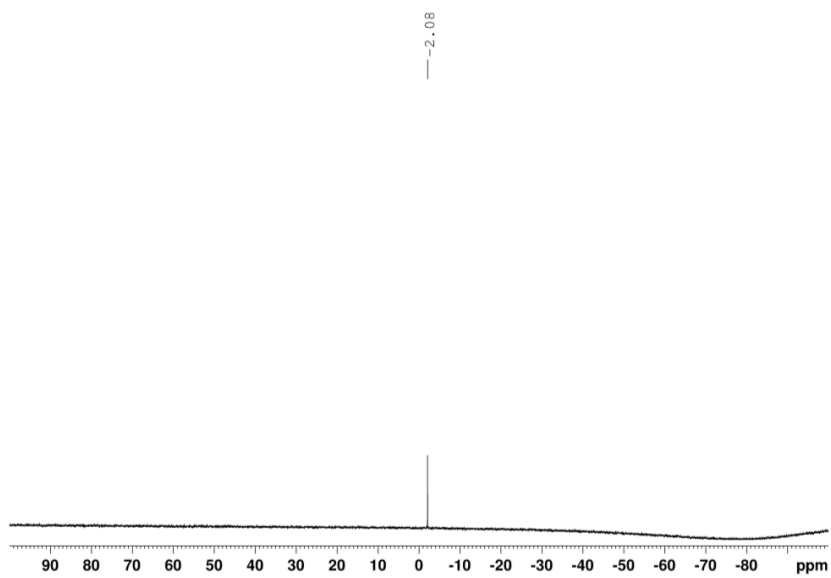


Figure S8. $^{29}\text{Si}\{^1\text{H}\}$ NMR (79.5 MHz, C_6D_6 , 300 K) spectrum of compound **3**.

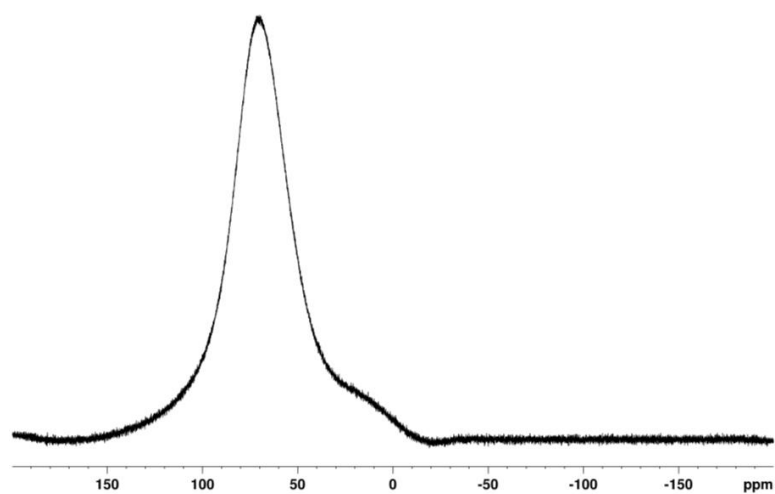


Figure S9. $^{27}\text{Al}\{^1\text{H}\}$ NMR (104.26MHz, C_6D_6 , 300 K) spectrum of compound **3**.

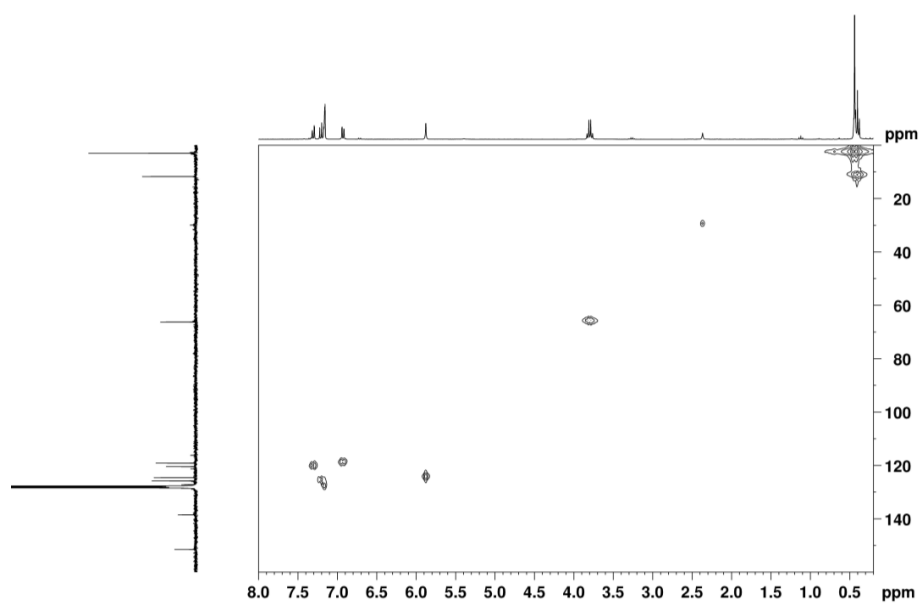
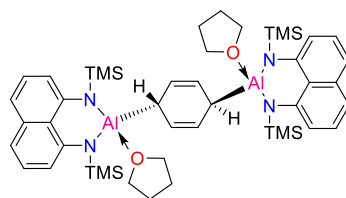


Figure S10. ^1H - ^{13}C HMQC NMR (C_6D_6 , 300 K) spectrum of compound **3**.



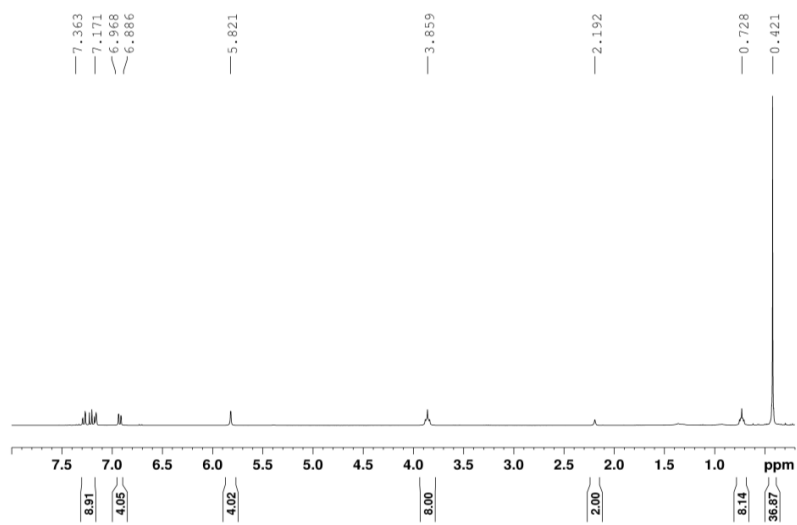


Figure S11. ^1H NMR (300 MHz, C_6D_6 , 300 K) spectrum of compound 4.

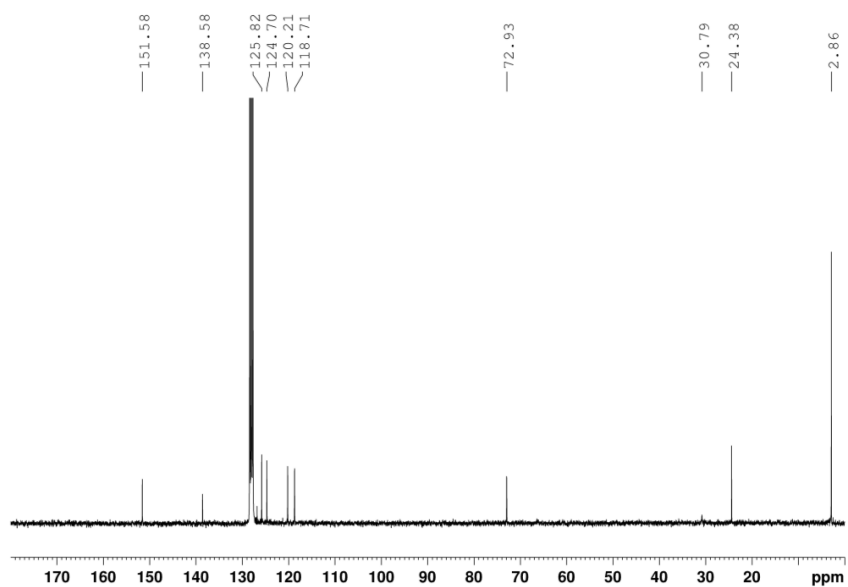


Figure S12. $^{13}\text{C}\{^1\text{H}\}$ NMR (75.46 MHz, C_6D_6 , 300 K) spectrum of compound 4.

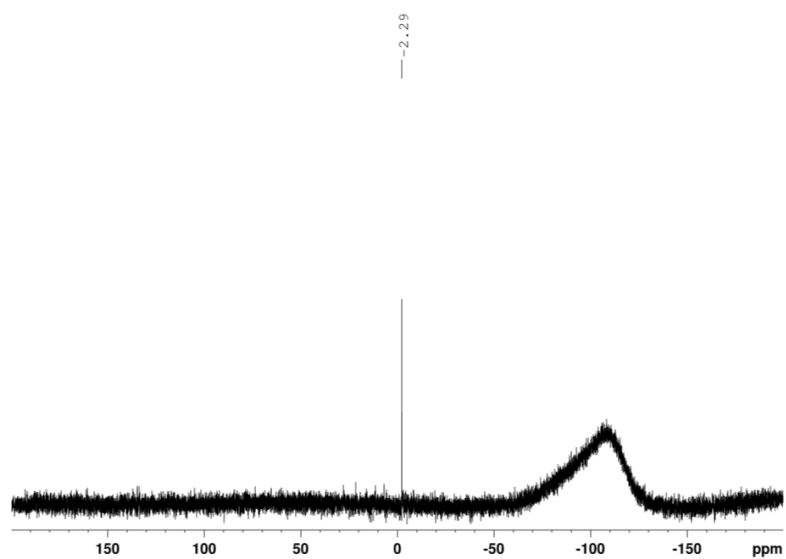


Figure S13. $^{29}\text{Si}\{^1\text{H}\}$ NMR (59.62 MHz, C_6D_6 , 300 K) spectrum of compound 4.

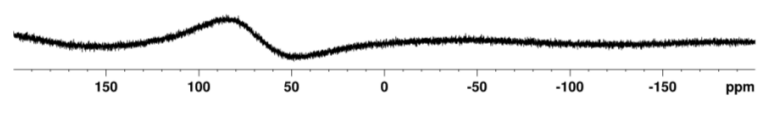
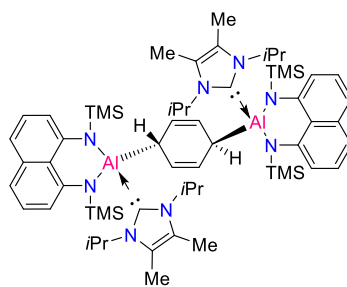


Figure S14. $^{27}\text{Al}\{^1\text{H}\}$ NMR (78.20 MHz, C_6D_6 , 300 K) spectrum of compound 4.



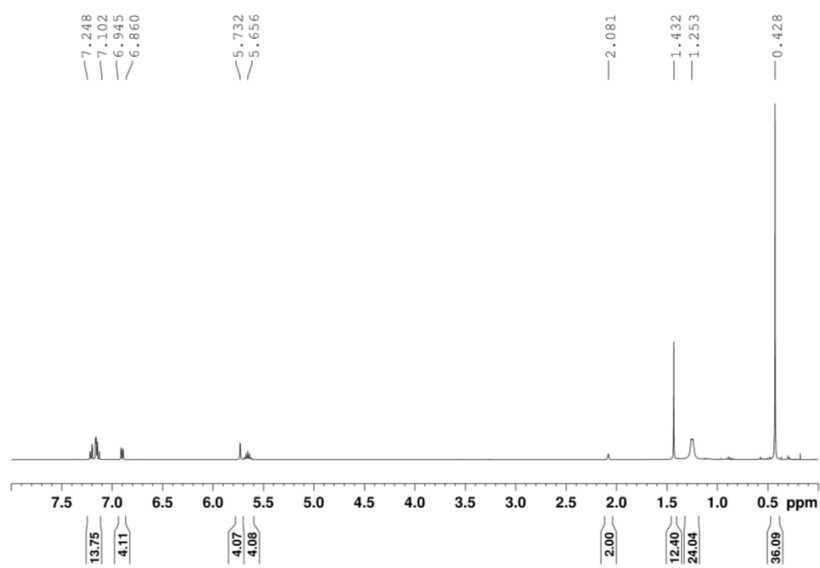


Figure S15. ^1H NMR (300 MHz, C_6D_6 , 300 K) spectrum of compound **5**.

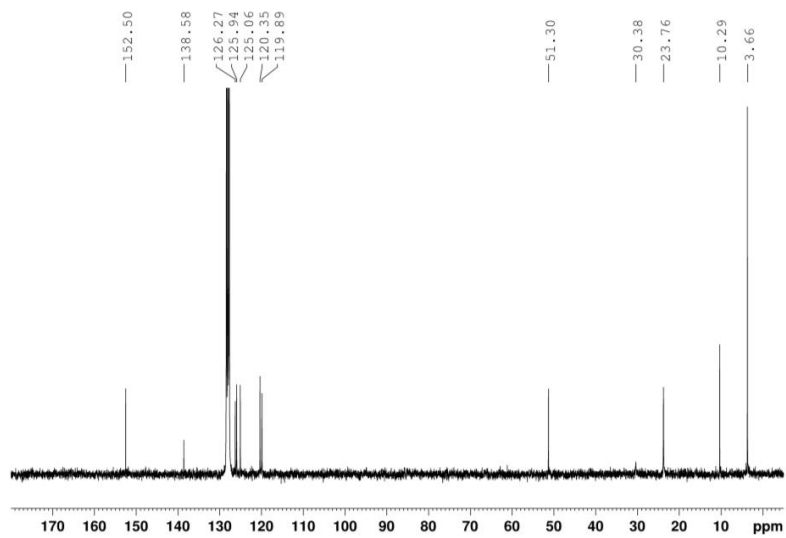


Figure S16. $^{13}\text{C}\{^1\text{H}\}$ NMR (75.46 MHz, C_6D_6 , 300 K) spectrum of compound **5**.

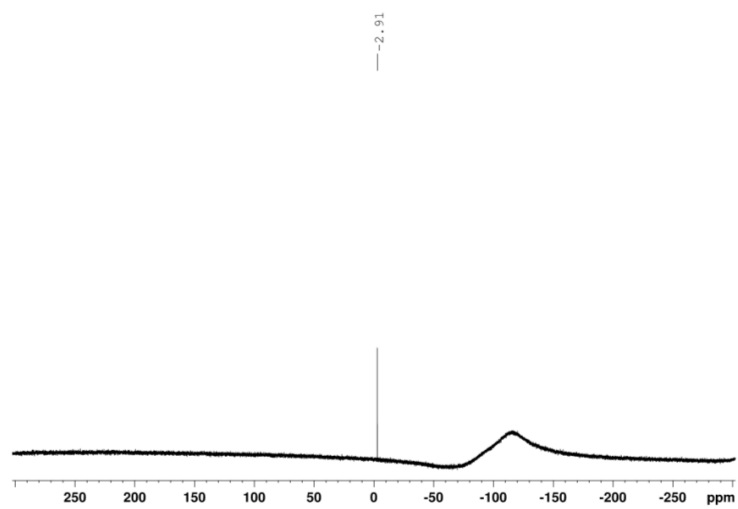


Figure S17. $^{29}\text{Si}\{^1\text{H}\}$ NMR (59.62 MHz, C_6D_6 , 300 K) spectrum of compound **5**.

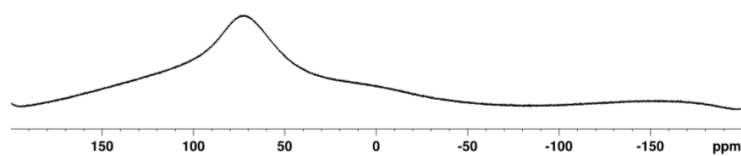


Figure S18. $^{27}\text{Al}\{^1\text{H}\}$ NMR (78.20 MHz, C_6D_6 , 300 K) spectrum of compound **5**.

UV-Visible Spectra

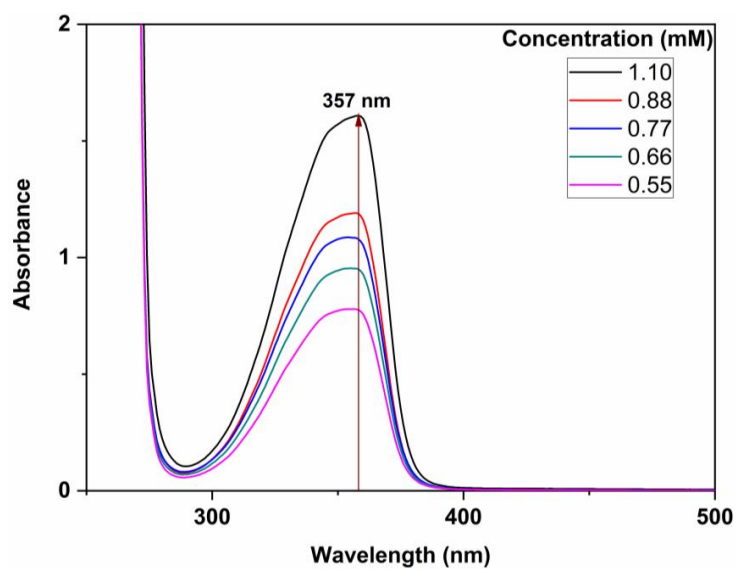


Figure S19: UV/vis spectrum of compound 2 in benzene at different concentrations.

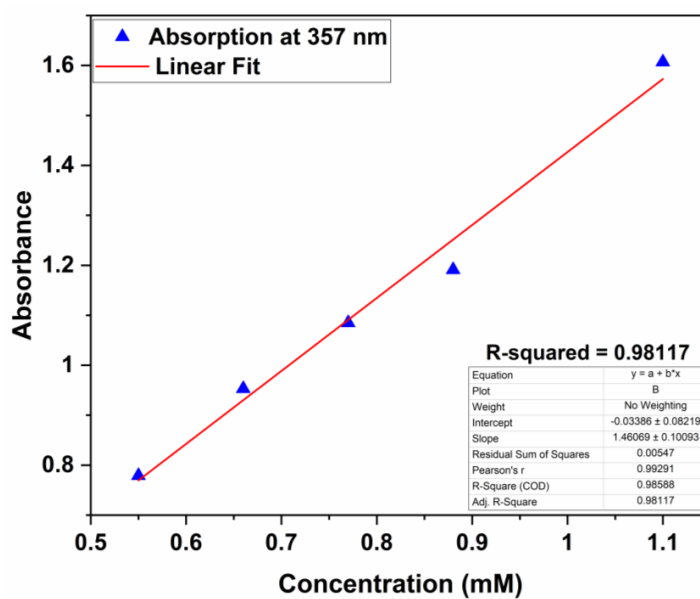


Figure S20: Linear regression of 2 in benzene at 357 nm.

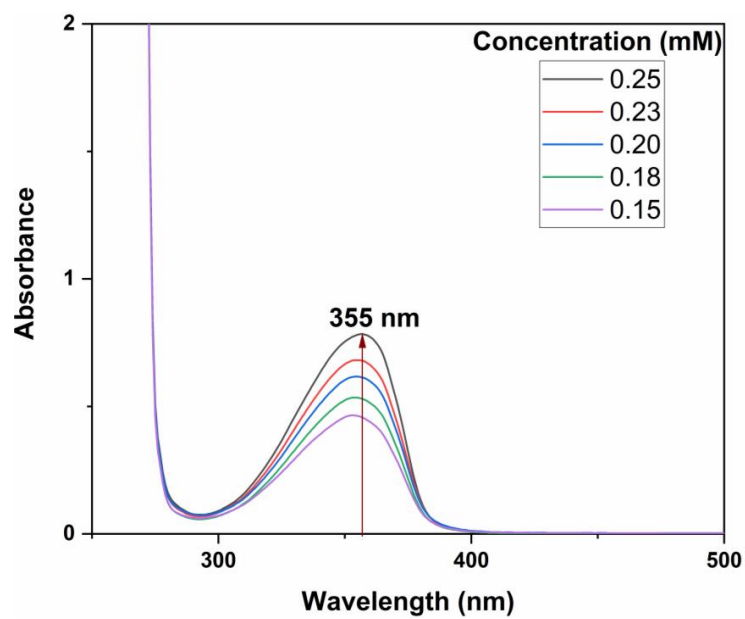


Figure S21: UV/vis spectrum of compound 3 in benzene at different concentrations.

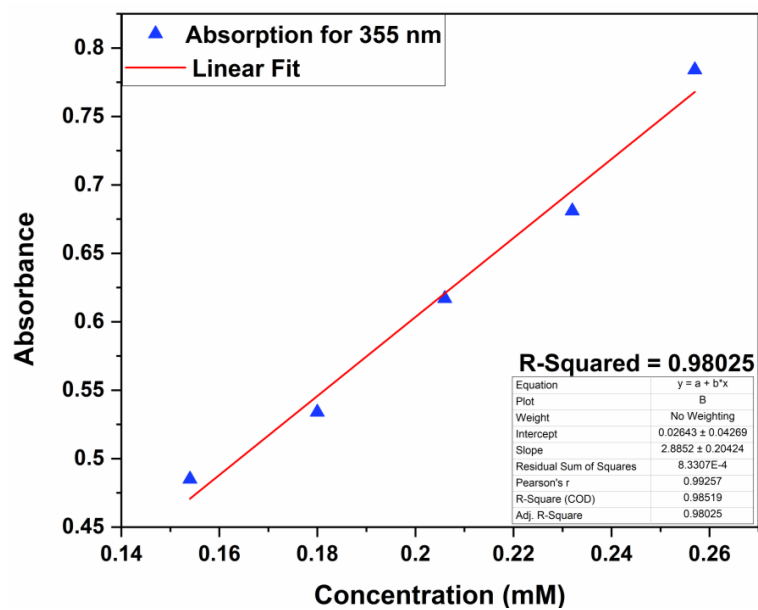


Figure S22: Linear regression of 3 in benzene at 355 nm.

IR Spectra

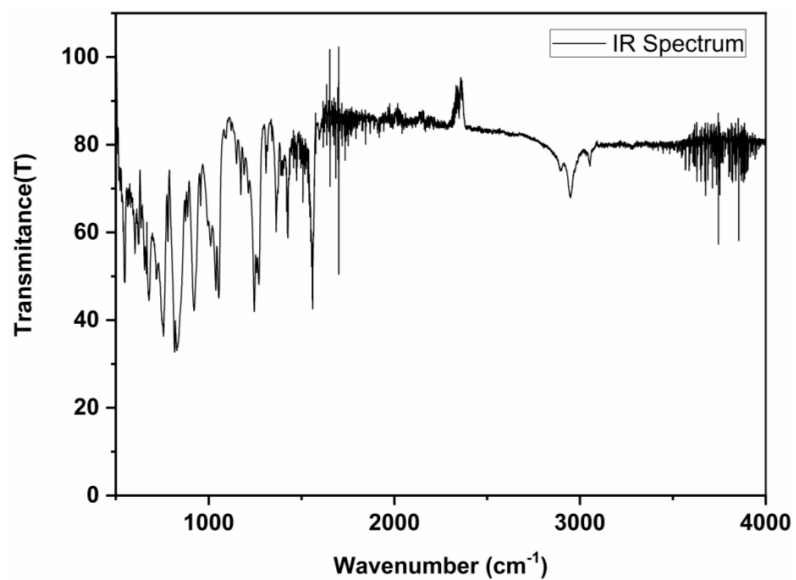


Figure S23: IR spectrum of 2.

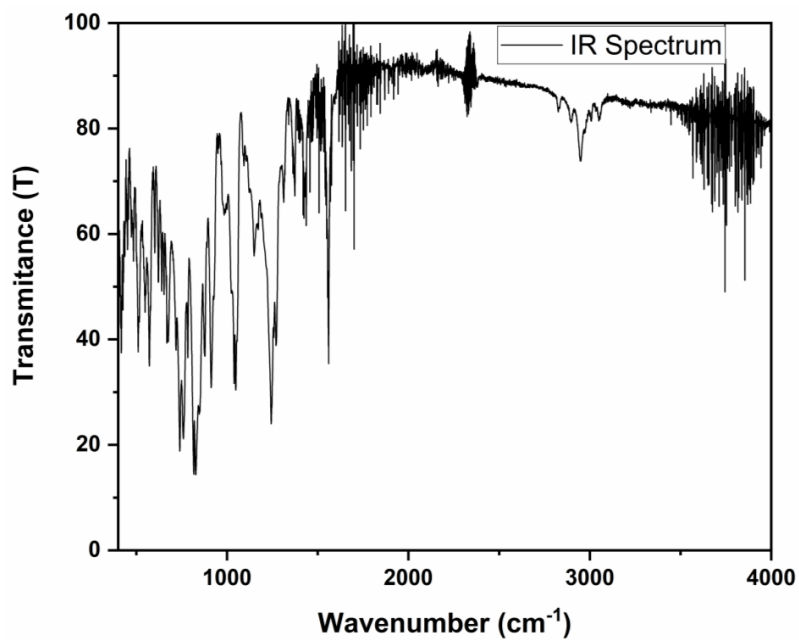


Figure S24: IR spectrum of 3.

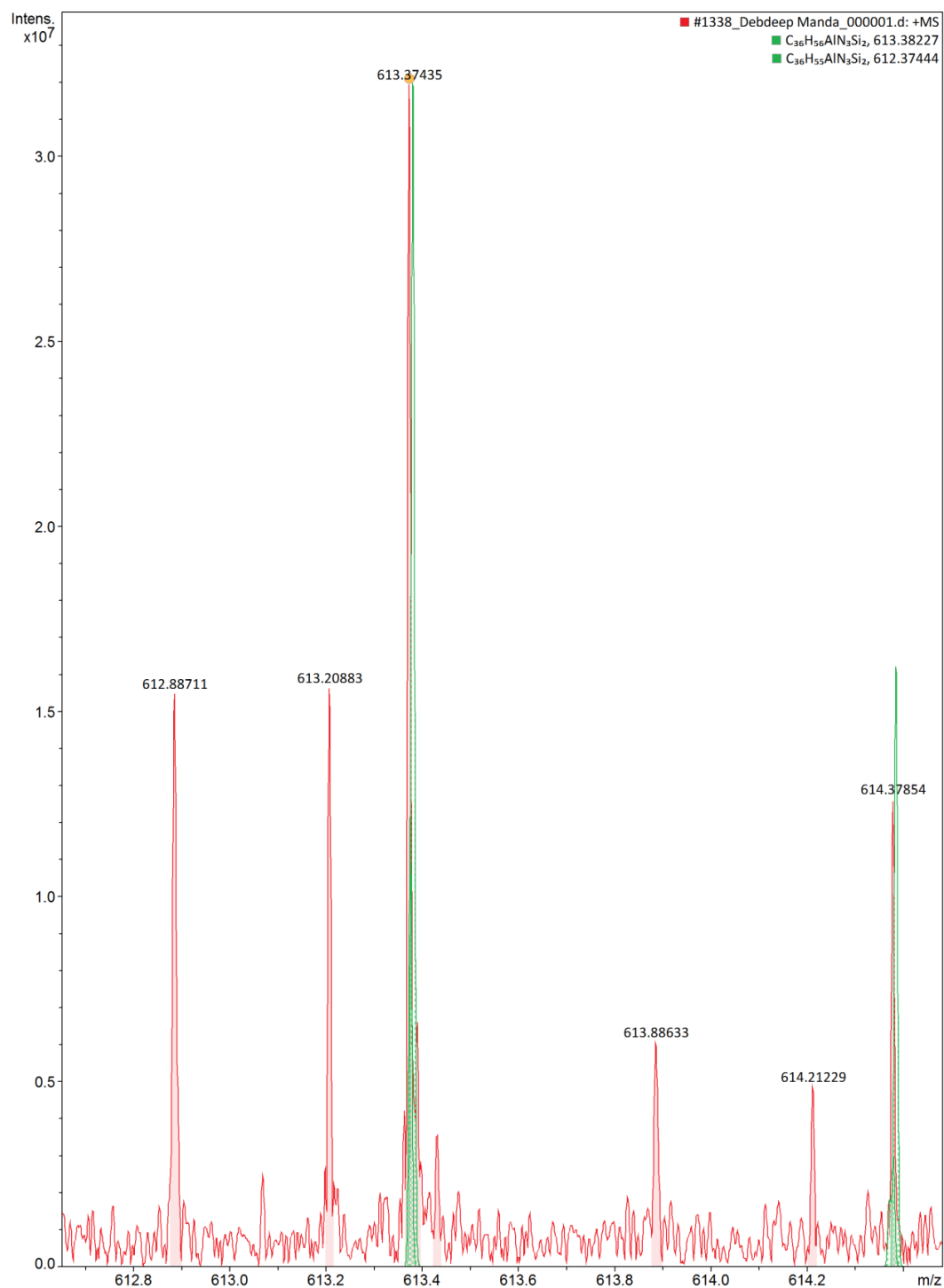


Figure S25: Mass spectrum of **6**. The peaks at m/z 613.38 and 614.38 is assignable to $[\text{LAl}(\text{cAAC})]^+$ and $[\text{LAl}(\text{cAAC}) + \text{H}]^+$, respectively.

XRD structure

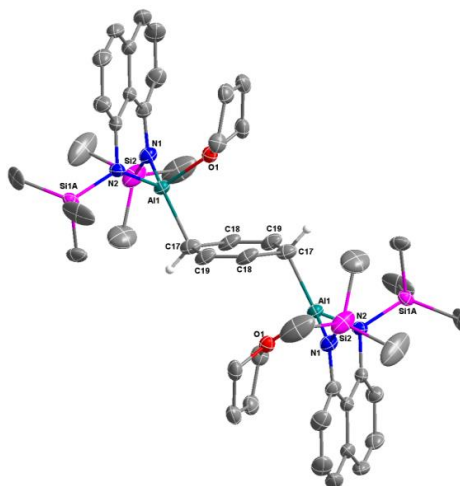


Figure S26. Molecular structures of **4** in the solid state as determined by X-ray crystallography. Thermal ellipsoids set at 50% probability. Nonessential hydrogen atoms have been omitted. Selected experimental bond lengths (Å) and bond angles (°): Al1-N1 1.8252(17), Al1-N2 1.8249(17), Al1-O1 1.8910(14), Al1-C17 1.986(2); N2-Al1-N1 100.83(8).

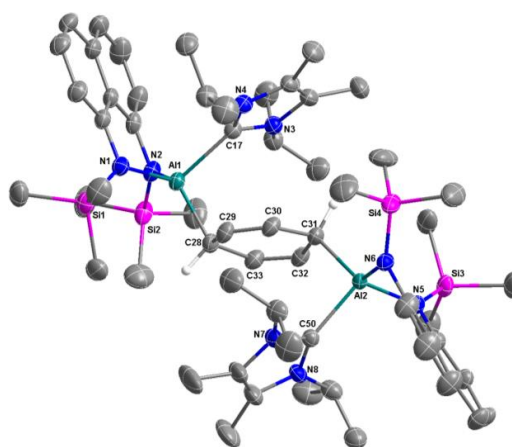


Figure S27. Molecular structures of **5** in the solid state as determined by X-ray crystallography. Thermal ellipsoids set at 50% probability. Nonessential hydrogen atoms have been omitted. Selected experimental bond lengths (Å) and bond angles (°): Al1-N1 1.8597(19), Al1-N2 1.851(2), Al1-C17 2.093(2), Al1-C28 2.007(2), Al2-N5 1.8524(19), Al2-N6 1.855(2), Al2-C50 2.082(2), Al1-C31 2.011(2); N2-Al1-N1 97.85(9), N5-Al2-N6 98.19(9).

Crystallographic Details

Table S1. Crystal data and structure refinement for **2**.

CCDC reference number	2193647	
Identification code	sh4310_a	
Empirical formula	C ₂₀ H ₃₄ Al I N ₂ O Si ₂	
Formula weight	528.55	
Temperature	132(2) K	
Wavelength	0.71073 Å	
Crystal system	Monoclinic	
Space group	P2 ₁ /n	
Unit cell dimensions	a = 7.6036(3) Å	α = 90°.
	b = 16.8547(7) Å	β = 96.621(2)°.
	c = 19.6806(7) Å	γ = 90°.
Volume	2505.37(17) Å ³	
Z	4	
Density (calculated)	1.401 Mg/m ³	
Absorption coefficient	1.421 mm ⁻¹	
F(000)	1080	
Crystal size	0.555 x 0.364 x 0.134 mm ³	
Theta range for data collection	1.595 to 25.681°.	
Index ranges	-9 ≤ h ≤ 9, -20 ≤ k ≤ 20, -24 ≤ l ≤ 24	
Reflections collected	17393	
Independent reflections	4761 [R(int) = 0.0429]	
Completeness to theta = 25.242°	100.0 %	
Absorption correction	Semi-empirical from equivalents	
Max. and min. transmission	0.7455 and 0.5969	
Refinement method	Full-matrix least-squares on F ²	
Data / restraints / parameters	4761 / 0 / 252	
Goodness-of-fit on F ²	1.202	
Final R indices [I > 2σ(I)]	R1 = 0.0620, wR2 = 0.1453	
R indices (all data)	R1 = 0.0655, wR2 = 0.1467	
Extinction coefficient	n/a	
Largest diff. peak and hole	1.349 and -1.357 e.Å ⁻³	

Table S2. Crystal data and structure refinement for **3**.

CCDC reference number	2193648	
Identification code	sh4347_a	
Empirical formula	C ₄₆ H ₇₄ Al ₂ N ₄ O ₂ Si ₄	
Formula weight	881.41	
Temperature	133(2) K	
Wavelength	0.71073 Å	
Crystal system	Triclinic	
Space group	P-1	
Unit cell dimensions	a = 9.9698(3) Å	α = 91.2350(10)°.
	b = 14.2981(4) Å	β = 102.6520(10)°.
	c = 19.0331(5) Å	γ = 102.7880(10)°.
Volume	2574.61(13) Å ³	
Z	2	
Density (calculated)	1.137 Mg/m ³	
Absorption coefficient	0.188 mm ⁻¹	
F(000)	952	
Crystal size	0.839 x 0.730 x 0.384 mm ³	
Theta range for data collection	2.152 to 29.605°.	
Index ranges	-13 ≤ h ≤ 13, -19 ≤ k ≤ 19, -26 ≤ l ≤ 26	
Reflections collected	98274	
Independent reflections	14462 [R(int) = 0.0240]	
Completeness to theta = 25.242°	99.8 %	
Absorption correction	Semi-empirical from equivalents	
Max. and min. transmission	0.7459 and 0.7008	
Refinement method	Full-matrix least-squares on F ²	
Data / restraints / parameters	14462 / 0 / 745	
Goodness-of-fit on F ²	1.041	
Final R indices [I > 2σ(I)]	R1 = 0.0286, wR2 = 0.0774	
R indices (all data)	R1 = 0.0307, wR2 = 0.0791	
Extinction coefficient	n/a	
Largest diff. peak and hole	0.394 and -0.219 e.Å ⁻³	

Table S3. Crystal data and structure refinement for **4**.

CCDC reference number	2193649	
Identification code	4444_a_sq	
Empirical formula	C ₄₆ H ₇₀ Al ₂ N ₄ O ₂ Si ₄	
Formula weight	877.38	
Temperature	133(2) K	
Wavelength	0.71073 Å	
Crystal system	Monoclinic	
Space group	C2/c	
Unit cell dimensions	a = 20.6409(7) Å b = 21.0142(7) Å c = 13.6378(5) Å	α = 90°. β = 113.819(2)°. γ = 90°.
Volume	5411.6(3) Å ³	
Z	4	
Density (calculated)	1.077 Mg/m ³	
Absorption coefficient	0.178 mm ⁻¹	
F(000)	1888	
Crystal size	0.513 x 0.147 x 0.108 mm ³	
Theta range for data collection	1.450 to 27.938°.	
Index ranges	-27 ≤ h ≤ 27, -27 ≤ k ≤ 27, -17 ≤ l ≤ 17	
Reflections collected	66779	
Independent reflections	6488 [R(int) = 0.0706]	
Completeness to theta = 25.242°	100.0 %	
Absorption correction	Semi-empirical from equivalents	
Max. and min. transmission	0.7456 and 0.6945	
Refinement method	Full-matrix least-squares on F ²	
Data / restraints / parameters	6488 / 114 / 302	
Goodness-of-fit on F ²	1.028	
Final R indices [I > 2σ(I)]	R1 = 0.0478, wR2 = 0.1113	
R indices (all data)	R1 = 0.0804, wR2 = 0.1285	
Extinction coefficient	n/a	
Largest diff. peak and hole	0.583 and -0.711 e.Å ⁻³	

Table S4. Crystal data and structure refinement for **5**.

CCDC reference number	2193650	
Identification code	sh4952_a	
Empirical formula	C ₆₈ H ₁₁₀ Al ₂ N ₈ O ₂ Si ₄	
Formula weight	1237.95	
Temperature	133(2) K	
Wavelength	0.71073 Å	
Crystal system	Monoclinic	
Space group	P2 ₁ /c	
Unit cell dimensions	a = 19.7117(16) Å	α = 90°.
	b = 19.6113(16) Å	β = 115.399(3)°.
	c = 20.8564(18) Å	γ = 90°.
Volume	7283.2(11) Å ³	
Z	4	
Density (calculated)	1.129 Mg/m ³	
Absorption coefficient	0.152 mm ⁻¹	
F(000)	2688	
Crystal size	0.200 x 0.120 x 0.100 mm ³	
Theta range for data collection	1.965 to 27.114°.	
Index ranges	-25 ≤ h ≤ 25, -25 ≤ k ≤ 25, -26 ≤ l ≤ 26	
Reflections collected	178283	
Independent reflections	16076 [R(int) = 0.0950]	
Completeness to theta = 25.242°	100.0 %	
Absorption correction	Semi-empirical from equivalents	
Max. and min. transmission	0.7393 and 0.7027	
Refinement method	Full-matrix least-squares on F ²	
Data / restraints / parameters	16076 / 380 / 873	
Goodness-of-fit on F ²	1.071	
Final R indices [I > 2σ(I)]	R1 = 0.0549, wR2 = 0.1318	
R indices (all data)	R1 = 0.0791, wR2 = 0.1472	
Extinction coefficient	n/a	
Largest diff. peak and hole	0.494 and -0.418 e.Å ⁻³	

EPR Details

The continuous wave (CW) EPR experiments were performed at room temperature (298 K) on a Bruker Magnetech Miniscope MS-5000 spectrometer. The microwave (MW) frequency was 9.48 GHz, the MW power was 10 mW (10dB) and the modulation amplitude was 0.8 mT for all experiments.

The simulation of the EPR spectra were conducted with the Easyspin-Toolbox^[5] in Matlab. To analyze the hyperfine coupling constant, we simulated the spectra for all reaction times (Figure S28). The hyperfine constant for the hyperfine coupling of the electron to the aluminium atom was calculated to be 45.7(1.3) MHz. The experimental and calculated signal widths are almost identical, and the conformity with the experiment could be further improved by taking into account the hyperfine broadening, which could be estimated by simulating with several radical species, two between 0 and 25 hours, and three from 50 to 435 hours.

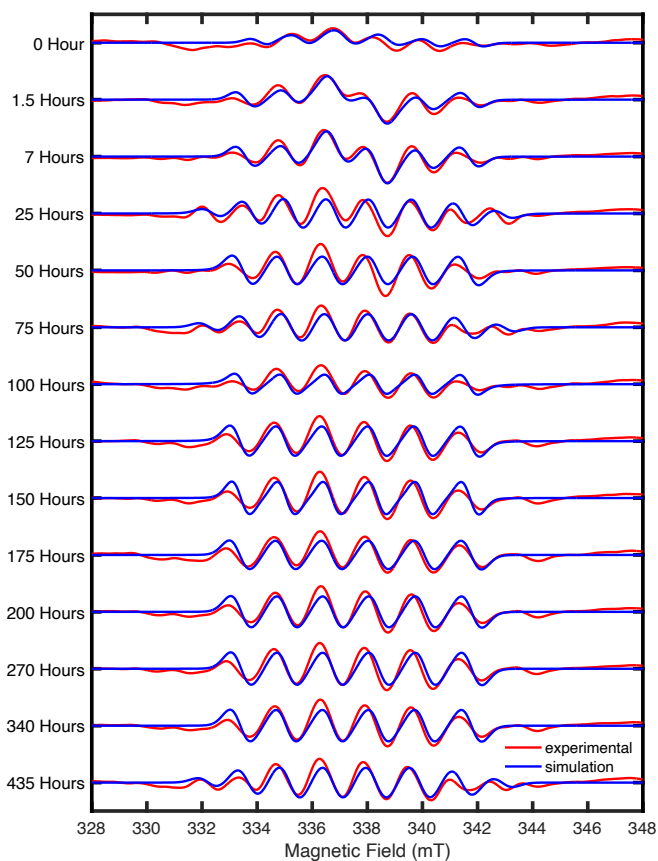


Figure S28. Time dependant EPR spectra of filtered compound **2** with KC_8 in C_6D_6 . The experimental spectra are colored in red, the simulated spectra are colored in blue. The microwave (MW) frequency was 9.48 GHz, the MW power was 10 mW (10dB) and the modulation amplitude was 0.8 mT.

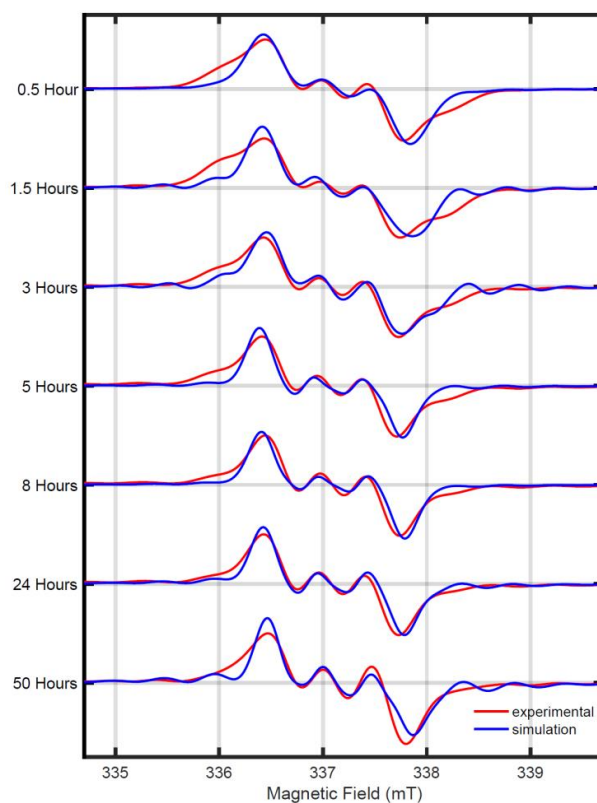


Figure S29. Time dependant EPR spectra of filtered compound **2** with KC_8 in C_6D_6 in the presence of cAAC. The experimental spectra are colored in red, the simulated spectra are colored in blue. The microwave (MW) frequency was 9.48 GHz, the MW power was 3.162 mW (15dB) and the modulation amplitude was 0.1 mT.

Computational Details

All geometries were optimized without symmetry constraint within the DFT (density functional theory) framework using the TPSSh^[6] in combination with the Ahlrichs def2-SVPP basis function.^[7] These calculations were performed using the Gaussian 16 C.01 software.^[8] The stationary points were located with the Berny algorithm^[9] using redundant internal coordinates. Analytical Hessians were computed to determine the nature of stationary points (one and zero imaginary frequencies for transition states and minima, respectively)^[10] and to calculate unscaled zero-point energies (ZPEs) as well as thermal corrections and entropy effects using the standard statistical-mechanics relationships for an ideal gas. The energy has been improved at the TPSSh/def2-TZVPP level of theory using benzene within the polarizable continuum model.^[11]

The Wiberg Bond Indices (WBI)^[12] and NPA^[13] atomic partial charges have been calculated at the TPSSh/def2-TZVPP level of theory using GENNBO 7.0 programs.^[14] The Atoms-in-Molecule (AIM) method^[15] was performed at the TPSSh/def2-TZVPP level of theory with the program AIMAll program package.^[16]

EPR parameters (g-tensors) and hyperfine coupling constants (*hfc*) were computed with the ORCA 4.2 software.^[17] These calculations were performed with the functional TPSSh in combination with the basis set aug-cc-pVTZ-J for N and Al atoms, and aug-cc-pVDZ for H, C, and Si atoms.^[17-18]

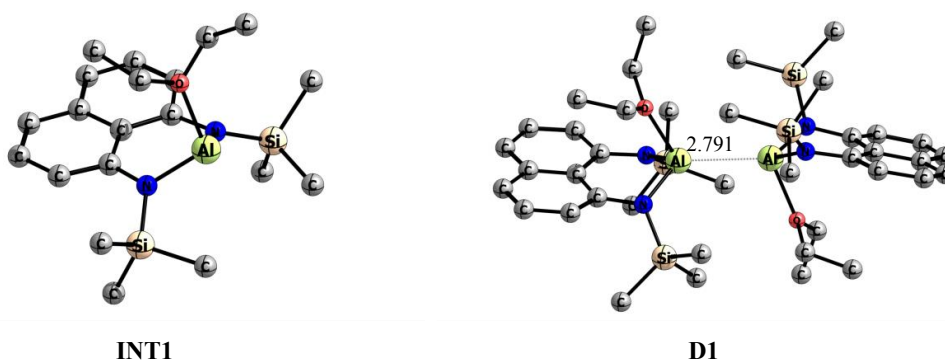
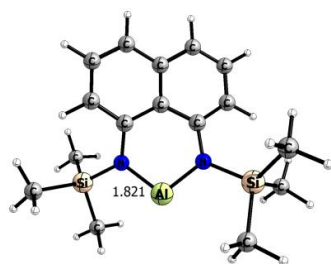
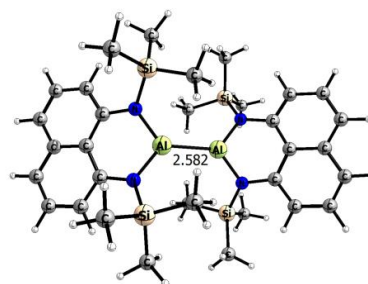


Figure S30. Optimized structures of **INT1** and **D1** at the TPSSh/def2-SVP level of theory. Bond lengths are in Å. Hydrogen atoms were omitted for clarity.



INT3



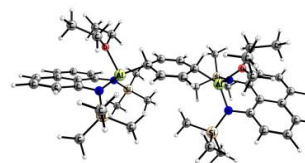
D2

Figure S31. Optimized structures of **INT3** and **D2** at the TPSSh/def2-SVP level of theory. Bond lengths are in Å. Hydrogen atoms were omitted for clarity.



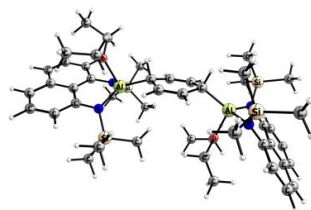
3

$\Delta G_r = 0.0$ kcal/mol



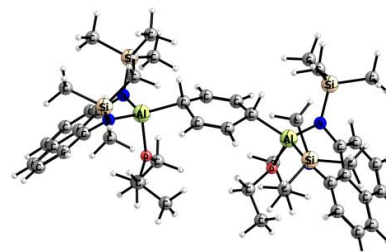
3A

$\Delta G_r = +15.6$ kcal/mol



3B

$\Delta G_r = +11.4$ kcal/mol



3C

$\Delta G_r = +8.3$ kcal/mol

Figure S32. Optimized structures of **3** isomers at the PCM(benzene)-TPSSh/def2-TZVPP//TPSSh/def2-SVP level of theory. The relative Gibbs energy (ΔG_r) is in kcal/mol.

Table S5. NBO results calculated at TPSSh/def2-TZVPP//TPSSh/def2-SVP level of theory: partial charges, Q (in e), Wiberg bond order, P (in a.u.).^a

	3
Q(C17/C17')	-0.89
Q(C18/C18')	-0.22
Q(C19/C19')	-0.22
Q(Al)	+2.14
Q(C₆H₆)	-1.37
Q(OEt₂)	+0.12
Q(AlL)^b	0.57
P(Al-C17)	0.41
P(C17-C19)	1.05
P(C19-18)	1.86

^a Numbering according to Figure 2 of the main text. ^b L = ligand.

Table S6. Electron density, Laplacian, ellipticity, delocalization index, and QTAIM Local topological parameters [in a.u.] of the charge density at the main Bond Critical Points calculated at TPSSh/def2-TZVPP//TPSSh/def2-SVP level of theory: Local kinetic energy density (G), Local potential energy density (V), and local electronic energy density (H).

BCP	$\rho(r)$ ($e/\text{\AA}^3$)	$\nabla^2\rho(r)$ ($e/\text{\AA}^5$)	ϵ	DI	V	G	H
Al1-C17	0.53	5.25	0.01	0.32	-0.1002	0.0773	-0.0229
C17-C19	1.70	-15.21	0.09	1.07	-0.2922	0.0672	-0.2250
C19-C18	2.29	-23.99	0.37	1.70	-0.5253	0.1382	-0.3871

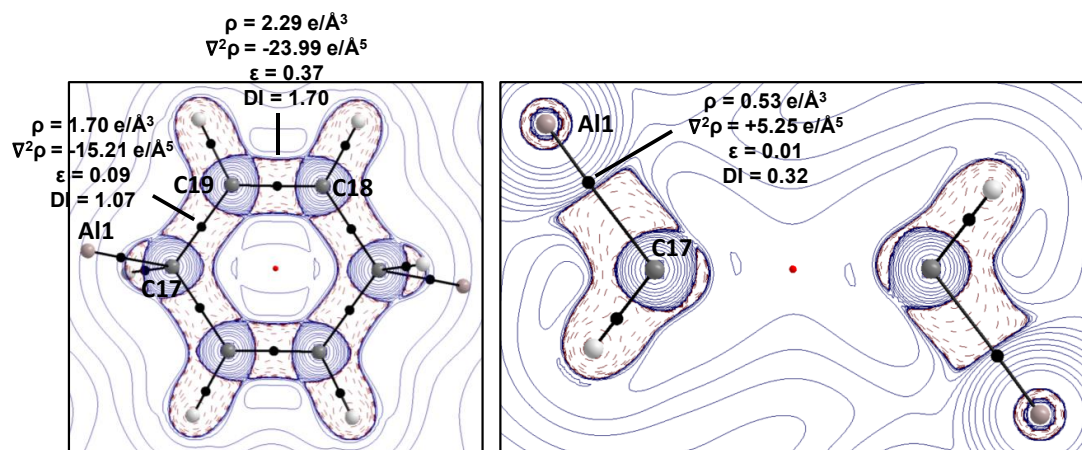


Figure S33. Laplacian distribution of the electron density of **3** (TPSSh/def2-TZVPP//TPSSh/def2-SVP). Contour line diagrams of the Laplacian distribution $\nabla^2\rho(r)$ in the plane of the C_6H_6 fragment and perpendicular to it. Dashed red lines indicate areas of charge concentration ($\nabla^2\rho(r)<0$) while solid blue lines show areas of charge depletion ($\nabla^2\rho(r)>0$). The thick solid lines connecting the atomic nuclei are the bond paths and the small dots are the critical points. Bond Critical Points (in black), Ring Critical Points (in red), Cage Critical Point (in Blue).

Table S7. Calculated g -factor hfc constants (A in mT), Löwdin and Mulliken (in parenthesis) spin densities for the radical species **INT1-4** and compound **6** at the PCM(benz)-TPSSH/aug-cc-pVDZ&aug-cc-pVTZ-J level of theory.

	INT1	INT2	INT3	INT4	6	D1^{•-}	D2^{•-}
g -factor	2.0016604	2.0028688	2.0010980	2.0029461	2.0026056	2.0021219	2.001744
$A_{\text{iso}}(\text{Al})$	36.6 (0.83/0.88)	7.7 (0.08/0.09)	41.8 (0.84/0.86)	8.8 (0.24/0.27)	0.34 (0.21/0.24)	-0.10 (0.10/0.13) -0.10 (0.10/0.13)	10.1 (0.46/0.53) 9.8 (0.43/0.46)
$A_{\text{iso}}(\text{N})$	0.78 (0.03/0.03)	0.09 (0.00/0.00)	0.9 (0.04/0.04)	0.08 (0.00/0.00)	0.06 (0.00/0.00)	0.04/0.03 (0.00/-0.01) (0.00/-0.01)	0.17/0.16 (0.01/0.00) (0.01/0.00)
$A_{\text{iso}}(\text{N})$	0.76 (0.03/0.03)	0.08 (0.00/0.00)	0.9 (0.04/0.04)	0.08 (0.00/0.00)	0.02 (0.00/0.00)	0.00/0.00 (0.00/0.00) (0.00/0.00)	0.06/0.08 (0.01/0.00) (0.01/0.00)
$A_{\text{iso}}(\text{N})_{\text{CAAC}}$					0.62 (0.22/0.22)		

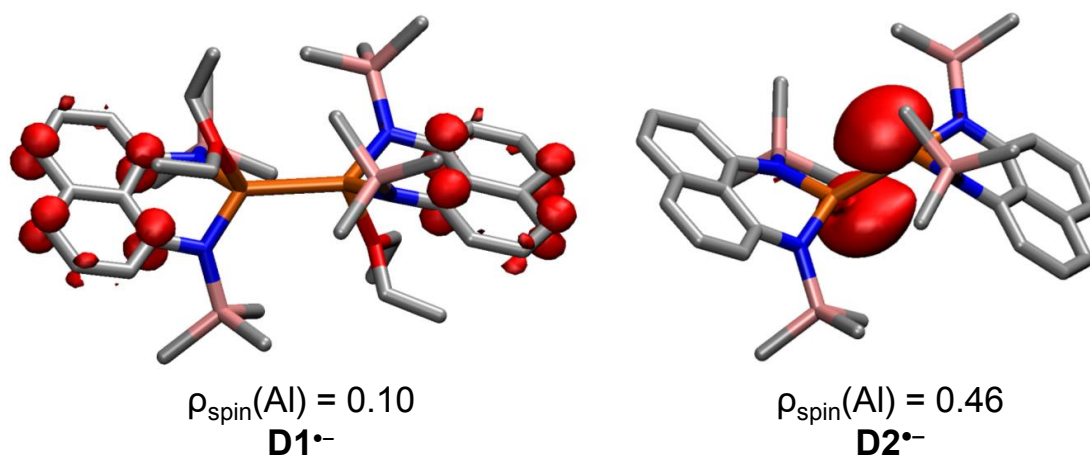


Figure S34. Spin density (isovalue 0.003 a.u.) and Mulliken spin-density plots of **D1^{•-}** and **D2^{•-}**. H atoms have been omitted for clarity.

Cartesian xyz coordinates and Energies in Hartrees

Benzene

Energy (PCM(benzene)-[TPSSh/def2-TZVPP//TPSSh/def2-SVP])= -232.352118546

C	0.000000000000	1.399616000000	0.000000000000
C	1.212103000000	0.699808000000	0.000000000000
C	-1.212103000000	0.699808000000	0.000000000000
H	2.158708000000	1.246331000000	0.000000000000
H	-2.158708000000	1.246331000000	0.000000000000
C	1.212103000000	-0.699808000000	0.000000000000
C	-1.212103000000	-0.699808000000	0.000000000000
H	2.158708000000	-1.246331000000	0.000000000000
H	-2.158708000000	-1.246331000000	0.000000000000
C	0.000000000000	-1.399616000000	0.000000000000
H	0.000000000000	-2.492662000000	0.000000000000
H	0.000000000000	2.492662000000	0.000000000000

Et₂O

Energy (PCM(benzene)-[TPSSh/def2-TZVPP//TPSSh/def2-SVP])= -233.765527787

O	0.000047000000	-0.000770000000	-0.810645000000
C	-1.002755000000	-0.657068000000	-0.051984000000
H	-0.568428000000	-1.138962000000	0.846202000000
H	-1.388803000000	-1.465274000000	-0.694028000000
C	2.140899000000	-0.278660000000	0.345224000000
H	2.586353000000	-0.737895000000	-0.550595000000
H	2.927727000000	0.275064000000	0.883108000000
H	1.787752000000	-1.087510000000	1.004890000000
C	1.002618000000	0.656933000000	-0.052853000000
H	1.388392000000	1.464423000000	-0.695965000000
H	0.568120000000	1.139877000000	0.844675000000
C	-2.140783000000	0.279364000000	0.344861000000
H	-2.586125000000	0.737544000000	-0.551556000000
H	-2.927742000000	-0.273507000000	0.883428000000
H	-1.787500000000	1.088978000000	1.003517000000

2

Energy (TPSSh/def2-SVP)= -2085.82996583

I	-3.130835000000	-0.030878000000	0.763056000000
O	0.002841000000	-0.042773000000	2.046617000000
N	0.172785000000	-1.434862000000	-0.543906000000
Si	-0.516371000000	-2.706521000000	-1.579696000000
Al	-0.652514000000	0.014462000000	0.201701000000
C	2.264655000000	-0.049318000000	-0.264041000000
C	1.569644000000	-1.330095000000	-0.327398000000
N	0.236263000000	1.450128000000	-0.505759000000
Si	-0.426331000000	2.799330000000	-1.463070000000
C	2.302645000000	-2.507333000000	-0.135413000000
H	1.757345000000	-3.453450000000	-0.127714000000
C	3.696749000000	-2.516783000000	0.050153000000
H	4.218164000000	-3.468801000000	0.180160000000
C	4.388084000000	-1.326546000000	0.073021000000
H	5.471968000000	-1.306801000000	0.209011000000
C	3.702789000000	-0.088058000000	-0.076522000000
C	4.470275000000	1.108905000000	-0.051552000000
H	5.552096000000	1.031959000000	0.079805000000
C	1.637671000000	1.264244000000	-0.383910000000
C	2.457806000000	2.398766000000	-0.330793000000
H	1.981497000000	3.379164000000	-0.378823000000
C	3.854714000000	2.332432000000	-0.186681000000
H	4.437193000000	3.257149000000	-0.161681000000
C	-2.028763000000	-2.017258000000	-2.478783000000
H	-2.834362000000	-1.697494000000	-1.799898000000
H	-2.442116000000	-2.801107000000	-3.137275000000
H	-1.756221000000	-1.159687000000	-3.116607000000
C	-1.073056000000	-4.211866000000	-0.571164000000
H	-1.544013000000	-4.967953000000	-1.222918000000
H	-1.819071000000	-3.916138000000	0.186247000000
H	-0.236839000000	-4.702793000000	-0.045711000000
C	0.715329000000	-3.228545000000	-2.915707000000

S31

H	0.190129000000	-3.858157000000	-3.654915000000
H	1.575281000000	-3.800882000000	-2.538119000000
H	1.107946000000	-2.345194000000	-3.446347000000
C	-2.167221000000	2.363306000000	-2.051609000000
H	-2.202243000000	1.403659000000	-2.593220000000
H	-2.493624000000	3.149934000000	-2.754559000000
H	-2.906709000000	2.319480000000	-1.237696000000
C	0.617834000000	3.083822000000	-3.013690000000
H	0.668414000000	2.158566000000	-3.611796000000
H	1.649626000000	3.404107000000	-2.807700000000
H	0.139967000000	3.860219000000	-3.635889000000
C	-0.583586000000	4.406231000000	-0.464911000000
H	-1.202652000000	4.244345000000	0.434244000000
H	-1.083094000000	5.180421000000	-1.073005000000
H	0.382776000000	4.819964000000	-0.134194000000
C	-0.191257000000	1.123227000000	2.911236000000
H	-0.951137000000	1.738731000000	2.407545000000
H	-0.631606000000	0.751644000000	3.849646000000
C	1.088409000000	1.904040000000	3.134024000000
H	1.517996000000	2.228658000000	2.176277000000
H	1.843359000000	1.317843000000	3.675637000000
H	0.851514000000	2.798245000000	3.732711000000
C	0.090919000000	-1.341242000000	2.715167000000
H	0.021729000000	-2.064447000000	1.891955000000
H	-0.803573000000	-1.439728000000	3.351900000000
C	1.379764000000	-1.520117000000	3.491834000000
H	2.252749000000	-1.366864000000	2.841259000000
H	1.411482000000	-2.552737000000	3.873727000000
H	1.444284000000	-0.844200000000	4.357720000000

INT1

Energy (PCM(benzene)-[TPSSh/def2-TZVPP//TPSSh/def2-SVP])= -1789.43858005

Al	-0.135772000000	1.228817000000	0.655355000000
Si	-2.879254000000	1.215607000000	-0.946576000000
Si	2.686629000000	1.763715000000	-0.677740000000

O	-0.108305000000	0.030096000000	2.268780000000
N	1.403570000000	0.645662000000	-0.185004000000
N	-1.462757000000	0.370968000000	-0.303966000000
C	0.179216000000	-1.508718000000	-0.664644000000
C	-1.180393000000	-0.985452000000	-0.570870000000
C	-2.253070000000	-1.871472000000	-0.738176000000
H	-3.265059000000	-1.478339000000	-0.625648000000
H	-2.961005000000	-3.873766000000	-1.158464000000
C	-2.082383000000	-3.235877000000	-1.029748000000
C	0.325893000000	-2.921447000000	-0.960935000000
H	-0.652762000000	-4.812866000000	-1.364680000000
C	-0.812886000000	-3.755853000000	-1.139175000000
C	2.635494000000	-1.380646000000	-0.651947000000
H	3.545999000000	-0.799358000000	-0.498074000000
C	2.749231000000	-2.748572000000	-0.954523000000
H	3.741206000000	-3.196586000000	-1.057926000000
C	1.613093000000	-3.512084000000	-1.099998000000
H	1.674382000000	-4.578925000000	-1.327632000000
C	1.403478000000	-0.727880000000	-0.507550000000
C	2.001632000000	3.521325000000	-0.510998000000
H	1.109829000000	3.682020000000	-1.140113000000
H	2.772839000000	4.241076000000	-0.838562000000
H	1.729864000000	3.778462000000	0.526716000000
C	4.235724000000	1.698492000000	0.422459000000
H	4.937952000000	2.498399000000	0.129124000000
H	4.783037000000	0.743937000000	0.362060000000
H	3.972841000000	1.865760000000	1.481481000000
C	3.170672000000	1.486728000000	-2.483013000000
H	2.290225000000	1.604145000000	-3.136420000000
H	3.924813000000	2.230702000000	-2.792413000000
H	3.589229000000	0.485205000000	-2.665737000000
C	-4.467110000000	0.934124000000	0.060544000000
H	-4.825219000000	-0.107961000000	0.035732000000
H	-5.280674000000	1.570035000000	-0.330294000000
H	-4.315452000000	1.209954000000	1.118676000000

C	-2.519329000000	3.072643000000	-0.856694000000
H	-3.378983000000	3.631324000000	-1.267362000000
H	-1.630655000000	3.348619000000	-1.449250000000
H	-2.357390000000	3.427680000000	0.175195000000
C	-3.179696000000	0.755933000000	-2.754067000000
H	-2.287851000000	0.985968000000	-3.360339000000
H	-3.409013000000	-0.311868000000	-2.891424000000
H	-4.025061000000	1.338943000000	-3.158298000000
C	-1.358785000000	-0.285887000000	2.939180000000
H	-1.286751000000	-1.316757000000	3.314770000000
H	-2.105019000000	-0.267823000000	2.133265000000
C	1.359393000000	-1.827662000000	2.996651000000
H	1.362495000000	-2.250879000000	1.982274000000
H	2.344592000000	-2.013664000000	3.452644000000
H	0.609598000000	-2.355389000000	3.605815000000
C	1.124855000000	-0.328611000000	2.955412000000
H	1.906397000000	0.172928000000	2.369464000000
H	1.097365000000	0.117365000000	3.962876000000
C	-1.693614000000	0.707106000000	4.038755000000
H	-1.758523000000	1.728906000000	3.634321000000
H	-2.669323000000	0.444735000000	4.477293000000
H	-0.949869000000	0.698557000000	4.850315000000

D1

Energy (PCM(benzene)-[TPSSh/def2-TZVPP//TPSSh/def2-SVP])= -3578.92849321

Al	-1.368418000000	-0.049882000000	-0.047076000000
Si	-2.044959000000	2.824819000000	-1.461946000000
Si	-2.171435000000	-2.496726000000	-2.092406000000
O	-2.064496000000	-0.392984000000	1.888009000000
N	-2.540238000000	-1.308508000000	-0.828375000000
N	-2.396735000000	1.495249000000	-0.343802000000
C	-4.482317000000	0.114041000000	-0.052665000000
C	-3.758823000000	1.368613000000	0.023728000000
C	-4.431305000000	2.506497000000	0.488297000000
H	-3.859532000000	3.428593000000	0.596127000000

H	-6.265709000000	3.420047000000	1.191199000000
C	-5.792772000000	2.498315000000	0.841684000000
C	-5.886506000000	0.128853000000	0.311691000000
H	-7.572307000000	1.295018000000	1.017421000000
C	-6.512390000000	1.327894000000	0.753925000000
C	-4.749030000000	-2.266537000000	-0.555227000000
H	-4.317143000000	-3.225807000000	-0.840475000000
C	-6.114498000000	-2.225334000000	-0.223534000000
H	-6.712264000000	-3.137671000000	-0.298210000000
C	-6.678004000000	-1.048857000000	0.217380000000
H	-7.733206000000	-0.994688000000	0.495287000000
C	-3.904303000000	-1.147683000000	-0.490753000000
C	-0.389612000000	-2.220237000000	-2.626168000000
H	-0.189576000000	-1.180767000000	-2.929378000000
H	-0.164335000000	-2.876469000000	-3.484593000000
H	0.310596000000	-2.481825000000	-1.817832000000
C	-2.249851000000	-4.330228000000	-1.566921000000
H	-1.501061000000	-4.904627000000	-2.139228000000
H	-3.227426000000	-4.797976000000	-1.769055000000
H	-2.015315000000	-4.468781000000	-0.498678000000
C	-3.281798000000	-2.233921000000	-3.599732000000
H	-3.142715000000	-1.219397000000	-4.009337000000
H	-3.024236000000	-2.958497000000	-4.391710000000
H	-4.350217000000	-2.356152000000	-3.365030000000
C	-1.934926000000	4.569040000000	-0.711881000000
H	-2.925944000000	5.007314000000	-0.512180000000
H	-1.423740000000	5.237655000000	-1.426904000000
H	-1.358342000000	4.588209000000	0.226809000000
C	-0.358370000000	2.462840000000	-2.221559000000
H	-0.100556000000	3.229230000000	-2.972248000000
H	-0.355597000000	1.482630000000	-2.724381000000
H	0.435955000000	2.460708000000	-1.458058000000
C	-3.334101000000	2.863143000000	-2.843055000000
H	-3.372729000000	1.896832000000	-3.372739000000
H	-4.343074000000	3.070475000000	-2.452591000000

H	-3.089142000000	3.648784000000	-3.578616000000
C	-2.555881000000	0.665376000000	2.765152000000
H	-3.654270000000	0.617946000000	2.755297000000
H	-2.260205000000	1.590081000000	2.259235000000
C	-3.757392000000	-1.991908000000	2.842182000000
H	-4.520780000000	-1.680895000000	2.117071000000
H	-3.872427000000	-3.074944000000	3.006954000000
H	-3.945593000000	-1.492255000000	3.803844000000
C	-2.347557000000	-1.760826000000	2.323583000000
H	-2.169045000000	-2.361538000000	1.423673000000
H	-1.597054000000	-2.025023000000	3.083189000000
C	-2.006938000000	0.611103000000	4.180376000000
H	-0.912854000000	0.701512000000	4.205449000000
H	-2.431505000000	1.461079000000	4.737956000000
H	-2.292823000000	-0.307874000000	4.713082000000
Al	1.422786000000	-0.057250000000	-0.084275000000
Si	2.023263000000	2.850208000000	1.338392000000
Si	1.852982000000	-2.454121000000	2.002195000000
O	2.296267000000	-0.249689000000	-1.976866000000
N	2.453767000000	-1.426063000000	0.690275000000
N	2.489698000000	1.419976000000	0.392086000000
C	4.527568000000	-0.072616000000	0.229204000000
C	3.878988000000	1.229451000000	0.189953000000
C	4.673788000000	2.352643000000	-0.078950000000
H	4.178857000000	3.319415000000	-0.174281000000
H	6.629281000000	3.209644000000	-0.436804000000
C	6.068668000000	2.290301000000	-0.247211000000
C	5.963695000000	-0.117837000000	0.025201000000
H	7.790794000000	0.996062000000	-0.328644000000
C	6.709619000000	1.073695000000	-0.191451000000
C	4.583547000000	-2.521315000000	0.366562000000
H	4.041700000000	-3.465512000000	0.443157000000
C	5.977312000000	-2.542641000000	0.184624000000
H	6.503539000000	-3.500493000000	0.152809000000
C	6.662102000000	-1.357713000000	0.027459000000

H	7.744682000000	-1.346139000000	-0.119895000000
C	3.841725000000	-1.334737000000	0.448170000000
C	1.019453000000	-1.314567000000	3.263247000000
H	1.779475000000	-0.641989000000	3.696136000000
H	0.555281000000	-1.876434000000	4.092161000000
H	0.246425000000	-0.685837000000	2.797095000000
C	0.627714000000	-3.730245000000	1.322063000000
H	0.007140000000	-4.181803000000	2.114653000000
H	1.177425000000	-4.549342000000	0.826643000000
H	-0.043265000000	-3.294585000000	0.564007000000
C	3.176666000000	-3.372977000000	2.995340000000
H	4.025048000000	-2.719830000000	3.254791000000
H	2.706306000000	-3.703584000000	3.938864000000
H	3.578695000000	-4.267494000000	2.496143000000
C	1.970238000000	4.507666000000	0.401602000000
H	2.968303000000	4.940022000000	0.224635000000
H	1.404386000000	5.240466000000	1.003345000000
H	1.463032000000	4.424614000000	-0.573149000000
C	0.281695000000	2.563866000000	1.998691000000
H	-0.016012000000	3.414993000000	2.635489000000
H	0.252315000000	1.655545000000	2.619718000000
H	-0.475275000000	2.464526000000	1.203950000000
C	3.161731000000	3.050679000000	2.835454000000
H	3.144451000000	2.141468000000	3.459423000000
H	4.208312000000	3.243851000000	2.555287000000
H	2.815782000000	3.895223000000	3.456566000000
C	2.691153000000	0.921278000000	-2.746550000000
H	3.787497000000	0.995750000000	-2.704567000000
H	2.284805000000	1.766937000000	-2.182386000000
C	4.218574000000	-1.548167000000	-2.953189000000
H	4.896961000000	-1.237850000000	-2.148360000000
H	4.463724000000	-2.589311000000	-3.215560000000
H	4.408530000000	-0.932451000000	-3.845142000000
C	2.762206000000	-1.526140000000	-2.521741000000
H	2.589504000000	-2.237278000000	-1.705369000000

H	2.101598000000	-1.784370000000	-3.361702000000
C	2.182529000000	0.905666000000	-4.178103000000
H	1.089372000000	0.802323000000	-4.221429000000
H	2.451162000000	1.862772000000	-4.652285000000
H	2.634432000000	0.101926000000	-4.778101000000

TS1

Energy (PCM(benzene)-[TPSSh/def2-TZVPP//TPSSh/def2-SVP])= -2021.77290562

Al	-0.675431000000	0.093431000000	0.397661000000
Si	0.374235000000	2.799393000000	1.737853000000
Si	0.105636000000	-2.674320000000	1.842630000000
O	-0.791027000000	0.129003000000	-1.592741000000
N	0.377522000000	-1.416076000000	0.627981000000
N	0.580799000000	1.444269000000	0.619657000000
C	2.236622000000	-0.111702000000	-0.471039000000
C	1.775297000000	1.221680000000	-0.097099000000
C	2.535705000000	2.328132000000	-0.499942000000
H	2.165399000000	3.324160000000	-0.250693000000
H	4.282669000000	3.115845000000	-1.506499000000
C	3.732484000000	2.212866000000	-1.228339000000
C	3.465541000000	-0.201433000000	-1.236752000000
H	5.113091000000	0.853116000000	-2.171712000000
C	4.189778000000	0.968395000000	-1.599054000000
C	2.149558000000	-2.568683000000	-0.545704000000
H	1.624758000000	-3.496640000000	-0.311322000000
C	3.345326000000	-2.628880000000	-1.282927000000
H	3.744255000000	-3.600817000000	-1.585587000000
C	3.992939000000	-1.463943000000	-1.628718000000
H	4.922261000000	-1.483830000000	-2.202975000000
C	1.578023000000	-1.363784000000	-0.114901000000
C	-1.145120000000	-2.023526000000	3.108663000000
H	-0.814677000000	-1.072652000000	3.558914000000
H	-1.238433000000	-2.759816000000	3.926278000000
H	-2.155775000000	-1.875019000000	2.696701000000
C	-0.622531000000	-4.282908000000	1.140101000000

H	-0.904194000000	-4.964730000000	1.961493000000
H	0.082203000000	-4.827196000000	0.490290000000
H	-1.532187000000	-4.084077000000	0.547904000000
C	1.701740000000	-3.058334000000	2.778234000000
H	2.101005000000	-2.143508000000	3.246989000000
H	1.500826000000	-3.790465000000	3.579308000000
H	2.490409000000	-3.472296000000	2.131872000000
C	-0.113041000000	4.429873000000	0.890593000000
H	0.674716000000	4.837688000000	0.236485000000
H	-0.340145000000	5.199088000000	1.649358000000
H	-1.020015000000	4.296828000000	0.275442000000
C	-1.053224000000	2.372847000000	2.908186000000
H	-1.166133000000	3.183922000000	3.649093000000
H	-0.867473000000	1.439869000000	3.465903000000
H	-2.020125000000	2.273110000000	2.388526000000
C	1.923809000000	3.058224000000	2.787434000000
H	2.166123000000	2.137531000000	3.343880000000
H	2.807927000000	3.327782000000	2.189922000000
H	1.752989000000	3.863860000000	3.522106000000
C	-3.328899000000	-0.006357000000	0.798490000000
H	-3.061858000000	0.013840000000	1.857205000000
C	-4.586083000000	1.111664000000	-0.985589000000
H	-4.994992000000	2.029178000000	-1.418665000000
C	-3.885482000000	1.174259000000	0.212652000000
H	-3.755089000000	2.136771000000	0.714811000000
C	-0.576417000000	1.359020000000	-2.346691000000
H	0.393625000000	1.270617000000	-2.857831000000
H	-0.471686000000	2.124808000000	-1.568068000000
C	0.100728000000	-1.347548000000	-3.392547000000
H	1.100684000000	-1.337775000000	-2.936165000000
H	-0.065792000000	-2.346180000000	-3.826254000000
H	0.071159000000	-0.621164000000	-4.218910000000
C	-0.983086000000	-1.099276000000	-2.359111000000
H	-0.976856000000	-1.884143000000	-1.591433000000
H	-1.986860000000	-1.054549000000	-2.808048000000

C	-1.706649000000	1.684801000000	-3.303896000000
H	-2.670567000000	1.722636000000	-2.777377000000
H	-1.509629000000	2.672895000000	-3.748859000000
H	-1.783804000000	0.960262000000	-4.128723000000
C	-4.812603000000	-0.123491000000	-1.626007000000
H	-5.376334000000	-0.166861000000	-2.560652000000
C	-3.663759000000	-1.258889000000	0.193404000000
H	-3.363804000000	-2.190147000000	0.681073000000
C	-4.358987000000	-1.305107000000	-1.010654000000
H	-4.585291000000	-2.274317000000	-1.464393000000

INT2

Energy (PCM(benzene)-[TPSSh/def2-TZVPP//TPSSh/def2-SVP])= -2021.79104529

Al	0.760729000000	-0.102222000000	-0.241629000000
Si	0.242761000000	2.674522000000	-1.850526000000
Si	-0.448488000000	-2.717059000000	-1.756244000000
O	0.756880000000	-0.052017000000	1.721489000000
N	-0.517457000000	-1.391335000000	-0.579497000000
N	-0.151053000000	1.454828000000	-0.626235000000
C	-2.140820000000	0.283032000000	0.392587000000
C	-1.393400000000	1.488178000000	0.050543000000
C	-1.911521000000	2.730478000000	0.438491000000
H	-1.319023000000	3.621687000000	0.222585000000
H	-3.496914000000	3.872675000000	1.371761000000
C	-3.141119000000	2.873885000000	1.105106000000
C	-3.400325000000	0.457872000000	1.091409000000
H	-4.832454000000	1.840061000000	1.950074000000
C	-3.875889000000	1.755641000000	1.428938000000
C	-2.568678000000	-2.136409000000	0.468667000000
H	-2.234326000000	-3.156123000000	0.270148000000
C	-3.793356000000	-1.939708000000	1.130700000000
H	-4.402365000000	-2.805005000000	1.405649000000
C	-4.202966000000	-0.662948000000	1.443925000000
H	-5.146592000000	-0.484442000000	1.964883000000
C	-1.733653000000	-1.082272000000	0.075200000000

C	0.953511000000	-2.392722000000	-2.988064000000
H	0.859568000000	-1.406948000000	-3.472383000000
H	0.891376000000	-3.154423000000	-3.784677000000
H	1.961907000000	-2.468195000000	-2.552957000000
C	-0.095627000000	-4.413113000000	-0.976183000000
H	0.063283000000	-5.168313000000	-1.765601000000
H	-0.916832000000	-4.775639000000	-0.336582000000
H	0.817616000000	-4.385004000000	-0.357397000000
C	-2.044191000000	-2.795743000000	-2.766548000000
H	-2.228971000000	-1.829202000000	-3.264477000000
H	-1.947977000000	-3.566933000000	-3.550219000000
H	-2.933238000000	-3.034950000000	-2.164384000000
C	1.092501000000	4.214279000000	-1.134094000000
H	0.432606000000	4.797798000000	-0.471163000000
H	1.419448000000	4.886201000000	-1.946679000000
H	1.987955000000	3.939313000000	-0.550866000000
C	1.438642000000	1.920067000000	-3.111185000000
H	1.604237000000	2.654715000000	-3.918288000000
H	1.017927000000	1.013389000000	-3.576495000000
H	2.428679000000	1.667610000000	-2.701419000000
C	-1.301548000000	3.184600000000	-2.813380000000
H	-1.787425000000	2.298869000000	-3.255615000000
H	-2.051574000000	3.702869000000	-2.197661000000
H	-1.014889000000	3.860035000000	-3.637910000000
C	2.734138000000	-0.393796000000	-0.658760000000
H	2.743882000000	-0.464688000000	-1.765347000000
C	4.393944000000	0.679180000000	0.893379000000
H	4.939749000000	1.571564000000	1.215500000000
C	3.530302000000	0.771242000000	-0.173366000000
H	3.421760000000	1.728928000000	-0.690754000000
C	0.788980000000	1.213981000000	2.450412000000
H	-0.214273000000	1.378207000000	2.870953000000
H	0.948624000000	1.961264000000	1.662976000000
C	-0.547256000000	-1.265530000000	3.462870000000
H	-1.489551000000	-1.068332000000	2.932544000000

H	-0.618674000000	-2.261814000000	3.926784000000
H	-0.427492000000	-0.532145000000	4.274612000000
C	0.633508000000	-1.276426000000	2.509523000000
H	0.517854000000	-2.060979000000	1.750512000000
H	1.591868000000	-1.429440000000	3.028127000000
C	1.876349000000	1.272682000000	3.505396000000
H	2.858482000000	1.036879000000	3.072047000000
H	1.907377000000	2.296454000000	3.910204000000
H	1.684605000000	0.590862000000	4.347650000000
C	4.622868000000	-0.554964000000	1.563271000000
H	5.322610000000	-0.613248000000	2.399340000000
C	3.137022000000	-1.679353000000	-0.015053000000
H	2.722501000000	-2.612162000000	-0.408839000000
C	3.998239000000	-1.727020000000	1.057813000000
H	4.235966000000	-2.695974000000	1.507961000000

TS3 (estimated from a scan on the Al-C the energy profile)

Al	-3.341550000000	0.056462000000	-0.232323000000
Si	-4.261395000000	2.988451000000	-1.279059000000
Si	-4.101313000000	-2.351426000000	-2.278695000000
O	-3.413893000000	-0.311759000000	1.700520000000
N	-4.409273000000	-1.309807000000	-0.879363000000
N	-4.483901000000	1.505136000000	-0.337604000000
C	-6.291322000000	-0.127034000000	0.321348000000
C	-5.729766000000	1.217997000000	0.267427000000
C	-6.441113000000	2.265336000000	0.867010000000
H	-5.987830000000	3.258487000000	0.864505000000
H	-8.203104000000	2.948075000000	1.924593000000
C	-7.692518000000	2.088080000000	1.482952000000
C	-7.577917000000	-0.284913000000	0.972907000000
H	-9.223652000000	0.667636000000	2.013670000000
C	-8.254194000000	0.832368000000	1.537445000000
C	-6.344708000000	-2.545608000000	-0.111684000000
H	-5.854567000000	-3.442948000000	-0.493213000000
C	-7.599353000000	-2.670173000000	0.510825000000

H	-8.074248000000	-3.652908000000	0.574175000000
C	-8.206944000000	-1.558979000000	1.051024000000
H	-9.178088000000	-1.630907000000	1.546451000000
C	-5.672439000000	-1.323022000000	-0.241557000000
C	-2.703965000000	-1.603804000000	-3.318316000000
H	-2.910898000000	-0.559744000000	-3.604889000000
H	-2.618557000000	-2.189166000000	-4.250453000000
H	-1.720785000000	-1.637923000000	-2.823762000000
C	-3.533635000000	-4.108513000000	-1.826379000000
H	-3.228502000000	-4.653410000000	-2.736893000000
H	-4.317927000000	-4.706902000000	-1.334888000000
H	-2.662955000000	-4.084237000000	-1.148683000000
C	-5.623681000000	-2.442018000000	-3.395516000000
H	-5.915621000000	-1.431252000000	-3.726247000000
H	-5.392230000000	-3.038963000000	-4.294517000000
H	-6.497023000000	-2.895933000000	-2.903792000000
C	-3.701284000000	4.476701000000	-0.239866000000
H	-4.471444000000	4.815488000000	0.472413000000
H	-3.460659000000	5.332509000000	-0.894481000000
H	-2.794231000000	4.239572000000	0.342011000000
C	-2.914831000000	2.692550000000	-2.579550000000
H	-2.844694000000	3.587902000000	-3.221467000000
H	-3.161967000000	1.839354000000	-3.232741000000
H	-1.913915000000	2.521616000000	-2.154140000000
C	-5.839178000000	3.429629000000	-2.221663000000
H	-6.153575000000	2.586575000000	-2.859299000000
H	-6.683875000000	3.681464000000	-1.563183000000
H	-5.649591000000	4.297603000000	-2.876569000000
C	-1.351973000000	0.155350000000	-0.559246000000
H	-1.248655000000	0.303432000000	-1.656381000000
C	0.227845000000	1.190643000000	1.122458000000
H	0.574663000000	2.091100000000	1.641029000000
C	-0.743298000000	1.316346000000	0.182248000000
H	-1.122962000000	2.319915000000	-0.039689000000
C	-3.512685000000	0.770957000000	2.673337000000

H	-4.508176000000	0.709696000000	3.137842000000
H	-3.487093000000	1.677341000000	2.054916000000
C	-4.540446000000	-2.006560000000	3.131523000000
H	-5.503936000000	-1.816829000000	2.637221000000
H	-4.488016000000	-3.078592000000	3.378050000000
H	-4.502393000000	-1.448317000000	4.079360000000
C	-3.376669000000	-1.676955000000	2.214900000000
H	-3.405877000000	-2.294464000000	1.307899000000
H	-2.401094000000	-1.820025000000	2.703871000000
C	-2.392844000000	0.760449000000	3.695642000000
H	-1.412157000000	0.773540000000	3.199164000000
H	-2.481886000000	1.666061000000	4.315992000000
H	-2.445266000000	-0.107864000000	4.369881000000
C	0.842567000000	-0.091626000000	1.474679000000
H	1.147502000000	-0.221274000000	2.519377000000
C	-0.722737000000	-1.148049000000	-0.136874000000
H	-1.091411000000	-2.068402000000	-0.604680000000
C	0.240505000000	-1.251022000000	0.813932000000
H	0.598375000000	-2.249011000000	1.093286000000
Al	3.593526000000	-0.080793000000	0.507657000000
Si	4.877292000000	-2.574335000000	2.039342000000
Si	4.359496000000	2.895601000000	1.441939000000
O	3.033867000000	-0.412118000000	-1.333189000000
N	4.561265000000	1.477177000000	0.402326000000
N	4.897731000000	-1.359449000000	0.748023000000
C	6.320303000000	0.096197000000	-0.754942000000
C	6.005676000000	-1.178308000000	-0.115903000000
C	6.807963000000	-2.287570000000	-0.413660000000
H	6.550327000000	-3.246440000000	0.038818000000
H	8.492761000000	-3.131803000000	-1.477401000000
C	7.904218000000	-2.229336000000	-1.292113000000
C	7.436497000000	0.121226000000	-1.681436000000
H	9.046052000000	-0.981259000000	-2.626822000000
C	8.209420000000	-1.047251000000	-1.927347000000
C	6.017494000000	2.490112000000	-1.241067000000

H	5.451841000000	3.412221000000	-1.091677000000
C	7.098607000000	2.484879000000	-2.140298000000
H	7.369181000000	3.405133000000	-2.664888000000
C	7.801568000000	1.320629000000	-2.354413000000
H	8.649898000000	1.292590000000	-3.042312000000
C	5.623432000000	1.355609000000	-0.520174000000
C	3.543308000000	2.301200000000	3.043358000000
H	4.225920000000	1.641946000000	3.605941000000
H	3.300601000000	3.161134000000	3.691346000000
H	2.608967000000	1.744897000000	2.864422000000
C	3.248102000000	4.225667000000	0.670919000000
H	3.082611000000	5.055552000000	1.379872000000
H	3.684840000000	4.657004000000	-0.245157000000
H	2.260327000000	3.812339000000	0.405018000000
C	6.029297000000	3.649150000000	1.904650000000
H	6.700770000000	2.877341000000	2.316048000000
H	5.879264000000	4.416725000000	2.683729000000
H	6.546838000000	4.125646000000	1.058617000000
C	4.469213000000	-4.329766000000	1.438446000000
H	5.255200000000	-4.778375000000	0.809791000000
H	4.321822000000	-4.997764000000	2.305039000000
H	3.532562000000	-4.335189000000	0.854626000000
C	3.495927000000	-2.099481000000	3.241957000000
H	3.522529000000	-2.788658000000	4.104356000000
H	3.612391000000	-1.075126000000	3.633826000000
H	2.494127000000	-2.179455000000	2.790192000000
C	6.509111000000	-2.576736000000	2.991266000000
H	6.701615000000	-1.579741000000	3.421280000000
H	7.373941000000	-2.840955000000	2.363954000000
H	6.460214000000	-3.300882000000	3.822640000000
C	3.391018000000	-1.577929000000	-2.136311000000
H	3.993881000000	-1.224431000000	-2.985924000000
H	4.042820000000	-2.158999000000	-1.473669000000
C	2.783084000000	1.265062000000	-3.144077000000
H	3.760345000000	1.701350000000	-2.890478000000

H	2.113430000000	2.074336000000	-3.475161000000
H	2.908818000000	0.574353000000	-3.992040000000
C	2.159110000000	0.590317000000	-1.938122000000
H	1.974762000000	1.305068000000	-1.124304000000
H	1.203235000000	0.100131000000	-2.170334000000
C	2.184209000000	-2.384004000000	-2.577054000000
H	1.554573000000	-2.652061000000	-1.715697000000
H	2.540505000000	-3.310327000000	-3.054122000000
H	1.562178000000	-1.851509000000	-3.312429000000

INT3

Energy (PCM(benzene)-[TPSSh/def2-TZVPP//TPSSh/def2-SVP])= -1555.64922787

Al	-0.000045000000	-1.669347000000	0.000042000000
Si	3.070494000000	-1.273742000000	0.218090000000
Si	-3.070567000000	-1.273652000000	-0.218088000000
N	-1.453828000000	-0.575571000000	0.076046000000
N	1.453777000000	-0.575633000000	-0.076083000000
C	0.000021000000	1.471921000000	-0.000069000000
C	1.248176000000	0.803653000000	-0.321516000000
C	2.309473000000	1.568716000000	-0.815483000000
H	3.219909000000	1.056490000000	-1.129317000000
H	3.129115000000	3.522609000000	-1.259263000000
C	2.261850000000	2.973441000000	-0.883950000000
C	0.000073000000	2.918598000000	-0.000026000000
H	1.099014000000	4.733834000000	-0.446238000000
C	1.140365000000	3.642174000000	-0.447655000000
C	-2.309382000000	1.568835000000	0.815471000000
H	-3.219815000000	1.056652000000	1.129384000000
C	-2.261667000000	2.973554000000	0.883988000000
H	-3.128869000000	3.522762000000	1.259391000000
C	-1.140159000000	3.642231000000	0.447668000000
H	-1.098725000000	4.733888000000	0.446323000000
C	-1.248173000000	0.803726000000	0.321386000000
C	-2.778420000000	-3.010211000000	-0.920192000000
H	-2.309252000000	-3.702253000000	-0.200219000000

H	-3.758276000000	-3.443384000000	-1.189788000000
H	-2.164942000000	-3.003724000000	-1.837831000000
C	-4.007924000000	-0.268944000000	-1.511237000000
H	-4.969945000000	-0.758332000000	-1.741159000000
H	-4.221692000000	0.759158000000	-1.182346000000
H	-3.426955000000	-0.207322000000	-2.446279000000
C	-4.106896000000	-1.497344000000	1.351069000000
H	-3.528474000000	-2.030382000000	2.124340000000
H	-5.000009000000	-2.104777000000	1.123249000000
H	-4.457619000000	-0.550757000000	1.791630000000
C	4.106842000000	-1.497540000000	-1.351043000000
H	4.457809000000	-0.550997000000	-1.791505000000
H	4.999804000000	-2.105195000000	-1.123227000000
H	3.528337000000	-2.030382000000	-2.124386000000
C	2.778311000000	-3.010261000000	0.920280000000
H	3.758152000000	-3.443384000000	1.190015000000
H	2.164733000000	-3.003741000000	1.837852000000
H	2.309247000000	-3.702362000000	0.200298000000
C	4.007852000000	-0.268962000000	1.511178000000
H	3.426986000000	-0.207475000000	2.446292000000
H	4.221407000000	0.759190000000	1.182298000000
H	4.969981000000	-0.758201000000	1.740958000000

D2

Energy (PCM(benzene)-[TPSSh/def2-TVPP//TPSSh/def2-SVP])= -3111.37999725

Al	-1.267353000000	-0.000051000000	-0.245247000000
Si	-2.044719000000	2.755199000000	-1.500450000000
Si	-2.045158000000	-2.755249000000	-1.500428000000
N	-2.386385000000	-1.437533000000	-0.352831000000
N	-2.386339000000	1.437482000000	-0.352917000000
C	-4.276757000000	0.000046000000	0.512942000000
C	-3.673330000000	1.292078000000	0.231137000000
C	-4.379694000000	2.452163000000	0.560177000000
H	-3.897906000000	3.415144000000	0.389006000000
H	-6.169782000000	3.369115000000	1.361377000000

C	-5.665617000000	2.427418000000	1.129761000000
C	-5.598127000000	0.000078000000	1.109695000000
H	-7.263026000000	1.174056000000	1.848708000000
C	-6.267174000000	1.220613000000	1.402022000000
C	-4.379337000000	-2.452071000000	0.561285000000
H	-3.897403000000	-3.415044000000	0.390481000000
C	-5.665217000000	-2.427265000000	1.130970000000
H	-6.169203000000	-3.368933000000	1.363093000000
C	-6.266969000000	-1.220424000000	1.402634000000
H	-7.262823000000	-1.173805000000	1.849308000000
C	-3.673220000000	-1.292028000000	0.231582000000
C	-0.404386000000	-2.298535000000	-2.337212000000
H	-0.439315000000	-1.316426000000	-2.843738000000
H	-0.188206000000	-3.043872000000	-3.122429000000
H	0.457718000000	-2.301425000000	-1.648110000000
C	-1.831111000000	-4.480007000000	-0.742339000000
H	-1.267578000000	-5.122783000000	-1.440646000000
H	-2.795414000000	-4.977997000000	-0.551242000000
H	-1.273688000000	-4.449698000000	0.206979000000
C	-3.400209000000	-2.817736000000	-2.811475000000
H	-3.466456000000	-1.861297000000	-3.355781000000
H	-3.191199000000	-3.615188000000	-3.545016000000
H	-4.387383000000	-3.018702000000	-2.366153000000
C	-1.831123000000	4.479912000000	-0.742101000000
H	-2.795560000000	4.978209000000	-0.552471000000
H	-1.266288000000	5.122538000000	-1.439486000000
H	-1.275181000000	4.449345000000	0.208079000000
C	-0.403675000000	2.298588000000	-2.336745000000
H	-0.187420000000	3.043831000000	-3.122033000000
H	-0.438380000000	1.316400000000	-2.843140000000
H	0.458305000000	2.301668000000	-1.647492000000
C	-3.399238000000	2.817503000000	-2.812055000000
H	-3.464229000000	1.861469000000	-3.357229000000
H	-4.386821000000	3.017064000000	-2.367014000000
H	-3.190707000000	3.615793000000	-3.544822000000

Al	1.267393000000	-0.000012000000	0.245150000000
Si	2.044781000000	2.755309000000	1.500280000000
Si	2.044980000000	-2.755121000000	1.500428000000
N	2.386280000000	-1.437609000000	0.352629000000
N	2.386439000000	1.437441000000	0.352939000000
C	4.276832000000	-0.000109000000	-0.512853000000
C	3.673437000000	1.291954000000	-0.231117000000
C	4.379832000000	2.452003000000	-0.560199000000
H	3.898056000000	3.415004000000	-0.389104000000
H	6.169993000000	3.368878000000	-1.361333000000
C	5.665798000000	2.427203000000	-1.129689000000
C	5.598264000000	-0.000134000000	-1.109480000000
H	7.263260000000	1.173774000000	-1.848394000000
C	6.267364000000	1.220373000000	-1.401810000000
C	4.379340000000	-2.452237000000	-0.561141000000
H	3.897327000000	-3.415177000000	-0.390373000000
C	5.665287000000	-2.427486000000	-1.130663000000
H	6.169286000000	-3.369168000000	-1.362703000000
C	6.267101000000	-1.220664000000	-1.402298000000
H	7.263006000000	-1.174089000000	-1.848863000000
C	3.673222000000	-1.292153000000	-0.231563000000
C	0.403975000000	-2.298525000000	2.336842000000
H	0.438621000000	-1.316331000000	2.843216000000
H	0.187904000000	-3.043790000000	3.122163000000
H	-0.458044000000	-2.301760000000	1.647641000000
C	1.831290000000	-4.480014000000	0.742543000000
H	1.267141000000	-5.122608000000	1.440516000000
H	2.795654000000	-4.978168000000	0.552197000000
H	1.274539000000	-4.449706000000	-0.207174000000
C	3.399746000000	-2.817167000000	2.811788000000
H	3.465468000000	-1.860774000000	3.356238000000
H	3.190882000000	-3.614802000000	3.545173000000
H	4.387104000000	-3.017681000000	2.366668000000
C	1.830713000000	4.479816000000	0.741622000000
H	2.794995000000	4.978063000000	0.551088000000

H	1.266440000000	5.122617000000	1.439304000000
H	1.274001000000	4.449013000000	-0.208097000000
C	0.403942000000	2.298575000000	2.336904000000
H	0.187771000000	3.043890000000	3.122147000000
H	0.438880000000	1.316449000000	2.843395000000
H	-0.458175000000	2.301481000000	1.647822000000
C	3.399455000000	2.818122000000	2.811703000000
H	3.465031000000	1.862023000000	3.356694000000
H	4.386881000000	3.018290000000	2.366590000000
H	3.190581000000	3.616164000000	3.544640000000

TS3

Energy (PCM(benzene)-[TPSSh/def2-TZVPP//TPSSh/def2-SVP])= -1787.99721556

C	2.481329000000	-0.627935000000	2.887851000000
H	3.232498000000	0.065803000000	3.269771000000
C	1.939807000000	-2.764658000000	1.853178000000
H	2.249650000000	-3.739516000000	1.469277000000
C	2.874271000000	-1.884519000000	2.364574000000
H	3.929621000000	-2.168676000000	2.381957000000
C	0.545455000000	-2.393792000000	1.782239000000
H	-0.195183000000	-3.194104000000	1.676041000000
C	1.120401000000	-0.303013000000	2.960788000000
H	0.805891000000	0.635853000000	3.421736000000
C	0.150013000000	-1.183049000000	2.474657000000
H	-0.910314000000	-0.951855000000	2.598342000000
Al	0.113042000000	-1.194465000000	-0.008840000000
Si	-2.911305000000	-1.540458000000	-0.727106000000
Si	2.601760000000	-0.204807000000	-1.593339000000
N	1.209641000000	0.155172000000	-0.555092000000
N	-1.581022000000	-0.521504000000	-0.150060000000
C	-0.601176000000	1.792969000000	0.101083000000
C	-1.716304000000	0.854029000000	0.151542000000
C	-2.978988000000	1.328308000000	0.524999000000
H	-3.797414000000	0.611012000000	0.602508000000
H	-4.244728000000	2.986763000000	1.101587000000

C	-3.234163000000	2.678498000000	0.820960000000
C	-0.893659000000	3.180816000000	0.408930000000
H	-2.379583000000	4.648943000000	0.985212000000
C	-2.208547000000	3.593238000000	0.762131000000
C	1.723247000000	2.496422000000	-0.280451000000
H	2.757709000000	2.237809000000	-0.509799000000
C	1.409788000000	3.835992000000	0.006776000000
H	2.196753000000	4.593686000000	-0.034100000000
C	0.122088000000	4.174965000000	0.352226000000
H	-0.146934000000	5.207138000000	0.588392000000
C	0.775772000000	1.467379000000	-0.252964000000
C	2.483003000000	-2.059200000000	-1.980618000000
H	1.563378000000	-2.322423000000	-2.531344000000
H	3.336247000000	-2.348317000000	-2.619672000000
H	2.536424000000	-2.689309000000	-1.075220000000
C	4.303417000000	0.066011000000	-0.800873000000
H	5.082164000000	-0.382608000000	-1.442220000000
H	4.562545000000	1.128379000000	-0.667249000000
H	4.359646000000	-0.418947000000	0.187050000000
C	2.495796000000	0.757291000000	-3.214851000000
H	1.555841000000	0.525396000000	-3.742334000000
H	3.335397000000	0.487249000000	-3.878134000000
H	2.528415000000	1.846397000000	-3.056027000000
C	-4.109241000000	-2.103792000000	0.632996000000
H	-4.718436000000	-1.286149000000	1.050124000000
H	-4.805465000000	-2.859946000000	0.230146000000
H	-3.562794000000	-2.569526000000	1.470945000000
C	-2.113352000000	-3.119339000000	-1.414817000000
H	-2.905531000000	-3.766926000000	-1.831175000000
H	-1.401978000000	-2.909658000000	-2.232256000000
H	-1.585941000000	-3.714214000000	-0.648944000000
C	-3.859944000000	-0.705235000000	-2.129552000000
H	-3.178618000000	-0.461135000000	-2.961313000000
H	-4.348908000000	0.229170000000	-1.814637000000
H	-4.640659000000	-1.382527000000	-2.516273000000

INT3

Energy (PCM(benzene)-[TPSSh/def2-TZVPP//TPSSh/def2-SVP])= -1787.99861938

C	2.857144000000	-0.898327000000	2.763904000000
H	3.565645000000	-0.241115000000	3.270577000000
C	2.452308000000	-2.766418000000	1.243517000000
H	2.829617000000	-3.589898000000	0.631739000000
C	3.325599000000	-1.947088000000	1.918069000000
H	4.401784000000	-2.117289000000	1.825934000000
C	1.000192000000	-2.542229000000	1.298692000000
H	0.371664000000	-3.432408000000	1.152561000000
C	1.478211000000	-0.780341000000	3.009625000000
H	1.118056000000	-0.050567000000	3.739374000000
C	0.555602000000	-1.607707000000	2.369737000000
H	-0.498723000000	-1.583841000000	2.659627000000
Al	0.290413000000	-1.024567000000	0.134219000000
Si	-2.595675000000	-1.883067000000	-0.772050000000
Si	2.476054000000	0.411720000000	-1.603207000000
N	1.135935000000	0.469291000000	-0.443743000000
N	-1.486590000000	-0.695264000000	-0.063808000000
C	-0.924783000000	1.746530000000	0.275466000000
C	-1.865024000000	0.631877000000	0.263484000000
C	-3.198307000000	0.871852000000	0.609874000000
H	-3.883772000000	0.023425000000	0.642005000000
H	-4.738968000000	2.271485000000	1.203900000000
C	-3.684053000000	2.147849000000	0.945606000000
C	-1.450035000000	3.049877000000	0.635901000000
H	-3.175231000000	4.222327000000	1.223022000000
C	-2.824297000000	3.221673000000	0.960343000000
C	1.263020000000	2.837404000000	0.004331000000
H	2.331599000000	2.757378000000	-0.201659000000
C	0.726741000000	4.090555000000	0.348762000000
H	1.379599000000	4.966834000000	0.376935000000
C	-0.609145000000	4.196961000000	0.660271000000
H	-1.049830000000	5.158155000000	0.934894000000

C	0.491847000000	1.673324000000	-0.060025000000
C	2.527005000000	-1.384419000000	-2.210967000000
H	1.596935000000	-1.673177000000	-2.731032000000
H	3.351583000000	-1.508629000000	-2.934139000000
H	2.711382000000	-2.104531000000	-1.395170000000
C	4.177516000000	0.811158000000	-0.874426000000
H	4.966374000000	0.575614000000	-1.609966000000
H	4.290297000000	1.872704000000	-0.601156000000
H	4.366730000000	0.210665000000	0.030100000000
C	2.127719000000	1.534515000000	-3.080296000000
H	1.173219000000	1.261179000000	-3.559524000000
H	2.928935000000	1.431790000000	-3.832244000000
H	2.066295000000	2.596354000000	-2.796185000000
C	-3.730406000000	-2.733558000000	0.486063000000
H	-4.479506000000	-2.055775000000	0.925655000000
H	-4.278288000000	-3.560763000000	0.002126000000
H	-3.145089000000	-3.163101000000	1.316777000000
C	-1.502441000000	-3.241396000000	-1.522257000000
H	-2.145254000000	-3.965317000000	-2.052952000000
H	-0.787652000000	-2.844044000000	-2.263800000000
H	-0.934966000000	-3.815280000000	-0.770649000000
C	-3.613075000000	-1.119159000000	-2.166526000000
H	-2.949701000000	-0.702207000000	-2.942227000000
H	-4.270418000000	-0.307662000000	-1.819362000000
H	-4.246444000000	-1.889853000000	-2.638434000000

TS4

Energy (PCM(benzene)-[TPSSh/def2-TZVPP//TPSSh/def2-SVP])= -3343.65257972

Al	-3.130378000000	0.330455000000	-0.621973000000
Si	-4.641854000000	3.071919000000	-0.055951000000
Si	-2.808380000000	-2.757846000000	-1.107004000000
N	-3.552949000000	-1.400728000000	-0.220769000000
N	-4.640403000000	1.285872000000	-0.172543000000
C	-5.800761000000	-0.771040000000	0.679964000000
C	-5.827812000000	0.567442000000	0.126531000000

C	-7.068238000000	1.195635000000	-0.020687000000
H	-7.111126000000	2.164501000000	-0.520483000000
H	-9.196198000000	1.196010000000	0.378655000000
C	-8.257646000000	0.649010000000	0.500209000000
C	-7.007633000000	-1.273624000000	1.294595000000
H	-9.123770000000	-0.952866000000	1.653410000000
C	-8.223248000000	-0.541606000000	1.191334000000
C	-4.674571000000	-2.819434000000	1.402402000000
H	-3.777277000000	-3.439220000000	1.433139000000
C	-5.830395000000	-3.246370000000	2.085965000000
H	-5.804670000000	-4.180829000000	2.652533000000
C	-6.991126000000	-2.510163000000	1.999078000000
H	-7.914474000000	-2.855294000000	2.470313000000
C	-4.650352000000	-1.646784000000	0.643493000000
C	-1.946424000000	-1.981782000000	-2.602564000000
H	-2.679774000000	-1.584869000000	-3.325646000000
H	-1.351650000000	-2.749346000000	-3.128239000000
H	-1.250332000000	-1.166653000000	-2.338695000000
C	-1.519766000000	-3.739485000000	-0.125493000000
H	-1.059748000000	-4.501535000000	-0.778875000000
H	-1.947901000000	-4.267679000000	0.741159000000
H	-0.714997000000	-3.084410000000	0.243800000000
C	-4.142412000000	-3.930385000000	-1.746190000000
H	-4.886204000000	-3.381186000000	-2.346743000000
H	-3.683278000000	-4.698267000000	-2.392679000000
H	-4.680638000000	-4.447144000000	-0.937131000000
C	-5.540135000000	3.674694000000	1.491562000000
H	-6.634454000000	3.583002000000	1.436552000000
H	-5.297204000000	4.738936000000	1.655974000000
H	-5.201038000000	3.110462000000	2.376055000000
C	-2.824189000000	3.559319000000	0.121272000000
H	-2.698320000000	4.648545000000	0.236290000000
H	-2.255883000000	3.245815000000	-0.773321000000
H	-2.385389000000	3.073592000000	1.020819000000
C	-5.298171000000	3.930020000000	-1.611702000000

H	-4.672812000000	3.672602000000	-2.483383000000
H	-6.336443000000	3.660643000000	-1.861126000000
H	-5.261311000000	5.026084000000	-1.485028000000
C	-0.315655000000	1.034735000000	-0.669757000000
H	-0.757803000000	1.870298000000	-0.134923000000
C	1.106846000000	-0.959053000000	-0.552906000000
H	1.435892000000	-1.849061000000	-0.007221000000
C	0.229351000000	-0.081513000000	0.043708000000
H	-0.075629000000	-0.255422000000	1.079282000000
C	1.686349000000	-0.694535000000	-1.905815000000
H	1.893667000000	-1.601215000000	-2.495601000000
C	0.096624000000	1.218616000000	-2.043454000000
H	-0.341797000000	2.040465000000	-2.616409000000
C	0.993737000000	0.386366000000	-2.645358000000
H	1.248688000000	0.532790000000	-3.698576000000
Al	3.339956000000	-0.114955000000	-0.903588000000
Si	4.044059000000	2.923190000000	-1.245668000000
Si	5.265097000000	-2.581453000000	-0.910588000000
N	4.416212000000	-1.291253000000	-0.036006000000
N	3.727261000000	1.512918000000	-0.217121000000
C	4.413009000000	0.326344000000	1.907966000000
C	3.970420000000	1.508529000000	1.181507000000
C	3.769468000000	2.700114000000	1.883333000000
H	3.385391000000	3.561658000000	1.334183000000
H	3.849436000000	3.784416000000	3.755983000000
C	4.018163000000	2.824170000000	3.261850000000
C	4.659361000000	0.481137000000	3.328884000000
H	4.660465000000	1.802675000000	5.045728000000
C	4.459890000000	1.733153000000	3.974128000000
C	5.082294000000	-2.023734000000	2.168805000000
H	5.211839000000	-3.018445000000	1.739428000000
C	5.330975000000	-1.843043000000	3.540945000000
H	5.675857000000	-2.688910000000	4.141118000000
C	5.120042000000	-0.610967000000	4.115094000000
H	5.296410000000	-0.446976000000	5.180601000000

C	4.643610000000	-0.992940000000	1.332841000000
C	5.014049000000	-2.208339000000	-2.756265000000
H	5.298254000000	-1.176207000000	-3.028781000000
H	5.664706000000	-2.878640000000	-3.344494000000
H	3.982790000000	-2.385804000000	-3.103498000000
C	4.566272000000	-4.316446000000	-0.610938000000
H	5.047195000000	-5.039688000000	-1.292268000000
H	4.722532000000	-4.678999000000	0.417430000000
H	3.481400000000	-4.342217000000	-0.809457000000
C	7.118248000000	-2.539737000000	-0.555761000000
H	7.531049000000	-1.541933000000	-0.778348000000
H	7.639818000000	-3.273968000000	-1.193448000000
H	7.358276000000	-2.772626000000	0.492630000000
C	2.670143000000	4.225950000000	-1.247629000000
H	2.680575000000	4.858974000000	-0.345441000000
H	2.783404000000	4.894444000000	-2.118731000000
H	1.678913000000	3.748988000000	-1.313906000000
C	4.175692000000	2.225098000000	-3.005448000000
H	4.491019000000	3.025769000000	-3.696624000000
H	4.933795000000	1.425236000000	-3.082777000000
H	3.215167000000	1.838742000000	-3.385322000000
C	5.694587000000	3.718558000000	-0.794693000000
H	6.518775000000	2.994532000000	-0.903992000000
H	5.711844000000	4.090262000000	0.241324000000
H	5.899117000000	4.572009000000	-1.463752000000

INT5

Energy (PCM(benzene)-[TPSSh/def2-TZVPP//TPSSh/def2-SVP])=-3343.70287006

Al	-0.497361000000	2.417748000000	1.745099000000
Si	0.931349000000	4.997218000000	0.741876000000
Si	-2.915174000000	2.062704000000	3.677985000000
N	-1.161844000000	2.178436000000	3.415471000000
N	0.796122000000	3.676864000000	1.923218000000
C	1.027780000000	3.022048000000	4.353146000000
C	1.518358000000	3.668096000000	3.144750000000

C	2.766303000000	4.296639000000	3.175667000000
H	3.148430000000	4.732427000000	2.251196000000
H	4.524802000000	4.875315000000	4.297536000000
C	3.559394000000	4.364158000000	4.334895000000
C	1.870100000000	3.094037000000	5.531411000000
H	3.718793000000	3.806554000000	6.409237000000
C	3.119087000000	3.773669000000	5.496732000000
C	-0.559207000000	1.728034000000	5.710398000000
H	-1.484970000000	1.154800000000	5.781475000000
C	0.270207000000	1.820405000000	6.842136000000
H	-0.038816000000	1.344750000000	7.776452000000
C	1.466057000000	2.495076000000	6.756635000000
H	2.130660000000	2.577554000000	7.619711000000
C	-0.237728000000	2.315419000000	4.483636000000
C	-3.710254000000	2.509853000000	2.011051000000
H	-3.398250000000	3.506661000000	1.650742000000
H	-4.805286000000	2.554355000000	2.143222000000
H	-3.522105000000	1.777624000000	1.208880000000
C	-3.539829000000	0.340664000000	4.158742000000
H	-4.640539000000	0.305930000000	4.083703000000
H	-3.272510000000	0.060454000000	5.190293000000
H	-3.131705000000	-0.434504000000	3.489599000000
C	-3.487257000000	3.340787000000	4.943163000000
H	-3.202306000000	4.356795000000	4.623793000000
H	-4.586172000000	3.309497000000	5.039469000000
H	-3.055695000000	3.171657000000	5.941307000000
C	2.451003000000	4.910139000000	-0.385263000000
H	3.387499000000	5.166309000000	0.135585000000
H	2.337163000000	5.619090000000	-1.223628000000
H	2.575543000000	3.901277000000	-0.811907000000
C	-0.603173000000	4.849624000000	-0.368956000000
H	-0.631696000000	5.722225000000	-1.044488000000
H	-1.546222000000	4.870028000000	0.206529000000
H	-0.610242000000	3.955260000000	-1.013030000000
C	0.851931000000	6.674155000000	1.603954000000

H	-0.080167000000	6.766463000000	2.185499000000
H	1.693265000000	6.835602000000	2.294779000000
H	0.868002000000	7.484554000000	0.855065000000
C	-0.836108000000	1.266573000000	0.142589000000
H	-1.630085000000	1.706846000000	-0.491253000000
C	1.242164000000	0.084670000000	-0.669375000000
H	2.206713000000	0.160017000000	-1.181354000000
C	0.475050000000	1.190783000000	-0.595208000000
H	0.845513000000	2.107251000000	-1.065361000000
C	0.836108000000	-1.266573000000	-0.142589000000
H	1.630085000000	-1.706846000000	0.491253000000
C	-1.242164000000	-0.084670000000	0.669375000000
H	-2.206713000000	-0.160017000000	1.181354000000
C	-0.475050000000	-1.190783000000	0.595208000000
H	-0.845513000000	-2.107251000000	1.065361000000
Al	0.497361000000	-2.417748000000	-1.745099000000
Si	-0.931349000000	-4.997218000000	-0.741876000000
Si	2.915174000000	-2.062704000000	-3.677985000000
N	1.161844000000	-2.178436000000	-3.415471000000
N	-0.796122000000	-3.676864000000	-1.923218000000
C	-1.027780000000	-3.022048000000	-4.353146000000
C	-1.518358000000	-3.668096000000	-3.144750000000
C	-2.766303000000	-4.296639000000	-3.175667000000
H	-3.148430000000	-4.732427000000	-2.251196000000
H	-4.524802000000	-4.875315000000	-4.297536000000
C	-3.559394000000	-4.364158000000	-4.334895000000
C	-1.870100000000	-3.094037000000	-5.531411000000
H	-3.718793000000	-3.806554000000	-6.409237000000
C	-3.119087000000	-3.773669000000	-5.496732000000
C	0.559207000000	-1.728034000000	-5.710398000000
H	1.484970000000	-1.154800000000	-5.781475000000
C	-0.270207000000	-1.820405000000	-6.842136000000
H	0.038816000000	-1.344750000000	-7.776452000000
C	-1.466057000000	-2.495076000000	-6.756635000000
H	-2.130660000000	-2.577554000000	-7.619711000000

C	0.237728000000	-2.315419000000	-4.483636000000
C	3.710254000000	-2.509853000000	-2.011051000000
H	3.398250000000	-3.506661000000	-1.650742000000
H	4.805286000000	-2.554355000000	-2.143222000000
H	3.522105000000	-1.777624000000	-1.208880000000
C	3.539829000000	-0.340664000000	-4.158742000000
H	4.640539000000	-0.305930000000	-4.083703000000
H	3.272510000000	-0.060454000000	-5.190293000000
H	3.131705000000	0.434504000000	-3.489599000000
C	3.487257000000	-3.340787000000	-4.943163000000
H	3.202306000000	-4.356795000000	-4.623793000000
H	4.586172000000	-3.309497000000	-5.039469000000
H	3.055695000000	-3.171657000000	-5.941307000000
C	-2.451003000000	-4.910139000000	0.385263000000
H	-3.387499000000	-5.166309000000	-0.135585000000
H	-2.337163000000	-5.619090000000	1.223628000000
H	-2.575543000000	-3.901277000000	0.811907000000
C	0.603173000000	-4.849624000000	0.368956000000
H	0.631696000000	-5.722225000000	1.044488000000
H	1.546222000000	-4.870028000000	-0.206529000000
H	0.610242000000	-3.955260000000	1.013030000000
C	-0.851931000000	-6.674155000000	-1.603954000000
H	0.080167000000	-6.766463000000	-2.185499000000
H	-1.693265000000	-6.835602000000	-2.294779000000
H	-0.868002000000	-7.484554000000	-0.855065000000

3

Energy (PCM(benzene)-[TPSSh/def2-TZVPP//TPSSh/def2-SVP])= -3811.29514707

Al	0.099710000000	2.182164000000	2.309083000000
Si	1.007706000000	5.076680000000	1.154204000000
Si	-2.696585000000	2.256966000000	3.965336000000
O	1.509950000000	0.941646000000	2.907091000000
N	-0.929314000000	2.296279000000	3.842188000000
N	1.026374000000	3.780474000000	2.360757000000
C	1.084040000000	3.432812000000	4.859431000000

C	1.632677000000	3.979423000000	3.623352000000
C	2.829783000000	4.704385000000	3.685518000000
H	3.258057000000	5.066265000000	2.748761000000
H	4.432815000000	5.546118000000	4.873302000000
C	3.506999000000	4.964816000000	4.889881000000
C	1.808709000000	3.704747000000	6.086489000000
H	3.516578000000	4.656664000000	7.022624000000
C	3.006896000000	4.471966000000	6.074006000000
C	-0.540514000000	2.198418000000	6.229851000000
H	-1.433173000000	1.573819000000	6.293975000000
C	0.171693000000	2.488102000000	7.407083000000
H	-0.195177000000	2.111068000000	8.365491000000
C	1.332366000000	3.225704000000	7.338932000000
H	1.907420000000	3.458305000000	8.238350000000
C	-0.143081000000	2.649735000000	4.964184000000
C	-3.448776000000	2.518920000000	2.245877000000
H	-3.081672000000	3.442040000000	1.768227000000
H	-4.541826000000	2.622269000000	2.361274000000
H	-3.276310000000	1.680698000000	1.553274000000
C	-3.389820000000	0.604560000000	4.599170000000
H	-4.491023000000	0.600542000000	4.519911000000
H	-3.137137000000	0.403014000000	5.652919000000
H	-3.012685000000	-0.242701000000	4.001000000000
C	-3.322173000000	3.669865000000	5.053999000000
H	-2.979690000000	4.639503000000	4.655530000000
H	-4.425818000000	3.676334000000	5.059006000000
H	-2.979659000000	3.599529000000	6.097193000000
C	2.537013000000	5.089691000000	0.027051000000
H	3.465449000000	5.338943000000	0.566623000000
H	2.414512000000	5.835929000000	-0.777283000000
H	2.687281000000	4.107268000000	-0.452603000000
C	-0.497783000000	4.844035000000	0.026919000000
H	-0.551579000000	5.700823000000	-0.667093000000
H	-1.437928000000	4.829214000000	0.602666000000
H	-0.458235000000	3.932325000000	-0.588874000000

C	0.809709000000	6.765244000000	1.979975000000
H	-0.098722000000	6.781532000000	2.605025000000
H	1.659926000000	7.040007000000	2.621898000000
H	0.702712000000	7.545568000000	1.206751000000
C	-0.543332000000	1.293280000000	0.617747000000
H	-1.376852000000	1.927213000000	0.249688000000
C	1.048033000000	0.090452000000	-0.938407000000
H	1.866314000000	0.174938000000	-1.663523000000
C	0.545447000000	1.230665000000	-0.420367000000
H	0.970296000000	2.180550000000	-0.765444000000
C	2.909360000000	1.152092000000	2.553412000000
H	3.451607000000	1.401923000000	3.477404000000
H	2.885538000000	2.052359000000	1.926261000000
C	2.004178000000	-0.274551000000	5.021944000000
H	1.899240000000	0.651740000000	5.604681000000
H	1.617781000000	-1.106836000000	5.630829000000
H	3.071700000000	-0.469300000000	4.837920000000
C	1.193607000000	-0.214483000000	3.740360000000
H	0.125239000000	-0.089433000000	3.959216000000
H	1.320349000000	-1.114941000000	3.120238000000
C	3.523169000000	-0.024097000000	1.819448000000
H	2.936684000000	-0.270948000000	0.923085000000
H	4.540476000000	0.255893000000	1.504107000000
H	3.608849000000	-0.919761000000	2.453170000000
C	0.543332000000	-1.293280000000	-0.617747000000
H	1.376852000000	-1.927213000000	-0.249688000000
C	-1.048033000000	-0.090452000000	0.938407000000
H	-1.866314000000	-0.174938000000	1.663523000000
C	-0.545447000000	-1.230665000000	0.420367000000
H	-0.970296000000	-2.180550000000	0.765444000000
Al	-0.099710000000	-2.182164000000	-2.309083000000
Si	-1.007706000000	-5.076680000000	-1.154204000000
Si	2.696585000000	-2.256966000000	-3.965336000000
O	-1.509950000000	-0.941646000000	-2.907091000000
N	0.929314000000	-2.296279000000	-3.842188000000

N	-1.026374000000	-3.780474000000	-2.360757000000
C	-1.084040000000	-3.432812000000	-4.859431000000
C	-1.632677000000	-3.979423000000	-3.623352000000
C	-2.829783000000	-4.704385000000	-3.685518000000
H	-3.258057000000	-5.066265000000	-2.748761000000
H	-4.432815000000	-5.546118000000	-4.873302000000
C	-3.506999000000	-4.964816000000	-4.889881000000
C	-1.808709000000	-3.704747000000	-6.086489000000
H	-3.516578000000	-4.656664000000	-7.022624000000
C	-3.006896000000	-4.471966000000	-6.074006000000
C	0.540514000000	-2.198418000000	-6.229851000000
H	1.433173000000	-1.573819000000	-6.293975000000
C	-0.171693000000	-2.488102000000	-7.407083000000
H	0.195177000000	-2.111068000000	-8.365491000000
C	-1.332366000000	-3.225704000000	-7.338932000000
H	-1.907420000000	-3.458305000000	-8.238350000000
C	0.143081000000	-2.649735000000	-4.964184000000
C	3.448776000000	-2.518920000000	-2.245877000000
H	3.081672000000	-3.442040000000	-1.768227000000
H	4.541826000000	-2.622269000000	-2.361274000000
H	3.276310000000	-1.680698000000	-1.553274000000
C	3.389820000000	-0.604560000000	-4.599170000000
H	4.491023000000	-0.600542000000	-4.519911000000
H	3.137137000000	-0.403014000000	-5.652919000000
H	3.012685000000	0.242701000000	-4.001000000000
C	3.322173000000	-3.669865000000	-5.053999000000
H	2.979690000000	-4.639503000000	-4.655530000000
H	4.425818000000	-3.676334000000	-5.059006000000
H	2.979659000000	-3.599529000000	-6.097193000000
C	-2.537013000000	-5.089691000000	-0.027051000000
H	-3.465449000000	-5.338943000000	-0.566623000000
H	-2.414512000000	-5.835929000000	0.777283000000
H	-2.687281000000	-4.107268000000	0.452603000000
C	0.497783000000	-4.844035000000	-0.026919000000
H	0.551579000000	-5.700823000000	0.667093000000

H	1.437928000000	-4.829214000000	-0.602666000000
H	0.458235000000	-3.932325000000	0.588874000000
C	-0.809709000000	-6.765244000000	-1.979975000000
H	0.098722000000	-6.781532000000	-2.605025000000
H	-1.659926000000	-7.040007000000	-2.621898000000
H	-0.702712000000	-7.545568000000	-1.206751000000
C	-2.909360000000	-1.152092000000	-2.553412000000
H	-3.451607000000	-1.401923000000	-3.477404000000
H	-2.885538000000	-2.052359000000	-1.926261000000
C	-2.004178000000	0.274551000000	-5.021944000000
H	-1.899240000000	-0.651740000000	-5.604681000000
H	-1.617781000000	1.106836000000	-5.630829000000
H	-3.071700000000	0.469300000000	-4.837920000000
C	-1.193607000000	0.214483000000	-3.740360000000
H	-0.125239000000	0.089433000000	-3.959216000000
H	-1.320349000000	1.114941000000	-3.120238000000
C	-3.523169000000	0.024097000000	-1.819448000000
H	-2.936684000000	0.270948000000	-0.923085000000
H	-4.540476000000	-0.255893000000	-1.504107000000
H	-3.608849000000	0.919761000000	-2.453170000000

3A

Energy (PCM(benzene)-[TPSSh/def2-TZVPP//TPSSh/def2-SVP])= -3811.26954505

C	1.550593000000	0.097610000000	1.361260000000
C	-0.596471000000	-1.239002000000	1.277854000000
H	-1.064567000000	-2.228811000000	1.251002000000
C	0.749162000000	-1.178772000000	1.285403000000
H	1.299921000000	-2.126744000000	1.243484000000
C	-1.505769000000	-0.040761000000	1.363279000000
H	-1.959376000000	-0.087097000000	2.383053000000
C	0.642333000000	1.296575000000	1.313880000000
H	1.109969000000	2.286610000000	1.322355000000
C	-0.702923000000	1.237102000000	1.321582000000
H	-1.253300000000	2.185739000000	1.320074000000
Al	-3.313181000000	-0.016924000000	0.426370000000

Si	-3.716889000000	-3.020410000000	-0.754006000000
Si	-3.112955000000	2.221409000000	-1.894633000000
O	-4.358550000000	0.497024000000	2.088234000000
N	-4.016634000000	1.269145000000	-0.698997000000
N	-4.302155000000	-1.505658000000	-0.041602000000
C	-6.226387000000	0.100260000000	-0.338658000000
C	-5.688307000000	-1.216871000000	-0.023818000000
C	-6.576305000000	-2.238605000000	0.334706000000
H	-6.154541000000	-3.204033000000	0.623096000000
H	-8.616985000000	-2.905250000000	0.628575000000
C	-7.972436000000	-2.066483000000	0.352034000000
C	-7.667763000000	0.253027000000	-0.311801000000
H	-9.593014000000	-0.682127000000	0.035180000000
C	-8.511924000000	-0.840821000000	0.031386000000
C	-6.100422000000	2.466633000000	-0.984522000000
H	-5.499559000000	3.351984000000	-1.200362000000
C	-7.501788000000	2.582019000000	-0.980812000000
H	-7.963432000000	3.541478000000	-1.229302000000
C	-8.277228000000	1.495593000000	-0.641548000000
H	-9.367384000000	1.564739000000	-0.617930000000
C	-5.430008000000	1.272621000000	-0.686025000000
C	-1.463546000000	1.352421000000	-2.174085000000
H	-1.605023000000	0.368870000000	-2.650204000000
H	-0.833448000000	1.958142000000	-2.847551000000
H	-0.889884000000	1.204750000000	-1.244992000000
C	-2.740990000000	3.992124000000	-1.315484000000
H	-2.126265000000	4.517070000000	-2.067405000000
H	-3.649755000000	4.594815000000	-1.153540000000
H	-2.170147000000	3.987992000000	-0.371193000000
C	-4.013482000000	2.273559000000	-3.556999000000
H	-4.274200000000	1.253192000000	-3.884007000000
H	-3.341535000000	2.709030000000	-4.317001000000
H	-4.939400000000	2.867499000000	-3.546204000000
C	-3.399424000000	-4.360772000000	0.553363000000
H	-4.326192000000	-4.655053000000	1.074133000000

H	-2.978929000000	-5.269195000000	0.088011000000
H	-2.683682000000	-4.021197000000	1.321357000000
C	-2.097039000000	-2.657755000000	-1.659318000000
H	-1.618630000000	-3.601476000000	-1.973920000000
H	-2.298716000000	-2.068551000000	-2.569414000000
H	-1.359763000000	-2.105341000000	-1.056079000000
C	-4.912973000000	-3.691947000000	-2.055468000000
H	-5.210177000000	-2.894600000000	-2.756680000000
H	-5.831766000000	-4.130605000000	-1.639234000000
H	-4.397764000000	-4.476542000000	-2.636984000000
C	-4.567451000000	-0.535973000000	3.090830000000
H	-4.306772000000	-1.464349000000	2.562967000000
H	-3.834787000000	-0.369472000000	3.900193000000
C	-5.606095000000	2.565053000000	2.730211000000
H	-6.219369000000	2.464346000000	1.823849000000
H	-5.418702000000	3.637370000000	2.900967000000
H	-6.168557000000	2.182226000000	3.591870000000
C	-4.264812000000	1.875313000000	2.546726000000
H	-3.696337000000	2.381463000000	1.754075000000
H	-3.661476000000	1.877995000000	3.470872000000
C	-5.988309000000	-0.620668000000	3.621014000000
H	-6.244584000000	0.216865000000	4.284427000000
H	-6.079091000000	-1.548969000000	4.207259000000
H	-6.710123000000	-0.667071000000	2.793454000000
Al	3.354162000000	0.043763000000	0.429788000000
Si	3.055999000000	-1.952802000000	-2.091208000000
Si	3.900400000000	3.113866000000	-0.464348000000
O	4.340437000000	-0.710182000000	2.020168000000
N	4.422061000000	1.517033000000	0.104571000000
N	4.001509000000	-1.162634000000	-0.814130000000
C	6.265198000000	-0.146049000000	-0.343898000000
C	5.412736000000	-1.241585000000	-0.793670000000
C	6.023058000000	-2.441197000000	-1.183590000000
H	5.378683000000	-3.272757000000	-1.475438000000
H	7.830513000000	-3.585038000000	-1.516561000000

C	7.416835000000	-2.626830000000	-1.190783000000
C	7.697531000000	-0.371930000000	-0.333473000000
H	9.330167000000	-1.736103000000	-0.753088000000
C	8.244802000000	-1.611209000000	-0.767846000000
C	6.728468000000	2.102782000000	0.536628000000
H	6.353978000000	3.057199000000	0.913660000000
C	8.114340000000	1.862033000000	0.532941000000
H	8.798874000000	2.639645000000	0.882446000000
C	8.593737000000	0.644860000000	0.102199000000
H	9.665744000000	0.433707000000	0.089188000000
C	5.791678000000	1.162879000000	0.087999000000
C	2.294870000000	2.899855000000	-1.442243000000
H	2.508368000000	2.406910000000	-2.405454000000
H	1.853020000000	3.886514000000	-1.665402000000
H	1.523977000000	2.307937000000	-0.924623000000
C	3.597090000000	4.319652000000	0.969826000000
H	3.213886000000	5.285811000000	0.598144000000
H	4.524104000000	4.525182000000	1.531366000000
H	2.858644000000	3.923715000000	1.687563000000
C	5.144274000000	3.876515000000	-1.667655000000
H	5.448157000000	3.141034000000	-2.430834000000
H	4.656669000000	4.719262000000	-2.188519000000
H	6.058009000000	4.260525000000	-1.190737000000
C	2.595564000000	-3.750632000000	-1.684033000000
H	3.471601000000	-4.413911000000	-1.593854000000
H	1.948635000000	-4.165345000000	-2.476758000000
H	2.031626000000	-3.809395000000	-0.737388000000
C	1.452004000000	-0.979723000000	-2.270893000000
H	0.785534000000	-1.484544000000	-2.990461000000
H	1.640295000000	0.037101000000	-2.650935000000
H	0.895623000000	-0.894339000000	-1.323441000000
C	3.958056000000	-1.890213000000	-3.751795000000
H	4.250341000000	-0.854024000000	-3.990399000000
H	4.866329000000	-2.510086000000	-3.788233000000
H	3.277923000000	-2.240101000000	-4.547815000000

C	4.502388000000	-2.142466000000	2.211769000000
H	5.580116000000	-2.357287000000	2.258416000000
H	4.118065000000	-2.574023000000	1.278545000000
C	6.258171000000	-0.071994000000	3.470182000000
H	6.918097000000	-0.005819000000	2.593384000000
H	6.556262000000	0.712936000000	4.182554000000
H	6.407974000000	-1.042616000000	3.967378000000
C	4.810051000000	0.166503000000	3.083155000000
H	4.680537000000	1.173360000000	2.663565000000
H	4.131269000000	0.052654000000	3.944976000000
C	3.759741000000	-2.672108000000	3.426356000000
H	2.687325000000	-2.430517000000	3.379109000000
H	3.863144000000	-3.768263000000	3.449299000000
H	4.168054000000	-2.283266000000	4.371815000000
H	2.017729000000	0.116781000000	2.375845000000

3B

Energy (PCM(benzene)-[TPSSh/def2-TZVPP//TPSSh/def2-SVP])= -3811.27641286

C	1.564873000000	0.308682000000	1.419951000000
C	-0.627407000000	-0.941424000000	1.295758000000
H	-1.136318000000	-1.913402000000	1.304099000000
C	0.715024000000	-0.938399000000	1.403313000000
H	1.220432000000	-1.907436000000	1.495048000000
C	-1.474302000000	0.307771000000	1.183037000000
H	-1.893216000000	0.489605000000	2.203582000000
C	0.742519000000	1.506312000000	1.009209000000
H	1.269802000000	2.447846000000	0.811844000000
C	-0.599763000000	1.506085000000	0.897333000000
H	-1.092524000000	2.447512000000	0.632685000000
Al	-3.301636000000	0.101942000000	0.322751000000
Si	-3.024844000000	-2.376136000000	-1.726986000000
Si	-3.865579000000	2.912806000000	-1.224137000000
O	-4.285362000000	-0.216681000000	2.060502000000
N	-4.362493000000	1.476119000000	-0.314025000000
N	-3.958856000000	-1.339183000000	-0.634274000000

C	-6.216065000000	-0.233901000000	-0.389344000000
C	-5.371612000000	-1.400666000000	-0.617972000000
C	-5.991925000000	-2.645831000000	-0.788225000000
H	-5.355546000000	-3.523814000000	-0.914330000000
H	-7.808638000000	-3.816881000000	-0.908669000000
C	-7.387351000000	-2.818662000000	-0.762474000000
C	-7.649070000000	-0.443811000000	-0.328360000000
H	-9.292539000000	-1.850188000000	-0.483074000000
C	-8.206662000000	-1.737437000000	-0.526039000000
C	-6.659579000000	2.144446000000	0.047281000000
H	-6.276524000000	3.152082000000	0.225025000000
C	-8.046564000000	1.915406000000	0.108256000000
H	-8.723717000000	2.749191000000	0.312278000000
C	-8.535849000000	0.642579000000	-0.082772000000
H	-9.608956000000	0.439922000000	-0.046994000000
C	-5.733581000000	1.130714000000	-0.227257000000
C	-2.274692000000	2.492423000000	-2.160338000000
H	-2.498041000000	1.794488000000	-2.984595000000
H	-1.839843000000	3.404685000000	-2.604122000000
H	-1.499461000000	2.034201000000	-1.526497000000
C	-3.537697000000	4.404756000000	-0.098283000000
H	-3.169232000000	5.265552000000	-0.682878000000
H	-4.453406000000	4.728757000000	0.424578000000
H	-2.780941000000	4.179070000000	0.672177000000
C	-5.137764000000	3.390188000000	-2.538753000000
H	-5.444031000000	2.506777000000	-3.123153000000
H	-4.672463000000	4.109979000000	-3.234908000000
H	-6.048724000000	3.855491000000	-2.134358000000
C	-2.576206000000	-4.061450000000	-0.975337000000
H	-3.459975000000	-4.678764000000	-0.745391000000
H	-1.945308000000	-4.637254000000	-1.674865000000
H	-2.004001000000	-3.939837000000	-0.039851000000
C	-1.403915000000	-1.486053000000	-2.120862000000
H	-0.784438000000	-2.142965000000	-2.756524000000
H	-1.587696000000	-0.556965000000	-2.684341000000

H	-0.813985000000	-1.236943000000	-1.223506000000
C	-3.917309000000	-2.631039000000	-3.374977000000
H	-4.200783000000	-1.658621000000	-3.811064000000
H	-4.829824000000	-3.240517000000	-3.299333000000
H	-3.234698000000	-3.132058000000	-4.083385000000
C	-4.077365000000	-1.482919000000	2.750854000000
H	-3.331123000000	-2.016236000000	2.145472000000
H	-3.624361000000	-1.253018000000	3.729869000000
C	-5.957857000000	0.924139000000	3.519529000000
H	-6.732561000000	0.765561000000	2.755888000000
H	-6.134054000000	1.904734000000	3.989403000000
H	-6.052489000000	0.159594000000	4.304345000000
C	-4.577198000000	0.943710000000	2.890422000000
H	-4.482622000000	1.789293000000	2.195400000000
H	-3.780590000000	1.017014000000	3.651736000000
C	-5.336319000000	-2.322395000000	2.876934000000
H	-6.085019000000	-1.863154000000	3.535612000000
H	-5.059070000000	-3.299048000000	3.305544000000
H	-5.787825000000	-2.492780000000	1.889761000000
Al	3.343968000000	0.125642000000	0.506005000000
Si	4.695424000000	2.959879000000	1.372771000000
Si	4.507060000000	-2.403232000000	2.202547000000
O	2.910098000000	-0.121228000000	-1.398558000000
N	4.451375000000	-1.328426000000	0.793475000000
N	4.569812000000	1.505444000000	0.366599000000
C	6.022395000000	-0.186414000000	-0.820166000000
C	5.596353000000	1.183276000000	-0.553288000000
C	6.206637000000	2.222440000000	-1.267910000000
H	5.848070000000	3.239437000000	-1.098848000000
H	7.678962000000	2.867442000000	-2.718433000000
C	7.236914000000	2.011657000000	-2.201158000000
C	7.075303000000	-0.378495000000	-1.799627000000
H	8.459824000000	0.539839000000	-3.192383000000
C	7.665379000000	0.730787000000	-2.466996000000
C	5.997091000000	-2.628584000000	-0.541257000000

H	5.555812000000	-3.516652000000	-0.085252000000
C	7.027105000000	-2.787873000000	-1.485173000000
H	7.387814000000	-3.791546000000	-1.725747000000
C	7.557854000000	-1.681069000000	-2.109038000000
H	8.355301000000	-1.778377000000	-2.849593000000
C	5.486394000000	-1.377583000000	-0.170459000000
C	3.565837000000	-1.610188000000	3.642157000000
H	3.947808000000	-0.603781000000	3.880081000000
H	3.717876000000	-2.237356000000	4.537966000000
H	2.479476000000	-1.538280000000	3.479718000000
C	3.701486000000	-4.099273000000	1.905568000000
H	3.661311000000	-4.670512000000	2.849524000000
H	4.248285000000	-4.715340000000	1.173057000000
H	2.665454000000	-3.993273000000	1.540511000000
C	6.288611000000	-2.642838000000	2.788437000000
H	6.752665000000	-1.667167000000	3.009862000000
H	6.295684000000	-3.239431000000	3.717016000000
H	6.926253000000	-3.154944000000	2.052533000000
C	4.008446000000	4.525705000000	0.542781000000
H	4.593652000000	4.845002000000	-0.335054000000
H	4.007333000000	5.365462000000	1.259511000000
H	2.966822000000	4.376246000000	0.209965000000
C	3.688095000000	2.714102000000	2.957152000000
H	3.870387000000	3.578860000000	3.618788000000
H	3.997993000000	1.810678000000	3.507728000000
H	2.601427000000	2.660806000000	2.789043000000
C	6.485561000000	3.253495000000	1.905081000000
H	6.877542000000	2.367451000000	2.431940000000
H	7.162755000000	3.467245000000	1.064775000000
H	6.529284000000	4.108286000000	2.601953000000
C	2.848075000000	1.009246000000	-2.317594000000
H	3.622091000000	0.857578000000	-3.083967000000
H	3.154580000000	1.862093000000	-1.698581000000
C	3.445195000000	-1.803248000000	-3.154035000000
H	4.520628000000	-1.702816000000	-2.948375000000

H	3.242957000000	-2.855702000000	-3.407439000000
H	3.183725000000	-1.197130000000	-4.034860000000
C	2.614816000000	-1.446795000000	-1.934996000000
H	2.844329000000	-2.118716000000	-1.097335000000
H	1.534829000000	-1.490312000000	-2.139151000000
C	1.468773000000	1.212466000000	-2.911430000000
H	0.714034000000	1.323424000000	-2.120044000000
H	1.478487000000	2.134462000000	-3.513595000000
H	1.168642000000	0.386703000000	-3.573970000000
H	1.890163000000	0.475191000000	2.472006000000

3C

Energy (PCM(benzene)-[TPSSh/def2-TZVPP//TPSSh/def2-SVP])= -3811.28132735

C	-1.526818000000	0.068536000000	-1.392839000000
C	0.700807000000	-1.101266000000	-1.197937000000
H	1.245343000000	-2.044138000000	-1.056024000000
C	-0.644907000000	-1.141474000000	-1.171288000000
H	-1.127046000000	-2.112379000000	-1.005445000000
C	1.505544000000	0.161518000000	-1.416200000000
H	1.832470000000	0.176460000000	-2.480087000000
C	-0.720712000000	1.334811000000	-1.203818000000
H	-1.262461000000	2.280836000000	-1.073647000000
C	0.626662000000	1.375598000000	-1.208535000000
H	1.111644000000	2.351289000000	-1.082703000000
Al	3.270061000000	0.074588000000	-0.459357000000
Si	4.494918000000	2.957220000000	-1.274070000000
Si	4.596002000000	-2.429928000000	-2.070076000000
O	2.694462000000	-0.330790000000	1.399080000000
N	4.471632000000	-1.313364000000	-0.695659000000
N	4.399752000000	1.518689000000	-0.239382000000
C	5.915588000000	-0.085535000000	0.979791000000
C	5.417888000000	1.256578000000	0.705529000000
C	5.951903000000	2.329754000000	1.431309000000
H	5.542889000000	3.325413000000	1.247971000000
H	7.347214000000	3.055858000000	2.919204000000

C	6.966261000000	2.176896000000	2.392326000000
C	6.949178000000	-0.218800000000	1.989593000000
H	8.239096000000	0.774579000000	3.420607000000
C	7.455980000000	0.921303000000	2.672980000000
C	6.049111000000	-2.521227000000	0.689573000000
H	5.683973000000	-3.432674000000	0.213426000000
C	7.054252000000	-2.624051000000	1.667755000000
H	7.466375000000	-3.605987000000	1.915332000000
C	7.498268000000	-1.491441000000	2.311684000000
H	8.277093000000	-1.544529000000	3.076144000000
C	5.475404000000	-1.301749000000	0.304262000000
C	3.576276000000	-1.763084000000	-3.517909000000
H	3.851270000000	-0.730670000000	-3.789103000000
H	3.780694000000	-2.397101000000	-4.398261000000
H	2.489822000000	-1.798622000000	-3.341340000000
C	3.910865000000	-4.169106000000	-1.719649000000
H	3.899128000000	-4.759441000000	-2.652580000000
H	4.499728000000	-4.737472000000	-0.981548000000
H	2.871641000000	-4.120666000000	-1.351107000000
C	6.387595000000	-2.556248000000	-2.658932000000
H	6.767863000000	-1.559828000000	-2.939650000000
H	6.442225000000	-3.203199000000	-3.551378000000
H	7.067274000000	-2.969845000000	-1.898927000000
C	3.642882000000	4.479320000000	-0.522163000000
H	4.139754000000	4.837083000000	0.394678000000
H	3.641129000000	5.314816000000	-1.243680000000
H	2.592051000000	4.262375000000	-0.264712000000
C	3.639236000000	2.597094000000	-2.924844000000
H	3.788673000000	3.466304000000	-3.588923000000
H	4.085196000000	1.722897000000	-3.427764000000
H	2.553627000000	2.434167000000	-2.848784000000
C	6.291059000000	3.373883000000	-1.693181000000
H	6.793582000000	2.497965000000	-2.136438000000
H	6.886611000000	3.695609000000	-0.826216000000
H	6.311209000000	4.187484000000	-2.438884000000

C	1.853362000000	0.645504000000	2.079493000000
H	1.335243000000	1.197183000000	1.280846000000
H	1.093109000000	0.076028000000	2.636649000000
C	3.302501000000	-1.850738000000	3.264294000000
H	4.351781000000	-1.525143000000	3.223152000000
H	3.283988000000	-2.916689000000	3.540969000000
H	2.777969000000	-1.292418000000	4.055035000000
C	2.636912000000	-1.695585000000	1.911031000000
H	3.153054000000	-2.288762000000	1.146285000000
H	1.573317000000	-1.987587000000	1.929603000000
C	2.644406000000	1.575535000000	2.978597000000
H	3.144090000000	1.034180000000	3.793946000000
H	1.954624000000	2.312294000000	3.421323000000
H	3.409011000000	2.113038000000	2.402047000000
Al	-3.290985000000	0.024352000000	-0.443159000000
Si	-4.799442000000	2.498433000000	-1.918832000000
Si	-4.325801000000	-2.895709000000	-1.436260000000
O	-2.821566000000	0.316992000000	1.463690000000
N	-4.293229000000	-1.522248000000	-0.313123000000
N	-4.607244000000	1.315772000000	-0.608662000000
C	-5.926180000000	-0.119969000000	1.002224000000
C	-5.614214000000	1.160714000000	0.374567000000
C	-6.315904000000	2.296369000000	0.801093000000
H	-6.049873000000	3.258917000000	0.361241000000
H	-7.836958000000	3.179908000000	2.062346000000
C	-7.322107000000	2.257010000000	1.782210000000
C	-6.952926000000	-0.130161000000	2.027440000000
H	-8.405741000000	1.008511000000	3.164975000000
C	-7.634286000000	1.063778000000	2.393282000000
C	-5.702425000000	-2.541770000000	1.368928000000
H	-5.195319000000	-3.481288000000	1.141228000000
C	-6.704532000000	-2.526361000000	2.355354000000
H	-6.978765000000	-3.455969000000	2.861284000000
C	-7.320067000000	-1.338947000000	2.683072000000
H	-8.100972000000	-1.299928000000	3.446270000000

C	-5.303035000000	-1.395600000000	0.669012000000
C	-3.510935000000	-2.388835000000	-3.068204000000
H	-3.994958000000	-1.500255000000	-3.506317000000
H	-3.634700000000	-3.216064000000	-3.788724000000
H	-2.431191000000	-2.190657000000	-2.988033000000
C	-3.390099000000	-4.423191000000	-0.801744000000
H	-3.351516000000	-5.197796000000	-1.587429000000
H	-3.864015000000	-4.878091000000	0.083627000000
H	-2.349000000000	-4.177383000000	-0.531254000000
C	-6.107912000000	-3.376810000000	-1.843072000000
H	-6.658362000000	-2.508731000000	-2.242609000000
H	-6.109989000000	-4.163982000000	-2.616732000000
H	-6.667709000000	-3.755022000000	-0.974647000000
C	-4.255209000000	4.258122000000	-1.447138000000
H	-4.889993000000	4.727013000000	-0.677836000000
H	-4.283353000000	4.910618000000	-2.337251000000
H	-3.217507000000	4.263460000000	-1.070746000000
C	-3.708525000000	1.996394000000	-3.380960000000
H	-3.937820000000	2.671373000000	-4.223936000000
H	-3.910476000000	0.968179000000	-3.723072000000
H	-2.629917000000	2.088892000000	-3.179526000000
C	-6.584130000000	2.520668000000	-2.541107000000
H	-6.880208000000	1.514951000000	-2.883431000000
H	-7.310013000000	2.839386000000	-1.778274000000
H	-6.670053000000	3.208738000000	-3.399702000000
C	-2.922932000000	1.626688000000	2.092983000000
H	-3.671160000000	1.556834000000	2.895598000000
H	-3.339953000000	2.261642000000	1.301742000000
C	-3.156010000000	-0.947551000000	3.582664000000
H	-4.237513000000	-1.006040000000	3.393258000000
H	-2.843314000000	-1.887198000000	4.064266000000
H	-2.953077000000	-0.130167000000	4.291398000000
C	-2.381242000000	-0.802082000000	2.285712000000
H	-2.539651000000	-1.675155000000	1.638338000000
H	-1.299361000000	-0.685699000000	2.459549000000

C	-1.589366000000	2.154314000000	2.585765000000
H	-0.858411000000	2.192508000000	1.764767000000
H	-1.736592000000	3.176585000000	2.967713000000
H	-1.175817000000	1.551320000000	3.409081000000
H	-1.852816000000	0.041060000000	-2.457520000000

6

Energy (PCM(benzene)-[TPSSh/def2-TZVPP//TPSSh/def2-SVP])= -2391.56838432

Al	0.570718000000	-0.321782000000	-0.115171000000
Si	2.212144000000	-2.684611000000	-1.449955000000
Si	0.856490000000	2.322475000000	-1.993849000000
N	1.208893000000	1.341229000000	-0.559641000000
N	2.082999000000	-1.362219000000	-0.273630000000
C	3.346251000000	0.632005000000	0.600691000000
C	3.236055000000	-0.790759000000	0.317503000000
C	4.289912000000	-1.631797000000	0.689548000000
H	4.185769000000	-2.701114000000	0.503735000000
H	6.234457000000	-1.869311000000	1.609802000000
C	5.445791000000	-1.162069000000	1.339767000000
C	4.531566000000	1.087130000000	1.299855000000
H	6.441465000000	0.555769000000	2.177355000000
C	5.561436000000	0.172929000000	1.655241000000
C	2.597876000000	2.970949000000	0.568549000000
H	1.838180000000	3.707132000000	0.303588000000
C	3.748746000000	3.387195000000	1.262686000000
H	3.872797000000	4.443574000000	1.515112000000
C	4.703734000000	2.462112000000	1.619481000000
H	5.609989000000	2.763301000000	2.150385000000
C	2.375364000000	1.639120000000	0.203490000000
C	-0.305124000000	1.281171000000	-3.058513000000
H	0.171199000000	0.345183000000	-3.396500000000
H	-0.601610000000	1.839314000000	-3.962743000000
H	-1.234509000000	1.033733000000	-2.518912000000
C	-0.024053000000	3.971049000000	-1.682396000000
H	-0.308713000000	4.415206000000	-2.652674000000

H	0.605716000000	4.708095000000	-1.158956000000
H	-0.946203000000	3.827557000000	-1.097524000000
C	2.457364000000	2.655407000000	-2.938642000000
H	2.957072000000	1.711420000000	-3.211979000000
H	2.246849000000	3.213658000000	-3.867048000000
H	3.168267000000	3.248989000000	-2.342263000000
C	2.665883000000	-4.404207000000	-0.781828000000
H	3.733877000000	-4.495060000000	-0.526175000000
H	2.457547000000	-5.151508000000	-1.567795000000
H	2.079722000000	-4.686914000000	0.106771000000
C	0.499960000000	-2.852500000000	-2.244542000000
H	0.531304000000	-3.641991000000	-3.015444000000
H	0.174286000000	-1.927575000000	-2.750518000000
H	-0.277730000000	-3.132747000000	-1.515180000000
C	3.477110000000	-2.225897000000	-2.776021000000
H	3.184664000000	-1.300274000000	-3.298755000000
H	4.473697000000	-2.059476000000	-2.336042000000
H	3.569716000000	-3.029228000000	-3.526798000000
N	-2.320410000000	-0.743153000000	0.847031000000
C	-2.010178000000	-1.909370000000	2.852187000000
H	-2.185169000000	-2.859883000000	3.379579000000
H	-2.028580000000	-1.105569000000	3.606709000000
C	-3.217527000000	2.626031000000	3.043523000000
H	-3.455851000000	3.647750000000	2.706471000000
H	-2.783393000000	2.706635000000	4.053315000000
H	-4.166233000000	2.073095000000	3.120435000000
C	-0.945455000000	-0.956858000000	0.910029000000
C	-0.648768000000	-1.882779000000	2.113829000000
C	-3.093486000000	-1.621773000000	1.796740000000
C	-3.574783000000	-2.928364000000	1.129550000000
H	-3.907777000000	-3.632995000000	1.908267000000
H	-2.774404000000	-3.411013000000	0.552780000000
H	-4.425876000000	-2.750026000000	0.459883000000
C	-4.309816000000	-0.907017000000	2.390989000000
H	-5.023202000000	-0.607990000000	1.607572000000

H	-4.020474000000	-0.012213000000	2.956898000000
H	-4.830140000000	-1.591818000000	3.078742000000
C	-0.173638000000	-3.294100000000	1.708912000000
H	-0.887819000000	-3.805976000000	1.048781000000
H	-0.026737000000	-3.920535000000	2.605170000000
H	0.788681000000	-3.222343000000	1.182769000000
C	0.439353000000	-1.265093000000	3.019902000000
H	0.583549000000	-1.876393000000	3.927540000000
H	0.165664000000	-0.244915000000	3.331360000000
H	1.412270000000	-1.220275000000	2.501451000000
C	-2.899207000000	0.368151000000	0.140147000000
C	-3.537334000000	0.177733000000	-1.116368000000
C	-4.078660000000	1.295295000000	-1.774147000000
H	-4.570982000000	1.157149000000	-2.740205000000
C	-4.000792000000	2.571805000000	-1.223297000000
H	-4.426130000000	3.427571000000	-1.753374000000
C	-3.383507000000	2.748401000000	0.014340000000
H	-3.337935000000	3.748789000000	0.452285000000
C	-2.830962000000	1.668452000000	0.719935000000
C	-2.217460000000	1.940763000000	2.092067000000
H	-1.944410000000	0.968297000000	2.526590000000
C	-0.930750000000	2.778414000000	1.996024000000
H	-0.198525000000	2.316977000000	1.318901000000
H	-0.468611000000	2.883342000000	2.991029000000
H	-1.147143000000	3.792773000000	1.621032000000
C	-3.701349000000	-1.191637000000	-1.768793000000
H	-3.143976000000	-1.911936000000	-1.154770000000
C	-5.185782000000	-1.607740000000	-1.792710000000
H	-5.762887000000	-0.957943000000	-2.470861000000
H	-5.650809000000	-1.536857000000	-0.797474000000
H	-5.293022000000	-2.644736000000	-2.150789000000
C	-3.124046000000	-1.261897000000	-3.193004000000
H	-3.248550000000	-2.279029000000	-3.598568000000
H	-2.053219000000	-1.019521000000	-3.210394000000
H	-3.639066000000	-0.567609000000	-3.876747000000

6-Et₂O

Energy (PCM(benzene)-[TPSSh/def2-TZVPP//TPSSh/def2-SVP])= -2625.31807256

Al	0.501852000000	0.374048000000	0.144552000000
Si	2.962130000000	2.694794000000	0.713820000000
Si	1.596521000000	-1.347005000000	2.685051000000
N	1.225677000000	-1.163309000000	0.954321000000
N	2.141156000000	1.314821000000	-0.069725000000
C	3.093060000000	-0.940689000000	-0.733705000000
C	3.010277000000	0.505576000000	-0.859995000000
C	3.808879000000	1.129330000000	-1.826211000000
H	3.690465000000	2.206320000000	-1.967731000000
H	5.363162000000	0.984620000000	-3.329885000000
C	4.752217000000	0.435301000000	-2.608415000000
C	4.066419000000	-1.638405000000	-1.546618000000
H	5.617491000000	-1.487477000000	-3.057362000000
C	4.889308000000	-0.927654000000	-2.465303000000
C	2.440266000000	-3.118236000000	0.186131000000
H	1.767931000000	-3.704217000000	0.813236000000
C	3.424995000000	-3.774344000000	-0.578022000000
H	3.532073000000	-4.859777000000	-0.502407000000
C	4.221003000000	-3.048852000000	-1.437366000000
H	4.976332000000	-3.540065000000	-2.055846000000
C	2.252243000000	-1.732485000000	0.144893000000
C	0.332793000000	-0.371600000000	3.697381000000
H	0.210321000000	0.665381000000	3.347333000000
H	0.664026000000	-0.329639000000	4.748994000000
H	-0.659010000000	-0.849512000000	3.680917000000
C	1.610637000000	-3.116430000000	3.381305000000
H	1.657648000000	-3.040050000000	4.482796000000
H	2.506219000000	-3.669689000000	3.056931000000
H	0.725558000000	-3.717590000000	3.128307000000
C	3.346723000000	-0.719487000000	3.043264000000
H	3.492171000000	0.328455000000	2.746635000000
H	3.575107000000	-0.806456000000	4.119697000000

S78

H	4.085909000000	-1.327847000000	2.495850000000
C	2.601777000000	4.355655000000	-0.136485000000
H	2.911298000000	4.342539000000	-1.195199000000
H	3.171344000000	5.158234000000	0.364608000000
H	1.537751000000	4.637768000000	-0.105273000000
C	2.525785000000	2.870967000000	2.568848000000
H	3.438145000000	2.697821000000	3.163579000000
H	1.767742000000	2.162089000000	2.929303000000
H	2.170980000000	3.888105000000	2.804540000000
C	4.847900000000	2.487511000000	0.727884000000
H	5.141769000000	1.486216000000	1.083459000000
H	5.338367000000	2.654993000000	-0.241445000000
H	5.251379000000	3.227969000000	1.441606000000
N	-2.610427000000	0.583198000000	0.552513000000
C	-3.036332000000	2.832947000000	1.047020000000
H	-3.180328000000	3.563300000000	1.858610000000
H	-3.650520000000	3.172231000000	0.196520000000
C	-5.500021000000	1.353151000000	-2.343637000000
H	-5.866060000000	0.731770000000	-3.176805000000
H	-5.680053000000	2.406675000000	-2.613157000000
H	-6.113611000000	1.113891000000	-1.463320000000
C	-1.333237000000	1.190894000000	0.389379000000
C	-1.547608000000	2.712246000000	0.627721000000
C	-3.477083000000	1.416811000000	1.457400000000
C	-3.134269000000	1.146603000000	2.936808000000
H	-3.605681000000	1.908802000000	3.578240000000
H	-2.049916000000	1.175399000000	3.102689000000
H	-3.504113000000	0.162958000000	3.258903000000
C	-4.976124000000	1.190398000000	1.262208000000
H	-5.256295000000	0.142231000000	1.445619000000
H	-5.308122000000	1.465227000000	0.254821000000
H	-5.526914000000	1.817216000000	1.980834000000
C	-0.637211000000	3.301621000000	1.712435000000
H	-0.783230000000	2.817578000000	2.688748000000
H	-0.823405000000	4.382043000000	1.835854000000

H	0.415652000000	3.184224000000	1.432105000000
C	-1.285133000000	3.496135000000	-0.678539000000
H	-1.483687000000	4.573515000000	-0.537039000000
H	-1.926320000000	3.136726000000	-1.496777000000
H	-0.236037000000	3.387396000000	-0.996197000000
C	-3.145754000000	-0.504991000000	-0.228191000000
C	-3.141464000000	-1.831516000000	0.288104000000
C	-3.618297000000	-2.887827000000	-0.506862000000
H	-3.602832000000	-3.903735000000	-0.104893000000
C	-4.115872000000	-2.668684000000	-1.787571000000
H	-4.474960000000	-3.503567000000	-2.394630000000
C	-4.184265000000	-1.363428000000	-2.269004000000
H	-4.622235000000	-1.181019000000	-3.254178000000
C	-3.733606000000	-0.269889000000	-1.511893000000
C	-3.993526000000	1.116856000000	-2.099708000000
H	-3.639121000000	1.854519000000	-1.367366000000
C	-3.250334000000	1.368010000000	-3.421158000000
H	-2.164897000000	1.270262000000	-3.299895000000
H	-3.458213000000	2.384928000000	-3.791415000000
H	-3.568662000000	0.657601000000	-4.201615000000
C	-2.688373000000	-2.161326000000	1.702846000000
H	-2.201829000000	-1.260538000000	2.102864000000
C	-3.900026000000	-2.500516000000	2.593998000000
H	-4.389610000000	-3.427945000000	2.253402000000
H	-4.658163000000	-1.703036000000	2.581746000000
H	-3.580391000000	-2.652851000000	3.637966000000
C	-1.670505000000	-3.309340000000	1.746741000000
H	-1.384898000000	-3.512273000000	2.790257000000
H	-0.759311000000	-3.052568000000	1.187064000000
H	-2.088359000000	-4.243728000000	1.338201000000
O	0.408489000000	-0.283266000000	-1.759578000000
C	0.555555000000	0.732471000000	-2.791466000000
H	1.146461000000	1.515210000000	-2.299796000000
H	-0.445342000000	1.135564000000	-3.002310000000
C	1.240460000000	0.261484000000	-4.060403000000

H	0.609496000000	-0.416081000000	-4.654100000000
H	2.200116000000	-0.225898000000	-3.838088000000
H	1.444583000000	1.149368000000	-4.679996000000
C	-0.397507000000	-1.456735000000	-2.084446000000
H	-1.245264000000	-1.116868000000	-2.698405000000
H	-0.799040000000	-1.789725000000	-1.119132000000
C	0.374040000000	-2.587650000000	-2.743657000000
H	0.690480000000	-2.353202000000	-3.767925000000
H	1.256661000000	-2.863252000000	-2.151652000000
H	-0.294894000000	-3.462365000000	-2.789197000000

D1⁻

Energy (PCM(benzene)-[TPSSh/def2-TZVPP//TPSSh/def2-SVP])= -3578.96014364

Al	1.354447000000	-0.008648000000	0.039555000000
Si	2.147584000000	2.891208000000	1.333091000000
Si	1.990257000000	-2.213735000000	2.346490000000
O	2.070977000000	-0.361128000000	-1.877463000000
N	2.411979000000	-1.323822000000	0.893116000000
N	2.505955000000	1.454880000000	0.380810000000
C	4.465400000000	-0.118376000000	0.086422000000
C	3.872373000000	1.206350000000	0.061574000000
C	4.671251000000	2.293795000000	-0.358981000000
H	4.202821000000	3.276692000000	-0.430166000000
H	6.589848000000	3.034087000000	-1.021171000000
C	6.016879000000	2.153126000000	-0.714568000000
C	5.860018000000	-0.248570000000	-0.311069000000
H	7.659063000000	0.765826000000	-0.975208000000
C	6.610902000000	0.898821000000	-0.692463000000
C	4.439468000000	-2.568895000000	0.392564000000
H	3.868391000000	-3.474071000000	0.617097000000
C	5.784222000000	-2.671028000000	0.024386000000
H	6.266615000000	-3.653024000000	-0.008792000000
C	6.491961000000	-1.524958000000	-0.320546000000
H	7.543473000000	-1.581192000000	-0.616142000000
C	3.765625000000	-1.328945000000	0.474074000000

C	0.990964000000	-1.056196000000	3.466214000000
H	1.660540000000	-0.269615000000	3.854139000000
H	0.551594000000	-1.583248000000	4.331448000000
H	0.178058000000	-0.558894000000	2.916949000000
C	0.977804000000	-3.781202000000	1.989584000000
H	0.622030000000	-4.261136000000	2.918899000000
H	1.587875000000	-4.521026000000	1.442963000000
H	0.100657000000	-3.554436000000	1.361735000000
C	3.490395000000	-2.705731000000	3.399844000000
H	4.191538000000	-1.860341000000	3.496819000000
H	3.132798000000	-2.969699000000	4.411957000000
H	4.057776000000	-3.561970000000	3.005868000000
C	2.053246000000	4.550764000000	0.392844000000
H	3.041045000000	4.924691000000	0.077198000000
H	1.608898000000	5.317842000000	1.052366000000
H	1.417592000000	4.480131000000	-0.504584000000
C	0.458707000000	2.681712000000	2.156985000000
H	0.212923000000	3.587235000000	2.739344000000
H	0.468047000000	1.826530000000	2.850111000000
H	-0.350469000000	2.518898000000	1.426894000000
C	3.422652000000	3.103332000000	2.721509000000
H	3.446802000000	2.205084000000	3.361315000000
H	4.439408000000	3.258058000000	2.327760000000
H	3.163396000000	3.969477000000	3.355927000000
C	2.655918000000	0.693267000000	-2.692829000000
H	3.747682000000	0.566052000000	-2.671630000000
H	2.421888000000	1.611656000000	-2.142416000000
C	3.675055000000	-2.019308000000	-2.880515000000
H	4.471322000000	-1.731727000000	-2.181127000000
H	3.746780000000	-3.107536000000	-3.036568000000
H	3.848480000000	-1.534069000000	-3.853374000000
C	2.290855000000	-1.735403000000	-2.321929000000
H	2.110782000000	-2.329438000000	-1.415974000000
H	1.510666000000	-1.969961000000	-3.062125000000
C	2.125076000000	0.750731000000	-4.115740000000

H	1.046027000000	0.949959000000	-4.146275000000
H	2.640147000000	1.575903000000	-4.634041000000
H	2.325412000000	-0.172108000000	-4.680833000000
Al	-1.354500000000	-0.008753000000	-0.039610000000
Si	-2.148386000000	2.890931000000	-1.333408000000
Si	-1.989915000000	-2.213323000000	-2.346777000000
O	-2.070497000000	-0.361069000000	1.877652000000
N	-2.411861000000	-1.323904000000	-0.893147000000
N	-2.506092000000	1.454808000000	-0.380588000000
C	-4.465351000000	-0.118713000000	-0.086217000000
C	-3.872424000000	1.206031000000	-0.061102000000
C	-4.671270000000	2.293331000000	0.359921000000
H	-4.202801000000	3.276192000000	0.431347000000
H	-6.589812000000	3.033346000000	1.022593000000
C	-6.016843000000	2.152514000000	0.715626000000
C	-5.859941000000	-0.249070000000	0.311386000000
H	-7.658947000000	0.765062000000	0.975990000000
C	-6.610820000000	0.898182000000	0.693179000000
C	-4.439331000000	-2.569174000000	-0.392945000000
H	-3.868229000000	-3.474259000000	-0.617757000000
C	-5.784040000000	-2.671454000000	-0.024674000000
H	-6.266402000000	-3.653470000000	0.008298000000
C	-6.491804000000	-1.525492000000	0.320610000000
H	-7.543282000000	-1.581859000000	0.616302000000
C	-3.765556000000	-1.329163000000	-0.474170000000
C	-0.990355000000	-1.055585000000	-3.466105000000
H	-1.659890000000	-0.268918000000	-3.853913000000
H	-0.551153000000	-1.582611000000	-4.331448000000
H	-0.177327000000	-0.558478000000	-2.916856000000
C	-0.977789000000	-3.781006000000	-1.989943000000
H	-0.622354000000	-4.261390000000	-2.919149000000
H	-1.587920000000	-4.520440000000	-1.442867000000
H	-0.100434000000	-3.554256000000	-1.362369000000
C	-3.490000000000	-2.704831000000	-3.400429000000
H	-4.191266000000	-1.859505000000	-3.497012000000

H	-3.132403000000	-2.968349000000	-4.412660000000
H	-4.057257000000	-3.561320000000	-3.006806000000
C	-2.054296000000	4.550907000000	-0.393874000000
H	-3.042017000000	4.924352000000	-0.077424000000
H	-1.611072000000	5.317975000000	-1.054167000000
H	-1.417703000000	4.481073000000	0.502955000000
C	-0.459418000000	2.681554000000	-2.157051000000
H	-0.212759000000	3.587438000000	-2.738452000000
H	-0.468669000000	1.826868000000	-2.850769000000
H	0.349053000000	2.517779000000	-1.426367000000
C	-3.423984000000	3.102097000000	-2.721471000000
H	-3.448437000000	2.203355000000	-3.360570000000
H	-4.440533000000	3.257026000000	-2.327262000000
H	-3.165167000000	3.967788000000	-3.356681000000
C	-2.655386000000	0.693240000000	2.693040000000
H	-3.747173000000	0.566203000000	2.671839000000
H	-2.421201000000	1.611621000000	2.142667000000
C	-3.674588000000	-2.019529000000	2.880353000000
H	-4.470816000000	-1.732071000000	2.180871000000
H	-3.746212000000	-3.107763000000	3.036423000000
H	-3.848172000000	-1.534277000000	3.853174000000
C	-2.290368000000	-1.735497000000	2.321924000000
H	-2.110175000000	-2.329366000000	1.415890000000
H	-1.510220000000	-1.970043000000	3.062155000000
C	-2.124523000000	0.750600000000	4.115957000000
H	-1.045384000000	0.949381000000	4.146414000000
H	-2.639242000000	1.575996000000	4.634236000000
H	-2.325202000000	-0.172150000000	4.681080000000

D2⁻

Energy (PCM(benzene)-[TPSSh/def2-TZVPP//TPSSh/def2-SVP])= -3111.45650204

Al	-1.096229000000	0.205893000000	-0.666211000000
Si	-2.505056000000	2.971926000000	-1.325114000000
Si	-1.943680000000	-2.422160000000	-2.242969000000
N	-2.155574000000	-1.327231000000	-0.878178000000

N	-2.486630000000	1.453756000000	-0.429457000000
C	-3.854566000000	-0.343427000000	0.681171000000
C	-3.542924000000	1.055770000000	0.405114000000
C	-4.328966000000	2.040460000000	1.025812000000
H	-4.075658000000	3.086538000000	0.849097000000
H	-5.951665000000	2.559022000000	2.357611000000
C	-5.385495000000	1.741093000000	1.901364000000
C	-4.939518000000	-0.625677000000	1.600509000000
H	-6.494172000000	0.172864000000	2.885783000000
C	-5.684448000000	0.429295000000	2.197330000000
C	-3.593188000000	-2.775230000000	0.420826000000
H	-3.052706000000	-3.619631000000	-0.011079000000
C	-4.637853000000	-3.021583000000	1.327022000000
H	-4.907709000000	-4.054085000000	1.569384000000
C	-5.305330000000	-1.966172000000	1.909164000000
H	-6.124999000000	-2.133297000000	2.613215000000
C	-3.186203000000	-1.480547000000	0.059991000000
C	-0.950352000000	-1.525399000000	-3.584927000000
H	-1.449562000000	-0.598878000000	-3.915874000000
H	-0.849965000000	-2.186337000000	-4.465306000000
H	0.064966000000	-1.257456000000	-3.248870000000
C	-0.982190000000	-4.019842000000	-1.875919000000
H	-0.853422000000	-4.603261000000	-2.805239000000
H	-1.477707000000	-4.673157000000	-1.139344000000
H	0.022090000000	-3.781406000000	-1.488532000000
C	-3.625344000000	-2.879153000000	-2.994947000000
H	-4.165698000000	-1.968328000000	-3.303433000000
H	-3.483320000000	-3.511236000000	-3.889294000000
H	-4.271474000000	-3.425991000000	-2.290682000000
C	-2.186305000000	4.549988000000	-0.305433000000
H	-3.031527000000	4.833305000000	0.342859000000
H	-1.996432000000	5.397846000000	-0.987626000000
H	-1.298538000000	4.434771000000	0.337524000000
C	-1.120257000000	2.907320000000	-2.616873000000
H	-1.117762000000	3.852878000000	-3.189433000000

H	-1.259070000000	2.081355000000	-3.334390000000
H	-0.120878000000	2.785281000000	-2.166719000000
C	-4.147973000000	3.186660000000	-2.249574000000
H	-4.300080000000	2.353417000000	-2.956043000000
H	-5.010706000000	3.203984000000	-1.564958000000
H	-4.150499000000	4.128581000000	-2.825965000000
Al	1.114236000000	0.186028000000	0.560495000000
Si	2.335976000000	3.005623000000	1.270794000000
Si	1.873722000000	-2.473603000000	2.107825000000
N	2.177993000000	-1.335880000000	0.794146000000
N	2.489509000000	1.461853000000	0.429900000000
C	3.997789000000	-0.285427000000	-0.573351000000
C	3.635189000000	1.101106000000	-0.294967000000
C	4.466649000000	2.112116000000	-0.805030000000
H	4.183300000000	3.150334000000	-0.628144000000
H	6.208357000000	2.689452000000	-1.948127000000
C	5.611361000000	1.851342000000	-1.575480000000
C	5.172568000000	-0.527627000000	-1.387785000000
H	6.837079000000	0.326317000000	-2.486667000000
C	5.958714000000	0.552727000000	-1.876312000000
C	3.742552000000	-2.726570000000	-0.416604000000
H	3.172688000000	-3.589042000000	-0.065995000000
C	4.873710000000	-2.933999000000	-1.223174000000
H	5.178054000000	-3.955477000000	-1.471312000000
C	5.583911000000	-1.854044000000	-1.700069000000
H	6.471918000000	-1.990469000000	-2.323221000000
C	3.289653000000	-1.447999000000	-0.053872000000
C	0.765503000000	-1.628840000000	3.392188000000
H	1.216473000000	-0.698593000000	3.777817000000
H	0.620711000000	-2.312164000000	4.249048000000
H	-0.230929000000	-1.378477000000	2.992395000000
C	0.968155000000	-4.070251000000	1.618461000000
H	0.787601000000	-4.690570000000	2.514613000000
H	1.522053000000	-4.687276000000	0.892320000000
H	-0.012033000000	-3.830070000000	1.175063000000

C	3.498187000000	-2.929953000000	2.976645000000
H	4.002088000000	-2.021352000000	3.347110000000
H	3.293798000000	-3.583890000000	3.842760000000
H	4.203684000000	-3.454063000000	2.313335000000
C	2.058284000000	4.525105000000	0.155776000000
H	2.961980000000	4.843461000000	-0.388909000000
H	1.724241000000	5.380789000000	0.769071000000
H	1.274006000000	4.324606000000	-0.592455000000
C	0.820495000000	2.904131000000	2.402964000000
H	0.706655000000	3.866917000000	2.934158000000
H	0.923016000000	2.112742000000	3.164330000000
H	-0.116929000000	2.711674000000	1.855041000000
C	3.845087000000	3.334418000000	2.373491000000
H	3.952140000000	2.530055000000	3.120574000000
H	4.783946000000	3.382825000000	1.799895000000
H	3.726577000000	4.289290000000	2.915479000000

INT3⁻

Energy (PCM(benzene)-[TPSSh/def2-TZVPP//TPSSh/def2-SVP])= -1555.74192469

Al	0.000016000000	1.906290000000	0.000011000000
Si	-3.047577000000	1.220842000000	0.234864000000
Si	3.047597000000	1.220818000000	-0.234864000000
N	1.418695000000	0.593379000000	0.042830000000
N	-1.418679000000	0.593397000000	-0.042832000000
C	-0.000006000000	-1.442469000000	-0.000011000000
C	-1.226329000000	-0.752234000000	-0.353598000000
C	-2.245771000000	-1.511820000000	-0.962141000000
H	-3.132981000000	-0.993605000000	-1.330709000000
H	-3.022731000000	-3.454039000000	-1.512041000000
C	-2.186638000000	-2.913080000000	-1.056080000000
C	-0.000020000000	-2.887976000000	-0.000006000000
H	-1.075843000000	-4.695992000000	-0.545525000000
C	-1.107809000000	-3.602607000000	-0.538920000000
C	2.245745000000	-1.511857000000	0.962144000000
H	3.132955000000	-0.993656000000	1.330731000000

C	2.186588000000	-2.913115000000	1.056086000000
H	3.022664000000	-3.454087000000	1.512063000000
C	1.107752000000	-3.602625000000	0.538917000000
H	1.075765000000	-4.696009000000	0.545530000000
C	1.226329000000	-0.752255000000	0.353578000000
C	2.992085000000	2.838550000000	-1.223874000000
H	2.515422000000	3.660758000000	-0.668612000000
H	4.031006000000	3.131544000000	-1.470387000000
H	2.436210000000	2.718499000000	-2.168763000000
C	4.086726000000	0.033578000000	-1.299664000000
H	5.058366000000	0.502895000000	-1.537717000000
H	4.282435000000	-0.937595000000	-0.821161000000
H	3.566404000000	-0.164888000000	-2.252355000000
C	4.014374000000	1.636033000000	1.356002000000
H	3.436361000000	2.358225000000	1.957806000000
H	4.986828000000	2.100666000000	1.111253000000
H	4.212959000000	0.758218000000	1.992642000000
C	-4.014339000000	1.636103000000	-1.356000000000
H	-4.212921000000	0.758306000000	-1.992664000000
H	-4.986793000000	2.100733000000	-1.111247000000
H	-3.436318000000	2.358308000000	-1.957780000000
C	-2.992067000000	2.838549000000	1.223917000000
H	-4.030990000000	3.131540000000	1.470428000000
H	-2.436202000000	2.718470000000	2.168809000000
H	-2.515395000000	3.660769000000	0.668683000000
C	-4.086720000000	0.033576000000	1.299618000000
H	-3.566408000000	-0.164920000000	2.252309000000
H	-4.282426000000	-0.937583000000	0.821085000000
H	-5.058361000000	0.502888000000	1.537675000000

References

- [1] G. R. Fulmer, A. J. M. Miller, N. H. Sherden, H. E. Gottlieb, A. Nudelman, B. M. Stoltz, J. E. Bercaw, K. I. Goldberg, *Organometallics* **2010**, *29*, 2176-2179.

- [2] (a) G. M. Sheldrick, *Acta Crystallogr. A* **2008**, *64*, 112-122; (b) G. M. Sheldrick, *Acta Crystallographica a-Foundation and Advances* **2015**, *71*, 3-8; (c) G. M. Sheldrick, *Acta Crystallogr. C* **2015**, *71*, 3-8.
- [3] I. S. Weitz, M. Rabinovitz, *J. Chem. Soc.-Perkin Trans. 1* **1993**, 117-120.
- [4] C. H. Lee, Y. H. La, S. J. Park, J. W. Park, *Organometallics* **1998**, *17*, 3648-3655.
- [5] S. Stoll, A. Schweiger, *Journal of Magnetic Resonance* **2006**, *178*, 42-55.
- [6] (a) J. Tao, J. P. Perdew, V. N. Staroverov, G. E. Scuseria, *Phys. Rev. Lett.* **2003**, *91*, 146401; (b) V. N. Staroverov, G. E. Scuseria, J. Tao, J. P. Perdew, **2003**, *119*, 12129-12137.
- [7] F. Weigend, R. Ahlrichs, *Phys. Chem. Chem. Phys.* **2005**, *7*, 3297-3305.
- [8] M. J. Frisch, G. W. Trucks, H. B. Schlegel, G. E. Scuseria, M. A. Robb, J. R. Cheeseman, G. Scalmani, V. Barone, G. A. Petersson, H. Nakatsuji, X. Li, M. Caricato, A. V. Marenich, J. Bloino, B. G. Janesko, R. Gomperts, B. Mennucci, H. P. Hratchian, J. V. Ortiz, A. F. Izmaylov, J. L. Sonnenberg, D. Williams-Young, F. Ding, F. Lipparini, F. Egidi, J. Goings, B. Peng, A. Petrone, T. Henderson, D. Ranasinghe, V. G. Zakrzewski, J. Gao, N. Rega, G. Zheng, W. Liang, M. Hada, M. Ehara, K. Toyota, R. Fukuda, J. Hasegawa, M. Ishida, T. Nakajima, Y. Honda, O. Kitao, H. Nakai, T. Vreven, K. Throssell, J. J. A. Montgomery, J. E. Peralta, F. Ogliaro, M. J. Bearpark, J. J. Heyd, E. N. Brothers, K. N. Kudin, V. N. Staroverov, T. A. Keith, R. Kobayashi, J. Normand, K. Raghavachari, A. P. Rendell, J. C. Burant, S. S. Iyengar, J. Tomasi, M. Cossi, J. M. Millam, M. Klene, C. Adamo, R. Cammi, J. W. Ochterski, R. L. Martin, K. Morokuma, O. Farkas, J. B. Foresman, D. J. Fox, Gaussian 16, Revision C.01. Gaussian, Inc., Wallingford CT, **2019**.
- [9] C. Y. Peng, P. Y. Ayala, H. B. Schlegel, M. J. Frisch, *J. Comp. Chem.* **1996**, *17*, 49-56.
- [10] J. W. McIver, Komornic, A., *J. Am. Chem. Soc.* **1972**, *94*, 2625-2633.
- [11] J. Tomasi, B. Mennucci, R. Cammi, *Chem. Rev.* **2005**, *105*, 2999-3094.
- [12] (a) J. P. Foster, F. Weinhold, *J. Am. Chem. Soc.* **1980**, *102*, 7211-7218; (b) A. E. Reed, F. Weinhold, *J. Chem. Phys.* **1985**, *83*, 1736-1740.
- [13] A. E. Reed, R. B. Weinstock, F. Weinhold, *J. Chem. Phys.* **1985**, *83*, 735-746.
- [14] E. D. Glendening, J. K. Badenhoop, A. E. Reed, J. E. Carpenter, J. A. Bohmann, C. M. Morales, P. Karafiloglou, C. R. Landis, F. Weinhold, GENNBO 7.0 ed., Theoretical Chemistry Institute, University of Wisconsin, Madison, WI, **2018**.
- [15] (a) R. F. W. Bader, *Atoms in Molecules: A Quantum Theory*, Clarendon, Oxford, **1990**; (b) R. F. W. Bader, *Chem. Rev.* **1991**, *91*, 893-928.
- [16] T. A. Keith, T. K. Gristmill, 19.02.13 ed., Overland Park KS, USA (aim.tkgristmill.com), **2019**.
- [17] F. Neese, 4.2.1 ed., Max-Planck-Institut für Kohlenforschung; Mulheim an der Ruhr, Germany, **2019**.
- [18] (a) E. D. Hedegård, J. Kongsted, S. P. A. Sauer, *J. Chem. Theory Comput.* **2013**, *9*, 2380-2388; (b) E. D. Hedegård, J. Kongsted, S. P. A. Sauer, *J. Chem. Theory Comput.* **2011**, *7*, 4077-4087.